The Dissertation Committee for Joshua Benjamin White
certifies that this is the approved version of the following dissertation:

Evaluation of Fatigue Design Load Models for Cross-Frames in Steel I-Girder Bridges

Committee:

Michael D. Engelhardt, Supervisor

Todd A. Helwig, Co-Supervisor

Krishnaswa Ravi-Chandar

Eric B. Williamson

Evaluation of Fatigue Design Load Models for Cross-Frames in Steel I-Girder Bridges

by

Joshua Benjamin White

Dissertation

Presented to the Faculty of the Graduate School of

The University of Texas at Austin

in Partial Fulfillment

of the Requirements

for the Degree of

Doctor of Philosophy

The University of Texas at Austin

August 2020

Dedication

Amy, this is for you. Thank you for your unwavering support and your unending love.

Acknowledgements

I would like to acknowledge my committee members, whose keen insight, experience, and encouragement have made this work possible. Dr. Engelhardt, it has been my greatest academic honor to work under your advisement. Thank you for your support, I have learned much from you that will make me a better engineer and a better person. Dr. Helwig, I have thoroughly enjoyed learning from you over the past several years, your knowledge in all things stability never ceases to impress me. Dr. Ravi-Chandar and Dr. Williamson - I appreciate the time, effort, and feedback you have provided to me.

It has been a privilege to work with my fellow researchers on this project: Matt Reichenbach, Sunghyun Park, Esteban Zecchin, Matthew Moore, Yangqing Liu, Chen Liang, and Balázs Kövesdi. Matt R., I'd especially like to thank you for your friendship and your support. You were the glue that held this team together.

There have been many colleagues and experts in this field that have taken their time to weigh in on my research. I am indebted to you all. Dr. Robert Connor and Mike Grubb, thank you for providing your valuable feedback and contributing your expertise to help shape this work. Dr. John Kulicki, Dr. Andrzej Nowak, and Dr. Tom Murphy, I appreciate you all taking the time to share your experiences and offer your suggestions. Thank you to the NCHRP 12-113 project panel and the TRB staff for your guidance and your expertise, as well as the engineers and staff at TxDOT for your support. To Debbie Walker, thank you for your efforts in providing me the WIM records.

To my WJE family - thank you for your constant support. You have believed in me, invested in me, and have always had my back. I'd like to acknowledge the Houston office for their encouragement and support; particularly Justin, Ammie, and my S12 family: Jacob, Kurt, Anna, Daniel, Casey, and Ahmad. Your friendship has meant everything to me.

It would be impossible to list the countless family and friends whose love and support have encouraged and supported me in this endeavor. To Mom and Dad, thank you

for your love. Kathy and Tom, you have always believed in me. To all of my brothers and sisters and extended family, thank you from the bottom of my heart. To Dale and Gail, my extended parents, I appreciate everything you have done for me and your constant support. Dr. Borg, you have been a true friend; thank you for being a constant source of support and beer. Dr. Fry, I'd like to thank you for your mentorship throughout the years. I am profoundly grateful to have your friendship.

To my wife, Amy. Thank you for your endless support. I owe everything to you. To Phin and Sophie, I know you're too young to fully grasp how thankful I am for the countless hours you've sacrificed as daddy worked late. Don't worry, we'll make up tons of time playing "monsters" and "hide-and-seek".

Finally, I'd like to acknowledge my Creator. You have been the lamp to my feet and the light to my path.

Abstract

Evaluation of Fatigue Design Load Models for Cross-Frames in Steel I-Girder Bridges

Joshua Benjamin White, Ph.D.

The University of Texas at Austin, 2020

Supervisor: Michael D. Engelhardt

Co-Supervisor: Todd A. Helwig

There have been a number of advances in the level of understanding of cross-frame systems for steel I-girder bridges; however, very little work has focused on the proper loading conditions to produce an adequate estimate of the fatigue load in cross-frames. The goal of this research is to provide an improved definition of the fatigue loading for cross-frames in straight, horizontally-curved, and skewed steel I-girder bridges which will be analyzed using refined analysis techniques.

In order to compare load effects, three bridges were instrumented and monitored. The bridges include: i) a straight bridge with normal supports, ii) a straight bridge with skewed supports, and iii) a horizontally curved bridge with radial supports. Data gathered from the field instrumentation was used to validate three-dimensional finite element analysis (FEA) models that were used to carry out extensive parametric analyses to improve the understanding of the behavior of cross-frame stresses as a function of truck position on the bridge. A wide range of geometrical parameters of straight and horizontally curved bridges were used to understand the general behavior of the bridges.

The primary objectives of this research include the following:

1) Investigate the adequacy of the current AASHTO (American Association of State Highway and Transportation Officials) fatigue load model for the design of cross-

frames in steel I-girder bridges.

2) Investigate the effects of multiple presence on the design of cross-frames in steel I-girder bridges.

3) Investigate the reliability of the developed load model and identify the gaps in knowledge of cross-frame detail resistance data as it relates to the reliability of current design practices.

These objectives were accomplished by examining recently collected, high-resolution, multi-lane weigh-in-motion (WIM) data, which represent actual truck traffic records in the US. The current AASHTO fatigue design load model was evaluated by comparing cross-frame load effects caused by the fatigue load model to load effects caused by simulated truck traffic representing actual live load. Influence surfaces generated from three-dimensional FEA models provided information on the stresses in select cross-frame members as a function on truck position on the bridge deck. WIM data representing real truck traffic (tens of millions of truck records) were filtered and analyzed; multi-lane data were analyzed using a cluster analysis. The statistical parameters of this WIM study were used to simulate actual live load on the three-dimensional bridge models and compare load effects to those generated by a fatigue design truck. The outcome of this study indicates the current fatigue design truck axle and weight configuration and placement of the fatigue design truck to maximize design-controlling fatigue effects for both the Fatigue I and Fatigue II AASHTO limit states is overly conservative. Stochastic techniques were used to investigate the implications of new load factors in the context of reliability-based fatigue design.

Table of Contents

List of Tables

List of Figures

Chapter 1: Introduction

1.1 Research Overview and Objectives

The American Association of State Highway Transportation Officials (AASHTO) defines a cross-frame as a "*transverse truss framework connecting adjacent longitudinal flexural components*"; these members are used to transfer and distribute vertical and lateral loads, as well as provide stability to the compression flanges of longitudinal flexural members (AASHTO 2014). A photo of a cross-frame in a steel I-girder bridge is shown in Figure 1-1. Cross-frames serve an important role in the behavior of a bridge throughout its life, beginning with construction. Prior to the development of composite action between longitudinal flexural members and the concrete deck, cross-frames serve as primary stability braces to resist girder lateral torsional buckling. In service, the cross-frames serve to distribute vertical (e.g., truck traffic) and lateral (e.g., wind) loads to other primary members.

Under cyclic or repetitive loads caused by highway traffic, cross-frames and their connections are susceptible to distortion-induced and load-induced fatigue, which must be accounted for in design. Distortion-induced fatigue issues, which are estimated to be responsible for approximately 90% of all reported fatigue issues (Connor and Fisher 2006), are a topic that has been primarily addressed in the 1970s and 1980s by enhanced detailing practices. Load-induced fatigue (the aspect of fatigue that is considered in this research) is an issue that requires an understanding of the loading conditions and the associated accumulation of fatigue damage in a member over its lifetime.

It is important to consider modern transportation loads in the design of cross-frames for new bridges, as well as the evaluation of cross-frames in older bridges. According to the United States Department of Transportation (USDOT) Bureau of Transportation Statistics, of the various modes of transportation available today, more freight is transported via roadways than any other mode (e.g., rail, water, air, pipeline, etc.) for short distance trips (i.e., less than 750 total miles). In addition, truck weights are at historic highs, with total truck tonnage having increased 5 to 10 percent annually for the past 20 years (USDOT 2018). The significant growth of highway traffic volume has an impact on the fatigue performance of steel members, which requires periodic review to ensure the standards and details used in their design reflect these loads.

State by state, standard details for the design of cross-frames have been inextricably linked to the successful performance of these members in older bridges, and these standard details are often used as a starting point in the design (Reichenbach, et al. 2021). The standard details for various Departments of Transportation (DOTs) are generally based on bridge geometry and minimum member cross-sections that have worked well in the past. The older bridges for which these standard details have been based were typically designed using different load models that are not representative of the truck traffic in use today (Nowak 1999 and Kulicki, et al. 2015). In addition, cross-frame standards and details have seen little improvement or incorporation of recent research over the past several decades pertaining to more accurate cross-frame analysis techniques (Wang 2013 and Battistini, et al. 2016).

While the design of cross-frames for load-induced fatigue has remained relatively unchanged over the years, advancements and refinements in bridge design and analysis have created an opportunity for improvement related to cross-frame design and analysis. Recent work has considered the effects of modern traffic loads on fatigue design of primary longitudinal bridge members (Kulicki, Wassef, et al. 2015), but very little work has focused on understanding the proper loading conditions to produce an adequate estimate of the load-induced fatigue in cross-frames.

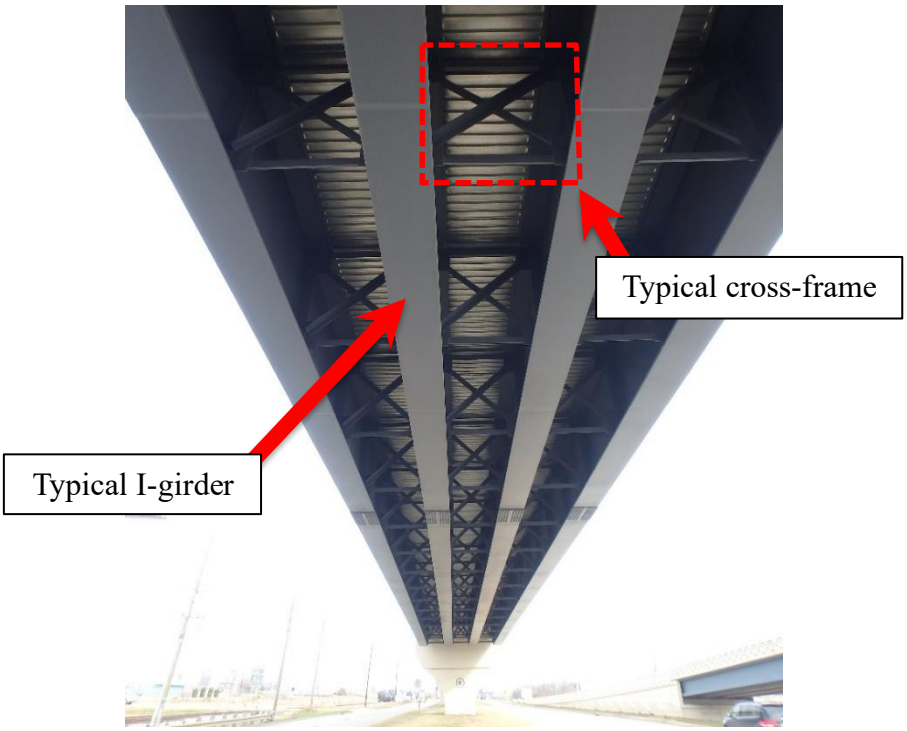

Figure 1-1: Typical cross-frames in a steel I-girder bridge span.

Based on a survey of bridge owners and consultants across the country (Reichenbach et al. 2021), there are no reported widespread issues related to load-induced fatigue of cross-frames. The nation's older bridges appear to be successfully carrying the increased traffic volume and weights that were not considered by the design load models of their day. The fact that standard cross-frame designs are generally based on empirical performance data and have generally performed well over the years suggests they are adequately designed for fatigue. However, the traffic demand on both new and existing bridges continues to grow rapidly. As bridges are maintained for longer periods of service life, the effect of increased truck weight and quantity on fatigue design and assessment becomes increasingly important. Since cross-frames are an important component of a bridge, they require an updated review as it relates to modern-day traffic loading to ensure the design of these members is not overly conservative (i.e., unduly expensive) or unconservative (i.e., unsafe).

The goal of this research is to provide an improved definition of the fatigue loading for cross-frames, with a particular focus on curved and/or severely skewed steel I-girder bridges, for which cross-frame forces are known to produce larger force effects (Wang 2013, Battistini, et al. 2016, Keating, Saindon and Wilson 1997, McConnell, Radovic and Ambrose 2016). The primary objectives of this research include the following:

1. Investigate the adequacy of the current AASHTO fatigue load model for the design of cross-frames in steel I-girder bridges.
2. Investigate the effects of multiple presence on the design of cross-frames in steel I-girder bridges.
3. Investigate the reliability of the developed load model and identify the gaps in knowledge of cross-frame detail resistance data as it relates to the reliability of current design practices.

These objectives will be accomplished using field experimentation and validation; refined analysis techniques; and recently collected, high-resolution, multi-lane weigh-in-motion (WIM) data, which represent actual truck traffic records in the US. Stochastic techniques will be used to investigate the implications of these findings in the context of reliability-based fatigue design.

1.2 PROJECT DESCRIPTION

This research was performed in conjunction with the National Cooperative Highway Research Program (NCHRP) Project 12-113, "*Proposed Modification to AASHTO Cross-Frame*

Analysis and Design" (referenced herein as the project). The objective of the project was to propose modifications to the AASHTO *Load and Resistance Factor Design (LRFD) Bridge Design Specifications* (AASHTO 2014, referenced herein as AASHTO *LRFD*) to provide quantitative guidance on 1) the calculation of the fatigue design forces in cross-frames for steel I-girder bridges; 2) the calculation of strength and stiffness requirements for stability bracing; and 3) the influence of cross-frame member end connections upon cross-frame stiffness.

The project team included graduate researchers, faculty advisors, and consultants. Due to the wide range of topics, the project scope was divided into two additional doctoral dissertations (Reichenbach 2020 and Park 2020). While the scopes of all three dissertations include overlap, each had a specific focus relevant the project objectives. Reichenbach investigated the influence of composite geometry and cross-frame layout on the fatigue behavior of cross-frame systems, including the dissemination of the experimental data and compilation of the analytical testing matrix discussed in Chapter 3. In addition, Reichenbach evaluated commercial software programs regarding their ability to accurately predict cross-frame behavior for various bridge geometries and cross-frame configurations. Park evaluated the influence of cross-frame end connections on member stiffness using refined analysis techniques, specifically developing a three-dimensional modeling approach for accurately representing the effective cross-frame stiffness in composite systems.

The project included four phases, with the following key tasks:

Phase I: Planning

1. Review Pertinent Literature
2. Synthesize the Current Body of Knowledge
3. Propose 2-Part Analytical Program
    a. Part 1: Preliminary Analysis of Three Bridges for Instrumentation and Testing in Phase II
    b. Part 2: Development of a Preliminary Plan for Comprehensive Parametric Finite Element Analysis (FEA) Studies in Phase III
4. Propose Field Experiments
5. Identification of AASHTO *LRFD* Provisions for Modification
6. Present Findings in Interim Report

Phase II: Part 1 Analytical Program

7. Perform Preliminary Analysis of Bridges to be Instrumented and Tested
8. Perform Field Experiments
9. Validate FEA Models
10. Present Findings in Interim Report

Phase III: Part 2 Analytical Program

11. Parametric FEA Studies
12. Develop Proposed Changes to AASHTO *LRFD* Bridge Design Specifications
13. Synthesize Findings in Interim Report

Phase IV: Final Products

14. Development of Ballots for AASHTO *LRFD* Bridge Design Specifications
15. Final Report Preparation

For the research presented in this dissertation, the overlap with Reichenbach (2020) and Park (2020) is primarily contained in Chapter 3 as it pertains the experimental program (i.e., field instrumentation and load tests) and model validation. The following section discusses the specific focus of this dissertation as it relates to the project scope.

1.3 DISSERTATION FOCUS

In the context of the project objectives and tasks discussed in the previous section, the primary focus of this dissertation is to provide an appropriate definition of fatigue loading for cross-frames. The scope of this study specifically includes straight bridges with both normal and skewed supports (Figure 1-2 and Figure 1-3), as well as horizontally-curved bridges with both normal (Figure 1-4) and skewed supports, since both skew and curvature add complexity to the behavior of cross-frames.

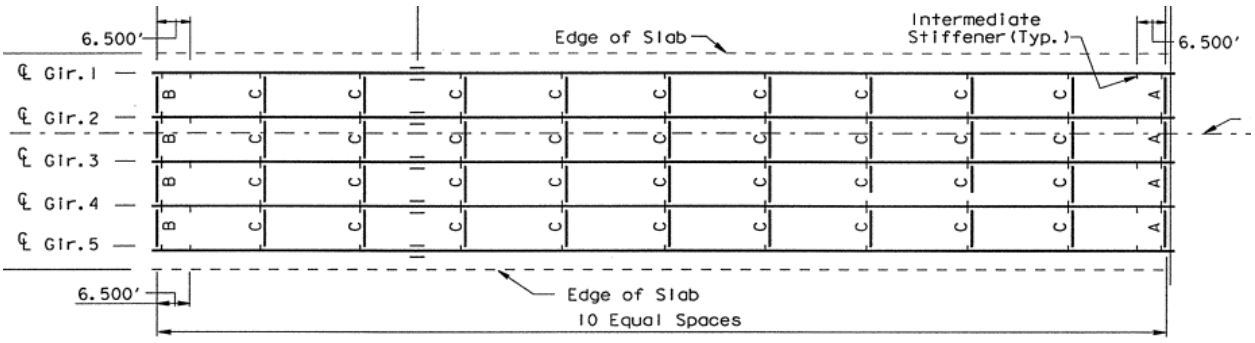

Figure 1-2: Typical cross-frame framing plan for a straight bridge with normal supports.

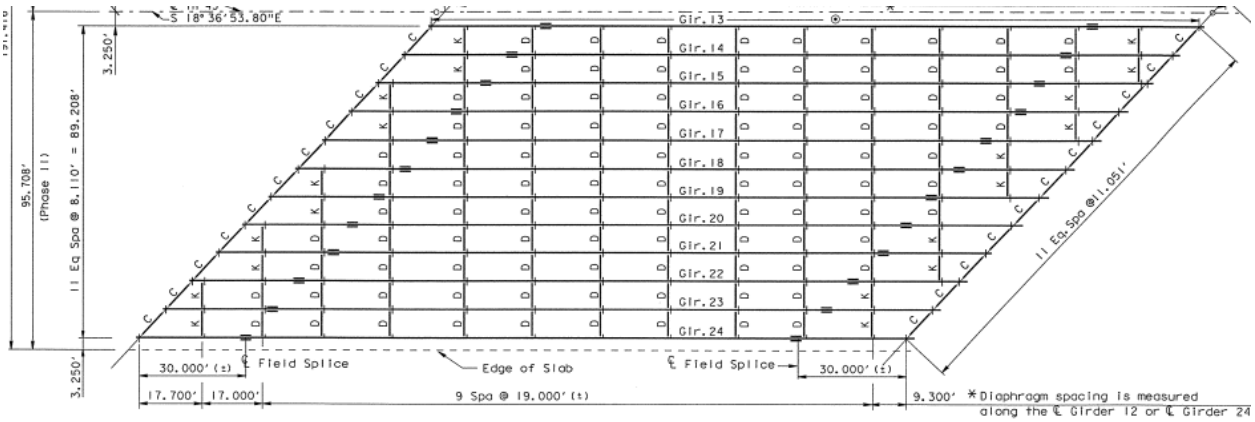

Figure 1-3: Typical cross-frame framing plan for a straight bridge with skewed supports.

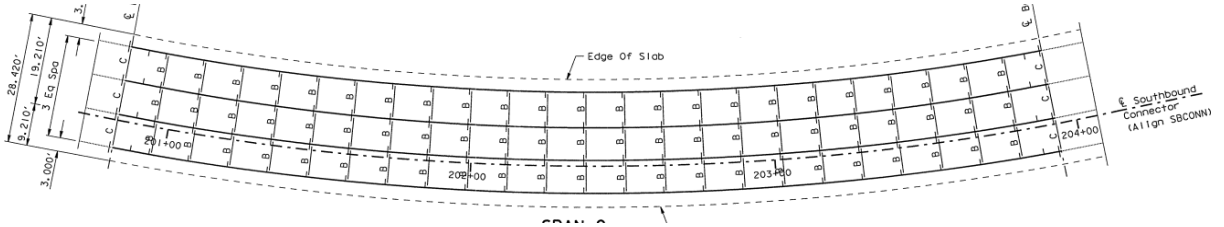

Figure 1-4: Typical cross-frame framing plan for a curved bridge span with normal supports.

To better understand modern traffic loading, WIM records were obtained from the Federal Highway Administration (FHWA) for 16 sites in the US. Current WIM technologies, which are discussed in greater detail in Chapter 2, allow agencies to collect axle weights and spacing from vehicles traveling at driving speeds. A primary benefit of the WIM records obtained for this study is the high resolution of the recorded time stamps, which allow for more accurate placement of the

vehicles on a simulated bridge deck to study effects such as multiple presence and sensitivity of lane positions. Another benefit of the WIM records obtained for this study is the fact that, since they were recorded in 2014 and were obtained from various roadways with a variety of traffic counts, these records should represent a relatively current national sample of vehicle loading. A comparison is made in Chapter 4 to WIM records studied by others to support this assumption. The raw WIM records were obtained without substantial pre-filtering, which allowed this research to control various aspects of data filtering. This research desired to control the removal of light weight vehicles and records, which are commonly removed for fatigue evaluation. This research also evaluates the truncation of smaller stress cycles and its effect on the fatigue performance of cross-frames.

To date, the effect of modern-day loading conditions on cross-frame forces has not been studied. The implications of this research will allow bridge designers to more accurately predict realistic cross-frame forces based on modern traffic. The findings of this research are provided in the context of a reliability analysis that should allow for a more optimal design of bridge cross-frames. Since cross-frames are, per pound of steel, among the most labor intensive and expensive components of a bridge (Mahmoud 2011), this has the potential to provide significant cost savings to the bridge owner.

1.4 DISSERTATION ORGANIZATION

This dissertation is presented in seven chapters with supporting appendices. Chapter 2 provides a background of key concepts related to this research, including a summary of the body of knowledge pertaining to fatigue behavior in steel I-girder bridges, resistance and load models for fatigue, reliability-based design and calibration of Load and Resistance Factor Design (LRFD) codes, and analysis techniques for design of cross-frames.

Chapter 3 outlines the selection process of the bridges instrumented and load tested for the purposes of FEA model validation. These bridges are assumed to be representative of the population investigated in this research. The FEA model validation was performed prior to extensive parametric studies, which allowed for selecting a number of models that are assumed to be the most critical for cross-frame force effects.

Chapter 4 uses the WIM records obtained from sites throughout the US to simulate realistic traffic on bridges representative of the model data set discussed in Chapter 3. In general, since

WIM analyses for cross-frames have four degrees of freedom, each simulation for a particular bridge and cross-frame member must consider longitudinal and transverse vehicle placement, the measured cross-frame force effects, and time. Since these analyses present significant computational time constraints, preliminary studies are discussed that utilize a single WIM record that is generally representative of other records, in order to explore the sensitivities of vehicle lane placement, multiple presence, and vehicle weight filters on the fatigue parameters for computing the Fatigue I and II limit states, as defined in AASHTO *LRFD*. The Fatigue I and II limit states are described in Chapter 2.

Building on the findings from the sensitivity studies provided in Chapter 4, Chapter 5 discusses the simulation of 18 WIM records with "drive lane" data (i.e., the instrumented lane is the right lane, or drive lane, where a majority of the heavy traffic is driven) on the drive lanes of the subset of bridges chosen to be representative of the analytical testing matrix. These advanced studies aim to develop appropriate statistical parameters for the reliability evaluation of the Fatigue I and Fatigue II limit states. The variation of cycles per passage for various bridge geometries is investigated using the WIM records with various traffic counts applied to the same set of bridges.

Chapter 6 implements the statistical parameters developed in Chapter 5 in a reliability study of proposed load factors for the Fatigue I and II limit states. The inherent reliability indices of the existing code are reviewed, and the proposed load factors are presented in the context of meeting the same level of reliability.

Finally, Chapter 7 provides a synthesis of the primary findings and conclusions of this research. Recommendations for additional studies are provided.

Chapter 2: Background and Literature Review

This chapter provides a background of key concepts related to this research, including a summary of the body of knowledge pertaining to fatigue behavior in steel I-girder bridges, resistance and load models for fatigue, reliability-based design and calibration of current LRFD codes, and analysis techniques for design of cross-frames.

2.1 FATIGUE IN STEEL BRIDGES

Crack growth in steel members or weldments is a complex phenomenon whose process can be described as 1) **initiation** of a defect (which is generally localized), and 2) **propagation** of a formed crack under cyclic or repetitive loading until 3) a state of **equilibrium** is reached (e.g., unstable fracture). In the context of this discussion, a defect is defined as an unwanted feature that is larger than a pre-defined acceptable size, such as cracks, porosity, lack of fusion, or incomplete penetration (typically found in welds, but also relevant to base metals). Fracture is defined as a sudden rupture or extension of the crack length that leads to loss of functionality or serviceability of the bridge member.

The initiation and propagation of cracks or crack-like flaws and the subsequent dynamic fracture have been well studied in steel members; summaries of the current body of knowledge can be found in Chowdhury and Sehitoglu (2016), and a review of fundamental concepts can be found in Fisher et al. (1998) and Freund (1990). In general, the initiation and subsequent propagation of cracks or crack-like flaws in steel bridge members typically results from one or a combination of unfavorable conditions that can be broadly categorized as follows: design (e.g., poor detailing), construction (e.g., poor quality of welds), and material (e.g., poor toughness characteristics) (Zhou and Biegalski 2010). Some aspects of these considerations are unavoidable, such as welding of steel members, during which residual (internal) stresses lead to unintended but anticipated stress concentrations. Local stress concentrations created by the uneven heating and cooling of the welding process can consequently facilitate crack growth, and the welding process itself can introduce defects (e.g., lack of fusion, undercutting, etc.). Openings, fillets, threads, or attachments are examples of other stress concentrations that are generally unavoidable. A typical aspect of design that is unavoidable but can be intentionally controlled is the creation of a stress riser due to a discontinuity when joining one material to another. Finally, a material's fracture toughness defines a material's susceptibility to fracture.

When a crack or crack-life flaw is present in a steel member, it is susceptible to crack growth. In order for a flaw to propagate in steel bridge members, a cyclical or repetitive load with a tensile component must be applied to the member (Fisher et al. 1998, FHWA 2016). In particular, the tensile component of the load must be generally normal to the direction of crack growth, a so-called *Mode I* crack (Fisher et al. 1998). Stated more precisely, crack growth orientation is encouraged by the direction of the tensile component of an applied load.

Crack growth in primary and secondary steel members in bridges is predominantly driven by stress ranges caused by the passage of truck traffic. The stress levels associated with fatigue crack growth are generally well below the yield strength of the material. In the context of this discussion, primary members in non-horizontally curved bridges are defined as longitudinal members that are key elements of a bridge superstructure and provide a direct load path from the bridge deck to the bridge substructure (see Figure 2-1 for an illustration of these typical elements in a straight bridge). Secondary members in non-horizontally curved bridges are defined as members that are typically constructed transverse to the primary members (e.g., cross-frames and diaphragm systems); in general, these secondary members 1) enhance the lateral torsional buckling resistance of primary members by reducing their unbraced length, 2) resist the torsion applied to girders due to deck overhang or curvature, and 3) distribute lateral loads (e.g., wind loads) across the structure and into the substructure. In the context of AASHTO *LRFD* design, cross-frames and diaphragms in horizontally-curved bridges (Figure 2-2) are considered primary members due to their increased importance in overall structural stability due to the curved bridge geometry (Stith et al. 2010).

Cracks continue to propagate under cyclic loading until they are either arrested or complete member fracture occurs. The arrest of cracks in steel bridges is commonly achieved intentionally, when upon their discovery, bridge owners or inspectors intervene by alleviating the stress concentration at the crack tip. One method of crack arrest that is commonly utilized in steel bridges consists of coring a sufficiently large diameter hole at the crack tip. The arrest of cracks in bolted or riveted connections sometimes happens naturally through a cross-boundary separation, when a crack cannot continue to propagate due to the discontinuous member construction. When the failure of an individual element does not lead to a system failure (e.g., the loads are redistributed throughout the structure), this is referred to as a stable fracture.

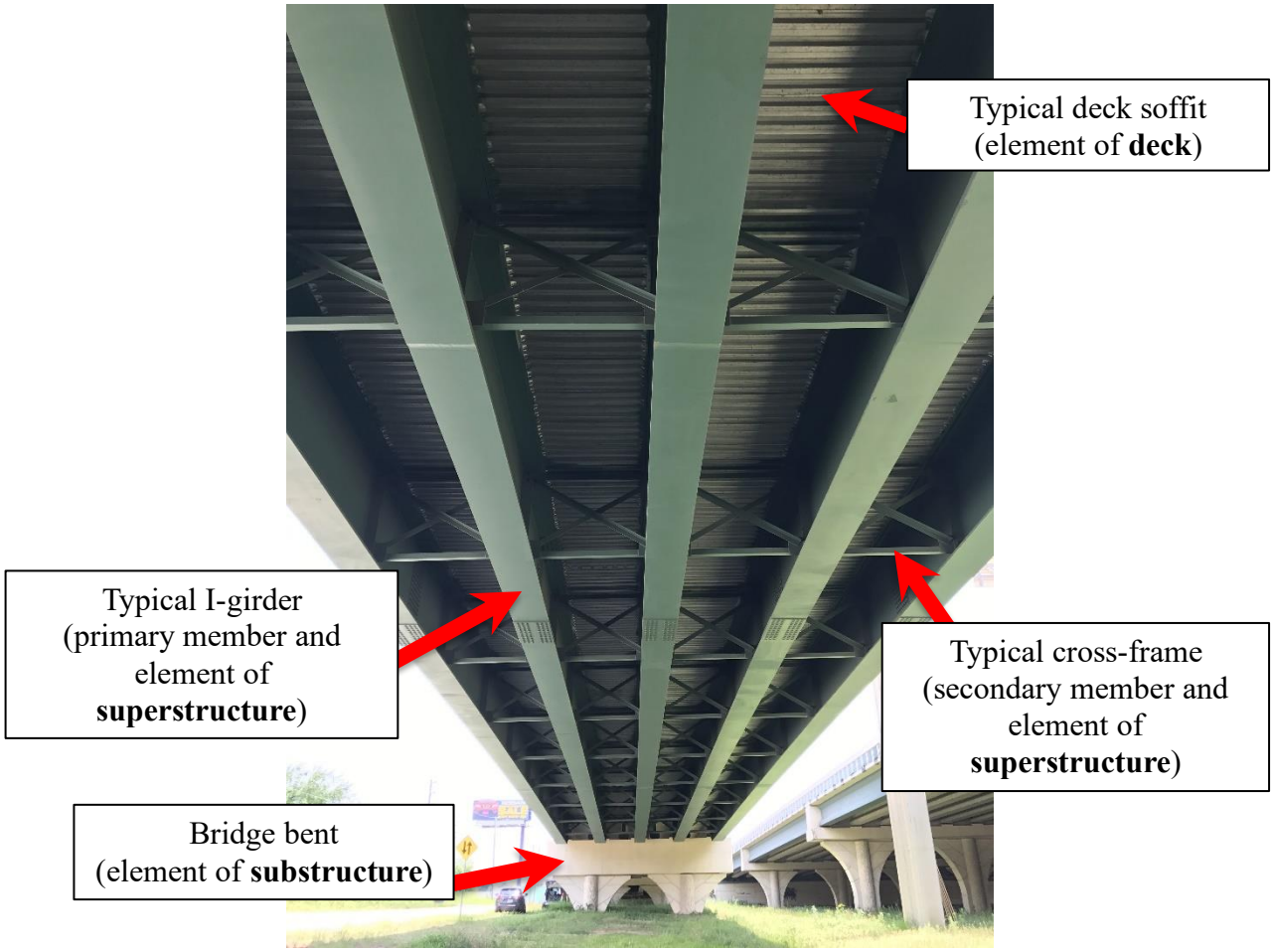

Figure 2-1: Typical cross-frames in a straight, steel I-girder bridge span. Also shown are typical elements of a bridge's deck, superstructure, and substructure.

Unfortunately, unstable fractures do occur which can lead to localized failures in bridge systems, or in the worst case, entire failure of the bridge. The collapse of the Silver Bridge (connecting Point Pleasant, West Virginia and Kanauga, Ohio) is an example of an unstable fracture that occurred at a critical member due to mechanisms associated with stress corrosion cracking (NBS 1969). The bridge, constructed in 1929, was designed as an eye bar chain suspension bridge that utilized twin-member eye bar "links" to carry loads from both the superstructure and deck. Due to the high-strength material characteristics of the eye bar and the design of the links as non-redundant members, the flaw initiation, propagation, and ultimate fracture of one eye bar led to the complete bridge collapse and the loss of 46 lives (Witcher 2017). The collapse of this bridge resulted in the passage of the first national bridge inspection standards in 1968, which would later become the National Bridge Inspection Standards (NBIS).

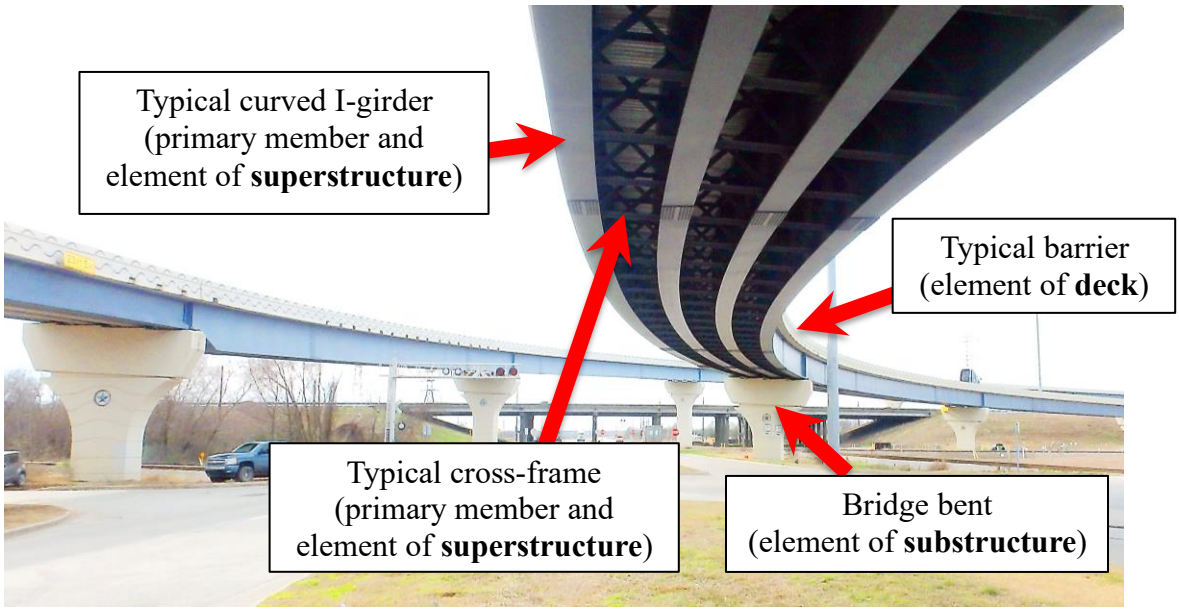

Figure 2-2: Typical cross-frames in a horizontally-curved steel I-girder bridge span. Also shown are typical elements of a bridge's deck, superstructure, and substructure.

To date, very little documented research has been performed considering the effects of modern traffic loads on the fatigue behavior of cross-frames. The fatigue behavior of steel details specific to bridges was studied extensively by Fisher and Keating (1986, discussed in more detail in Section 2.2) in order to characterize the applied cyclic loading (stress ranges) relative to the quantity of load cycles to failure; however, limited research has been performed for typical cross-frame connections. The following is a summary of research efforts related to the fatigue behavior of cross-frames.

2.1.1 Influence of Member End Connection Eccentricity to Cross-Frame Stiffness and Fatigue

For a given maximum design moment, design equations referenced in Yura (1992, 2001) related to stability bracing can be used to solve for the required stiffness of the torsional bracing system (i.e., the stiffness of the cross-frame system). There are generally three components of the bracing system that impact the bracing behavior for torsional bracing systems (represented by β_{Ts}): i) the stiffness of the brace (cross-frame), β_b, ii) the effective resistance of cross-sectional distortion, β_{sec}, and iii) the in-plane stiffness of the brace, β_g. From a stiffness perspective, bracing systems often follow the behavior of springs in series. Considering these three stiffness

components of a torsional bracing system, the total system stiffness is given by the following expression from Yura et. al. (1992):

$$\frac{1}{\beta_{Ts}} = \frac{1}{\beta_b} + \frac{1}{\beta_{sec}} + \frac{1}{\beta_g} \qquad \text{Eq. 2.1}$$

This expression shows that the effective stiffness of a cross-frame will be less than the least stiff component in the system. If the stiffness related to cross sectional distortion, β_{sec}, and the in-plane stiffness of the girder, β_g, are sufficient, but if the stiffness of the brace, β_b, is low, then the effective stiffness of the torsional bracing system, β_{Ts}, will suffer due to the flexible brace. This could potentially render the cross-frame inadequate from a stiffness standpoint. This example illustrates the importance of each component of the total system stiffness.

If the total system stiffness of a cross-frame is underestimated, that is, if the actual cross-frame stiffness is greater than assumed in the analysis, the result will be conservative as it relates to stability bracing. However, this same situation may be unconservative from a fatigue standpoint. If the cross-frame is stiffer than considered in analysis, then the actual stress ranges experienced by the cross-frame will be higher than those computed in the analysis, which could potentially result in fatigue issues during the life of a bridge. The opposite is also true; if the total system stiffness is overestimated, the constructed cross-frame will have less stiffness than assumed in the design. This is unconservative as it relates to stability, and conservative for fatigue considerations. This overestimate of the total system stiffness can lead to the prediction of stress ranges that the actual cross-frame will not experience, potentially leading a designer to believe the cross-frame will not pass the fatigue checks. Thus, it is important that the actual stiffness of a cross-frame be represented with reasonable accuracy in the analysis of steel I-girder bridge systems.

As part of the NCHRP 12-113 project scope, Park (2020), Reichenbach (2020), and Reichenbach et al. (2021) discuss in detail the estimation of actual cross-frame stiffness using various models that more accurately reflect the stress ranges associated with fatigue.

2.1.2 Use of Bent Plate Connections in Skewed Bridges

Cross-frames close to abutments experience significant live-load induced forces due to differential deflections of the girders. Quadrato (2010, 2014) investigated reducing girder end twist in skewed steel I-girder bridges such that the first row of cross-frames could be located further

from the abutment. By moving the first row of cross-frames away from the abutment, the research suggested that the load-induced fatigue forces experienced by the cross-frames might be reduced.

The most common detail used for cross-frame to girder connections at the time the research was performed was a bent plate connection. One objective of the project was to investigate the behavior of the bent plate connection, and another objective was to propose an alternate, improved connection. The research described in the previous references included field instrumentation, laboratory testing programs, and parametric studies that led to proposing a split pipe connection as an alternative to the bent plate.

One of the laboratory tests was performed to evaluate the fatigue performance of the proposed split pipe connection, as well as normal and skewed plate stiffeners. The testing was performed under cyclic loading and demonstrated that the tension flange stress range met the AASHTO fatigue category C for all test specimens. In terms of fatigue behavior (cycles to failure under a given stress range), the split pipe stiffener behaved the best, followed by the normal plate stiffener, and finally the skewed plate stiffener.

2.1.3 Impact of Single-Angle Members on Cross-Frame Stiffness

McDonald and Frank (2009) performed testing on single-angle members that were welded to connection plates. The goals of the study were to confirm that the detail was in the appropriate fatigue category in AASHTO and to compare the performance of balanced welds and unbalanced welds.

The testing program was intended to evaluate the performance of single-angle members with gusset plates welded to each side of the angle. Each specimen was intended to be uniaxially loaded under tension; however, upon loading the first specimen, large amounts of bending were observed, even though the angle was loaded in tension. To avoid damaging the testing machine, further tests were performed by placing angles back-to-back. This created a system that performed similarly to a double-angle member, which may have unintentionally improved the performance of the angles. While this research was not performed to study the impact of eccentricity on connection stiffness, it was apparent from the testing that the use of single-angle members resulted in large amounts of out-of-plane bending (McDonald and Frank 2009).

The research outlined by Wang (2013) and Battistini, et. al. (2016) also investigated the stiffness and fatigue behavior of cross-frames, specifically three types: X-type frames, K-type

frames, and Z-type frames. Z-type frames are not commonly used but were investigated as a possible alternative to X-type and K-type frames. The researchers also tested a variety of cross-frame member types, including single angles, double angles, and HSS sections. As part of the research program described in these studies, large scale tests were performed on the three types of cross-frames and six different cross-frame configurations: X-type cross-frames composed of equal leg, single-angle members; X-type cross-frames composed of unequal leg, single-angle members; K-type cross-frames composed of single angle members; Z-type cross-frames with a double-angle diagonal member and single angle struts; Z-type cross-frames composed of double-angle members; and Z-type cross-frames with HSS section members for both the diagonal and struts.

Each of the cross-frame specimens was tested in a setup that replicated the deformations and forces that would be experienced by a cross-frame in a steel bridge as one girder displaced relative to an adjacent girder. This allowed for a system-based test to characterize the interaction of the various cross-frame assemblies with the overall structure. Previous to this research, single angle fatigue details were only studied on an element basis. Each cross-frame was instrumented with strain gauges to measure axial strains in each member and linear potentiometers to measure the rotation of the cross-frame. The axial forces experienced by each member were calculated from the strain data using the numerical regression technique outlined in (Helwig and Fan 2000). The rotations were used to calculate the brace stiffness provided by each cross-frame using the following equation (Wang 2013; Battistini et. al. 2016):

$$\beta_b = \frac{M}{\theta} \qquad \text{Eq. 2.2}$$

In this equation, M is the moment created by the force couples applied to the cross-frame by actuators, and θ is the measured rotation of the cross-frame. Data collected from parametric studies led to the stiffness reduction factors that can be used for single-angle cross-frames, and can be used to modify the stiffness estimates made by analytical solutions or line element solutions. Once a designer has calculated the reduction coefficient using the equation for the appropriate cross-frame type, the coefficient can be multiplied by the area of the cross-frame members to account for the reduction in stiffness caused by the eccentricity of the connection.

Applying this reduction in stiffness allows for a more accurate determination of actual fatigue forces in these members. Battistini describes the full-scale cross-frame tests to evaluate the behavior of the cross-frame system for fatigue. In these tests, the single angle detail for the various

types of cross-frame configurations mentioned above (25 separate specimens) were tested, and found to be unconservative for Category E. Due to the eccentricity of the cross-frame connection, the single angle detail is reported to better fit the lower bound of Category E', which was subsequently adopted by AASHTO.

2.1.4 Field Experiments

Several researchers have conducted field load tests on cross-frames. In these investigations, cross-fame members are usually instrumented with strain gages, and then trucks with a known weight are placed at various locations along the bridge. For the given truck locations and truck axle configurations/weights, the forces in the cross-frame members are measured. These types of studies provide data that can be compared to finite element bridge models in order to assess capabilities and limitations of various modeling approaches and assumptions. Such studies include work by Keating et al. (1997), Romage (2008), McConnell et al. (2016), Rowles (2014), Zwerneman (1997), Azizinamini (1995), and Tedesko et al. (1995). In general, these studies were more focused on the characteristics of cross-frames as it relates to girder distribution factors, rather than the fatigue behavior of cross-frames.

2.2 LOAD AND RESISTANCE MODELS FOR FATIGUE

Various studies were pivotal in the development of the load and resistance factored design philosophy in use today. This section summarizes many of the studies used to characterize load and resistance models used for fatigue design.

2.2.1 Development of the Fatigue Design Curves

Fatigue resistance testing for riveted, bolted and butt-welded connections was first performed in the US in the 1930s and 1940s (Wilson and Coombe 1939, and Wilson 1940), which included computational analyses and small-scale tests; however, it wasn't until the ninth edition of the AASHTO *Standard Specifications for Highway Bridges* (1965) that design provisions were included for fatigue. Under NCHRP Project 12-15 (Report 286, Keating and Fisher 1986), the fatigue behavior of steel details specific to bridges was studied extensively in order to characterize applied stress ranges relative to the quantity of load cycles to failure. The 12-15 project considered and added to test data performed in the early 1970s (Fisher et al. 1970, Fisher et al. 1974). This

work was predominately performed on small scale tests using hundreds of specimens with various common details. The tests included applying a constant amplitude load to selected details until fracture was observed. Figure 2-3 represents the fatigue design curves developed from this test data, showing the relationship between stress range and the total quantity of cycles to failure (referred to as an S-N curve). Using a lognormal regression analysis on the test data, it was determined that various details could be represented by various categories with different fatigue parameters. An exponential relationship between stress range and each of the detail categories was developed, which led to constants for each of the categories, and ultimately, the fatigue design curves, which represent a lower bound on fatigue life. Another key observation from this study was that under certain stress ranges for each detail category, no fatigue damage was observed after a large number of cycles (generally in the 5 to 15 million cycle range and referred to as a "run out" test); this ultimately led to identifying threshold stress ranges for each detail category, below which fatigue life is assumed to be relatively infinite. The results of this work led to the current detail categories provided in AASHTO *LRFD* Table 6.6.1.2.3-1 (2015), which provides fatigue resistance parameters for eight details ranging from A to E'. The use of these curves to design for fatigue in steel bridges is discussed in Section 2.4.

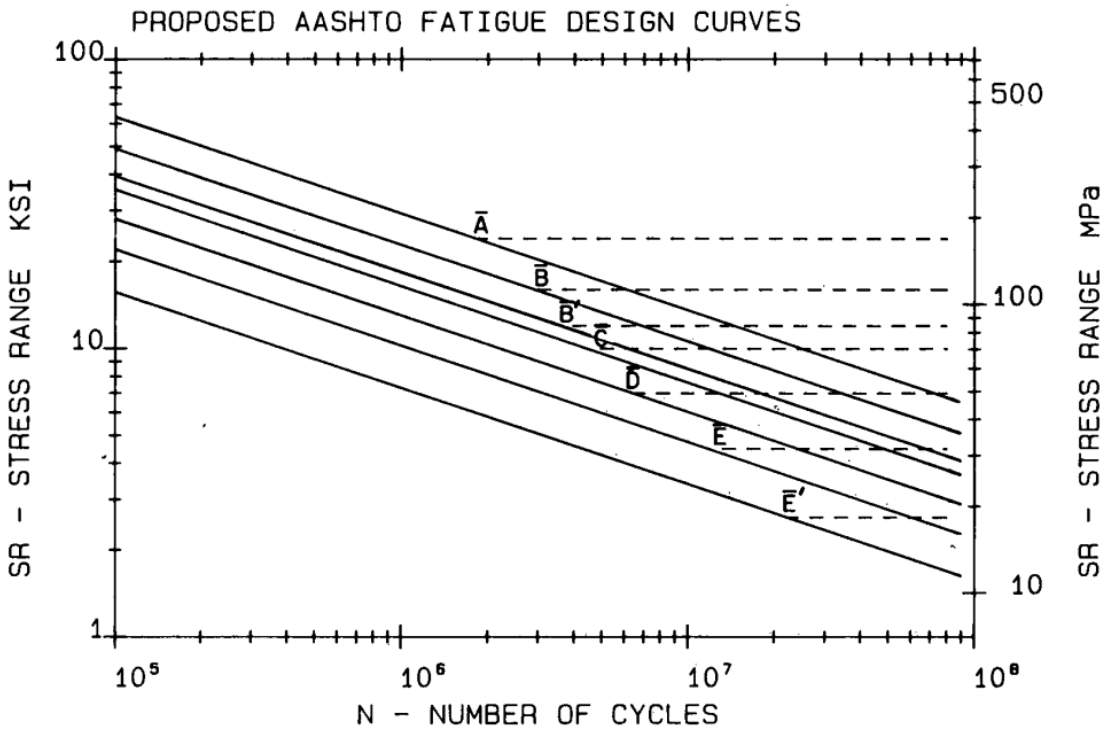

Figure 2-3: Fatigue design curves proposed by Keating and Fisher (1986) and currently used in AASHTO *LRFD*.

2.2.2 Recent Efforts to Characterize the Statistical Parameters for Load and Resistance

The Second Strategic Highway Research Program (SHRP 2) project R19B developed calibrated service limit states (SLSs) for bridges with a 100-year design life, in addition to developing a framework for future calibration efforts related to SLSs (Kulicki et al. 2015). As part of the investigation of the fatigue limit states, the R19B project reviewed the test data from earlier fatigue studies summarized by Keating and Fisher (1986) in order to summarize key statistical parameters for the purposes of reliability studies. For the reliability studies (discussed in more detail in Section 2.3), it is necessary to describe the bias (denoted by λ) and the coefficient of variation (CV). The bias is merely the ratio of the measured value divided by the nominal (or design) value. For resistance, this is equivalent to the ratio of the fatigue test data to the design value for the detail. Because the original resistance studies only reported the relationship between stress ranges and number of cycles to failure, and each specimen group tested was often tested over small increments of stress ranges and limited in number, this made it difficult to fit one statistical distribution to the available data. It is commonly accepted to relate constant amplitude stress ranges to an effective constant amplitude stress range, S_{eff}, using the following relationship (AASHTO *LRFD* 2015 and Fisher et al. 1998):

$$S_{eff} = (\sum \gamma_i * S_{ri}^3)^{\frac{1}{3}} \quad \text{Eq. 2.3}$$

where:

γ_i = percentage of cycles at a given stress range, and

S_{ri} = constant amplitude stress range for a group of cycles (ksi).

Using this relationship, the R19B project calculated a fatigue damage parameter, S_{fi}, using the constant amplitude stress ranges for each of the individual test specimens:

$$S_{fi} = (N * S_{ri}^3)^{\frac{1}{3}} \quad \text{Eq. 2.4}$$

where:

N = number of cycles.

The distribution of this fatigue damage parameter for each of the detail categories was then used to calculate the statistical parameters for that detail category. Table 2-1 summarizes the

statistical parameters R19B developed for all eight detail categories. Note that the design value used to calculate the bias was obtained by taking the cube root of the constant, A, for the respective detail category found in AASHTO Table 6.6.1.2.5-1 (2015).

Table 2-1: Statistical parameters for resistance as calculated from SHRP 2 R19B (Kulicki et al. 2015).

Category	Standard Deviation	CV	Bias, λ	Measured Fatigue Parameter	Design Fatigue Parameter
A	1000.0	0.24	1.43	4,167.40	2,924
B	666.7	0.22	1.34	3,077.47	2,289
B’	250.0	0.11	1.28	2,336.10	1,827
C and C’	454.6	0.21	1.35	2,210.77	1,638
D	185.2	0.10	1.36	1,773.69	1,300
E	140.9	0.12	1.17	1,207.41	1,032
E’	232.6	0.20	1.56	1,1140.28	730

The statistical parameters of the loads for fatigue design of primary longitudinal members were also developed by the R19B project. Using a compilation of WIM records collected from approximately 2004 to 2008 for 15 sites across the nation, the researchers simulated truck records over bridges using an influence line analysis. The bridges considered ranged in span lengths of 30 to 200 feet, and the simulation calculated the positive bending moments at midspan of simply supported bridges, negative bending moments at the interior support of a two-span continuous bridge, and positive bending moments at 0.4 of the span length of a two-span continuous bridge. The distribution of moment cycles was assumed to be similar to the distribution in resulting stresses, so the research team used the statistical parameters describing these force effects in the subsequent reliability analysis.

2.2.3 Weigh-in-Motion Technology

Weigh-in-motion (WIM) technology has been used in numerous applications to study current traffic loads in developing bridge load models (Davis 2007), calibrating partial safety factors for new design (Fu and van de Lindt 2006, Nassif et al. 2008, Mertz 2008, Kwon et al. 2011, Sivakumar et al. 2009 and 2011), and calibrating partial safety factors for evaluating existing

bridges (Fu and Hag-Elsafi 1997 and 2000, Pelphrey et al. 2008, Curtis and till 2008, Fu et al. 2019, Ghosn et al. 2011, Uddin et al. 2011, Moses 2001, Sivakumar et al. 2007). This section provides a background of WIM technology, its development over the decades, and its benefits for use in load studies.

WIM technology was largely introduced in the early 1950s (Normann and Hopkins 1952), which was a result of the Bureau of Public Roads (BPR, a predecessor of the FHWA) researching ways to incorporate electronic scales in the measurements of vehicle weights at driving speeds. The researchers developed an electronic weighing device that measured truck weights and axle spacings using a large reinforced concrete platform built within an area of pavement and supported by load cells. The load cells measured the weight of vehicles at roadway speeds, and the resulting measurement was captured via an oscilloscope. A "road detector tube" was used as a measurement trigger, which allowed a link to be made between the passing vehicle's axles and the oscilloscope's signal sweep. A camera would then be used to photograph the oscilloscope readout for analysis - a process that reportedly took approximately 10 seconds per vehicle. Prior to WIM technology, traffic weights were estimated by either randomly stopping a truck and using portable scales or diverting trucks to a dedicated stationary weighing station. Normann and Hopkins describe a typical static weight measuring crew as a six-person party that could weigh approximately 200 trucks per day.

Many advancements have been made over the past 70 years as it relates to WIM technology. In 1965, Dr. Clyde Lee obtained a patent for the first WIM sensor in the US (Lee 1966). This apparatus, developed at the University of Texas at Austin in collaboration with the Texas Department of Transportation (TxDOT), consisted of steel plates supported by strain gage load cells. These steel plate platforms were considerably smaller and lighter than the reinforced concrete pads used in the BPR studies; the concrete pads used in the original studies tended to cause inertial effects that complicated the accurate measurement of closely-spaced axles or vehicles. During the same time frame, researchers in Germany utilized bending plates with strain gages installed on the bottom face of the plate (Lee and Garner 1996). Almost a decade after the first US patent, Goble et al. (1976) used strain gages installed on a bridge to allow the bridge itself to become a measurement platform. This concept, developed through the years, is known as bridge weigh-in-motion, or B-WIM. B-WIM has been adapted and utilized by various researchers and some state agencies, but it has not become as popular as systems that are permanently located in

the roadway.

Modern WIM systems are significantly more robust and accurate than the initial versions discussed previously and are used in a variety of transportation applications: pavement and bridge design/monitoring, enforcement of size/weight overload policies, collection and management of tollways, and development of legislation and regulation (Al-Qadi et al. 2016 and ASTM 2017). In addition to drive-by axle weights and spacings, many modern WIM systems can classify vehicle type per FHWA categories (Table 2-2), as well as measure vehicle track widths (transverse dimension between wheels on a single axle), wheel lateral location on a particular lane, license plate numbers, and digital images. While most modern WIM systems provide time stamps with a resolution on the order of 1 second, advancements in signal processing allow many systems to report timestamp resolution within 0.01 seconds.

ASTM E1318-09 (reapproved in 2017), *Standard Specification for Highway Weigh-in-Motion (WIM) Systems with User Requirements and Test Methods*, provides minimum data that WIM systems shall provide, depending on the *type* of WIM system (ASTM 2017). For Type I systems, which are predominantly used in highway applications for speeds from 10 to 80 miles per hour (mph), the WIM system is required to calculate, store, and reproduce for immediate review the following data: wheel loads, axle loads, axle-group loads, gross vehicle weight, speed, center-to-center spacing between axles, vehicle class (typically FHWA), site identification code, lane and direction of travel, date and time of passage, sequential vehicle record number, wheelbase (front-most axle to rear-most axle), equivalent single axle loads (ESALs), and violation codes, as appropriate. Type II systems essentially require the same as Type I, except they are not required to produce wheel loads, and the minimum vehicle speed is 15 mph rather than 10. Type III systems are typically used by enforcement agencies and have specific requirements for measuring vehicle acceleration. Type IV systems are not yet approved for use in the US but are also intended to be used for enforcement.

Table 2-2: FHWA classification system (adapted from TMG 2016).

Class	Description
1	*Motorcycles*: all two or three-wheeled motorized vehicles. Typical vehicles in this category have saddle type seats and are steered by handlebars rather than steering wheels. This category includes motorcycles, motor scooters, mopeds, motor-powered bicycles, and three-wheel motorcycles
2	*Passenger cars*: All sedans, coupes, and station wagons manufactured primarily for the purpose of carrying passengers and including those passenger cars pulling recreational or other light trailers.
3	*Four tire, single unit*: All two-axle, four-tire, vehicles other than passenger cars. Included in this classification are pickups, panels, vans, and other vehicles such as campers, motor homes, ambulances, hearses, carryalls, and minibuses. Other two-axle, four-tire single-unit vehicles pulling recreational or other light trailers are included in this classification. Because automatic vehicle classifiers have difficulty distinguishing class 3 from class 2, these two classes may be combined into class 2.
4	*Buses*: All vehicles manufactured as traditional passenger-carrying buses with two axles and six tires or three or more axles. This category includes only traditional buses (including school buses) functioning as passenger-carrying vehicles. Modified buses should be considered to be a truck and should be appropriately classified.
5	*Two axle, six tire, single unit*[1]: All vehicles on a single frame including trucks, camping and recreational vehicles, motor homes, etc., with two axles and dual rear wheels.
6	*Three axle, single unit*[1]: All vehicles on a single frame including trucks, camping and recreational vehicles, motor homes, etc., with three axles.
7	*Four or more axle, single unit*[1]: All trucks on a single frame with four or more axles.
8	*Four or less axle, single trailer*[1]: All vehicles with four or fewer axles consisting of two units, one of which is a tractor or straight truck power unit.
9	*Five axle tractor semitrailer*[1]: All five-axle vehicles consisting of two units, one of which is a tractor or straight truck power unit.
10	*Six or more axle, single trailer*[1]: All vehicles with six or more axles consisting of two units, one of which is a tractor or straight truck power unit.
11	*Five or less axle, multi-trailer*[1]: All vehicles with five or fewer axles consisting of three or more units, one of which is a tractor or straight truck power unit.
12	*Six axle, multi-trailer*[1]: All six-axle vehicles consisting of three or more units, one of which is a tractor or straight truck power unit.
13	*Seven or more axle, multi-trailer*[1]: All vehicles with seven or more axles consisting of three or more units, one of which is a tractor or straight truck power unit.

[1]In reporting trucks, FHWA provides the following criteria: truck tractor units traveling without a trailer will be considered single-axle units; A truck tractor unit pulling other such units in a saddle mount configuration will be considered one single-unit truck and will be defined only by the axles on the pulling unit; Vehicles are defined by the number of axles in contact with the road. Therefore, floating axles are counted only when in the down position; and the term "trailer" includes both semi- and full trailers.

In general, a modern WIM system consists of the following three primary components:

- **Weight sensor**. There are three primary types of sensors in use today, with various advantages and disadvantages to their use (see Table 2-3).
    - *Load cells*. The original weight sensor technology used a primitive version of today's load cell. Modern load cells convert strains (using strain gages attached to load cell fixtures) or pressure (using hydraulic rams) into an equivalent static weight. Temperature effects require consideration, and usually involve the installment of temperature sensors along with the load cell to compensate for temperature differentials within the manufacturer's stated operational range.
    - *Bending plates*. A series of plates (also called "weighpads") are used as the contact surface, and these plates typically span an opening or slot cut into the roadway surface. The underside of the plates are generally instrumented with strain gages to relate bending stresses to static vehicle weights. Similar to load cells, temperature sensors are usually installed along with the bending plate to compensate for temperature differentials within the manufacturer's stated operational range.
    - *Piezoelectric sensors*. There are three common piezoelectric sensors in use today that utilize various primary constituents: quartz, ceramic, and polymer. Regardless of the constituents of the actual sensor, all piezoelectric sensors convert a pressure applied to the sensor into a proportional voltage; the three types all have different enclosures or methods of installation depending on the manufacturer. The specific design of each type tends to be proprietary. All three are typically installed in narrow strips in the roadway surface. Of the three, the quartz piezoelectric elements (piezoquartz) tend to be the most commonly use piezoelectric element for weight measurements; the other two tend to be used more commonly for vehicle classification purposes and are less accurate for measuring weight. Piezoquartz elements do not generally require temperature compensation.

Table 2-3: Comparison of various WIM weight sensors (adapted from Zhang 2007).

Characteristic		Bending Plate	Single Load Cell	Piezoelectric Sensor
Cost (USD)	**Initial Installation per Lane**	Medium ~$20,000	High ~$50,000	Low to Medium ~$9,000 to $20,000 (quartz)
	Annual Maintenance and Operation	Medium ~$6,000	High ~$8,000	Low to High ~$5,000 to $8,000 (quartz)
Accuracy[1]		± 10%	± 6%	± 10% (quartz) -15%
Sensitivity		Medium	Medium	High
Service Life (years)		6	12	4 to over 15 (quartz)
Overall Reliability		Medium	High	Low to Medium (quartz)

[1]*Accuracy is stated in terms of GVW using a 95% confidence interval.*

For every lane that is instrumented, corresponding sensor types are either installed in-line or staggered (Figure 2-4). An in-line installation requires the use of a trigger or set of triggers (discussed next) in order to calculate vehicle speed and axle spacing information. A staggered installation, which tends to be more common, allows vehicle speed and axle spacing to be captured by the weight sensor, since the offset sensors are separated by a known value and the time stamp associated with the weight record is stored. Regardless of in-line or staggered installation, every sensor is installed with a trigger to define the beginning and ending periods for data collection for the sensor.

- **Trigger**. An installed vehicle trigger is typically in the form of an inductive loop; these are electromagnetic communication systems that are charged by a nearby controller. When a metallic body enters the loop (such as a vehicle's chassis), the periphery of the metallic body induces eddy currents, which decreases the inductance of the loop. This decrease in inductance allows the controller to sense the metallic body and communicate to the weight sensor to begin or stop recording. Inductive loops are usually installed on both sides of the weight sensors in order to communicate both the arrival and departure of a vehicle.
- **Data Acquisition System (DAQ)**. The DAQ collects the measurements obtained from the weight sensor and trigger, as well as additional information obtained with

optional components (discussed next). This information is either stored locally or communicated via cellular modem to an end user. The DAQ is generally located in close proximity to the roadway within a weatherproof housing (roadside cabinet) and is powered either by a local power supply, batteries, or solar energy. DAQs also typically provide power to the weight sensors and triggers.

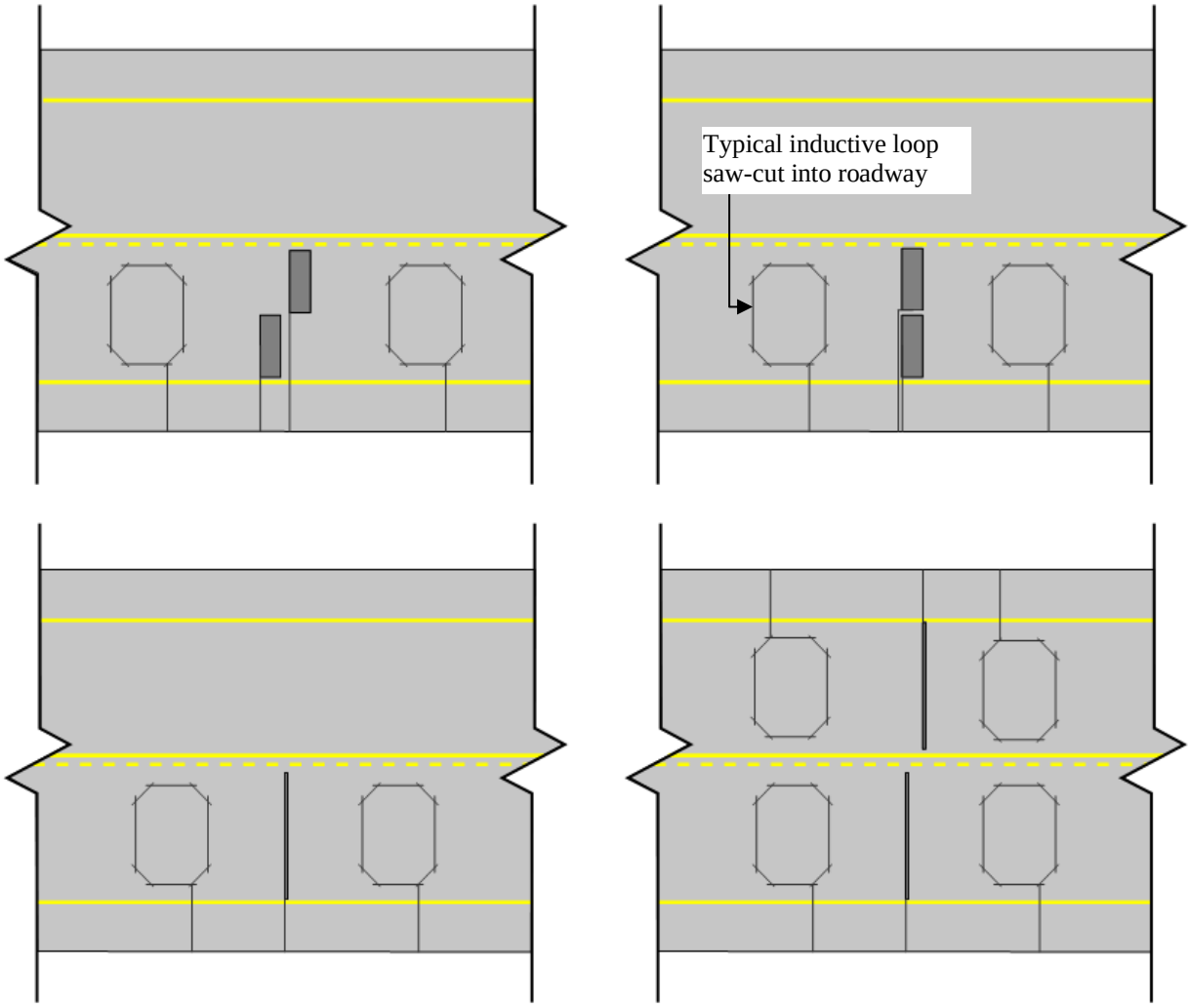

Figure 2-4: Typical configurations of various weight sensors and triggers. Top left is a single-lane staggered bending plate or load cell; top right is a single-lane in-line bending plate or load cell (requires triggers for vehicle speed and classification); bottom right is a two-lane piezoelectric sensor; and bottom left is a single-lane piezoelectric sensor. All configurations shown with typical inductive loop triggers saw-cut into roadway.

Optional components of a modern WIM system may include:

- **Laser Scanner**. A scanner will collect a 3D image or profile of the passing vehicle in order to classify the event in one of the thirteen different FHWA classifications (see Table 2-2). Because the imaging of the laser is sensitive to vehicle leading edges, laser scanners can also be designed to report vehicle speed.
- **Cameras**. Onboard cameras (commonly installed in combination with tollway plazas) collect digital images of vehicles, primarily for the purpose of digitizing and compiling a list of license plate tags for passing vehicles. The use of cameras specific to license plates is regional - that is, various plate designs require specific camera configurations in order for the automated reader to properly identify the plate characters. Cameras may also be used as a backup for confirming vehicle classification.
- **Automated Vehicle Classification (AVC) System**. An AVC utilizes timestamps and axle records for a given vehicle record to characterize the FHWA classification of the vehicle. This usually involves specialized software to recognize typical axle configurations and sort the series of axle records into appropriate bins belonging to each classification type.

WIM systems require careful calibration in order to provide reliable data. Calibration of WIM sensors is performed annually (at a minimum) in accordance with ASTM E1318. Per the standard, calibration involves using the static weights of two semi-trailer test vehicles measured per the standard to correlate the WIM-system calculations to the static vehicles. Calibration is performed for the installed system, such that the effects of dynamic tire forces and road surface profiles are considered. In addition to calibrations, WIM system owners may require periodic on-site acceptance or verification tests.

There are four primary benefits of WIM systems compared to static weighing: 1) WIM systems can capture an increased sample population at much lower costs than static weigh stations, 2) the systems are capable of continuous recording using a high processing rate, 3) WIM systems are safer than static weigh stations since, besides maintenance and operation, they minimize human interaction with roadway traffic, and 4) an installed WIM system on a typically roadway is generally not apparent to the traveling public, therefore scale bias (the tendency for operators of heavy trucks to avoid roadways with known weigh stations and enforcement present) is minimized.

The disadvantages of WIM systems are: 1) in general, WIM systems are less accurate than static weigh stations, 2) they require frequent calibration, and 3) there is generally less data recorded for individual trucks.

A sample of raw WIM data output is provided in Appendix A.

2.3 RELIABILITY-BASED DESIGN AND CALIBRATION EFFORTS

The following sections provide a brief review of key concepts in reliability-based design and the introduction of reliability-based designs in AASHTO specifications.

2.3.1 Concepts in Reliability-Based Design

An illustration of the fundamental concepts used in reliability-based design philosophies is shown in Figure 2-5 and Figure 2-6. In these figures, a sample distribution of loads and resistances with their respective coefficients of variation are illustrated. The coefficient of variation, or CV, is a measure of the variability of the distribution, and is equal to the distribution's standard deviation divided by the mean.

For the illustration in Figure 2-5, the total distribution of loads is mostly less than the total distribution of resistances. The nominal loads and resistances are *design values* used in the limit state. These nominal values are related to the actual means of the respective distributions by a bias factor, denoted by λ. The bias is the ratio of the actual load (or resistance) effect to the nominal load (or resistance) effect. The design point is a location on the failure boundary described by the limit state equation. For the distributions illustrated, the limit state takes the form of many of the LRFD limit states with appropriate partial safety factors applied to both the load and resistance side of the equation:

$$\gamma_R R_N \geq \gamma_Q Q_N \qquad \text{Eq. 2.5}$$

where:

γ_R = resistance factor applied to the nominal resistance, R_N, and

γ_Q = load factor applied to the nominal load effect, Q_N.

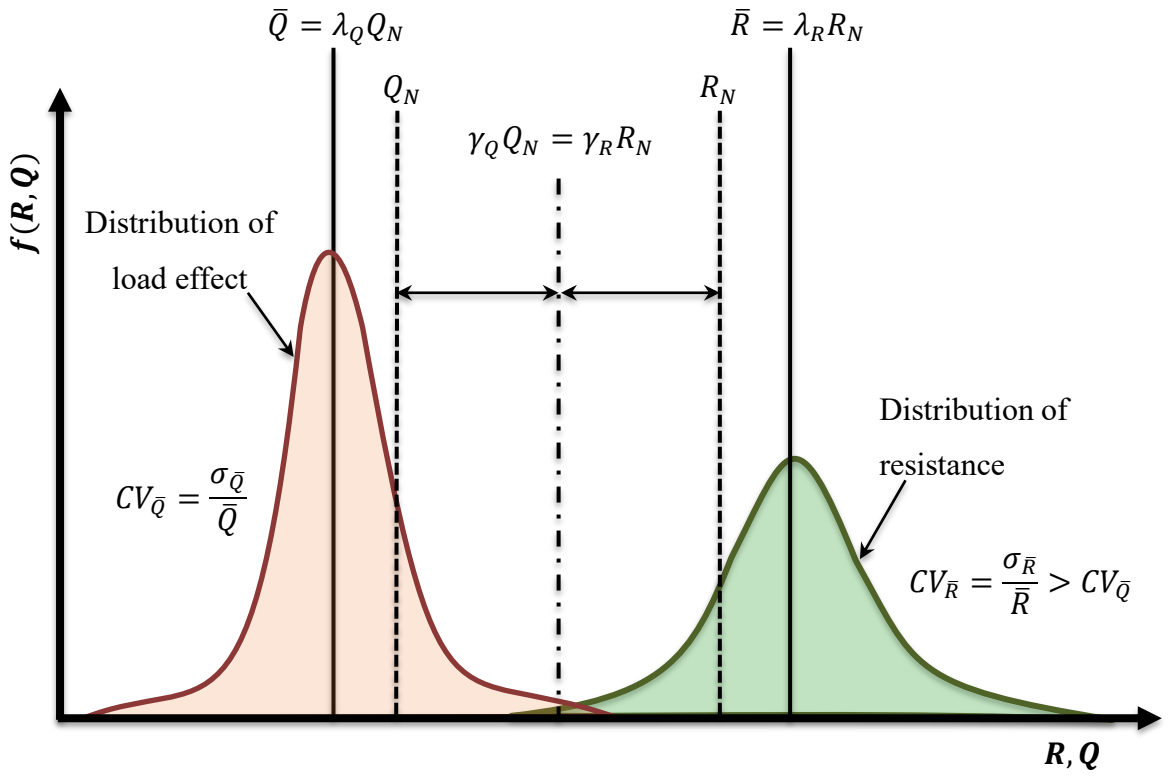

Figure 2-5: Fundamental concepts in a reliability-based design: relationship between distribution of actual resistances ($\bar{R}$) and actual load effects ($\bar{Q}$) with nominal loads (Q_N) and nominal resistances (R_N). The CV for resistance is shown to be qualitatively larger than the CV for loads due to the wider distribution.

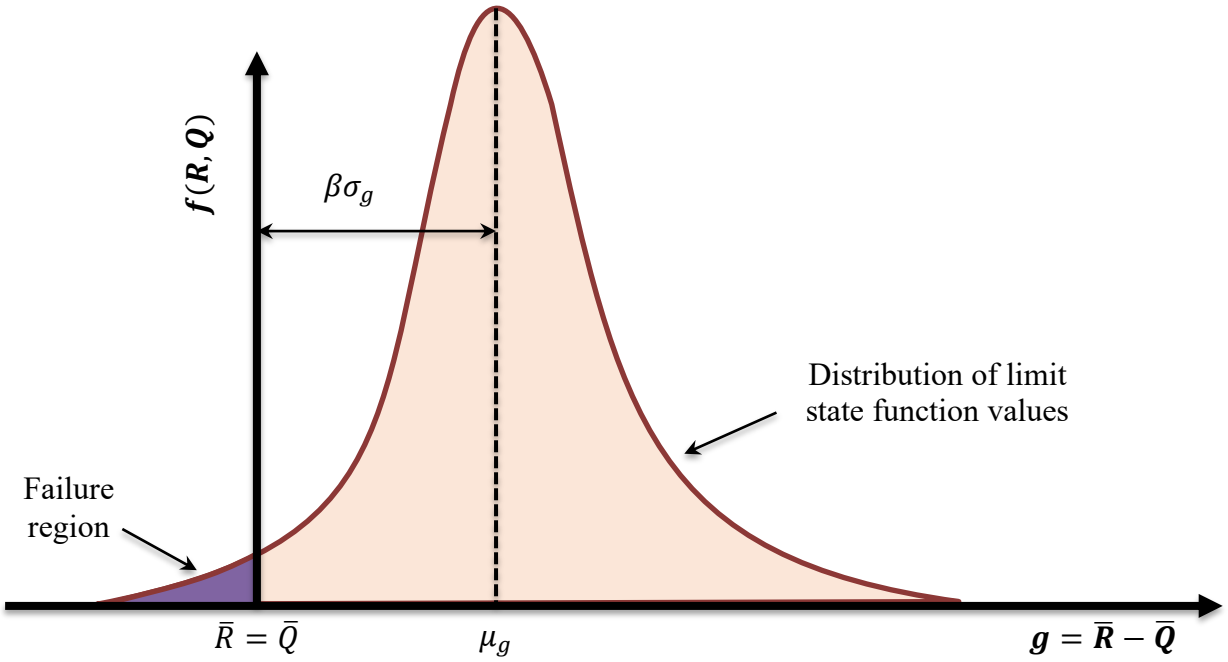

Figure 2-6: Fundamental reliability concepts: relationship between distribution of limit state function and failure region.

Defining this relationship between the load and resistance $g(R,Q)$, the limit state can be rearranged to indicate the failure boundary (i.e., when the actual load effect just equals the actual resistance):

$$g(R,Q) = \gamma_R R_N - \gamma_Q Q_N = 0 \qquad \text{Eq. 2.6}$$

Figure 2-6 illustrates the qualitative limit state function $g(R,Q)$ for the distributions shown in Figure 2-5. As stated previously, the total distribution of loads in Figure 2-5 is mostly less than the total distribution of resistances; however, there is slight overlap of these distributions. If a structural component that has an exceptionally low strength defined by the left tail of the resistance distribution experiences an exceptionally large load effect defined by the right tail of the load distribution, failure will occur. This is illustrated in Figure 2-6 as the negative portions of the limit state function. The limit state function can be described with statistical parameters μ_g (mean) and σ_g (standard deviation); and the distance from the mean of this distribution to the location where the limit state equals zero can be defined as $\beta\sigma_g$, where β is a measure of reliability for normal distributions, termed the reliability index. Because the distributions of loads and resistances in the

preceding illustrations are normal, the probability of failure, P_f, can be determined by evaluating the standard normal distribution (denoted by Φ) at $-\beta$:

$$P_f = \Phi(-\beta) \qquad \text{Eq. 2.7}$$

Conversely, if the probability of failure is known, the reliability index can be calculated by evaluating the inverse of the standard normal distribution (denoted by Φ^{-1}) calculated at P_f:

$$\beta = \Phi^{-1}(P_f) \qquad \text{Eq. 2.8}$$

The same calculation of β can also be accomplished by plotting the cumulative distribution function on a normal probability plot ($\Phi^{-1}(P_f)$ on the y-axis versus a ranked list of the limit state values $g(R, Q)$ on the x-axis). The value of β is equal to the negative value of the plotted CDF evaluated at $g(R, Q) = 0$. This is demonstrated in Figure 2-7 for two sample distributions of load and resistance.

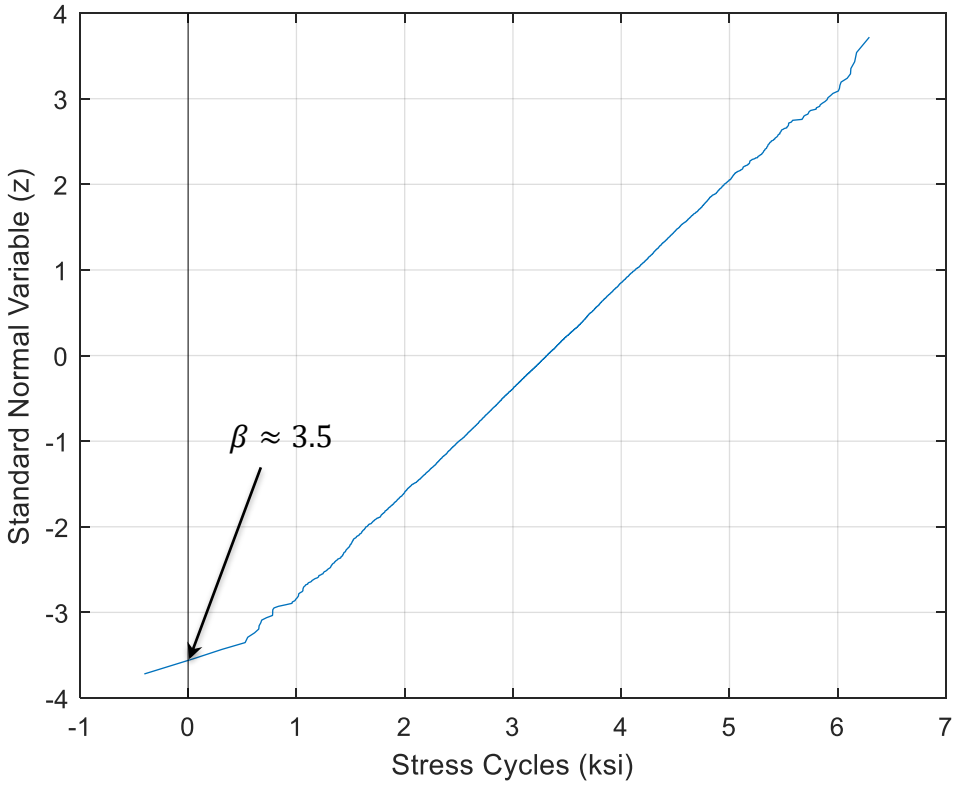

Figure 2-7: CDF of sample limit state function values for two distributions load and resistance $g(R, Q)$. The value of β is taken as the negative value of the CDF at $g(R, Q) = 0$.

The examples provided above demonstrate the calculation of the reliability index

conceptually and graphically for normal distributions. By converting the load and resistance distributions to a standard form (called reduced variables), Hasofer and Lind (1974) demonstrated that the reliability index can be expressed as the shortest distance from the limit state function failure boundary to the origin in reduced variable space. The derivation is beyond the scope of this discussion; however, an important concept from this derivation is that, for normal distributions, the reliability index can be expressed as the following:

$$\beta = \frac{\overline{R} - \overline{Q}}{\sqrt{\left(CV_R R_N \lambda_R\right)^2 + \left(CV_Q Q_N \lambda_Q\right)^2}} \qquad \text{Eq. 2.9}$$

where the values are as defined previously. When both load and resistance distributions can be expressed as perfectly normal, the closed-form solution in Eq. 2.9 is exact. When the distributions are both lognormal (and provided there is only one load distribution), the closed-form solution becomes (Allen et al. 2005):

$$\beta = \frac{LN\left[\frac{\overline{R}}{\overline{Q}}\sqrt{\left(1 + CV_Q^2\right)/\left(1 + CV_R^2\right)}\right]}{\sqrt{LN\left[\left(1 + CV_Q^2\right)\left(1 + CV_R^2\right)\right]}} \qquad \text{Eq. 2.10}$$

For more complicated distributions, more rigorous analytical computations may involve the Rackwitz-Fiessler procedure (1978) or a Monte Carlo simulation.

2.3.2 Development of AASHTO's Calibrated, Reliability-Based Limit State Specifications

Up until the early 1970s, AASHTO *Standard Specifications* (the minimum code requirements for bridge design in the US prior to AASHTO *Load and Resistance Factor Design*, or *LRFD*, assuming this role in 2007) required bridges to be designed based on the working stress design (WSD) philosophy. This philosophy (also called the Allowable Stress Design, or ASD), had been practiced for decades, and requires the loads applied to a member must be less than or equal to the nominal strength of a member, divided by a factor of safety. In essence, the WSD philosophy sought to ensure that the actual stresses placed on a member never approached the allowable stress of a member by using a "one-size-fits-all" factor of safety that reduced the capacity of a member to a point below yielding. The disadvantage of this design philosophy is that

the uncertainty in loads versus materials resistance can be highly variable. There are a wide variety of loads on bridges ranging from relatively predictable self-weight to complicated dynamic loads that have considerable variability. Working stress designs based on certain load combinations (which may or may not be simultaneous) and applied to systems comprised of various material combinations were often not optimal, resulting in effective factors of safety that were quite inconsistent across the bridge system. In addition, the factors of safety used in WSD were all applied to the resistance side of the equation; meaning it varies only with the type of force being designed (e.g., axial, bending moment). The factor of safety did not take into consideration variability in either the loads or resistances.

Beginning in the 1970s, the AASHTO *Standard Specifications* began to incorporate a design philosophy called load factor design (LFD) into the existing WSD design provisions (Kulicki and Mertz 1998). This philosophy attempted to acknowledge that design factors should be varied based on the predictability of certain loads.

By the mid-1970s, many researchers and practitioners were considering the benefits of using a reliability-based design approach that employed the use of partial safety factors, or factors that were applied to both the load and resistance. The Ontario Ministry of Transportation and Communication (currently Canada's Ministry of Transportation) was the first to develop a calibrated, reliability-based limit state specification (Kulicki and Mertz 1998) in North America. In this context, a limit state is broadly defined as the relationship between loads and other actions on a structure (e.g., strength, deflection) that implicitly defines a design point, or design criteria (e.g., loads above this point no longer meet the limit state). In the development of reliability-based limit states, partial safety factors are used to take into account the statistical distribution of the loads and resistances for various limit states in order to provide a rational and consistent means of designing a system to a more uniform level of reliability. Nowak and Collins describe this code approach to limit state equations as a *Level I code*: the safety margin is applied through the use of partial safety factors and deterministic design formulas (2013). In the development of the *Ontario Highway Bridge Design Code* (OHBDC) in the late 1970s, as well as the subsequent development of the first reliability-based AASHTO code (AASHTO *LRFD* 1994), the partial safety factors were generally developed using a *Level 2 code* philosophy: design acceptance criterion is usually provided by judging how closely the safety parameters for a given limit state equation are with

respect to the target reliability index (Nowak and Collins 2013)[1]. Using a reliability-based approach, an approximate probability of failure can be calculated by considering the mean resistance, mean loads, nominal (design) values of resistance, nominal values of loads, and the variation of resistances and loads. By setting the probability of failure at an acceptable level, this design philosophy allows engineers to design to a better understood level of risk.

When the first reliability-based AASHTO code was published in 1994, AASHTO merely allowed this design philosophy to be optional to the existing AASHTO *Standard Specifications*, which was still written in the context of WSD and LFD. During this period, most engineers continued to design bridges using the AASHTO Standard Specifications, despite the improved reliability associated with the AASHTO *LRFD* approach. A great deal of effort was put forth in developing and revising the AASHTO *LRFD*. The formation of AASHTO *LRFD* 1994 was a direct result of NCHRP Project 12-33 (Kulicki and Mertz 1998), which was the first attempt to create specifications on a probabilistic load and resistance factor design philosophy for bridges in the US. The 12-33 project team, led by Dr. John Kulicki with Modjeski and Masters, included four contractors and forty-seven consultants. The outcome of this project was three draft specifications with commentary released to AASHTO bridge engineers, the FHWA, and private authorities for review and comment. The fourth draft was submitted in 1993 and was balloted by the AASHTO Highway Subcommittee on Bridges and Structures (HSCOBS), culminating in the 1994 version of AASHTO *LRFD*. A significant calibration effort was undertaken in the development of the first AASHTO *LRFD* for the ultimate limit states (ULSs); the intention of the calibration effort was to provide partial load factors for limit state equations that produced a consistent and acceptable level of reliability. Note that the serviceability limit states (SLSs) were not calibrated during this work. The calibration effort for the ULSs is summarized in NCHRP Report 368 (Nowak 1999) and the follow-up report for NCHRP Project 20-7/186 (Kulicki et al. 2007). Kulicki and Mertz (1998) note that in the calibration of 1994 AASHTO *LRFD*, WIM data were available, but not directly usable in the development of the live load model; Nowak reports that due to the unreliable WIM records available, the live load was calibrated using truck measurements collected in 1975 by the Ontario

[1] Nowak and Collins go on to define *Level III codes* as a full reliability review of code limit states in order to quantify and optimize probability of failure; *Level IV codes* are developed taking into consideration the optimization of a utility function balancing benefits and costs of a particular design.

Ministry of Transportation. The records consisted of approximately 10,000 trucks (generally randomly selected for static weighing) collected over a time period of approximately 2 weeks. As noted earlier, there was a major problem associated with too many active specifications with WSD, LFD, and LRFD approaches permissible. The AASHTO *LRFD* was the primary specification with ongoing updates to provisions compared to the antiquated methods in the WSD and LFD approaches. Many designers continued to utilize the WSD and LFD approaches, mainly due to familiarity with the specifications. In 2007, AASHTO mandated that new bridge designs after January 2007 would conform to current AASHTO *LRFD*, rather than the then-optional *Standard Specifications*.

As discussed earlier in this chapter, recommendations from the SHRP 2 Project R19B, research conducted by Modjeski and Masters (Kulicki et al. 2015), led to Fatigue I and Fatigue II load factor changes in the 8th Edition of AASHTO *LRFD* (2017). The research by R19B (as well as that conducted under NCHRP Project 12-83, Wassef et al. 2014) was focused on providing guidance for 100-year design life by developing design and detailing guidelines, as well as calibrated SLSs using reliability theory. Based on a survey of bridge owners and a review of national and international literature, the following SLSs were developed for calibration: foundation deformations, reinforced concrete component cracking, live load deflections, permanent deflections, prestressed concrete component cracking, reinforced concrete component fatigue, and steel fatigue. The researchers for this work used WIM data from 32 bridge sites across the country that included over 35 million useful records (after filtering) to form their final recommendations.

Three primary outcomes of the R19B project are of particular interest to this research: the first outcome is the aforementioned Fatigue I and Fatigue II load factor changes. In the 6th Edition of AASHTO *LRFD* (2012), the load factors for Fatigue I and Fatigue II limit states were 1.5 and 0.75, respectively. One of the objectives of the R19B research was the development of statistical parameters (i.e. bias and coefficient of variation) of fatigue loading by using WIM data (discussed previously). Based on the findings from the WIM data, truck traffic simulation, rain-flow cycle-counting, and Monte Carlo simulation, R19B proposed to update the respective load factors for the fatigue limit states to 2.0 and 0.8 for Fatigue I and II to account for current and projected truck loads. As noted by Russo (2017), further analysis of the WIM data and other parameters determined that a value of 1.75 for the Fatigue I limit state was more appropriate. Accordingly, the 8th Edition of AASHTO currently specifies load factors of 1.75 for the Fatigue I limit state

(per the additional analysis of the WIM data), and 0.8 for the Fatigue II limit state, based on the original recommendation made by R19B.

The second outcome was the design and detailing recommendations to change the constant A for fatigue categories D, E, and E′. R19B also recommended changing the constant amplitude fatigue limit (CAFL, or threshold) values for categories B′, D, and E′. These changes were due to the fact that when the proposed load factor changes were applied to the statistical data, the reliability indices were too large (exceeding +/- 0.2 for the target reliability of 1.0). Instead of changing the resistance factor for select detail categories (inherently taken as 1.0), R19B recommended altering the constant A and CAFL appropriately. The recommended changes to A and CAFL were not made in the 8th Edition of AASHTO *LRFD*.

The third outcome was the validation of the single truck, single lane placement for the fatigue limit state design. While R19B indicated this placement is appropriate (even with the rare occurrence of passing trucks), the WIM data suggested the cycles per passage approach currently used in AASHTO could be simplified.

2.4 ANALYSIS TECHNIQUES FOR CROSS-FRAMES

The bridge engineer is responsible for the design of the structural components and systems comprising the bridge. Regarding fatigue of cross-frames, the bridge engineer must consider the strength of the members used in construction and how these members will be loaded. Choice of materials includes an appropriate fracture toughness that permits a reliable detection of cracks less than $a_{critical}$ during inspections (reference Section 2.1.1). Current AASHTO *LRFD* design (2015) requires that all primary longitudinal superstructure components, connections, and transverse floor beams sustaining tensile stresses due to Strength Load Combination I be verified for fracture toughness via Charpy V-notch testing; testing of members (e.g., cross-frames) that are transverse to the primary components (other than floor beams) is at the discretion of the owner. The use of modern fabrication techniques with modern high-strength fine-grained steels result in higher material toughness, and consequently, larger critical crack lengths. The available strength of a member must also be evaluated in terms of its resistance to applied loads.

In addition, AASHTO *LRFD* requires that the engineer identify facture-critical members, or FCMs. FCMs are components in tension whose failure is expected to result in the collapse of the bridge or the inability of the bridge to perform its function. The location of FCMs must be

identified on the bridge's contract plans.

In general, all steel members have discontinuities due to fabrication processes that can facilitate the growth of fatigue cracks. These discontinuities are generally benign, provided the magnitude of the cyclic loading is relatively low. The fatigue behavior of steel details specific to bridges was studied extensively by Fisher and Keating (1986, discussed in more detail in Section 2.2) in order to characterize the applied cyclic loading (stress ranges) relative to the quantity of load cycles to failure. This work was predominately performed on primary member connections. Limited data exists for the actual resistance data for cross-frame connections. The following subsections provide a summary of recent research related to the fatigue behavior of cross-frames. Recent work establishing proper fatigue categories for the members that mostly comprise the cross-frames include McDonald and Frank (2009) and Battistini et al. (2013).

2.4.1 Legacy Code Provisions

Since 1949, AASHTO *Standard Specifications* limited the maximum cross-frame spacing in steel-girder bridges to 25 feet. While this limit generally ensured satisfactory performance of steel bridge superstructure over the years, it was essentially an arbitrary limit that was based on the experience and knowledge that existed at the time. The limit was generally targeted at shorter spans than is commonly achieved with modern I-girder bridges and for girders that were generally designed for lower stress levels.

The 25-foot spacing limit was removed in the 1st Edition of AASHTO *LRFD* (1994). Instead, the need for cross-frames or diaphragms at all stages of construction and the final condition of the bridge was to be established by a rational analysis. Based upon this requirement, cross-frames or diaphragms may currently be designed with spacing exceeding 25 feet, where rational analysis and investigation indicates that such a spacing is acceptable. Caution should be exercised when extending the spacing significantly beyond 25 feet since the demand on the cross-frames will increase and standard details may not be suitable. The 2005 AASHTO *LRFD* unified the design provisions for straight and horizontally-curved girders by including an upper limit that was established on the cross-frame spacing for horizontally curved I-girder bridges (to limit flange lateral bending stresses resulting from torsion), and also to theoretically preclude elastic lateral torsional buckling of the compression flange in curved I-girders.

All modern bridges generally make use of composite action between the steel girders and

the concrete bridge deck. As a result, the top flange of the girder in the finished bridge is continuously braced in the positive moment regions of the composite bridge, and the critical stage for stability generally occurs during construction. The critical stages for stability can occur during erection when partial bracing is provided, or during placement of the bridge deck when the fresh concrete does not provide restraint to the girder. Though the cured concrete deck can provide torsional restraint in the negative moment regions with proper shear stud detailing, in most designs this deck restraint is conservatively neglected and the cross-frame spacing in the negative moment regions is usually based on the resistance of the girder alone and the factored design moment in the final condition at the strength limit state. Although the approach in the positive and negative moment regions is "rational" with respect to the girder buckling resistance, such an approach does not address the required size of the cross-frames from the perspective of the minimum required stiffness or strength for adequate bracing.

Historically, cross-frame locations were often regions of cracking in the girder webs as a result of distortion-induced fatigue. While cross-frame connections to main elements are evaluated for load induced fatigue, the wide-spread tendencies for distortion-induced fatigue cracking in the girder webs around the cross-frames were alleviated in the 1970s and 1980s with the requirement to positively attach the connection plates (i.e., transverse web stiffeners that connect the cross-frames to the girders) by welding or bolting to the girder flanges. An exception is permitted to this requirement where cross-frames are used on rolled beams in straight bridges with composite concrete decks and with support cross-frames that are normal (or not skewed more than 10 degrees from normal), and with intermediate cross-frames placed in contiguous lines parallel to the supports. This relaxation appears to be completely based on good performance observed with this detail and girder arrangement. Cross-frame and diaphragm locations still pose a fatigue concern in steel bridges, however, particularly in systems with significant support skew or horizontal curvature. The primary concerns in these systems are related to the fatigue behavior of the cross-frame members and their connections, which typically experience larger loads in these systems.

As discussed in Section 2.1.2, there have been a number of advances in the body of knowledge in recent years related to the stability of bridge components as well as the fatigue performance related to cross-frame systems. Some of these improvements in understanding include the recognition of system buckling modes (Yura et al. 2008, Han and Helwig 2015), issues with detailing and fit-up of cross-frames in skewed and curved I-girder bridges (Chavel and Earls

2006, Chavel et al., 2016, White et al. 2015), lean-on bracing concepts for straight skewed I-girder bridges (Helwig and Wang 2003; Romage 2008), corrections in the stiffness modelling of the cross-frames (Wang 2013, Battistini et al. 2016, White et. al. 2012), and establishing proper fatigue categories for the members that comprise the cross-frames (McDonald and Frank 2009, Battistini et al. 2013). Improvements in computational resources over the last few decades allow engineers to carry out sophisticated analyses on bridge systems that can produce efficient and reliable structural systems satisfying both construction and in-service design requirements. Though the computational resources and analytical programs permit relatively sophisticated analyses on bridge systems, the accuracy of any analysis is limited by the modeling assumptions and level of understanding of the fundamental behavior of the structure. While some commercial software packages may provide an evaluation of the fatigue performance of the girders and cross-frames, many analytical models that are used for design may consist of either line-girder models or grillage models (in which the girders and braces are modeled using 2-D line/beam elements). These models are often not capable of accurately evaluating the stability bracing behavior of the cross-frames or diaphragms and the accuracy of a fatigue evaluation is questionable. Even the most detailed "three-dimensional" finite element (FEA) models generally represent the cross-frame members as axially-loaded truss elements and do not reflect the impact of eccentric connections. Recent research has shown this can significantly reduce the cross-frame stiffness (Battistini et al 2016). Neglecting the reduction in stiffness due to eccentric connections will generally be unconservative from a stability or torsional behavior perspective and overly-conservative from a fatigue standpoint, since modeling stiffer cross-frames will result in larger live-load induced forces than occur in reality. Cross-frame stiffness modifications for fatigue applications that are consistent with deformational modes in the composite girders are discussed by Park (2020).

2.4.2 AASHTO LRFD Bridge Design Specifications (7th Edition)

The following sub-sections provide an overview of the current design requirements for cross-frames according to the 7th Edition of AASHTO and the 2015 and 2016 interim revisions (AASHTO 2016). Note that during this research effort, the 8th Edition of AASHTO was released (2017). Those changes are discussed specifically where relevant in the following subsections.

2.4.2.1 Analysis of Cross-Frames

Article 4.6.3.3.4 of AASHTO states that when performing a static analysis of cross-frames using a grillage type model (i.e., a model that converts cross-frames to equivalent, single line beam elements), both cross-frame flexure and shear deformation must be considered when calculating the equivalent beam stiffness. Neglecting to account for shear deformations can lead to significant error in the calculation of cross-frame stiffness.

This article also states that the influence of end-connection eccentricities must be considered when calculating the equivalent axial stiffness to be used when a cross-frame is composed of single-angle or tee-section members. The stiffness of cross-frames composed of these members can be significantly reduced because of end connection eccentricity (Wang 2013; Battistini et. al. 2016). The AASHTO *LRFD* Chapter 4 commentary related to analysis methods currently recommends applying a reduction factor of 0.65 to the axial stiffness of equal leg angles, unequal leg angles connected to the long leg, and flange-connected tee-section members. This recommendation was based upon early results from the work of Wang and Battistini. Equations (presented in Section 2.4.2 of this report) were developed for the reduction in stiffness of single-angle cross-frames that consider the geometry and member sizes of the specific cross-frame. These equations provide improved accuracy over the current commentary language that uses the fixed factor of 0.65.

2.4.2.2 General Requirements for Cross-Frames in Steel I-Girder Bridges

Article 6.7.4.1 requires the need for cross-frames to be investigated at both the construction stage and during the in-service condition of a steel I-girder bridge. Permanent cross-frames must be designed for all applicable limit states. AASHTO defines a primary member as:

"…a member designed to carry the loads applied to the structure as determined from an analysis,"

and therefore cross-frames in horizontally curved girders are considered primary members. In the 8th Edition of AASHTO, the definition of a primary member was changed to:

"…a steel member or component that transmits gravity loads through a necessary as-designed load path. These members are therefore subjected to more stringent fabrication and testing requirements; considered synonymous with the term main member."

At a minimum, the cross-frames in straight steel I-girder bridges must be designed to

transfer wind loads in the finished condition of the bridge. However, because the cross-frames in horizontally curved bridges are considered primary members, they must be designed for all limit states, including fatigue.

Article C6.7.4.1 states that previous versions of AASHTO required cross-frames to not be spaced at a distance greater than 25 feet. This provision was replaced by the requirement for a rational analysis. However, for horizontally curved bridges, Article 6.7.4.2 requires that the cross-frame spacing not exceed the spacing calculated by the following equation, or 30 feet, whichever is less:

$$L_b < L_r < \frac{R}{10} \qquad \text{Eq. 2.11}$$

for which, L_b is the spacing of the cross-frames, L_r is the limiting unbraced length determined from AASHTO Eq. 6.10.8.2.3-5, and R is the minimum girder radius within the panel. The limit of R/10 in Eq. 2.11 is consistent with past practice. Limiting the unbraced length to L_r theoretically precludes elastic lateral torsional buckling of the compression flange and helps to limit flange lateral bending stresses resulting from torsion.

Article 6.7.4.2 requires that braces such as cross-frames or diaphragms used in systems with rolled beams be a minimum of 0.5 of the depth of the girders, and the braces used in systems with plate girders be a minimum of 0.75 of the depth of the girders.

Where the supports of a steel I-girder bridge are not skewed, the intermediate cross-frames should be placed in contiguous lines perpendicular to the girders. If the supports of a steel I-girder bridge are skewed at an angle less than 20 degrees from normal, then intermediate cross-frames may be placed in continuous lines parallel to the supports, as shown in Figure 2-8 (top). For small skew angles, this arrangement permits the cross-frames to be attached to the girders at points of nearly similar length along the girders (i.e., points of nearly equal stiffness), thus reducing the relative deflection between the cross-frame ends and the restoring forces in these members. If the supports of a steel I-girder bridge are skewed at an angle greater than 20 degrees from normal, intermediate cross-frames must be oriented perpendicular to the girders, as shown in Figure 2-8 (middle). This requirement is consistent with past practice and is likely related, in part, to fabrication difficulties and problems encountered when braces were oriented parallel to the skew angles at larger support skews. The fabrication difficulties are related to issues with welding access to the acute corner between the connection plate and the web. As a result, for braces at the support

locations that are typically oriented parallel to the skew, a common detail is to use a perpendicular connection plate (web stiffener connected the cross-frame to the girder), combined with a bent plate to account for the skew. Another reason for requiring perpendicular braces for larger skew angles is likely the result of observed problems when typical cross-frame sizes were used with parallel braces. The parallel orientation results in substantial reductions in the brace stiffness due to the longer brace and skewed orientation.

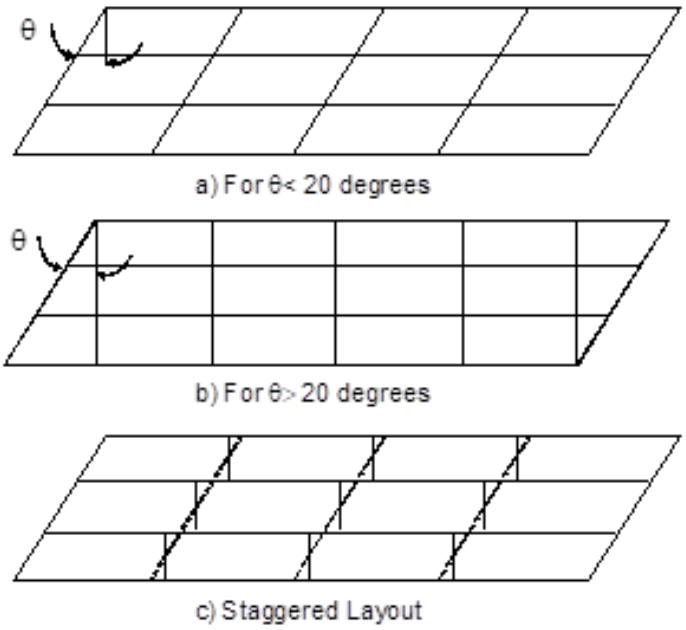

Figure 2-8: Cross-Frame Layout as a Function of Skew Angle, θ.

Where support lines are skewed more than 20 degrees from normal, it may be advantageous to orient the intermediate diaphragms or cross-frames normal to the girders in discontinuous lines, to selectively omit certain diaphragms or cross-frames, and/or to stagger the diaphragms or cross-frames in adjacent bays between the girders Figure 2-8 (bottom). In highly-skewed bridge systems, a perpendicular line of braces will result in very significant differences in the girder displacements at the two ends of the bracing line. For example, with skews greater than 45 degrees, one end of the bracing line may frame into one fascia girder near midspan while the other end of the bracing line may frame into the other fascia girder near the support, thereby resulting in very large forces induced in the braces. One particularly problematic situation can occur when a bracing line frames into the support with a highly-skewed girder system, as shown in Figure 2-8 (middle). Improved

behavior with the bracing line near the support can be achieved with the omission of highly-stressed diaphragms or cross-frames near the obtuse corners of a span, provided the potentially larger unbraced length in this region does not compromise the buckling behavior.

In the 8th Edition of AASHTO, additional language is provided in Article C6.7.4.2 discussing potential framing arrangements to both reduce the number of cross-frames or diaphragms within the bridge as well as to reduce the overall transverse stiffness effects in skewed I-girder bridges. In addition, a recommended offset of the first intermediate cross-frames or diaphragms placed normal to the girders adjacent to a skewed support is provided to alleviate the introduction of a stiff load path that will attract and transfer large transverse forces to the skewed support, particularly at the obtuse corners of a skewed span. At skewed interior piers in continuous-span bridges, transverse stiffness effects are alleviated most effectively by placing diaphragms or cross-frames along the skewed bearing line, and locating normal intermediate diaphragms or cross-frames at distances greater than or equal to the minimum offset from the bearing lines discussed above. Framing of a normal intermediate cross-frame into or near a bearing location along a skewed support line is strongly discouraged unless the cross-frame diagonals are omitted.

2.4.2.3 Design for Fatigue

2.4.2.3.1 Limit States

The fatigue limit state was not explicitly added to the Specifications until the 1st Edition of AASHTO *LRFD* (1994). In 2009, this original single load combination was replaced with what is currently provided as the Fatigue I and Fatigue II limit states.

Article 1.3.2.3 of AASHTO states that the fatigue limit states shall limit the stress range that results from the passing of a single design truck occurring over a given number of cycles.

Articles 3.4.1 and C3.4.1 describe two limit states for load-induced fatigue design: Fatigue I and Fatigue II, for the respective cases of infinite fatigue life and finite fatigue life. Because fatigue behavior is a function of the cyclic stress range, only live loads, the dynamic load allowance, and centrifugal forces are considered in both limit states.

According to the 7th Edition of AASHTO, the Fatigue I limit state is related to infinite load-induced fatigue life. If a member has infinite fatigue life, then it will theoretically be able to withstand an infinite number of cycles, provided the applied effective stress range amplified by the Fatigue I load factor does not exceed the specified constant amplitude fatigue limit (CAFL) of

the specific detail. The load factor to be used with the Fatigue I limit state is 1.5 and results in what is sometimes referred to as the Fatigue Limit State Load. This load factor, when applied to the effective fatigue design truck (i.e., the HS-20 with a load factor of 0.75) discussed in the next section, corresponds to a truck or stress range with a return period of about 1 in 10,000. Variable amplitude fatigue testing has shown that if the CAFL is exceeded at a frequency of less than 1 in 10,000, infinite life can be expected. It can be seen that the ratio between Fatigue I and Fatigue II limit state load factors is 2.0.

The Fatigue II limit state is related to finite load-induced fatigue life. If a member has a finite fatigue life, then it will theoretically fail due to fatigue when a given number of cycles at a given stress range are completed. The AASHTO fatigue design curves correspond to a probability of failure of approximately 2.5% (a 97.5% probability of survival). The load factor to be used with the Fatigue II limit state is 0.75. This value is representative of the effective stress range produced by the general truck population.

As previously discussed, the findings of SHRP 2 R19B resulted in the Fatigue I and Fatigue II load factors in the 8th Edition of AASHTO to be updated to 1.75 and 0.8, respectively. This change, which is a result of an analysis of WIM data from around the country, reflects the fact that there are a greater number of vehicles now that produce large bending moments when compared to the moments produced by the effective fatigue design truck. In other words, trucks are getting heavier. Historically, the ratio between the load factors for the Fatigue I and Fatigue II limit states has been 2:1, but considering the findings of the R19B, this ratio is now closer to 2.2:1.

2.4.2.3.2 Fatigue Loading

Article 3.6.1.4.1 states that one design truck, as specified in Article 3.6.1.2.2, is to be used to calculate the fatigue design stress range. The use of a single truck in a single design lane was confirmed in the R19B project for the case of fatigue in bridge girders. It is also specified that the rear axles of the truck shall have a constant spacing of 30 feet. The dynamic load allowance specified in Article 3.6.2 is applied to the fatigue load. The fatigue design truck is shown in Figure 2-9. Article 3.6.1.4.3a states that if using a refined analysis method, one must consider a single design truck positioned both longitudinally and transversely on the bridge to produce the maximum stress range on a given component. The position of design lanes is ignored because it is often difficult to predict any future changes that might result in the shifting of design lanes on the bridge deck.

The dynamic load allowance, IM, to be applied to the design truck is specified in Article 3.6.2.1. When evaluating fatigue (in a girder or other "global" components such as a cross-frame), a value of 1.15 is to be used for the dynamic load allowance per AASHTO *LRFD* Table 3.6.2.1-1. The dynamic load allowance is used to account for "average" wheel load impact from moving vehicles. Peak impacts, such as 1.33, are not appropriate for fatigue since fatigue is intended to represent stress ranges produced during normal in-service conditions. This dynamic response may be caused by either hammering effects resulting from moving wheel loads and/or from the dynamic response of the bridge. Interestingly, field studies consistently show that even 1.15 is not frequently exceeded.

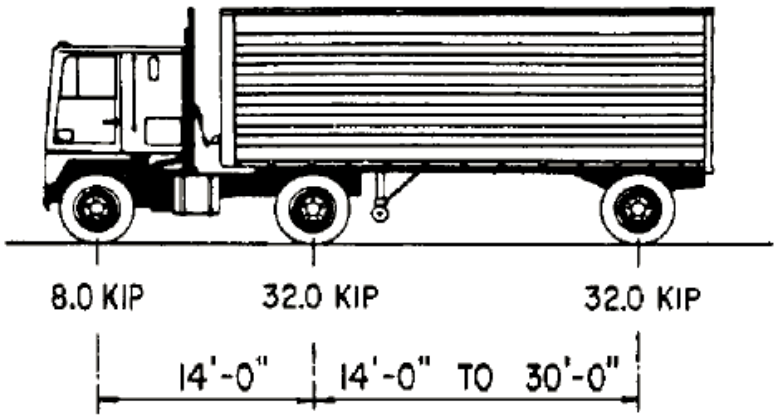

Figure 2-9: Characteristics of the Design Truck - Profile Only (AASHTO 2016).

Article 3.6.3 discusses the provisions for centrifugal force (CE) that accounts for the overturning effect due to lateral forces created when a truck is rounding a horizontally-curved bridge. This will generally apply only to horizontally-curved bridges since straight bridges will likely not experience significant lateral forces from vehicular traffic.

Article 3.6.1.4.2 discusses the methodology for determining the frequency of the fatigue load if the information is not available from other sources. The frequency of the fatigue load is to be taken as the single-lane average daily truck traffic, $ADTT_{SL}$. The $ADTT_{SL}$ is the expected number of trucks per day in a single lane averaged over the life of the bridge, which is best determined in consultation with traffic engineers. This frequency is to be applied to all components of the bridge being designed for fatigue. In lieu of more accurate information, the single-lane average daily truck traffic may be calculated as follows:

$$ADTT_{SL} = p * ADTT \quad \text{Eq. 2.12}$$

where, p is the fraction of truck traffic in a single lane, and $ADTT$ is the total number of trucks in one direction per day over the life of the bridge. As the number of lanes increase, the value of p decreases. As mentioned in Article C3.6.1.4.2, consultation with traffic engineers regarding any directionality of truck traffic may lead to the conclusion that one direction carries more than one-half of the bidirectional ADTT. If such data are not available, designing for 55 percent of the bidirectional ADTT is suggested. Guidance is also given in Article C3.6.1.4.2 regarding the extrapolation of available traffic growth data for the fatigue design life of the bridge (taken as 75 years in AASHTO).

2.4.2.3.3 Design for Load-Induced Fatigue

Article 6.6.1 discusses how to check the limit states of fatigue and fracture. Fatigue is categorized as either load-induced fatigue or distortion-induced fatigue. Load-induced fatigue is characterized by the application of repeated in-plane tensile stresses to an element. Distortion-induced fatigue represents fatigue effects due to out-of-plane secondary stresses not quantified in the analysis and is often the result of improper detailing. Historically, cracking in the webs in the vicinity of cross-frame locations is one of the most common cases of distortion-induced fatigue. Prior to the 1980s, distortion-induced cracks in the webs were relatively common and caused by the lack of a rigid load or stress path to transmit the force in the cross-frame members from the web to the flange. Distortion-induced fatigue is not a topic of this research and will not be discussed further.

Articles 6.6.1.2.1 and C6.6.1.2.1 state that only the live load stress range is to be considered for fatigue design, and that residual stresses caused by fabrication are not to be considered when investigating fatigue. Permanent loads do not contribute to the stress range. Residual stresses are not included explicitly because they are included implicitly through the specification of the stress range as the sole dominant parameter for fatigue design. Growth in the fatigue cracks is caused by cyclic tensile stresses. However, for cases with a stress reversal (i.e., stress ranges including both tensile and compressive components) the complete live load stress range, consisting of the full range including both the tensile and compressive stress components, is used to check fatigue. The reason the compression component is included is because the residual stresses locked in during fabrication may cause the entire stress range cycle to be shifted into the tensile stress region. Even

if there is only a small component of tension in the stress range, the crack can propagate. In the case of stress reversal, even if the compression component of the stress range is much larger than the tensile portion, the fatigue limit states must be considered.

If the live load tensile stress calculated using the Fatigue I limit state load factor is smaller than the compressive stress due to the unfactored compressive permanent loads, then there is no net tensile stress, and there is no need to further consider fatigue. The Fatigue I limit state is used for this check because it is associated with the upper bound (i.e., the 1 in 10,000 return period) stress range an element may experience.

In calculating section properties for the design of composite steel girders, the concrete deck is converted to an equivalent amount of steel based on the modular ratio, $n=E_s/E_c$, where E_s and E_c are the respective elastic moduli of the steel and concrete. Depending on the nature of the calculations, either "short-term" or "long-term" composite section properties may be used. In calculations utilizing "short-term" composite properties, the deck is transformed into an equivalent steel section using the modular ratio, n. For "long-term" composite section properties, the effects of creep and shrinkage are approximated, and the concrete is transformed using $3n$. According to Article 6.6.1.2.1, dead and live load stresses and live load stress ranges for fatigue design at all sections in the member due to loads applied to the composite section may be computed using the long-term composite section for dead loads and the short-term composite section for the live loads, assuming the concrete deck is effective for both positive and negative flexure. Shear connectors must be provided throughout the entire length of the member, and the longitudinal reinforcement must satisfy the provisions of Article 6.10.1.7 in order for the concrete to be considered effective for negative flexure. Properly reinforced concrete can provide significant resistance to tensile stress at service load levels. Recognizing this behavior will have a significantly beneficial effect on the computation of fatigue stress ranges for details located on or near the top of the girder in regions of stress reversal and in regions of negative flexure.

The primary guidance for the application of the fatigue loads in cross-frames can be found in Article C6.6.1.2.1; however, the guidance has changed in recent years. Prior to 2015, AASHTO Article C6.6.1.2.1 described a possible fatigue loading condition for cross-frames when these effects are determined from a refined analysis. Stresses are created in cross-frames when one girder deflects with respect to an adjacent girder. The proposed loading condition involves the passing of two trucks simultaneously, with one truck traveling along one girder and the other truck traveling

along an adjacent girder (slightly behind the first truck). It was further suggested that a factor of 0.75 be applied to the resulting stress range to account for the low probability of occurrence of two vehicles located in these critical relative positions. In no case was the calculated stress range to be less than the stress range caused by the loading of only one lane. While this loading condition creates the worst possible fatigue stress range in a cross-frame, a 2015 interim revision noted that it is highly unlikely that this loading condition is a common occurrence throughout the service life of the bridge. As a result, the 2015 interim revisions recommended positioning a single fatigue truck in one transverse position for each longitudinal position evaluated. This was determined solely on the consensus of AASHTO T-14 members and advisors to this subcommittee based on experiences and an informal review of available data. The group subsequently agreed that this loading more accurately represents the typical loading condition that will be experienced by the cross-frames throughout the design service life of the bridge.

All details being evaluated for load-induced fatigue are to satisfy the following equation from Article 6.6.1.2.2 of AASHTO:

$$\gamma(\Delta f) \leq (\Delta F)_n \qquad \text{Eq. 2.13}$$

where, γ is the load factor pertaining to either the Fatigue I limit state or the Fatigue II limit state, (Δf) is the calculated stress range experienced by the detail under consideration, and $(\Delta F)_n$ is the nominal fatigue resistance of the detail determined as specified in Article 6.6.1.2.5.

The nominal fatigue resistance, $(\Delta F)_n$, can be calculated using one of two equations, depending on which limit state is being checked. The limit state and equation to check depends on the value of the calculated $ADTT_{SL}$ relative to the value specified in Table 6.6.1.2.3-2 for the component or detail under consideration. If the component or detail is to be checked for infinite life using the Fatigue I limit state, the nominal fatigue resistance is to be calculated as follows:

$$(\Delta F)_n = (\Delta F)_{TH} \qquad \text{Eq. 2.14}$$

$(\Delta F)_{TH}$ is the constant amplitude fatigue threshold (CAFL). If it is determined that the stress range in a given detail is lower than the CAFL, then the detail is considered to have an infinite fatigue life. Article 6.6.1.2.3 further recommends that components and details on fracture-critical members should always be designed for infinite life.

If the component or details is to be checked for finite life using the Fatigue II limit state, the nominal fatigue resistance is to be calculated as follows:

$$(\Delta F)_n = \left(\frac{A}{N}\right)^{\frac{1}{3}} \quad \text{Eq. 2.15}$$

Where A is a detail-category constant specified in Table 6.6.1.2.5-1 representing the y-axis intercept of the S-N curve (Figure C6.6.1.2.5-1) for each detail category, and N is an estimate of the total number of cycles the detail can expect to experience over the 75-year fatigue design life based on $ADTT_{SL}$. The value of N for cross-frames depends on the number of stress cycles per truck passage, *n*, which for transverse members is affected by the spacing of the cross-frames (Table 6.6.1.2.5-2). The 75-year $ADTT_{SL}$ values above which the infinite life check governs given in Table 6.6.1.2.3-2 assume one stress range cycle per truck passage (i.e., *n*=1.0). For other values of *n*, the values in the table must be divided by *n*. If a fatigue life other than 75 years is sought, the table values must be multiplied by the ratio of 75 divided by the fatigue life sought in years.

All details are categorized according to Table 6.6.1.2.3-1 of AASHTO. There are eight detail categories ranging from A to E′. Detail Category A is associated with base metal, and is considered the best fatigue detail category. Detail Category E′ is considered the worst detail category.

In the 7th Edition of AASHTO, a detail in Table 6.6.1.2.3-1 (Condition 7.2) is provided for single angles and tee-section members welded to gusset plates by longitudinal fillet welds along both sides of the connected element, and this detail was listed as Category E. However, research performed by McDonald and Frank (2009) and Battistini (2014) showed that this detail is actually a Category E′ detail due to the effects of connection eccentricity. This detail category was revised accordingly in the 2016 interim revisions.

2.4.2.3.4 Multiple Presence

AASHTO does not currently require the consideration of multiple presence specific to cross-frame design.

2.4.2.3.5 Stability Bracing Requirements

AASHTO does not currently provide minimum strength or stiffness requirements that are specific to cross-frames.

2.5 CHAPTER SUMMARY

The following three points outline the current gaps of knowledge recognized from a review of the literature:

- Recent research has advanced the state of knowledge regarding the effects of connection eccentricity and modeling assumptions as it relates to fatigue behavior in cross-frames; however, virtually no research has investigated the effects of modern traffic loads on cross-frames, or the proper loading conditions to estimate force effects in cross-frame design. Specifically, recent traffic records (i.e., WIM data) are generally available and should be utilized to better understand the appropriateness of the fatigue load model. Recent updates to the load factors for the fatigue limit states are based on primary longitudinal members. This research did not consider if these load factors are reasonable for cross-frame fatigue design.
- The effects of multiple presence on primary girders has been investigated, and due to recent research, current AASHTO *LRFD* requirements have removed this from discussion in the Commentary; however, the effects of multiple presence on cross-frames has not been directly evaluated.
- While recent efforts have evaluated the AASHTO *LRFD* fatigue limit states from a context of reliability, these efforts have been focused on primary longitudinal girders - not secondary members such as cross-frames.

Chapter 3: Studies of Representative Bridges and Development of Model Data Set

3.1 INTRODUCTION

This chapter summarizes the components of the larger NCHRP Project 12-113 research efforts that serve as a basis for the advanced loading studies addressed in this research. Specifically, this chapter summarizes the selection of three representative bridges that were instrumented and load tested, the use of the field tests to validate three-dimensional finite element analysis (FEA) models, the extensive parametric studies performed to improve the understanding of the behavior of cross-frame stresses, and the development of a comprehensive analytical testing matrix and model data set that attempted to include a wide range of geometrical parameters of straight and horizontally-curved bridges with and without skewed supports. The combination of the validated FEA models (performed by and documented in Park 2020) and the development of an analytical testing matrix and model data set (performed by and documented in Reichenbach 2020) provided the framework for the fatigue loading study represented in this dissertation.

3.2 SELECTION OF REPRESENTATIVE BRIDGES AND FIELD TESTS

This section summarizes the basic information of the three bridges that were instrumented and monitored as part of the study. The information that is provided includes location, geometry, and cross-frame details. The instrumented bridges include 1) a straight bridge with normal supports, 2) a straight bridge with skewed supports, and 3) a horizontally-curved bridge with normal supports. Pertinent information for the three bridges is summarized in Table 3-1. The bridge number corresponds to the order in which the bridges were instrumented, monitored, and tested.

Table 3-1: Pertinent information of three instrumented bridges.

Bridge No.	Type	Location
1	Straight; normal supports	Conroe, TX
2	Straight; skewed supports	Conroe, TX
3	Horizontally-curved, normal supports	Seabrook, TX

3.2.1 Bridge 1

The first bridge instrumented as part of the study is a portion of an Interstate Highway (IH) 45 off-ramp in Conroe, Texas. Conroe is located approximately 45 miles north of Houston. The middle spans of this bridge are comprised of continuous, built-up steel plate girders acting compositely with an nominally 8-inch thick concrete deck. Bridge 1 is straight with supports oriented normal to the girder lines. The respective lengths of the continuous plate girder spans range between approximately 200 to 250 feet, and the total width of the bridge is approximately 40 feet. According to the construction drawings, the estimated average daily traffic (ADT) for this bridge is 3,300.

There are three types of cross-frame configurations used on Bridge 1. The end cross-frames are K-type frames that consist of a WT top strut compositely connected to the deck and single angle L4x4x1/2 bottom strut and diagonal sections. Cross-frames at interior bents are X-type frames with single angle L4x4x1/2 sections for the top struts, bottom struts, and diagonal members.

The intermediate cross-frames (i.e., between bents) are the primary focus for the NCHRP 12-113 project, and consist of X-type frames with single angle L4x4x3/8 sections for the top struts, bottom struts, and diagonal members. All member-to-gusset and gusset-to-connection plate connections are welded, similar to the standard detail illustrated in Figure 3-1. Based upon the results of the Phase I industry survey documented in Reichenbach et al. 2021, aside from the welded connections, the layout of the cross frame is consistent with one of the most popular cross-frame geometries used by bridge owners throughout the US. The cross-frames for Bridge 1 are typically spaced at approximately 20 feet on center.

In selecting the bridges for instrumentation during Phase I of the NCHRP 12-113 project, Bridge 1 offered several advantages, including the following:

- The spans are long and relatively narrow but still support three striped lanes. The system is not overly redundant, and three lanes offer a variety of potential load positions for the controlled live load tests;
- The IH 45 corridor has a high traffic volume with large ADTT.

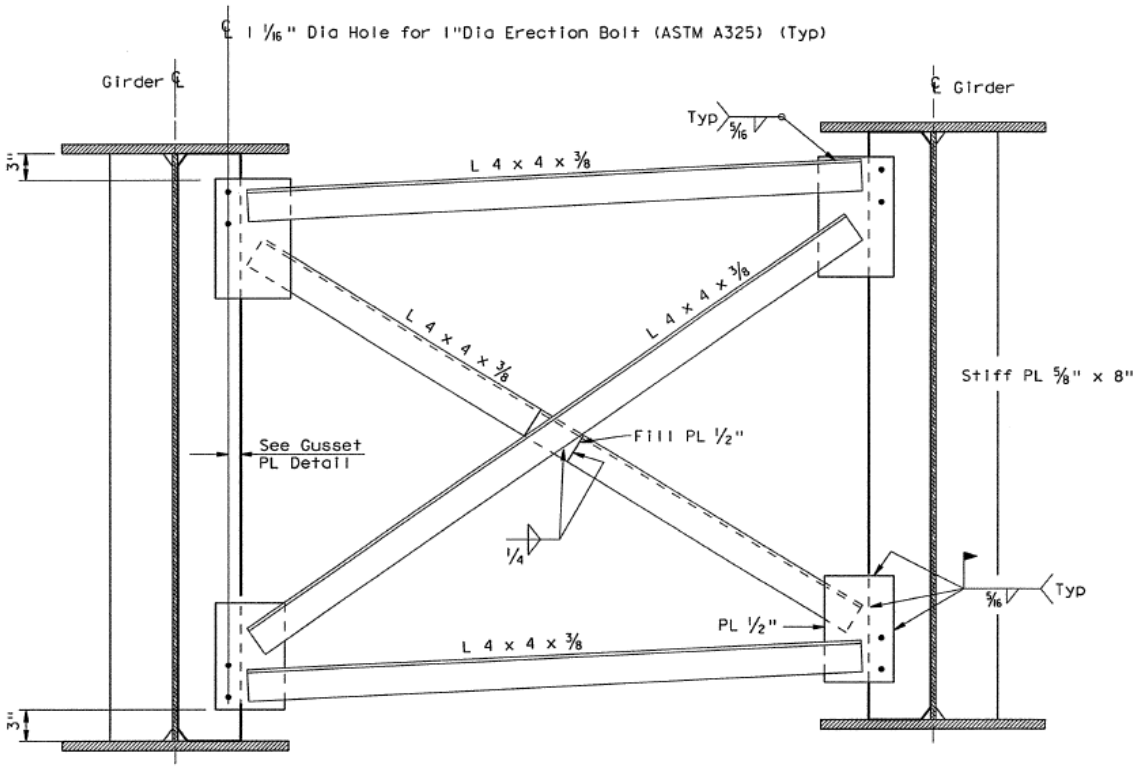

Figure 3-1: Intermediate cross-frame configuration similar to that used for all bridges.

3.2.2 Bridge 2

The second bridge that was instrumented is an IH 45 main lane in Conroe, Texas. Bridge 2 includes a three-span continuous, steel I-girder unit with a total length of approximately 450 feet. Each span is constructed with steel plate girders acting compositely with a nominally 8-inch thick concrete deck. The bridge supports are skewed relative to the centerline of the bridge (approximately 40 degrees). The span lengths for the continuous girder portion of the bridge range from approximately 100 to 200 feet, and a bridge width of approximately 96 feet. According to available traffic records, the ADT for this bridge is approximately 120,000.

There are four types of cross-frame configurations used in Bridge 2. End cross-frames are X-type frames that consist of a WT top strut compositely connected to the deck and single angle L5x5x1/2 bottom strut and diagonal sections. Cross-frames at interior bents are X-type frames with single angle L5x5x1/2 sections for the top struts, bottom struts, and diagonal members.

Similar to Bridge 1, the intermediate cross-frames are the primary focus of the NCHRP 12-113 project. Typical intermediate cross-frames are X-type frames with single angle L5x5x1/2 sections for the top struts, bottom struts, and diagonal members. Unique to Bridge 2, the designer

employed lean-on bracing near the interior skewed support lines. Lean-on braces utilize only top and bottom struts, thereby eliminating the diagonal members. Lean-on braces are double angle (2L5x5x1/2) sections for top and bottom struts only with one intermediate spacer plate. The first line of cross-frames are offset at least 3 feet from the girder support, and the typical spacing for intermediate cross-frame lines is approximately 17 feet for the instrumented span.

Figure 3-2 illustrates typical lean-on braces used in Bridge 2. Similar to Bridge 1, Figure 3-1 illustrates typical intermediate cross-frames without lean-on braces. In bridges with skewed supports and cross-frames oriented perpendicular to the girder lines, cross-frames connect to the girders at different locations along the individual girder lengths. As a result, there can be relatively large forces induced in the cross-frames due to differential girder deflections under truck traffic. This is of particular concern for cross-frames that frame into or near skewed supports where the differential deflection between adjacent girders can be large since deflection of one girder is relatively small or negligible. By removing the diagonal members in these select cross-frames, the bracing line is softened, and the live-load-induced forces are reduced. Despite the fact that lean-on bracing schemes can be used throughout an entire framing system, the designer in this case opted to only apply the concepts in the regions around interior supports. All member-to-gusset and gusset-to-connection plate connections are welded. The detailing of the intermediate cross-frames are identical to the standard TxDOT intermediate cross-frame detail as shown in Figure 3-1.

In selecting the bridges for instrumentation during Phase I of the NCHRP 12-113 project, Bridge 2 offered several advantages, including the following:

- The span lengths are reasonably representative of steel bridge systems;
- The girders support five striped lanes, which offers a variety of potential load positions for the controlled live load tests;
- The IH 45 corridor is high volume with large ADTT.

In contrast, the only difficulty identified with Bridge 2 is that it is a highly redundant system given the number of girders.

3.2.3 Bridge 3

The third bridge that was instrumented is a State Highway (SH) 146 Direct Connector near La Porte, TX. Bridge 3 primarily serves large trucks traveling to nearby shipping ports. According to available traffic data, the ADT is 40,000.

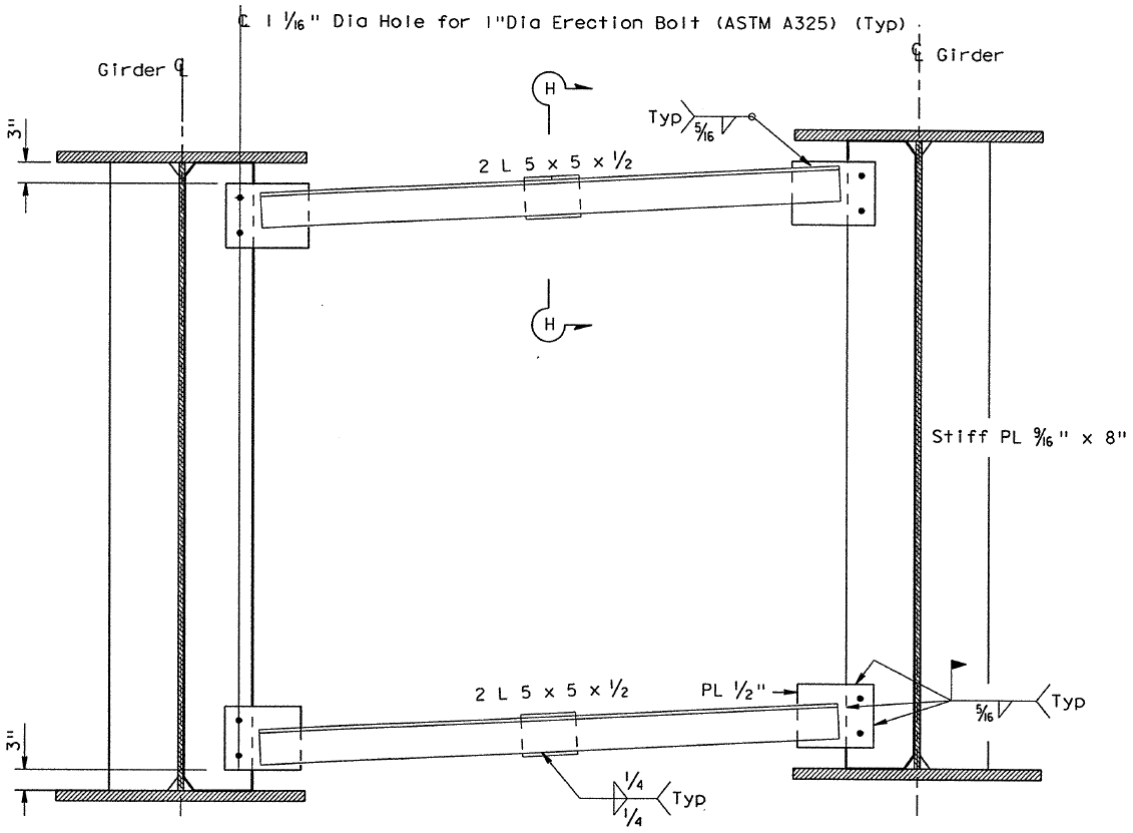

Figure 3-2: Typical lean-on cross-frame bracing using in Bridge 2.

The bridge includes a 4-span continuous, built-up steel plate girder system acting compositely with a nominally 8-inch thick concrete deck. Bridge 3 is horizontally-curved with an approximate 800-foot radius of curvature. The supports are normal to the centerline of the bridge. The span lengths vary between approximately 200 to 300 feet, and the total width of the bridge is approximately 30 feet. The bridge is striped for one 14-foot lane of traffic and two shoulders. Based on the width of the bridge, this bridge could have two design lanes. The design of all four girders is identical, except for small variations in flange transition locations as well as the radius and corresponding girder span.

There are three types of cross-frame configurations used on Bridge 3. End cross-frames are K-type frames that consist of a WT top strut compositely connected to the deck and single angle L5x5x1/2 bottom strut and diagonal sections. Cross-frames at interior bents are X-type frames with single angle L5x5x1/2 sections for the top struts, bottom struts, and diagonal members.

The intermediate cross-frames are X-type frames with single angle L5x5x1/2 sections for the top struts, bottom struts, and diagonal members. Like the other two bridges, all member-to-gusset and gusset-to-connection plate connections are welded, similar as illustrated in Figure 3-1. All connections were welded, and cross-frames are typically spaced radially at approximately 12 feet on center.

In selecting the bridges for instrumentation during Phase I of the NCHRP 12-113 project, Bridge 3 offered several advantages, including the following:

- The spans are long and the bridge has significant curvature (radius of curvature is 800 feet);
- Since the bridge has only four girders, every cross-frame should be engaged for all loading conditions;
- The direct connector services large volumes of heavy trucks.
- The bridge has a single striped lane, but two design lanes. Data can be obtained considering both the striped lanes as well as likely design lane positions during the controlled live load tests.

The only disadvantage of this bridge is that the relatively narrow deck width limits the number of load cases that can be considered during the controlled live load tests.

3.2.4 Field Instrumentation and Load Test

Preliminary models were developed in Abaqus for the three bridges (documented in Park 2020 and Reichenbach 2020) in order to address the following:

- Identify cross-frames that are likely to experience the largest stress ranges due to truck traffic.
- Identify girder flanges to be instrumented to determine flange stress and vertical displacements.
- Identify truck positions and orientation likely to provide the most meaningful data for validating the FEA models.
- Confirmation that the expected load test truck weight would likely create significant cross-frame forces and provide meaningful data.

Based on the preliminary modeling, an instrumentation plan was developed unique for each bridge to best capture this data. Each bridge was instrumented with approximately 70 Micro-

Measurements LWK-Series weldable strain gages. The gages were installed on both the cross-frame members and girder flanges. The use of the weldable gages simplified the surface preparation in the field and expedited the instrumentation process. Weldable gages require very little energy and have shown to have no discernible fatigue effects on the bridge components during or after instrumentation. Figure 3-3 shows a typical strain gage after the steel surface has been prepped and the gage welded. The final stage of the instrumentation consists of protecting the gage from the environment with wax and silicone, which is not shown in the picture. Figure 3-4 shows the project team instrumenting Bridge 1 with the use of an articulating boom lift and temporary working platform stations installed on top of the girder bottom flanges and adjacent to the line of instrumented cross-frames. Figure 3-5 illustrates a typical line of cross frames after they are instrumented and Figure 3-6 illustrates a single cross-frames after it is instrumented. The specific instrumentation plan for each bridge can be found in Reichenbach et al. 2021.

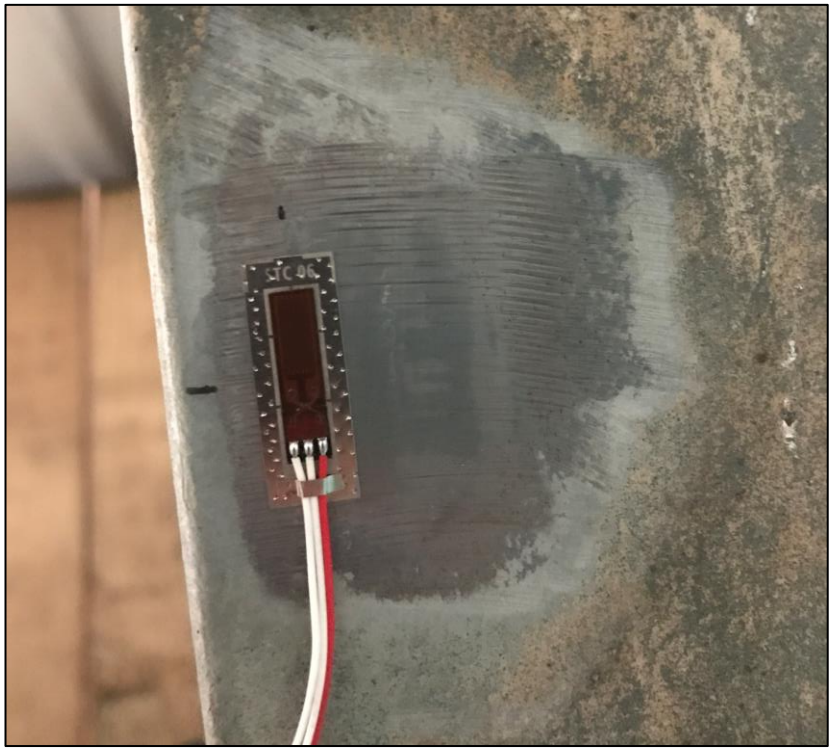

Figure 3-3: Typical welded strain gage used for instrumentation (wax and silicon for environmental protection are not shown).

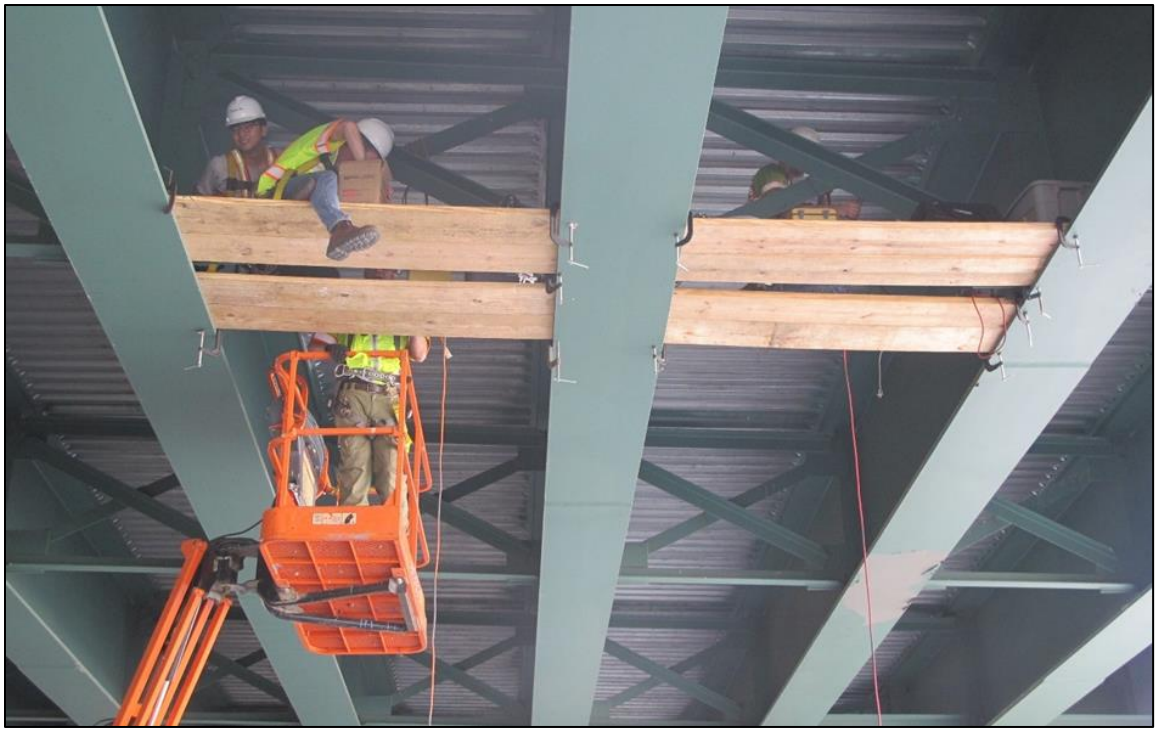

Figure 3-4: Articulating boom lift and working platform stations utilized during instrumentation of Bridge 1.

Figure 3-5: View of a typical line of cross-frames after instrumentation.

Figure 3-6: View of a typical cross-frame after instrumentation.

3.2.5 Controlled Live Load Tests

The Texas Department of Transportation (TxDOT) provided full bridge closures for each subject bridge during controlled live load tests. TxDOT also provided four loaded, three-axle dump trucks for use during testing. The trucks were weighed before the test, and the gross weight was typically around 50 kips. Based on previous experience, multiple 50-kip trucks are generally heavy enough to provide reliable data from strain gages.

The load tests for Bridges 1 and 2 were performed during a nighttime closure, whereas the load test for Bridge 3 was performed during a morning closure. The data collected during the controlled live load tests include strain data for cross-frames and girder bottom flanges and girder vertical deflection measurements at predetermined points along the bridge. In total, eight different load cases were performed for each bridge: one moving case and seven static cases.

Strain data were measured by the strain gages; the data were measured continuously as trucks were moved onto the bridge to their final predetermined locations for all eight cases. This enabled the project team to understand the influence line effects for the full spectrum of data collected.

Deflection data were measured for the seven static load cases using a Hilti PD-E (+/- 1/25

inch accuracy) laser distance meter. Deflections were documented at pre-selected cross-frame lines. The laser distance meter was positioned directly below the girder bottom flanges at the desired reading locations, on a level base constructed prior to the load test using Hydrostone. Three independent readings were recorded at each location and averaged for improved reliability in the measurements. Distance readings were recorded in the unloaded state prior to testing and loaded state for all seven static load cases, and the corresponding displacement was the net change in the average of these readings.

The controlled live load testing and data collection was carried out systematically for each load case and for each bridge according to the steps shown in Table 3-2: Procedural outline for controlled live load testing. Step 0, the closure of the bridge and other necessary traffic control procedures, occurred only one time and was handled by TxDOT. The complexity and magnitude of the lane closures differed between the bridges. Steps 1 and 2 included preparation efforts below the bridge as well as on the bridge deck (e.g., marking truck stopping positions on the deck, positioning traffic cones to improve guidance for truck drivers, documenting the wheel base and tracks of each truck, and obtaining baseline strain and deflection readings of the unloaded bridge).

Steps 3 through 5 were repeated for each load case performed during the test. One by one, each truck was positioned as close as possible to the predetermined position as marked with the colored tape and traffic cones. Incrementally introducing the trucks afforded the opportunity to obtain additional intermediate load cases and yielded cleaner data. The vertical deflection measurements were taken after all four of the trucks was positioned, and the position of the truck wheels were documented. Finally, all four trucks were removed from the bridge. Vertical deflections at select locations along the bridge were measured and evaluated for the static load cases only. Figure 3-7 represents a stress history of a cross-frame diagonal member measured during a load case. The cross-frame angle was instrumented with four strain gages, and since the gusset plate is connected to only a single leg of the angle, two strain gages were placed on the loaded leg and two gages were placed on the unloaded (unwelded) leg. Since it is desirable to reference the axial stress component of the loaded cross-frame, a linear regression algorithm detailed in Reichenbach et al. 2021 was used to convert the combined bending and axial responses (due to the cross-frame connection eccentricity) to an axial response comparable to AASHTO *LRFD* idealization (i.e., the Category E′ fatigue designation inherently considers bending effects). The axial component of the stress, derived by the linear regression algorithm, always falls within

the bounds set by the extreme stress states measured from free edge to free edge of an angle's two legs. Bending effects on angle sections due to eccentrically-applied loads were studied and are documented in greater depth in Reichenbach et al. 2021.

Table 3-2: Procedural outline for controlled live load testing.

Step #	Description	Approximate Duration
0	*Road Closure*: Traffic is stopped and all vehicles are removed from bridge. The bridge is shut down for the entire duration of testing.	N/A
1	*Prep Work*: The bridge deck is prepped with colored tape and traffic cones. The wheelbases of the truck are measured and documented.	~30 mins
2	*Baseline Measurements at Unloaded Condition*: Baseline strain readings of the unloaded bridge are recorded; baseline laser distance readings of the unloaded bridge are recorded. Five locations minimum were used for deflection readings.	~ 30 mins
3	*Truck Positioning*: The trucks are moved onto the bridge one at a time to the predetermined locations.	~ 12 mins
4	*Loaded Measurements at Specific Load Condition*: Strain measurements are recorded continuously, laser distance measurements are taken for the loaded condition of the bridge, and the exact position of the trucks on the deck is measured and documented.	~ 12 mins
5	*Removal of Trucks*: All vehicles are removed from the bridge.	~ 3 mins
6	*Road Reopened*: Traffic control is removed, and the bridge is opened back up to traffic	N/A

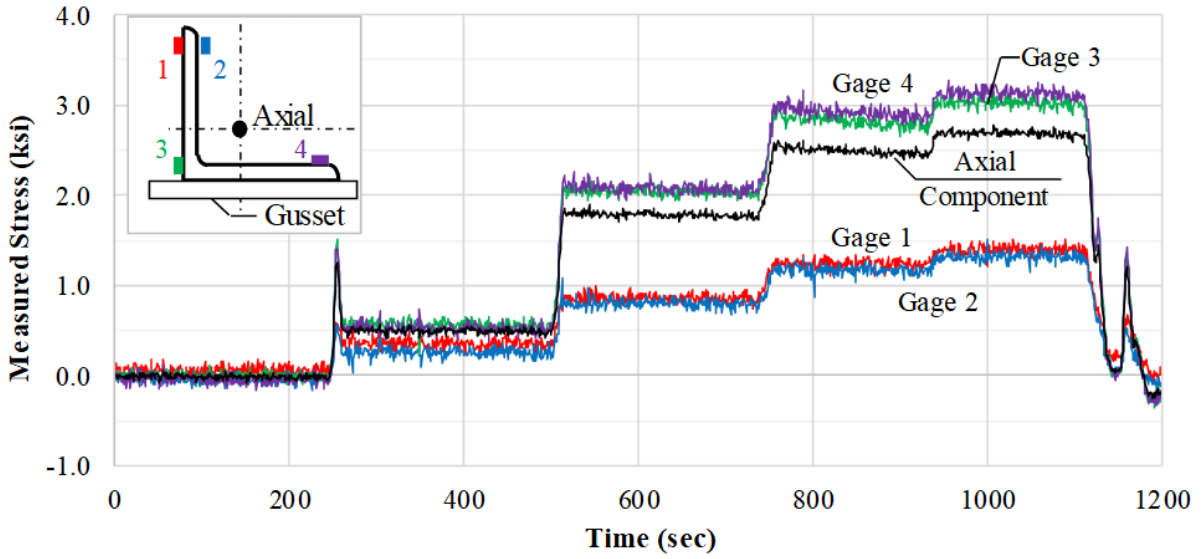

Figure 3-7: Example showing the axial stress component of a cross-frame angle section versus the individual strain gage responses.

A single load case generally took 25-30 minutes to complete. In total, eight iterations of Steps 3 through 5 took approximately 4 hours to complete once traffic control was in place and prep work was finished. At the completion of the live load test, TxDOT crews reopened the bridge to traffic. Figure 3-8 shows the typical three-axle dump truck provided by TxDOT and loaded with sand. The truck consists of one front steer axle and two rear drive axles. The individual load cases used for each bridge are summarized in Reichenbach et al. 2021. The results of the controlled live load test served as a vital component towards the validation of the FEA models.

Figure 3-8: Typical TxDOT dump truck used for the controlled live load test.

3.2.6 In-Service Monitoring

At each instrumented bridge, stress cycle spectra were obtained for various cross-frame members and girder flanges during a one-month monitoring period. These spectra provide useful insight on the stress cycle magnitudes that a component typically experiences due to live loads. The relative difference in truck traffic volume between different bridges can also be inferred from the data, as well as a calculation of the accumulated fatigue damage for instrumented bridge components caused by real traffic. The spectra, however, are limited in that they provide no indication of the load spectrum (i.e., the weight and axle configuration of the vehicles causing those cycles) or the corresponding transverse lane positions, which is especially critical for cross-frames given their observed sensitivity to load position. The primary goal for obtaining this data

was to establish effective and maximum stress range metrics, by which the computational studies and fatigue criteria developed in this research can be assessed in future studies. Consequently, the monitoring data is not further discussed in this dissertation, but a summary of results is provided in Reichenbach et al. (2021).

3.3 FEA Model Validation

The preliminary FEA models discussed in Section 3.2 were compared with the measured strain and vertical deflection readings from the load test using simulated truck properties and loading positions. Appropriate modifications were applied based on this comparison, including adjusting the models to match the as-built conditions in order to obtain good agreement with the composite stiffness of the deck and I-girders. The model validation is documented in Park (2020) and Reichenbach (2020). The validated models adopted a consistent set of assumptions across the three models, and generally reported errors of approximately +/-10% when compared to the field measured data.

3.4 Analytical Testing Matrix and Model Data Set

Reichenbach (2020) developed an analytical testing matrix that attempted to encompass the parameters primarily affecting cross-frame force effects. Developing a testing matrix that represents the thousands of steel I-girder bridges in the US is challenging. This was accomplished by outlining a range of possible parameters and categorized them as independent or dependent parameters. Independent parameters were then further classified as either constants or variables. Table 3-3 provides a comprehensive breakdown of parameters considered by Reichenbach in the development of the testing matrix. Parameters are divided into four categories: overall geometry, cross-section, cross-frame detail, and materials. The parameter designation (independent parameter, constant parameter, or dependent parameter) is also shown. Dependent variables, although not independently varied in the FEA models, are important values that are commonly used to describe the geometry of a bridge and the cross-section proportions of I-girders; hence, they are included in the table for reference. These variables are simply a function of other independent variables and constants. For example, the span length is a function of the girder depth and the span-to-depth ratio of the bridge. Table 3-4 and Table 3-5 describe the range of variable(s) considered for independent variables and constants, respectively.

Using the validated models discussed in the previous section, Reichenbach (2020) generated a 4,104-model matrix based on assumed parameters that could likely be most influential in cross-frame force effects; most of the parameter boundaries were based on limits per AASHTO *LRFD* design provisions. The 4,104-model matrix is discussed in detail in Reichenbach 2020 and Reichenbach et al. 2021. Based on a detailed review of this model matrix, Reichenbach (2020) and Park (2020) executed a large-scale parametric study, which Reichenbach used to comprehensively identify and study critical cross-frame members within each model. The model matrix included producing over 65,000 influence surface plots for various cross-frames. Reichenbach developed interactive, Excel-based data visualization workbooks to:

- Display an influence surface for the axial-force response of cross-frames in the form of a color contour plot;
- Display the global and localized displacement of the cross-frame panel of interest;
- Simulate the passage of an individual truck or truck(s) along the length of the influence surface to develop an influence-line plot at a discrete transverse position; and
- Tabulate all relevant parameters describing the geometry and details of the superstructure.

Table 3-3: Parameters considered in development of analytical testing matrix.

Parameters and Type							
Geometry	**Type**	**Cross-Section**	**Type**	**Cross-Frame Detail**	**Type**	**Material**	**Type**
No. spans	IND	Web depth	IND	Cross-frame type	IND	Concrete modulus	IND
L/d ratio	IND	Deck thickness	IND	Cross-frame area	IND	Steel modulus	CON
Girder spacing	IND	Web slenderness	CON	Connection plate width	CON		
No. girders	IND	Top flange width	CON	Conn. plate thickness	CON		
Support skew	IND	Bottom flange width	CON	Vertical offset dimension	CON		
Radius of curvature	IND	Flange slenderness	CON	Modification factor	CON		
Cross-frame spacing	IND	Degree of monosymmetry	CON				
Cross-frame layout	IND	Flange transitions	CON				
Barrier joint spacing	CON	Haunch thickness	CON				
Overhang width	CON	Barrier thickness	CON				
Span length	DEP	Barrier height	CON				
Bridge width	DEP	Bearing stiffness	CON				
Skew index	DEP	Web thickness	DEP				
Curvature index	DEP	Top flange thickness	DEP				
		Bottom flange thickness	DEP				

Note: IND = independent variable, CON = constant value, DEP = dependent variable

Table 3-4: Range of values used for independent variables in Fatigue Loading Study.

Parameter	Range of Values
No. spans	{1, 2, 3}
L/d ratio	{25, 30, 35}
Girder spacing [ft]	{6, 8, 10}
No. girders	{3, 5, 7}
Support skew	{0, 30, 60}; {Parallel, Trapezoidal}
Radius of curvature [ft]	{Infinite, 1500, 750}
Cross-frame spacing [ft]	{20, 30}
Cross-frame layout	{Contiguous, Staggered}
Web depth [in]	{72, 96}
Deck thickness [in]	{8, 10}
Cross-frame type	{X, K}
Cross-frame area [in^2]	{2.86, 4.79}; {L4x4x3/8, L5x5x1/2}
Concrete modulus [ksi]	{3600, 5000}

Table 3-5: Constant values used in Fatigue Loading Study.

Parameter	Value
Barrier joint spacing [ft]	20
Overhang width [ft]	3
Web slenderness	128
Top flange width [in]	24
Bottom flange width [in]	24
Flange slenderness	8
Degree of monosymmetry	0.5
Flange transitions	None
Haunch thickness [in]	3 (Including flange)
Barrier thickness [in]	18
Barrier height [in]	36
Bearing stiffness	As-validated
Connection plate width [in]	8
Connection plate thickness [in]	0.5
Vertical offset dimension [in]	6
Stiffness modification factor	0.6
Steel modulus [ksi]	29000

Using these interactive visualization workbooks, Reichenbach selected 20 bridge models from the 4,104-model set that attempted to represent the extreme bridge geometries and configurations that most influence cross-frame force effects. This subset of bridge models,

summarized in Appendix B along with the 4,104-model bridge set, provided the framework for the fatigue loading study represented in this dissertation.

3.5 CHAPTER SUMMARY

This chapter discussed the components of the larger NCHRP Project 12-113 research efforts that serve as a basis for the advanced loading studies addressed in the remainder of the dissertation. Three representative bridges were selected for instrumentation and load testing. The instrumented bridges included 1) a straight bridge with normal supports, 2) a straight bridge with skewed supports, and 3) a horizontally-curved bridge with normal supports. The field tests were used to validate three-dimensional FEA models for the purposes of conducting a comprehensive parametric study to evaluate the impact of various bridge characteristics on the force-effects of cross-frames.

The FEA models and subsequent parametric studies assisted Reichenbach (2020) in the development of a comprehensive analytical testing matrix and a 4,104-model data set that attempted to include a wide range of geometrical parameters of straight and horizontally-curved bridges with and without skewed supports. Reichenbach developed and utilized data visualization tools to comprehensively review critical cross-frame members within each of the models. Based on assumed extreme cross-frame force effects, Reichenbach developed a 20-model data set that provided the framework for the fatigue loading study represented in this dissertation.

Chapter 4: WIM Sensitivity Study and Preliminary Findings

4.1 INTRODUCTION

The focus of this chapter is to use weigh-in-motion (WIM) records obtained from sites throughout the US to simulate realistic traffic on bridges representative of the model data set discussed in Chapter 3. In general, WIM analyses for cross-frames have four degrees of freedom: each simulation for a particular bridge and cross-frame member must consider longitudinal and transverse vehicle placement, the measured cross-frame force effects, and time. Since these analyses present significant computational time constraints, it is desirable to perform preliminary studies on a single WIM record that is generally representative of all records, in order to explore the sensitivities of vehicle lane placement, multiple presence, and vehicle weight filters on the fatigue parameters for computing the Fatigue I and II limit states. The findings from the sensitivity studies provide guidance on the advanced WIM analyses performed in Chapter 5 that will encompass a larger number of WIM records.

This chapter discusses the available WIM records and subsequent filtering; the development of automated scripts to simulate these records on FEA bridge models in order to study cross-frame force effects; development and implementation of four sensitivity studies based on one representative WIM record; a multiple presence study considering all available 2-lane high-resolution traffic records; and primary findings.

4.2 WIM RECORDS AND FILTERING

High-resolution WIM records were obtained by reaching out directly to the FHWA for 16 specific pavement study (SPS) sites across the US. The records are summarized in Table 4-1, and generally include a full year's worth of measurements collected in 2014. The record timestamps are reported with 0.01-second measurement resolution. Table 4-1 includes the SPS identification and site ID, the WIM sensor type, the number of days missing from the record (if any), and number of lanes recorded. Note that the SPS identification refers to a special materials focus of the Long-Term Pavement Performance program (Al-Qadi et al. 2016). For example, SPS-1 is a strategic study of structural factors for flexible pavements, and SPS-5 is a rehabilitation of asphalt concrete pavements. In total, the unfiltered records include approximately 46 million vehicle records from 16 sites over 15 states. Since some sites have multiple lanes, the records include 23 one-lane

records.

Table 4-1: SPS Sites with WIM data obtained by FHWA.

State	Road & Site ID	SPS ID	Sensor Type	Number of Days Missing[a]	Number of Lanes Recorded
AR	I-30, 050200	SPS-1	Bending plate	--	1
AZ	I-10, 040200	SPS-2	Bending plate	23	1
CA	SR-99, 060200	SPS-1	Bending plate	2	1
CO	I-76, 080200	SPS-2	Bending plate	--	1
IL	I-57, 170600	SPS-1	Bending plate	8	1
IN	US-31, 180600	SPS-1	Quartz	--	4
KS	I-70, 200200	SPS-1	Bending plate	--	1
LA	US-171, 220100	SPS-1	Quartz	--	1
MD	US-15, 240500	SPS-1	Bending plate	14	1
MN	US-2, 270500	SPS-035	Quartz	--	1
NM	I-25, 350100	SPS-1	Quartz	4	1
NM	I-10, 350500	SPS-2	Quartz	6	1
PA	I-80, 420600	SPS-158	Quartz	90	1
TN	I-40, 470600	SPS-1	Quartz	97	4
VA	US-29, 510100	SPS-1	Bending plate	--	2
WI	SH-29, 550100	SPS-1	Bending plate	--	1

[a]Data were collected at all sites from January 2014 through December 2014; value indicates the number of days missing from the full-year data set.

Consistent with SHRP 2 Project R19B (Kulicki et al. 2015), the same filters the R19B project used were applied to this data set in an attempt to eliminate questionable records (i.e., unrealistic geometry or erroneous data) and apparent permit vehicles or illegally loaded vehicles. Many of these filters were based on NCHRP 12-76 (Sivakumar et al. 2011). Accordingly, the following filtering criteria were used:

- Records were eliminated when axle weight were less than 2 kips or greater than 70 kips (based on NCHRP 12-76);
- Records were eliminated when first axle spacing was less than 5 feet (based on NCHRP 12-76);
- Records were eliminated when any axle spacing was less than 3.4 feet (based on NCHRP

12-76);

- Records were eliminated when the gross vehicle weight (GVW) varies from the sum of the axle weights by more than 10 percent (based on NCHRP 12-76);
- Records were eliminated when the length of the truck varies from the sum of the spacing between axles by more than 1 foot (based on NCHRP 12-76);
- Records were eliminated when the steering axle is less than 6 kips (based on NCHRP 12-76);
- Records were eliminated when the sum of the axle spacing lengths is less than 7 feet (based on Pelphrey et al. (2008));
- Records were eliminated when the vehicle speed was less than 10 mph or greater than 100 mph (based on NCHRP 12-76);
- Records were eliminated when the GVW was greater than 50 kips with total number of axles less than three;
- Records were eliminated when the steering axle weights were more than 35 kips; and
- Records were eliminated when the individual axle weights were more than 45 kips.

After the above filtering was applied, the records still contained lightweight vehicle records (i.e., GVWs less than 20 kips). These entries are traditionally eliminated in fatigue studies for primary longitudinal members, since previous research has indicated that light vehicles have negligible effects on the accumulated fatigue damage in a member or detail (Connor and Fisher 2006). In order to study the effects of including these light vehicles on cross-frame members, these records (prior to eliminating light vehicles) were set aside for the sensitivity studies discussed in Section 4.4. To be consistent with previous studies, the lightweight traffic records were then removed to form a second set of records. Throughout this dissertation, the filtered records with the light vehicles retained are designated Class AV records ("**A**ll **V**ehicles"), and the filtered records with the light vehicles removed are designated Class T records ("**T**rucks"). Class T records included the following filtering criteria:

- Records were eliminated when the assigned FHWA vehicle classification was less than Class 3 or greater than Class 14 (i.e., to filter out passenger cars, motorcycles, etc.);
- Records were eliminated when the GVW was less than 20 kips.

Table 4-2 provides a summary of WIM records prior to filtering, as well as total number of vehicle records and average daily traffic counts for each SPS site for both Class AV and Class

T records. After all appropriate filters were applied, the Class AV records used for the fatigue study contained over 44 million vehicle measurements, and the Class T records contained over 11 million truck measurements. Figure 4-5 shows the cumulative distribution functions (CDFs) of GVWs captured by the WIM sensors for all SPS sites for Class AV records, and Figure 4-6 shows the CDFs of GVWs for Class T records for MN US-2 and AR I-30, respectively. The GVWs are shown as a normal probability plot, in which the horizontal axis is GVW (in kips), and the vertical axis is the standard normal variable (i.e., axis values are "Z-values" indicating the number of standard deviations the GVW value is from the mean). A normal probability plot can be used to determine how well the data represents a normal distribution; nonlinear data sets indicate departures from a normal distribution. As shown, the GVW populations for both classes of vehicles are clearly not normal. Figure 4-1 through Figure 4-4 provide sample PDFs of GVWs for the WIM sites for both Class AV and Class T records. Due to the domination of lightweight vehicles in the Class AV records (passenger vehicle traffic obviously makes up a large percentage of total ADT), the PDFs for Class AV records are shown with a lognormal vertical axis; for many sites, it appears that the GVW distributions are multi-modal. After the lightweight vehicles are filtered, many of the distributions appear bi-modal (see Minnesota US-2 data in Figure 4-1 and Figure 4-2). In Chapter 5, the effects of this bi-modal distribution on the parameters used to calculate the Fatigue I and II limit states are further explored.

As noted in the SHRP 2 R19B study, the irregularity of the CDFs representing modern truck traffic is a result of different types of vehicles within the WIM traffic streams (e.g., variety of vehicle lengths, payload, etc.). The shape of the Class T CDFs appears to be generally consistent with the CDFs of WIM data used in the SHRP 2 R19B project (recreated with the same filters described above and shown in Figure 4-7).

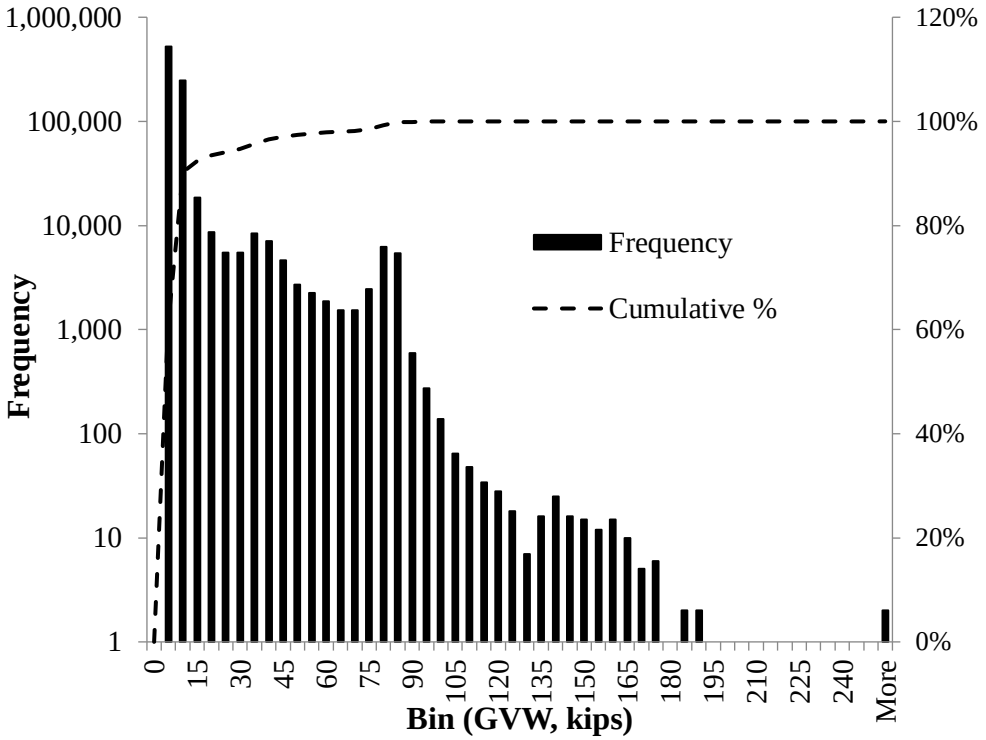

Figure 4-1: PDF of MN US-2 Class AV records.

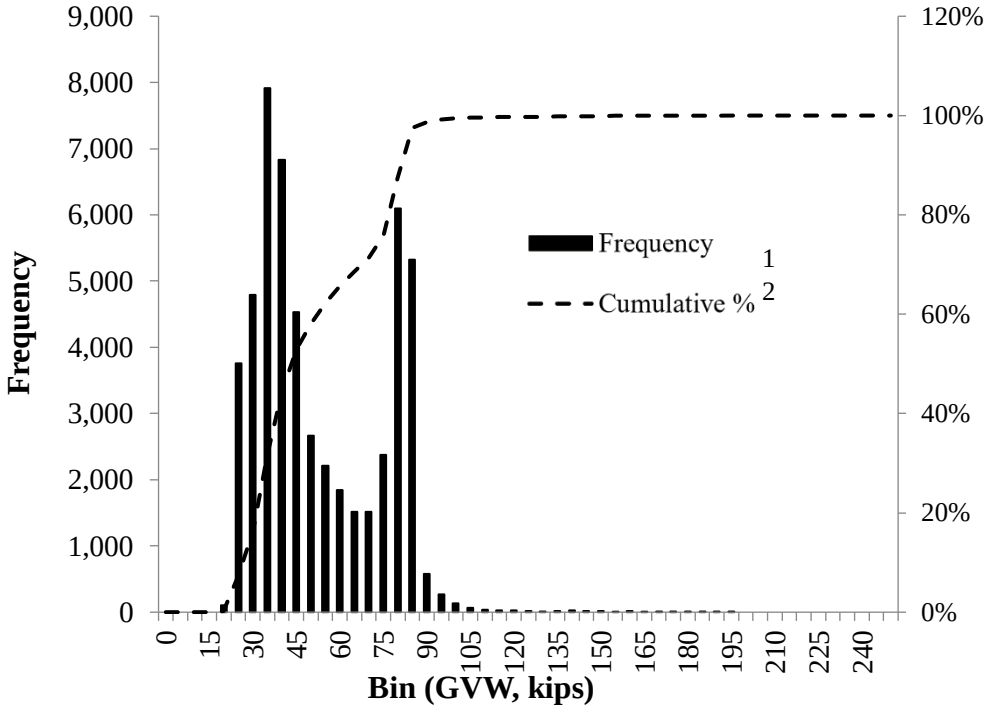

Figure 4-2: PDF of MN US-2 Class T records.

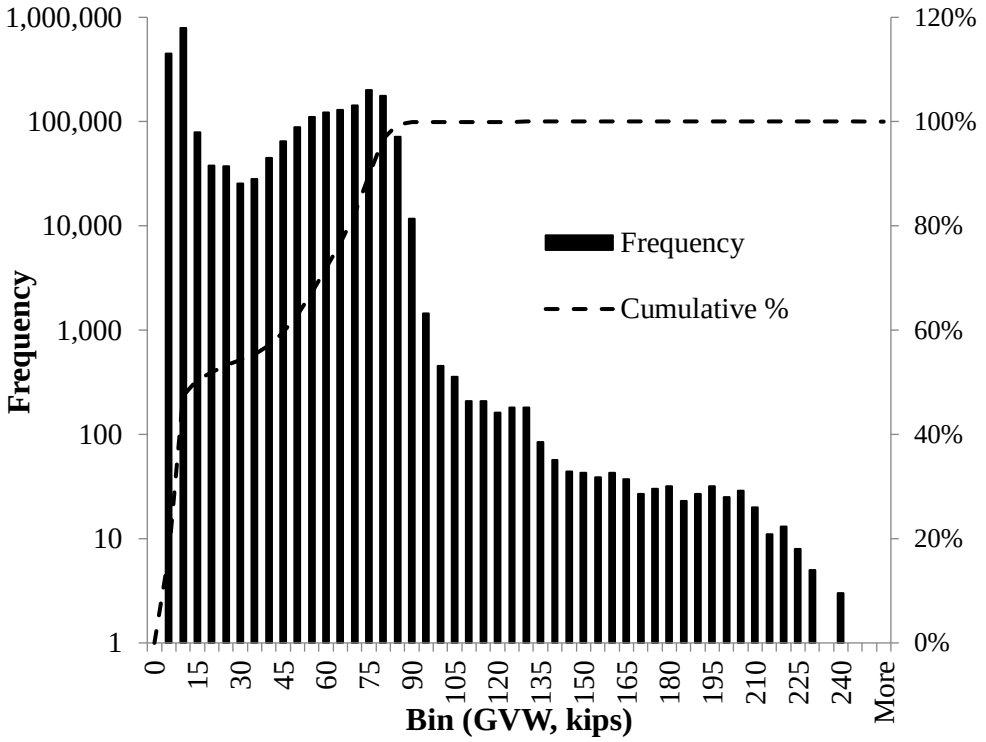

Figure 4-3: PDF of AR I-30 Class AV records.

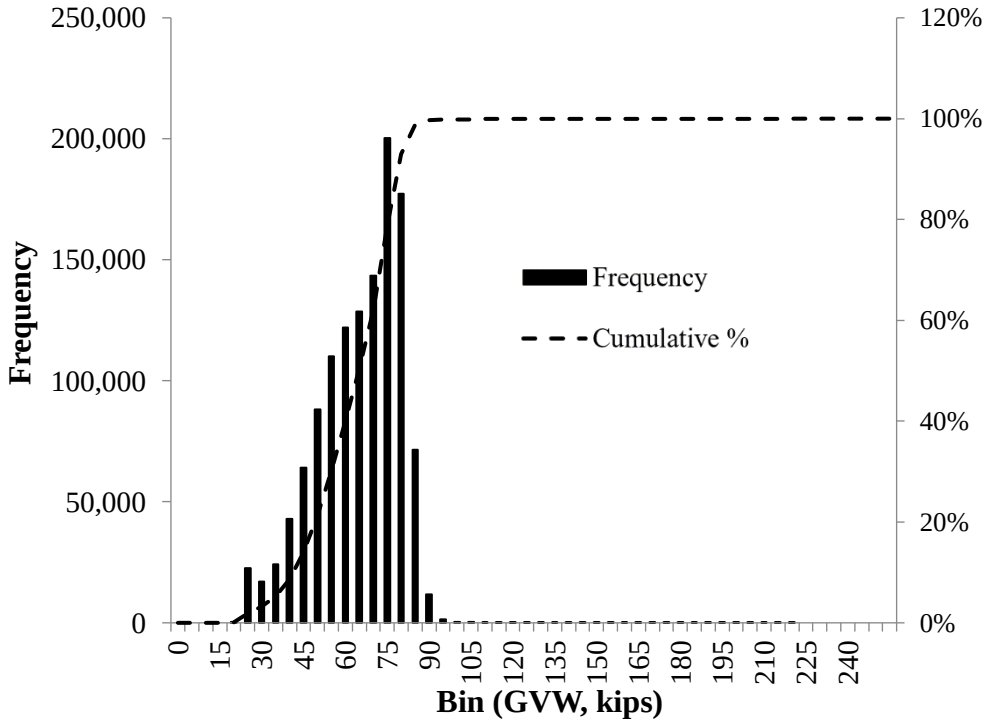

Figure 4-4: PDF of AR I-30 Class T records.

Table 4-2: Number of records in WIM data.

State	Initial Number of Records (Before Filtering)	Class AV Records		Class T Records	
		Total Number of Records	Lane ADT	Total Number of Truck Records	Lane ADTT
AR	3,529,952	3,414,934	9,356	1,704,481	4,670
AZ	2,711,532	2,626,954	7,704	1,227,567	3,600
CA	4,873,640	4,779,602	13,167	1,380,075	3,802
CO	1,675,744	1,645,722	4,509	352,198	965
IL	2,807,183	2,707,469	7,584	798,935	2,238
IN (Lane 1)	1,886,428	1,865,543	5,111	370,241	1,014
IN (Lane 2)	500,621	471,291	1,302	21,340	59
IN (Lane 3)	1,843,395	1,802,053	4,937	360,458	988
IN (Lane 4)	548,382	524,003	1,460	20,158	56
KS	2,312,975	2,262,526	6,199	436,913	1,197
LA	1,734,519	1,722,311	4,719	76,547	210
MD	3,040,831	3,005,933	8,564	108,881	310
MN	864,803	857,522	2,349	52,757	145
NM1	1,018,250	1,005,887	2,786	147,077	407
NM2	1,675,090	1,609,947	4,485	892,295	2,486
PA	2,292,235	2,251,316	8,187	873,903	3,178
TN (Lane 1)	2,792,715	2,120,750	7,913	550,858	2,055
TN (Lane 2)	1,945,926	1,842,295	6,874	118,000	440
TN (Lane 3)	2,042,591	1,942,114	7,247	191,330	714
TN (Lane 4)	2,757,569	2,690,197	10,038	1,182,136	4,411
VA (Lane 1)	1,462,016	1,445,614	3,961	224,928	616
VA (Lane 2)	438,126	430,438	1,179	19,300	53
WI	1,468,798	1,358,660	5,435	120,079	480
Total	**46,223,321**	**44,383,081**		**11,230,457**	

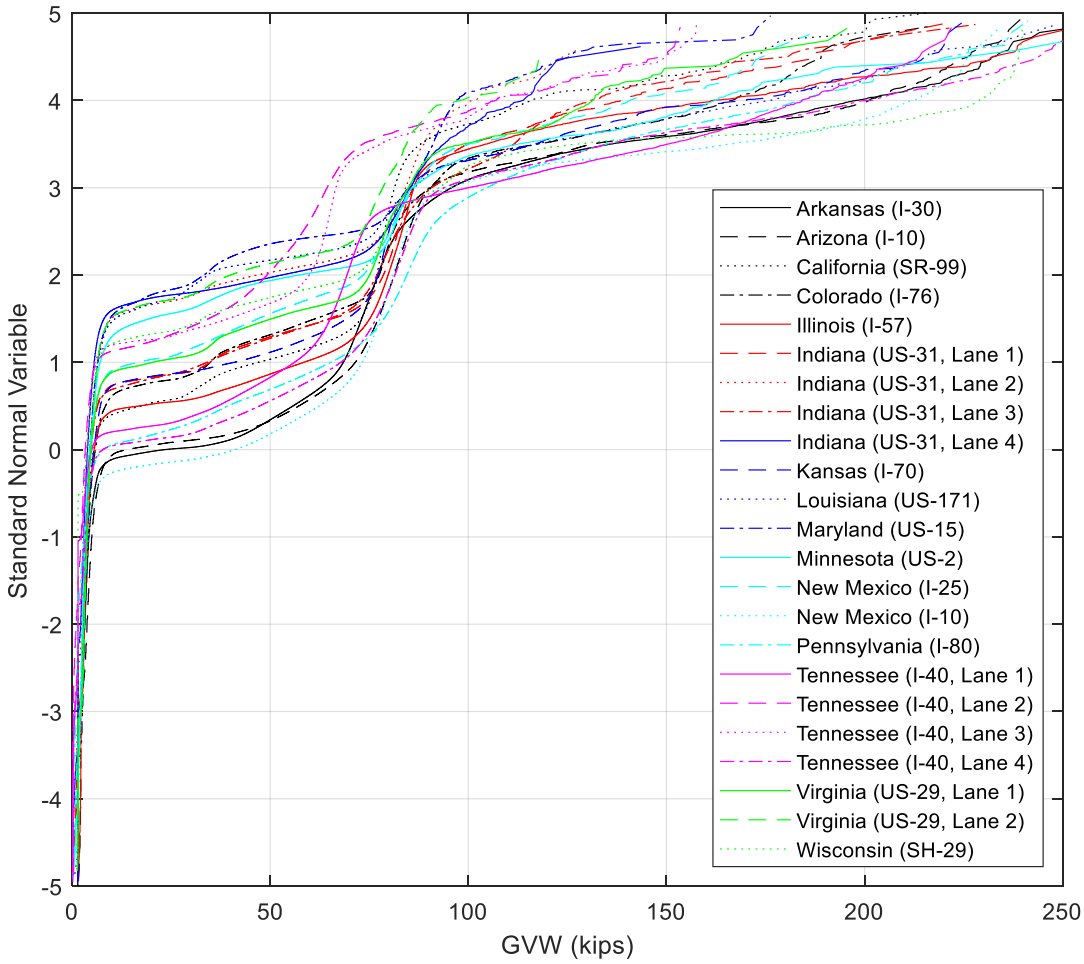

Figure 4-5: CDF of GVWs from FHWA 2014 Data (including light vehicles).

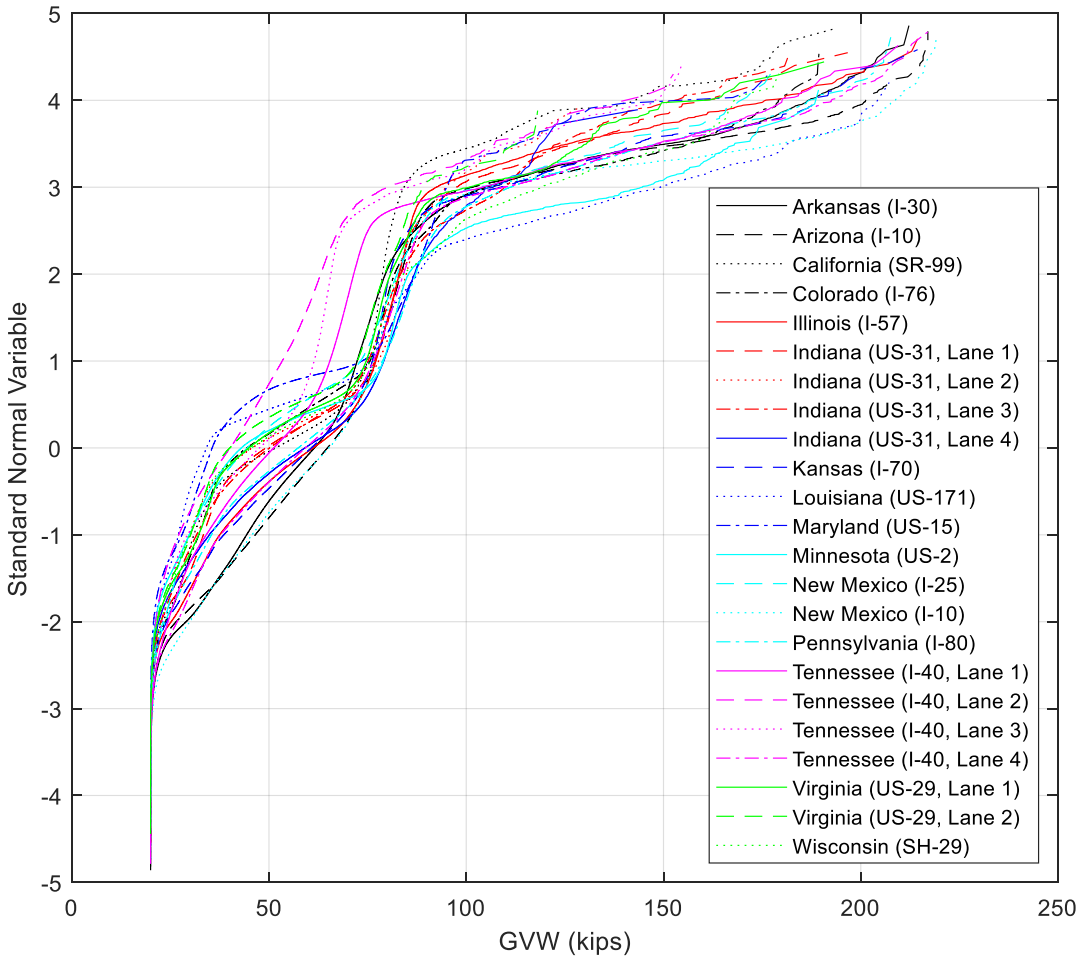

Figure 4-6: CDF of GVWs from FHWA 2014 Data (excluding light vehicles).

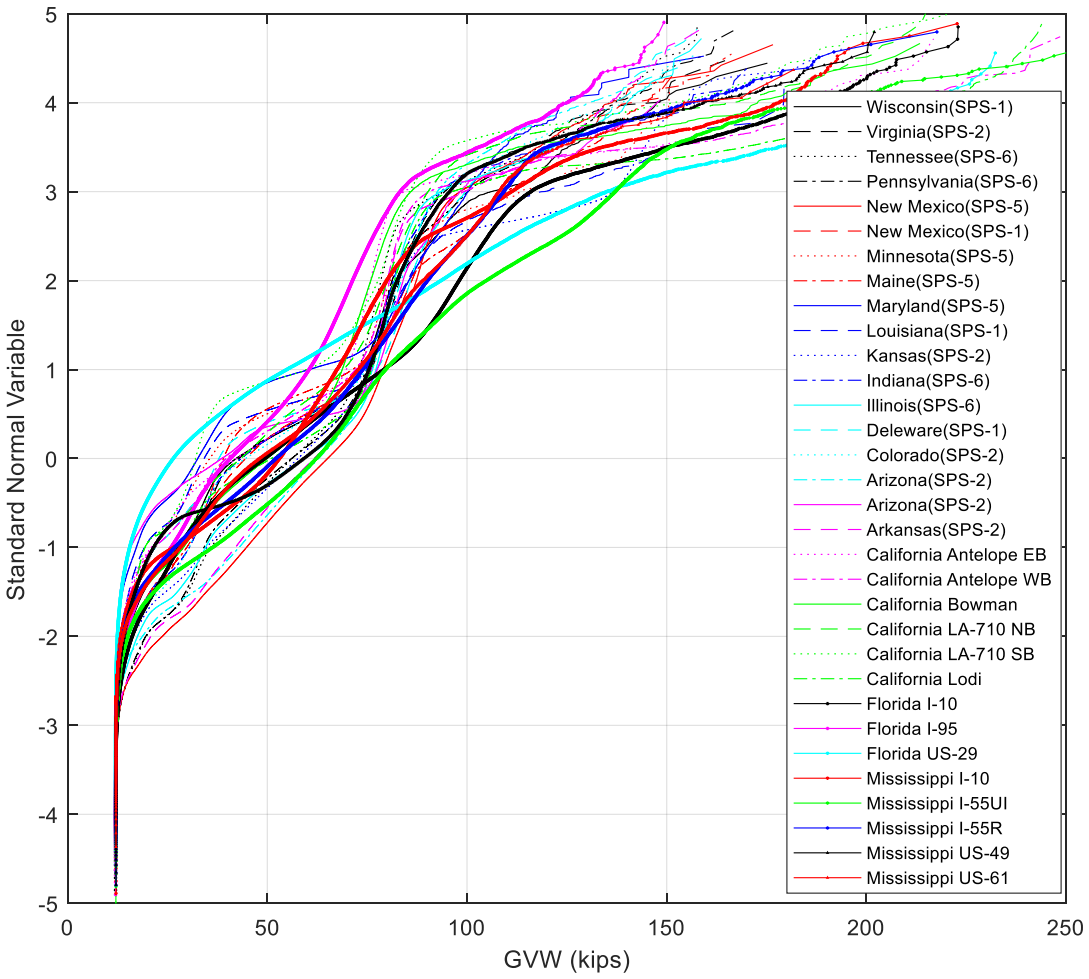

Figure 4-7: CDF of GVWs from SHRP 2 R19B WIM Data (excluding light vehicles).

4.3 WIM TRAFFIC STREAM SIMULATION

As previously discussed, the WIM data were filtered to eliminate questionable records (i.e., unrealistic geometry or erroneous data) and apparent permit vehicles or illegally loaded vehicles. Additionally, the data were separated into two families: Class AV records represent filtered data that includes all vehicles (including passenger vehicles), and Class T records represent filtered data that excludes light vehicles (i.e., GVWs less than 20 kips). Using MATLAB, a script was then created to read and format the two databases. Since the axle tracks (i.e., the distance between the centerline of two roadwheels on the same axle) are not recorded in the WIM records, all axle tracks were set to 6 feet and the weight of each axle is assumed to be evenly distributed between the driver and passenger side wheels. Automated scripts were then created to perform the following basic load configuration routines:

Load Configuration 1 - Single Traffic Stream: This routine steps a stream of user-defined WIM traffic along a user-defined bridge deck's influence surface at 1-foot longitudinal intervals in any user-defined transverse position (also 1-foot intervals). This script uses a cluster analysis, which means the analysis includes the effects of groups of vehicles in the same traffic stream, provided any of a following vehicle's tires are on the bridge during the time window that a vehicle in the cluster ahead of the following vehicle is still on the bridge. Time windows are calculated based on the respective vehicle speeds.

Load Configuration 2 - Two Traffic Streams: Similar to Load Configuration 1, a user-defined WIM traffic stream is stepped along a user-defined bridge deck in a user-defined transverse position. The script uses a cluster analysis to include the effects of groups of vehicles in any adjacent user-defined transverse position, provided any of a following vehicle's tires are on the bridge during the time window that a leading vehicle is still on the bridge. An individual load event can include numerous vehicles in the drive lane and passing lane, provided any vehicles' tires in the cluster are still on the bridge while another vehicle's tires in the cluster are still on the bridge. As per Load Configuration 1, time windows are calculated based on the respective vehicle speeds.

Load Configuration 3 - Realistic "Meandering" Traffic Stream: This routine steps a stream of user-defined WIM traffic along a user-defined bridge deck's influence surface at 1-foot longitudinal intervals in any user-defined 12-foot wide lane position. The routine randomly selects a transverse position (within the 12-foot wide lane) for each vehicle record based on a user-defined distribution, such that effects of lane meandering are recognized. Since cross-frames are highly sensitive to transverse position (Reichenbach 2020), the slight variation in vehicle location in a lane is a feature that will be studied. This script uses a cluster analysis to include the effects of groups of vehicles, provided any of a following vehicle's tires are on the bridge during the time window that a vehicle in the cluster ahead of the following vehicle is still on the bridge. Time windows are calculated based on the respective vehicle speeds.

In order to apply any WIM traffic stream in any of the load configurations described above, the influence surface output by Abaqus needs to be re-meshed to represent the surface of the actual bridge deck. Recalling that the Abaqus output provides influence surfaces that are relatively

sparsely gridded, the scripts use the defined bridge geometries and bi-linear interpolation to re-mesh the influence surfaces to a 1-foot by 1-foot grid. The output of each of the load configuration routines above includes the following:

- A sample load event history (see Figure 4-8);
- The total number of stress cycles (using rainflow counting techniques);
- The average number of cycles per passage;
- The maximum stress and stress cycle recorded;
- The equivalent stress range using the Palmgren-Miner damage accumulation model (i.e., stress range corresponding to the Fatigue II limit state); and
- The lowest stress range from the top 99.99th percentile of all stress ranges (i.e., 1/10,000th exceedance criteria corresponding to the Fatigue I limit state).

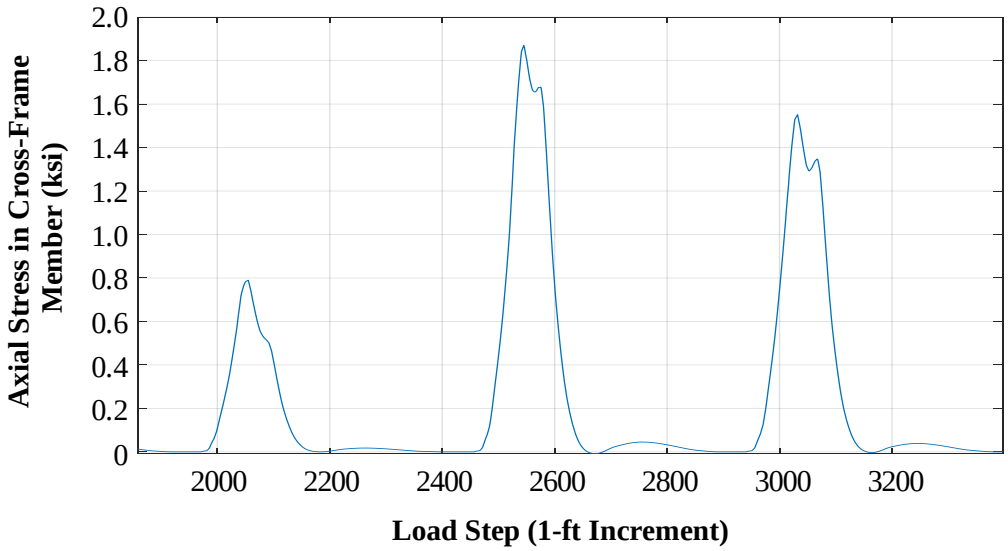

Figure 4-8: Sample load event history showing three vehicles back to back.

For calculating the total number of stress cycles, a rainflow counting script was created that is consistent with ASTM E1049-85 (ASTM 2017): "*Standard Practices for Cycle Counting in Fatigue Analysis*." This script includes counting half-cycles in addition to full cycles, which is consistent with previous research on load factor calibration (Kulicki et al. 2017). Following this method, rainflow counting is generally performed on complete data sets (i.e., no live counting). Keeping all stress cycle histories in a computer's memory is not feasible, as this would both decrease computation speed and be costly to maintain. A preliminary analysis was completed to perform cycle counting at various load increments (e.g., every 10th truck, every 100th truck, etc.)

in order to balance computational time and accuracy. This is because cycle counting at smaller load increments is computationally faster, but less accurate when compared to cycle counting a complete data set. Typical results from this analysis are shown in Figure 4-9. These analyses indicated that performing rainflow counting after every 30th load event consistently produced an accuracy higher than 99.5%; therefore, the scripts were designed to perform rainflow counting every 30th load event, store the cycle counts and magnitudes, and delete the load history prior to continuing.

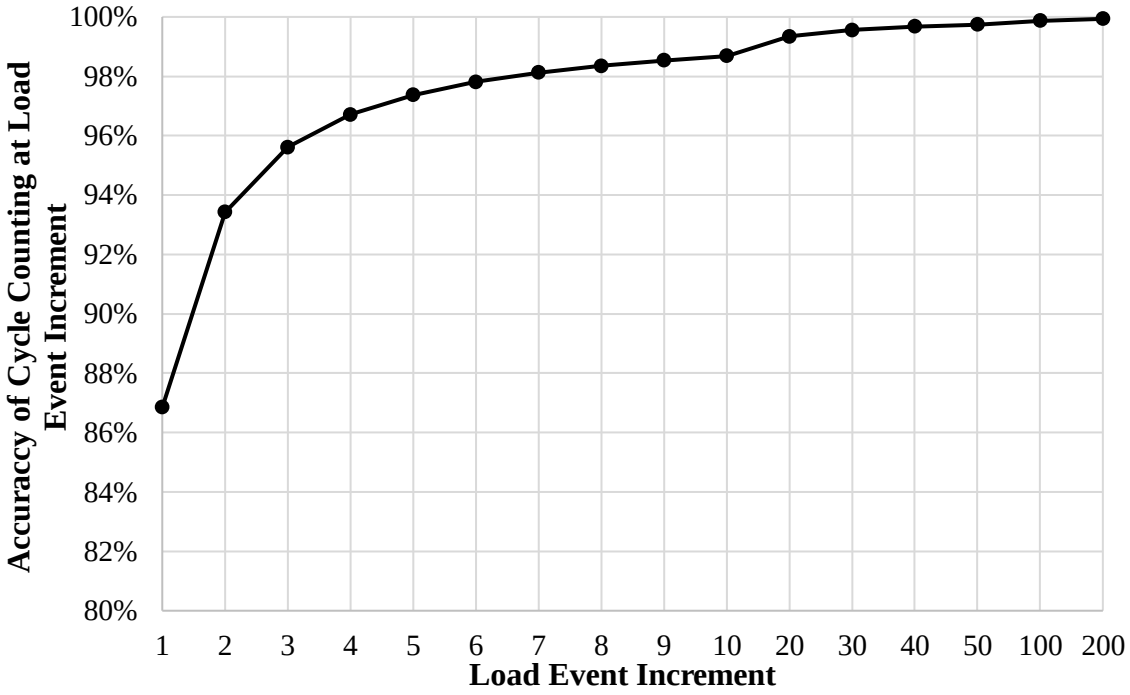

Figure 4-9: Typical results showing the accuracy of cycle counting at various load event increments when compared to cycle counting on the complete data set.

Past research has indicated that eliminating smaller stress cycles of a variable-amplitude loading source has negligible effect on the damage accumulated in a fatigue detail. Connor and Fisher (2006) showed that stress cycle magnitudes less than 25% of the constant amplitude fatigue limit (CAFL) generally have little impact on the long-term fatigue performance. For this reason, the results of each loading iteration (as listed above) were compiled for two different conditions: (i) including the effects of stress magnitudes less than 25% of the CAFL and (ii) filtering out those effects. For the purposes of this study, a detail category E' is assumed based on the results of McDonald and Frank (2009) and AASHTO Table 6.6.1.2.3-1. The corresponding CAFL value for this detail is 2.6 ksi; thus, all stress cycles less than 0.65 ksi are truncated when the filter is applied.

Each of the routines discussed in the previous section marches a defined traffic stream in a specific load configuration over a defined influence surface for one cross frame member in one bridge. Based on preliminary results applying the AASHTO fatigue truck to the 4,104 bridge models discussed in Chapter 3, 16 to 20 cross-frames were selected for each bridge that are assumed to include the governing, critical cross-frame for the design of that particular bridge. Using this subset of 20 models, this results in more than 320 influence surfaces for consideration.

For each influence surface, the script can position wheel loads on any defined 1-foot wide transverse lane position for a particular traffic stream. Since bridge widths of the 20 models range from 30 to 45 feet, this results in 25 to 41 possible transverse positions for selection (incorporating a 6-foot wide vehicle track), resulting in approximately 8,000 to 13,000 iterations for unique transverse load positions. Considering the computational time for each iteration varies from several minutes to multiple hours (depending on the total number of vehicle entries and bridge length), and this doesn't consider other variables such as adjacent lanes containing vehicles or the inclusion of passenger vehicles, etc., the number of potential iterations becomes unmanageable. For this reason, the sensitivity studies discussed in the next section were completed using a single site chosen to be representative of all WIM sites.

4.4 SENSITIVITY STUDIES

The objective of the sensitivity studies was to understand the effects of various variables to the overall force effects calculated for critical cross-frames. A single WIM site, Indiana US-31, was chosen to be representative of all WIM sites for the sensitivity studies, since this site has two-lane data available, and the distribution of GVWs appears to be generally representative of the remaining WIM sites, as shown in Figure 4-10. Figure 4-11 shows the mean GVW of all WIM sites (after filtering) and supports the use of the Indiana site for these initial studies.

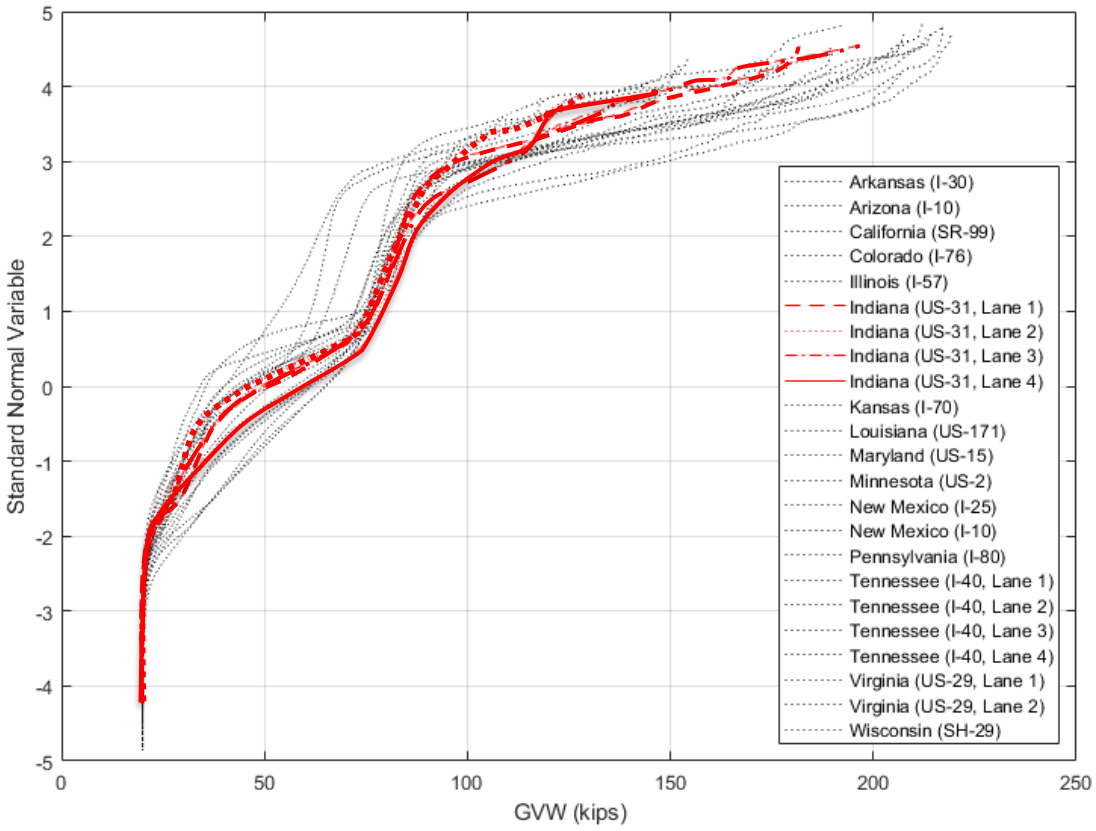

Figure 4-10: CDF of FHWA 2014 WIM Records. Indiana sites highlighted by red dashed lines.

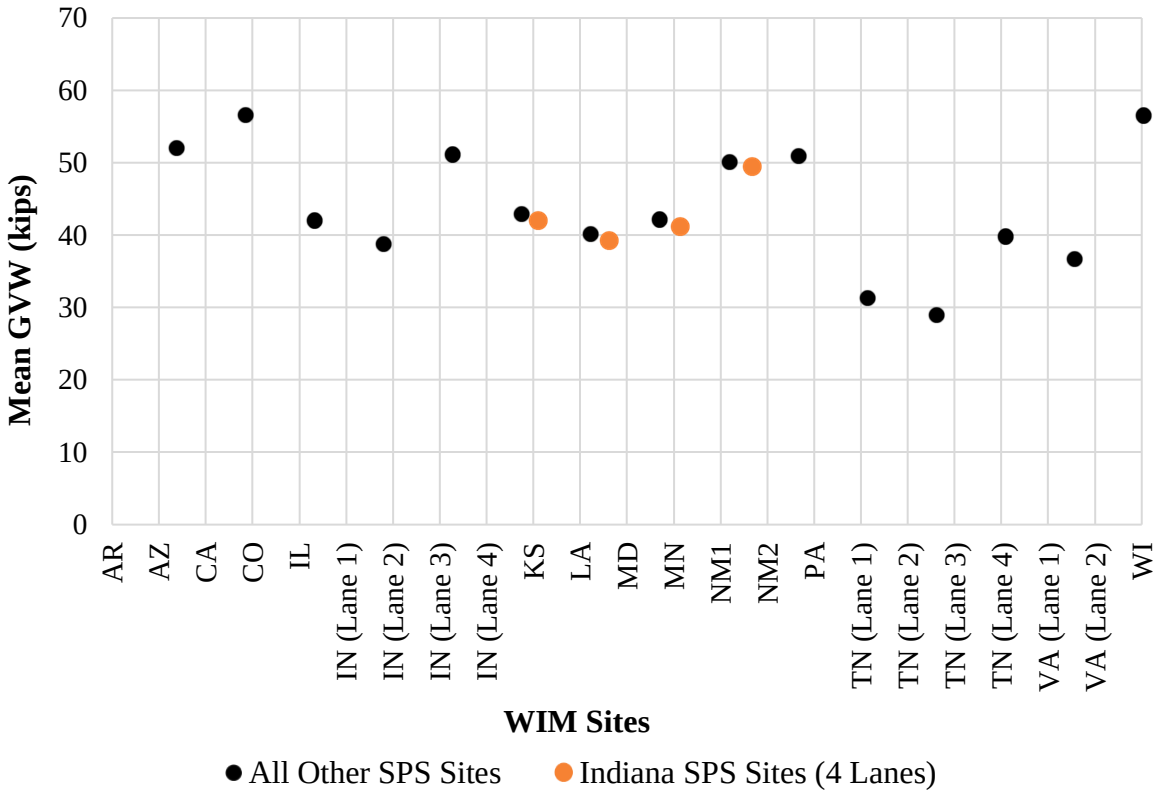

Figure 4-11: Mean GVW of WIM sites (after filtering).

The following subsections present four sensitivity studies conducted using the Indiana site. The first study places the Indiana WIM traffic stream (using Class T records) in what is estimated to be the worst-case lane position to maximize force effects in a cross-frame. Note, however, that the worst lane position may not necessarily be a realistic lane given the bridge width (i.e., the right tire of a truck may be at the bridge deck's edge where a traffic barrier would be placed). Using an example influence surface, the most critical lane position to maximize tension in a cross-frame diagonal is shown to be when the truck is positioned as close to the deck edge as possible. This is illustrated in Figure 4-12.

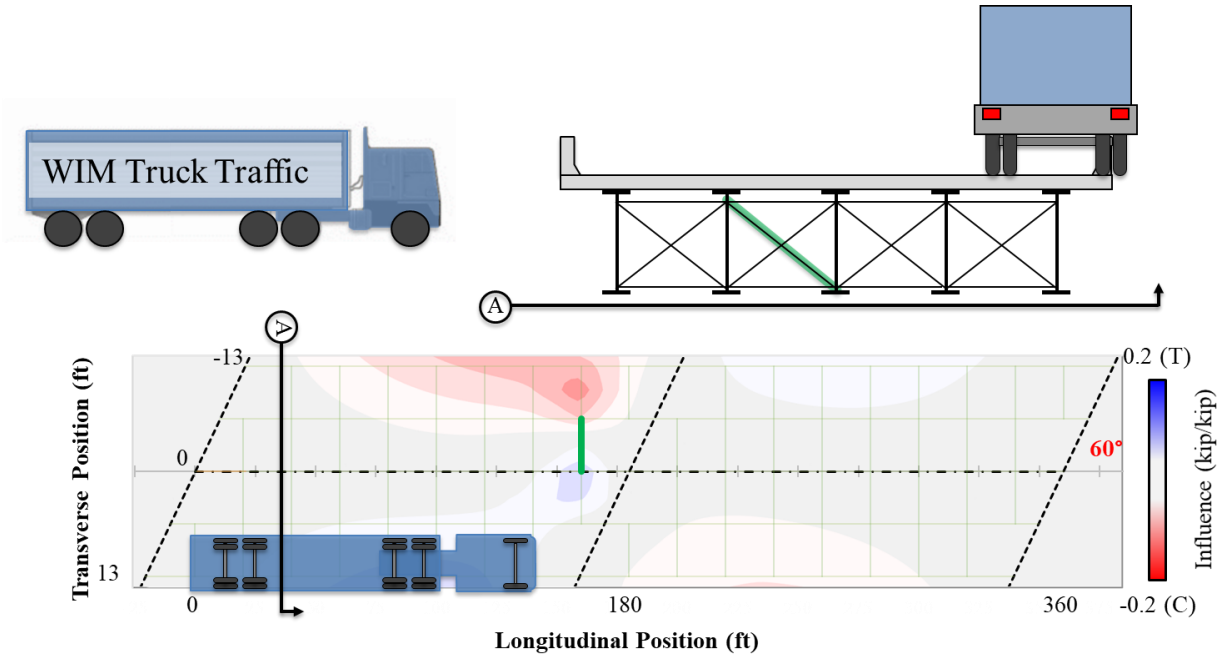

Figure 4-12: Illustration of worst-case truck position to maximize cross-frame force effects.

The second study places the Indiana WIM traffic stream (using Class T records) in what is considered a realistic lane position, based on the actual bridge width and recommendations from AASHTO Section 3.6.1.1.1. Since the largest governing tensile stress ranges in cross-frames are typically experienced when a vehicle is located on the overhang (note the tensile portion of the influence surface is largest at the edge of the deck), locating the vehicles in realistic lanes tends to produce much smaller stress ranges. This is illustrated in Figure 4-13 using the same influence surface as the first sensitivity study, where the truck positioned in the realistic lane does not produce the largest tensile stress range for the selected cross-frame.

The third study places the Indiana WIM traffic stream (using Class T records) in the same realistic lane position as the second study, but also includes passing lane traffic. Passing lane traffic is taken directly from the WIM site's instrumented passing lane using that lane's Class T records.

Finally, the fourth study places the Indiana WIM traffic stream (using Class AV records) in the "realistic" lane position and includes passing lane traffic. Passing lane traffic is taken directly from the WIM site's instrumented passing lane using that lane's Class AV records.

For the actual location of each 6-foot vehicle track width within the realistic lane, a distribution was created where 55 percent of the time the vehicle is located in the center of the lane; 30 percent of the time the vehicle is located plus or minus 1 foot of the center of the lane; 10

percent of the time the vehicle is located plus or minus 2 feet of the center of the lane; and 5 percent of the time the vehicle is located on the edges (boundaries) of the lane. This is illustrated in Figure 4-14. No data is available of the actual transverse distribution of vehicle locations within a lane. Consequently, the distribution was chosen somewhat arbitrarily, based on judgement.

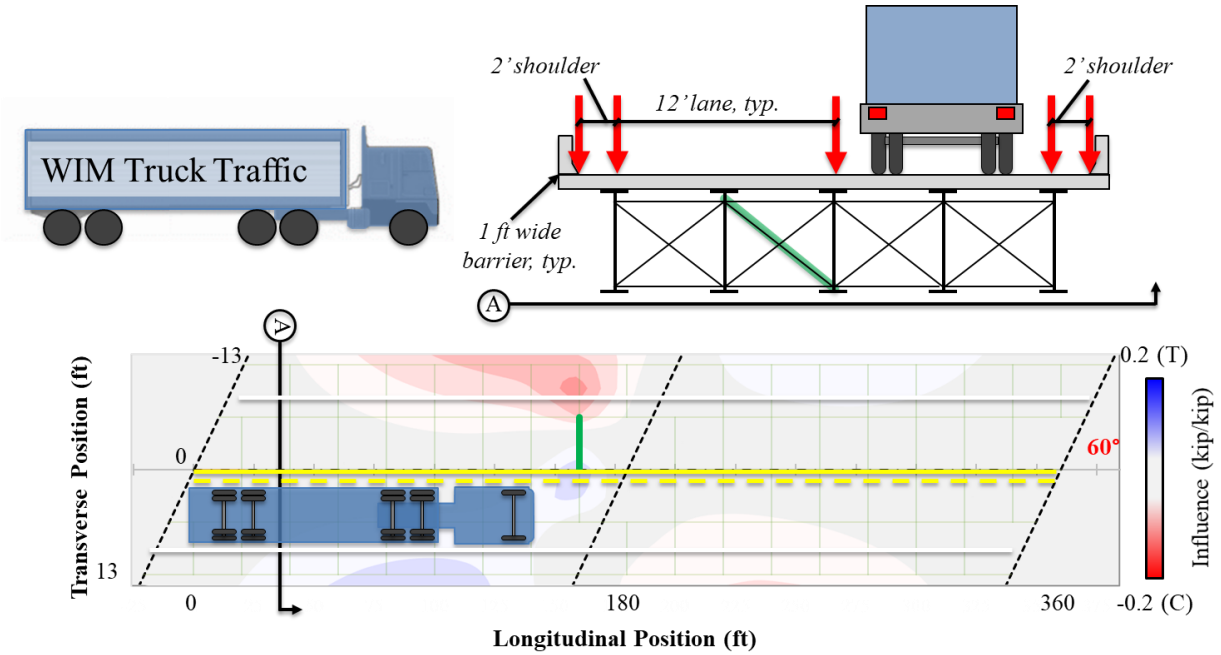

Figure 4-13: Illustration of realistic truck position in drive lane.

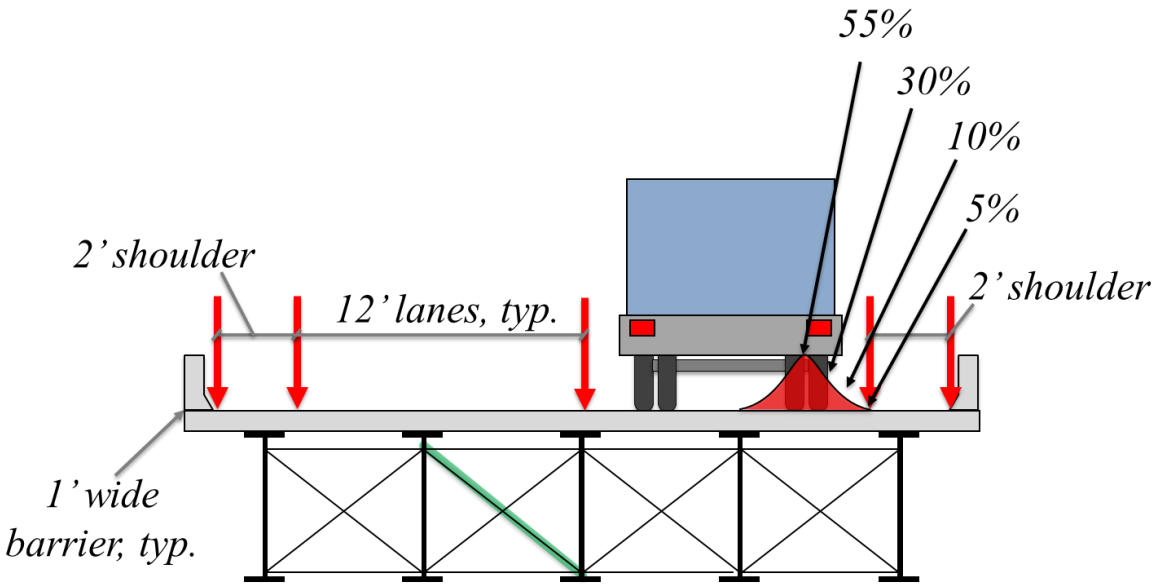

Figure 4-14: Illustration showing distribution of vehicle transverse location within 12-foot design lane for a 30-foot wide bridge.

To estimate real world force effects on cross-frame members, the filtered WIM traffic streams specific to each of the four sensitivity studies were applied to a subset of the filtered analytical testing matrix discussed in Chapter 3. As discussed in Chapter 3, the parametric studies identified 4,104 unique bridge geometries (i.e., the filtered analytical testing matrix) that included various girder and cross-frame layouts, girder cross-sections, and cross-frame details. This 4,104-model data set is intended to represent a wide variety of steel I-girder bridges currently in service in the US. Due to the significant computation effort involved in these sensitivity studies, approximately 20 models were selected from the 4,104 model data set. While the models were somewhat arbitrarily selected, models were chosen that would likely represent extreme cross-frame force effects based on preliminary studies applying the AASHTO fatigue design truck to the entire 4,104-model data set.

4.4.1 Sensitivity Study 1: Indiana Drive Lane Truck Traffic Positioned to Maximize Force Effects

This simulation utilized the Class T records. A worst-case lane position to maximize force effects in a cross-frame is determined by stepping the WIM stream over every available transverse lane per the Load Configuration 1 discussed above (Single Traffic Stream). This simulation is computationally very time consuming, since the bridge widths of the 20 models range from 30 to 45 feet, which results in 25 to 41 possible transverse positions (incorporating a 6-foot wide vehicle track) that would need to be performed for each of the 16 to 20 cross-frames per bridge. In order to optimize the simulation approach, the AASHTO fatigue truck was used as a predictor for critical transverse lane positions that maximize force effects in each cross-frame. This was done by placing the fatigue truck in each available transverse lane (a computation that takes seconds to run per bridge), and ranking the transverse positions corresponding to the largest force effects for each of the 16 to 20 cross frames. The ranked force effects were filtered to ensure the largest stress ranges included a tensile component that is necessary for crack growth (Fisher et al. 1998). For a few cross-frames in a few bridges, the WIM traffic stream was marched over every possible lane position, and rankings from this analysis were compared to the rankings produced from the fatigue truck. The top five transverse positions produced by both iterations were almost always in agreement, with an occasional re-ordering of the top five. Since actual WIM traffic records have variable axle spacings that may or may not produce the same transverse lane position rankings, the

top seven transverse lane positions ranked by the fatigue truck were used for the WIM traffic stream positioning.

For each of the top seven transverse locations of the WIM traffic stream, the values for calculating the Fatigue I and II stress ranges were collected. The pertinent values for calculating the Fatigue I and II parameters are introduced in Section 2.4.2.3, and the process used to collect this information from the automated scripts is provided in greater detail in Section 5.2. Table 4-3 and Table 4-4 summarize the pertinent values associated with the maximum Fatigue I and II parameters, respectively (i.e., 99.99th percentile stress range for Fatigue I, and equivalent stress range and fatigue damage ratio for Fatigue II).

All results were normalized to the maximum stress range in any cross-frame produced by applying the unfactored AASHTO design load (i.e., the fatigue truck) to the same bridge in all possible transverse positions within the clear distance of the barriers. For the fatigue truck loading, the refined design truck footprint was utilized as discussed in AASHTO Section 3.6.1.4.1.

Table 4-3: Pertinent values for calculating Fatigue I parameters for Sensitivity Study 1.

Bridge ID	Fatigue I: 99.99th Percentile Stress Range (ksi)		Fatigue I: 99.99th Percentile Stress Range (Normalized)	
	Before filtering	**After filtering**	**Before filtering**	**After filtering**
59-2	7.71	9.68	1.59	2.00
83-3	3.86	4.22	1.58	1.72
115-2	2.97	3.23	0.95	1.04
233-2	3.27	3.62	1.47	1.63
253-3	3.29	3.51	1.62	1.73
277-2	2.26	2.58	1.58	1.80
747-2	6.18	6.28	1.64	1.67
753-2	5.27	6.21	1.60	1.88
755-2	3.23	3.77	0.73	0.85
755-4	4.31	4.89	0.87	0.98
761-2	3.96	4.39	0.94	1.05
825-3	4.03	4.20	1.42	1.48
909-2	3.18	3.55	0.93	1.04
1179-2	5.79	6.49	1.34	1.50
1181-2	9.49	10.01	1.75	1.85
1181-4	10.37	11.47	1.50	1.65
1183-2	4.33	4.57	1.76	1.85
1187-2	2.36	2.86	0.99	1.20
1213-3	3.28	3.55	1.59	1.72
1249-2	2.26	2.59	1.55	1.78
		Mean	**1.37**	**1.52**
		Mean + 1.5 Standard Deviations	**1.87**	**2.06**

Table 4-4: Pertinent values for calculating Fatigue II parameters for Sensitivity Study 1.

Bridge ID	Maximum Number of Cycles		Fatigue II: Effective Stress Range (ksi)		Fatigue II: Effective Stress Range (Normalized)		Fatigue II: Fatigue Damage Ratio	
	Before filtering	After filtering	Before filtering	After filtering	Before filtering	After filtering	Before filtering	After filtering
59-2	1,337,527	380,352	2.19	4.10	0.45	0.85	0.69	0.86
83-3	881,406	361,525	1.44	1.89	0.59	0.77	0.79	0.77
115-2	813,511	357,047	1.13	1.45	0.36	0.46	0.47	0.46
233-2	1,154,292	279,117	1.07	1.66	0.48	0.75	0.71	0.68
253-3	759,916	365,441	1.28	1.60	0.63	0.79	0.80	0.78
277-2	1,289,040	307,805	0.79	1.21	0.55	0.85	0.84	0.80
747-2	456,965	370,241	2.48	2.64	0.66	0.70	0.71	0.70
753-2	2,032,332	370,241	1.61	2.70	0.49	0.82	0.86	0.82
755-2	2,093,983	369,820	0.99	1.73	0.22	0.39	0.40	0.39
755-4	1,599,013	272,238	1.31	2.22	0.26	0.45	0.43	0.40
761-2	1,023,708	370,229	1.45	1.96	0.35	0.47	0.48	0.47
825-3	549,715	370,170	1.69	1.90	0.60	0.67	0.68	0.67
909-2	956,720	362,603	1.17	1.56	0.34	0.46	0.47	0.45
1179-2	1,059,584	231,877	1.77	2.75	0.41	0.63	0.58	0.54
1181-2	741,267	376,118	3.68	4.47	0.68	0.83	0.86	0.83
1181-4	1,076,887	376,370	4.14	5.65	0.60	0.81	0.85	0.82
1183-2	742,628	372,410	1.68	2.05	0.68	0.83	0.86	0.83
1187-2	2,182,026	343,295	0.74	1.32	0.31	0.55	0.56	0.54
1213-3	809,575	366,458	1.27	1.61	0.62	0.78	0.80	0.78
1249-2	1,585,997	314,283	0.76	1.23	0.52	0.84	0.85	0.80
						Mean	**0.68**	**0.67**
						Mean + 1.5 Standard Deviations	**0.93**	**0.92**

4.4.2 Sensitivity Study 2: Indiana Drive Lane Truck Traffic Positioned in Realistic Drive Lanes

This simulation utilized the Class T records. As previously discussed, a realistic drive lane was determined based on the actual bridge width and recommendations from AASHTO Section 3.6.1.1.1. This simulation utilized the Load Configuration 3 (Realistic Meandering Traffic Stream)

with the custom distribution illustrated in Figure 4-14.

For each of the 16 to 20 cross-frames per bridge, the values for calculating the Fatigue I and II stress ranges were collected. Table 4-5 and Table 4-6 summarize the relevant values associated with the maximum Fatigue I and II parameters, respectively (i.e., 99.99th percentile stress range for Fatigue I, and equivalent stress range and fatigue damage ratio for Fatigue II). For many bridges, the realistic drive lane did not always produce stress ranges with a tensile component for all of the 16 to 20 cross-frames; therefore, the cross-frames with the largest Fatigue I and II parameters were filtered to ensure the governing cross-frame reported in the table included a tensile component due to passage of the vehicles.

All results were normalized to the maximum stress range in any cross-frame produced by applying the unfactored AASHTO design load (i.e., the fatigue truck) to the same bridge in all possible transverse positions within the clear distance of the barriers. For the fatigue truck loading, the refined design truck footprint was utilized as discussed in AASHTO Section 3.6.1.4.1.

4.4.3 Sensitivity Study 3: Indiana Drive Lane Truck Traffic Positioned in Realistic Drive Lanes and Including Passing Lane Truck Traffic

This simulation utilized the Class T records. Similar to Sensitivity Study 2, a realistic drive lane was determined based on the actual bridge width and recommendations from AASHTO Section 3.6.1.1.1. This simulation utilized the Load Configuration 3 (Realistic Meandering Traffic Stream) with the custom distribution illustrated in Figure 4-14, as well as Load Configuration 2 (Two Traffic Streams) in order to account for truck traffic in the passing lane.

For each of the 16 to 20 cross-frames per bridge, the values for calculating the Fatigue I and II stress ranges were collected. Table 4-7 and Table 4-8 summarize the relevant values associated with the maximum Fatigue I and II parameters, respectively (i.e., 99.99th percentile stress range for Fatigue I, and equivalent stress range and fatigue damage ratio for Fatigue II). For many bridges, the realistic drive lane and passing lanes did not always produce stress ranges with a tensile component for all of the 16 to 20 cross-frames; therefore, the cross-frames with the largest Fatigue I and II parameters were filtered to ensure the governing cross-frame reported in the table included a tensile component due to passage of the vehicles.

Table 4-5: Pertinent values for calculating Fatigue I parameters for Sensitivity Study 2.

Bridge ID	Fatigue I: 99.99th Percentile Stress Range (ksi)		Fatigue I: 99.99th Percentile Stress Range (Normalized)	
	Before filtering	**After filtering**	**Before filtering**	**After filtering**
59-2	4.71	5.30	0.97	1.10
83-3	2.88	3.06	1.18	1.25
115-2	3.04	3.25	0.98	1.05
233-2	2.99	3.61	1.35	1.63
253-3	2.29	2.63	1.13	1.29
277-2	1.74	2.01	1.21	1.41
747-2	4.59	5.18	1.22	1.38
753-2	3.72	4.34	1.13	1.32
755-2	5.06	5.90	1.14	1.33
755-4	5.76	6.41	1.16	1.29
761-2	5.14	5.85	1.22	1.39
825-3	2.95	3.12	1.04	1.10
909-2	3.25	3.61	0.95	1.06
1179-2	5.21	5.24	1.20	1.21
1181-2	5.67	6.49	1.05	1.20
1181-4	7.44	8.51	1.07	1.23
1183-2	2.86	3.37	1.16	1.37
1187-2	2.96	3.45	1.24	1.45
1213-3	2.35	2.70	1.14	1.31
1249-2	1.77	2.13	1.21	1.46
		Mean	**1.14**	**1.29**
		Mean + 1.5 Standard Deviations	**1.29**	**1.51**

Table 4-6: Pertinent values for calculating Fatigue II parameters for Sensitivity Study 2.

Bridge ID	Maximum Number of Cycles		Fatigue II: Effective Stress Range (ksi)		Fatigue II: Effective Stress Range (Normalized)		Fatigue II: Fatigue Damage Ratio	
	Before filtering	After filtering	Before filtering	After filtering	Before filtering	After filtering	Before filtering	After filtering
59-2	1,244,510	370,237	1.54	2.23	0.32	0.46	0.48	0.46
83-3	701,292	328,236	1.08	1.35	0.44	0.55	0.54	0.53
115-2	810,697	354,964	1.14	1.47	0.37	0.47	0.48	0.47
233-2	974,544	63,845	0.60	1.38	0.27	0.62	0.37	0.00
253-3	945,473	252,126	0.80	1.17	0.39	0.58	0.53	0.51
277-2	1,466,016	136,464	0.46	0.95	0.32	0.67	0.51	0.48
747-2	456,965	367,789	1.53	2.12	0.41	0.56	0.44	0.56
753-2	2,456,531	341,382	0.91	1.66	0.28	0.50	0.52	0.49
755-2	2,269,889	369,471	1.37	2.39	0.31	0.54	0.57	0.54
755-4	1,494,166	369,753	1.73	2.64	0.35	0.53	0.55	0.53
761-2	1,309,166	370,319	1.63	2.39	0.39	0.57	0.59	0.57
825-3	689,219	341,106	1.15	1.41	0.40	0.50	0.50	0.48
909-2	986,329	363,042	1.17	1.58	0.34	0.46	0.47	0.46
1179-2	414,433	373,659	2.25	2.32	0.52	0.54	0.54	0.54
1181-2	1,491,218	375,635	1.91	2.88	0.35	0.53	0.56	0.53
1181-4	1,452,974	376,241	2.50	3.74	0.36	0.54	0.57	0.54
1183-2	1,862,665	320,768	0.78	1.32	0.31	0.53	0.54	0.51
1187-2	1,298,571	326,219	0.94	1.42	0.39	0.60	0.60	0.57
1213-3	1,062,583	293,424	0.68	1.23	0.33	0.60	0.47	0.55
1249-2	1,268,964	137,178	0.50	0.96	0.34	0.66	0.52	0.47
						Mean	**0.52**	**0.49**
						Mean + 1.5 Standard Deviations	**0.60**	**0.67**

All results were normalized to the maximum stress range in any cross-frame produced by applying the unfactored AASHTO design load (i.e., the fatigue truck) to the same bridge in all possible transverse positions within the clear distance of the barriers. For the fatigue truck loading, the refined design truck footprint was utilized as discussed in AASHTO Section 3.6.1.4.1.

Table 4-7: Pertinent values for calculating Fatigue I parameters for Sensitivity Study 3.

Bridge ID	Fatigue I: 99.99th Percentile Stress Range (ksi)		Fatigue I: 99.99th Percentile Stress Range (Normalized)	
	Before filtering	**After filtering**	**Before filtering**	**After filtering**
59-2	4.15	5.24	0.86	1.08
83-3	3.49	3.76	1.43	1.54
115-2	3.15	3.48	1.01	1.12
233-2	2.97	4.01	1.34	1.81
253-3	2.75	2.92	1.35	1.44
277-2	1.77	2.06	1.24	1.44
747-2	4.74	5.20	1.26	1.39
753-2	3.79	4.23	1.15	1.28
755-2	5.10	5.88	1.15	1.33
755-4	5.78	6.41	1.16	1.29
761-2	5.12	5.76	1.22	1.37
825-3	3.61	3.76	1.27	1.33
909-2	3.33	3.67	0.97	1.07
1179-2	5.17	5.27	1.19	1.22
1181-2	4.71	6.36	0.87	1.17
1181-4	7.43	8.44	1.07	1.22
1183-2	3.22	3.59	1.31	1.45
1187-2	2.91	3.34	1.22	1.40
1213-3	2.65	3.23	1.29	1.57
1249-2	1.78	2.05	1.22	1.41
		Mean	**1.18**	**1.35**
		Mean + 1.5 Standard Deviations	**1.41**	**1.62**

Table 4-8: Pertinent values for calculating Fatigue II parameters for Sensitivity Study 3.

Bridge ID	Maximum Number of Cycles		Fatigue II: Effective Stress Range (ksi)		Fatigue II: Effective Stress Range (Normalized)		Fatigue II: Fatigue Damage Ratio	
	Before filtering	After filtering	Before filtering	After filtering	Before filtering	After filtering	Before filtering	After filtering
59-2	2,289,386	190,625	0.94	1.95	0.19	0.40	0.36	0.32
83-3	97,975	27,359	0.81	1.17	0.33	0.48	0.21	0.20
115-2	817,731	349,976	1.13	1.47	0.36	0.47	0.48	0.46
233-2	2,093,549	32,337	0.35	1.31	0.16	0.59	0.28	0.26
253-3	951,653	253,734	0.80	1.19	0.39	0.58	0.54	0.51
277-2	1,477,929	137,434	0.46	0.96	0.32	0.67	0.51	0.48
747-2	1,098,110	368,723	1.53	2.12	0.41	0.56	0.58	0.56
753-2	2,483,967	341,307	0.91	1.67	0.28	0.51	0.52	0.49
755-2	2,300,314	369,540	1.37	2.39	0.31	0.54	0.57	0.54
755-4	1,519,403	369,822	1.72	2.64	0.35	0.53	0.55	0.53
761-2	1,363,663	370,386	1.61	2.39	0.38	0.57	0.59	0.57
825-3	695,990	344,778	1.16	1.43	0.41	0.50	0.51	0.49
909-2	991,300	364,183	1.18	1.59	0.34	0.46	0.48	0.46
1179-2	432,038	376,238	2.23	2.32	0.52	0.54	0.54	0.54
1181-2	1,505,876	378,115	1.11	2.67	0.20	0.49	0.33	0.50
1181-4	1,463,921	379,529	2.50	3.73	0.36	0.54	0.57	0.54
1183-2	1,873,448	320,345	0.82	1.40	0.33	0.57	0.57	0.54
1187-2	1,342,276	326,113	0.93	1.42	0.39	0.60	0.60	0.57
1213-3	1,090,130	296,357	0.67	1.24	0.33	0.60	0.47	0.56
1249-2	1,300,444	137,627	0.50	0.96	0.34	0.66	0.52	0.47
						Mean	**0.49**	**0.48**
						Mean + 1.5 Standard Deviations	**0.65**	**0.63**

4.4.4 Sensitivity Study 4: All Indiana Drive Lane Traffic Positioned in Realistic Drive Lanes and Including All Passing Lane Traffic

This simulation utilized the Class AV records to study the effects of lightweight vehicles on the calculated fatigue parameters. Similar to Sensitivity Study 2, a realistic drive lane was determined based on the actual bridge width and recommendations from AASHTO Section

3.6.1.1.1. This simulation utilized the Load Configuration 3 (Realistic Meandering Traffic Stream) with the custom distribution illustrated in Figure 4-14, as well as Load Configuration 2 (Two Traffic Streams) in order to account for traffic in the passing lane.

For each of the 16 to 20 cross-frames per bridge, the values for calculating the Fatigue I and II stress ranges were collected. Table 4-9 and Table 4-10 summarize the relevant values associated with the maximum Fatigue I and II parameters, respectively (i.e., 99.99th percentile stress range for Fatigue I, and equivalent stress range and fatigue damage ratio for Fatigue II). For many bridges, the realistic drive lane and passing lanes did not always produce stress ranges with a tensile component for all of the 16 to 20 cross-frames; therefore, the cross-frames with the largest Fatigue I and II parameters were filtered to ensure the governing cross-frame reported in the table included a tensile component due to passage of the vehicles.

All results were normalized to the maximum stress range in any cross-frame produced by applying the unfactored AASHTO design load (i.e., the fatigue truck) to the same bridge in all possible transverse positions within the clear distance of the barriers. For the fatigue truck loading, the refined design truck footprint was utilized as discussed in AASHTO Section 3.6.1.4.1.

4.4.5 Cycles Per Passage Using Sensitivity Study 2

Current design provisions for the Fatigue II limit state require knowledge of the total cycles expected for a particular detail. The total number of cycles, N, for a 75-year design life is defined as:

$$N = (365)(75)n(ADTT)_{SL} \qquad \text{Eq. 4.16}$$

Where:

n = cycles per truck passage, calculated from AASHTO Table 6.6.1.2.5-2, and

$(ADTT)_{SL}$ = Annual Daily Truck Traffic for a single lane.

The cycles per passage for cross-frames is not explicitly listed in the current design provisions; rather, an entry for “transverse members” specifies 1 cycle per passage for member spacing greater than 20 feet, and 2 cycles per passage for member spacing less than or equal to 20 feet. Using the total number of cycles recorded for Sensitivity Study 2 both before and after truncating stresses below 25% CAFL, the average number of cycles per passage due to the WIM

truck records can be calculated by dividing the total number of cycles counted via rainflow techniques by the lane's ADTT and number of days recorded in the year (365 total days for Indiana traffic per Table 4-1). Figure 4-15 shows the results for Sensitivity Study 2 (Class T records in a realistic drive lane). The bins in this plot represent the "mean number of cycles per truck passage" for the given bridge, and the dashed lines represent the average of all mean cycles per passage. The values are represented for both before and after truncation of stresses below 25% CAFL.

Before filtering, the cycles per passage varies per bridge, has a mean of 3.3 cycles per passage, but ranges between just over 1 to nearly 7 cycles per passage. After filtering, the mean cycles per passage varies much less considerably across all bridges, with very few bridges indicating an average cycle per passage above unity. After filtering, the mean cycles per passage per bridge varies between 0.2 and 1.02, with an overall mean of 0.8. From this plot, it is evident that the effect of truncating stress ranges below 0.65 ksi (25% CAFL) significantly reduces the number of cycles counted; furthermore, since the average cycles per passage for the filtered case includes many values less than unity, it is clear that the majority of cycles caused by the WIM traffic are actually less than 0.65 ksi (i.e., it is physically impossible to have a truck passage with less than 1 cycle per passage). This is demonstrated in Figure 4-16, which shows a CDF of the stress ranges for Bridge ID 277-2; it can be seen that the percentage of stress ranges below 0.65 ksi is approximately 91% of the total stress ranges counted. Bridge ID 277-2 was demonstrated, since it is shown in Figure 4-15 to have an average cycles per passage much less than one. This trend will be studied more in Chapter 5, when a large number of WIM records (and thus ADTTs) will be simulated over the same bridges.

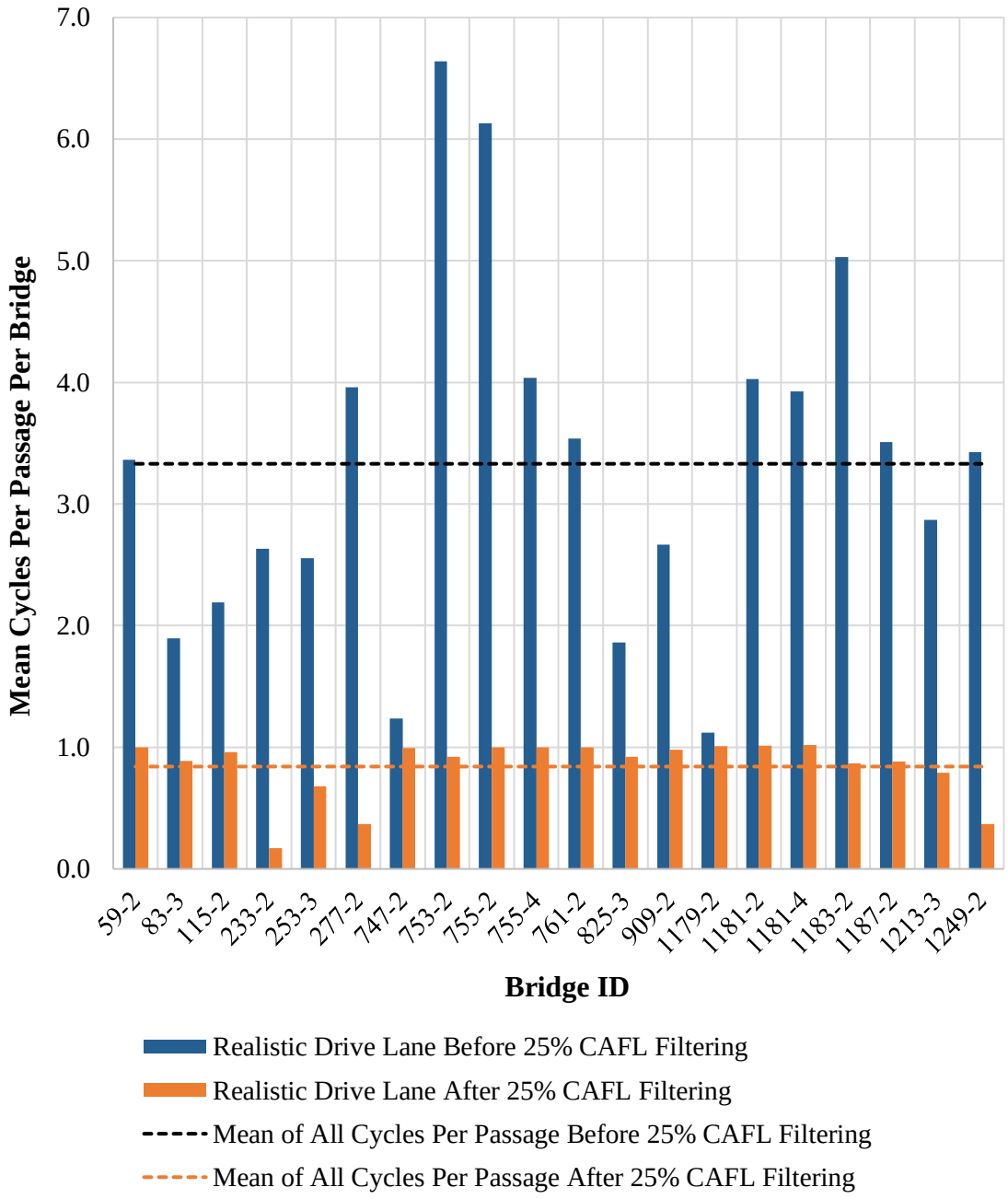

Figure 4-15: Summary of cycles per passage (CPP) for Sensitivity Study 2 (Realistic Drive Lane with Truck Traffic). Includes results both before and after stress truncation (i.e., removing stress ranges less than 25% CAFL).

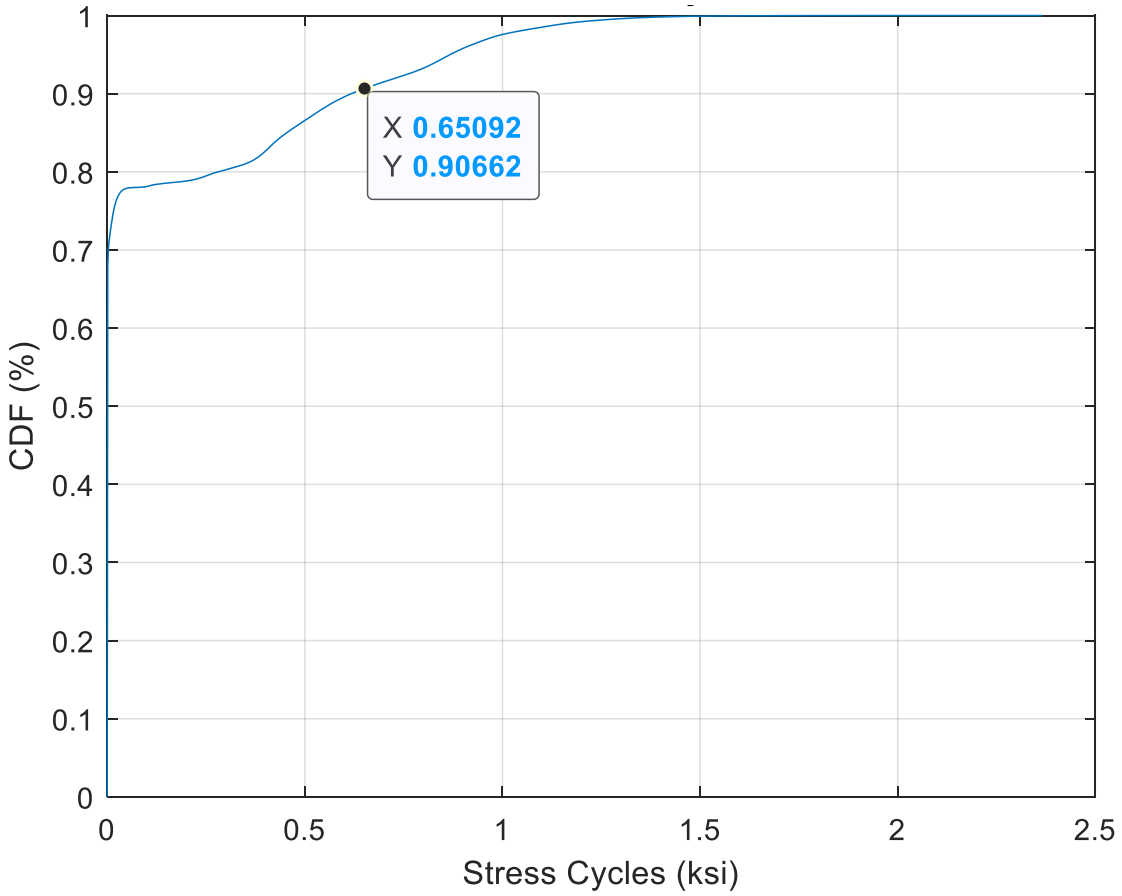

Figure 4-16: Example CDF of stress cycles (before 25% CAFL filtering) for Bridge ID 277-2, showing approximately 91% of total cycles are less than 0.65 ksi.

4.4.6 Findings

Figure 4-17 compares the normalized Fatigue I 99.99th percentile stress ranges for the four sensitivity studies prior to truncating the lower stress ranges (i.e., removing stress ranges less than 25% CAFL), and Figure 4-18 compares the same stress ranges after truncating the lower stress ranges. The stress ranges are normalized by dividing the Fatigue I 99.99th percentile WIM stress ranges by the unfactored fatigue truck stress range for each bridge.

Table 4-9: Pertinent values for calculating Fatigue I parameters for Sensitivity Study 4.

Bridge ID	Fatigue I: 99.99th Percentile Stress Range (ksi)		Fatigue I: 99.99th Percentile Stress Range (Normalized)	
	Before filtering	**After filtering**	**Before filtering**	**After filtering**
59-2	8.21	10.12	1.70	2.09
83-3	3.14	3.67	1.28	1.50
115-2	2.75	3.31	0.89	1.06
233-2	2.59	3.50	1.17	1.58
253-3	2.37	2.98	1.17	1.46
277-2	1.60	2.13	1.12	1.49
747-2	4.18	5.02	1.11	1.33
753-2	3.49	4.24	1.06	1.29
755-2	4.66	5.85	1.05	1.32
755-4	5.33	6.48	1.07	1.30
761-2	4.59	5.72	1.09	1.36
825-3	3.01	3.73	1.06	1.32
909-2	2.94	3.65	0.86	1.06
1179-2	4.31	5.17	1.00	1.19
1181-2	4.71	6.36	0.87	1.17
1181-4	6.25	8.16	0.90	1.18
1183-2	3.27	3.85	1.32	1.56
1187-2	2.62	3.43	1.10	1.44
1213-3	2.63	3.30	1.28	1.60
1249-2	1.57	2.05	1.08	1.41
		Mean	**1.11**	**1.39**
		Mean + 1.5 Standard Deviations	**1.40**	**1.73**

Table 4-10: Pertinent values for calculating Fatigue II parameters for Sensitivity Study 4.

Bridge ID	Maximum Number of Cycles		Fatigue II: Effective Stress Range (ksi)		Fatigue II: Effective Stress Range (Normalized)		Fatigue II: Fatigue Damage Ratio	
	Before filtering	After filtering	Before filtering	After filtering	Before filtering	After filtering	Before filtering	After filtering
59-2	13,439,031	286,727	1.06	3.38	0.22	0.70	0.73	0.64
83-3	2,446,959	342,955	0.77	1.37	0.32	0.56	0.59	0.55
115-2	3,845,507	363,961	0.73	1.47	0.24	0.47	0.52	0.47
233-2	6,407,954	80,698	0.35	1.28	0.16	0.58	0.40	0.35
253-3	3,598,307	264,389	0.55	1.18	0.27	0.58	0.58	0.52
277-2	5,025,926	138,759	0.33	0.94	0.23	0.66	0.54	0.47
747-2	5,558,926	395,398	0.95	2.04	0.25	0.54	0.62	0.55
753-2	11,744,643	347,673	0.57	1.62	0.17	0.49	0.55	0.48
755-2	11,971,218	396,677	0.84	2.28	0.19	0.51	0.60	0.53
755-4	7,343,472	407,956	1.07	2.50	0.22	0.50	0.59	0.52
761-2	7,672,235	403,315	0.96	2.27	0.23	0.54	0.63	0.56
825-3	5,880,185	43,313	0.37	1.52	0.13	0.54	0.33	0.26
909-2	4,309,806	375,360	0.77	1.56	0.22	0.45	0.51	0.46
1179-2	2,806,641	423,840	1.28	2.18	0.30	0.50	0.58	0.53
1181-2	9,177,942	440,550	1.11	2.67	0.20	0.49	0.60	0.52
1181-4	6,960,685	467,037	1.56	3.41	0.23	0.49	0.60	0.53
1183-2	9,019,861	123,599	0.25	0.81	0.10	0.33	0.29	0.23
1187-2	7,091,287	329,057	0.57	1.39	0.24	0.58	0.64	0.56
1213-3	4,819,235	53,232	0.44	1.31	0.21	0.63	0.50	0.33
1249-2	10,180,415	139,086	0.12	0.94	0.09	0.65	0.26	0.47
						Mean	**0.53**	**0.48**
						Mean + 1.5 Standard Deviations	**0.72**	**0.63**

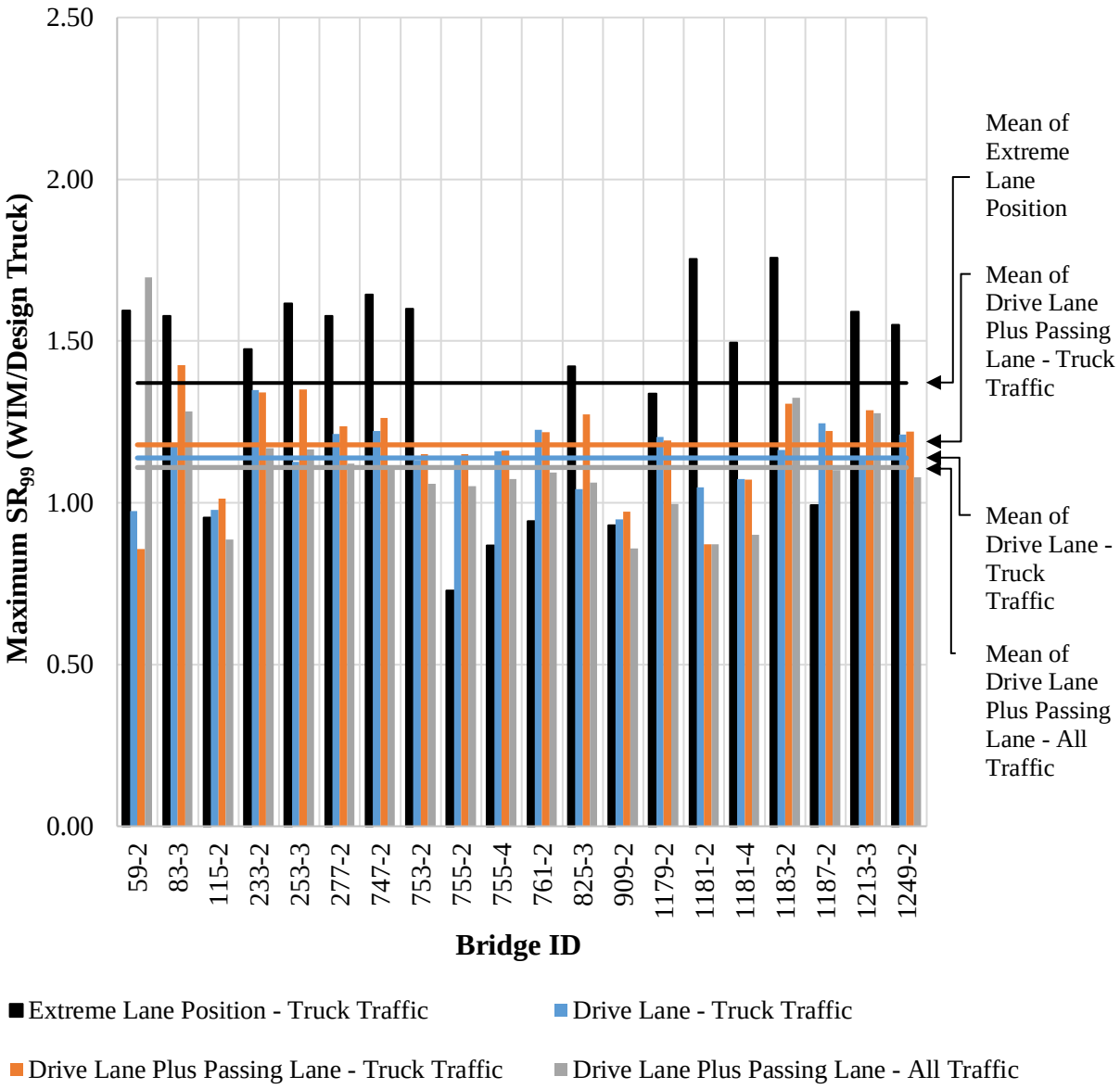

Figure 4-17: Normalized Fatigue I 99.99th percentile stress ranges for the four sensitivity studies prior to truncating the lower stress ranges (i.e., prior to removing stress ranges less than 25% CAFL).

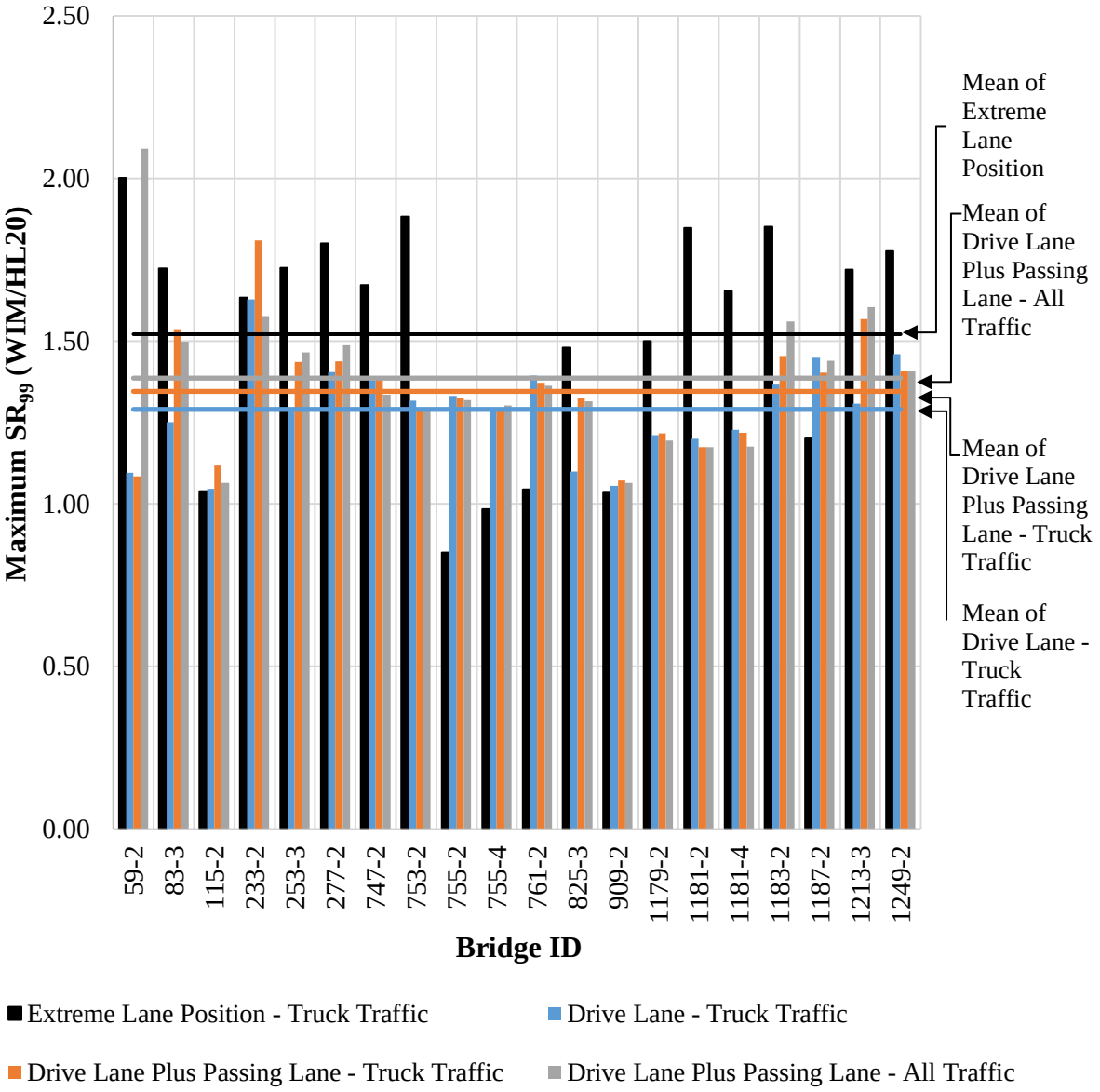

Figure 4-18: Normalized Fatigue I 99.99th percentile stress ranges for the four sensitivity studies after truncating the lower stress ranges (i.e., removing stress ranges less than 25% CAFL).

For both of these figures, each bin value represents the Fatigue I stress range for the given sensitivity study (the sensitivity studies are color coded per the legend). Four solid lines in each figure represents the arithmetic mean of Fatigue I stress ranges for all bridges for the given sensitivity study (the lines are color coded to match the appropriate sensitivity study). The following observations can be made regarding the comparison of the Fatigue I stress ranges for

the four sensitivity studies:

1. Sensitivity Study 1 is intended to represent the "worst-case" lane position that maximizes force effects in any given cross-frame. The "worst-case" lane positions used in this analysis were selected by using the stress ranges produced by the fatigue truck as a predictor of critical positions. It is apparent from Figure 4-17 and Figure 4-18 that for five bridges (specifically, bridges 755-2, 755-4, 761-2, 909-2, and 1187-2), the realistic lane position from Sensitivity Study 2 produces a worse Fatigue I stress range than the lane position selected for Sensitivity Study 1. This indicates that the maximum stress ranges produced by the fatigue truck are not always a reliable predictor of the actual worst-case transverse positions for the WIM traffic.
2. When comparing Sensitivity Studies 2 and 3 (Class T realistic drive lane records with passing lane included, and Class AV realistic drive lane records with passing lane included) with Sensitivity Study 1 (Class T realistic drive lane with no passing lanes included), it is apparent that including the effects of passing lane traffic (regardless of whether the traffic streams include lightweight vehicles or not) produces a negligible effect on the Fatigue I stress ranges when compared to just the drive lane traffic. This is true regardless if the comparison is made between records with and without truncating stress ranges below 25% CAFL. Figure 4-18 illustrates that the Fatigue I stress ranges are generally within +/-5% of the values calculated by only considering truck traffic in the realistic drive lane.
3. Within each individual Sensitivity Study, the effects of truncating the stresses below 25% CAFL obviously produces larger Fatigue I stress ranges, since removing any lower stresses will result in a higher top 99.99th percentile population. On average, across all Sensitivity Studies, the effect of removing stresses below 25% CAFL caused the Fatigue I stresses to increase by 11 to 25%. Since the Fatigue I limit state is intended to represent the maximum stress ranges produced by the general truck population, it is most likely not appropriate to consider Fatigue I stress ranges calculated from records where light weight vehicles make up a considerable portion of the population. This finding is supported by the analysis of average "cycles per passage", or CPP for Sensitivity Study 2. From the CPP study, it is evident that the effect of truncating stress ranges below 0.65 ksi (25% CAFL) significantly reduces the number of cycles counted;

furthermore, since the average cycles per passage for the filtered case includes many values less than unity, it is clear that the majority of cycles caused by the WIM traffic are actually less than 0.65 ksi (i.e., it is physically impossible to have a truck passage with less than 1 cycle per passage). This trend will be studied more in Chapter 5 to determine if various WIM records (and thus ADTTs) will provide similar results when simulated over the same bridges.

4. For Sensitivity Studies 2 and 3, the mean and "mean plus 1.5 standard deviations" (for normal distributions, "mean plus 1.5 standard deviations" includes approximately 93% of the population) implies an appropriate load bias[2] for the Fatigue I limit state design of cross-frames falls between 1.3 to 1.6 (these values are not shown in the plots). This is generally less than the current Fatigue I load factor of 1.75. Sensitivity Study 1 and 4 results were omitted in this statement based on the discussion provided in items 1 and 3 above.

Figure 4-19 compares the normalized Fatigue II damage ratios for the four sensitivity studies prior to truncating the lower stress ranges (i.e., removing stress ranges less than 25% CAFL), and Figure 4-20 compares the same damage ratios after truncating the lower stress ranges. The damage ratios are normalized by dividing the damage caused by the WIM traffic by the damage caused by the unfactored fatigue truck for each bridge. For both of these figures, each bin value represents the Fatigue II damage ratio for the given sensitivity study (the sensitivity studies are color coded per the legend). Four solid lines in each figure represents the arithmetic mean of Fatigue II damage ratios for all bridges for the given sensitivity study (the lines are color coded to match the appropriate sensitivity study).

[2]"Load bias" refers to the ratio between the actual load effects to the design load effects (i.e., the WIM load effects divided by the load effects caused by the fatigue design truck).

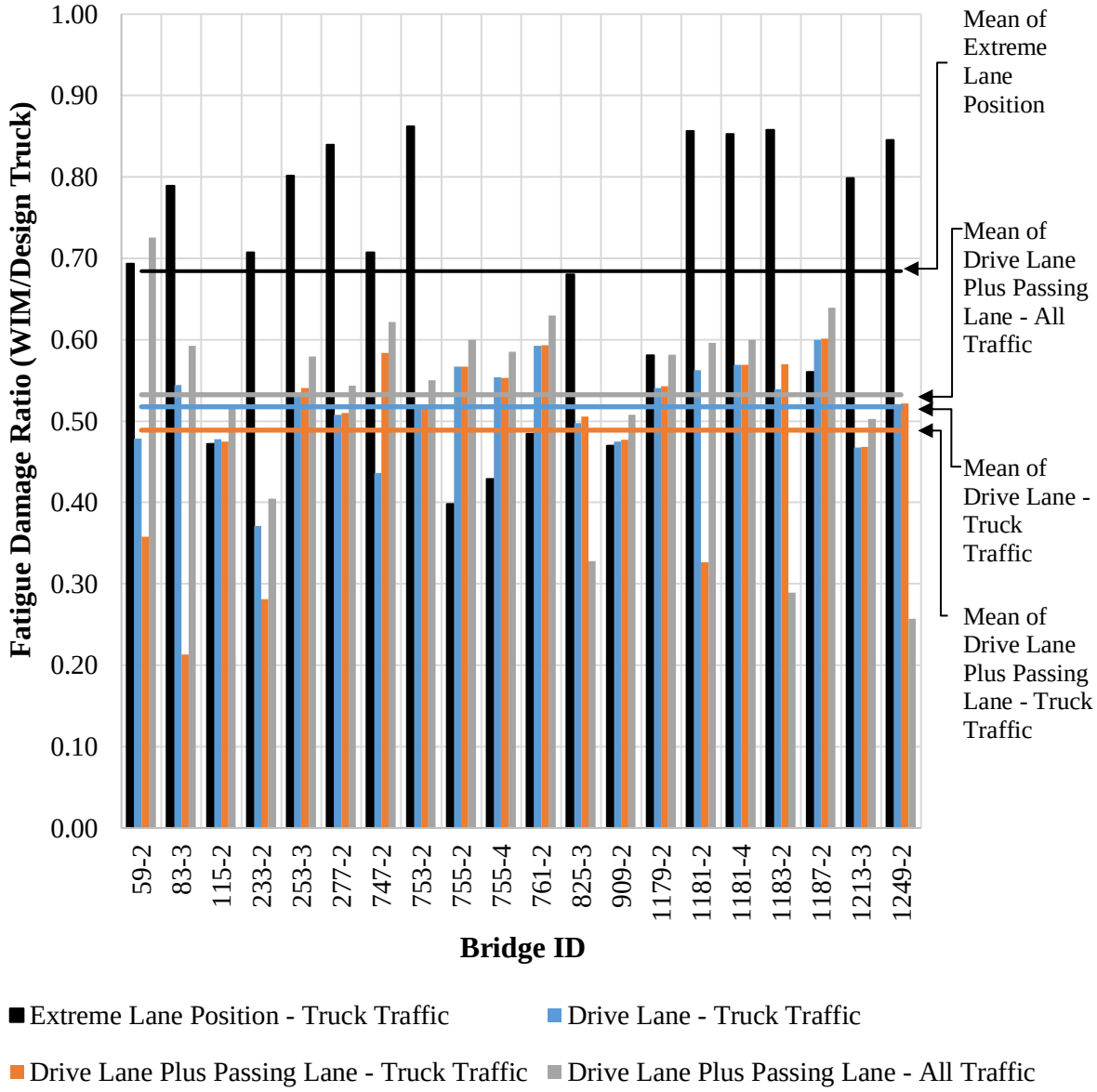

Figure 4-19: Normalized Fatigue II damage ratios for the four sensitivity studies prior to truncating the lower stress ranges (i.e., prior to removing stress ranges less than 25% CAFL).

The following observations can be made regarding the comparison of the Fatigue II damage ratios for the four sensitivity studies:

1. Similar to the observations made with the Fatigue I stress ranges, Sensitivity Study 1 is intended to represent the "worst-case" lane position that maximizes force effects in

any given cross-frame; however, for the same five bridges (specifically, bridges 755-2, 755-4, 761-2, 909-2, and 1187-2), the realistic lane position from Sensitivity Study 2 produces a worse Fatigue II damage ratio than the lane position selected for Sensitivity Study 1. This indicates that the stress ranges produced by the fatigue truck are not always a reliable predictor of the actual worst-case transverse positions.

2. Similar to the observations made with the Fatigue I stress ranges, when comparing Sensitivity Studies 2 and 3 with Sensitivity Study 1, it is apparent that including the effects of passing lane traffic produces a negligible effect on the Fatigue II damage ratios when compared to just the drive lane traffic. This is true regardless if the comparison is made between records with and without truncating stress ranges below 25% CAFL. Figure 4-20 illustrates that the Fatigue II damage ratio ranges are generally within +/-5% of the values calculated by only considering truck traffic in the realistic drive lane (i.e., Sensitivity Study 2).
3. Within each individual Sensitivity Study, the effects of truncating the stresses below 25% CAFL produces smaller Fatigue II damage ratios, since less traffic counts are available to contribute to the overall accumulation of damage. On average, across all Sensitivity Studies, the effect of removing stresses below 25% CAFL caused the Fatigue II damage ratios to decrease by 2 to 11%.
4. On average, when comparing Sensitivity Studies 2 through 3 after truncating stresses below 25% CAFL, it is apparent that the differences in Fatigue II damage ratios are negligible (within 2%).
5. For Sensitivity Studies 2 through 4, the mean and "mean plus 1.5 standard deviations" implies an appropriate load bias for the Fatigue II limit state design of cross-frames falls between 0.6 to 0.72 (these values are not shown in the plots). This is generally less than the current Fatigue II load factor of 0.8. Sensitivity Study 1 results were omitted in this statement based on the discussion provided in item 1 above.

Based on these findings, locating the traffic stream in the worst-case lane position produces overly conservative results when compared to traffic records in realistic drive lanes. If it is desirable to locate an actual worst-case lane position, these findings suggest the force effects produced by the fatigue truck are not a reliable predictor of the transverse lane position corresponding to the most critical cross-frame force effects produced by realistic traffic records.

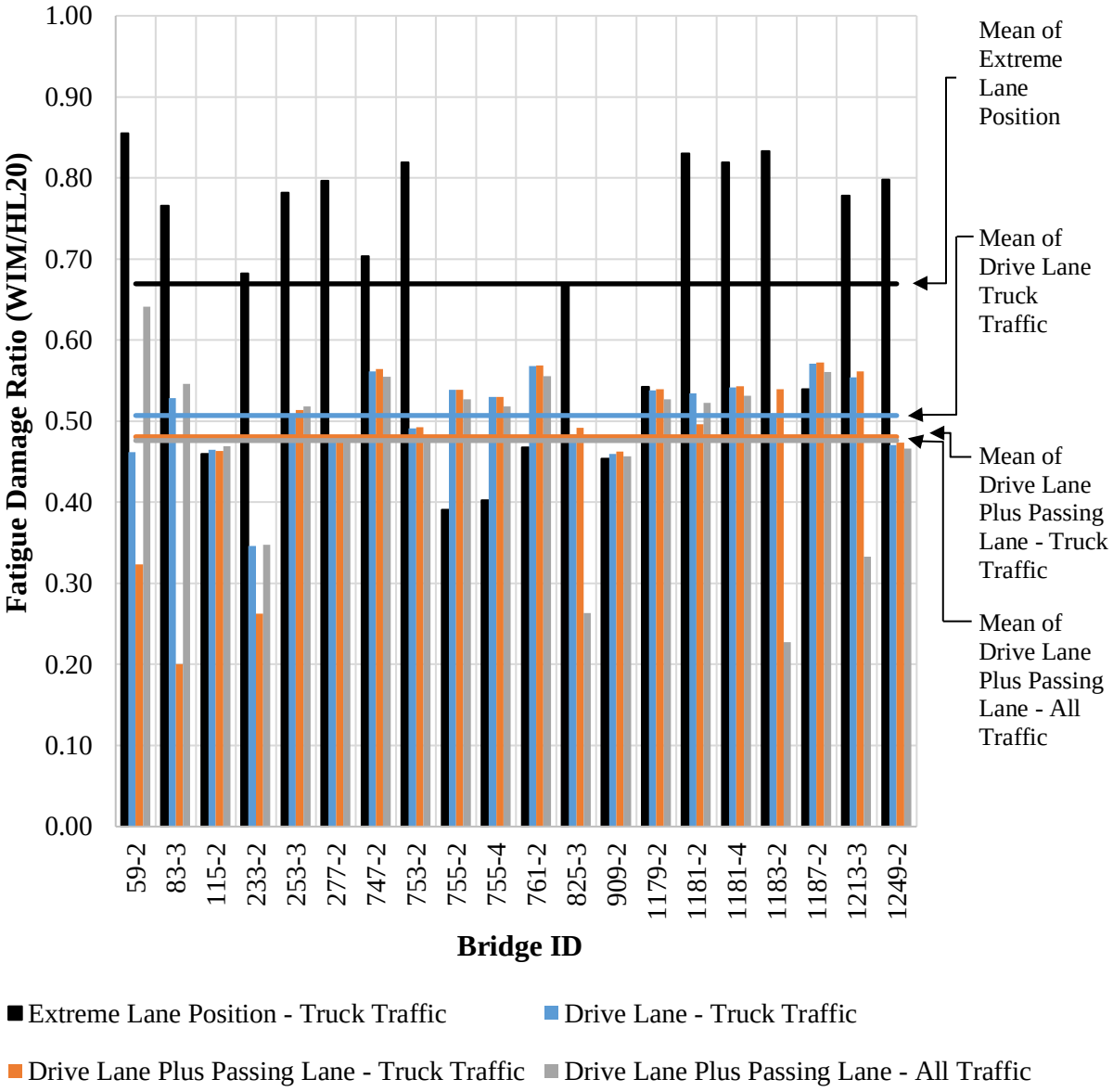

Figure 4-20: Normalized Fatigue II damage ratios for the four sensitivity studies after truncating the lower stress ranges (i.e., removing stress ranges less than 25% CAFL).

For the calculations of the Fatigue I and II parameters in the advanced studies in Chapter 5, the results of the sensitivity studies support the use of the truck traffic (i.e., the Class T records) located in realistic drive lanes; excluding the effects of passing lane traffic produces negligible results. Due to the effects of truncating stresses below 25% CAFL on both Fatigue I and II

parameters, the advanced studies performed in Chapter 5 will be performed both with and without this filter.

4.5 MULTIPLE PRESENCE STUDY

The assumptions of multiple presence in the original LRFD calibration studies (Nowak 1999) were initially based on engineering judgement and visual observations of truck traffic with unknown weights. These initial assumptions were that a "side by side" scenario (i.e., adjacent lane loaded with a passing truck in general alignment with the drive lane truck) occurred once every 15 load events. More recent studies have shown this assumption to be excessively conservative (Sivakumar et al. 2011). The research presented in the SHRP 2 R19B project attempted to verify certain statistical assumptions of multiple presence; however, the WIM records used in these studies have a time resolution of 1 second. At 70 miles per hour, plus or minus 0.5 seconds is equivalent to approximately plus or minus 50 feet. Since at this resolution it is impossible to determine if another truck is even on the same span as the truck in question, higher-resolution data is essential to evaluate the frequency of occurrence of multiple presence. At 70 miles per hour, the 0.01 second resolution data obtained from the FHWA generally provided a resolution of plus or minus 0.5 feet.

The obtained WIM records include multi-lane records for three sites. As two of the sites (Indiana US-31 and Tennessee IH-40) include two lanes of traffic in two directions, the multi-lane data consists of five two-lane data sets. Table 4-11 provides the 2-lane distribution of Average Daily Traffic (ADT) and Average Daily Truck Traffic (ADTT) counts for the years' worth of data. With the availability of this higher resolution multi-lane data, a multiple presence study was performed to better understand the statistical parameters surrounding multiple presence. This was performed using a cluster analysis to consider when a bridge may be loaded with other truck traffic during a primary drive lane load event (i.e., passage of one or more axles of a vehicle). The cluster analysis is performed based on the time stamps of the individual truck events, the lengths of the individual trucks, and the speed of the individual trucks. Since bridge lengths vary, the following study incorporates multiple presence load events that occur within a plus or minus 1000-foot window of the primary drive lane load event.

This study involved developing a script to determine how many times a second truck is in a lane adjacent to the primary drive lane truck (i.e., a second truck is passing or is being passed by

the truck in the drive lane, anywhere along an arbitrary length of 1000 feet). This scenario is illustrated schematically in Figure 4-21. Clear distances are measured from the rear axle of the drive lane truck to the front axle of the passing lane truck. Positive values indicate the passing lane truck's front axles are behind the drive lane truck's rear axles, and negative values indicate the passing lane truck's front axles are ahead of the drive lane truck's rear axles. This provides a smooth, continuous function of clear distances, with increasing clear distances (positive or negative) indicating a larger separation between vehicles. Note that a clear distance of zero corresponds to a staggered configuration, which was deemed critical to cross-frame force effects in the 7th Ed. AASHTO LRFD Specifications. This provision has since been removed in the current 8th Ed., with the Commentary citing that this was an infrequent occurrence.

Table 4-11: Two-lane distribution of ADT and ADTT counts for the multi-lane WIM data records (full years' worth of data).

WIM Record	ADT		ADTT	
	Fraction of Traffic in Drive Lane	**Fraction of Traffic in Passing Lane**	**Fraction of Traffic in Drive Lane**	**Fraction of Traffic in Passing Lane**
IN (Lanes 1/2)	80%	20%	95%	5%
IN (Lanes 3/4)	77%	23%	95%	5%
TN (Lanes 1/2)	54%	46%	82%	18%
TN (Lanes 3/4)	58%	42%	86%	14%
VA (Lanes 1/2)	77%	23%	92%	8%

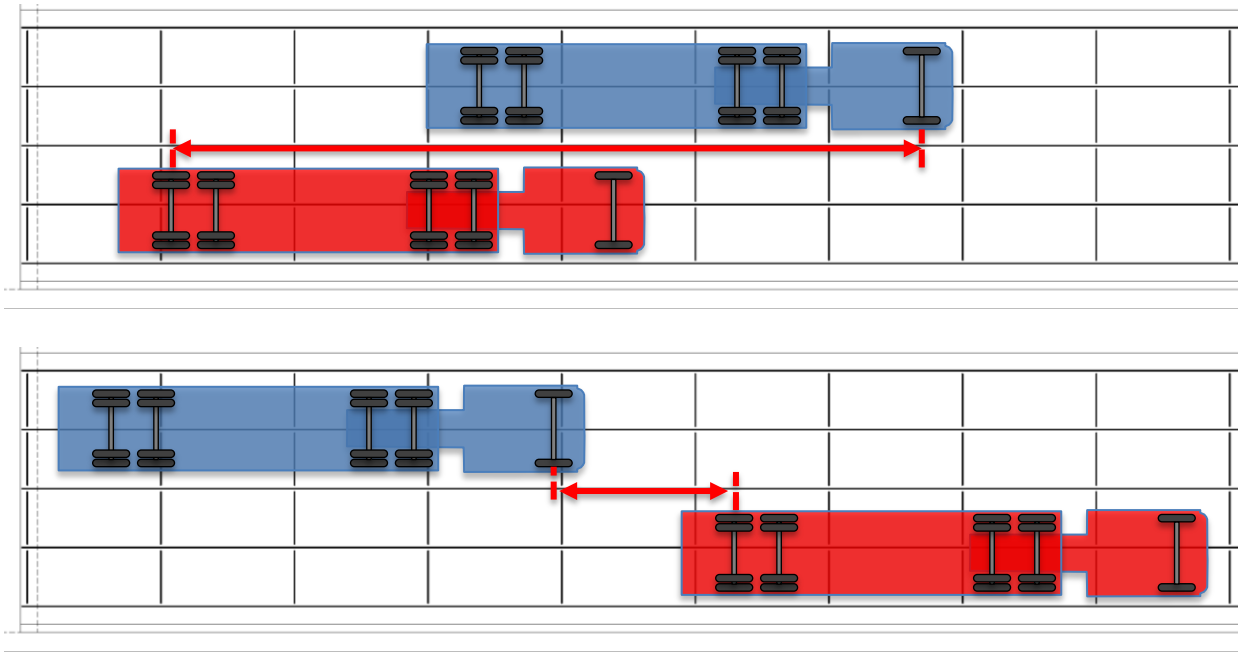

Figure 4-21: Illustration of an adjacent lanes (truck-passing-truck) scenario; negative (bottom figure) and positive (top figure) clear distances indicate the passing truck's front axle is ahead or behind the drive lane truck's rear axle, respectively.

The results of this adjacent lane scenario are summarized in Figure 4-22 through Figure 4-36, which provide histograms illustrating various aspects of multiple presence studied. For various load position parameters (e.g., clear distance between drive-lane and passing truck), the number of occurrences for each multi-lane WIM site is compiled and plotted. Specifically, Figure 4-22 through Figure 4-26 illustrate the clear distances between passing lane trucks and drive lane trucks. Using information from these histograms, Table 4-12 summarizes how often (for the year of data considered) any truck was within a certain window of the drive lane truck, relative to the total volume of traffic in the drive lane. Figure 4-27 through Figure 4-31 illustrate the spectrum of GVW for passing lane trucks, and Figure 4-32 through Figure 4-36 illustrate the ratio of passing lane truck GVW to drive lane truck GVW.

Based on these results, it is evident that a passing truck in close proximity to a drive lane truck is a rare occurrence. This is reflected in the findings from the sensitivity studies, where the inclusion of passing lane traffic produced negligible results on the Fatigue I and II parameters. The frequency of occurrence for multiple presence is less than the assumptions used in the original calibration studies (Nowak et al. 1999). The largest frequency of occurrence is demonstrated by the Tennessee IH-40 WB data, where approximately 30% of traffic is accompanied by another vehicle located with a headway distance of less than 1000 feet, and 1.8% of traffic is accompanied

by another vehicle located with a headway distance less than 20 feet. This higher percentage of multiple presence for the Tennessee data is consistent with these records also having the higher percentage of total one-way truck traffic in the passing lane when compared to the other 2-lane data sets (Table 4-11). Recalling that cross-frame forces generally reduce rapidly as a truck moves away from the cross-frame in the longitudinal direction (Reichenbach 2020), it is apparent that, for cross-frames, the largest frequency of occurrence for passing vehicles occurring simultaneously is approximately 1.8% (i.e., larger headway distances generally do not result in superimposed cross-frame forces). Another observation is that the distribution of the passing lane truck's GVW appears to be bi-modal for several sites, with the heavier truck mode being equal or heavier to the drive lane truck's GVW.

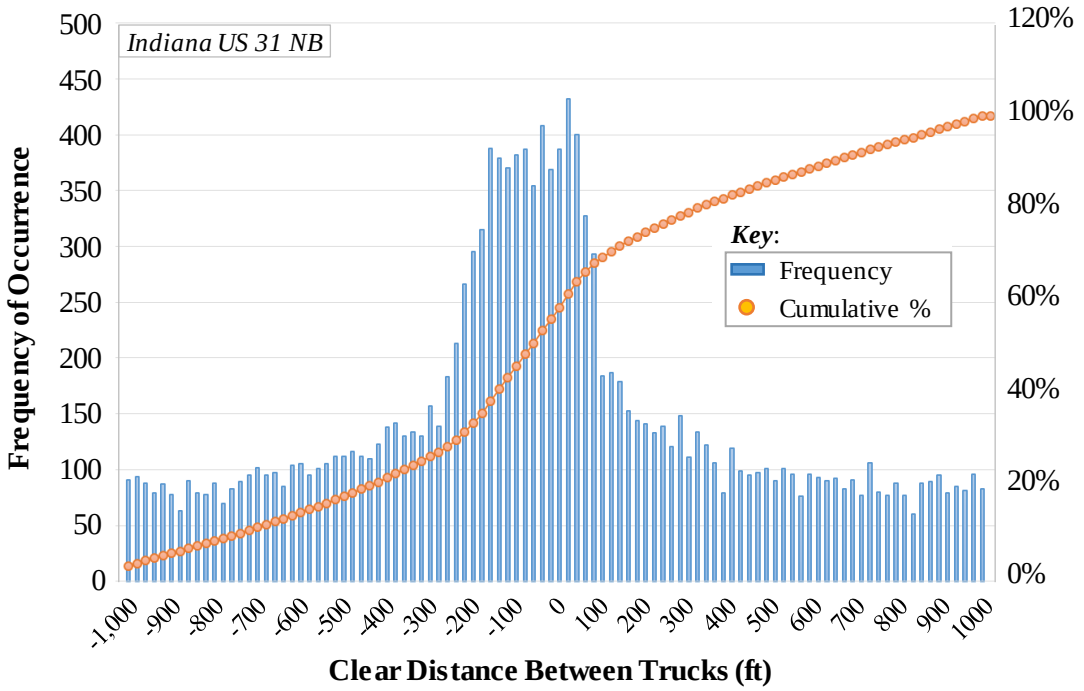

Figure 4-22: Histogram from two-lane WIM records, showing the clear distance between a passing truck and the drive lane truck (Indiana US-31 NB).

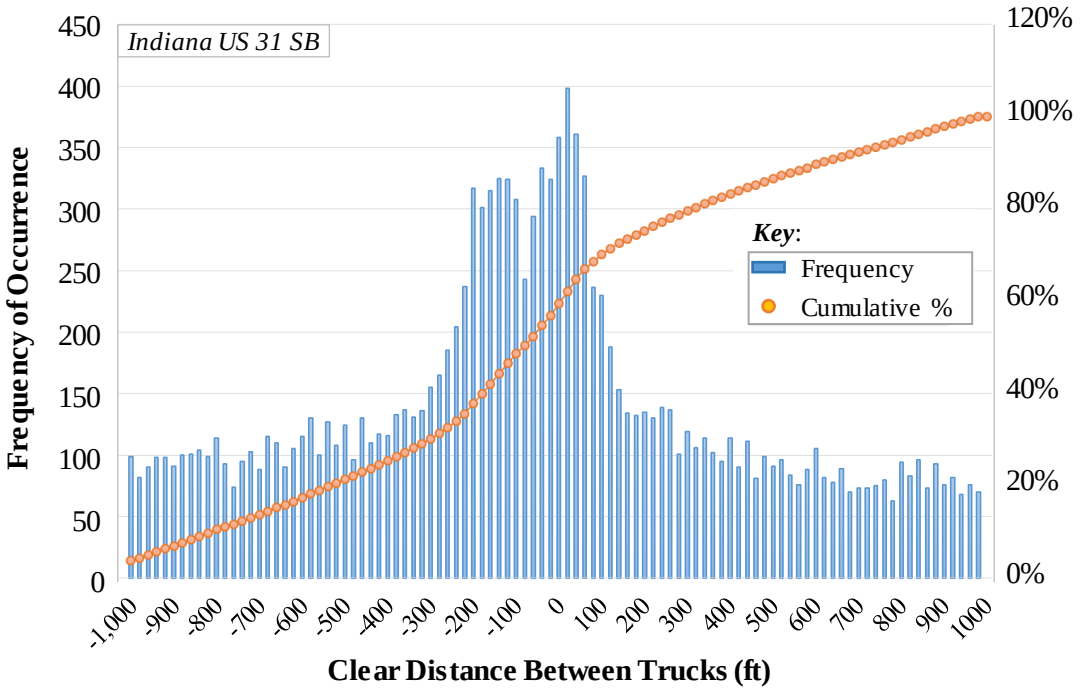

Figure 4-23: Histogram from two-lane WIM records, showing the clear distance between a passing truck and the drive lane truck (Indiana US-31 SB).

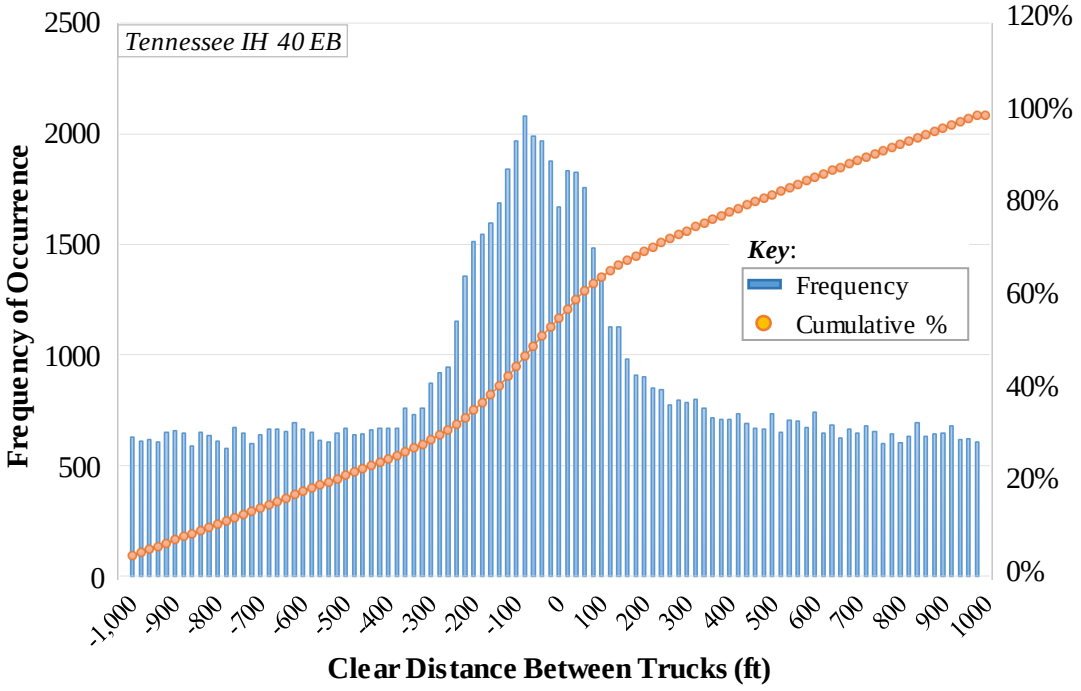

Figure 4-24: Histogram from two-lane WIM records, showing the clear distance between a passing truck and the drive lane truck (Tennessee IH-40 EB).

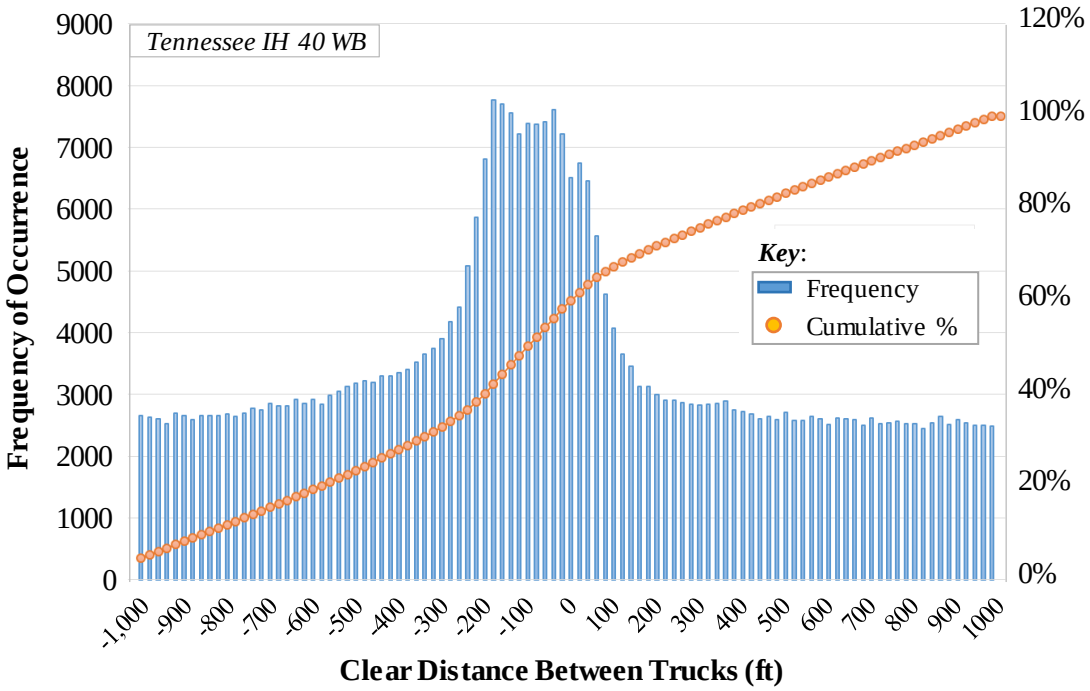

Figure 4-25: Histogram from two-lane WIM records, showing the clear distance between a passing truck and the drive lane truck (Tennessee IH-40 WB).

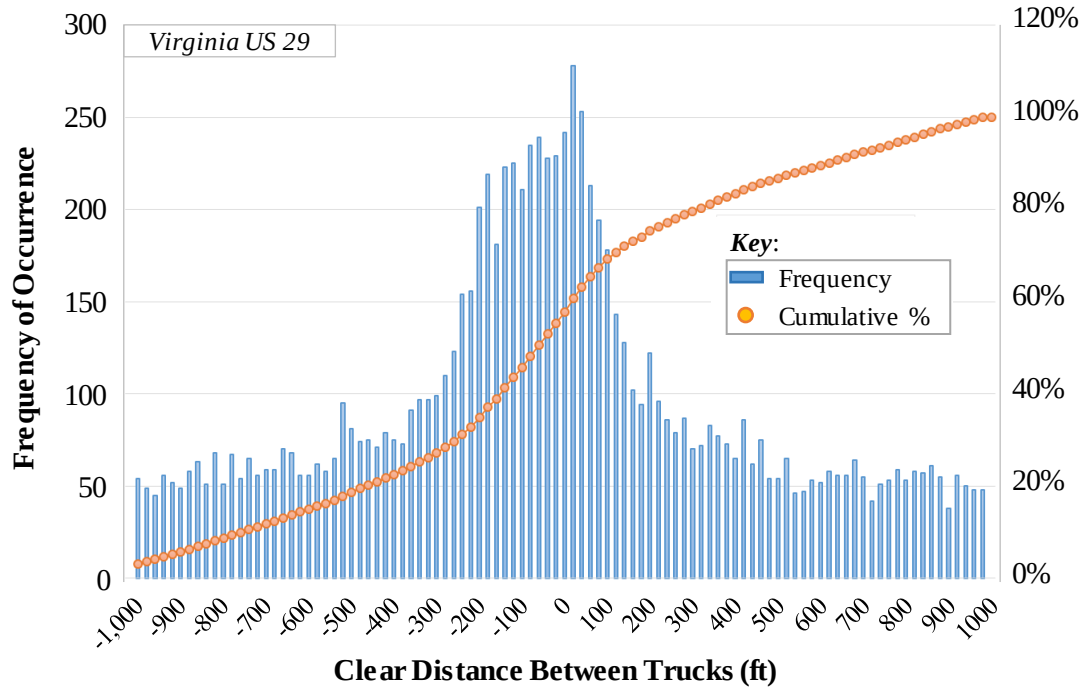

Figure 4-26: Histogram from two-lane WIM records, showing the clear distance between a passing truck and the drive lane truck (Virginia US-29).

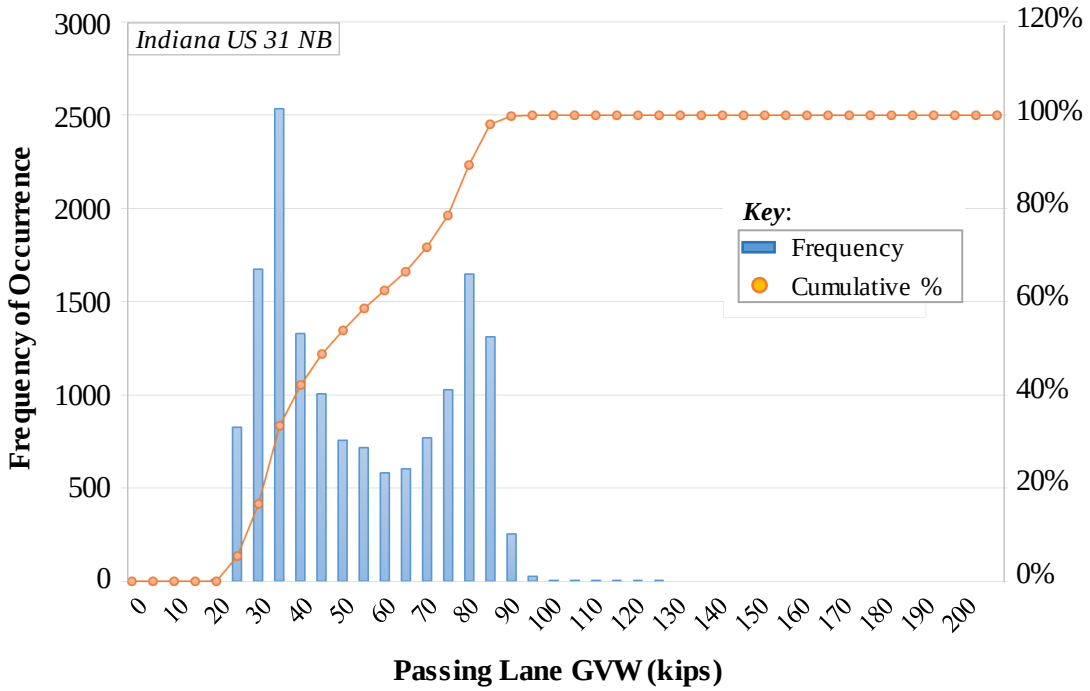

Figure 4-27: Histogram from two-lane WIM records, showing GVW of a passing truck (Indiana US-31 NB).

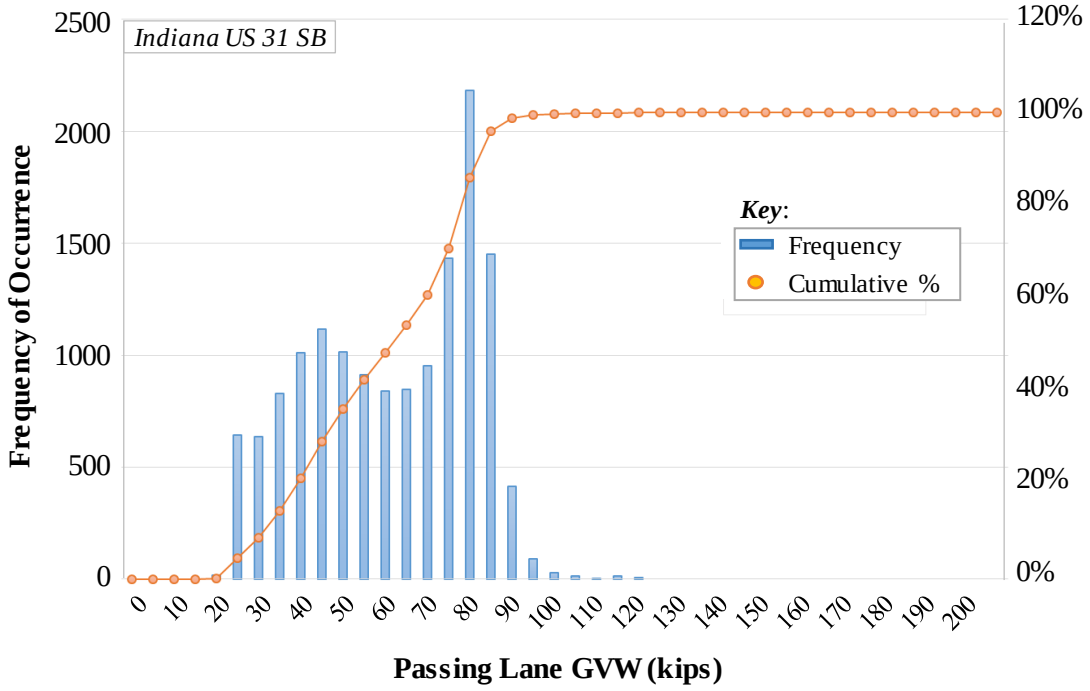

Figure 4-28: Histogram from two-lane WIM records, showing GVW of a passing truck (Indiana US-31 SB).

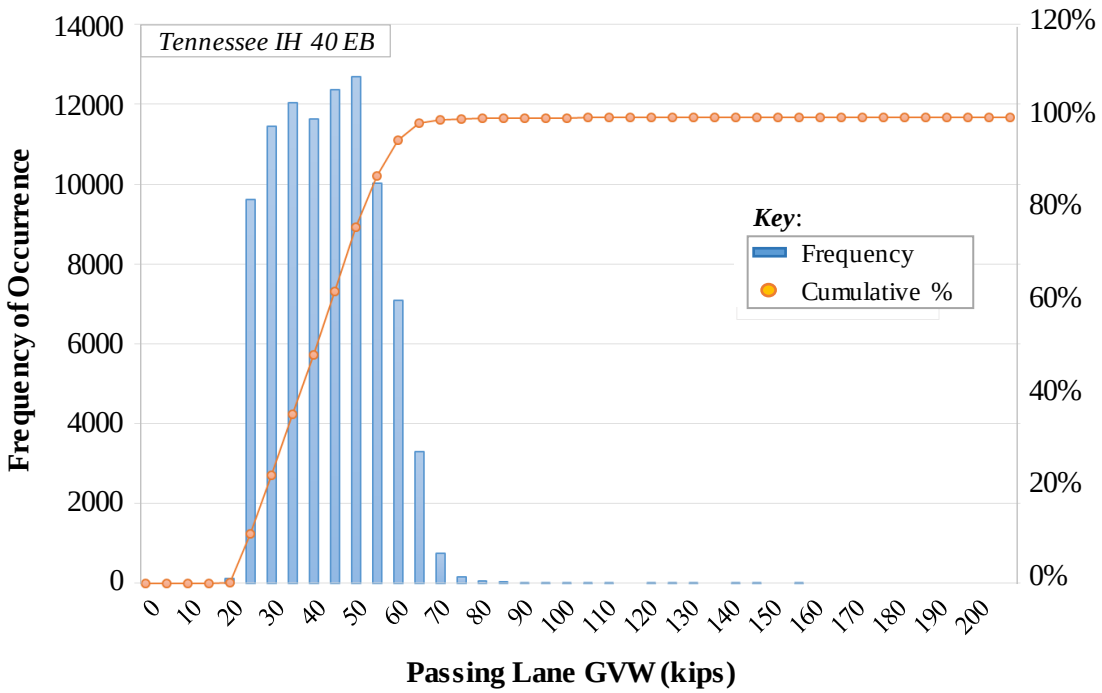

Figure 4-29: Histogram from two-lane WIM records, showing GVW of a passing truck (Tennessee IH-40 EB).

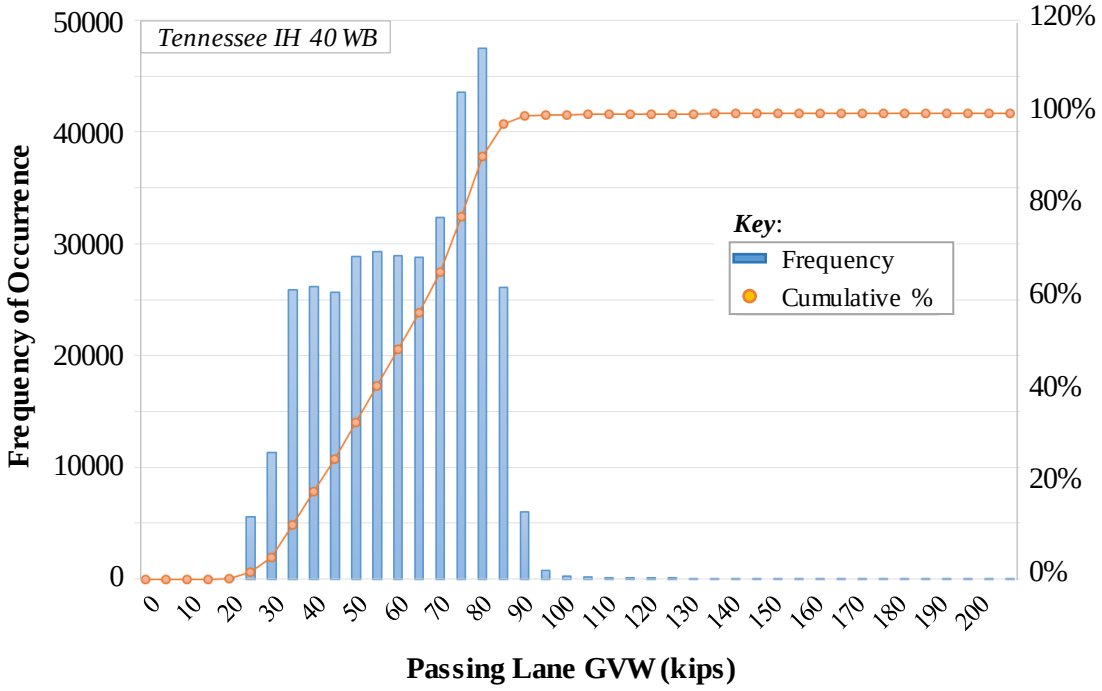

Figure 4-30: Histogram from two-lane WIM records, showing GVW of a passing truck (Tennessee IH-40 WB).

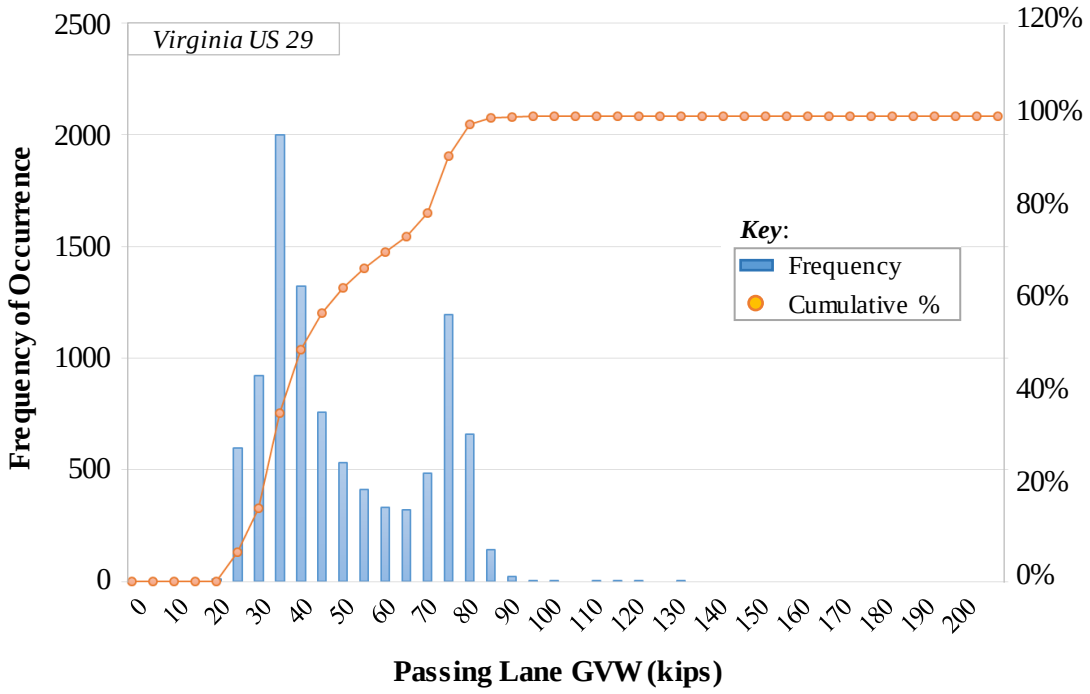

Figure 4-31: Histogram from two-lane WIM records, showing GVW of a passing truck (Virginia US-29).

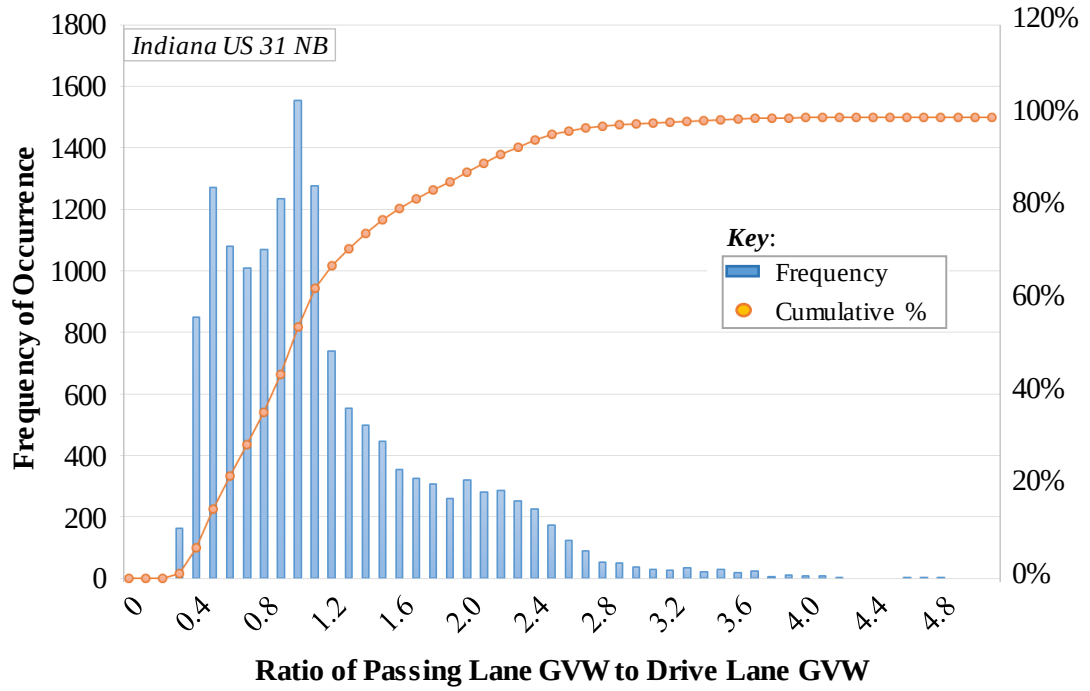

Figure 4-32: Histogram from two-lane WIM records, showing the ratio of the passing lane GVW to the drive lane GVW (Indiana US-31 NB)

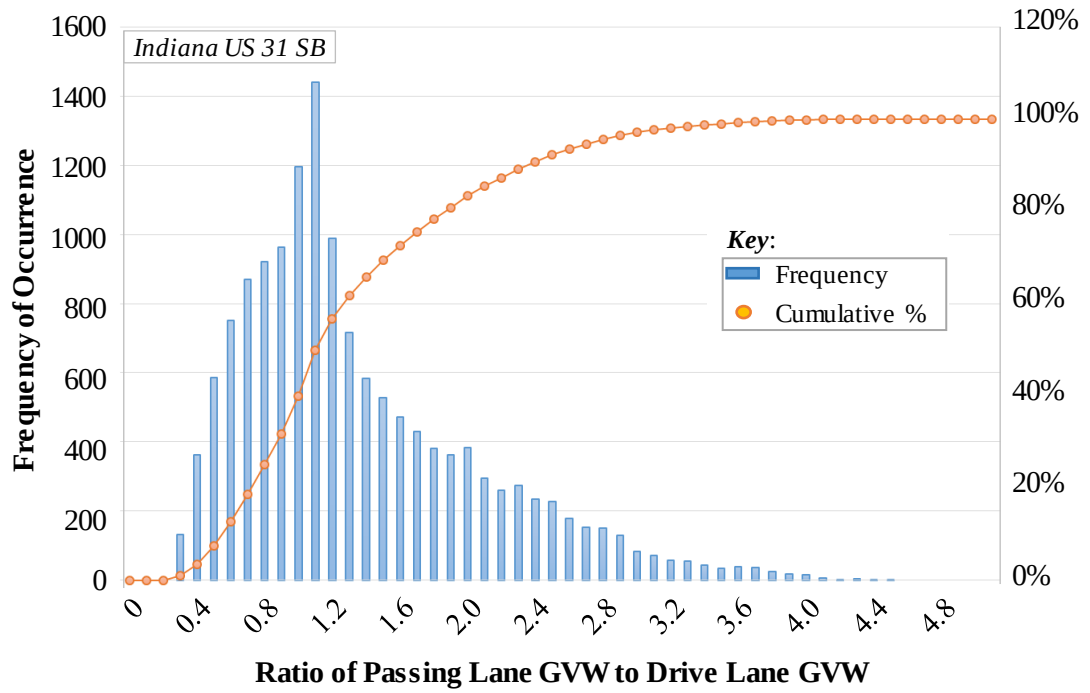

Figure 4-33: Histogram from two-lane WIM records, showing the ratio of the passing lane GVW to the drive lane GVW (Indiana US-31 SB).

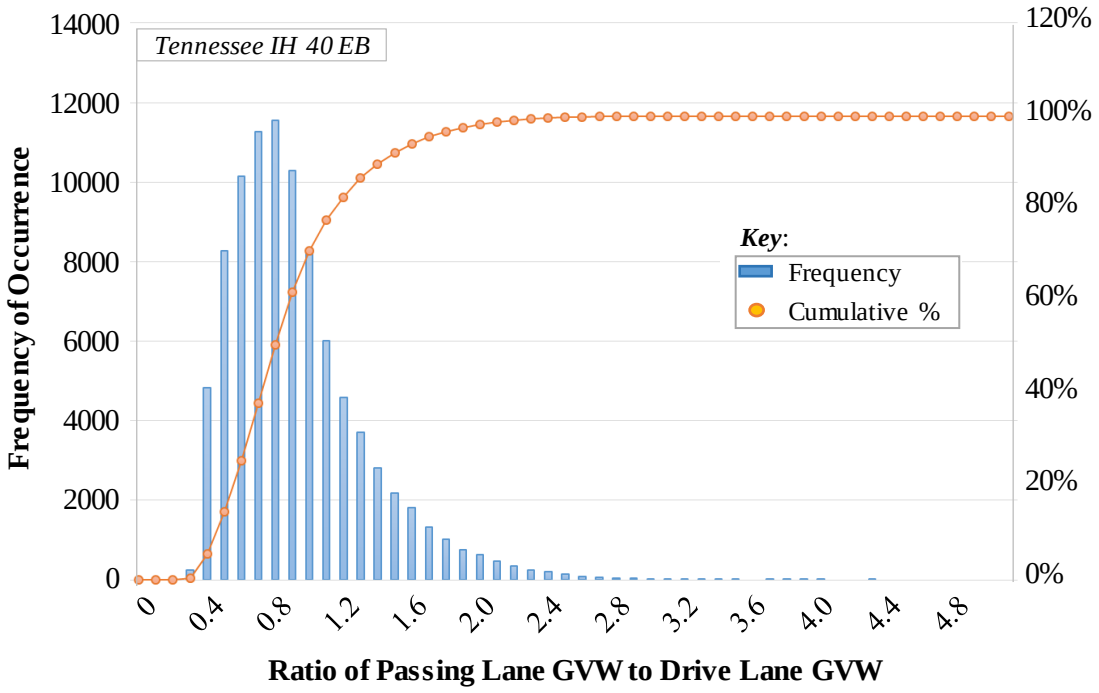

Figure 4-34: Histogram from two-lane WIM records, showing the ratio of the passing lane GVW to the drive lane GVW (Tennessee IH-40 EB).

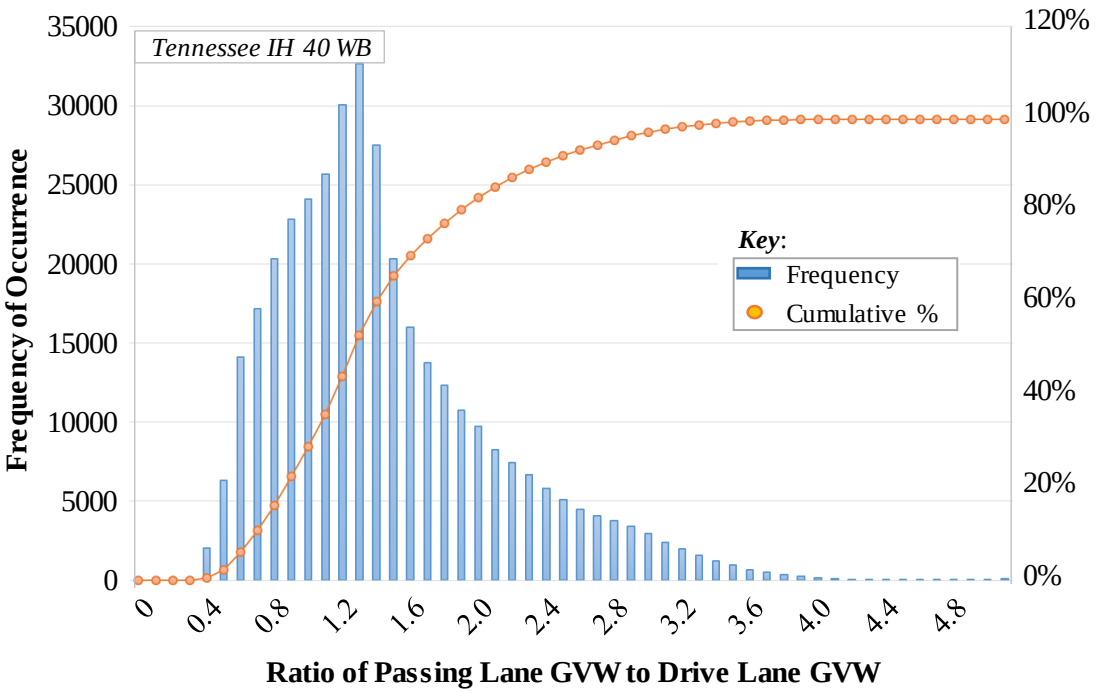

Figure 4-35: Histogram from two-lane WIM records, showing the ratio of the passing lane GVW to the drive lane GVW (Tennessee IH-40 WB).

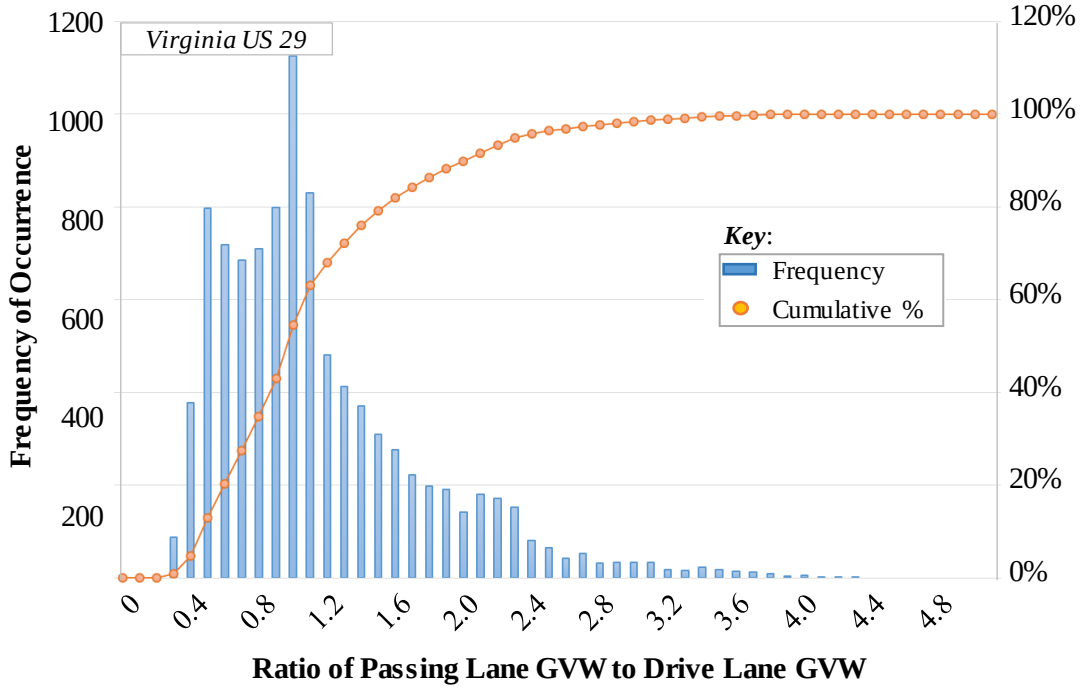

Figure 4-36: Histogram from two-lane WIM records, showing the ratio of the passing lane GVW to the drive lane GVW (Virginia US-29)

Table 4-12: Summary of multiple presence statistics for the adjacent lane loaded scenario.

WIM Site	Frequency of Occurrence within Clear Distance Window, Relative to Drive Lane Annual Truck Traffic (ATT)[a]				
	+/- 1000 ft	+/- 280 ft	+/- 50 ft	+/- 20 ft	+/- 0 ft
Indiana US-31 NB	4.0%	2.1%	0.5%	0.3%	0.01%
Indiana US-31 SB	4.2%	2.2%	0.5%	0.3%	0.00%
Tennessee IH-40 EB	16.0%	7.4%	1.7%	1.0%	0.02%
Tennessee IH-40 WB	29.9%	13.2%	3.0%	1.8%	0.03%
Virginia US-29	3.9%	2.0%	0.5%	0.3%	0.01%

[a]*Reference Figure 4-21 for illustration of positive and negative clear distances.*

4.6 CHAPTER SUMMARY

Based on the sensitivity studies presented in this chapter, there are several conclusions that can be drawn with respect to the fatigue stress ranges in cross-frame systems:

- The critical lane position for designing a governing cross-frame member for fatigue in a particular bridge depends on a variety of parameters. In general, truck passages along the outer edges of the deck (i.e., overhang loads) tend to maximize cross-frame forces in skewed and curved bridges, since the load applies a net torque on the superstructure, which engages cross-frames. Consequently, truck passages in actual design lanes may produce significantly smaller stress ranges and contribute significantly less to fatigue damage. The fatigue truck is not always a good predictor of which lane position actually produces the extreme cross-frame force effects exhibited by real traffic records.
- The effects of passing lane traffic (with or without light weight vehicles) cause negligible differences in the calculation of the Fatigue I and II parameters. A comprehensive multiple lane analysis using all available 2-lane traffic records

demonstrates that the probability of a single truck record (regardless of GVW) being located in a critical position for magnifying cross-frame force effects is exceptionally low: less than 0.02% for the most critical location (i.e., one truck's steering axle located just behind another truck's rear axles in an adjacent lane); and less than 3% when the truck is located within 20 to 50 feet from the rear axle of another truck in an adjacent lane.

- Truncating stresses (e.g., stresses below 25% CAFL) produces an effect that may or may not be negligible in the calculation of the Fatigue I and II parameters, which will be further studied in Chapter 5.
- Using the truck traffic records positioned in the realistic drive lane, the total number of average cycles per passage for all bridges (prior to truncating stresses below 25% CAFL) is 3.3; however, this actual average per bridge varies considerably (approximately 1 to 7). After truncating stresses below 25% CAFL, the average is more uniform, but well below unity, which indicates the threshold for truncating stresses (0.65 ksi) represents a significant portion of the total number of cycles contributing to damage, even when only considering truck traffic. The variation of cycles per passage per bridge will be further explored in Chapter 5, when a number of WIM records with various ADTTs will be simulated on the same subset of bridges.
- This chapter explored the Fatigue I and II load biases in the context of cross-frames through an analysis of WIM data. By analyzing a 20-model subset of the analytical testing matrix with one WIM site assumed to be representative of the remaining WIM sites, it was determined that current AASHTO fatigue load factors may be overly conservative for cross-frame design. This is largely attributed to the fact that current AASHTO design criteria requires all possible lane positions be considered in accordance with AASHTO Article 3.6.1.4.3a, regardless of design lanes or actual lane striping. A more realistic scenario is to consider only "drive lanes", where the large majority of truck traffic traverses.

Chapter 5: Advanced WIM Studies

5.1 INTRODUCTION

Recalling from Chapter 4 that the WIM records were obtained from 16 SPS sites, and some sites have multiple lanes, there are a total of 18 records with drive lane data. At a WIM site, the instrumented lane is the right lane, or drive lane, where a majority of the heavy traffic is driven. This chapter discusses advanced studies using these 18 WIM drive lane records simulated over the drive lanes of all 20 bridges chosen to be representative of the analytical testing matrix.[3] The advanced studies aim to develop appropriate load biases for the Fatigue I and Fatigue II limit states. In addition, the variation of cycles per passage for various bridge geometries studied in Chapter 4 will be further investigated using the WIM records with various ADTTs applied to the same bridge set.

The sensitivity studies discussed in Chapter 4 investigated various load configurations that affect fatigue parameters due to vehicle lane placement, multiple presence, and vehicle weight filters. To optimize the significant computational efforts involved with WIM analyses, the results of the sensitivity studies were used to provide guidance on the implementation of advanced WIM studies. The findings of the sensitivity studies (discussed in full in Chapter 4) led to the following decisions regarding the parameters for the advanced WIM analysis:

- Load Placement: Since a worst-case lane position may lead to unnecessary conservatism, the advanced WIM studies use Load Configuration 3 (i.e., realistic meandering traffic stream) to more accurately capture the effects of cross-frame stress ranges. The meandering traffic streams were defined over a realistic drive lane based on the width of the bridge and guidance provided by AASHTO Section 3.6.1.1.1.
- Multiple Presence: the advanced WIM studies ignore the negligible effects of multiple

[3] The results herein are from one arbitrary drive lane (i.e., the analysis does not consider that traffic could be flowing the opposite direction); the symmetry of the bridge is assumed to produce similar maximum effects for one of the 16 to 20 critical cross-frames selected per bridge. This assumption was partly verified at the conclusion of this study, when selected bridges and WIM records were chosen to simulate the WIM records on a bridge deck surface rotated by 180 degrees (i.e., traffic was located on the drive lane nearest the opposite edge of the bridge). The results of this spot check indicated there was very little difference in maximum force effects for fatigue.

lanes occupied by passing or passed traffic.

- Vehicle Weight Filters: Based on the observations that lightweight vehicles do not contribute significantly to the overall fatigue damage of cross-frames, the traffic streams for the advanced WIM studies use the Class T records (i.e., excluding vehicles with GVW less than 20 kips).

Additionally, since the controlling cross-frames for vehicles located in transverse positions to maximize cross-frame force effects are not necessarily the same controlling cross-frames for vehicles located in a realistic drive lane, the advanced WIM studies evaluate all 16 to 20 potentially critical cross-frame members selected as described in Section 3.4.

For the advanced WIM studies, all cross-frame force effects were normalized to the unfactored AASHTO design load (i.e., the fatigue truck). This was accomplished to determine the bias of the load effects. The force effects used in design were taken as the maximum stress range produced in any cross-frame that results from placing the fatigue truck at every transverse position (using a 1-foot increment) within the clear distance of the barriers. As discussed in Section 3.5 and 4.6, the sensitivity of a cross-frame to a wheel load is very localized; for this reason, the refined design truck footprint was utilized as prescribed in AASHTO Section 3.6.1.4.1 for the fatigue design of orthotropic decks.

Similar to the sensitivity study discussed in Section 4.4.2, the actual location of each 6-foot vehicle track width (i.e., transverse distance between left and right wheel lines) within the realistic lane utilized a distribution for which the vehicle is located in the center of the lane 55% of the time; 30% of the time, the vehicle is located plus or minus 1 foot of the lane centerline; 10% of the time, the vehicle is located plus or minus 2 feet of the lane centerline; and 5% of the time, the vehicle is riding along one of the lane edges. This is illustrated in Figure 5-1 for a sample 30-foot wide bridge, although the procedure is the same for different bridge widths and lane configurations. The intent of this assumed distribution is to consider the inherent variability of drivers locating their vehicle in a defined lane.

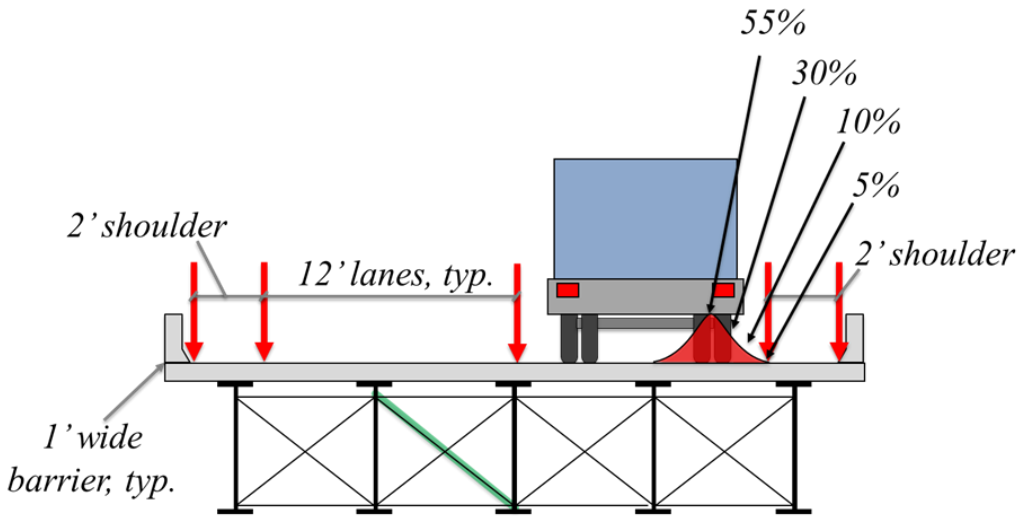

Figure 5-1: Illustration showing distribution of vehicle transverse location within 12-foot design lane for a 30-foot wide bridge.

5.2 REALISTIC DRIVE LANE ANALYSIS

The following subsections describe the advanced WIM analyses to calculate appropriate load biases for the Fatigue I and II limit states with respect to cross-frame design. Recalling from Chapter 2 that the load bias is defined as the ratio of the actual force effects to the force effects calculated in design, this was accomplished by comparing the WIM-related force effects to the maximum force effects created by the unfactored AASHTO design load to the same bridge in all possible transverse positions within the clear distance of the barriers. Note that the following results do not include a dynamic impact factor, since the WIM stations attempt to correct for dynamic effects and relate measured drive-by weights to static weights. It may be prudent to include a portion of the typical 0.15 impact factor (as specified in AASHTO Article 3.6.2.1), since the effects of bridge dynamics are not accounted for explicitly in the finite-element analyses that produced the influence surface plots for WIM analyses. The dynamic impact factor will be considered in the reliability study conducted in Chapter 6. The following sections discuss in detail the procedures used to simulate the stress ranges used in the Fatigue I and II limit states.

5.2.1 Fatigue I Stress Ranges

The governing Fatigue I stress range calculated for all WIM sites was determined based on 99.99th percentile criteria (i.e., the 1-in-10,000 exceedance stress range of all 16 to 20 critical

cross-frames for each bridge). This stress range corresponds to the lowest magnitude of the top 99.99th percentile of all stress ranges recorded (for the governing cross-frame for each bridge given the defined lane position). Figure 5-2 illustrates the selection of a Fatigue I stress range from a CDF of stress ranges for a given WIM site, cross-frame member, and bridge. In this figure, the stress range corresponding to the largest stress range recorded is approximately 7 ksi; however, the lowest stress range within the top 99.99th percentile stress ranges is shown to be 5.15 ksi. Thus, 5.15 ksi is considered the maximum stress for which AASHTO Fatigue I load criteria is evaluated.

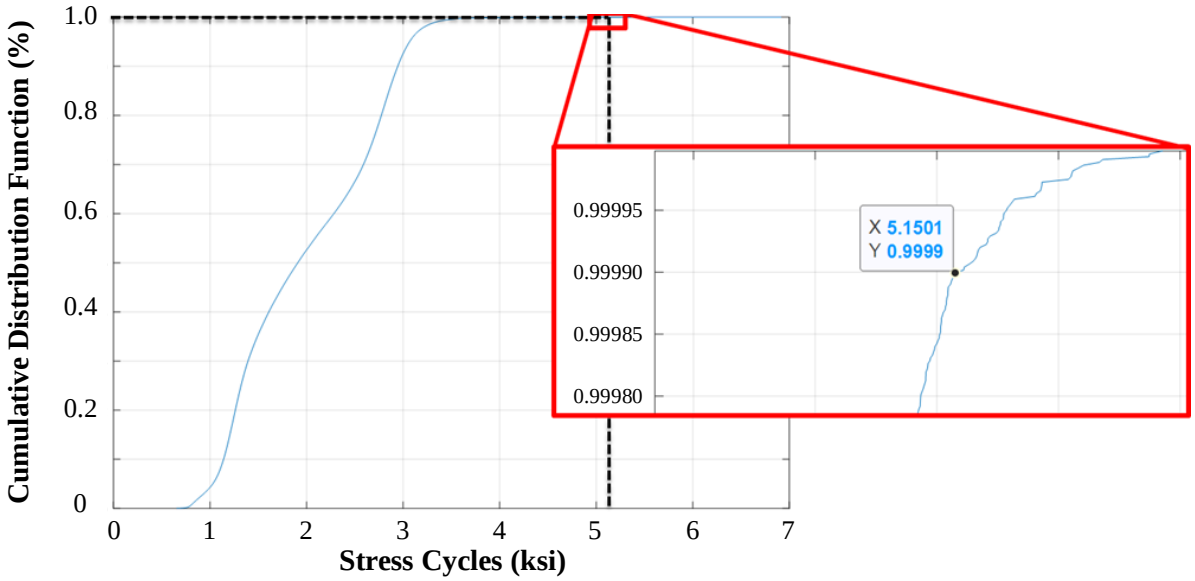

Figure 5-2: Illustration showing selection of 99.99th percentile stress range.

Once all Fatigue I stress ranges were calculated for each WIM site and each bridge (i.e., one value per cross-frame per bridge per WIM record), the stress ranges were normalized to the largest stress range produced by applying the unfactored AASHTO fatigue truck to the same bridge in all possible transverse positions within the clear distance of the barriers. Note that the positioning of the fatigue truck to create the largest stress range does not necessarily correspond to the location of the WIM traffic stream - this is consistent with a likely design approach, where the bridge (and its cross-frames) is designed based on the maximum stress range produced by locating the fatigue truck in the critical position between the barriers (in accordance to AASHTO Article 3.6.1.4.3).

The Fatigue I stress ranges and biases were calculated for each of the 20 bridges (see Appendix B) using all WIM site records, as well as the arithmetic mean of all stress ranges

produced by the 18 WIM site records, the standard deviation of all stress ranges produced by the 18 WIM site records, and the "mean plus 1.5 standard deviations" of all stress ranges produced by the 18 WIM site records. The average of all "mean plus 1.5 standard deviation" values is a convenient way to express a single bias value that encompasses the majority of all Fatigue I WIM stress ranges. In other words, the probability of a WIM site causing a Fatigue I stress range that exceeds this bias value is appreciably low (i.e., approximately 7 percent).

Figure 5-3 and Figure 5-4 summarize the ratios of the 99.99th percentile WIM stress ranges divided by the unfactored fatigue truck stress range for each bridge, before and after applying a stress range filter of 0.65 ksi (i.e., 0.25*CAFL for detail category E′), respectively. For both of these figures, each bin value represents the average of all Fatigue I stress ranges for all WIM sites applied to the identified bridge (as explained in the preceding paragraph). A solid line in each figure represents the arithmetic mean of all Fatigue I stress ranges for all WIM sites applied to the identified bridge. A dashed line in each figure represents the mean value of all "mean plus 1.5 standard deviations" (i.e., the mean plus 1.5 standard deviation for all values represented by the individual bars). The mean value of all "mean plus 1.5 standard deviations" would represent a single bias value that encompasses the majority of all Fatigue I stress ranges; consistent with previous research, this value would also correspond to an appropriate Fatigue I load factor for cross-frames. In other words, the stress ranges produced by the unfactored fatigue truck must be amplified by this factor to produce an equivalent 99.99th percentile stress range that represents the 99.99th percentile load effects caused by the WIM traffic streams. Without consideration of material fatigue resistances (and therefore the reliability index), the values in Figure 5-3 and Figure 5-4 associated with the mean value and "mean plus 1.5 standard deviations" value implies an appropriate load factor for the Fatigue I limit state is between 1.01 to 1.35 (with no stress range filtering), and a load factor of 1.24 to 1.63 (with stress range filtering), respectively. All values are less than the current Fatigue I load factor (1.75), which indicates a potential source of conservatism in the design load criteria.

Recall from Section 4.2 that the GVWs for the WIM records are not normal; rather, many WIM sites appear to have multi-modal distributions that likely correspond to natural groupings of different vehicle types and payload. Rather than solely use standard arithmetic equations to calculate the pertinent statistical values associated with a distribution, it is prudent to plot all normalized Fatigue I stress ranges on a normal probability scale to assess the normality of these

maximum stress ranges. Figure 5-5 represents a CDF of the normalized stress ranges plotted on a normal probability scale prior to truncating the stresses below 25% CAFL, and Figure 5-6 represents the same data after truncating stresses below 25% CAFL.

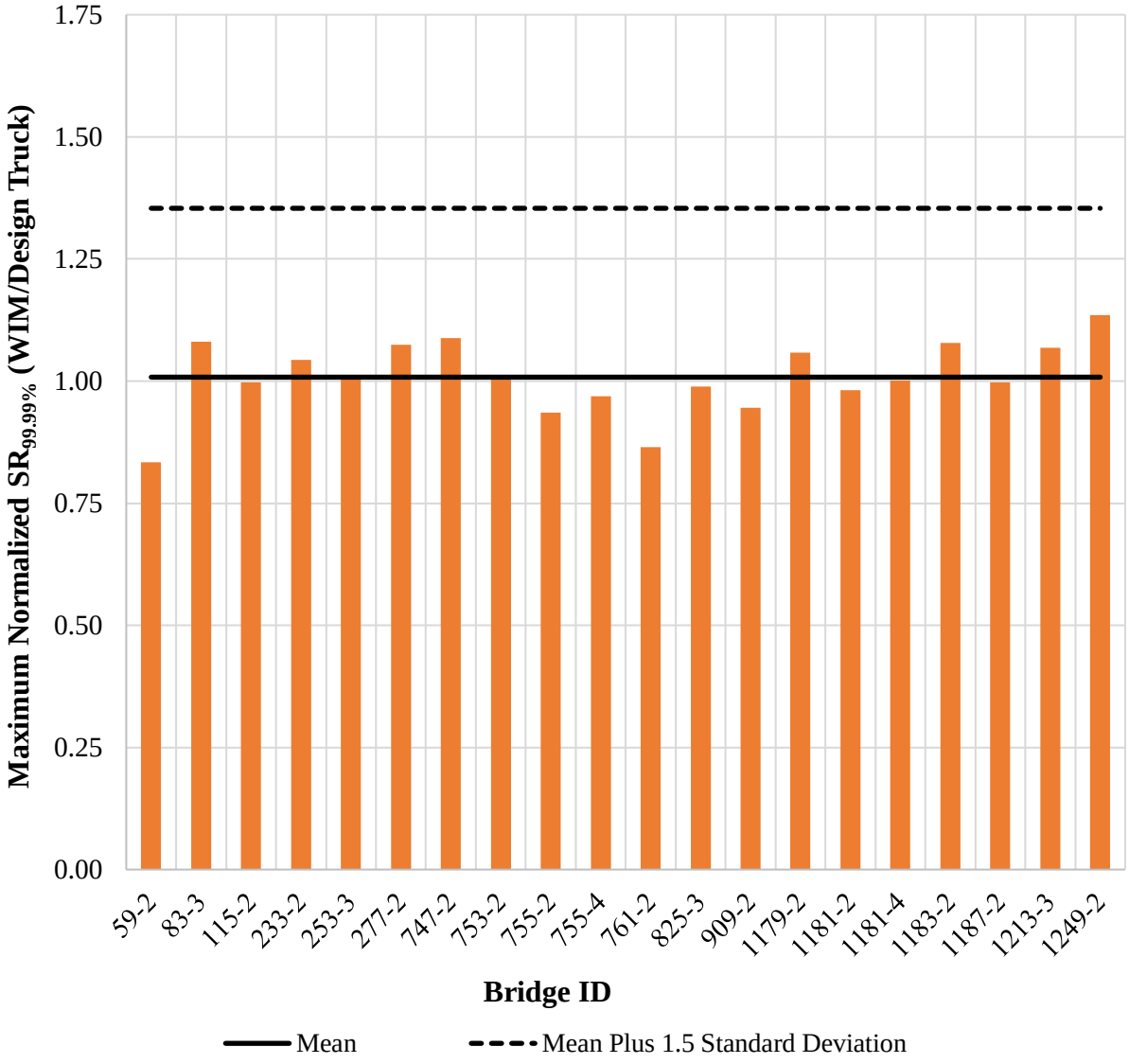

Figure 5-3: Summary of Fatigue I normalized 99.99% stress ranges ($SR_{99.99\%}$) for 18 WIM records and 20 sites prior to truncating the lower stress ranges (i.e., removing stress ranges less than 25% CAFL).

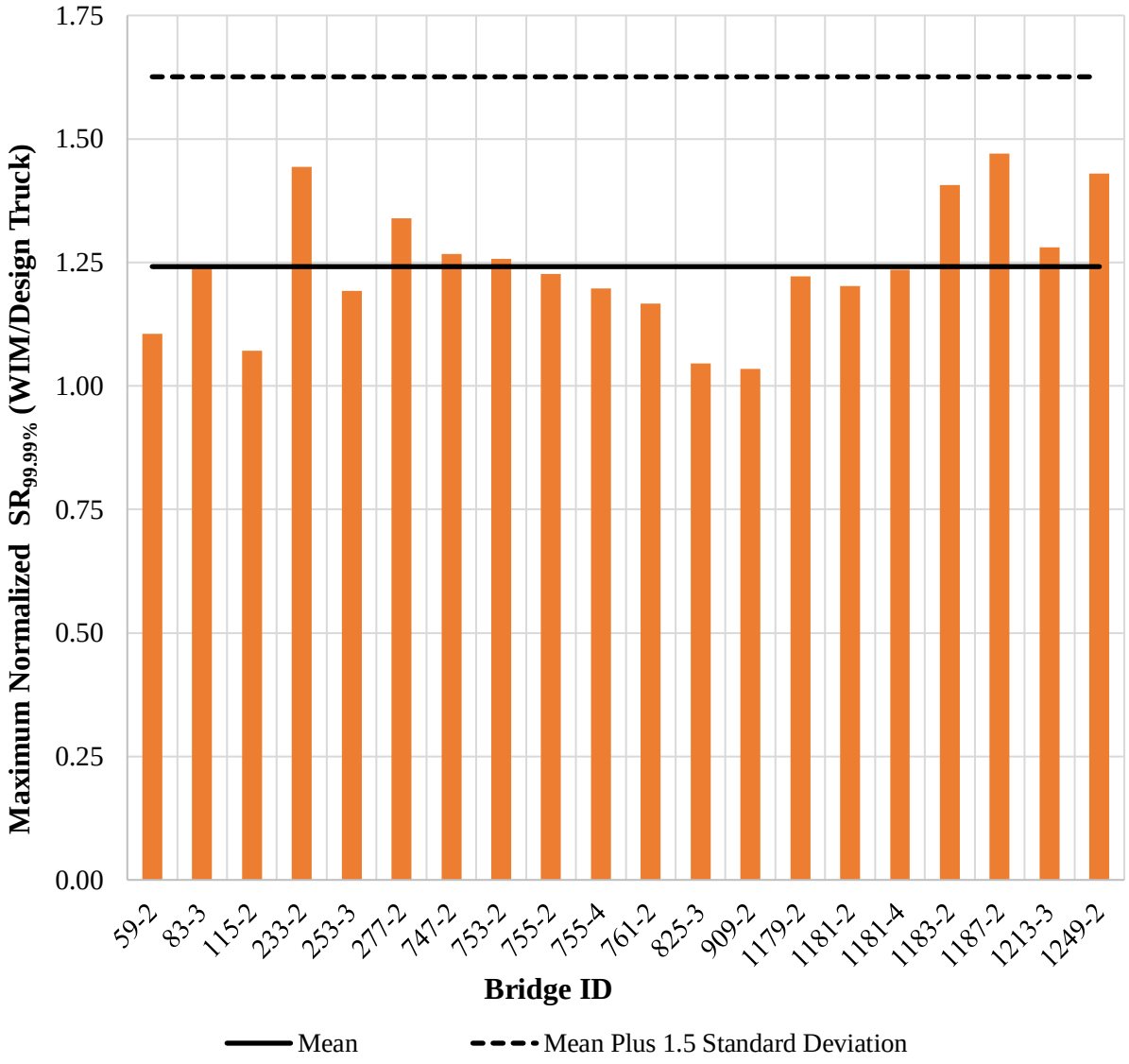

Figure 5-4: Summary of Fatigue I normalized 99.99% stress ranges ($SR_{99.99\%}$) for 18 WIM records and 20 sites after truncating the lower stress ranges (i.e., removing stress ranges less than 25% CAFL).

It is apparent that the distribution of normalized Fatigue I stress ranges prior to truncating the stresses is not normal; however, the Fatigue I stress ranges after removal of these lower stresses can be adequately described as normal distributions. By performing a linear regression analysis on the normalized values, the mean of the distributions corresponds to the horizontal axis value where the best fit line equals zero on the vertical axis (i.e., the standard normal variable is zero for a normal distribution). Additionally, the standard deviations of the data sets can be approximated by the inverse of the slope of the best fit line. Table 5-1 compares the standard deviations and means

obtained by the direct arithmetic calculation (represented in Figure 5-3 and Figure 5-4) and the normal probability scale approach.

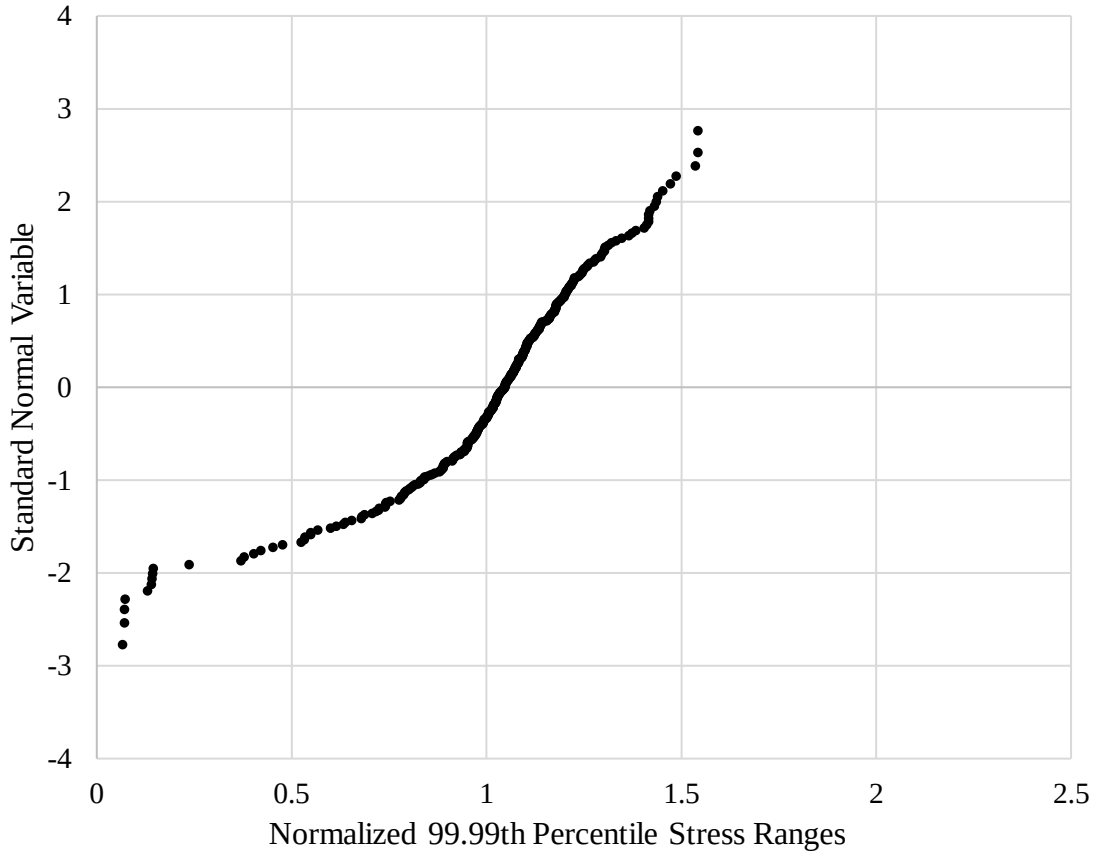

Figure 5-5: CDF of Fatigue I normalized 99.99th percentile stress ranges for 18 WIM records and 20 bridge sites prior to truncating the lower stress ranges (i.e., removing stress ranges less than 25% CAFL.

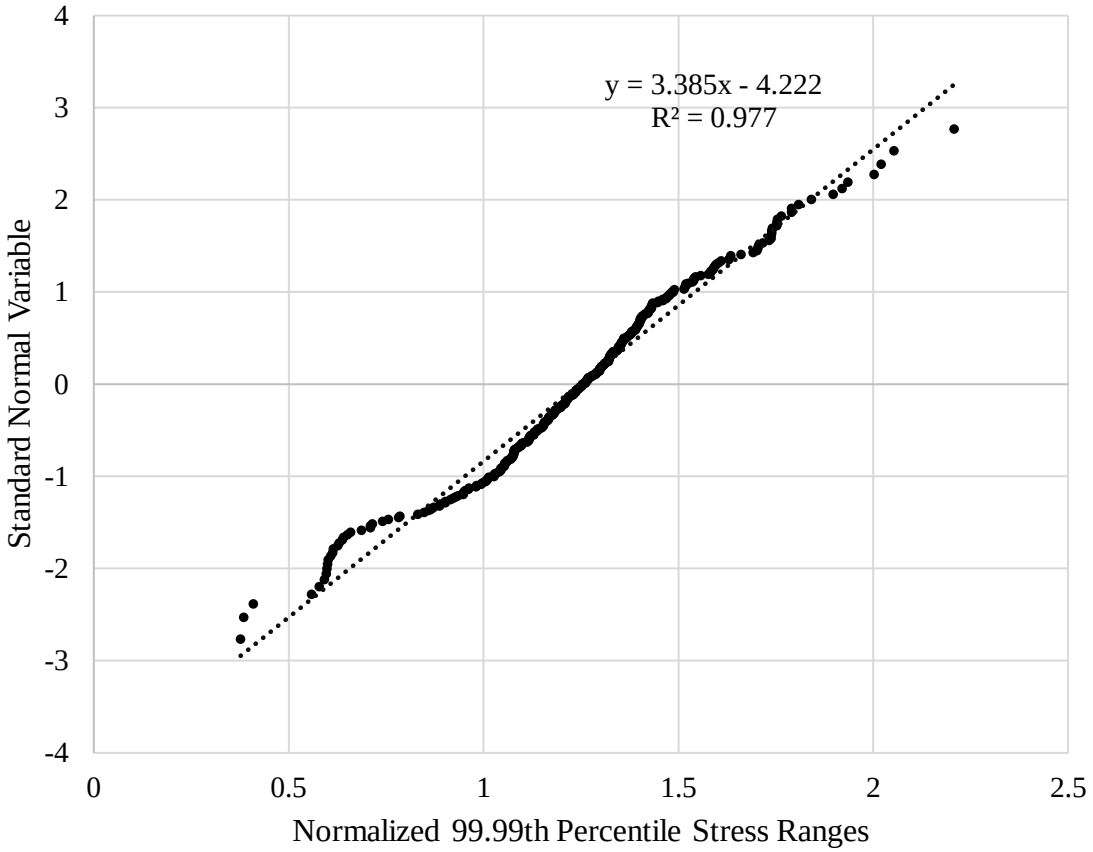

Figure 5-6: CDF of Fatigue I normalized 99.99th percentile stress ranges for 18 WIM records and 20 bridge sites after truncating the lower stress ranges (i.e., removing stress ranges less than 25% CAFL). A best fit line is demonstrated via linear regression.

Table 5-1: Comparison of statistical parameters obtained for the Fatigue I stress ranges by two methods.

		Mean	Standard Deviation	Mean Plus 1 Standard Deviation	Mean Plus 1.5 Standard Deviations
Prior to Removing Stresses Below 25% CAFL	Value Obtained by Direct Calculation	1.01	0.23	1.24	1.35
	Value Obtained from Normal Probability Scale	1.04	0.18	1.22	1.31
After Removing Stresses Below 25% CAFL	Value Obtained by Direct Calculation	1.24	0.25	1.50	1.63
	Value Obtained from Normal Probability Scale	1.24	0.30	1.54	1.69

As documented in the SHRP 2 R19B report (Kulicki, Wassef, et al. 2015), the value

associated with the "mean plus 1.5 standard deviations" was taken as both the bias of the data (R19B states this was a conservative measure, since it was unknown how accurately the WIM records used in the project reflected truck traffic across the nation), as well as an appropriate load factor. This resulted in a proposed load factor of 2.0 for Fatigue I; however, the load factor adopted in the 8th Edition of AASHTO *LRFD* was 1.75. Based on discussions with individuals knowledgeable on the selection of this load factor, it appears that the value of 1.75 was achieved by using the arithmetic mean of the normalized stress ranges produced by the WIM site records (i.e., the bias and load factor are both taken to be equal to the mean bias value). This was rationalized by acknowledging perceived conservatism inherent in the resistance data for Fatigue I and the fact that the WIM data reviewed was deemed to be sufficiently abundant to represent national traffic loads. Note that while the SHRP 2 R19B report indicates the bias and load factors were developed using the lightweight vehicle filtering (i.e., the removal of vehicles below 20 kips GVW similar to what was done in this advanced study), the report does not indicate whether the researchers truncated lower stress cycles directly.

5.2.2 Fatigue II Stress Ranges

In calculating the load bias of the Fatigue II stress ranges, it is possible to make this comparison by normalizing the effective stress range caused by the WIM traffic to the maximum stress range caused by the passage of the fatigue truck in the controlling transverse lane. However, since this comparison does not explicitly consider the stress cycle counts, it is more prudent to calculate the Fatigue II load bias by comparing the *fatigue damage* caused by the WIM traffic to the projected fatigue damage used in the design of the bridge. In the following sections, the results of the Fatigue II effective stress ranges are presented as both a normalization to the appropriate fatigue truck stress ranges as well as a normalization to fatigue damage caused by the fatigue truck.

Similar to the Fatigue I stress ranges, the governing Fatigue II stress ranges calculated for all WIM sites were determined based on the effective stress range for all 16 to 20 cross-frames for each bridge. In other words, one critical cross-frame produced WIM effective stress ranges that exceeded the remainder of the cross-frames in the bridge and thus served as the governing case. Recall that the Fatigue II limit state is intended to be representative of the effective or "average" effect of the traffic population. These effects are generally characterized by the effective stress range (or equivalent stress range) of the variable-amplitude response.

Recall from Section 2.4.2.3.1 that the number of stress cycles can be expressed to be inversely proportional to the cube of the stress range magnitude. Using the same relationship, the effective stress range can be expressed mathematically by the following equation:

$$S_{re} = \left(\frac{A}{N_R}\right)^{\frac{1}{3}} \quad \text{Eq. 5.17}$$

where:

N_R = number of cycles at the effective stress range, S_{re}, until failure, and

S_{re} = effective stress range (ksi).

In the equation above, the effective stress range, S_{re}, represents the fatigue damage caused by WIM traffic and is determined using Palmgren-Miner's rule using rainflow counting techniques on real stress cycles. The effective stress range mathematically characterizes a variable-amplitude response in terms of a constant-amplitude stress range of equal cycle count. Refer to Section 2.4.2.3 for a more detailed description of this calculation as in pertains to the Fatigue II limit state.

Once all Fatigue II effective stress ranges were calculated for each WIM site and each bridge using Eq. 5.17, the stress ranges were then normalized to the largest stress range produced by applying the unfactored fatigue truck to the same bridge in all possible transverse positions within the clear distance of the barriers (similar to Section 5.2.1 for Fatigue I criteria). Note that the positioning of the fatigue truck to create the largest stress range did not necessarily correspond to the location of the WIM traffic stream, which is consistent with the typical design approach.

The Fatigue II stress ranges and biases were calculated for each of the 20 bridges (see Appendix B) using all WIM site records, as well as the arithmetic mean of all stress ranges produced by the 18 WIM site records, the standard deviation of all stress ranges produced by the 18 WIM site records, and the "mean plus 1.5 standard deviations" of all stress ranges produced by the 18 WIM site records. The average of all "mean plus 1.5 standard deviation" values is a convenient way to express a single bias value that encompasses the majority of all Fatigue II WIM effective stress ranges. In other words, the probability of a WIM site causing a Fatigue II effective stress range that exceeds this bias value is appreciably low (i.e., approximately 7 percent).

Figure 5-7 and Figure 5-8 summarize the ratios of the effective WIM stress ranges divided by the unfactored fatigue truck stress range for each bridge, both before and after applying a stress range filter of 0.65 ksi (i.e., 0.25*CAFL for detail category E′). For both of these figures, each bin

value represents the mean of all Fatigue II effective stress ranges for all WIM sites applied to the identified bridge (as explained in the preceding paragraph). A solid line in each figure represents the arithmetic mean of all Fatigue II effective stress ranges for all WIM sites applied to the identified bridge. A dashed line in each figure represents the mean value of all "mean plus 1.5 standard deviations" (i.e., the mean plus 1.5 standard deviation for all values represented by the individual bars); this dashed line is the single bias value that encompasses the majority of all Fatigue II effective stress ranges. In other words, the stress ranges produced by the unfactored fatigue truck must be amplified by this factor to produce an equivalent effective stress range that represents the maximum load effects caused by the WIM traffic streams. Using the effective stress range as the metric for comparison, an appropriate load factor for Fatigue II in the context of these 20 representative bridges is 0.34 (prior to applying the CAFL filter) and 0.55 (after applying the CAFL filter) based on the "mean plus 1.5 standard deviations" criteria. Note that an appropriate load factor (without consideration of material resistances, and therefore the reliability index) should consider the actual damage accumulation given the effective stress range and number of cycles experienced by the member. This comparison is discussed in the next section.

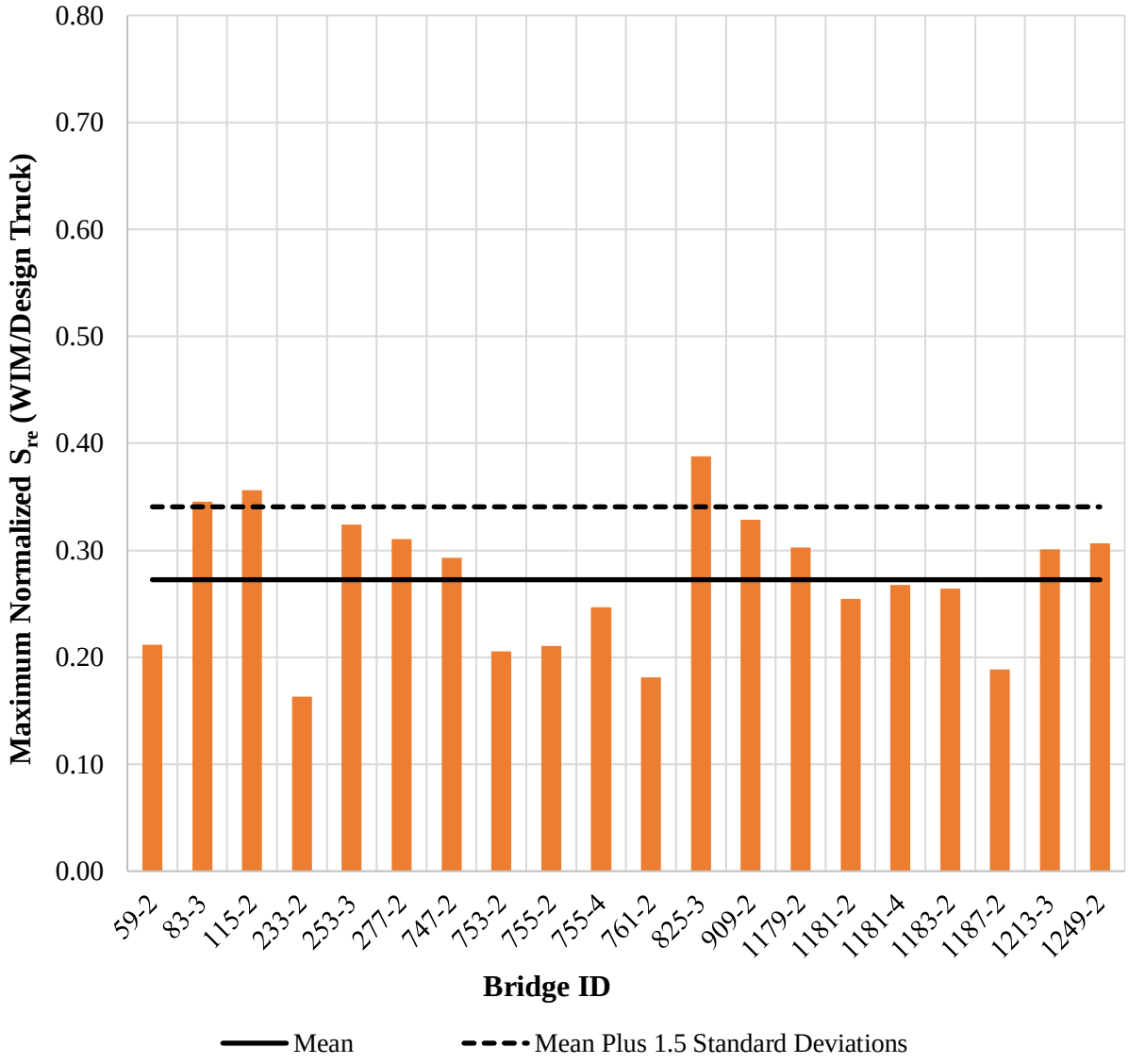

Figure 5-7: Summary of Fatigue II normalized effective stress ranges (S_{re}) for 18 WIM records and 20 sites prior to truncating the lower stress ranges (i.e., removing stress ranges less than 25% CAFL).

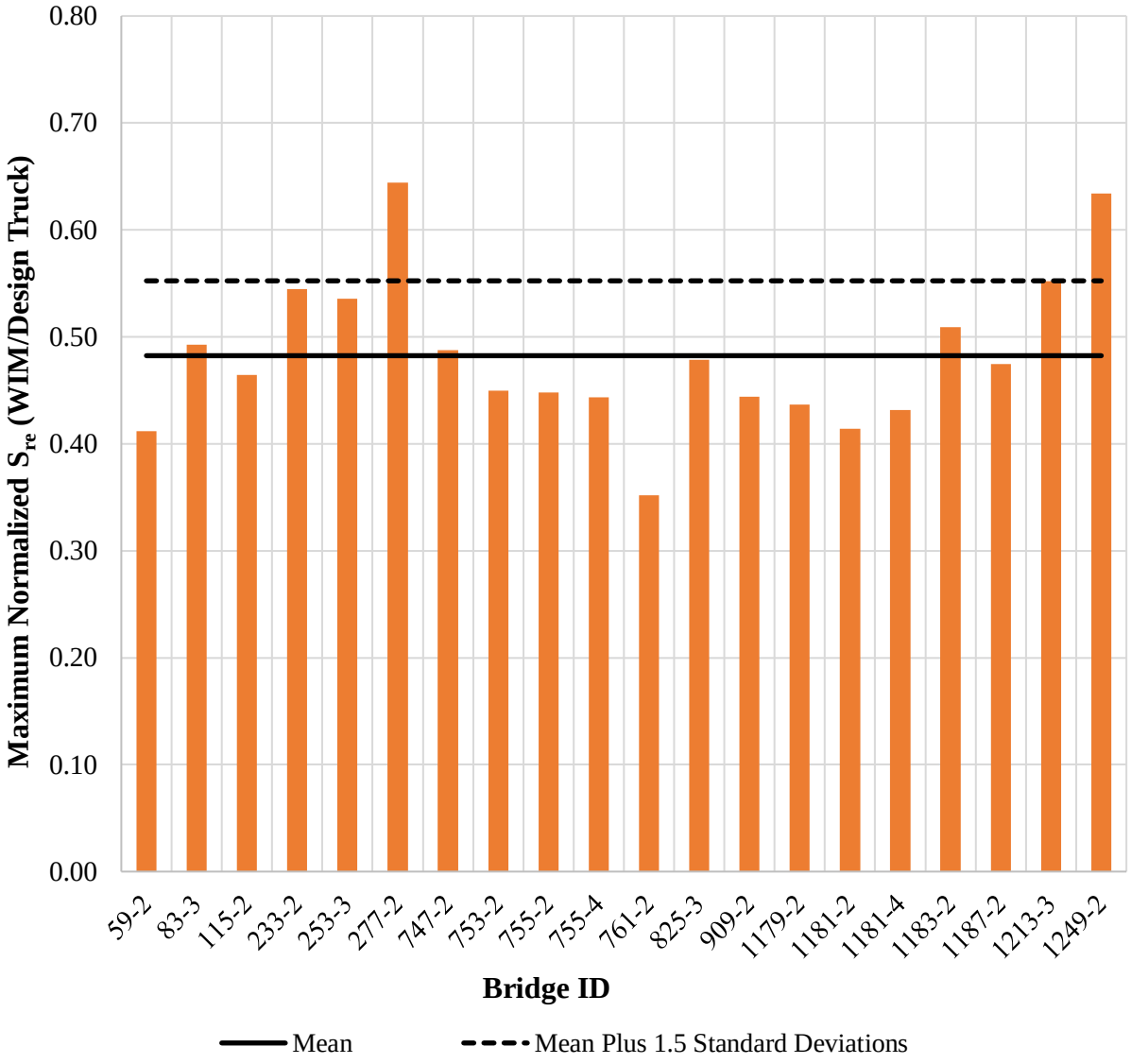

Figure 5-8: Summary of Fatigue II normalized effective stress ranges (S_{re}) for 18 WIM records and 20 sites after truncating the lower stress ranges (i.e., removing stress ranges less than 25% CAFL).

5.2.3 Fatigue II Damage Ratios

Similar to the previous section, the Fatigue II design criteria can also be evaluated in terms of accumulated damage, as opposed to simply the normalized effective stress range of the truck population spectra. The accumulated damage metric inherently considers both the variable stress range magnitudes and the number of cycles. Thus, the total damage accumulated by the various WIM traffic streams on the critical, governing cross-frame members is compared to the damage accumulated by the AASHTO fatigue truck (based on AASHTO criteria for the relationship

between number of trucks and number of cycles).

With that in mind, the fatigue damage caused by the AASHTO design load can by expressed by the following equation (in terms of stress range, similar to Eq. 5.17 for the effective stress range caused by WIM traffic):

$$S = \left(\frac{A}{N}\right)^{\frac{1}{3}} \quad \text{Eq. 5.18}$$

where:

N = number of total design cycles $= (365)(75)n(ADTT)_{SL}$,

S = governing design stress range caused by the AASHTO fatigue truck (ksi),

n = cycles per truck passage, calculated from AASHTO Table 6.6.1.2.5-2; taken as 1.0 for the results herein, and

$(ADTT)_{SL}$ = Annual Daily Truck Traffic for a single lane.

The boundaries of fatigue damage caused by the WIM traffic stream and the fatigue design truck can be related by equating Eq. 5.19 and Eq. 5.20 to form Eq. 5.21:

$$1 = \left(\frac{A}{N_R}\right)^{\frac{1}{3}} * \frac{1}{S_{re}} \quad \text{Eq. 5.19}$$

$$1 = \left(\frac{A}{N}\right)^{\frac{1}{3}} * \frac{1}{S} \quad \text{Eq. 5.20}$$

$$\left(\frac{A}{N_R}\right)^{\frac{1}{3}} * \frac{1}{S_{re}} = \left(\frac{A}{N}\right)^{\frac{1}{3}} * \frac{1}{S} \quad \text{Eq. 5.21}$$

Eq. 5.21 can be rearranged to form the ratio of actual (WIM) fatigue damage to the fatigue damage caused by the design truck. Consistent with SHRP 2 Project R19B studies, we will define this ratio, λ, as the "fatigue damage ratio":

$$\lambda = \frac{\left(\frac{A}{N_R}\right)^{\frac{1}{3}} * \frac{1}{S_{re}}}{\left(\frac{A}{N}\right)^{\frac{1}{3}} * \frac{1}{S}} = \sqrt[3]{\frac{N_R}{N}} * \frac{S_{re}}{S} \quad \text{Eq. 5.22}$$

Values of λ less than unity indicate that the damage accumulated by the WIM data is less

than that of the assumed values based on AASHTO design criteria (i.e., the design criteria is overly conservative); the opposite is true to values of λ larger than unity.

Table D-37 through Table D-54 summarizes the results from applying all 18 WIM site records to each of the 20 selected bridges for the advanced WIM studies (i.e., one table per WIM record). The 20 representative bridges are identified numerically.

Each table provides the fatigue damage ratio and biases calculated for the bridge using all WIM site records, the arithmetic mean of all stress ranges produced by the 18 WIM site records, the standard deviation of all stress ranges produced by the 18 WIM site records, and the "mean plus 1.5 standard deviations" of all stress ranges produced by the 18 WIM site records. The average of all "mean plus 1.5 standard deviation" values is a convenient way to express a single bias value that encompasses the majority of all Fatigue II WIM fatigue damage ratios. In other words, the probability of a WIM site causing a fatigue damage ratio that exceeds this bias value is appreciably low (i.e., approximately 7 percent).

Figure 5-9 and Figure 5-10 summarize the ratios of the WIM fatigue damage divided by the maximum fatigue damage due to the unfactored fatigue truck for each bridge, both before and after applying a stress range filter of 0.65 ksi (i.e., 0.25*CAFL for detail category E′). For both of these figures, each bin value represents the "mean plus 1.5 standard deviations" of all fatigue damage ratios for all WIM sites applied to the identified bridge (as explained in the preceding paragraph). A solid line in each figure represents the arithmetic mean of all fatigue damage ratios for all WIM sites applied to the identified bridge. A dashed line in each figure represents the mean value of all "mean plus 1.5 standard deviations" (i.e., the mean plus 1.5 standard deviation for all values represented by the individual bars); this dashed line is the single bias value that encompasses the majority of all fatigue damage ratios, and corresponds to an appropriate Fatigue II load factor for cross-frames. In other words, the fatigue damage produced by the unfactored fatigue truck must be amplified by this factor to produce an equivalent fatigue damage caused by the WIM traffic streams.

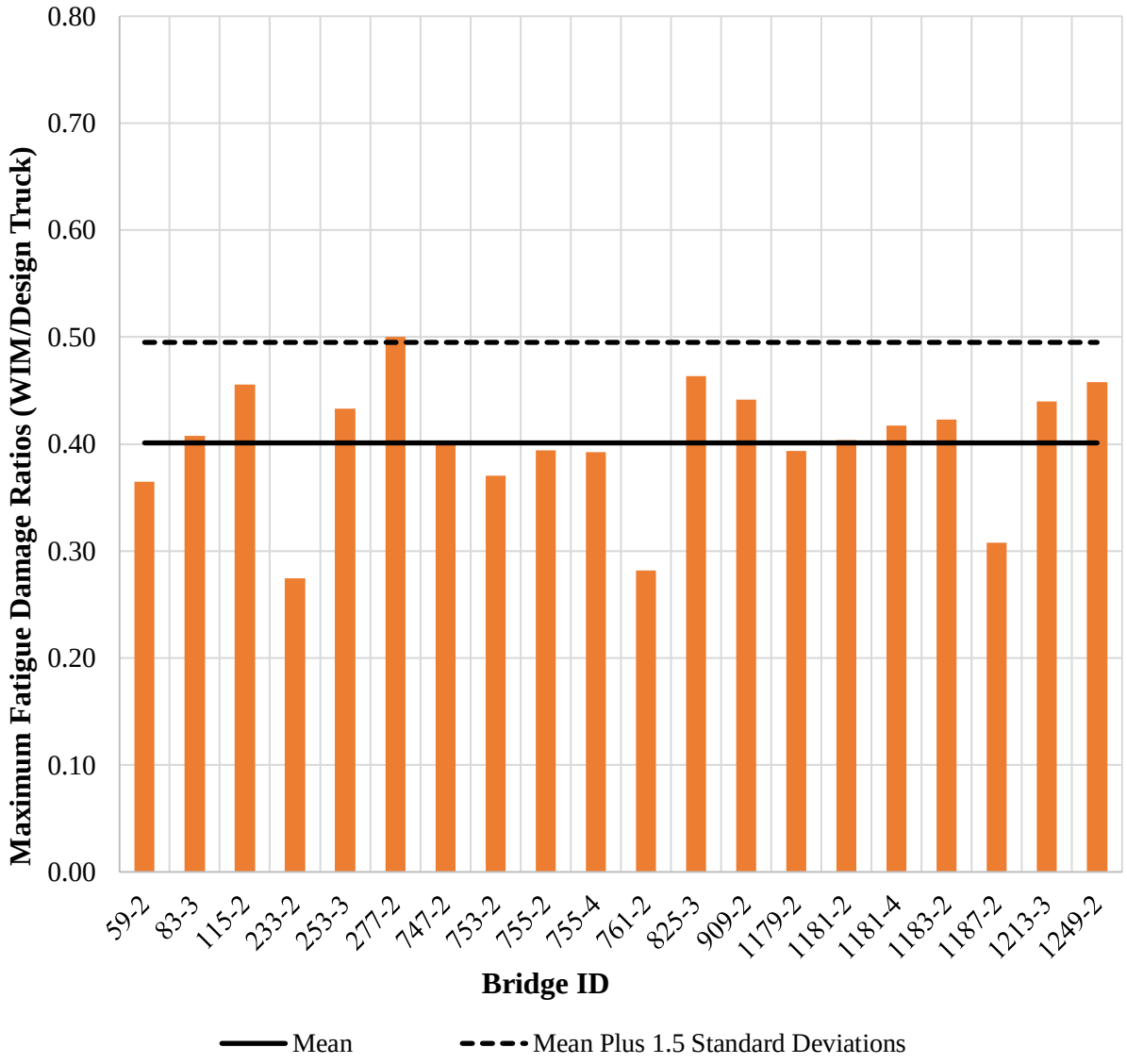

Figure 5-9: Summary of Fatigue II damage ratios for 18 WIM records and 20 sites prior to truncating the lower stress ranges (i.e., removing stress ranges less than 25% CAFL).

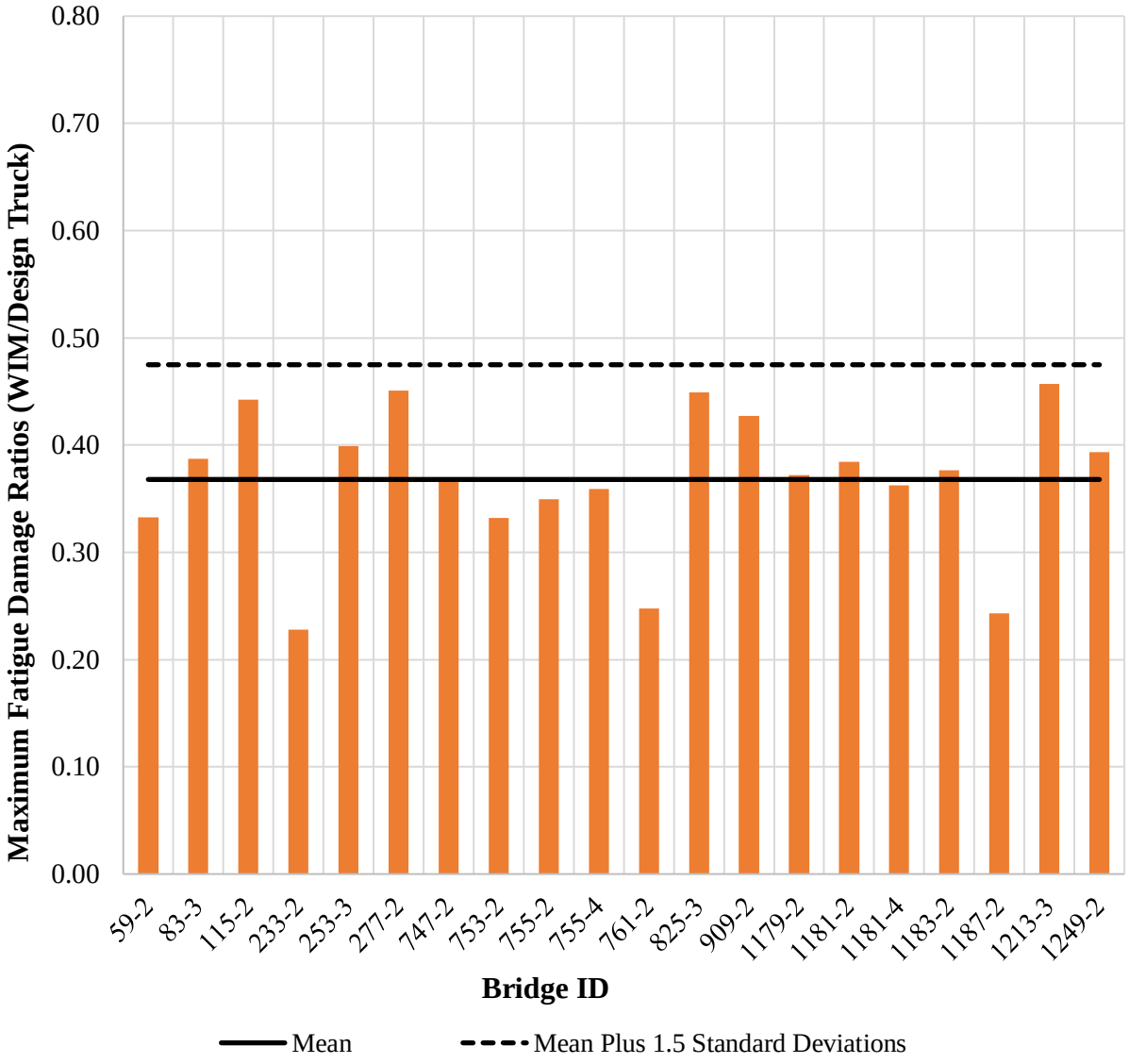

Figure 5-10: Summary of maximum Fatigue II damage ratios for 18 WIM records and 20 sites after truncating the lower stress ranges (i.e., removing stress ranges less than 25% CAFL).

Without consideration of material fatigue resistances (and therefore the reliability index), the value associated with the "mean plus 1.5 standard deviations" implies an appropriate load factor for the Fatigue II limit state is 0.50 to 0.53 (prior to 25% CAFL filtering) and 0.47 to 0.52 (after 25% CAFL filtering). Both values are less than the current Fatigue II load factor of 0.8, which suggests that the current load factor may be quite conservative for cross-frames.

Similar to the comparison made in Section 5.2.1, the fatigue damage ratios for all WIM records and all bridges were plotted on a normal probability scale to assess the normality of the damage ratios. Figure 5-11 represents a CDF of the fatigue damage ratios plotted on a normal

probability scale prior to truncating the stresses below 25% CAFL, and Figure 5-12 represents the same data after truncating stresses below 25% CAFL.

It is apparent that both distributions of Fatigue II damage ratios can be adequately described as normal distributions. By performing a linear regression analysis on the normalized values as described in Section 5.2.1, the mean and standard deviations of the distributions are calculated. Table 5-2 compares the standard deviations and means obtained by the direct arithmetic calculation (represented in Figure 5-7 and Figure 5-8) and the normal probability scale approach.

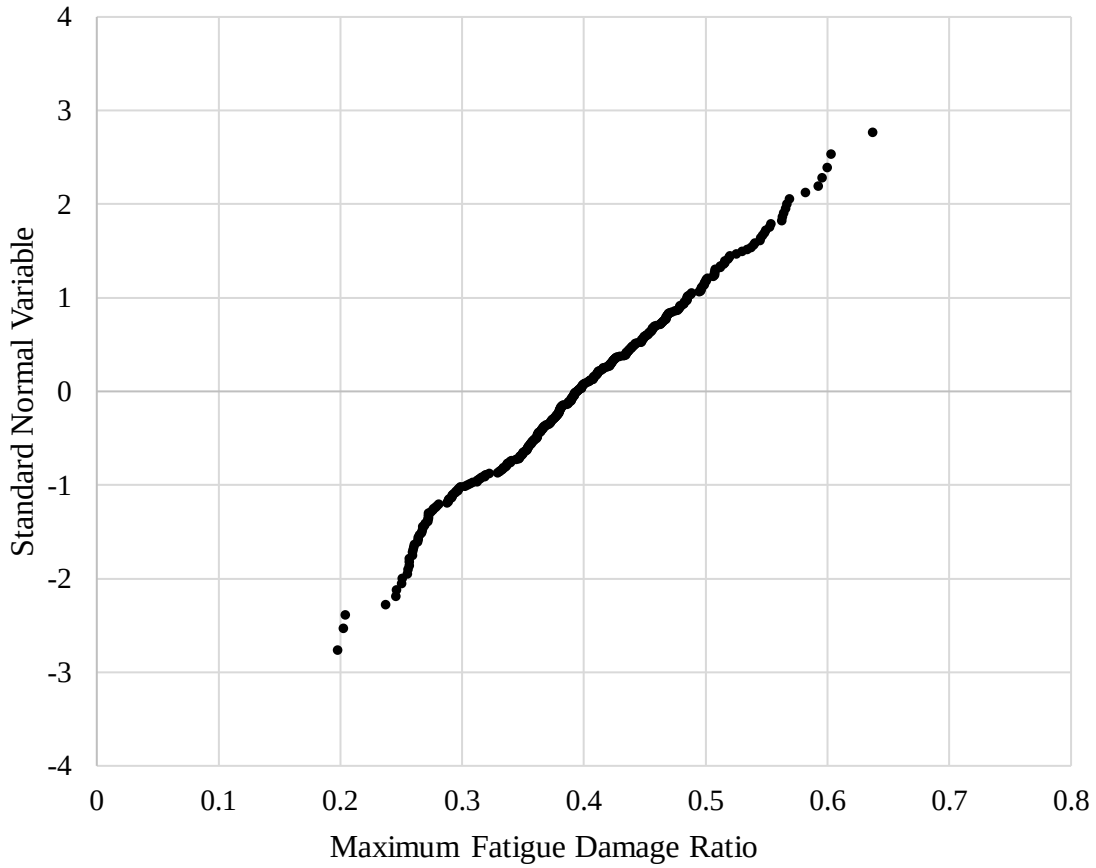

Figure 5-11: CDF of maximum Fatigue II damage ratios for 18 WIM records and 20 bridge sites prior to truncating the lower stress ranges (i.e., removing stress ranges less than 25% CAFL).

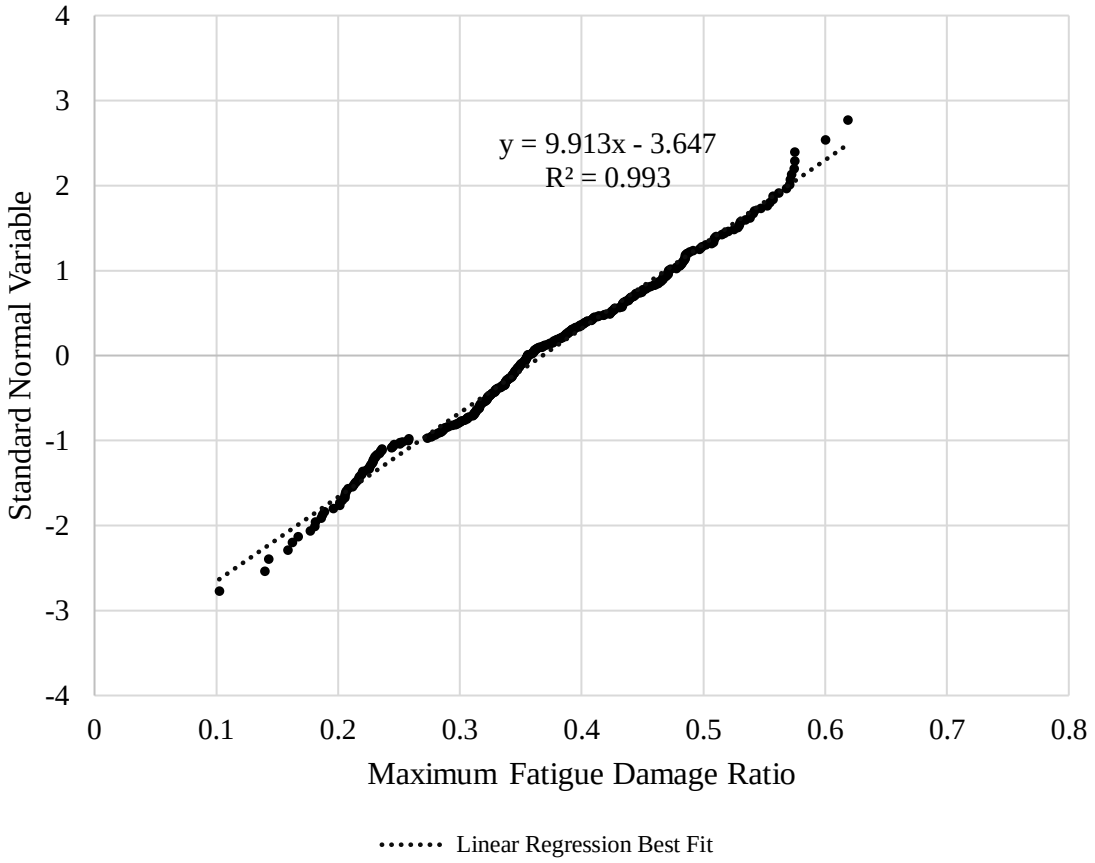

Figure 5-12: CDF of maximum Fatigue II damage ratios for 18 WIM records and 20 bridge sites after truncating the lower stress ranges (i.e., removing stress ranges less than 25% CAFL). A best fit line is demonstrated via linear regression.

Table 5-2: Comparison of statistical parameters obtained for the Fatigue II damage ratios by two methods.

		Mean	Standard Deviation	Mean Plus 1 Standard Deviation	Mean Plus 1.5 Standard Deviations
Prior to Removing Stresses Below 25% CAFL	Value Obtained by Direct Calculation	0.40	0.06	0.46	0.50
	Value Obtained from Normal Probability Scale	0.40	0.09	0.49	0.53
After Removing Stresses Below 25% CAFL	Value Obtained by Direct Calculation	0.37	0.07	0.43	0.47
	Value Obtained from Normal Probability Scale	0.37	0.10	0.47	0.52

The use of the "mean plus 1.5 standard deviations" as an indicator of an appropriate load factor is consistent with research documented in SHRP 2 Project R19B and the subsequent development of the 0.8 load factor for Fatigue II. Note that while the SHRP 2 Project R19B report indicates this load factor was developed using the lightweight vehicle filtering (i.e., the removal of vehicles below 20 kips GVW similar to what was done in this advanced study), the report does not indicate whether the researchers truncated lower stress cycles directly.

5.2.4 Comparative Study using Primary Member Calibration Data

The calibration of the current AASHTO LRFD load factors for the Fatigue I and II limit states was based entirely on the moment responses of primary girders to WIM traffic streams as described in the project report for SHRP 2 R19B. In order to directly compare the results of the advanced Fatigue I and Fatigue II WIM analyses discussed in this chapter to the results obtained by the SHRP 2 R19B project, the automated scripts discussed in Section 4.3 were modified to simulate the WIM traffic streams over a bridge in order to calculate the Fatigue I and II parameters (i.e., the maximum 99.99th percentile stress range and the maximum fatigue damage ratio). The published data in the SHRP 2 R19B report includes primary girder force effects for simply supported bridges (positive bending moment at midspan) and two-span continuous bridges (negative bending moment at the interior support and positive bending moment at 0.4 times the span length); in addition, the published data provides these bending moment values for 30, 60, 90, 120, and 200 foot long spans. For this comparative study, a simply supported bridge was chosen from the 20-model subset with a span length of 200 feet (i.e., this is the only simply supported bridge with a common span length for direct comparison). It is important to note that the WIM traffic streams used in this comparison are distinctly different WIM records than those used in the SHRP 2 R19B calibration.

The Fatigue I and II parameters published in the SHRP 2 R19B report for positive bending moment at midspan for a 200-foot long simply supported bridge are summarized in Table 5-3, and include 15 WIM records. At the bottom of this table, the statistical parameters for this data set are provided, including the mean of the Fatigue I and II parameters, the "mean plus 1 standard deviation" of the Fatigue I and II parameters, and the "mean plus 1.5 standard deviations" of the Fatigue I and II parameters. Note that the process used in the SHRP 2 study for choosing the mean and standard deviation of the data set is slightly more rigorous than the method used in this study

- the SHRP 2 study obtained this statistical data by plotting the various data on normal probability plots, and this study performed calculations on the data set directly using standard formulas for normal distributions. The use of standard formulas is justified, since the distributions of the Fatigue I and II parameters are demonstrated to be approximately normal, and the method of using normal probability plots was found to yield very similar results. When using normal probability plots, a regression analysis is performed on the various data, and the mean is taken as the intersection of the fitted line and the Y=0 axis; the standard deviation is taken as the slope of the fitted line.

Instead of calculating stress ranges in individual cross-frames due to a moving load fixed to a transverse position or range of positions, the automated scripts were modified to calculate the maximum positive bending moment at midspan of the selected bridge using a 1-dimensional influence line.

In order to maintain consistency with the approach to cross-frames, the process used to filter WIM records, obtain the load history, perform cycle counts, and calculate the various results is exactly the same as done with cross-frames. Besides the use of completely different WIM records, another primary difference between the two simulation approaches involves the level of detail in modeling the fatigue design truck. The SHRP 2 study used the fatigue design truck footprint as specified in AASHTO LRFD Article 3.6.1.2.2 (i.e., the individual axle loads are taken as clustered point loads - an 8 kip steering axle followed by two 32 kip axles, spaced at 14 and 30 feet, respectively); this study uses the refined design truck footprint as specified in AASHTO LRFD Article 3.6.1.4.1 (i.e., the individual axle loads are modeled in greater detail as an 8 kip steering axle followed by four 16 kip axles, spaced at 12, 4, 26, and 4 feet, respectively). In the comparison study, the automated scripts also include a 10% dynamic load allowance, since it appears that the SHRP 2 study considers this in the published data.

Table 5-3: Fatigue I and II parameters published in the SHRP 2 R19B for positive bending of a simply-supported 200-foot long bridge. The statistical summary of the parameters is not taken from the SHRP 2 R19B report.

WIM Record Details		**Fatigue I Parameters**		**Fatigue II Parameters**		
Site	**No. of Vehicles**	**99.99th Percentile Moment Cycle (kip-ft)**	**99.99th Percentile Moment Cycle Normalized to AASHTO Fatigue Truck (kip-ft)**	**Equivalent Moment (kip-ft)**	**Equivalent Moment (kip-ft) Normalized to the AASHTO Fatigue Truck**	**Fatigue Damage Ratio**
New Mexico	26,501	5,640	1.84	2,594	0.85	0.85
Arizona	1,391,098	4,711	1.54	2,601	0.85	0.85
Arkansas	1,642,334	5,066	1.65	2,555	0.83	0.83
Colorado	326,017	4,854	1.58	2,311	0.75	0.76
Delaware	175,889	5,735	1.87	2,424	0.79	0.79
Illinois	821,809	5,033	1.64	2,533	0.83	0.83
Kansas	456,881	6,083	1.99	2,525	0.82	0.83
Louisiana	70,831	6,616	2.16	2,319	0.76	0.76
Maine	172,333	5,549	1.81	2,206	0.72	0.72
Maryland	124,474	5,061	1.65	1,983	0.65	0.65
Minnesota	47,794	6,225	2.03	2,220	0.72	0.72
Pennsylvania	1,458,818	5,291	1.73	2,469	0.81	0.81
Tennessee	1,583,151	4,906	1.60	2,418	0.79	0.79
Virginia	237,804	5,055	1.65	2,356	0.77	0.77
Wisconsin	209,239	5,396	1.76	2,350	0.77	0.77
Total Count	**8,744,973**	***Mean***	***1.77***		***Mean***	***0.78***
		Mean + 1SD	***1.95***		***Mean + 1SD***	***0.84***
		Mean + 1.5SD	***2.04***		***Mean + 1.5SD***	***0.87***

The results of the comparative study are summarized in Table 5-4 and represent the application of all 18 WIM site records used in this study to the selected bridge. At the bottom of this table, the statistical parameters for this data set are provided, including the mean of the Fatigue I and II parameters, the "mean plus 1 standard deviation" of the Fatigue I and II parameters, and the "mean plus 1.5 standard deviations" of the Fatigue I and II parameters. The good agreement between the responses provides confidence in the modeling approach (i.e., automated scripts), the

fatigue parameter calculations (e.g., rainflow counting methodology), as well as the general effects of two different WIM data sets.

5.3 CYCLES PER PASSAGE

Using the total number of cycles recorded for each of the drive lane analyses (i.e., 18 WIM record sites applied to 20 bridges), the average cycles per passage was computed both before and after truncating stresses below 25% CAFL. The average number of cycles per passage due to the WIM truck records is calculated by dividing the total number of cycles counted via rainflow techniques by the lane's ADTT and number of days recorded in the year. Figure 5-13 through Figure 5-30 show the results for all 18 sites applied to 20 bridges. The bins in these plots represent the mean number of cycles per truck passage for the given bridge, and the dashed lines represent the average of all mean cycles per passage. The values are represented for both before and after truncation of stresses below 25% CAFL.

The results are similar to the drive lane analysis performed in Chapter 4, in that the pre-filtered cycles per passage vary widely per bridge. Interestingly, the magnitude of the average cycles per passage is generally consistent across all WIM traffic records for individual bridges (e.g., Bridge ID 755-2 generally has a higher average cycle per passage than the other 20 bridges, and Bridge ID 83-3 generally has the lowest average cycles per passage). This is illustrated in Figure 5-31 and Figure 5-32, and implies that some of bridge's parameters have a greater propensity for inducing more cycles per passage than others. Because the 20 model data set is intended to represent a very large selection of bridges with widely-varying geometries and material composition, it is not possible to draw specific conclusions with regard to the specific features of a bridge that result in more cycles per passage.

Similar to the findings in Chapter 4, the truncation of stresses significantly lowers the mean cycle per passage for each bridge; the results tend to be more uniform across all bridges and WIM records, with mean values per bridge all less than unity. It is evident that the effect of truncating stress ranges below 0.65 ksi (25% CAFL) significantly reduces the number of cycles counted; furthermore, since the average cycles per passage for the filtered case includes many values less than unity, it is clear that the majority of cycles caused by the WIM traffic are actually less than 0.65 ksi (i.e., it is physically impossible to have a truck passage with less than 1 cycle per passage).

Table 5-4: Fatigue I and II parameters using 18 WIM records for positive bending of a simply-supported 200-foot long bridge.

WIM Record Details		Fatigue I Parameters		Fatigue II Parameters		
Site	**No. of Vehicles**	**99.99th Percentile Moment Cycle (kip-ft)**	**99.99th Percentile Moment Cycle Normalized to AASHTO Fatigue Truck (kip-ft)**	**Equivalent Moment (kip-ft)**	**Equivalent Moment (kip-ft) Normalized to the AASHTO Fatigue Truck**	**Fatigue Damage Ratio**
Arizona	1,227,567	6,133	2.00	2,568	0.84	0.84
Arkansas	1,704,481	6,667	2.17	2,727	0.89	0.87
California	1,380,075	4,881	1.59	2,480	0.81	0.81
Colorado	352,198	6,700	2.18	2,405	0.78	0.79
Illinois	798,935	6,061	1.98	2,628	0.86	0.85
Indiana L1	370,241	5,858	1.91	2,525	0.82	0.82
Indiana L3	21,340	5,158	1.68	2,500	0.82	0.82
Indiana L4	360,458	5,525	1.80	2,499	0.82	0.82
Indiana L2	20,158	5,510	1.80	2,695	0.88	0.88
Kansas	436,913	6,294	2.05	2,609	0.85	0.85
Louisiana	76,547	7,326	2.39	2,421	0.79	0.79
Maryland	108,881	5,286	1.72	2,274	0.74	0.73
Minnesota	52,757	7,162	2.34	2,550	0.83	0.83
New Mexico	147,077	5,925	1.93	2,348	0.77	0.76
New Mexico	892,295	7,033	2.29	2,708	0.88	0.88
Pennsylvania	873,903	6,439	2.10	2,623	0.86	0.78
Tennessee L1	550,858	6,750	2.20	2,246	0.73	0.66
Tennessee L2	118,000	4,844	1.58	1,845	0.60	0.54
Tennessee L3	191,330	4,890	1.59	2,106	0.69	0.62
Tennessee L4	1,182,136	6,423	2.09	2,609	0.85	0.77
Virginia L1	224,928	5,700	1.86	2,405	0.78	0.79
Virginia L2	19,300	4,641	1.51	2,286	0.75	0.75
Wisconsin	120,079	6,349	2.07	2,497	0.81	0.82
Total Count	**11,230,457**	***Mean***	***1.95***		***Mean***	***0.79***
		Mean + 1SD	***2.21***		***Mean + 1SD***	***0.87***
		Mean + 1.5SD	***2.34***		***Mean + 1.5SD***	***0.91***

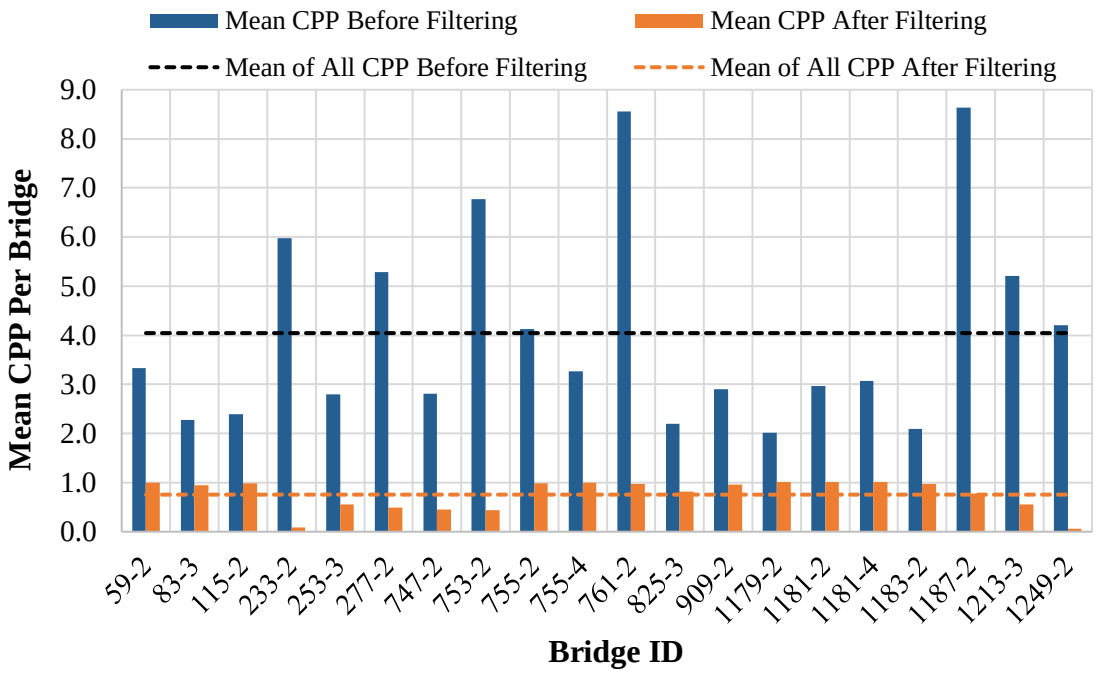

Figure 5-13: Summary of cycles per passage (CPP) for Arkansas I-30 (AR1). Includes results both before and after stress truncation (i.e., removing stress ranges less than 25% CAFL).

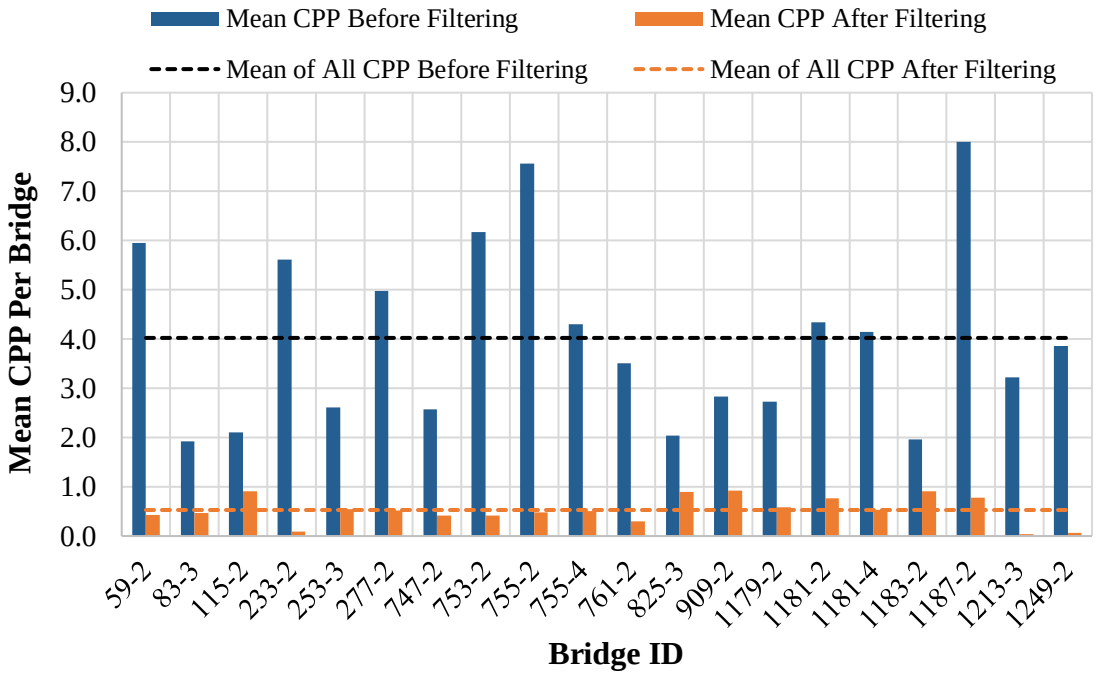

Figure 5-14: Summary of cycles per passage (CPP) for Arizona I-10 (AZ2). Includes results both before and after stress truncation (i.e., removing stress ranges less than 25% CAFL).

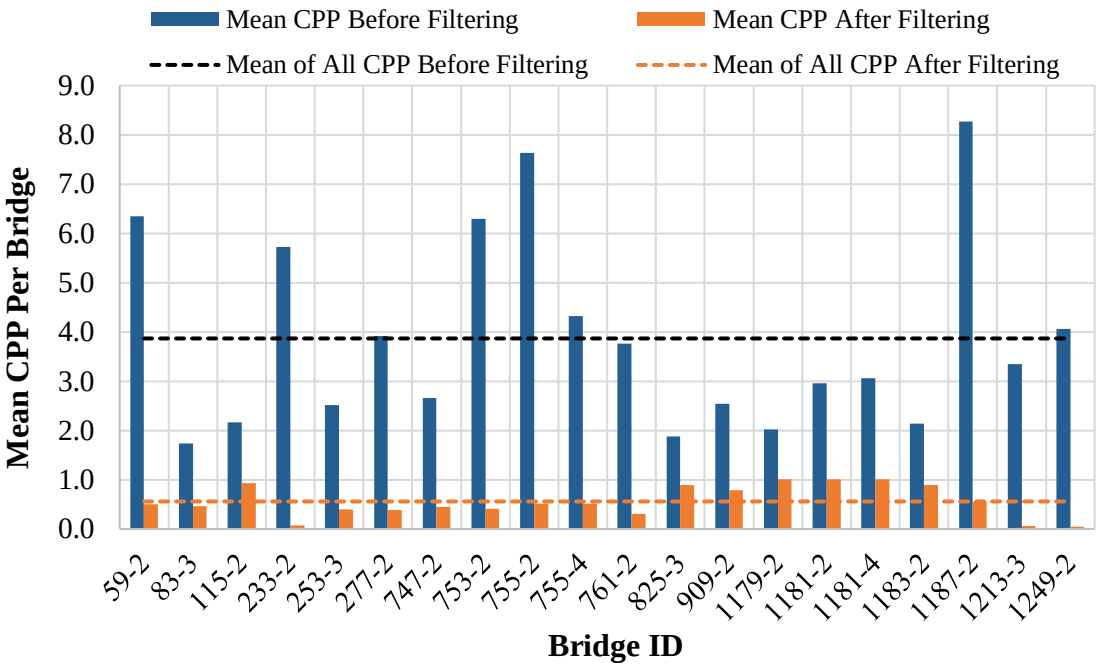

Figure 5-15: Summary of cycles per passage (CPP) for California SR-99 (CA1). Includes results both before and after stress truncation (i.e., removing stress ranges less than 25% CAFL).

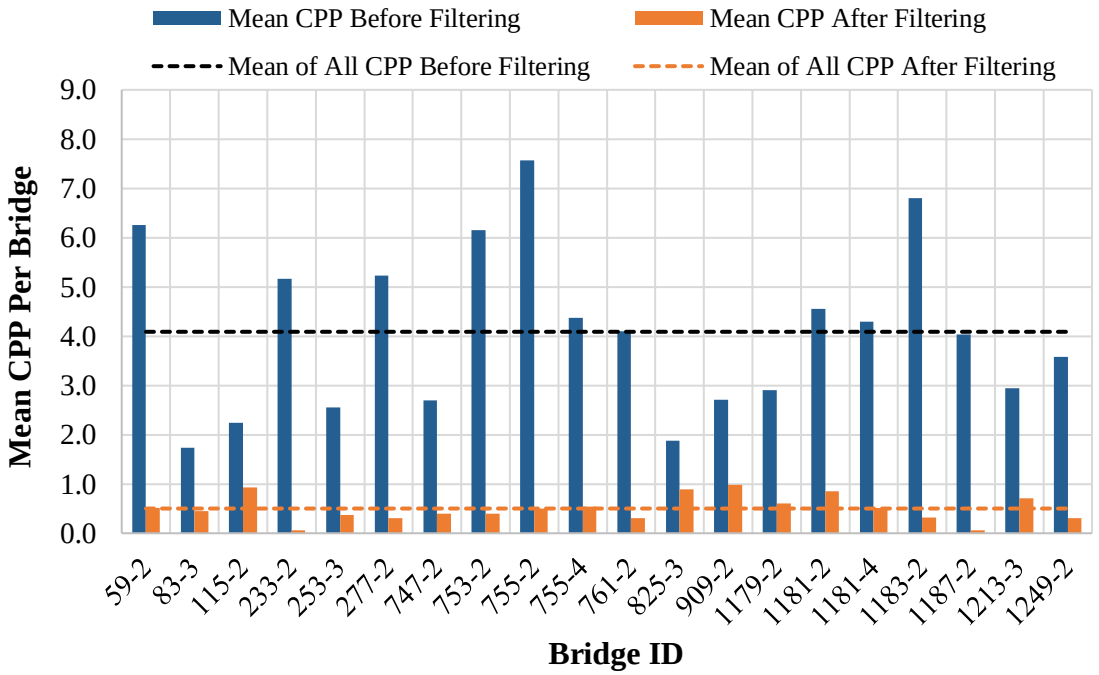

Figure 5-16: Summary of cycles per passage (CPP) for Colorado I-76 (CO2). Includes results both before and after stress truncation (i.e., removing stress ranges less than 25% CAFL).

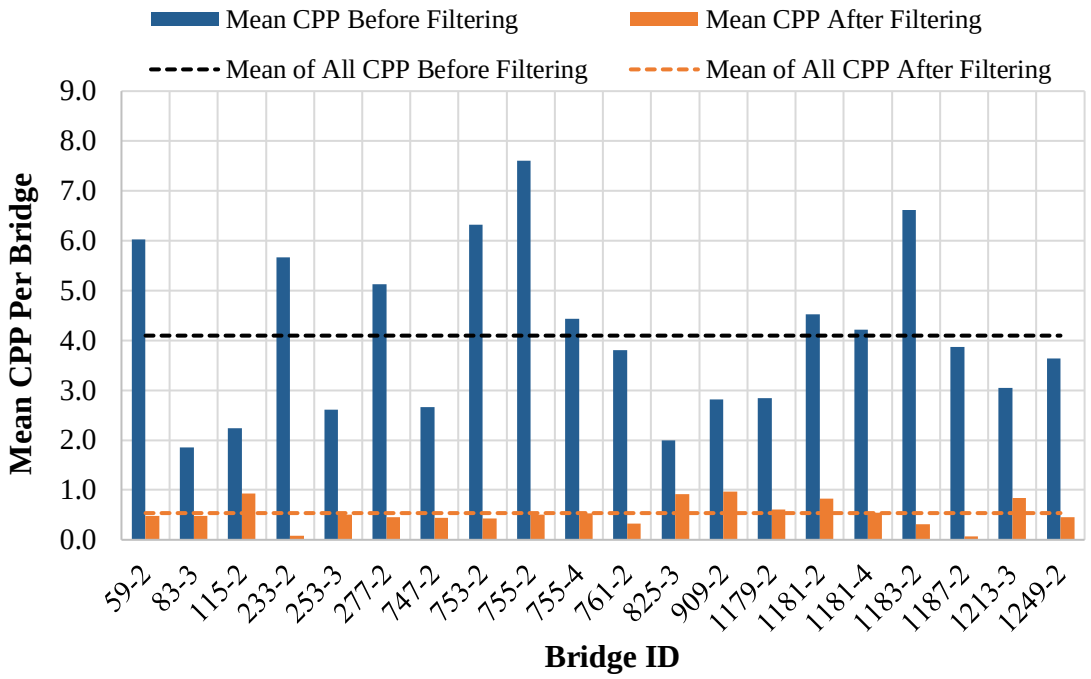

Figure 5-17: Summary of cycles per passage (CPP) for Illinois I-57 (IL1). Includes results both before and after stress truncation (i.e., removing stress ranges less than 25% CAFL).

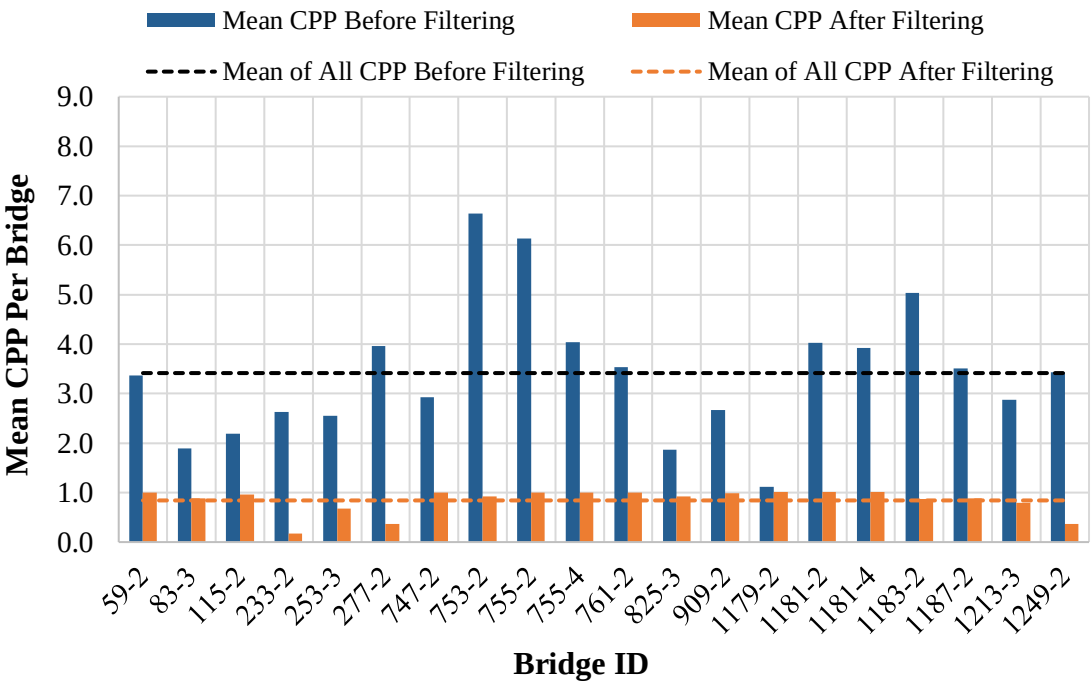

Figure 5-18: Summary of cycles per passage (CPP) for Indiana US-31 (IN1) Lane 1. Includes results both before and after stress truncation (i.e., removing stress ranges less than 25% CAFL).

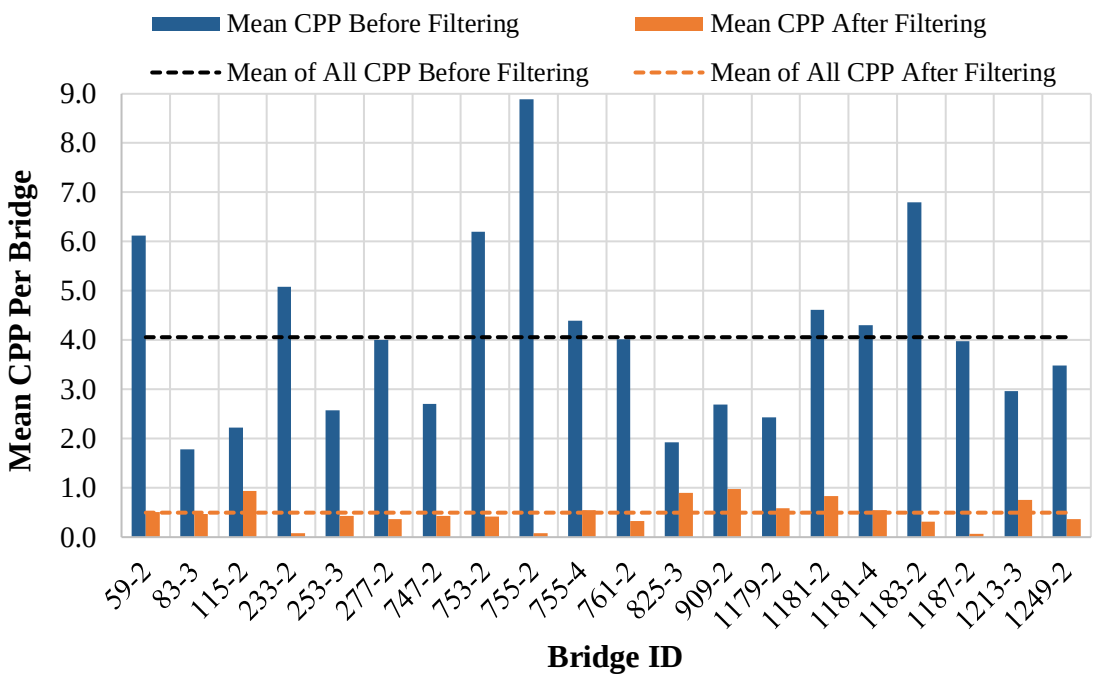

Figure 5-19: Summary of cycles per passage (CPP) for Indiana US-31 (IN1) Lane 3. Includes results both before and after stress truncation (i.e., removing stress ranges less than 25% CAFL).

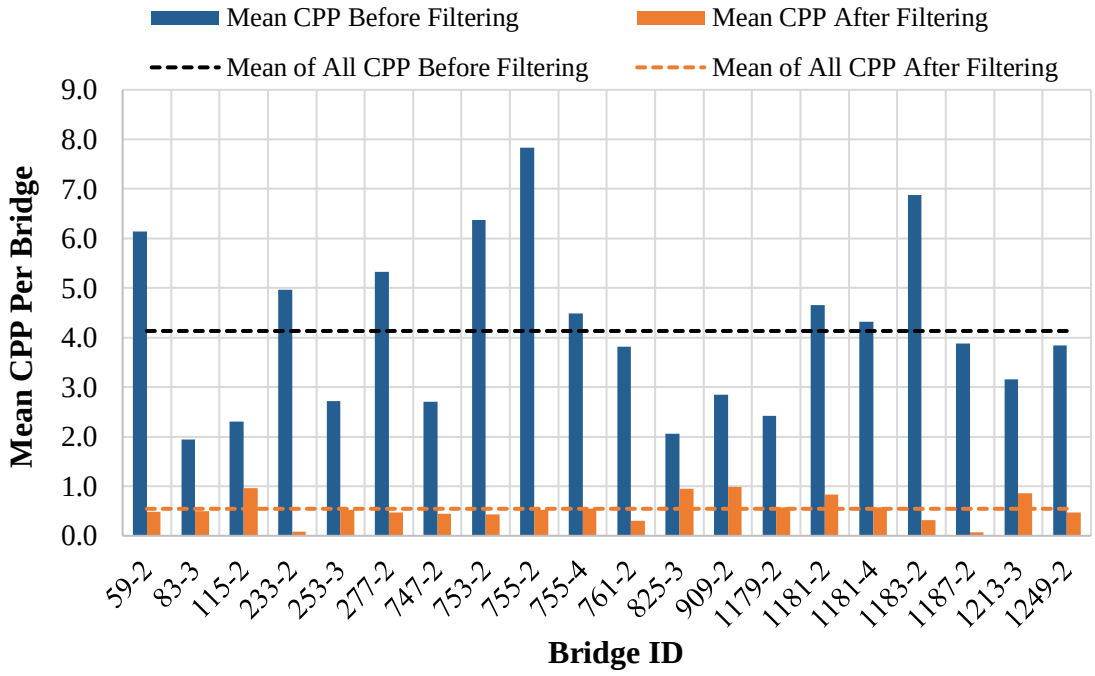

Figure 5-20: Summary of cycles per passage (CPP) for Kansas I-70 (KS1). Includes results both before and after stress truncation (i.e., removing stress ranges less than 25% CAFL).

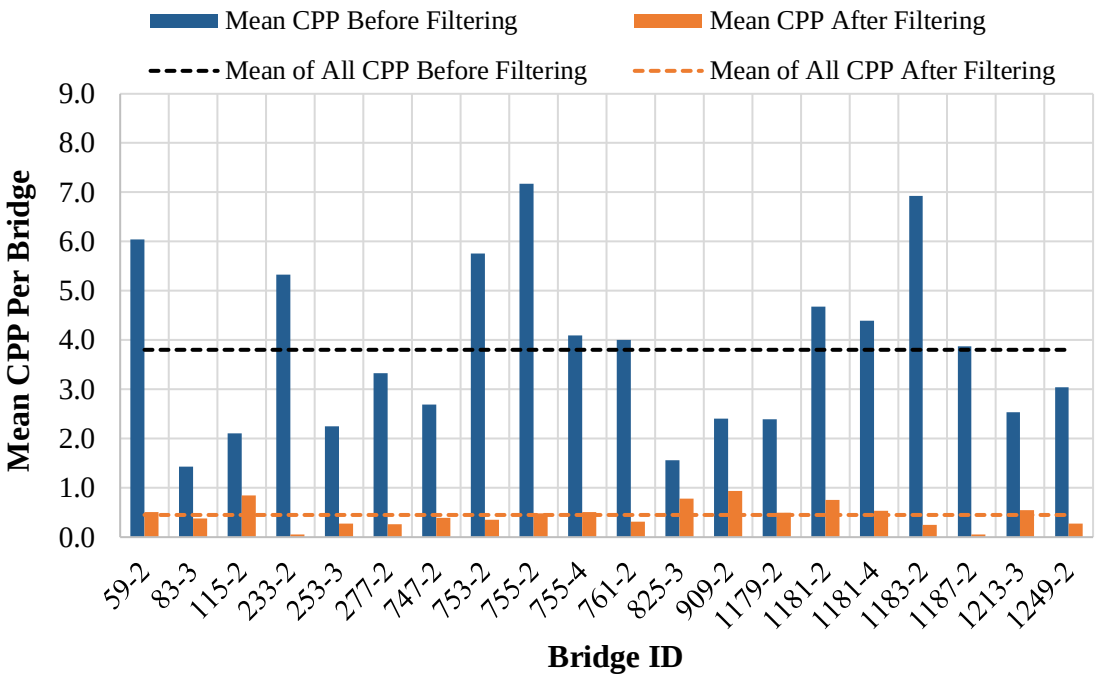

Figure 5-21: Summary of cycles per passage (CPP) for Louisiana US-171 (LA1). Includes results both before and after stress truncation (i.e., removing stress ranges less than 25% CAFL).

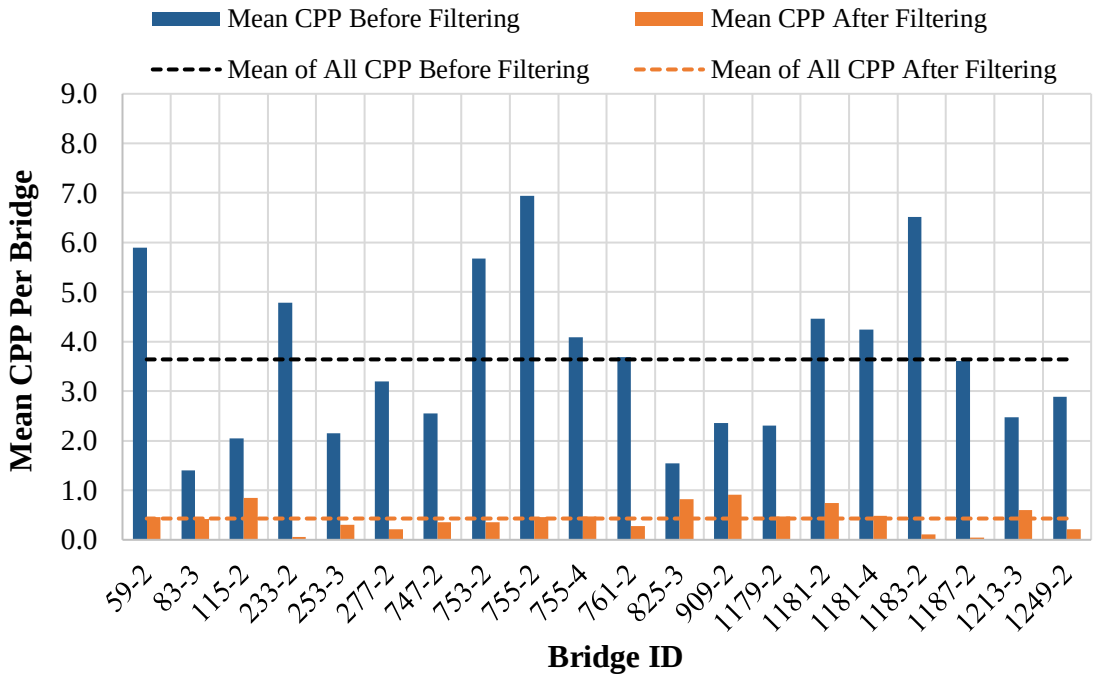

Figure 5-22: Summary of cycles per passage (CPP) for Maryland US-15 (MD5). Includes results both before and after stress truncation (i.e., removing stress ranges less than 25% CAFL).

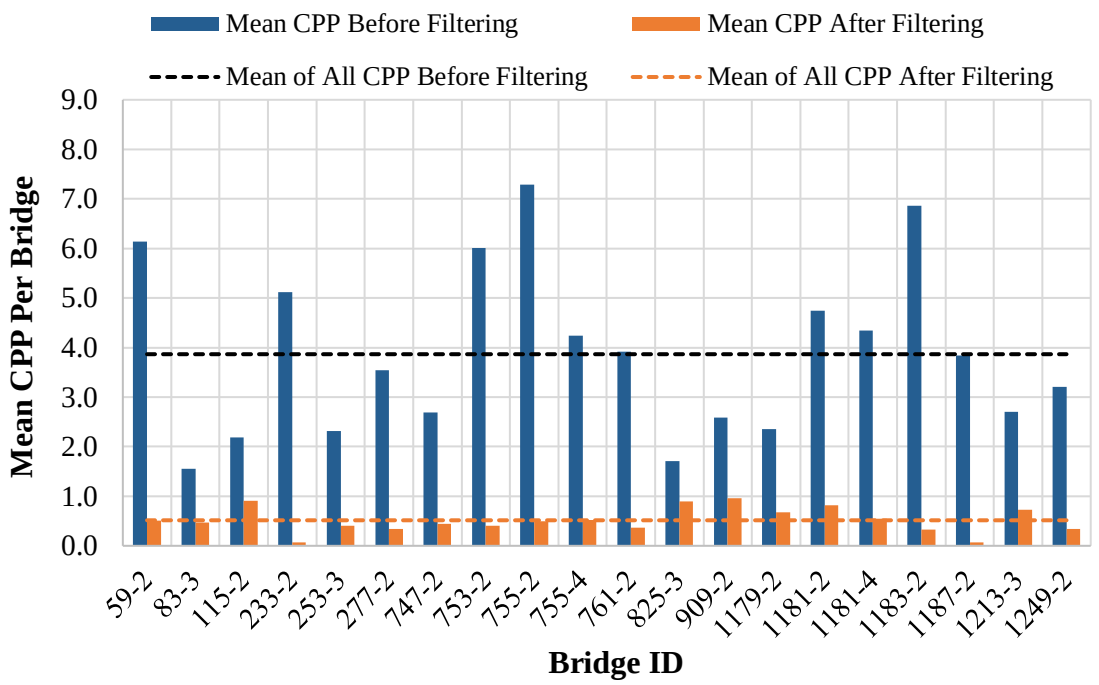

Figure 5-23: Summary of cycles per passage (CPP) for Minnesota US-2 (MN 035). Includes results both before and after stress truncation (i.e., removing stress ranges less than 25% CAFL).

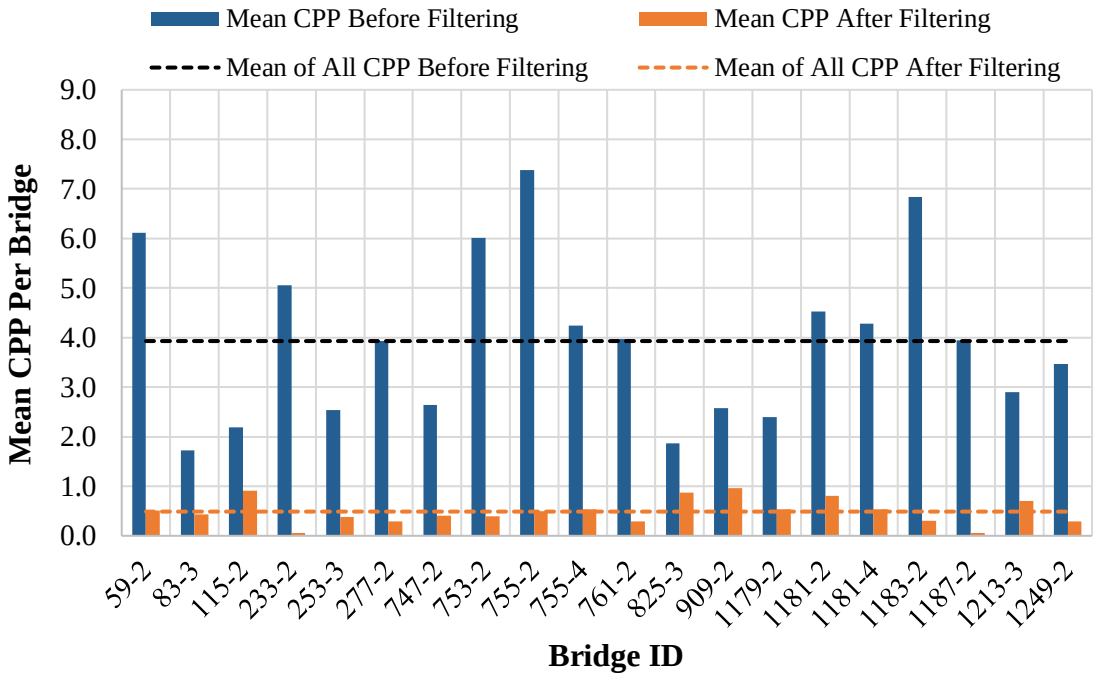

Figure 5-24: Summary of cycles per passage (CPP) for New Mexico I-25 (NM1). Includes results both before and after stress truncation (i.e., removing stress ranges less than 25% CAFL).

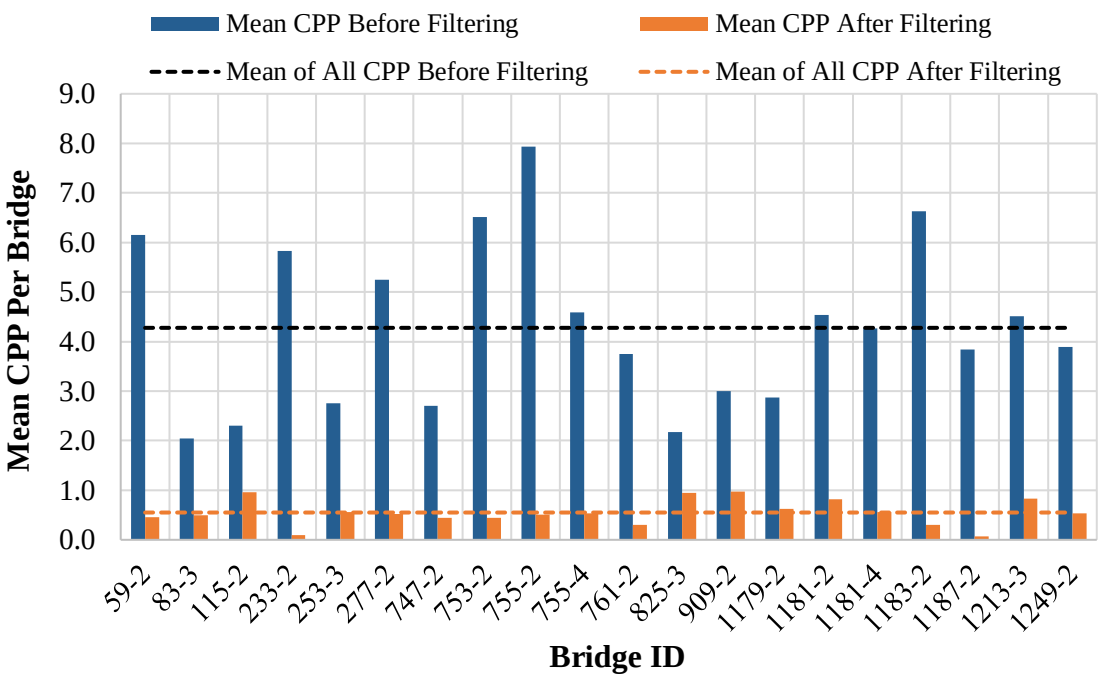

Figure 5-25: Summary of cycles per passage (CPP) for New Mexico I-10 (NM2). Includes results both before and after stress truncation (i.e., removing stress ranges less than 25% CAFL).

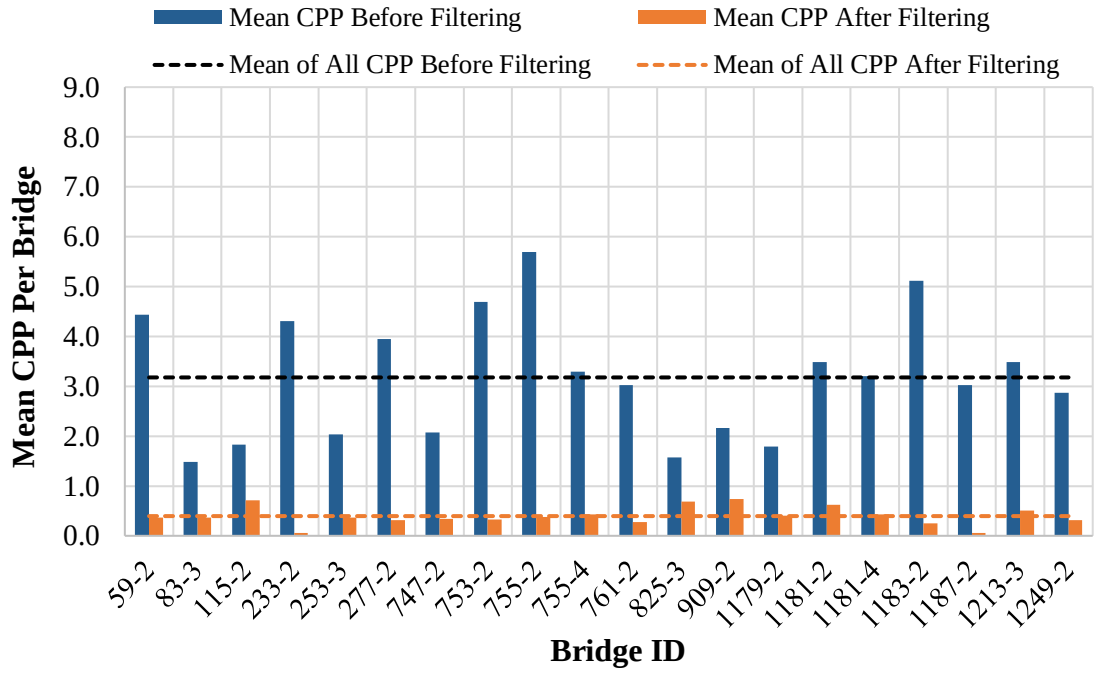

Figure 5-26: Summary of cycles per passage (CPP) for Pennsylvania I-80 (PA158). Includes results both before and after stress truncation (i.e., removing stress ranges less than 25% CAFL).

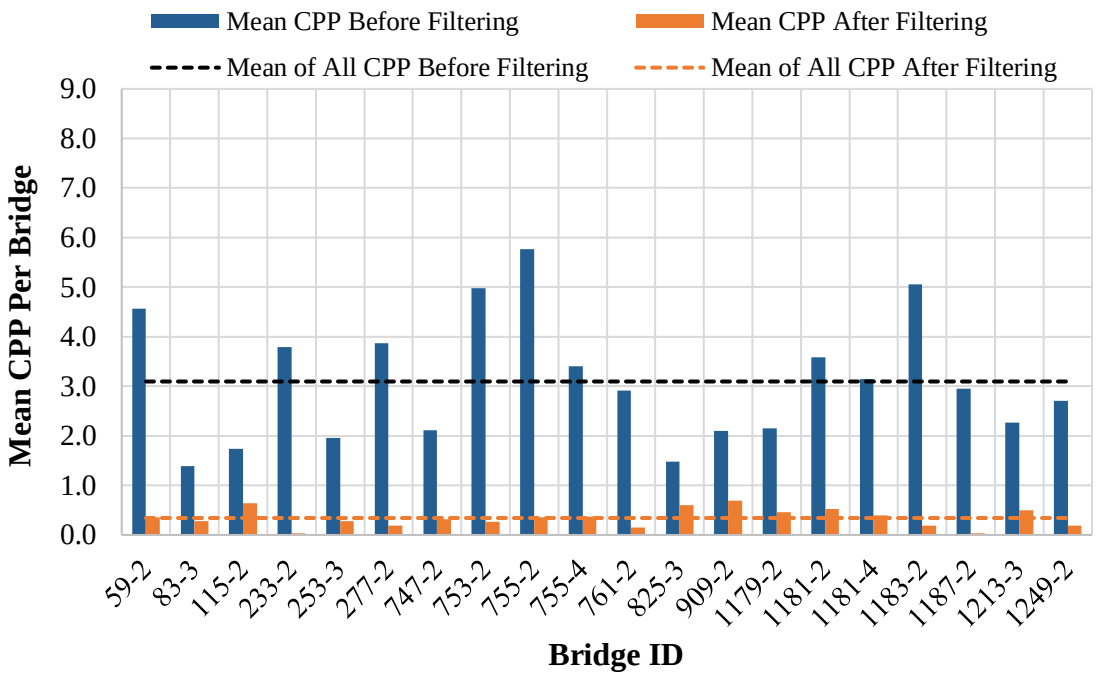

Figure 5-27: Summary of cycles per passage (CPP) for Tennessee I-40 (TN1) Lane 3. Includes results both before and after stress truncation (i.e., removing stress ranges less than 25% CAFL).

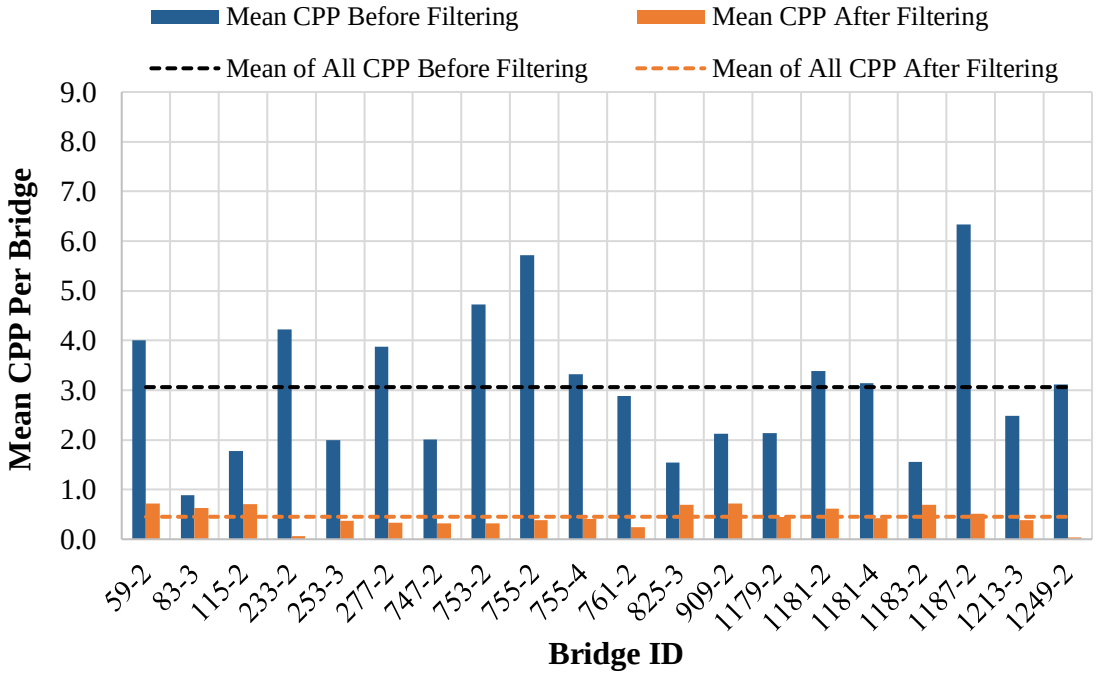

Figure 5-28: Summary of cycles per passage (CPP) for Tennessee I-40 (TN1) Lane 4. Includes results both before and after stress truncation (i.e., removing stress ranges less than 25% CAFL).

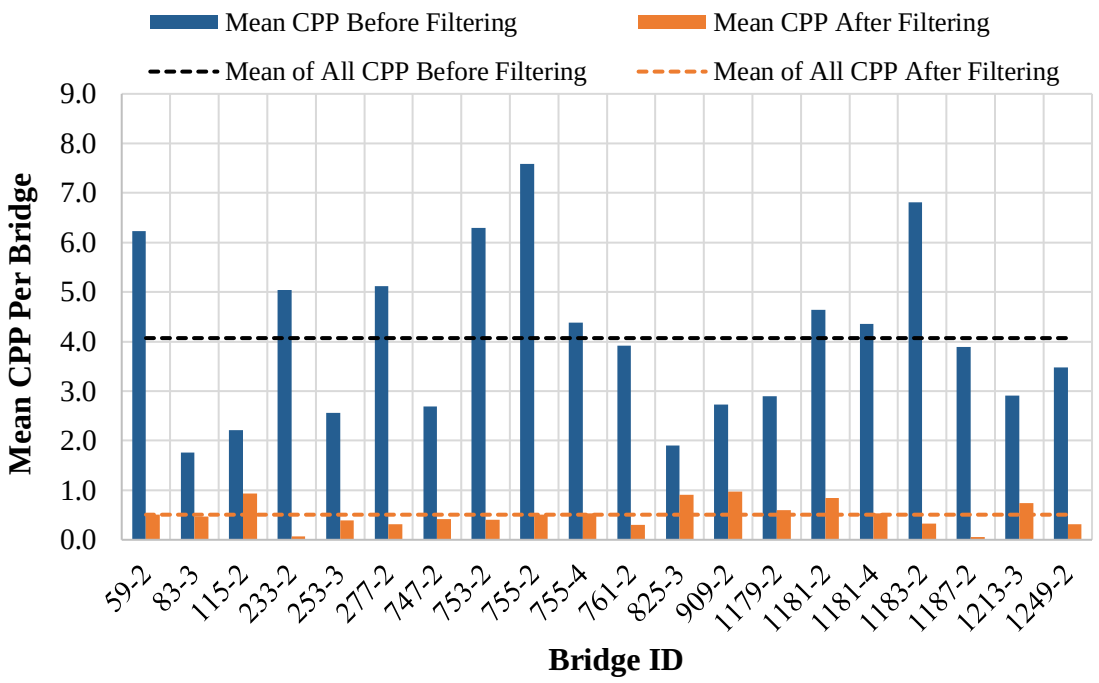

Figure 5-29: Summary of cycles per passage (CPP) for Virginia US-29 (VA1) Lane 1. Includes results both before and after stress truncation (i.e., removing stress ranges less than 25% CAFL).

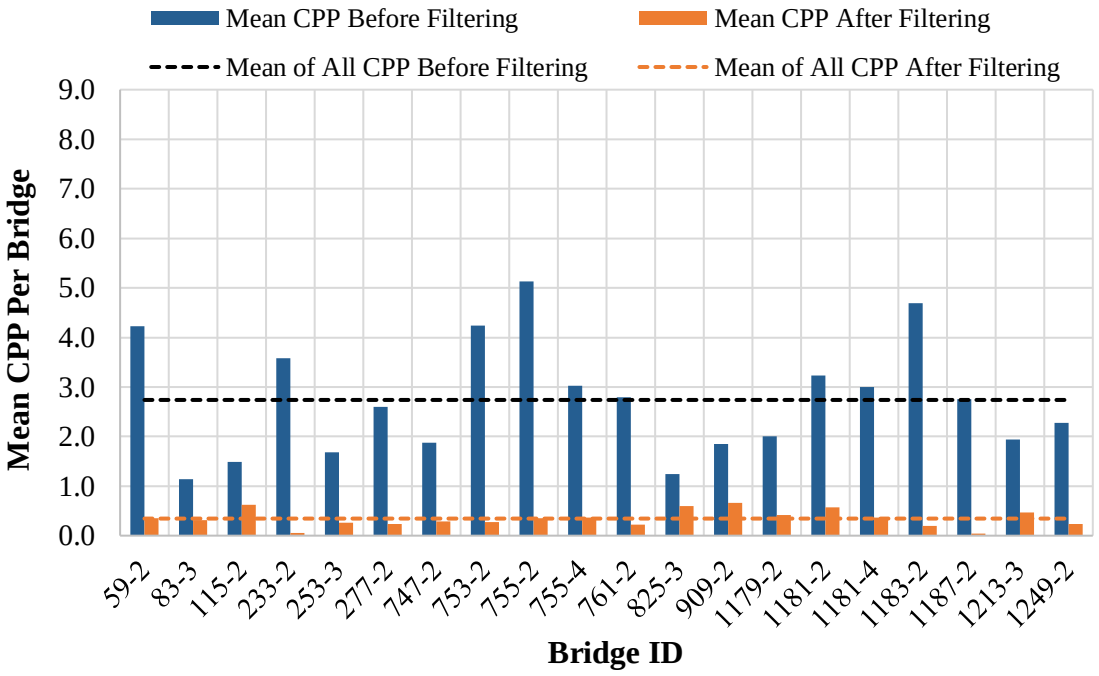

Figure 5-30: Summary of cycles per passage (CPP) for Wisconsin SH-29 (WI1). Includes results both before and after stress truncation (i.e., removing stress ranges less than 25% CAFL).

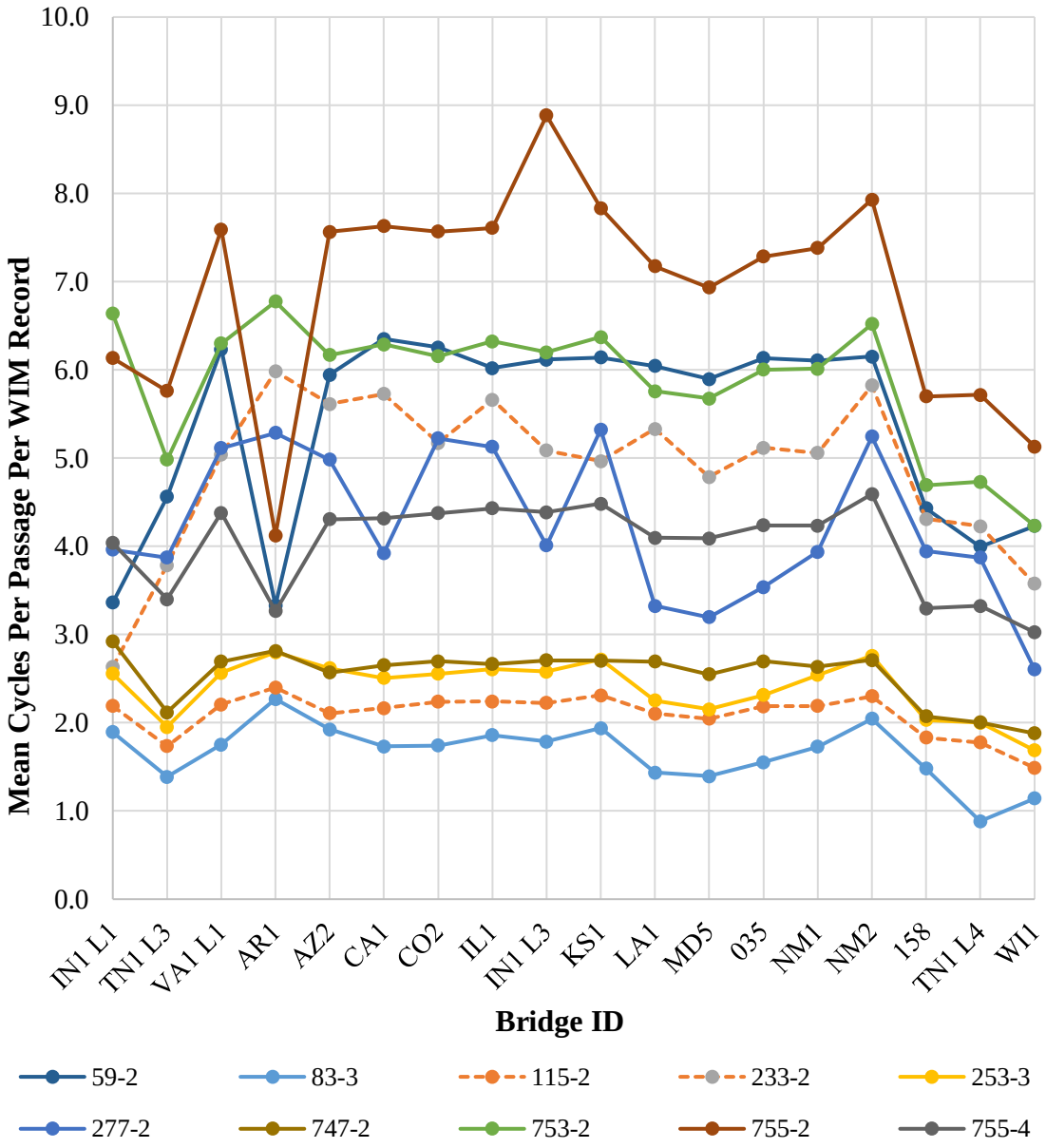

Figure 5-31: Comparison of average cycles per passage (CPP) per WIM record for select bridges. Includes only results before stress truncation (i.e., before removing stress ranges less than 25% CAFL).

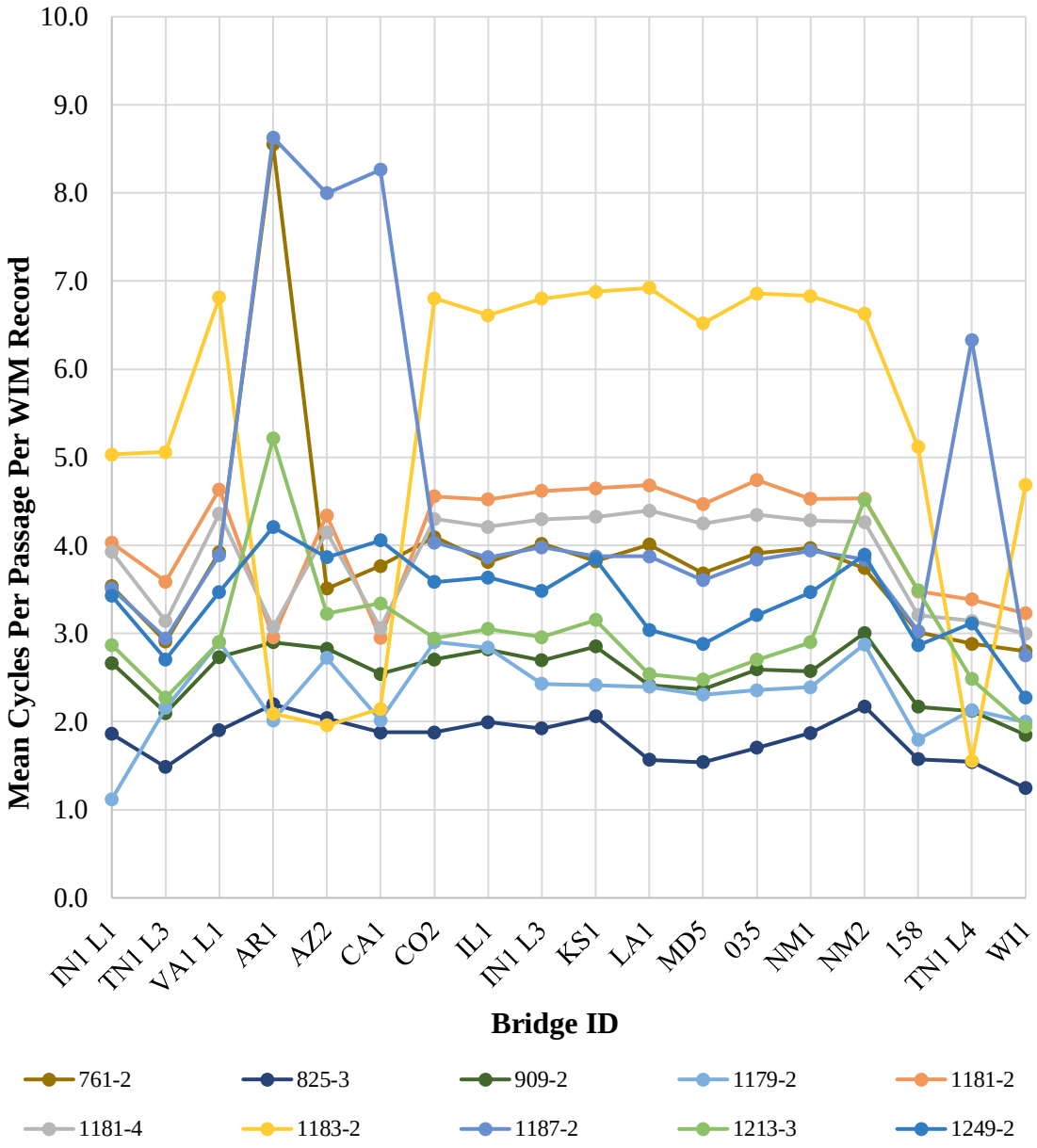

Figure 5-32: Comparison of average cycles per passage (CPP) per WIM record for select bridges. Includes only results before stress truncation (i.e., before removing stress ranges less than 25% CAFL).

5.4 CHAPTER SUMMARY

Based on the advanced studies presented in this chapter, there are several conclusions that can be drawn with respect to the appropriate fatigue design load factors for estimating design stress ranges in cross-frame systems:

- The current Fatigue I design load factor is conservative for the design of cross-frames.

To be consistent with AASHTO *LRFD*'s approach in basing the bias and load factor on the mean value of the bias (as opposed to the "mean plus 1.5 standard deviations"), the bias of the Fatigue I data was obtained by analyzing 18 WIM records simulated on 20 bridges selected to be representative of the analytical testing matrix. The mean value of the bias implies an appropriate load factor for the Fatigue I limit state design of cross-frames falls between 1.01 to 1.04 (prior to 25% CAFL filtering) and 1.24 (after 25% CAFL filtering). These are both less than the current Fatigue I load factor of 1.75. Without consideration of the material resistances pertinent to cross-frames, these values may represent a more appropriate load factor for fatigue design of cross-frames. Since the Fatigue I limit state is intended to represent the maximum stress ranges produced by the general truck population, and the truncated stresses were predominantly caused by the truck population, it is most likely appropriate to rely on the records obtained prior to the truncation of the 25% CAFL stresses. Due to the non-normality of the pre-filtered records, reliability studies would need to consider the potential multi-modal distribution of the Fatigue I load responses.

- The current Fatigue II design load factor is conservative for the design of cross-frames. Based on an analysis of 18 WIM records simulated on 20 bridge, the "mean plus 1.5 standard deviations" (for normal distributions, "mean plus 1.5 standard deviations" includes approximately 93% of the population; using this statistical characterization is consistent with the most recent Fatigue II load factor calibrations) implies an appropriate load factor for the Fatigue II limit state design of cross-frames falls between 0.50 to 0.53 (prior to 25% CAFL filtering) and 0.47 to 0.52 (after 25% CAFL filtering). Both of these values are less than the current Fatigue II load factor of 0.8. Without consideration of the material resistances pertinent to cross-frames, these values may represent a more appropriate Fatigue II load factor for design of cross-frames. The distribution of the fatigue damage ratios is approximately normal (i.e., the multi-modal GVW distributions discussed in Chapter 4 are not consequential to the Fatigue II limit state).

- The total number of cycles per passage varies widely for various bridge types. Because the 20-model bridge set intentionally contains a large number of various bridge parameters, it is generally not possible to ascertain which types of bridges tend to produce larger (or smaller) cycles per passage. Overall, the total number of cycles per passage prior to filtering ranges from 1.1 to 8.9, with an average of 3.7. After filtering, the average cycle per passage ranges from 0.03 to 1.02, with an average of 0.5; this implies that the majority of the truck stress range population is less than 0.65 ksi (the 25% CAFL filter) for each WIM record.

Chapter 6: Reliability Studies with Available Resistance Data

6.1 INTRODUCTION

This chapter discusses the implications of using the load statistics developed in Chapter 5 for fatigue of cross-frames in steel I-girder bridges in the context of a reliability-based design. Recall from Chapter 5 that the comprehensive study of WIM traffic records simulated over a range of bridge decks from the analytical testing matrix resulted in statistical parameters that describe the distribution of force effects in cross-frames. Using these statistical characterizations of the total load effect, it is possible to compare this to the statistical characterization of fatigue resistance provided in the literature (Kulicki et al. 2015). Stochastic models can be developed that utilize these characterizations of load and resistance to provide an indication of reliability, given a specific choice of design parameters.

The reliability study discussed in this chapter is performed via Monte Carlo simulation, in which values of load and resistance are obtained through a randomly determined process using the distribution parameters for load and resistance.

6.2 STATISTICAL CHARACTERIZATION OF AVAILABLE RESISTANCE DATA FOR CROSS-FRAMES

As discussed in Chapter 2, the SHRP 2 R19B project's recent calibration of AASHTO *LRFD*'s fatigue limit states (Kulicki et al. 2015) required a review of the resistance data originally collected by Keating and Fisher (1986). As part of the calibration, the R19B research required key statistical parameters from this data, which was not previously characterized. Because the original resistance studies only reported the relationship between stress ranges and number of cycles to failure, and each specimen group tested was often tested over small increments of stress ranges and limited in number, this made it difficult to fit one statistical distribution to the available data. By relating the constant amplitude stress ranges for a given test specimen to an effective constant amplitude stress range, the R19B project calculated a fatigue damage parameter, S_{fi} (refer to Section 2.2.2). The distribution of this fatigue damage parameter for each of the detail categories was then used to calculate the statistical parameters for that detail category. Table 2-1 summarizes the statistical parameters R19B developed for all eight detail categories. Note that the design value used to calculate the bias was obtained by taking the cube root of the constant, A, for the respective

detail category found in AASHTO Table 6.6.1.2.5-1 (2015).

Table 6-1: Statistical parameters for resistance as calculated from SHRP 2 R19B (Kulicki et al. 2015).

Category	Standard Deviation	CV	Bias, λ	Measured Fatigue Parameter	Design Fatigue Parameter
A	1000.0	0.24	1.43	4,167.40	2,924
B	666.7	0.22	1.34	3,077.47	2,289
B’	250.0	0.11	1.28	2,336.10	1,827
C and C’	454.6	0.21	1.35	2,210.77	1,638
D	185.2	0.10	1.36	1,773.69	1,300
E	140.9	0.12	1.17	1,207.41	1,032
E’	232.6	0.20	1.56	1,1140.28	730

For the purposes of this research, the statistical parameters developed by Kulicki et al. (2015) are assumed to accurately represent the various fatigue categories. While this research will consider all detail categories, the category E’ is of particularly importance to cross-frames, since most cross-frame members consist of single angle welded connections which are defined as a Category E’ detail.

6.3 TARGET RELIABILITY INDICES INHERENT IN CURRENT CODE

Based on the R19B project, the inherent reliability index of the 6th Edition AASHTO *LRFD* (2012) design provisions for fatigue was approximately 1.0, but as shown in Table 6-2, the indices exhibited variability between various categories. Using the R19B project’s recommended load factor and resistance constant changes (the resistance constant is effectively a load factor change on the resistance), the R19B project reported less variability between reliability indices, with all detail category indices within +/- 0.2 of unity.

Table 6-2: Inherent reliability of the 6th Edition AASHTO *LRFD* (2012) Fatigue I and II limit states as represented by Kulicki et al. (2015).

Detail Category	Reliability Index	
	Fatigue I	Fatigue II
A	1.2	1.0
B	1.1	0.9
B’	1.5	1.0
C	1.2	0.9
C’	1.2	0.9
D	2.0	1.3
E	0.9	0.7
E’	1.7	1.4

The load factors and resistance constants recommended by the SHRP 2 R19B project team were not all adopted in the 8th Edition of AASHTO *LRFD*. R19B recommended the Fatigue I load factor be increased to 2.0, and the value adopted by AASHTO *LRFD* is 1.75; the recommended changes to the resistance constants were also not adopted.

For the purposes of this study, it is useful to estimate the inherent reliability of the 8th Edition AASHTO *LRFD*. Assuming the loads and resistances can be represented by a normal distribution (this is the claim by the R19B project), the inherent reliability of the current AASHTO fatigue limit states can be verified by using the closed-form solution for the reliability index as discussed in Section 2.3.1. This equation (repeated here as Eq. 6.23) is exact when all distributions are considered perfectly normal:

$$\beta = \frac{\overline{R} - \overline{Q}}{\sqrt{(CV_R R_N \lambda_R)^2 + (CV_Q Q_N \lambda_Q)^2}} \qquad \text{Eq. 6.23}$$

Where all variables are defined here again for convenience:

$\bar{Q}$ = mean load effect, equal to $\mu_Q = \lambda_Q Q_N$,

λ_Q = bias factor for the mean load effect,

Q_N = nominal (design) load effect,

$\bar{R}$ = mean resistance, equal to $\mu_R = \lambda_R R_N$,

λ_R = bias factor for the total resistance,

R_N = nominal (design) resistance,

CV_R = coefficient of variation for resistance, equal to σ_R/μ_R ,

σ_R = standard deviation for resistance,

CV_Q = coefficient of variation for load, equal to σ_Q/μ_Q , and

σ_Q = standard deviation for load.

By using the limit state equation shown in Eq. 2.5 evaluated at the failure boundary (i.e., factored design load equals factored design resistance), the design resistance can be expressed as:

$$R_N = \frac{\gamma_Q}{\gamma_R} Q_N \qquad \text{Eq. 6.24}$$

where:

γ_R = load factor applied to the nominal resistance, R_N, and

γ_Q = load factor applied to the nominal load effect, Q_N.

Using the definitions above for the mean load and resistance effects and Eq. 6.24, the closed-form solution for the reliability index for normal distributions can be expresses as:

$$\beta = \frac{\lambda_R \frac{\gamma_Q}{\gamma_R} Q_N - \lambda_Q Q_N}{\sqrt{\left(CV_R \frac{\gamma_Q}{\gamma_R} Q_N \lambda_R\right)^2 + \left(CV_Q Q_N \lambda_Q\right)^2}} \qquad \text{Eq. 6.25}$$

The nominal load effect can be cancelled out, and since the load factor for resistance is taken as 1.0 in AASHTO *LRFD* for fatigue, the resulting equation is simplified, without needing input parameters for nominal load or resistance:

$$\beta = \frac{\lambda_R \gamma_Q - \lambda_Q}{\sqrt{\left(CV_R \gamma_Q \lambda_R\right)^2 + \left(CV_Q \lambda_Q\right)^2}} \qquad \text{Eq. 6.26}$$

Based on a review of the SHRP 2 R19B data, it appears that the biases calculated for the Fatigue I and II load effects were conservatively taken as one and a half standard deviations from the mean of the respective load effects. This assumption was confirmed with personal correspondence with the authors, who stated that the increase in the bias was considered a conservative measure due to the limited WIM data evaluated in this study. Coincidentally, the bias values align with R19B's *proposed* load factors; even though the load factors that were eventually adopted by AASHTO *LRFD* are not consistent with the R19B recommendations (the bias and load factors were based on the mean bias value). For evaluating the inherent reliability of AASHTO *LRFD* for the Fatigue I and II limit states, Table 6-1 summarizes the statistical parameters describing the resistance effects, and Table 6-3 summarizes the statistical parameters describing the load effects. Note the inclusion of the coefficient of variation for dynamic impact (per Kulicki et al. 2015). Applying Eq. 6.26 using the current AASHTO *LRFD* load factors (1.75 for Fatigue I and 0.8 for Fatigue II), the inherent reliability provided by the code is summarized in Table 6-4; the values in this table assume that the distributions of load and resistance are normal, as indicated in the SHRP 2 R19B project report, therefore justifying the use of Eq. 6.26.

Table 6-3: Statistical parameters describing the available load data per SHRP 2 R19B and load factors as provided in AASHTO *LRFD* (2017).

Limit State	Coefficient of Variation of Load	Bias for Load Data	Load Factor	Coefficient of Variation of Dynamic Impact
Fatigue I	0.12	1.75	1.75	0.8
Fatigue II	0.07	0.80	0.80	0.8

Table 6-4: Inherent reliability of 8th Edition AASHTO *LRFD* Fatigue I and II limit states.

Detail Category	Reliability Index	
	Fatigue I	**Fatigue II**
A	1.2	1.2
B	1.1	1.1
B’	1.5	1.8
C	1.1	1.2
C’	1.1	1.2
D	2.0	2.4
E	0.9	1.1
E’	1.7	1.8

6.4 STOCHASTIC SIMULATION VIA THE MONTE CARLO TECHNIQUE

The statistical parameters describing the load effects in cross-frames for the Fatigue I and II limit states was discussed in Chapter 5. Using the mean value of the bias implies an appropriate load factor for the Fatigue I limit state design of cross-frames falls between 1.01 (prior to 25% CAFL filtering) to 1.24 (after 25% CAFL filtering). These values bound a more appropriate load factor for fatigue design of cross-frames. The use of the mean value of the bias is consistent with the most recent adoption of load factors by AASHTO, recommendations from the NCHRP Project 12-113 panel, and personal correspondence with the R19B authors. Since the Fatigue I limit state is intended to represent the maximum stress ranges produced by the general truck population, and the truncated stresses were predominantly caused by the truck population (i.e., lightweight vehicles were discarded as discussed in Chapter 4 and the resulting records should be primarily truck traffic), it is most likely appropriate to rely on the records obtained prior to the truncation of the 25% CAFL stresses as a realistic population for examining the top 99.99% stress ranges. In other words, truncating lower stress ranges that are experienced in cross-frames by truck traffic artificially increases the 99.99th percentile of the realistic force effect spectrum. For Fatigue II, the “mean plus 1.5 standard deviations” (for normal distributions, “mean plus 1.5 standard deviations” includes approximately 93% of the population) implies an appropriate load factor for the Fatigue II limit state design of cross-frames falls between 0.50 to 0.53 (prior to 25% CAFL filtering) and 0.47 to 0.52 (after 25% CAFL filtering). These values bound a more appropriate Fatigue II load factor for design of cross-frames. The truncation of 25% CAFL stresses was an exercise to study

the overall effects of this simplification when performed on truck traffic (i.e., passenger vehicles are already removed, so this truncation is primarily affecting stress ranges caused by truck traffic). While this approach may be warranted when collecting rainflow data during in-service monitoring to preserve data storage and increase computational efficiency, for this project, the truncation of stresses removes data considered to accurately represent truck traffic. Therefore, for the reliability study, the values obtained without filtering will be used. The statistical parameters describing the load effects in cross-frames for the Fatigue I and II limit states used for additional reliability study are repeated in Table 6-5 for convenience.

Table 6-5: Statistical parameters describing the load effects in cross-frames for Fatigue I and II limit states.

Limit State	Coefficient of Variation of Load	Bias for Load Data	Load Factor
Fatigue I	0.26	1.01	1.01
Fatigue II	0.21	0.40	0.53

A Monte Carlo simulation was performed using the statistical summaries for resistance and cross-frame force effects previously described. For the simulation, a total of 10,000 samples were randomly generated from the distributions of load and resistance described by the statistical parameters. The following procedure was used in the development of this simulation:

1. **Define the nominal loads and nominal resistance**. For the purposes of this Monte Carlo simulation, this can merely be the relationship of nominal values per AASHTO *LRFD* (i.e., it is desirable to obtain a measure of reliability at the limit state failure boundary, where an element is allowed to be designed to be *just sufficient* for given a load). For both limit states, the relationship follows the generalized limit state, using the appropriate recommended load factors:

$$\gamma(\Delta f) \leq (\Delta F)_n \qquad \text{Eq. 6.27}$$

For Fatigue I, this relationship is as follows:

$$1.01 * (Q_N + IM) = R_n \qquad \text{Eq. 6.28}$$

For Fatigue II, this relationship is as follows:

$$0.53 * (Q_N + IM) = R_n \qquad \text{Eq. 6.29}$$

Note the inclusion of the dynamic allowance factor per AASHTO *LRFD*. This is equivalent to 1.15 of the fatigue stress range.

2. **Choose a selection of ADTTs.** In design, a member is first checked for infinite life (Fatigue I) using AASHTO *LRFD* Table 6.6.1.2.3-2. If the ADTT is equal to or below the value for the specific category, the member passes Fatigue I (infinite life) and only requires a check for Fatigue II. If the ADTT is above the value indicated for the specific category, then only the Fatigue I limit state is checked. For this step in the simulation, it is important to capture realistic ADTTs that fall above and below the thresholds that differentiate between requiring a Fatigue I or Fatigue II limit state check. In this manner, each detail category can be adequately sampled. The choice of ADTT ranges for consideration was balanced against how many failures occurred: for a Monte Carlo simulation, it is recommended that at least 10 failures are observed; otherwise, the sample size should be increased. For this study, the following range of ADTTs was chosen: 100, 1,000, 1,500, 2,500, 5,000, and 10,000.
3. **Perform the Monte Carlo simulation**. For the load effect being investigated, Q_N, define the associated resistance, R_N, through the relationship in Step 1. Then, for each ADTT in Step 2, a Monte Carlo simulation is performed by randomly selecting from these load and resistance distributions using the statistical parameters describing these distributions in Table 5-4. Note that the load effect chosen is arbitrary - the important consideration is that the relationship between load and resistance is maintained. It is necessary to generate a uniformly distributed random number, u_i, for randomly selecting nominal loads and resistances. The random number should be in the domain: $0 \leq u_i \leq 1$. The number of values generated, N, should generally be sufficient for at least 10 failures to occur. For this study, the number of values generated is taken as 10,000 (i.e., 10,000 random values for each random value calculated). For each of the N randomly selected values, the following steps are taken:
    a. Iteratively sample from the load and resistance distributions. An individual sample (Q_i for load and R_i for resistance) is calculated by randomly selecting a value on either side of the mean, (μ_Q for load and μ_R for

resistance). The location of this value relative to the mean is calculated by calculating the inverse normal distribution value associated with the uniformly distributed random number ($\phi^{-1}(u_{Qi})$ for load and $\phi^{-1}(u_{Ri})$ for resistance). This is performed by the following equation for live load:

$$Q_i = \mu_Q + \sigma_Q \phi^{-1}(u_{Qi}) \qquad \text{Eq. 6.30}$$

and a similar equation for resistance:

$$R_i = \mu_R + \sigma_R \phi^{-1}(u_{Ri}) \qquad \text{Eq. 6.31}$$

b. Calculate and store the evaluation of the limit state function: $G_i = R_i - Q_i$.

4. **Rank the limit state function values.** Rank the individual values calculated for the limit state function above in ascending order, and for each value i, calculate the individual probability of the occurrence, p_i, per **Error! Reference source not found.** and the corresponding value of the inverse standard normal distribution ($\phi^{-1}(p_i)$).

$$p_i = \frac{i}{i+N} \qquad \text{Eq. 6.32}$$

5. **Create a cumulative distribution plot (CDF) of the limit state function results**. This is done by plotting the inverse standard normal distribution values, $\phi^{-1}(p_i)$ versus the corresponding, ranked individual values, G_i.
6. **Calculate the reliability index**. This value can be obtained from the CDF above by taking the negative value of the CDF function where $G = 0$.

6.5 CHAPTER SUMMARY

The simulation described above was performed for the cross-frame statistics in Table 6-5. The resulting reliability indices are shown in Table 6-6. Based on the reliability analysis performed, the resulting reliability indices for cross-frames using the load factors developed in Chapter 5 exceeds the target reliability assumed inherent within the AASHTO *LRFD* code.

Table 6-6: Reliability of cross-frames for Fatigue I and II limit states using new load factors.

Detail Category	Reliability Index	
	Fatigue I	**Fatigue II**
A	1.0	1.8
B	0.9	1.7
B’	1.0	2.5
C	0.9	1.8
C’	0.9	1.8
D	1.3	2.9
E	0.6	2.0
E’	1.4	2.3

In order to obtain a reliability index close to the assumed target reliability of unity established in the SHRP 2 R19B study, adjustments to resistance factors are preferred. As an alternative to altering the resistance factors (or the associated changes in constant amplitude fatigue thresholds, $(\Delta F)_{TH}$, for Fatigue I, or detail constants, A, for Fatigue II) it is also possible to alter the load factor for fatigue such that the minimum target reliability of unity is achieved for each category. Additionally, as an alternative to introducing two new load factors for the fatigue limit state for cross-frames, it is possible to apply a single adjustment factor to the existing load factors. Using an adjustment factor of 0.65 applied to the Fatigue I load factor of 1.75 (i.e., a resultant load factor for cross-frames of 1.14 for Fatigue I) and the Fatigue II load factor of 0.8 (i.e., a resultant load factor for cross-frames of 0.52), the resulting reliability indices are calculated via Monte Carlo simulation and shown in Table 6-7. Each detail category satisfies the minimum assumed target reliability of 1.

Table 6-7: Reliability of cross-frames for Fatigue I and II limit states using new load factors.

Detail Category	Reliability Index	
	Fatigue I	**Fatigue II**
A	1.3	1.7
B	1.2	1.7
B’	1.5	2.4
C	1.3	1.8
C’	1.3	1.8
D	1.8	2.8
E	1.1	1.9
E’	1.8	2.3

As an academic exercise, it is possible to adjust the resistance factors (or the associated changes in constant amplitude fatigue thresholds, $(\Delta F)_{TH}$, for Fatigue I, or detail constants, A, for Fatigue II) for every detail category for both Fatigue I and II such that a uniform reliability index of unity is achieved. Table 6-8 indicates the changes to the Fatigue I and II nominal fatigue resistance that would be required in order to provide a consistent level of reliability across all detail categories for both limit states.

Table 6-8: Adjustments to resistance factors to achieve a uniform reliability.

Detail Category	Current Values in 8th Edition AASHTO *LRFD*		Nominal Fatigue Resistance for β = 1			
	$(\Delta F)_{TH}$ (ksi)	Constant A times 10^8 (ksi^3)	Fatigue I Resistance Factor (φ)	$(\Delta F)_{TH}$ (ksi)	Fatigue II Resistance Factor (φ)	Constant A times 10^8 (ksi^3)
A	24	250	1.17	28	1.07	306
B	16	120	1.12	18	1.03	131
B’	12	61	1.19	14	1.09	79
C	10	44	1.15	12	1.05	51
C’	12	44	1.14	14	1.05	51
D	7	22	1.28	9	1.16	34
E	4.5	11	1.08	4.9	0.99	11
E’	2.6	3.9	1.33	3.5	1.23	7.3

Chapter 7: Conclusions and Recommendations

7.1 SUMMARY

A primary goal of the research documented in this dissertation is to provide an improved definition of the fatigue loading for cross-frames in straight, horizontally-curved, and skewed steel I-girder bridges. The dissertation scope was one component of the larger NCHRP Project 12-113 documented in Reichenbach et al. 2021, with additional details in Park (2020) and Reichenbach (2020). In order to study the fatigue loading as part of the larger 12-113 project, three bridges were instrumented and monitored, and data gathered from the field instrumentation was used to validate three-dimensional finite element analysis (FEA) models; these FEA models were used to conduct extensive parametric studies to improve the understanding of the behavior of cross-frame stresses for a wide range of geometrical parameters of straight and horizontally-curved bridges with and without skewed supports. The FEA modeling and parametric studies were conducted by Park (2020) and Reichenbach (2020) and serve as a basis for the advanced loading analysis performed in this research.

The validated FEA models developed by Park and Reichenbach were used to carry out extensive fatigue loading studies to improve the understanding of cross-frame force effects as a function of truck traffic position on the bridge. The adequacy of the current AASHTO fatigue load model was investigated by examining recently collected, high-resolution, multi-lane weigh-in-motion (WIM) data, which represent actual truck traffic records in the US and is assumed to be representative of truck traffic in the US. The current AASHTO fatigue design load model was evaluated by comparing cross-frame load effects caused by the fatigue load model to load effects caused by simulated truck traffic representing actual live load. Influence surfaces generated from the three-dimensional FEA models provided information on the stresses in select cross-frame members as a function on truck position on the bridge deck. WIM data representing real truck traffic (tens of millions of truck records) was filtered and analyzed. Available multi-lane data were analyzed using a cluster analysis. The statistical parameters of this WIM study were used to simulate actual live load on the three-dimensional bridge models and compare load effects to those generated by a fatigue design truck.

The effects of multiple presence on the design of cross-frames in steel I-girder bridges was investigated by performing simulations on available 2-lane vehicle WIM traffic records. The

simulations considered both the probability of multiple presence occurring and the overall effects of multiple presence on the fatigue performance of cross-frames.

Stochastic techniques were used to investigate the implications of using improved load factors developed in this research in the context of reliability-based fatigue design.

7.2 CONCLUSIONS

7.2.1 Truck Placement for Fatigue Design of Cross-Frames

The research documented in this dissertation demonstrated that the current AASHTO *LRFD* Fatigue I and II load factors may be overly conservative for cross-frame design. This is largely attributed to the fact that current design criteria require all possible lane positions be considered in accordance with AASHTO Article 3.6.1.4.3a, regardless of design lanes or actual lane striping. A more realistic scenario is to consider only drive lanes, where the large majority of truck traffic traverses. Although the critical lane position for designing a governing cross-frame member for fatigue in a particular bridge depends on a variety of parameters, in general, truck passages along the outer edges of the deck (i.e., overhang loads) tend to maximize cross-frame forces in skewed and curved bridges, since the load engages cross-frames by applying a net torque on the superstructure. This loading scenario is often geometrically unrealistic. The results demonstrate that truck passages in realistic drive lanes generally produce significantly smaller stress ranges and contribute significantly less to fatigue damage, which can be optimized in the design of cross-frame members for fatigue.

Based on the study results that compared maximum stresses (Fatigue I) and fatigue damage (Fatigue II) in cross-frames caused by WIM traffic records to the same force effects caused by the AASHTO fatigue design truck, the recommended Fatigue I design load factor is 1.01, and the recommended Fatigue II design load factor is 0.53. Both of these values are less than the current AASHTO *LRFD* Fatigue I and II load factors of 1.75 and 0.8, respectively. As a simpler alternative to two new load factors, a single adjustment factor of 0.65 could also be applied to the existing load factors provided in AASHTO *LRFD*.

Using the 20-model bridge set and 18 WIM truck traffic records positioned in the realistic drive lane, the total number of average cycles per passage for all bridges (prior to truncating stresses below 25% CAFL) is 3.7. The total number of cycles per passage varies widely for various

bridge types; because the 20-model bridge set intentionally contains a large number of various bridge parameters, it is generally not possible with the data generated in this research to ascertain which types of bridges tend to produce larger (or smaller) cycles per passage. After truncating stresses below 25% CAFL, the average cycles per passage is more uniform but well below unity, indicating the threshold for truncating stresses (0.65 ksi) represents a significant portion of the total number of cycles contributing to damage, even when only considering truck traffic. While this influences the calculation of the maximum stress ranges for Fatigue I (i.e., the 99.99th percentile maximum stress ranges), the application of Palmgren-Miner's rule in the calculation of the Fatigue II effective stress ranges indicates that this truncation is generally negligible. Truncating stresses below 25% CAFL resulted in an approximate 20% increase in the maximum stresses considered for infinite life per Fatigue I.

The appeal for truncating stresses is generally twofold: 1) reducing the total number of stress cycles recorded and stored during in-service rainflow monitoring preserves data storage and increases computational efficiency, and 2) establishing a threshold for removal of low stress cycles often eliminates unwanted data that did not originate from the traffic loading (e.g., electrical noise, etc.). For this study, these effects are not present in the data, therefore the elimination of lower stress cycles provides insight as to the actual effects on the calculating fatigue parameters. For Fatigue I, the increase in calculated maximum stresses due to stress range truncation is a direct result of removing a significant portion of the lower stress cycles that make up a considerable portion of the force effect spectrum (i.e., the distribution of force effects shifts, resulting in a higher 99.99th percentile). Since the truncated cycles are low, even though there are a large number of these lower cycles, their contribution to accumulated fatigue damage is demonstrated to be low in comparison to the damage caused by the larger stress cycles. This was demonstrated in Chapter 5 per application of Palmgren-Miner's rule. The improved load factors developed and studied in Chapters 5 and 6 are based on the entire stress range of truck traffic.

7.2.2 Multiple Presence

The assumptions of multiple presence in the original LRFD calibration studies (Nowak 1999 and Kulicki et al. 2007) were initially based on engineering judgement and visual observations of truck traffic with unknown weights. These initial assumptions were that a "side by side" scenario (i.e., adjacent lane loaded with a passing truck in general alignment with the drive

lane truck) occurred once every 15 load events. More recent studies have shown this assumption to be excessively conservative (Sivakumar et al. 2007). While the research by Kulicki et al. (2015) confirmed this is an unlikely event, prior to this study the effect of multiple presence has not been reviewed in the context of actual cross-frame force effects.

The WIM study performed in this research confirmed that the dual truck event initially considered in the 7th Edition AASHTO *LRFD* is a rare occurrence. As such, the current load criteria (i.e., a single design truck positioned in all longitudinal and transverse positions) is more appropriate. This multiple presence study indicates that, even when considered, the effects of passing lane traffic on both the Fatigue I and Fatigue II limit state parameters is negligible. A comprehensive multiple lane analysis using all available 2-lane traffic records demonstrates that the probability of a single truck record (regardless of GVW) being located in a critical position for magnifying cross-frame force effects is exceptionally low: less than 0.02% for the most critical location (i.e., one truck's steering axle located just behind another truck's rear axles in an adjacent lane); and less than 3% when the truck is located within 20 to 50 feet from the rear axle of another truck in an adjacent lane.

7.2.3 Reliability of Improved Load Factors for Fatigue Design of Cross-Frames

The improved load factors developed in this research are based on a comprehensive WIM study utilizing calibrated bridge models representative of a variety of straight bridges with normal supports, straight bridges with skewed supports, and horizontally-curved bridges. Assuming the WIM records represent typical truck weights throughout the country, the improved load factors reflect more realistic force effects experienced by cross-frames in these types of bridges. Using published statistical data for resistance, the reliability of using these improved load factors was investigated. The Monte Carlo simulation using the cross-frame statistics in Table 6-5 and the resistance parameters in Table 6-1 resulted in reliability indices as shown in Table 6-6. Based on this analysis, the resulting reliability indices for cross-frames using the load factors developed in Chapter 5 exceeds the target reliability assumed inherent within the AASHTO *LRFD* code.

7.3 Recommendations for Future Research

1. This study reviewed approximately 20 cross-frames from each bridge model based on

extensive parametric studies by Reichenbach (2020). While this assumption is warranted given the considerable effort in understanding cross-frame behavior and the number of iterations required to exhaustively confirm individual cross-frames, it is an assumption that may or may not be accurate for a broad range of bridge designs. An additional study comparable to the sensitivity study conducted in Chapter 4 may be warranted. In this additional study, a selection of bridges and WIM traffic records that produce extreme force effects as shown in this study could be studied exhaustively, where every cross-frame member in the bridge model is reviewed. This study could also exhaustively review the placement of the WIM records in a wide range of realistic transverse positions.

2. Relatively little data exist for detail categories typical of cross-frames; as a result, the available, statistical data for resistance may not be representative of the actual resistance behavior of cross-frames. Recent work (Battistini et al. 2016, McDonald and Frank 2009) revealed that for a limited number of cross-frame tests, the actual resistance behavior for typical single-angle cross-frame details (i.e., single angles and tee-section members welded to gusset plates by longitudinal fillet welds along both sides of the connected element angle) were more appropriately categorized as and E' detail, rather than E. These data are limited, and it would be prudent for additional resistance studies to be performed in order to further understand the resistance behavior of common cross-frame details.
3. The balance of a cost-efficient design and a minimally-acceptable level of safety can be optimized though a reliability based design philosophy similar to AASHTO *LRFD*; however, it has been common practice in the early development of AASHTO *LRFD* to calibrate load and resistance factors to an assumed target reliability inherent in past design that has empirically worked well. This was considered a first step in code calibration; ultimately, code-writing bodies must establish a tolerable probability of failure. In order to more appropriately balance a cost-efficient bridge design and a bridge

design with a minimally-acceptable level of safety, it is important to look at the system reliability of bridge elements. In this approach, an element such as a cross-frame is not isolated from the bridge in the context of failure; rather, the system effect of the cross-frame, the girders to which they are attached, the contributions to stiffness from the bridge deck and other framing members, as well as deterioration models for these elements may result in decreased consequences of individual element failures. The system reliability of both cross-frames and girders requires additional research to improve this balance.

Appendix A: Sample of Raw WIM Data

Table A-1: WIM Data Entry Description for Table A-2.

Column Number	Description	Column Number	Description
1	Year	**23**	5th Axle Weight (kip)
2	Month	**24**	5-6 Axle Spacing (ft)
3	Day	**25**	6th Axle Weight (kip)
4	Hour (Military)	**26**	6-7 Axle Spacing (ft)
5	Minute	**27**	7th Axle Weight (kip)
6	Second	**28**	7-8 Axle Spacing (ft)
7	Hundredth of Second	**29**	8th Axle Weight (kip)
8	Error Number	**30**	8-9 Axle Spacing (ft)
9	Lane	**31**	9th Axle Weight (kip)
10	Speed	**32**	9-10 Axle Spacing (ft)
11	Class	**33**	10th Axle Weight (kip)
12	Length	**34**	10-11 Axle Spacing (ft)
13	GVW	**35**	11th Axle Weight (kip)
14	ESAL	**36**	11-12 Axle Spacing (ft)
15	1st Axle Weight (kip)	**37**	12th Axle Weight (kip)
16	1-2 Axle Spacing (ft)	**38**	12-13 Axle Spacing (ft)
17	2nd Axle Weight (kip)	**39**	13th Axle Weight (kip)
18	2-3 Axle Spacing (ft)	**40**	13-14 Axle Spacing (ft)
19	3rd Axle Weight (kip)	**41**	14th Axle Weight (kip)
20	3-4 Axle Spacing (ft)	**42**	-
21	4th Axle Weight (kip)	**43**	-
22	4-5 Axle Spacing (ft)	**44**	-

Table A-2: Sample WIM Data Entry (New Mexico I-25)[1].

14,1,1,0,6,8,29,0,11,1,79,2,12,3.4,0.000,2.0,8.6,1.4,0.0,0.0,0.0,0.0,0.0,0.0,0.0,0.0,0.0,0.0,0.0,0.0,0.0,0.0,0.0,0.0,0.0,0.0,…

14,1,1,0,8,58,21,0,11,1,75,2,15,6.1,0.002,3.0,9.6,3.2,0.0,0.0,0.0,0.0,0.0,0.0,0.0,0.0,0.0,0.0,0.0,0.0,0.0,0.0,0.0,0.0,0.0,0.0,0.0,…

14,1,1,0,9,1,52,0,11,1,76,2,14,4.4,0.000,2.3,8.8,2.0,0.0,0.0,0.0,0.0,0.0,0.0,0.0,0.0,0.0,0.0,0.0,0.0,0.0,0.0,0.0,0.0,0.0,0.0,0.0,…

14,1,1,0,11,50,81,0,11,1,72,3,15,4.2,0.000,2.3,10.6,1.9,0.0,0.0,0.0,0.0,0.0,0.0,0.0,0.0,0.0,0.0,0.0,0.0,0.0,0.0,0.0,0.0,0.0,0.0,…

14,1,1,0,17,0,36,0,11,1,69,2,30,6.3,0.001,1.6,8.7,2.5,16.0,2.2,0.0,0.0,0.0,0.0,0.0,0.0,0.0,0.0,0.0,0.0,0.0,0.0,0.0,0.0,0.0,0.0,…

14,1,1,0,17,1,86,0,11,1,70,2,15,3.6,0.000,2.0,9.0,1.6,0.0,0.0,0.0,0.0,0.0,0.0,0.0,0.0,0.0,0.0,0.0,0.0,0.0,0.0,0.0,0.0,0.0,0.0,…

14,1,1,0,20,23,45,0,11,1,76,2,13,2.5,0.000,1.6,8.6,1.0,0.0,0.0,0.0,0.0,0.0,0.0,0.0,0.0,0.0,0.0,0.0,0.0,0.0,0.0,0.0,0.0,0.0,0.0,…

14,1,1,0,24,34,74,0,11,1,63,11,72,38.3,0.191,8.4,12.6,9.6,20.8,6.6,9.4,6.6,22.0,7.2,0.0,0.0,0.0,0.0,0.0,0.0,0.0,0.0,0.0,0.0,…

14,1,1,0,26,39,71,0,11,1,87,2,13,3.4,0.000,1.9,8.7,1.4,0.0,0.0,0.0,0.0,0.0,0.0,0.0,0.0,0.0,0.0,0.0,0.0,0.0,0.0,0.0,0.0,0.0,0.0,…

14,1,1,0,27,44,67,0,11,1,68,9,73,78.3,3.566,12.0,16.1,16.6,4.3,16.4,33.6,17.2,4.1,16.2,0.0,0.0,0.0,0.0,0.0,0.0,0.0,0.0,…

14,1,1,0,29,40,93,0,11,1,68,6,24,20.5,0.196,11.6,15.8,4.8,4.5,4.1,0.0,0.0,0.0,0.0,0.0,0.0,0.0,0.0,0.0,0.0,0.0,0.0,0.0,0.0,0.0,0.0,…

14,1,1,0,30,15,94,0,11,1,77,2,13,3.6,0.000,2.1,8.6,1.5,0.0,0.0,0.0,0.0,0.0,0.0,0.0,0.0,0.0,0.0,0.0,0.0,0.0,0.0,0.0,0.0,0.0,0.0,…

14,1,1,0,33,18,99,0,11,1,71,3,17,6.4,0.002,3.5,11.9,2.9,0.0,0.0,0.0,0.0,0.0,0.0,0.0,0.0,0.0,0.0,0.0,0.0,0.0,0.0,0.0,0.0,0.0,0.0,…

14,1,1,0,34,38,76,0,11,1,75,3,17,4.5,0.001,2.7,11.9,1.9,0.0,0.0,0.0,0.0,0.0,0.0,0.0,0.0,0.0,0.0,0.0,0.0,0.0,0.0,0.0,0.0,0.0,0.0,…

14,1,1,0,39,9,68,0,11,1,77,2,13,3.2,0.000,1.8,8.4,1.5,0.0,0.0,0.0,0.0,0.0,0.0,0.0,0.0,0.0,0.0,0.0,0.0,0.0,0.0,0.0,0.0,0.0,0.0,…

14,1,1,0,42,9,10,0,11,1,80,3,17,6.3,0.002,3.0,10.9,3.4,0.0,0.0,0.0,0.0,0.0,0.0,0.0,0.0,0.0,0.0,0.0,0.0,0.0,0.0,0.0,0.0,0.0,0.0,…

14,1,1,0,45,30,21,0,11,1,73,9,67,43.3,0.346,8.8,11.1,10.2,4.3,9.4,35.7,7.5,4.1,7.4,0.0,0.0,0.0,0.0,0.0,0.0,0.0,0.0,0.0,…

14,1,1,0,53,0,64,0,11,1,80,2,14,4.1,0.000,2.3,9.3,1.8,0.0,0.0,0.0,0.0,0.0,0.0,0.0,0.0,0.0,0.0,0.0,0.0,0.0,0.0,0.0,0.0,0.0,0.0,…

14,1,1,0,57,18,77,0,11,1,73,2,14,3.7,0.000,2.2,9.3,1.5,0.0,0.0,0.0,0.0,0.0,0.0,0.0,0.0,0.0,0.0,0.0,0.0,0.0,0.0,0.0,0.0,0.0,0.0,…

14,1,1,1,5,45,13,0,11,1,63,2,15,5.9,0.002,3.1,9.8,2.8,0.0,0.0,0.0,0.0,0.0,0.0,0.0,0.0,0.0,0.0,0.0,0.0,0.0,0.0,0.0,0.0,0.0,0.0,…

14,1,1,1,6,18,42,0,11,1,78,2,15,3.9,0.000,2.2,9.2,1.7,0.0,0.0,0.0,0.0,0.0,0.0,0.0,0.0,0.0,0.0,0.0,0.0,0.0,0.0,0.0,0.0,0.0,0.0,…

14,1,1,1,7,40,47,0,11,1,74,2,13,3.2,0.000,1.9,9.0,1.3,0.0,0.0,0.0,0.0,0.0,0.0,0.0,0.0,0.0,0.0,0.0,0.0,0.0,0.0,0.0,0.0,0.0,0.0,…

14,1,1,1,14,42,31,0,11,1,76,2,13,3.7,0.000,2.0,8.9,1.6,0.0,0.0,0.0,0.0,0.0,0.0,0.0,0.0,0.0,0.0,0.0,0.0,0.0,0.0,0.0,0.0,0.0,0.0,…

[1]*End of data file truncated for viewing purposes.*

Appendix B: Bridge Model Summary

Table B-1 (adapted from Reichenbach 2020) summarizes all parameters used to describe and develop the 4,104-model data set from the analytical testing matrix. Only 13 independent variables are shown. Independent constants and dependent variables are discussed in Reichenbach 2020.

Several abbreviations are used in the table, which are identified as follows: "Mat'l" = material; n_{span} = number of spans; L/d ratio = span-to-depth ratio; s_g = girder spacing, n_g = number of girders; R = radius of horizontal curvature; s_{cf} = typical intermediate cross-frame spacing; "CF" = cross-frame; d_w = web depth; t_{deck} = deck thickness; A_{cf} = area of cross-frame member; E_c = elastic modulus of concrete deck; "Cont." = contiguous line of cross-frames; and "Stag." = staggered cross-frame layout.

Table B-1: Independent parameters that describe the bridge geometries and cross-frame layouts of all 4,104 unique bridges considered in the parametric study. Highlighted models correspond to the 20 model subset.

Model ID	Geometry									Cross-section		CF detail		Mat'l
	n_{span}	L/d ratio	s_g [ft]	n_{girder}	Support skew [deg]; Layout		R [ft]	s_{cf} [ft]	CF layout	d_w [in]	t_{deck} [in]	CF type	A_{cf} [in^2]	E_c [ksi]
1-1	1	25	6	3	0	Parallel	1500	20	Cont.	72	8	X	2.86	3600
1-2	1	25	6	3	0	Parallel	1500	20	Cont.	72	8	X	2.86	5000
1-3	1	25	6	3	0	Parallel	1500	20	Cont.	72	10	X	2.86	5000
1-4	1	25	6	3	0	Parallel	1500	20	Cont.	72	8	K	2.86	5000
1-5	1	25	6	3	0	Parallel	1500	20	Cont.	72	8	X	4.79	5000
2-1	1	25	6	3	0	Parallel	1500	30	Cont.	72	8	X	2.86	5000
3-1	1	25	6	3	0	Parallel	750	20	Cont.	72	8	X	2.86	3600
3-2	1	25	6	3	0	Parallel	750	20	Cont.	72	8	X	2.86	5000
3-3	1	25	6	3	0	Parallel	750	20	Cont.	72	10	X	2.86	5000
3-4	1	25	6	3	0	Parallel	750	20	Cont.	72	8	K	2.86	5000
3-5	1	25	6	3	0	Parallel	750	20	Cont.	72	8	X	4.79	5000
4-1	1	25	6	3	0	Parallel	750	30	Cont.	72	8	X	2.86	5000
5-1	1	25	6	3	30	Parallel	1500	20	Cont.	72	8	X	2.86	3600
5-2	1	25	6	3	30	Parallel	1500	20	Cont.	72	8	X	2.86	5000
5-3	1	25	6	3	30	Parallel	1500	20	Cont.	72	10	X	2.86	5000
5-4	1	25	6	3	30	Parallel	1500	20	Cont.	72	8	K	2.86	5000
5-5	1	25	6	3	30	Parallel	1500	20	Cont.	72	8	X	4.79	5000
6-1	1	25	6	3	30	Parallel	1500	30	Cont.	72	8	X	2.86	5000
7-1	1	25	6	3	30	Parallel	750	20	Cont.	72	8	X	2.86	3600
7-2	1	25	6	3	30	Parallel	750	20	Cont.	72	8	X	2.86	5000
7-3	1	25	6	3	30	Parallel	750	20	Cont.	72	10	X	2.86	5000
7-4	1	25	6	3	30	Parallel	750	20	Cont.	72	8	K	2.86	5000
7-5	1	25	6	3	30	Parallel	750	20	Cont.	72	8	X	4.79	5000
8-1	1	25	6	3	30	Parallel	750	30	Cont.	72	8	X	2.86	5000
9-1	1	25	6	3	60	Parallel	1500	20	Cont.	72	8	X	2.86	3600
9-2	1	25	6	3	60	Parallel	1500	20	Cont.	72	8	X	2.86	5000
9-3	1	25	6	3	60	Parallel	1500	20	Cont.	72	10	X	2.86	5000
9-4	1	25	6	3	60	Parallel	1500	20	Cont.	72	8	K	2.86	5000
9-5	1	25	6	3	60	Parallel	1500	20	Cont.	72	8	X	4.79	5000
10-1	1	25	6	3	60	Parallel	1500	30	Cont.	72	8	X	2.86	5000
11-1	1	25	6	3	60	Parallel	750	20	Cont.	72	8	X	2.86	3600
11-2	1	25	6	3	60	Parallel	750	20	Cont.	72	8	X	2.86	5000
11-3	1	25	6	3	60	Parallel	750	20	Cont.	72	10	X	2.86	5000
11-4	1	25	6	3	60	Parallel	750	20	Cont.	72	8	K	2.86	5000
11-5	1	25	6	3	60	Parallel	750	20	Cont.	72	8	X	4.79	5000
12-1	1	25	6	3	60	Parallel	750	30	Cont.	72	8	X	2.86	5000
13-1	1	25	6	3	60	Trap.	1500	20	Cont.	72	8	X	2.86	3600
13-2	1	25	6	3	60	Trap.	1500	20	Cont.	72	8	X	2.86	5000
13-3	1	25	6	3	60	Trap.	1500	20	Cont.	72	10	X	2.86	5000
13-4	1	25	6	3	60	Trap.	1500	20	Cont.	72	8	K	2.86	5000
13-5	1	25	6	3	60	Trap.	1500	20	Cont.	72	8	X	4.79	5000
14-1	1	25	6	3	60	Trap.	1500	30	Cont.	72	8	X	2.86	5000
15-1	1	25	6	3	60	Trap.	750	20	Cont.	72	8	X	2.86	3600
15-2	1	25	6	3	60	Trap.	750	20	Cont.	72	8	X	2.86	5000
15-3	1	25	6	3	60	Trap.	750	20	Cont.	72	10	X	2.86	5000
15-4	1	25	6	3	60	Trap.	750	20	Cont.	72	8	K	2.86	5000
15-5	1	25	6	3	60	Trap.	750	20	Cont.	72	8	X	4.79	5000
16-1	1	25	6	3	60	Trap.	750	30	Cont.	72	8	X	2.86	5000
17-1	1	25	6	5	0	Parallel	1500	20	Cont.	72	8	X	2.86	3600
17-2	1	25	6	5	0	Parallel	1500	20	Cont.	72	8	X	2.86	5000
17-3	1	25	6	5	0	Parallel	1500	20	Cont.	72	10	X	2.86	5000
17-4	1	25	6	5	0	Parallel	1500	20	Cont.	72	8	K	2.86	5000
17-5	1	25	6	5	0	Parallel	1500	20	Cont.	72	8	X	4.79	5000
18-1	1	25	6	5	0	Parallel	1500	30	Cont.	72	8	X	2.86	5000
19-1	1	25	6	5	0	Parallel	750	20	Cont.	72	8	X	2.86	3600
19-2	1	25	6	5	0	Parallel	750	20	Cont.	72	8	X	2.86	5000
19-3	1	25	6	5	0	Parallel	750	20	Cont.	72	10	X	2.86	5000
19-4	1	25	6	5	0	Parallel	750	20	Cont.	72	8	K	2.86	5000
19-5	1	25	6	5	0	Parallel	750	20	Cont.	72	8	X	4.79	5000
20-1	1	25	6	5	0	Parallel	750	30	Cont.	72	8	X	2.86	5000
21-1	1	25	6	5	30	Parallel	1500	20	Cont.	72	8	X	2.86	3600
21-2	1	25	6	5	30	Parallel	1500	20	Cont.	72	8	X	2.86	5000
21-3	1	25	6	5	30	Parallel	1500	20	Cont.	72	10	X	2.86	5000
21-4	1	25	6	5	30	Parallel	1500	20	Cont.	72	8	K	2.86	5000
21-5	1	25	6	5	30	Parallel	1500	20	Cont.	72	8	X	4.79	5000
22-1	1	25	6	5	30	Parallel	1500	30	Cont.	72	8	X	2.86	5000
23-1	1	25	6	5	30	Parallel	750	20	Cont.	72	8	X	2.86	3600

Model ID	Geometry									Cross-section		CF detail		Mat'l
	n_{span}	L/d ratio	s_g [ft]	n_{girder}	Support skew [deg]; Layout		R [ft]	s_{cf} [ft]	CF layout	d_w [in]	t_{deck} [in]	CF type	A_{cf} [in^2]	E_c [ksi]
23-2	1	25	6	5	30	Parallel	750	20	Cont.	72	8	X	2.86	5000
23-3	1	25	6	5	30	Parallel	750	20	Cont.	72	10	X	2.86	5000
23-4	1	25	6	5	30	Parallel	750	20	Cont.	72	8	K	2.86	5000
23-5	1	25	6	5	30	Parallel	750	20	Cont.	72	8	X	4.79	5000
24-1	1	25	6	5	30	Parallel	750	30	Cont.	72	8	X	2.86	5000
25-1	1	25	6	5	60	Parallel	1500	20	Cont.	72	8	X	2.86	3600
25-2	1	25	6	5	60	Parallel	1500	20	Cont.	72	8	X	2.86	5000
25-3	1	25	6	5	60	Parallel	1500	20	Cont.	72	10	X	2.86	5000
25-4	1	25	6	5	60	Parallel	1500	20	Cont.	72	8	K	2.86	5000
25-5	1	25	6	5	60	Parallel	1500	20	Cont.	72	8	X	4.79	5000
26-1	1	25	6	5	60	Parallel	1500	30	Cont.	72	8	X	2.86	5000
27-1	1	25	6	5	60	Parallel	750	20	Cont.	72	8	X	2.86	3600
27-2	1	25	6	5	60	Parallel	750	20	Cont.	72	8	X	2.86	5000
27-3	1	25	6	5	60	Parallel	750	20	Cont.	72	10	X	2.86	5000
27-4	1	25	6	5	60	Parallel	750	20	Cont.	72	8	K	2.86	5000
27-5	1	25	6	5	60	Parallel	750	20	Cont.	72	8	X	4.79	5000
28-1	1	25	6	5	60	Parallel	750	30	Cont.	72	8	X	2.86	5000
29-1	1	25	6	5	60	Trap.	1500	20	Cont.	72	8	X	2.86	3600
29-2	1	25	6	5	60	Trap.	1500	20	Cont.	72	8	X	2.86	5000
29-3	1	25	6	5	60	Trap.	1500	20	Cont.	72	10	X	2.86	5000
29-4	1	25	6	5	60	Trap.	1500	20	Cont.	72	8	K	2.86	5000
29-5	1	25	6	5	60	Trap.	1500	20	Cont.	72	8	X	4.79	5000
30-1	1	25	6	5	60	Trap.	1500	30	Cont.	72	8	X	2.86	5000
31-1	1	25	6	5	60	Trap.	750	20	Cont.	72	8	X	2.86	3600
31-2	1	25	6	5	60	Trap.	750	20	Cont.	72	8	X	2.86	5000
31-3	1	25	6	5	60	Trap.	750	20	Cont.	72	10	X	2.86	5000
31-4	1	25	6	5	60	Trap.	750	20	Cont.	72	8	K	2.86	5000
31-5	1	25	6	5	60	Trap.	750	20	Cont.	72	8	X	4.79	5000
32-1	1	25	6	5	60	Trap.	750	30	Cont.	72	8	X	2.86	5000
33-1	1	25	8	3	0	Parallel	1500	20	Cont.	72	8	X	2.86	3600
33-2	1	25	8	3	0	Parallel	1500	20	Cont.	72	8	X	2.86	5000
33-3	1	25	8	3	0	Parallel	1500	20	Cont.	72	10	X	2.86	5000
33-4	1	25	8	3	0	Parallel	1500	20	Cont.	72	8	K	2.86	5000
33-5	1	25	8	3	0	Parallel	1500	20	Cont.	72	8	X	4.79	5000
34-1	1	25	8	3	0	Parallel	1500	30	Cont.	72	8	X	2.86	5000
35-1	1	25	8	3	0	Parallel	750	20	Cont.	72	8	X	2.86	3600
35-2	1	25	8	3	0	Parallel	750	20	Cont.	72	8	X	2.86	5000
35-3	1	25	8	3	0	Parallel	750	20	Cont.	72	10	X	2.86	5000
35-4	1	25	8	3	0	Parallel	750	20	Cont.	72	8	K	2.86	5000
35-5	1	25	8	3	0	Parallel	750	20	Cont.	72	8	X	4.79	5000
36-1	1	25	8	3	0	Parallel	750	30	Cont.	72	8	X	2.86	5000
37-1	1	25	8	3	30	Parallel	1500	20	Cont.	72	8	X	2.86	3600
37-2	1	25	8	3	30	Parallel	1500	20	Cont.	72	8	X	2.86	5000
37-3	1	25	8	3	30	Parallel	1500	20	Cont.	72	10	X	2.86	5000
37-4	1	25	8	3	30	Parallel	1500	20	Cont.	72	8	K	2.86	5000
37-5	1	25	8	3	30	Parallel	1500	20	Cont.	72	8	X	4.79	5000
38-1	1	25	8	3	30	Parallel	1500	30	Cont.	72	8	X	2.86	5000
39-1	1	25	8	3	30	Parallel	750	20	Cont.	72	8	X	2.86	3600
39-2	1	25	8	3	30	Parallel	750	20	Cont.	72	8	X	2.86	5000
39-3	1	25	8	3	30	Parallel	750	20	Cont.	72	10	X	2.86	5000
39-4	1	25	8	3	30	Parallel	750	20	Cont.	72	8	K	2.86	5000
39-5	1	25	8	3	30	Parallel	750	20	Cont.	72	8	X	4.79	5000
40-1	1	25	8	3	30	Parallel	750	30	Cont.	72	8	X	2.86	5000
41-1	1	25	8	3	60	Parallel	1500	20	Cont.	72	8	X	2.86	3600
41-2	1	25	8	3	60	Parallel	1500	20	Cont.	72	8	X	2.86	5000
41-3	1	25	8	3	60	Parallel	1500	20	Cont.	72	10	X	2.86	5000
41-4	1	25	8	3	60	Parallel	1500	20	Cont.	72	8	K	2.86	5000
41-5	1	25	8	3	60	Parallel	1500	20	Cont.	72	8	X	4.79	5000
42-1	1	25	8	3	60	Parallel	1500	30	Cont.	72	8	X	2.86	5000
43-1	1	25	8	3	60	Parallel	750	20	Cont.	72	8	X	2.86	3600
43-2	1	25	8	3	60	Parallel	750	20	Cont.	72	8	X	2.86	5000
43-3	1	25	8	3	60	Parallel	750	20	Cont.	72	10	X	2.86	5000
43-4	1	25	8	3	60	Parallel	750	20	Cont.	72	8	K	2.86	5000
43-5	1	25	8	3	60	Parallel	750	20	Cont.	72	8	X	4.79	5000
44-1	1	25	8	3	60	Parallel	750	30	Cont.	72	8	X	2.86	5000
45-1	1	25	8	3	60	Trap.	1500	20	Cont.	72	8	X	2.86	3600
45-2	1	25	8	3	60	Trap.	1500	20	Cont.	72	8	X	2.86	5000
45-3	1	25	8	3	60	Trap.	1500	20	Cont.	72	10	X	2.86	5000
45-4	1	25	8	3	60	Trap.	1500	20	Cont.	72	8	K	2.86	5000
45-5	1	25	8	3	60	Trap.	1500	20	Cont.	72	8	X	4.79	5000
46-1	1	25	8	3	60	Trap.	1500	30	Cont.	72	8	X	2.86	5000
47-1	1	25	8	3	60	Trap.	750	20	Cont.	72	8	X	2.86	3600
47-2	1	25	8	3	60	Trap.	750	20	Cont.	72	8	X	2.86	5000

Model ID	Geometry									Cross-section		CF detail		Mat'l
	n_{span}	L/d ratio	s_g [ft]	n_{girder}	Support skew [deg];	Layout	R [ft]	s_{cf} [ft]	CF layout	d_w [in]	t_{deck} [in]	CF type	A_{cf} [in^2]	E_c [ksi]
47-3	1	25	8	3	60	Trap.	750	20	Cont.	72	10	X	2.86	5000
47-4	1	25	8	3	60	Trap.	750	20	Cont.	72	8	K	2.86	5000
47-5	1	25	8	3	60	Trap.	750	20	Cont.	72	8	X	4.79	5000
48-1	1	25	8	3	60	Trap.	750	30	Cont.	72	8	X	2.86	5000
49-1	1	25	8	5	0	Parallel	1500	20	Cont.	72	8	X	2.86	3600
49-2	1	25	8	5	0	Parallel	1500	20	Cont.	72	8	X	2.86	5000
49-3	1	25	8	5	0	Parallel	1500	20	Cont.	72	10	X	2.86	5000
49-4	1	25	8	5	0	Parallel	1500	20	Cont.	72	8	K	2.86	5000
49-5	1	25	8	5	0	Parallel	1500	20	Cont.	72	8	X	4.79	5000
50-1	1	25	8	5	0	Parallel	1500	30	Cont.	72	8	X	2.86	5000
51-1	1	25	8	5	0	Parallel	750	20	Cont.	72	8	X	2.86	3600
51-2	1	25	8	5	0	Parallel	750	20	Cont.	72	8	X	2.86	5000
51-3	1	25	8	5	0	Parallel	750	20	Cont.	72	10	X	2.86	5000
51-4	1	25	8	5	0	Parallel	750	20	Cont.	72	8	K	2.86	5000
51-5	1	25	8	5	0	Parallel	750	20	Cont.	72	8	X	4.79	5000
52-1	1	25	8	5	0	Parallel	750	30	Cont.	72	8	X	2.86	5000
53-1	1	25	8	5	30	Parallel	1500	20	Cont.	72	8	X	2.86	3600
53-2	1	25	8	5	30	Parallel	1500	20	Cont.	72	8	X	2.86	5000
53-3	1	25	8	5	30	Parallel	1500	20	Cont.	72	10	X	2.86	5000
53-4	1	25	8	5	30	Parallel	1500	20	Cont.	72	8	K	2.86	5000
53-5	1	25	8	5	30	Parallel	1500	20	Cont.	72	8	X	4.79	5000
54-1	1	25	8	5	30	Parallel	1500	30	Cont.	72	8	X	2.86	5000
55-1	1	25	8	5	30	Parallel	750	20	Cont.	72	8	X	2.86	3600
55-2	1	25	8	5	30	Parallel	750	20	Cont.	72	8	X	2.86	5000
55-3	1	25	8	5	30	Parallel	750	20	Cont.	72	10	X	2.86	5000
55-4	1	25	8	5	30	Parallel	750	20	Cont.	72	8	K	2.86	5000
55-5	1	25	8	5	30	Parallel	750	20	Cont.	72	8	X	4.79	5000
56-1	1	25	8	5	30	Parallel	750	30	Cont.	72	8	X	2.86	5000
57-1	1	25	8	5	60	Parallel	1500	20	Cont.	72	8	X	2.86	3600
57-2	1	25	8	5	60	Parallel	1500	20	Cont.	72	8	X	2.86	5000
57-3	1	25	8	5	60	Parallel	1500	20	Cont.	72	10	X	2.86	5000
57-4	1	25	8	5	60	Parallel	1500	20	Cont.	72	8	K	2.86	5000
57-5	1	25	8	5	60	Parallel	1500	20	Cont.	72	8	X	4.79	5000
58-1	1	25	8	5	60	Parallel	1500	30	Cont.	72	8	X	2.86	5000
59-1	1	25	8	5	60	Parallel	750	20	Cont.	72	8	X	2.86	3600
59-2	1	25	8	5	60	Parallel	750	20	Cont.	72	8	X	2.86	5000
59-3	1	25	8	5	60	Parallel	750	20	Cont.	72	10	X	2.86	5000
59-4	1	25	8	5	60	Parallel	750	20	Cont.	72	8	K	2.86	5000
59-5	1	25	8	5	60	Parallel	750	20	Cont.	72	8	X	4.79	5000
60-1	1	25	8	5	60	Parallel	750	30	Cont.	72	8	X	2.86	5000
61-1	1	25	8	5	60	Trap.	1500	20	Cont.	72	8	X	2.86	3600
61-2	1	25	8	5	60	Trap.	1500	20	Cont.	72	8	X	2.86	5000
61-3	1	25	8	5	60	Trap.	1500	20	Cont.	72	10	X	2.86	5000
61-4	1	25	8	5	60	Trap.	1500	20	Cont.	72	8	K	2.86	5000
61-5	1	25	8	5	60	Trap.	1500	20	Cont.	72	8	X	4.79	5000
62-1	1	25	8	5	60	Trap.	1500	30	Cont.	72	8	X	2.86	5000
63-1	1	25	8	5	60	Trap.	750	20	Cont.	72	8	X	2.86	3600
63-2	1	25	8	5	60	Trap.	750	20	Cont.	72	8	X	2.86	5000
63-3	1	25	8	5	60	Trap.	750	20	Cont.	72	10	X	2.86	5000
63-4	1	25	8	5	60	Trap.	750	20	Cont.	72	8	K	2.86	5000
63-5	1	25	8	5	60	Trap.	750	20	Cont.	72	8	X	4.79	5000
64-1	1	25	8	5	60	Trap.	750	30	Cont.	72	8	X	2.86	5000
65-1	1	25	10	3	0	Parallel	1500	20	Cont.	72	8	X	2.86	3600
65-2	1	25	10	3	0	Parallel	1500	20	Cont.	72	8	X	2.86	5000
65-3	1	25	10	3	0	Parallel	1500	20	Cont.	72	10	X	2.86	5000
65-4	1	25	10	3	0	Parallel	1500	20	Cont.	72	8	K	2.86	5000
65-5	1	25	10	3	0	Parallel	1500	20	Cont.	72	8	X	4.79	5000
66-1	1	25	10	3	0	Parallel	1500	30	Cont.	72	8	X	2.86	5000
67-1	1	25	10	3	0	Parallel	750	20	Cont.	72	8	X	2.86	3600
67-2	1	25	10	3	0	Parallel	750	20	Cont.	72	8	X	2.86	5000
67-3	1	25	10	3	0	Parallel	750	20	Cont.	72	10	X	2.86	5000
67-4	1	25	10	3	0	Parallel	750	20	Cont.	72	8	K	2.86	5000
67-5	1	25	10	3	0	Parallel	750	20	Cont.	72	8	X	4.79	5000
68-1	1	25	10	3	0	Parallel	750	30	Cont.	72	8	X	2.86	5000
69-1	1	25	10	3	30	Parallel	1500	20	Cont.	72	8	X	2.86	3600
69-2	1	25	10	3	30	Parallel	1500	20	Cont.	72	8	X	2.86	5000
69-3	1	25	10	3	30	Parallel	1500	20	Cont.	72	10	X	2.86	5000
69-4	1	25	10	3	30	Parallel	1500	20	Cont.	72	8	K	2.86	5000
69-5	1	25	10	3	30	Parallel	1500	20	Cont.	72	8	X	4.79	5000
70-1	1	25	10	3	30	Parallel	1500	30	Cont.	72	8	X	2.86	5000
71-1	1	25	10	3	30	Parallel	750	20	Cont.	72	8	X	2.86	3600
71-2	1	25	10	3	30	Parallel	750	20	Cont.	72	8	X	2.86	5000
71-3	1	25	10	3	30	Parallel	750	20	Cont.	72	10	X	2.86	5000

Model ID	Geometry									Cross-section		CF detail		Mat'l
	n_{span}	L/d ratio	s_g [ft]	n_{girder}	Support skew [deg]; Layout		R [ft]	s_{cf} [ft]	CF layout	d_w [in]	t_{deck} [in]	CF type	A_{cf} [in^2]	E_c [ksi]
71-4	1	25	10	3	30	Parallel	750	20	Cont.	72	8	K	2.86	5000
71-5	1	25	10	3	30	Parallel	750	20	Cont.	72	8	X	4.79	5000
72-1	1	25	10	3	30	Parallel	750	30	Cont.	72	8	X	2.86	5000
73-1	1	25	10	3	60	Parallel	1500	20	Cont.	72	8	X	2.86	3600
73-2	1	25	10	3	60	Parallel	1500	20	Cont.	72	8	X	2.86	5000
73-3	1	25	10	3	60	Parallel	1500	20	Cont.	72	10	X	2.86	5000
73-4	1	25	10	3	60	Parallel	1500	20	Cont.	72	8	K	2.86	5000
73-5	1	25	10	3	60	Parallel	1500	20	Cont.	72	8	X	4.79	5000
74-1	1	25	10	3	60	Parallel	1500	30	Cont.	72	8	X	2.86	5000
75-1	1	25	10	3	60	Parallel	750	20	Cont.	72	8	X	2.86	3600
75-2	1	25	10	3	60	Parallel	750	20	Cont.	72	8	X	2.86	5000
75-3	1	25	10	3	60	Parallel	750	20	Cont.	72	10	X	2.86	5000
75-4	1	25	10	3	60	Parallel	750	20	Cont.	72	8	K	2.86	5000
75-5	1	25	10	3	60	Parallel	750	20	Cont.	72	8	X	4.79	5000
76-1	1	25	10	3	60	Parallel	750	30	Cont.	72	8	X	2.86	5000
77-1	1	25	10	3	60	Trap.	1500	20	Cont.	72	8	X	2.86	3600
77-2	1	25	10	3	60	Trap.	1500	20	Cont.	72	8	X	2.86	5000
77-3	1	25	10	3	60	Trap.	1500	20	Cont.	72	10	X	2.86	5000
77-4	1	25	10	3	60	Trap.	1500	20	Cont.	72	8	K	2.86	5000
77-5	1	25	10	3	60	Trap.	1500	20	Cont.	72	8	X	4.79	5000
78-1	1	25	10	3	60	Trap.	1500	30	Cont.	72	8	X	2.86	5000
79-1	1	25	10	3	60	Trap.	750	20	Cont.	72	8	X	2.86	3600
79-2	1	25	10	3	60	Trap.	750	20	Cont.	72	8	X	2.86	5000
79-3	1	25	10	3	60	Trap.	750	20	Cont.	72	10	X	2.86	5000
79-4	1	25	10	3	60	Trap.	750	20	Cont.	72	8	K	2.86	5000
79-5	1	25	10	3	60	Trap.	750	20	Cont.	72	8	X	4.79	5000
80-1	1	25	10	3	60	Trap.	750	30	Cont.	72	8	X	2.86	5000
81-1	1	25	10	5	0	Parallel	1500	20	Cont.	72	8	X	2.86	3600
81-2	1	25	10	5	0	Parallel	1500	20	Cont.	72	8	X	2.86	5000
81-3	1	25	10	5	0	Parallel	1500	20	Cont.	72	10	X	2.86	5000
81-4	1	25	10	5	0	Parallel	1500	20	Cont.	72	8	K	2.86	5000
81-5	1	25	10	5	0	Parallel	1500	20	Cont.	72	8	X	4.79	5000
82-1	1	25	10	5	0	Parallel	1500	30	Cont.	72	8	X	2.86	5000
83-1	1	25	10	5	0	Parallel	750	20	Cont.	72	8	X	2.86	3600
83-2	1	25	10	5	0	Parallel	750	20	Cont.	72	8	X	2.86	5000
83-3	1	25	10	5	0	Parallel	750	20	Cont.	72	10	X	2.86	5000
83-4	1	25	10	5	0	Parallel	750	20	Cont.	72	8	K	2.86	5000
83-5	1	25	10	5	0	Parallel	750	20	Cont.	72	8	X	4.79	5000
84-1	1	25	10	5	0	Parallel	750	30	Cont.	72	8	X	2.86	5000
85-1	1	25	10	5	30	Parallel	1500	20	Cont.	72	8	X	2.86	3600
85-2	1	25	10	5	30	Parallel	1500	20	Cont.	72	8	X	2.86	5000
85-3	1	25	10	5	30	Parallel	1500	20	Cont.	72	10	X	2.86	5000
85-4	1	25	10	5	30	Parallel	1500	20	Cont.	72	8	K	2.86	5000
85-5	1	25	10	5	30	Parallel	1500	20	Cont.	72	8	X	4.79	5000
86-1	1	25	10	5	30	Parallel	1500	30	Cont.	72	8	X	2.86	5000
87-1	1	25	10	5	30	Parallel	750	20	Cont.	72	8	X	2.86	3600
87-2	1	25	10	5	30	Parallel	750	20	Cont.	72	8	X	2.86	5000
87-3	1	25	10	5	30	Parallel	750	20	Cont.	72	10	X	2.86	5000
87-4	1	25	10	5	30	Parallel	750	20	Cont.	72	8	K	2.86	5000
87-5	1	25	10	5	30	Parallel	750	20	Cont.	72	8	X	4.79	5000
88-1	1	25	10	5	30	Parallel	750	30	Cont.	72	8	X	2.86	5000
89-1	1	25	10	5	60	Parallel	1500	20	Cont.	72	8	X	2.86	3600
89-2	1	25	10	5	60	Parallel	1500	20	Cont.	72	8	X	2.86	5000
89-3	1	25	10	5	60	Parallel	1500	20	Cont.	72	10	X	2.86	5000
89-4	1	25	10	5	60	Parallel	1500	20	Cont.	72	8	K	2.86	5000
89-5	1	25	10	5	60	Parallel	1500	20	Cont.	72	8	X	4.79	5000
90-1	1	25	10	5	60	Parallel	1500	30	Cont.	72	8	X	2.86	5000
91-1	1	25	10	5	60	Parallel	750	20	Cont.	72	8	X	2.86	3600
91-2	1	25	10	5	60	Parallel	750	20	Cont.	72	8	X	2.86	5000
91-3	1	25	10	5	60	Parallel	750	20	Cont.	72	10	X	2.86	5000
91-4	1	25	10	5	60	Parallel	750	20	Cont.	72	8	K	2.86	5000
91-5	1	25	10	5	60	Parallel	750	20	Cont.	72	8	X	4.79	5000
92-1	1	25	10	5	60	Parallel	750	30	Cont.	72	8	X	2.86	5000
93-1	1	25	10	5	60	Trap.	1500	20	Cont.	72	8	X	2.86	3600
93-2	1	25	10	5	60	Trap.	1500	20	Cont.	72	8	X	2.86	5000
93-3	1	25	10	5	60	Trap.	1500	20	Cont.	72	10	X	2.86	5000
93-4	1	25	10	5	60	Trap.	1500	20	Cont.	72	8	K	2.86	5000
93-5	1	25	10	5	60	Trap.	1500	20	Cont.	72	8	X	4.79	5000
94-1	1	25	10	5	60	Trap.	1500	30	Cont.	72	8	X	2.86	5000
95-1	1	25	10	5	60	Trap.	750	20	Cont.	72	8	X	2.86	3600
95-2	1	25	10	5	60	Trap.	750	20	Cont.	72	8	X	2.86	5000
95-3	1	25	10	5	60	Trap.	750	20	Cont.	72	10	X	2.86	5000
95-4	1	25	10	5	60	Trap.	750	20	Cont.	72	8	K	2.86	5000

Model ID	Geometry									Cross-section		CF detail		Mat'l
	n_{span}	L/d ratio	s_g [ft]	n_{girder}	Support skew [deg]; Layout		R [ft]	s_{cf} [ft]	CF layout	d_w [in]	t_{deck} [in]	CF type	A_{cf} [in^2]	E_c [ksi]
95-5	1	25	10	5	60	Trap.	750	20	Cont.	72	8	X	4.79	5000
96-1	1	25	10	5	60	Trap.	750	30	Cont.	72	8	X	2.86	5000
97-1	1	25	6	3	0	Parallel	1500	20	Cont.	96	8	X	2.86	3600
97-2	1	25	6	3	0	Parallel	1500	20	Cont.	96	8	X	2.86	5000
97-3	1	25	6	3	0	Parallel	1500	20	Cont.	96	10	X	2.86	5000
97-4	1	25	6	3	0	Parallel	1500	20	Cont.	96	8	K	2.86	5000
97-5	1	25	6	3	0	Parallel	1500	20	Cont.	96	8	X	4.79	5000
98-1	1	25	6	3	0	Parallel	1500	30	Cont.	96	8	X	2.86	5000
99-1	1	25	6	3	0	Parallel	750	20	Cont.	96	8	X	2.86	3600
99-2	1	25	6	3	0	Parallel	750	20	Cont.	96	8	X	2.86	5000
99-3	1	25	6	3	0	Parallel	750	20	Cont.	96	10	X	2.86	5000
99-4	1	25	6	3	0	Parallel	750	20	Cont.	96	8	K	2.86	5000
99-5	1	25	6	3	0	Parallel	750	20	Cont.	96	8	X	4.79	5000
100-1	1	25	6	3	0	Parallel	750	30	Cont.	96	8	X	2.86	5000
101-1	1	25	6	3	30	Parallel	1500	20	Cont.	96	8	X	2.86	3600
101-2	1	25	6	3	30	Parallel	1500	20	Cont.	96	8	X	2.86	5000
101-3	1	25	6	3	30	Parallel	1500	20	Cont.	96	10	X	2.86	5000
101-4	1	25	6	3	30	Parallel	1500	20	Cont.	96	8	K	2.86	5000
101-5	1	25	6	3	30	Parallel	1500	20	Cont.	96	8	X	4.79	5000
102-1	1	25	6	3	30	Parallel	1500	30	Cont.	96	8	X	2.86	5000
103-1	1	25	6	3	30	Parallel	750	20	Cont.	96	8	X	2.86	3600
103-2	1	25	6	3	30	Parallel	750	20	Cont.	96	8	X	2.86	5000
103-3	1	25	6	3	30	Parallel	750	20	Cont.	96	10	X	2.86	5000
103-4	1	25	6	3	30	Parallel	750	20	Cont.	96	8	K	2.86	5000
103-5	1	25	6	3	30	Parallel	750	20	Cont.	96	8	X	4.79	5000
104-1	1	25	6	3	30	Parallel	750	30	Cont.	96	8	X	2.86	5000
105-1	1	25	6	3	60	Parallel	1500	20	Cont.	96	8	X	2.86	3600
105-2	1	25	6	3	60	Parallel	1500	20	Cont.	96	8	X	2.86	5000
105-3	1	25	6	3	60	Parallel	1500	20	Cont.	96	10	X	2.86	5000
105-4	1	25	6	3	60	Parallel	1500	20	Cont.	96	8	K	2.86	5000
105-5	1	25	6	3	60	Parallel	1500	20	Cont.	96	8	X	4.79	5000
106-1	1	25	6	3	60	Parallel	1500	30	Cont.	96	8	X	2.86	5000
107-1	1	25	6	3	60	Parallel	750	20	Cont.	96	8	X	2.86	3600
107-2	1	25	6	3	60	Parallel	750	20	Cont.	96	8	X	2.86	5000
107-3	1	25	6	3	60	Parallel	750	20	Cont.	96	10	X	2.86	5000
107-4	1	25	6	3	60	Parallel	750	20	Cont.	96	8	K	2.86	5000
107-5	1	25	6	3	60	Parallel	750	20	Cont.	96	8	X	4.79	5000
108-1	1	25	6	3	60	Parallel	750	30	Cont.	96	8	X	2.86	5000
109-1	1	25	6	3	60	Trap.	1500	20	Cont.	96	8	X	2.86	3600
109-2	1	25	6	3	60	Trap.	1500	20	Cont.	96	8	X	2.86	5000
109-3	1	25	6	3	60	Trap.	1500	20	Cont.	96	10	X	2.86	5000
109-4	1	25	6	3	60	Trap.	1500	20	Cont.	96	8	K	2.86	5000
109-5	1	25	6	3	60	Trap.	1500	20	Cont.	96	8	X	4.79	5000
110-1	1	25	6	3	60	Trap.	1500	30	Cont.	96	8	X	2.86	5000
111-1	1	25	6	3	60	Trap.	750	20	Cont.	96	8	X	2.86	3600
111-2	1	25	6	3	60	Trap.	750	20	Cont.	96	8	X	2.86	5000
111-3	1	25	6	3	60	Trap.	750	20	Cont.	96	10	X	2.86	5000
111-4	1	25	6	3	60	Trap.	750	20	Cont.	96	8	K	2.86	5000
111-5	1	25	6	3	60	Trap.	750	20	Cont.	96	8	X	4.79	5000
112-1	1	25	6	3	60	Trap.	750	30	Cont.	96	8	X	2.86	5000
113-1	1	25	6	5	0	Parallel	1500	20	Cont.	96	8	X	2.86	3600
113-2	1	25	6	5	0	Parallel	1500	20	Cont.	96	8	X	2.86	5000
113-3	1	25	6	5	0	Parallel	1500	20	Cont.	96	10	X	2.86	5000
113-4	1	25	6	5	0	Parallel	1500	20	Cont.	96	8	K	2.86	5000
113-5	1	25	6	5	0	Parallel	1500	20	Cont.	96	8	X	4.79	5000
114-1	1	25	6	5	0	Parallel	1500	30	Cont.	96	8	X	2.86	5000
115-1	1	25	6	5	0	Parallel	750	20	Cont.	96	8	X	2.86	3600
115-2	1	25	6	5	0	Parallel	750	20	Cont.	96	8	X	2.86	5000
115-3	1	25	6	5	0	Parallel	750	20	Cont.	96	10	X	2.86	5000
115-4	1	25	6	5	0	Parallel	750	20	Cont.	96	8	K	2.86	5000
115-5	1	25	6	5	0	Parallel	750	20	Cont.	96	8	X	4.79	5000
116-1	1	25	6	5	0	Parallel	750	30	Cont.	96	8	X	2.86	5000
117-1	1	25	6	5	30	Parallel	1500	20	Cont.	96	8	X	2.86	3600
117-2	1	25	6	5	30	Parallel	1500	20	Cont.	96	8	X	2.86	5000
117-3	1	25	6	5	30	Parallel	1500	20	Cont.	96	10	X	2.86	5000
117-4	1	25	6	5	30	Parallel	1500	20	Cont.	96	8	K	2.86	5000
117-5	1	25	6	5	30	Parallel	1500	20	Cont.	96	8	X	4.79	5000
118-1	1	25	6	5	30	Parallel	1500	30	Cont.	96	8	X	2.86	5000
119-1	1	25	6	5	30	Parallel	750	20	Cont.	96	8	X	2.86	3600
119-2	1	25	6	5	30	Parallel	750	20	Cont.	96	8	X	2.86	5000
119-3	1	25	6	5	30	Parallel	750	20	Cont.	96	10	X	2.86	5000
119-4	1	25	6	5	30	Parallel	750	20	Cont.	96	8	K	2.86	5000
119-5	1	25	6	5	30	Parallel	750	20	Cont.	96	8	X	4.79	5000

Model ID	Geometry									Cross-section		CF detail		Mat'l
	n_{span}	L/d ratio	s_g [ft]	n_{girder}	Support skew [deg]; Layout		R [ft]	s_{cf} [ft]	CF layout	d_w [in]	t_{deck} [in]	CF type	A_{cf} [in^2]	E_c [ksi]
120-1	1	25	6	5	30	Parallel	750	30	Cont.	96	8	X	2.86	5000
121-1	1	25	6	5	60	Parallel	1500	20	Cont.	96	8	X	2.86	3600
121-2	1	25	6	5	60	Parallel	1500	20	Cont.	96	8	X	2.86	5000
121-3	1	25	6	5	60	Parallel	1500	20	Cont.	96	10	X	2.86	5000
121-4	1	25	6	5	60	Parallel	1500	20	Cont.	96	8	K	2.86	5000
121-5	1	25	6	5	60	Parallel	1500	20	Cont.	96	8	X	4.79	5000
122-1	1	25	6	5	60	Parallel	1500	30	Cont.	96	8	X	2.86	5000
123-1	1	25	6	5	60	Parallel	750	20	Cont.	96	8	X	2.86	3600
123-2	1	25	6	5	60	Parallel	750	20	Cont.	96	8	X	2.86	5000
123-3	1	25	6	5	60	Parallel	750	20	Cont.	96	10	X	2.86	5000
123-4	1	25	6	5	60	Parallel	750	20	Cont.	96	8	K	2.86	5000
123-5	1	25	6	5	60	Parallel	750	20	Cont.	96	8	X	4.79	5000
124-1	1	25	6	5	60	Parallel	750	30	Cont.	96	8	X	2.86	5000
125-1	1	25	6	5	60	Trap.	1500	20	Cont.	96	8	X	2.86	3600
125-2	1	25	6	5	60	Trap.	1500	20	Cont.	96	8	X	2.86	5000
125-3	1	25	6	5	60	Trap.	1500	20	Cont.	96	10	X	2.86	5000
125-4	1	25	6	5	60	Trap.	1500	20	Cont.	96	8	K	2.86	5000
125-5	1	25	6	5	60	Trap.	1500	20	Cont.	96	8	X	4.79	5000
126-1	1	25	6	5	60	Trap.	1500	30	Cont.	96	8	X	2.86	5000
127-1	1	25	6	5	60	Trap.	750	20	Cont.	96	8	X	2.86	3600
127-2	1	25	6	5	60	Trap.	750	20	Cont.	96	8	X	2.86	5000
127-3	1	25	6	5	60	Trap.	750	20	Cont.	96	10	X	2.86	5000
127-4	1	25	6	5	60	Trap.	750	20	Cont.	96	8	K	2.86	5000
127-5	1	25	6	5	60	Trap.	750	20	Cont.	96	8	X	4.79	5000
128-1	1	25	6	5	60	Trap.	750	30	Cont.	96	8	X	2.86	5000
129-1	1	25	8	3	0	Parallel	1500	20	Cont.	96	8	X	2.86	3600
129-2	1	25	8	3	0	Parallel	1500	20	Cont.	96	8	X	2.86	5000
129-3	1	25	8	3	0	Parallel	1500	20	Cont.	96	10	X	2.86	5000
129-4	1	25	8	3	0	Parallel	1500	20	Cont.	96	8	K	2.86	5000
129-5	1	25	8	3	0	Parallel	1500	20	Cont.	96	8	X	4.79	5000
130-1	1	25	8	3	0	Parallel	1500	30	Cont.	96	8	X	2.86	5000
131-1	1	25	8	3	0	Parallel	750	20	Cont.	96	8	X	2.86	3600
131-2	1	25	8	3	0	Parallel	750	20	Cont.	96	8	X	2.86	5000
131-3	1	25	8	3	0	Parallel	750	20	Cont.	96	10	X	2.86	5000
131-4	1	25	8	3	0	Parallel	750	20	Cont.	96	8	K	2.86	5000
131-5	1	25	8	3	0	Parallel	750	20	Cont.	96	8	X	4.79	5000
132-1	1	25	8	3	0	Parallel	750	30	Cont.	96	8	X	2.86	5000
133-1	1	25	8	3	30	Parallel	1500	20	Cont.	96	8	X	2.86	3600
133-2	1	25	8	3	30	Parallel	1500	20	Cont.	96	8	X	2.86	5000
133-3	1	25	8	3	30	Parallel	1500	20	Cont.	96	10	X	2.86	5000
133-4	1	25	8	3	30	Parallel	1500	20	Cont.	96	8	K	2.86	5000
133-5	1	25	8	3	30	Parallel	1500	20	Cont.	96	8	X	4.79	5000
134-1	1	25	8	3	30	Parallel	1500	30	Cont.	96	8	X	2.86	5000
135-1	1	25	8	3	30	Parallel	750	20	Cont.	96	8	X	2.86	3600
135-2	1	25	8	3	30	Parallel	750	20	Cont.	96	8	X	2.86	5000
135-3	1	25	8	3	30	Parallel	750	20	Cont.	96	10	X	2.86	5000
135-4	1	25	8	3	30	Parallel	750	20	Cont.	96	8	K	2.86	5000
135-5	1	25	8	3	30	Parallel	750	20	Cont.	96	8	X	4.79	5000
136-1	1	25	8	3	30	Parallel	750	30	Cont.	96	8	X	2.86	5000
137-1	1	25	8	3	60	Parallel	1500	20	Cont.	96	8	X	2.86	3600
137-2	1	25	8	3	60	Parallel	1500	20	Cont.	96	8	X	2.86	5000
137-3	1	25	8	3	60	Parallel	1500	20	Cont.	96	10	X	2.86	5000
137-4	1	25	8	3	60	Parallel	1500	20	Cont.	96	8	K	2.86	5000
137-5	1	25	8	3	60	Parallel	1500	20	Cont.	96	8	X	4.79	5000
138-1	1	25	8	3	60	Parallel	1500	30	Cont.	96	8	X	2.86	5000
139-1	1	25	8	3	60	Parallel	750	20	Cont.	96	8	X	2.86	3600
139-2	1	25	8	3	60	Parallel	750	20	Cont.	96	8	X	2.86	5000
139-3	1	25	8	3	60	Parallel	750	20	Cont.	96	10	X	2.86	5000
139-4	1	25	8	3	60	Parallel	750	20	Cont.	96	8	K	2.86	5000
139-5	1	25	8	3	60	Parallel	750	20	Cont.	96	8	X	4.79	5000
140-1	1	25	8	3	60	Parallel	750	30	Cont.	96	8	X	2.86	5000
141-1	1	25	8	3	60	Trap.	1500	20	Cont.	96	8	X	2.86	3600
141-2	1	25	8	3	60	Trap.	1500	20	Cont.	96	8	X	2.86	5000
141-3	1	25	8	3	60	Trap.	1500	20	Cont.	96	10	X	2.86	5000
141-4	1	25	8	3	60	Trap.	1500	20	Cont.	96	8	K	2.86	5000
141-5	1	25	8	3	60	Trap.	1500	20	Cont.	96	8	X	4.79	5000
142-1	1	25	8	3	60	Trap.	1500	30	Cont.	96	8	X	2.86	5000
143-1	1	25	8	3	60	Trap.	750	20	Cont.	96	8	X	2.86	3600
143-2	1	25	8	3	60	Trap.	750	20	Cont.	96	8	X	2.86	5000
143-3	1	25	8	3	60	Trap.	750	20	Cont.	96	10	X	2.86	5000
143-4	1	25	8	3	60	Trap.	750	20	Cont.	96	8	K	2.86	5000
143-5	1	25	8	3	60	Trap.	750	20	Cont.	96	8	X	4.79	5000
144-1	1	25	8	3	60	Trap.	750	30	Cont.	96	8	X	2.86	5000

Model ID	Geometry									Cross-section		CF detail		Mat'l
	n_{span}	L/d ratio	s_g [ft]	n_{girder}	Support skew [deg]; Layout		R [ft]	s_{cf} [ft]	CF layout	d_w [in]	t_{deck} [in]	CF type	A_{cf} [in^2]	E_c [ksi]
145-1	1	25	8	5	0	Parallel	1500	20	Cont.	96	8	X	2.86	3600
145-2	1	25	8	5	0	Parallel	1500	20	Cont.	96	8	X	2.86	5000
145-3	1	25	8	5	0	Parallel	1500	20	Cont.	96	10	X	2.86	5000
145-4	1	25	8	5	0	Parallel	1500	20	Cont.	96	8	K	2.86	5000
145-5	1	25	8	5	0	Parallel	1500	20	Cont.	96	8	X	4.79	5000
146-1	1	25	8	5	0	Parallel	1500	30	Cont.	96	8	X	2.86	5000
147-1	1	25	8	5	0	Parallel	750	20	Cont.	96	8	X	2.86	3600
147-2	1	25	8	5	0	Parallel	750	20	Cont.	96	8	X	2.86	5000
147-3	1	25	8	5	0	Parallel	750	20	Cont.	96	10	X	2.86	5000
147-4	1	25	8	5	0	Parallel	750	20	Cont.	96	8	K	2.86	5000
147-5	1	25	8	5	0	Parallel	750	20	Cont.	96	8	X	4.79	5000
148-1	1	25	8	5	0	Parallel	750	30	Cont.	96	8	X	2.86	5000
149-1	1	25	8	5	30	Parallel	1500	20	Cont.	96	8	X	2.86	3600
149-2	1	25	8	5	30	Parallel	1500	20	Cont.	96	8	X	2.86	5000
149-3	1	25	8	5	30	Parallel	1500	20	Cont.	96	10	X	2.86	5000
149-4	1	25	8	5	30	Parallel	1500	20	Cont.	96	8	K	2.86	5000
149-5	1	25	8	5	30	Parallel	1500	20	Cont.	96	8	X	4.79	5000
150-1	1	25	8	5	30	Parallel	1500	30	Cont.	96	8	X	2.86	5000
151-1	1	25	8	5	30	Parallel	750	20	Cont.	96	8	X	2.86	3600
151-2	1	25	8	5	30	Parallel	750	20	Cont.	96	8	X	2.86	5000
151-3	1	25	8	5	30	Parallel	750	20	Cont.	96	10	X	2.86	5000
151-4	1	25	8	5	30	Parallel	750	20	Cont.	96	8	K	2.86	5000
151-5	1	25	8	5	30	Parallel	750	20	Cont.	96	8	X	4.79	5000
152-1	1	25	8	5	30	Parallel	750	30	Cont.	96	8	X	2.86	5000
153-1	1	25	8	5	60	Parallel	1500	20	Cont.	96	8	X	2.86	3600
153-2	1	25	8	5	60	Parallel	1500	20	Cont.	96	8	X	2.86	5000
153-3	1	25	8	5	60	Parallel	1500	20	Cont.	96	10	X	2.86	5000
153-4	1	25	8	5	60	Parallel	1500	20	Cont.	96	8	K	2.86	5000
153-5	1	25	8	5	60	Parallel	1500	20	Cont.	96	8	X	4.79	5000
154-1	1	25	8	5	60	Parallel	1500	30	Cont.	96	8	X	2.86	5000
155-1	1	25	8	5	60	Parallel	750	20	Cont.	96	8	X	2.86	3600
155-2	1	25	8	5	60	Parallel	750	20	Cont.	96	8	X	2.86	5000
155-3	1	25	8	5	60	Parallel	750	20	Cont.	96	10	X	2.86	5000
155-4	1	25	8	5	60	Parallel	750	20	Cont.	96	8	K	2.86	5000
155-5	1	25	8	5	60	Parallel	750	20	Cont.	96	8	X	4.79	5000
156-1	1	25	8	5	60	Parallel	750	30	Cont.	96	8	X	2.86	5000
157-1	1	25	8	5	60	Trap.	1500	20	Cont.	96	8	X	2.86	3600
157-2	1	25	8	5	60	Trap.	1500	20	Cont.	96	8	X	2.86	5000
157-3	1	25	8	5	60	Trap.	1500	20	Cont.	96	10	X	2.86	5000
157-4	1	25	8	5	60	Trap.	1500	20	Cont.	96	8	K	2.86	5000
157-5	1	25	8	5	60	Trap.	1500	20	Cont.	96	8	X	4.79	5000
158-1	1	25	8	5	60	Trap.	1500	30	Cont.	96	8	X	2.86	5000
159-1	1	25	8	5	60	Trap.	750	20	Cont.	96	8	X	2.86	3600
159-2	1	25	8	5	60	Trap.	750	20	Cont.	96	8	X	2.86	5000
159-3	1	25	8	5	60	Trap.	750	20	Cont.	96	10	X	2.86	5000
159-4	1	25	8	5	60	Trap.	750	20	Cont.	96	8	K	2.86	5000
159-5	1	25	8	5	60	Trap.	750	20	Cont.	96	8	X	4.79	5000
160-1	1	25	8	5	60	Trap.	750	30	Cont.	96	8	X	2.86	5000
161-1	1	25	10	3	0	Parallel	1500	20	Cont.	96	8	X	2.86	3600
161-2	1	25	10	3	0	Parallel	1500	20	Cont.	96	8	X	2.86	5000
161-3	1	25	10	3	0	Parallel	1500	20	Cont.	96	10	X	2.86	5000
161-4	1	25	10	3	0	Parallel	1500	20	Cont.	96	8	K	2.86	5000
161-5	1	25	10	3	0	Parallel	1500	20	Cont.	96	8	X	4.79	5000
162-1	1	25	10	3	0	Parallel	1500	30	Cont.	96	8	X	2.86	5000
163-1	1	25	10	3	0	Parallel	750	20	Cont.	96	8	X	2.86	3600
163-2	1	25	10	3	0	Parallel	750	20	Cont.	96	8	X	2.86	5000
163-3	1	25	10	3	0	Parallel	750	20	Cont.	96	10	X	2.86	5000
163-4	1	25	10	3	0	Parallel	750	20	Cont.	96	8	K	2.86	5000
163-5	1	25	10	3	0	Parallel	750	20	Cont.	96	8	X	4.79	5000
164-1	1	25	10	3	0	Parallel	750	30	Cont.	96	8	X	2.86	5000
165-1	1	25	10	3	30	Parallel	1500	20	Cont.	96	8	X	2.86	3600
165-2	1	25	10	3	30	Parallel	1500	20	Cont.	96	8	X	2.86	5000
165-3	1	25	10	3	30	Parallel	1500	20	Cont.	96	10	X	2.86	5000
165-4	1	25	10	3	30	Parallel	1500	20	Cont.	96	8	K	2.86	5000
165-5	1	25	10	3	30	Parallel	1500	20	Cont.	96	8	X	4.79	5000
166-1	1	25	10	3	30	Parallel	1500	30	Cont.	96	8	X	2.86	5000
167-1	1	25	10	3	30	Parallel	750	20	Cont.	96	8	X	2.86	3600
167-2	1	25	10	3	30	Parallel	750	20	Cont.	96	8	X	2.86	5000
167-3	1	25	10	3	30	Parallel	750	20	Cont.	96	10	X	2.86	5000
167-4	1	25	10	3	30	Parallel	750	20	Cont.	96	8	K	2.86	5000
167-5	1	25	10	3	30	Parallel	750	20	Cont.	96	8	X	4.79	5000
168-1	1	25	10	3	30	Parallel	750	30	Cont.	96	8	X	2.86	5000
169-1	1	25	10	3	60	Parallel	1500	20	Cont.	96	8	X	2.86	3600

Model ID	Geometry									Cross-section		CF detail		Mat'l
	n_{span}	L/d ratio	s_g [ft]	n_{girder}	Support skew [deg]; Layout		R [ft]	s_{cf} [ft]	CF layout	d_w [in]	t_{deck} [in]	CF type	A_{cf} [in^2]	E_c [ksi]
169-2	1	25	10	3	60	Parallel	1500	20	Cont.	96	8	X	2.86	5000
169-3	1	25	10	3	60	Parallel	1500	20	Cont.	96	10	X	2.86	5000
169-4	1	25	10	3	60	Parallel	1500	20	Cont.	96	8	K	2.86	5000
169-5	1	25	10	3	60	Parallel	1500	20	Cont.	96	8	X	4.79	5000
170-1	1	25	10	3	60	Parallel	1500	30	Cont.	96	8	X	2.86	5000
171-1	1	25	10	3	60	Parallel	750	20	Cont.	96	8	X	2.86	3600
171-2	1	25	10	3	60	Parallel	750	20	Cont.	96	8	X	2.86	5000
171-3	1	25	10	3	60	Parallel	750	20	Cont.	96	10	X	2.86	5000
171-4	1	25	10	3	60	Parallel	750	20	Cont.	96	8	K	2.86	5000
171-5	1	25	10	3	60	Parallel	750	20	Cont.	96	8	X	4.79	5000
172-1	1	25	10	3	60	Parallel	750	30	Cont.	96	8	X	2.86	5000
173-1	1	25	10	3	60	Trap.	1500	20	Cont.	96	8	X	2.86	3600
173-2	1	25	10	3	60	Trap.	1500	20	Cont.	96	8	X	2.86	5000
173-3	1	25	10	3	60	Trap.	1500	20	Cont.	96	10	X	2.86	5000
173-4	1	25	10	3	60	Trap.	1500	20	Cont.	96	8	K	2.86	5000
173-5	1	25	10	3	60	Trap.	1500	20	Cont.	96	8	X	4.79	5000
174-1	1	25	10	3	60	Trap.	1500	30	Cont.	96	8	X	2.86	5000
175-1	1	25	10	3	60	Trap.	750	20	Cont.	96	8	X	2.86	3600
175-2	1	25	10	3	60	Trap.	750	20	Cont.	96	8	X	2.86	5000
175-3	1	25	10	3	60	Trap.	750	20	Cont.	96	10	X	2.86	5000
175-4	1	25	10	3	60	Trap.	750	20	Cont.	96	8	K	2.86	5000
175-5	1	25	10	3	60	Trap.	750	20	Cont.	96	8	X	4.79	5000
176-1	1	25	10	3	60	Trap.	750	30	Cont.	96	8	X	2.86	5000
177-1	1	25	10	5	0	Parallel	1500	20	Cont.	96	8	X	2.86	3600
177-2	1	25	10	5	0	Parallel	1500	20	Cont.	96	8	X	2.86	5000
177-3	1	25	10	5	0	Parallel	1500	20	Cont.	96	10	X	2.86	5000
177-4	1	25	10	5	0	Parallel	1500	20	Cont.	96	8	K	2.86	5000
177-5	1	25	10	5	0	Parallel	1500	20	Cont.	96	8	X	4.79	5000
178-1	1	25	10	5	0	Parallel	1500	30	Cont.	96	8	X	2.86	5000
179-1	1	25	10	5	0	Parallel	750	20	Cont.	96	8	X	2.86	3600
179-2	1	25	10	5	0	Parallel	750	20	Cont.	96	8	X	2.86	5000
179-3	1	25	10	5	0	Parallel	750	20	Cont.	96	10	X	2.86	5000
179-4	1	25	10	5	0	Parallel	750	20	Cont.	96	8	K	2.86	5000
179-5	1	25	10	5	0	Parallel	750	20	Cont.	96	8	X	4.79	5000
180-1	1	25	10	5	0	Parallel	750	30	Cont.	96	8	X	2.86	5000
181-1	1	25	10	5	30	Parallel	1500	20	Cont.	96	8	X	2.86	3600
181-2	1	25	10	5	30	Parallel	1500	20	Cont.	96	8	X	2.86	5000
181-3	1	25	10	5	30	Parallel	1500	20	Cont.	96	10	X	2.86	5000
181-4	1	25	10	5	30	Parallel	1500	20	Cont.	96	8	K	2.86	5000
181-5	1	25	10	5	30	Parallel	1500	20	Cont.	96	8	X	4.79	5000
182-1	1	25	10	5	30	Parallel	1500	30	Cont.	96	8	X	2.86	5000
183-1	1	25	10	5	30	Parallel	750	20	Cont.	96	8	X	2.86	3600
183-2	1	25	10	5	30	Parallel	750	20	Cont.	96	8	X	2.86	5000
183-3	1	25	10	5	30	Parallel	750	20	Cont.	96	10	X	2.86	5000
183-4	1	25	10	5	30	Parallel	750	20	Cont.	96	8	K	2.86	5000
183-5	1	25	10	5	30	Parallel	750	20	Cont.	96	8	X	4.79	5000
184-1	1	25	10	5	30	Parallel	750	30	Cont.	96	8	X	2.86	5000
185-1	1	25	10	5	60	Parallel	1500	20	Cont.	96	8	X	2.86	3600
185-2	1	25	10	5	60	Parallel	1500	20	Cont.	96	8	X	2.86	5000
185-3	1	25	10	5	60	Parallel	1500	20	Cont.	96	10	X	2.86	5000
185-4	1	25	10	5	60	Parallel	1500	20	Cont.	96	8	K	2.86	5000
185-5	1	25	10	5	60	Parallel	1500	20	Cont.	96	8	X	4.79	5000
186-1	1	25	10	5	60	Parallel	1500	30	Cont.	96	8	X	2.86	5000
187-1	1	25	10	5	60	Parallel	750	20	Cont.	96	8	X	2.86	3600
187-2	1	25	10	5	60	Parallel	750	20	Cont.	96	8	X	2.86	5000
187-3	1	25	10	5	60	Parallel	750	20	Cont.	96	10	X	2.86	5000
187-4	1	25	10	5	60	Parallel	750	20	Cont.	96	8	K	2.86	5000
187-5	1	25	10	5	60	Parallel	750	20	Cont.	96	8	X	4.79	5000
188-1	1	25	10	5	60	Parallel	750	30	Cont.	96	8	X	2.86	5000
189-1	1	25	10	5	60	Trap.	1500	20	Cont.	96	8	X	2.86	3600
189-2	1	25	10	5	60	Trap.	1500	20	Cont.	96	8	X	2.86	5000
189-3	1	25	10	5	60	Trap.	1500	20	Cont.	96	10	X	2.86	5000
189-4	1	25	10	5	60	Trap.	1500	20	Cont.	96	8	K	2.86	5000
189-5	1	25	10	5	60	Trap.	1500	20	Cont.	96	8	X	4.79	5000
190-1	1	25	10	5	60	Trap.	1500	30	Cont.	96	8	X	2.86	5000
191-1	1	25	10	5	60	Trap.	750	20	Cont.	96	8	X	2.86	3600
191-2	1	25	10	5	60	Trap.	750	20	Cont.	96	8	X	2.86	5000
191-3	1	25	10	5	60	Trap.	750	20	Cont.	96	10	X	2.86	5000
191-4	1	25	10	5	60	Trap.	750	20	Cont.	96	8	K	2.86	5000
191-5	1	25	10	5	60	Trap.	750	20	Cont.	96	8	X	4.79	5000
192-1	1	25	10	5	60	Trap.	750	30	Cont.	96	8	X	2.86	5000
193-1	1	30	6	3	0	Parallel	Infinite	20	Cont.	72	8	X	2.86	3600
193-2	1	30	6	3	0	Parallel	Infinite	20	Cont.	72	8	X	2.86	5000

Model ID	Geometry									Cross-section		CF detail		Mat'l
	n_{span}	L/d ratio	s_g [ft]	n_{girder}	Support skew [deg]; Layout		R [ft]	s_{cf} [ft]	CF layout	d_w [in]	t_{deck} [in]	CF type	A_{cf} [in^2]	E_c [ksi]
193-3	1	30	6	3	0	Parallel	Infinite	20	Cont.	72	10	X	2.86	5000
193-4	1	30	6	3	0	Parallel	Infinite	20	Cont.	72	8	K	2.86	5000
193-5	1	30	6	3	0	Parallel	Infinite	20	Cont.	72	8	X	4.79	5000
194-1	1	30	6	3	0	Parallel	Infinite	30	Cont.	72	8	X	2.86	5000
195-1	1	30	6	3	30	Parallel	Infinite	20	Cont.	72	8	X	2.86	3600
195-2	1	30	6	3	30	Parallel	Infinite	20	Cont.	72	8	X	2.86	5000
195-3	1	30	6	3	30	Parallel	Infinite	20	Cont.	72	10	X	2.86	5000
195-4	1	30	6	3	30	Parallel	Infinite	20	Cont.	72	8	K	2.86	5000
195-5	1	30	6	3	30	Parallel	Infinite	20	Cont.	72	8	X	4.79	5000
196-1	1	30	6	3	30	Parallel	Infinite	30	Cont.	72	8	X	2.86	5000
197-1	1	30	6	3	60	Parallel	Infinite	20	Cont.	72	8	X	2.86	3600
197-2	1	30	6	3	60	Parallel	Infinite	20	Cont.	72	8	X	2.86	5000
197-3	1	30	6	3	60	Parallel	Infinite	20	Cont.	72	10	X	2.86	5000
197-4	1	30	6	3	60	Parallel	Infinite	20	Cont.	72	8	K	2.86	5000
197-5	1	30	6	3	60	Parallel	Infinite	20	Cont.	72	8	X	4.79	5000
198-1	1	30	6	3	60	Parallel	Infinite	30	Cont.	72	8	X	2.86	5000
199-1	1	30	6	3	60	Parallel	Infinite	20	Stag.	72	8	X	2.86	3600
199-2	1	30	6	3	60	Parallel	Infinite	20	Stag.	72	8	X	2.86	5000
199-3	1	30	6	3	60	Parallel	Infinite	20	Stag.	72	10	X	2.86	5000
199-4	1	30	6	3	60	Parallel	Infinite	20	Stag.	72	8	K	2.86	5000
199-5	1	30	6	3	60	Parallel	Infinite	20	Stag.	72	8	X	4.79	5000
200-1	1	30	6	3	60	Parallel	Infinite	30	Stag.	72	8	X	2.86	5000
201-1	1	30	6	3	60	Trap.	Infinite	20	Cont.	72	8	X	2.86	3600
201-2	1	30	6	3	60	Trap.	Infinite	20	Cont.	72	8	X	2.86	5000
201-3	1	30	6	3	60	Trap.	Infinite	20	Cont.	72	10	X	2.86	5000
201-4	1	30	6	3	60	Trap.	Infinite	20	Cont.	72	8	K	2.86	5000
201-5	1	30	6	3	60	Trap.	Infinite	20	Cont.	72	8	X	4.79	5000
202-1	1	30	6	3	60	Trap.	Infinite	30	Cont.	72	8	X	2.86	5000
203-1	1	30	6	3	60	Trap.	Infinite	20	Stag.	72	8	X	2.86	3600
203-2	1	30	6	3	60	Trap.	Infinite	20	Stag.	72	8	X	2.86	5000
203-3	1	30	6	3	60	Trap.	Infinite	20	Stag.	72	10	X	2.86	5000
203-4	1	30	6	3	60	Trap.	Infinite	20	Stag.	72	8	K	2.86	5000
203-5	1	30	6	3	60	Trap.	Infinite	20	Stag.	72	8	X	4.79	5000
204-1	1	30	6	3	60	Trap.	Infinite	30	Stag.	72	8	X	2.86	5000
205-1	1	30	6	5	0	Parallel	Infinite	20	Cont.	72	8	X	2.86	3600
205-2	1	30	6	5	0	Parallel	Infinite	20	Cont.	72	8	X	2.86	5000
205-3	1	30	6	5	0	Parallel	Infinite	20	Cont.	72	10	X	2.86	5000
205-4	1	30	6	5	0	Parallel	Infinite	20	Cont.	72	8	K	2.86	5000
205-5	1	30	6	5	0	Parallel	Infinite	20	Cont.	72	8	X	4.79	5000
206-1	1	30	6	5	0	Parallel	Infinite	30	Cont.	72	8	X	2.86	5000
207-1	1	30	6	5	30	Parallel	Infinite	20	Cont.	72	8	X	2.86	3600
207-2	1	30	6	5	30	Parallel	Infinite	20	Cont.	72	8	X	2.86	5000
207-3	1	30	6	5	30	Parallel	Infinite	20	Cont.	72	10	X	2.86	5000
207-4	1	30	6	5	30	Parallel	Infinite	20	Cont.	72	8	K	2.86	5000
207-5	1	30	6	5	30	Parallel	Infinite	20	Cont.	72	8	X	4.79	5000
208-1	1	30	6	5	30	Parallel	Infinite	30	Cont.	72	8	X	2.86	5000
209-1	1	30	6	5	60	Parallel	Infinite	20	Cont.	72	8	X	2.86	3600
209-2	1	30	6	5	60	Parallel	Infinite	20	Cont.	72	8	X	2.86	5000
209-3	1	30	6	5	60	Parallel	Infinite	20	Cont.	72	10	X	2.86	5000
209-4	1	30	6	5	60	Parallel	Infinite	20	Cont.	72	8	K	2.86	5000
209-5	1	30	6	5	60	Parallel	Infinite	20	Cont.	72	8	X	4.79	5000
210-1	1	30	6	5	60	Parallel	Infinite	30	Cont.	72	8	X	2.86	5000
211-1	1	30	6	5	60	Parallel	Infinite	20	Stag.	72	8	X	2.86	3600
211-2	1	30	6	5	60	Parallel	Infinite	20	Stag.	72	8	X	2.86	5000
211-3	1	30	6	5	60	Parallel	Infinite	20	Stag.	72	10	X	2.86	5000
211-4	1	30	6	5	60	Parallel	Infinite	20	Stag.	72	8	K	2.86	5000
211-5	1	30	6	5	60	Parallel	Infinite	20	Stag.	72	8	X	4.79	5000
212-1	1	30	6	5	60	Parallel	Infinite	30	Stag.	72	8	X	2.86	5000
213-1	1	30	6	5	60	Trap.	Infinite	20	Cont.	72	8	X	2.86	3600
213-2	1	30	6	5	60	Trap.	Infinite	20	Cont.	72	8	X	2.86	5000
213-3	1	30	6	5	60	Trap.	Infinite	20	Cont.	72	10	X	2.86	5000
213-4	1	30	6	5	60	Trap.	Infinite	20	Cont.	72	8	K	2.86	5000
213-5	1	30	6	5	60	Trap.	Infinite	20	Cont.	72	8	X	4.79	5000
214-1	1	30	6	5	60	Trap.	Infinite	30	Cont.	72	8	X	2.86	5000
215-1	1	30	6	5	60	Trap.	Infinite	20	Stag.	72	8	X	2.86	3600
215-2	1	30	6	5	60	Trap.	Infinite	20	Stag.	72	8	X	2.86	5000
215-3	1	30	6	5	60	Trap.	Infinite	20	Stag.	72	10	X	2.86	5000
215-4	1	30	6	5	60	Trap.	Infinite	20	Stag.	72	8	K	2.86	5000
215-5	1	30	6	5	60	Trap.	Infinite	20	Stag.	72	8	X	4.79	5000
216-1	1	30	6	5	60	Trap.	Infinite	30	Stag.	72	8	X	2.86	5000
217-1	1	30	8	3	0	Parallel	Infinite	20	Cont.	72	8	X	2.86	3600
217-2	1	30	8	3	0	Parallel	Infinite	20	Cont.	72	8	X	2.86	5000
217-3	1	30	8	3	0	Parallel	Infinite	20	Cont.	72	10	X	2.86	5000

Model ID	Geometry									Cross-section		CF detail		Mat'l
	n_{span}	L/d ratio	s_g [ft]	n_{girder}	Support skew [deg]; Layout		R [ft]	s_{cf} [ft]	CF layout	d_w [in]	t_{deck} [in]	CF type	A_{cf} [in^2]	E_c [ksi]
217-4	1	30	8	3	0	Parallel	Infinite	20	Cont.	72	8	K	2.86	5000
217-5	1	30	8	3	0	Parallel	Infinite	20	Cont.	72	8	X	4.79	5000
218-1	1	30	8	3	0	Parallel	Infinite	30	Cont.	72	8	X	2.86	5000
219-1	1	30	8	3	30	Parallel	Infinite	20	Cont.	72	8	X	2.86	3600
219-2	1	30	8	3	30	Parallel	Infinite	20	Cont.	72	8	X	2.86	5000
219-3	1	30	8	3	30	Parallel	Infinite	20	Cont.	72	10	X	2.86	5000
219-4	1	30	8	3	30	Parallel	Infinite	20	Cont.	72	8	K	2.86	5000
219-5	1	30	8	3	30	Parallel	Infinite	20	Cont.	72	8	X	4.79	5000
220-1	1	30	8	3	30	Parallel	Infinite	30	Cont.	72	8	X	2.86	5000
221-1	1	30	8	3	60	Parallel	Infinite	20	Cont.	72	8	X	2.86	3600
221-2	1	30	8	3	60	Parallel	Infinite	20	Cont.	72	8	X	2.86	5000
221-3	1	30	8	3	60	Parallel	Infinite	20	Cont.	72	10	X	2.86	5000
221-4	1	30	8	3	60	Parallel	Infinite	20	Cont.	72	8	K	2.86	5000
221-5	1	30	8	3	60	Parallel	Infinite	20	Cont.	72	8	X	4.79	5000
222-1	1	30	8	3	60	Parallel	Infinite	30	Cont.	72	8	X	2.86	5000
223-1	1	30	8	3	60	Parallel	Infinite	20	Stag.	72	8	X	2.86	3600
223-2	1	30	8	3	60	Parallel	Infinite	20	Stag.	72	8	X	2.86	5000
223-3	1	30	8	3	60	Parallel	Infinite	20	Stag.	72	10	X	2.86	5000
223-4	1	30	8	3	60	Parallel	Infinite	20	Stag.	72	8	K	2.86	5000
223-5	1	30	8	3	60	Parallel	Infinite	20	Stag.	72	8	X	4.79	5000
224-1	1	30	8	3	60	Parallel	Infinite	30	Stag.	72	8	X	2.86	5000
225-1	1	30	8	3	60	Trap.	Infinite	20	Cont.	72	8	X	2.86	3600
225-2	1	30	8	3	60	Trap.	Infinite	20	Cont.	72	8	X	2.86	5000
225-3	1	30	8	3	60	Trap.	Infinite	20	Cont.	72	10	X	2.86	5000
225-4	1	30	8	3	60	Trap.	Infinite	20	Cont.	72	8	K	2.86	5000
225-5	1	30	8	3	60	Trap.	Infinite	20	Cont.	72	8	X	4.79	5000
226-1	1	30	8	3	60	Trap.	Infinite	30	Cont.	72	8	X	2.86	5000
227-1	1	30	8	3	60	Trap.	Infinite	20	Stag.	72	8	X	2.86	3600
227-2	1	30	8	3	60	Trap.	Infinite	20	Stag.	72	8	X	2.86	5000
227-3	1	30	8	3	60	Trap.	Infinite	20	Stag.	72	10	X	2.86	5000
227-4	1	30	8	3	60	Trap.	Infinite	20	Stag.	72	8	K	2.86	5000
227-5	1	30	8	3	60	Trap.	Infinite	20	Stag.	72	8	X	4.79	5000
228-1	1	30	8	3	60	Trap.	Infinite	30	Stag.	72	8	X	2.86	5000
229-1	1	30	8	5	0	Parallel	Infinite	20	Cont.	72	8	X	2.86	3600
229-2	1	30	8	5	0	Parallel	Infinite	20	Cont.	72	8	X	2.86	5000
229-3	1	30	8	5	0	Parallel	Infinite	20	Cont.	72	10	X	2.86	5000
229-4	1	30	8	5	0	Parallel	Infinite	20	Cont.	72	8	K	2.86	5000
229-5	1	30	8	5	0	Parallel	Infinite	20	Cont.	72	8	X	4.79	5000
230-1	1	30	8	5	0	Parallel	Infinite	30	Cont.	72	8	X	2.86	5000
231-1	1	30	8	5	30	Parallel	Infinite	20	Cont.	72	8	X	2.86	3600
231-2	1	30	8	5	30	Parallel	Infinite	20	Cont.	72	8	X	2.86	5000
231-3	1	30	8	5	30	Parallel	Infinite	20	Cont.	72	10	X	2.86	5000
231-4	1	30	8	5	30	Parallel	Infinite	20	Cont.	72	8	K	2.86	5000
231-5	1	30	8	5	30	Parallel	Infinite	20	Cont.	72	8	X	4.79	5000
232-1	1	30	8	5	30	Parallel	Infinite	30	Cont.	72	8	X	2.86	5000
233-1	1	30	8	5	60	Parallel	Infinite	20	Cont.	72	8	X	2.86	3600
233-2	1	30	8	5	60	Parallel	Infinite	20	Cont.	72	8	X	2.86	5000
233-3	1	30	8	5	60	Parallel	Infinite	20	Cont.	72	10	X	2.86	5000
233-4	1	30	8	5	60	Parallel	Infinite	20	Cont.	72	8	K	2.86	5000
233-5	1	30	8	5	60	Parallel	Infinite	20	Cont.	72	8	X	4.79	5000
234-1	1	30	8	5	60	Parallel	Infinite	30	Cont.	72	8	X	2.86	5000
235-1	1	30	8	5	60	Parallel	Infinite	20	Stag.	72	8	X	2.86	3600
235-2	1	30	8	5	60	Parallel	Infinite	20	Stag.	72	8	X	2.86	5000
235-3	1	30	8	5	60	Parallel	Infinite	20	Stag.	72	10	X	2.86	5000
235-4	1	30	8	5	60	Parallel	Infinite	20	Stag.	72	8	K	2.86	5000
235-5	1	30	8	5	60	Parallel	Infinite	20	Stag.	72	8	X	4.79	5000
236-1	1	30	8	5	60	Parallel	Infinite	30	Stag.	72	8	X	2.86	5000
237-1	1	30	8	5	60	Trap.	Infinite	20	Cont.	72	8	X	2.86	3600
237-2	1	30	8	5	60	Trap.	Infinite	20	Cont.	72	8	X	2.86	5000
237-3	1	30	8	5	60	Trap.	Infinite	20	Cont.	72	10	X	2.86	5000
237-4	1	30	8	5	60	Trap.	Infinite	20	Cont.	72	8	K	2.86	5000
237-5	1	30	8	5	60	Trap.	Infinite	20	Cont.	72	8	X	4.79	5000
238-1	1	30	8	5	60	Trap.	Infinite	30	Cont.	72	8	X	2.86	5000
239-1	1	30	8	5	60	Trap.	Infinite	20	Stag.	72	8	X	2.86	3600
239-2	1	30	8	5	60	Trap.	Infinite	20	Stag.	72	8	X	2.86	5000
239-3	1	30	8	5	60	Trap.	Infinite	20	Stag.	72	10	X	2.86	5000
239-4	1	30	8	5	60	Trap.	Infinite	20	Stag.	72	8	K	2.86	5000
239-5	1	30	8	5	60	Trap.	Infinite	20	Stag.	72	8	X	4.79	5000
240-1	1	30	8	5	60	Trap.	Infinite	30	Stag.	72	8	X	2.86	5000
241-1	1	30	10	3	0	Parallel	Infinite	20	Cont.	72	8	X	2.86	3600
241-2	1	30	10	3	0	Parallel	Infinite	20	Cont.	72	8	X	2.86	5000
241-3	1	30	10	3	0	Parallel	Infinite	20	Cont.	72	10	X	2.86	5000
241-4	1	30	10	3	0	Parallel	Infinite	20	Cont.	72	8	K	2.86	5000

Model ID	Geometry									Cross-section		CF detail		Mat'l
	n_{span}	L/d ratio	s_g [ft]	n_{girder}	Support skew [deg];	Layout	R [ft]	s_{cf} [ft]	CF layout	d_w [in]	t_{deck} [in]	CF type	A_{cf} [in^2]	E_c [ksi]
241-5	1	30	10	3	0	Parallel	Infinite	20	Cont.	72	8	X	4.79	5000
242-1	1	30	10	3	0	Parallel	Infinite	30	Cont.	72	8	X	2.86	5000
243-1	1	30	10	3	30	Parallel	Infinite	20	Cont.	72	8	X	2.86	3600
243-2	1	30	10	3	30	Parallel	Infinite	20	Cont.	72	8	X	2.86	5000
243-3	1	30	10	3	30	Parallel	Infinite	20	Cont.	72	10	X	2.86	5000
243-4	1	30	10	3	30	Parallel	Infinite	20	Cont.	72	8	K	2.86	5000
243-5	1	30	10	3	30	Parallel	Infinite	20	Cont.	72	8	X	4.79	5000
244-1	1	30	10	3	30	Parallel	Infinite	30	Cont.	72	8	X	2.86	5000
245-1	1	30	10	3	60	Parallel	Infinite	20	Cont.	72	8	X	2.86	3600
245-2	1	30	10	3	60	Parallel	Infinite	20	Cont.	72	8	X	2.86	5000
245-3	1	30	10	3	60	Parallel	Infinite	20	Cont.	72	10	X	2.86	5000
245-4	1	30	10	3	60	Parallel	Infinite	20	Cont.	72	8	K	2.86	5000
245-5	1	30	10	3	60	Parallel	Infinite	20	Cont.	72	8	X	4.79	5000
246-1	1	30	10	3	60	Parallel	Infinite	30	Cont.	72	8	X	2.86	5000
247-1	1	30	10	3	60	Parallel	Infinite	20	Stag.	72	8	X	2.86	3600
247-2	1	30	10	3	60	Parallel	Infinite	20	Stag.	72	8	X	2.86	5000
247-3	1	30	10	3	60	Parallel	Infinite	20	Stag.	72	10	X	2.86	5000
247-4	1	30	10	3	60	Parallel	Infinite	20	Stag.	72	8	K	2.86	5000
247-5	1	30	10	3	60	Parallel	Infinite	20	Stag.	72	8	X	4.79	5000
248-1	1	30	10	3	60	Parallel	Infinite	30	Stag.	72	8	X	2.86	5000
249-1	1	30	10	3	60	Trap.	Infinite	20	Cont.	72	8	X	2.86	3600
249-2	1	30	10	3	60	Trap.	Infinite	20	Cont.	72	8	X	2.86	5000
249-3	1	30	10	3	60	Trap.	Infinite	20	Cont.	72	10	X	2.86	5000
249-4	1	30	10	3	60	Trap.	Infinite	20	Cont.	72	8	K	2.86	5000
249-5	1	30	10	3	60	Trap.	Infinite	20	Cont.	72	8	X	4.79	5000
250-1	1	30	10	3	60	Trap.	Infinite	30	Cont.	72	8	X	2.86	5000
251-1	1	30	10	3	60	Trap.	Infinite	20	Stag.	72	8	X	2.86	3600
251-2	1	30	10	3	60	Trap.	Infinite	20	Stag.	72	8	X	2.86	5000
251-3	1	30	10	3	60	Trap.	Infinite	20	Stag.	72	10	X	2.86	5000
251-4	1	30	10	3	60	Trap.	Infinite	20	Stag.	72	8	K	2.86	5000
251-5	1	30	10	3	60	Trap.	Infinite	20	Stag.	72	8	X	4.79	5000
252-1	1	30	10	3	60	Trap.	Infinite	30	Stag.	72	8	X	2.86	5000
253-1	1	30	10	5	0	Parallel	Infinite	20	Cont.	72	8	X	2.86	3600
253-2	1	30	10	5	0	Parallel	Infinite	20	Cont.	72	8	X	2.86	5000
253-3	1	30	10	5	0	Parallel	Infinite	20	Cont.	72	10	X	2.86	5000
253-4	1	30	10	5	0	Parallel	Infinite	20	Cont.	72	8	K	2.86	5000
253-5	1	30	10	5	0	Parallel	Infinite	20	Cont.	72	8	X	4.79	5000
254-1	1	30	10	5	0	Parallel	Infinite	30	Cont.	72	8	X	2.86	5000
255-1	1	30	10	5	30	Parallel	Infinite	20	Cont.	72	8	X	2.86	3600
255-2	1	30	10	5	30	Parallel	Infinite	20	Cont.	72	8	X	2.86	5000
255-3	1	30	10	5	30	Parallel	Infinite	20	Cont.	72	10	X	2.86	5000
255-4	1	30	10	5	30	Parallel	Infinite	20	Cont.	72	8	K	2.86	5000
255-5	1	30	10	5	30	Parallel	Infinite	20	Cont.	72	8	X	4.79	5000
256-1	1	30	10	5	30	Parallel	Infinite	30	Cont.	72	8	X	2.86	5000
257-1	1	30	10	5	60	Parallel	Infinite	20	Cont.	72	8	X	2.86	3600
257-2	1	30	10	5	60	Parallel	Infinite	20	Cont.	72	8	X	2.86	5000
257-3	1	30	10	5	60	Parallel	Infinite	20	Cont.	72	10	X	2.86	5000
257-4	1	30	10	5	60	Parallel	Infinite	20	Cont.	72	8	K	2.86	5000
257-5	1	30	10	5	60	Parallel	Infinite	20	Cont.	72	8	X	4.79	5000
258-1	1	30	10	5	60	Parallel	Infinite	30	Cont.	72	8	X	2.86	5000
259-1	1	30	10	5	60	Parallel	Infinite	20	Stag.	72	8	X	2.86	3600
259-2	1	30	10	5	60	Parallel	Infinite	20	Stag.	72	8	X	2.86	5000
259-3	1	30	10	5	60	Parallel	Infinite	20	Stag.	72	10	X	2.86	5000
259-4	1	30	10	5	60	Parallel	Infinite	20	Stag.	72	8	K	2.86	5000
259-5	1	30	10	5	60	Parallel	Infinite	20	Stag.	72	8	X	4.79	5000
260-1	1	30	10	5	60	Parallel	Infinite	30	Stag.	72	8	X	2.86	5000
261-1	1	30	10	5	60	Trap.	Infinite	20	Cont.	72	8	X	2.86	3600
261-2	1	30	10	5	60	Trap.	Infinite	20	Cont.	72	8	X	2.86	5000
261-3	1	30	10	5	60	Trap.	Infinite	20	Cont.	72	10	X	2.86	5000
261-4	1	30	10	5	60	Trap.	Infinite	20	Cont.	72	8	K	2.86	5000
261-5	1	30	10	5	60	Trap.	Infinite	20	Cont.	72	8	X	4.79	5000
262-1	1	30	10	5	60	Trap.	Infinite	30	Cont.	72	8	X	2.86	5000
263-1	1	30	10	5	60	Trap.	Infinite	20	Stag.	72	8	X	2.86	3600
263-2	1	30	10	5	60	Trap.	Infinite	20	Stag.	72	8	X	2.86	5000
263-3	1	30	10	5	60	Trap.	Infinite	20	Stag.	72	10	X	2.86	5000
263-4	1	30	10	5	60	Trap.	Infinite	20	Stag.	72	8	K	2.86	5000
263-5	1	30	10	5	60	Trap.	Infinite	20	Stag.	72	8	X	4.79	5000
264-1	1	30	10	5	60	Trap.	Infinite	30	Stag.	72	8	X	2.86	5000
265-1	1	30	6	3	0	Parallel	Infinite	20	Cont.	96	8	X	2.86	3600
265-2	1	30	6	3	0	Parallel	Infinite	20	Cont.	96	8	X	2.86	5000
265-3	1	30	6	3	0	Parallel	Infinite	20	Cont.	96	10	X	2.86	5000
265-4	1	30	6	3	0	Parallel	Infinite	20	Cont.	96	8	K	2.86	5000
265-5	1	30	6	3	0	Parallel	Infinite	20	Cont.	96	8	X	4.79	5000

Model ID	Geometry									Cross-section		CF detail		Mat'l
	n_{span}	L/d ratio	s_g [ft]	n_{girder}	Support skew [deg];	Layout	R [ft]	s_{cf} [ft]	CF layout	d_w [in]	t_{deck} [in]	CF type	A_{cf} [in^2]	E_c [ksi]
266-1	1	30	6	3	0	Parallel	Infinite	30	Cont.	96	8	X	2.86	5000
267-1	1	30	6	3	30	Parallel	Infinite	20	Cont.	96	8	X	2.86	3600
267-2	1	30	6	3	30	Parallel	Infinite	20	Cont.	96	8	X	2.86	5000
267-3	1	30	6	3	30	Parallel	Infinite	20	Cont.	96	10	X	2.86	5000
267-4	1	30	6	3	30	Parallel	Infinite	20	Cont.	96	8	K	2.86	5000
267-5	1	30	6	3	30	Parallel	Infinite	20	Cont.	96	8	X	4.79	5000
268-1	1	30	6	3	30	Parallel	Infinite	30	Cont.	96	8	X	2.86	5000
269-1	1	30	6	3	60	Parallel	Infinite	20	Cont.	96	8	X	2.86	3600
269-2	1	30	6	3	60	Parallel	Infinite	20	Cont.	96	8	X	2.86	5000
269-3	1	30	6	3	60	Parallel	Infinite	20	Cont.	96	10	X	2.86	5000
269-4	1	30	6	3	60	Parallel	Infinite	20	Cont.	96	8	K	2.86	5000
269-5	1	30	6	3	60	Parallel	Infinite	20	Cont.	96	8	X	4.79	5000
270-1	1	30	6	3	60	Parallel	Infinite	30	Cont.	96	8	X	2.86	5000
271-1	1	30	6	3	60	Parallel	Infinite	20	Stag.	96	8	X	2.86	3600
271-2	1	30	6	3	60	Parallel	Infinite	20	Stag.	96	8	X	2.86	5000
271-3	1	30	6	3	60	Parallel	Infinite	20	Stag.	96	10	X	2.86	5000
271-4	1	30	6	3	60	Parallel	Infinite	20	Stag.	96	8	K	2.86	5000
271-5	1	30	6	3	60	Parallel	Infinite	20	Stag.	96	8	X	4.79	5000
272-1	1	30	6	3	60	Parallel	Infinite	30	Stag.	96	8	X	2.86	5000
273-1	1	30	6	3	60	Trap.	Infinite	20	Cont.	96	8	X	2.86	3600
273-2	1	30	6	3	60	Trap.	Infinite	20	Cont.	96	8	X	2.86	5000
273-3	1	30	6	3	60	Trap.	Infinite	20	Cont.	96	10	X	2.86	5000
273-4	1	30	6	3	60	Trap.	Infinite	20	Cont.	96	8	K	2.86	5000
273-5	1	30	6	3	60	Trap.	Infinite	20	Cont.	96	8	X	4.79	5000
274-1	1	30	6	3	60	Trap.	Infinite	30	Cont.	96	8	X	2.86	5000
275-1	1	30	6	3	60	Trap.	Infinite	20	Stag.	96	8	X	2.86	3600
275-2	1	30	6	3	60	Trap.	Infinite	20	Stag.	96	8	X	2.86	5000
275-3	1	30	6	3	60	Trap.	Infinite	20	Stag.	96	10	X	2.86	5000
275-4	1	30	6	3	60	Trap.	Infinite	20	Stag.	96	8	K	2.86	5000
275-5	1	30	6	3	60	Trap.	Infinite	20	Stag.	96	8	X	4.79	5000
276-1	1	30	6	3	60	Trap.	Infinite	30	Stag.	96	8	X	2.86	5000
277-1	1	30	6	5	0	Parallel	Infinite	20	Cont.	96	8	X	2.86	3600
277-2	1	30	6	5	0	Parallel	Infinite	20	Cont.	96	8	X	2.86	5000
277-3	1	30	6	5	0	Parallel	Infinite	20	Cont.	96	10	X	2.86	5000
277-4	1	30	6	5	0	Parallel	Infinite	20	Cont.	96	8	K	2.86	5000
277-5	1	30	6	5	0	Parallel	Infinite	20	Cont.	96	8	X	4.79	5000
278-1	1	30	6	5	0	Parallel	Infinite	30	Cont.	96	8	X	2.86	5000
279-1	1	30	6	5	30	Parallel	Infinite	20	Cont.	96	8	X	2.86	3600
279-2	1	30	6	5	30	Parallel	Infinite	20	Cont.	96	8	X	2.86	5000
279-3	1	30	6	5	30	Parallel	Infinite	20	Cont.	96	10	X	2.86	5000
279-4	1	30	6	5	30	Parallel	Infinite	20	Cont.	96	8	K	2.86	5000
279-5	1	30	6	5	30	Parallel	Infinite	20	Cont.	96	8	X	4.79	5000
280-1	1	30	6	5	30	Parallel	Infinite	30	Cont.	96	8	X	2.86	5000
281-1	1	30	6	5	60	Parallel	Infinite	20	Cont.	96	8	X	2.86	3600
281-2	1	30	6	5	60	Parallel	Infinite	20	Cont.	96	8	X	2.86	5000
281-3	1	30	6	5	60	Parallel	Infinite	20	Cont.	96	10	X	2.86	5000
281-4	1	30	6	5	60	Parallel	Infinite	20	Cont.	96	8	K	2.86	5000
281-5	1	30	6	5	60	Parallel	Infinite	20	Cont.	96	8	X	4.79	5000
282-1	1	30	6	5	60	Parallel	Infinite	30	Cont.	96	8	X	2.86	5000
283-1	1	30	6	5	60	Parallel	Infinite	20	Stag.	96	8	X	2.86	3600
283-2	1	30	6	5	60	Parallel	Infinite	20	Stag.	96	8	X	2.86	5000
283-3	1	30	6	5	60	Parallel	Infinite	20	Stag.	96	10	X	2.86	5000
283-4	1	30	6	5	60	Parallel	Infinite	20	Stag.	96	8	K	2.86	5000
283-5	1	30	6	5	60	Parallel	Infinite	20	Stag.	96	8	X	4.79	5000
284-1	1	30	6	5	60	Parallel	Infinite	30	Stag.	96	8	X	2.86	5000
285-1	1	30	6	5	60	Trap.	Infinite	20	Cont.	96	8	X	2.86	3600
285-2	1	30	6	5	60	Trap.	Infinite	20	Cont.	96	8	X	2.86	5000
285-3	1	30	6	5	60	Trap.	Infinite	20	Cont.	96	10	X	2.86	5000
285-4	1	30	6	5	60	Trap.	Infinite	20	Cont.	96	8	K	2.86	5000
285-5	1	30	6	5	60	Trap.	Infinite	20	Cont.	96	8	X	4.79	5000
286-1	1	30	6	5	60	Trap.	Infinite	30	Cont.	96	8	X	2.86	5000
287-1	1	30	6	5	60	Trap.	Infinite	20	Stag.	96	8	X	2.86	3600
287-2	1	30	6	5	60	Trap.	Infinite	20	Stag.	96	8	X	2.86	5000
287-3	1	30	6	5	60	Trap.	Infinite	20	Stag.	96	10	X	2.86	5000
287-4	1	30	6	5	60	Trap.	Infinite	20	Stag.	96	8	K	2.86	5000
287-5	1	30	6	5	60	Trap.	Infinite	20	Stag.	96	8	X	4.79	5000
288-1	1	30	6	5	60	Trap.	Infinite	30	Stag.	96	8	X	2.86	5000
289-1	1	30	8	3	0	Parallel	Infinite	20	Cont.	96	8	X	2.86	3600
289-2	1	30	8	3	0	Parallel	Infinite	20	Cont.	96	8	X	2.86	5000
289-3	1	30	8	3	0	Parallel	Infinite	20	Cont.	96	10	X	2.86	5000
289-4	1	30	8	3	0	Parallel	Infinite	20	Cont.	96	8	K	2.86	5000
289-5	1	30	8	3	0	Parallel	Infinite	20	Cont.	96	8	X	4.79	5000
290-1	1	30	8	3	0	Parallel	Infinite	30	Cont.	96	8	X	2.86	5000

Model ID	Geometry									Cross-section		CF detail		Mat'l
	n_{span}	L/d ratio	s_g [ft]	n_{girder}	Support skew [deg]; Layout		R [ft]	s_{cf} [ft]	CF layout	d_w [in]	t_{deck} [in]	CF type	A_{cf} [in^2]	E_c [ksi]
291-1	1	30	8	3	30	Parallel	Infinite	20	Cont.	96	8	X	2.86	3600
291-2	1	30	8	3	30	Parallel	Infinite	20	Cont.	96	8	X	2.86	5000
291-3	1	30	8	3	30	Parallel	Infinite	20	Cont.	96	10	X	2.86	5000
291-4	1	30	8	3	30	Parallel	Infinite	20	Cont.	96	8	K	2.86	5000
291-5	1	30	8	3	30	Parallel	Infinite	20	Cont.	96	8	X	4.79	5000
292-1	1	30	8	3	30	Parallel	Infinite	30	Cont.	96	8	X	2.86	5000
293-1	1	30	8	3	60	Parallel	Infinite	20	Cont.	96	8	X	2.86	3600
293-2	1	30	8	3	60	Parallel	Infinite	20	Cont.	96	8	X	2.86	5000
293-3	1	30	8	3	60	Parallel	Infinite	20	Cont.	96	10	X	2.86	5000
293-4	1	30	8	3	60	Parallel	Infinite	20	Cont.	96	8	K	2.86	5000
293-5	1	30	8	3	60	Parallel	Infinite	20	Cont.	96	8	X	4.79	5000
294-1	1	30	8	3	60	Parallel	Infinite	30	Cont.	96	8	X	2.86	5000
295-1	1	30	8	3	60	Parallel	Infinite	20	Stag.	96	8	X	2.86	3600
295-2	1	30	8	3	60	Parallel	Infinite	20	Stag.	96	8	X	2.86	5000
295-3	1	30	8	3	60	Parallel	Infinite	20	Stag.	96	10	X	2.86	5000
295-4	1	30	8	3	60	Parallel	Infinite	20	Stag.	96	8	K	2.86	5000
295-5	1	30	8	3	60	Parallel	Infinite	20	Stag.	96	8	X	4.79	5000
296-1	1	30	8	3	60	Parallel	Infinite	30	Stag.	96	8	X	2.86	5000
297-1	1	30	8	3	60	Trap.	Infinite	20	Cont.	96	8	X	2.86	3600
297-2	1	30	8	3	60	Trap.	Infinite	20	Cont.	96	8	X	2.86	5000
297-3	1	30	8	3	60	Trap.	Infinite	20	Cont.	96	10	X	2.86	5000
297-4	1	30	8	3	60	Trap.	Infinite	20	Cont.	96	8	K	2.86	5000
297-5	1	30	8	3	60	Trap.	Infinite	20	Cont.	96	8	X	4.79	5000
298-1	1	30	8	3	60	Trap.	Infinite	30	Cont.	96	8	X	2.86	5000
299-1	1	30	8	3	60	Trap.	Infinite	20	Stag.	96	8	X	2.86	3600
299-2	1	30	8	3	60	Trap.	Infinite	20	Stag.	96	8	X	2.86	5000
299-3	1	30	8	3	60	Trap.	Infinite	20	Stag.	96	10	X	2.86	5000
299-4	1	30	8	3	60	Trap.	Infinite	20	Stag.	96	8	K	2.86	5000
299-5	1	30	8	3	60	Trap.	Infinite	20	Stag.	96	8	X	4.79	5000
300-1	1	30	8	3	60	Trap.	Infinite	30	Stag.	96	8	X	2.86	5000
301-1	1	30	8	5	0	Parallel	Infinite	20	Cont.	96	8	X	2.86	3600
301-2	1	30	8	5	0	Parallel	Infinite	20	Cont.	96	8	X	2.86	5000
301-3	1	30	8	5	0	Parallel	Infinite	20	Cont.	96	10	X	2.86	5000
301-4	1	30	8	5	0	Parallel	Infinite	20	Cont.	96	8	K	2.86	5000
301-5	1	30	8	5	0	Parallel	Infinite	20	Cont.	96	8	X	4.79	5000
302-1	1	30	8	5	0	Parallel	Infinite	30	Cont.	96	8	X	2.86	5000
303-1	1	30	8	5	30	Parallel	Infinite	20	Cont.	96	8	X	2.86	3600
303-2	1	30	8	5	30	Parallel	Infinite	20	Cont.	96	8	X	2.86	5000
303-3	1	30	8	5	30	Parallel	Infinite	20	Cont.	96	10	X	2.86	5000
303-4	1	30	8	5	30	Parallel	Infinite	20	Cont.	96	8	K	2.86	5000
303-5	1	30	8	5	30	Parallel	Infinite	20	Cont.	96	8	X	4.79	5000
304-1	1	30	8	5	30	Parallel	Infinite	30	Cont.	96	8	X	2.86	5000
305-1	1	30	8	5	60	Parallel	Infinite	20	Cont.	96	8	X	2.86	3600
305-2	1	30	8	5	60	Parallel	Infinite	20	Cont.	96	8	X	2.86	5000
305-3	1	30	8	5	60	Parallel	Infinite	20	Cont.	96	10	X	2.86	5000
305-4	1	30	8	5	60	Parallel	Infinite	20	Cont.	96	8	K	2.86	5000
305-5	1	30	8	5	60	Parallel	Infinite	20	Cont.	96	8	X	4.79	5000
306-1	1	30	8	5	60	Parallel	Infinite	30	Cont.	96	8	X	2.86	5000
307-1	1	30	8	5	60	Parallel	Infinite	20	Stag.	96	8	X	2.86	3600
307-2	1	30	8	5	60	Parallel	Infinite	20	Stag.	96	8	X	2.86	5000
307-3	1	30	8	5	60	Parallel	Infinite	20	Stag.	96	10	X	2.86	5000
307-4	1	30	8	5	60	Parallel	Infinite	20	Stag.	96	8	K	2.86	5000
307-5	1	30	8	5	60	Parallel	Infinite	20	Stag.	96	8	X	4.79	5000
308-1	1	30	8	5	60	Parallel	Infinite	30	Stag.	96	8	X	2.86	5000
309-1	1	30	8	5	60	Trap.	Infinite	20	Cont.	96	8	X	2.86	3600
309-2	1	30	8	5	60	Trap.	Infinite	20	Cont.	96	8	X	2.86	5000
309-3	1	30	8	5	60	Trap.	Infinite	20	Cont.	96	10	X	2.86	5000
309-4	1	30	8	5	60	Trap.	Infinite	20	Cont.	96	8	K	2.86	5000
309-5	1	30	8	5	60	Trap.	Infinite	20	Cont.	96	8	X	4.79	5000
310-1	1	30	8	5	60	Trap.	Infinite	30	Cont.	96	8	X	2.86	5000
311-1	1	30	8	5	60	Trap.	Infinite	20	Stag.	96	8	X	2.86	3600
311-2	1	30	8	5	60	Trap.	Infinite	20	Stag.	96	8	X	2.86	5000
311-3	1	30	8	5	60	Trap.	Infinite	20	Stag.	96	10	X	2.86	5000
311-4	1	30	8	5	60	Trap.	Infinite	20	Stag.	96	8	K	2.86	5000
311-5	1	30	8	5	60	Trap.	Infinite	20	Stag.	96	8	X	4.79	5000
312-1	1	30	8	5	60	Trap.	Infinite	30	Stag.	96	8	X	2.86	5000
313-1	1	30	10	3	0	Parallel	Infinite	20	Cont.	96	8	X	2.86	3600
313-2	1	30	10	3	0	Parallel	Infinite	20	Cont.	96	8	X	2.86	5000
313-3	1	30	10	3	0	Parallel	Infinite	20	Cont.	96	10	X	2.86	5000
313-4	1	30	10	3	0	Parallel	Infinite	20	Cont.	96	8	K	2.86	5000
313-5	1	30	10	3	0	Parallel	Infinite	20	Cont.	96	8	X	4.79	5000
314-1	1	30	10	3	0	Parallel	Infinite	30	Cont.	96	8	X	2.86	5000
315-1	1	30	10	3	30	Parallel	Infinite	20	Cont.	96	8	X	2.86	3600

Model ID	Geometry									Cross-section		CF detail		Mat'l
	n_{span}	L/d ratio	s_g [ft]	n_{girder}	Support skew [deg]; Layout		R [ft]	s_{cf} [ft]	CF layout	d_w [in]	t_{deck} [in]	CF type	A_{cf} [in^2]	E_c [ksi]
315-2	1	30	10	3	30	Parallel	Infinite	20	Cont.	96	8	X	2.86	5000
315-3	1	30	10	3	30	Parallel	Infinite	20	Cont.	96	10	X	2.86	5000
315-4	1	30	10	3	30	Parallel	Infinite	20	Cont.	96	8	K	2.86	5000
315-5	1	30	10	3	30	Parallel	Infinite	20	Cont.	96	8	X	4.79	5000
316-1	1	30	10	3	30	Parallel	Infinite	30	Cont.	96	8	X	2.86	5000
317-1	1	30	10	3	60	Parallel	Infinite	20	Cont.	96	8	X	2.86	3600
317-2	1	30	10	3	60	Parallel	Infinite	20	Cont.	96	8	X	2.86	5000
317-3	1	30	10	3	60	Parallel	Infinite	20	Cont.	96	10	X	2.86	5000
317-4	1	30	10	3	60	Parallel	Infinite	20	Cont.	96	8	K	2.86	5000
317-5	1	30	10	3	60	Parallel	Infinite	20	Cont.	96	8	X	4.79	5000
318-1	1	30	10	3	60	Parallel	Infinite	30	Cont.	96	8	X	2.86	5000
319-1	1	30	10	3	60	Parallel	Infinite	20	Stag.	96	8	X	2.86	3600
319-2	1	30	10	3	60	Parallel	Infinite	20	Stag.	96	8	X	2.86	5000
319-3	1	30	10	3	60	Parallel	Infinite	20	Stag.	96	10	X	2.86	5000
319-4	1	30	10	3	60	Parallel	Infinite	20	Stag.	96	8	K	2.86	5000
319-5	1	30	10	3	60	Parallel	Infinite	20	Stag.	96	8	X	4.79	5000
320-1	1	30	10	3	60	Parallel	Infinite	30	Stag.	96	8	X	2.86	5000
321-1	1	30	10	3	60	Trap.	Infinite	20	Cont.	96	8	X	2.86	3600
321-2	1	30	10	3	60	Trap.	Infinite	20	Cont.	96	8	X	2.86	5000
321-3	1	30	10	3	60	Trap.	Infinite	20	Cont.	96	10	X	2.86	5000
321-4	1	30	10	3	60	Trap.	Infinite	20	Cont.	96	8	K	2.86	5000
321-5	1	30	10	3	60	Trap.	Infinite	20	Cont.	96	8	X	4.79	5000
322-1	1	30	10	3	60	Trap.	Infinite	30	Cont.	96	8	X	2.86	5000
323-1	1	30	10	3	60	Trap.	Infinite	20	Stag.	96	8	X	2.86	3600
323-2	1	30	10	3	60	Trap.	Infinite	20	Stag.	96	8	X	2.86	5000
323-3	1	30	10	3	60	Trap.	Infinite	20	Stag.	96	10	X	2.86	5000
323-4	1	30	10	3	60	Trap.	Infinite	20	Stag.	96	8	K	2.86	5000
323-5	1	30	10	3	60	Trap.	Infinite	20	Stag.	96	8	X	4.79	5000
324-1	1	30	10	3	60	Trap.	Infinite	30	Stag.	96	8	X	2.86	5000
325-1	1	30	10	5	0	Parallel	Infinite	20	Cont.	96	8	X	2.86	3600
325-2	1	30	10	5	0	Parallel	Infinite	20	Cont.	96	8	X	2.86	5000
325-3	1	30	10	5	0	Parallel	Infinite	20	Cont.	96	10	X	2.86	5000
325-4	1	30	10	5	0	Parallel	Infinite	20	Cont.	96	8	K	2.86	5000
325-5	1	30	10	5	0	Parallel	Infinite	20	Cont.	96	8	X	4.79	5000
326-1	1	30	10	5	0	Parallel	Infinite	30	Cont.	96	8	X	2.86	5000
327-1	1	30	10	5	30	Parallel	Infinite	20	Cont.	96	8	X	2.86	3600
327-2	1	30	10	5	30	Parallel	Infinite	20	Cont.	96	8	X	2.86	5000
327-3	1	30	10	5	30	Parallel	Infinite	20	Cont.	96	10	X	2.86	5000
327-4	1	30	10	5	30	Parallel	Infinite	20	Cont.	96	8	K	2.86	5000
327-5	1	30	10	5	30	Parallel	Infinite	20	Cont.	96	8	X	4.79	5000
328-1	1	30	10	5	30	Parallel	Infinite	30	Cont.	96	8	X	2.86	5000
329-1	1	30	10	5	60	Parallel	Infinite	20	Cont.	96	8	X	2.86	3600
329-2	1	30	10	5	60	Parallel	Infinite	20	Cont.	96	8	X	2.86	5000
329-3	1	30	10	5	60	Parallel	Infinite	20	Cont.	96	10	X	2.86	5000
329-4	1	30	10	5	60	Parallel	Infinite	20	Cont.	96	8	K	2.86	5000
329-5	1	30	10	5	60	Parallel	Infinite	20	Cont.	96	8	X	4.79	5000
330-1	1	30	10	5	60	Parallel	Infinite	30	Cont.	96	8	X	2.86	5000
331-1	1	30	10	5	60	Parallel	Infinite	20	Stag.	96	8	X	2.86	3600
331-2	1	30	10	5	60	Parallel	Infinite	20	Stag.	96	8	X	2.86	5000
331-3	1	30	10	5	60	Parallel	Infinite	20	Stag.	96	10	X	2.86	5000
331-4	1	30	10	5	60	Parallel	Infinite	20	Stag.	96	8	K	2.86	5000
331-5	1	30	10	5	60	Parallel	Infinite	20	Stag.	96	8	X	4.79	5000
332-1	1	30	10	5	60	Parallel	Infinite	30	Stag.	96	8	X	2.86	5000
333-1	1	30	10	5	60	Trap.	Infinite	20	Cont.	96	8	X	2.86	3600
333-2	1	30	10	5	60	Trap.	Infinite	20	Cont.	96	8	X	2.86	5000
333-3	1	30	10	5	60	Trap.	Infinite	20	Cont.	96	10	X	2.86	5000
333-4	1	30	10	5	60	Trap.	Infinite	20	Cont.	96	8	K	2.86	5000
333-5	1	30	10	5	60	Trap.	Infinite	20	Cont.	96	8	X	4.79	5000
334-1	1	30	10	5	60	Trap.	Infinite	30	Cont.	96	8	X	2.86	5000
335-1	1	30	10	5	60	Trap.	Infinite	20	Stag.	96	8	X	2.86	3600
335-2	1	30	10	5	60	Trap.	Infinite	20	Stag.	96	8	X	2.86	5000
335-3	1	30	10	5	60	Trap.	Infinite	20	Stag.	96	10	X	2.86	5000
335-4	1	30	10	5	60	Trap.	Infinite	20	Stag.	96	8	K	2.86	5000
335-5	1	30	10	5	60	Trap.	Infinite	20	Stag.	96	8	X	4.79	5000
336-1	1	30	10	5	60	Trap.	Infinite	30	Stag.	96	8	X	2.86	5000
337-1	2	25	6	3	0	Parallel	1500	20	Cont.	72	8	X	2.86	3600
337-2	2	25	6	3	0	Parallel	1500	20	Cont.	72	8	X	2.86	5000
337-3	2	25	6	3	0	Parallel	1500	20	Cont.	72	10	X	2.86	5000
337-4	2	25	6	3	0	Parallel	1500	20	Cont.	72	8	K	2.86	5000
337-5	2	25	6	3	0	Parallel	1500	20	Cont.	72	8	X	4.79	5000
338-1	2	25	6	3	0	Parallel	1500	30	Cont.	72	8	X	2.86	5000
339-1	2	25	6	3	0	Parallel	750	20	Cont.	72	8	X	2.86	3600
339-2	2	25	6	3	0	Parallel	750	20	Cont.	72	8	X	2.86	5000

Model ID	Geometry									Cross-section		CF detail		Mat'l
	n_{span}	L/d ratio	s_g [ft]	n_{girder}	Support skew [deg]; Layout		R [ft]	s_{cf} [ft]	CF layout	d_w [in]	t_{deck} [in]	CF type	A_{cf} [in^2]	E_c [ksi]
339-3	2	25	6	3	0	Parallel	750	20	Cont.	72	10	X	2.86	5000
339-4	2	25	6	3	0	Parallel	750	20	Cont.	72	8	K	2.86	5000
339-5	2	25	6	3	0	Parallel	750	20	Cont.	72	8	X	4.79	5000
340-1	2	25	6	3	0	Parallel	750	30	Cont.	72	8	X	2.86	5000
341-1	2	25	6	3	30	Parallel	1500	20	Cont.	72	8	X	2.86	3600
341-2	2	25	6	3	30	Parallel	1500	20	Cont.	72	8	X	2.86	5000
341-3	2	25	6	3	30	Parallel	1500	20	Cont.	72	10	X	2.86	5000
341-4	2	25	6	3	30	Parallel	1500	20	Cont.	72	8	K	2.86	5000
341-5	2	25	6	3	30	Parallel	1500	20	Cont.	72	8	X	4.79	5000
342-1	2	25	6	3	30	Parallel	1500	30	Cont.	72	8	X	2.86	5000
343-1	2	25	6	3	30	Parallel	750	20	Cont.	72	8	X	2.86	3600
343-2	2	25	6	3	30	Parallel	750	20	Cont.	72	8	X	2.86	5000
343-3	2	25	6	3	30	Parallel	750	20	Cont.	72	10	X	2.86	5000
343-4	2	25	6	3	30	Parallel	750	20	Cont.	72	8	K	2.86	5000
343-5	2	25	6	3	30	Parallel	750	20	Cont.	72	8	X	4.79	5000
344-1	2	25	6	3	30	Parallel	750	30	Cont.	72	8	X	2.86	5000
345-1	2	25	6	3	60	Parallel	1500	20	Cont.	72	8	X	2.86	3600
345-2	2	25	6	3	60	Parallel	1500	20	Cont.	72	8	X	2.86	5000
345-3	2	25	6	3	60	Parallel	1500	20	Cont.	72	10	X	2.86	5000
345-4	2	25	6	3	60	Parallel	1500	20	Cont.	72	8	K	2.86	5000
345-5	2	25	6	3	60	Parallel	1500	20	Cont.	72	8	X	4.79	5000
346-1	2	25	6	3	60	Parallel	1500	30	Cont.	72	8	X	2.86	5000
347-1	2	25	6	3	60	Parallel	750	20	Cont.	72	8	X	2.86	3600
347-2	2	25	6	3	60	Parallel	750	20	Cont.	72	8	X	2.86	5000
347-3	2	25	6	3	60	Parallel	750	20	Cont.	72	10	X	2.86	5000
347-4	2	25	6	3	60	Parallel	750	20	Cont.	72	8	K	2.86	5000
347-5	2	25	6	3	60	Parallel	750	20	Cont.	72	8	X	4.79	5000
348-1	2	25	6	3	60	Parallel	750	30	Cont.	72	8	X	2.86	5000
349-1	2	25	6	3	60	Trap.	1500	20	Cont.	72	8	X	2.86	3600
349-2	2	25	6	3	60	Trap.	1500	20	Cont.	72	8	X	2.86	5000
349-3	2	25	6	3	60	Trap.	1500	20	Cont.	72	10	X	2.86	5000
349-4	2	25	6	3	60	Trap.	1500	20	Cont.	72	8	K	2.86	5000
349-5	2	25	6	3	60	Trap.	1500	20	Cont.	72	8	X	4.79	5000
350-1	2	25	6	3	60	Trap.	1500	30	Cont.	72	8	X	2.86	5000
351-1	2	25	6	3	60	Trap.	750	20	Cont.	72	8	X	2.86	3600
351-2	2	25	6	3	60	Trap.	750	20	Cont.	72	8	X	2.86	5000
351-3	2	25	6	3	60	Trap.	750	20	Cont.	72	10	X	2.86	5000
351-4	2	25	6	3	60	Trap.	750	20	Cont.	72	8	K	2.86	5000
351-5	2	25	6	3	60	Trap.	750	20	Cont.	72	8	X	4.79	5000
352-1	2	25	6	3	60	Trap.	750	30	Cont.	72	8	X	2.86	5000
353-1	2	25	6	5	0	Parallel	1500	20	Cont.	72	8	X	2.86	3600
353-2	2	25	6	5	0	Parallel	1500	20	Cont.	72	8	X	2.86	5000
353-3	2	25	6	5	0	Parallel	1500	20	Cont.	72	10	X	2.86	5000
353-4	2	25	6	5	0	Parallel	1500	20	Cont.	72	8	K	2.86	5000
353-5	2	25	6	5	0	Parallel	1500	20	Cont.	72	8	X	4.79	5000
354-1	2	25	6	5	0	Parallel	1500	30	Cont.	72	8	X	2.86	5000
355-1	2	25	6	5	0	Parallel	750	20	Cont.	72	8	X	2.86	3600
355-2	2	25	6	5	0	Parallel	750	20	Cont.	72	8	X	2.86	5000
355-3	2	25	6	5	0	Parallel	750	20	Cont.	72	10	X	2.86	5000
355-4	2	25	6	5	0	Parallel	750	20	Cont.	72	8	K	2.86	5000
355-5	2	25	6	5	0	Parallel	750	20	Cont.	72	8	X	4.79	5000
356-1	2	25	6	5	0	Parallel	750	30	Cont.	72	8	X	2.86	5000
357-1	2	25	6	5	30	Parallel	1500	20	Cont.	72	8	X	2.86	3600
357-2	2	25	6	5	30	Parallel	1500	20	Cont.	72	8	X	2.86	5000
357-3	2	25	6	5	30	Parallel	1500	20	Cont.	72	10	X	2.86	5000
357-4	2	25	6	5	30	Parallel	1500	20	Cont.	72	8	K	2.86	5000
357-5	2	25	6	5	30	Parallel	1500	20	Cont.	72	8	X	4.79	5000
358-1	2	25	6	5	30	Parallel	1500	30	Cont.	72	8	X	2.86	5000
359-1	2	25	6	5	30	Parallel	750	20	Cont.	72	8	X	2.86	3600
359-2	2	25	6	5	30	Parallel	750	20	Cont.	72	8	X	2.86	5000
359-3	2	25	6	5	30	Parallel	750	20	Cont.	72	10	X	2.86	5000
359-4	2	25	6	5	30	Parallel	750	20	Cont.	72	8	K	2.86	5000
359-5	2	25	6	5	30	Parallel	750	20	Cont.	72	8	X	4.79	5000
360-1	2	25	6	5	30	Parallel	750	30	Cont.	72	8	X	2.86	5000
361-1	2	25	6	5	60	Parallel	1500	20	Cont.	72	8	X	2.86	3600
361-2	2	25	6	5	60	Parallel	1500	20	Cont.	72	8	X	2.86	5000
361-3	2	25	6	5	60	Parallel	1500	20	Cont.	72	10	X	2.86	5000
361-4	2	25	6	5	60	Parallel	1500	20	Cont.	72	8	K	2.86	5000
361-5	2	25	6	5	60	Parallel	1500	20	Cont.	72	8	X	4.79	5000
362-1	2	25	6	5	60	Parallel	1500	30	Cont.	72	8	X	2.86	5000
363-1	2	25	6	5	60	Parallel	750	20	Cont.	72	8	X	2.86	3600
363-2	2	25	6	5	60	Parallel	750	20	Cont.	72	8	X	2.86	5000
363-3	2	25	6	5	60	Parallel	750	20	Cont.	72	10	X	2.86	5000

Model ID	Geometry									Cross-section		CF detail		Mat'l
	n_{span}	L/d ratio	s_g [ft]	n_{girder}	Support skew [deg]; Layout		R [ft]	s_{cf} [ft]	CF layout	d_w [in]	t_{deck} [in]	CF type	A_{cf} [in^2]	E_c [ksi]
363-4	2	25	6	5	60	Parallel	750	20	Cont.	72	8	K	2.86	5000
363-5	2	25	6	5	60	Parallel	750	20	Cont.	72	8	X	4.79	5000
364-1	2	25	6	5	60	Parallel	750	30	Cont.	72	8	X	2.86	5000
365-1	2	25	6	5	60	Trap.	1500	20	Cont.	72	8	X	2.86	3600
365-2	2	25	6	5	60	Trap.	1500	20	Cont.	72	8	X	2.86	5000
365-3	2	25	6	5	60	Trap.	1500	20	Cont.	72	10	X	2.86	5000
365-4	2	25	6	5	60	Trap.	1500	20	Cont.	72	8	K	2.86	5000
365-5	2	25	6	5	60	Trap.	1500	20	Cont.	72	8	X	4.79	5000
366-1	2	25	6	5	60	Trap.	1500	30	Cont.	72	8	X	2.86	5000
367-1	2	25	6	5	60	Trap.	750	20	Cont.	72	8	X	2.86	3600
367-2	2	25	6	5	60	Trap.	750	20	Cont.	72	8	X	2.86	5000
367-3	2	25	6	5	60	Trap.	750	20	Cont.	72	10	X	2.86	5000
367-4	2	25	6	5	60	Trap.	750	20	Cont.	72	8	K	2.86	5000
367-5	2	25	6	5	60	Trap.	750	20	Cont.	72	8	X	4.79	5000
368-1	2	25	6	5	60	Trap.	750	30	Cont.	72	8	X	2.86	5000
369-1	2	25	6	7	0	Parallel	1500	20	Cont.	72	8	X	2.86	3600
369-2	2	25	6	7	0	Parallel	1500	20	Cont.	72	8	X	2.86	5000
369-3	2	25	6	7	0	Parallel	1500	20	Cont.	72	10	X	2.86	5000
369-4	2	25	6	7	0	Parallel	1500	20	Cont.	72	8	K	2.86	5000
369-5	2	25	6	7	0	Parallel	1500	20	Cont.	72	8	X	4.79	5000
370-1	2	25	6	7	0	Parallel	1500	30	Cont.	72	8	X	2.86	5000
371-1	2	25	6	7	0	Parallel	750	20	Cont.	72	8	X	2.86	3600
371-2	2	25	6	7	0	Parallel	750	20	Cont.	72	8	X	2.86	5000
371-3	2	25	6	7	0	Parallel	750	20	Cont.	72	10	X	2.86	5000
371-4	2	25	6	7	0	Parallel	750	20	Cont.	72	8	K	2.86	5000
371-5	2	25	6	7	0	Parallel	750	20	Cont.	72	8	X	4.79	5000
372-1	2	25	6	7	0	Parallel	750	30	Cont.	72	8	X	2.86	5000
373-1	2	25	6	7	30	Parallel	1500	20	Cont.	72	8	X	2.86	3600
373-2	2	25	6	7	30	Parallel	1500	20	Cont.	72	8	X	2.86	5000
373-3	2	25	6	7	30	Parallel	1500	20	Cont.	72	10	X	2.86	5000
373-4	2	25	6	7	30	Parallel	1500	20	Cont.	72	8	K	2.86	5000
373-5	2	25	6	7	30	Parallel	1500	20	Cont.	72	8	X	4.79	5000
374-1	2	25	6	7	30	Parallel	1500	30	Cont.	72	8	X	2.86	5000
375-1	2	25	6	7	30	Parallel	750	20	Cont.	72	8	X	2.86	3600
375-2	2	25	6	7	30	Parallel	750	20	Cont.	72	8	X	2.86	5000
375-3	2	25	6	7	30	Parallel	750	20	Cont.	72	10	X	2.86	5000
375-4	2	25	6	7	30	Parallel	750	20	Cont.	72	8	K	2.86	5000
375-5	2	25	6	7	30	Parallel	750	20	Cont.	72	8	X	4.79	5000
376-1	2	25	6	7	30	Parallel	750	30	Cont.	72	8	X	2.86	5000
377-1	2	25	6	7	60	Parallel	1500	20	Cont.	72	8	X	2.86	3600
377-2	2	25	6	7	60	Parallel	1500	20	Cont.	72	8	X	2.86	5000
377-3	2	25	6	7	60	Parallel	1500	20	Cont.	72	10	X	2.86	5000
377-4	2	25	6	7	60	Parallel	1500	20	Cont.	72	8	K	2.86	5000
377-5	2	25	6	7	60	Parallel	1500	20	Cont.	72	8	X	4.79	5000
378-1	2	25	6	7	60	Parallel	1500	30	Cont.	72	8	X	2.86	5000
379-1	2	25	6	7	60	Parallel	750	20	Cont.	72	8	X	2.86	3600
379-2	2	25	6	7	60	Parallel	750	20	Cont.	72	8	X	2.86	5000
379-3	2	25	6	7	60	Parallel	750	20	Cont.	72	10	X	2.86	5000
379-4	2	25	6	7	60	Parallel	750	20	Cont.	72	8	K	2.86	5000
379-5	2	25	6	7	60	Parallel	750	20	Cont.	72	8	X	4.79	5000
380-1	2	25	6	7	60	Parallel	750	30	Cont.	72	8	X	2.86	5000
381-1	2	25	6	7	60	Trap.	1500	20	Cont.	72	8	X	2.86	3600
381-2	2	25	6	7	60	Trap.	1500	20	Cont.	72	8	X	2.86	5000
381-3	2	25	6	7	60	Trap.	1500	20	Cont.	72	10	X	2.86	5000
381-4	2	25	6	7	60	Trap.	1500	20	Cont.	72	8	K	2.86	5000
381-5	2	25	6	7	60	Trap.	1500	20	Cont.	72	8	X	4.79	5000
382-1	2	25	6	7	60	Trap.	1500	30	Cont.	72	8	X	2.86	5000
383-1	2	25	6	7	60	Trap.	750	20	Cont.	72	8	X	2.86	3600
383-2	2	25	6	7	60	Trap.	750	20	Cont.	72	8	X	2.86	5000
383-3	2	25	6	7	60	Trap.	750	20	Cont.	72	10	X	2.86	5000
383-4	2	25	6	7	60	Trap.	750	20	Cont.	72	8	K	2.86	5000
383-5	2	25	6	7	60	Trap.	750	20	Cont.	72	8	X	4.79	5000
384-1	2	25	6	7	60	Trap.	750	30	Cont.	72	8	X	2.86	5000
385-1	2	25	8	3	0	Parallel	1500	20	Cont.	72	8	X	2.86	3600
385-2	2	25	8	3	0	Parallel	1500	20	Cont.	72	8	X	2.86	5000
385-3	2	25	8	3	0	Parallel	1500	20	Cont.	72	10	X	2.86	5000
385-4	2	25	8	3	0	Parallel	1500	20	Cont.	72	8	K	2.86	5000
385-5	2	25	8	3	0	Parallel	1500	20	Cont.	72	8	X	4.79	5000
386-1	2	25	8	3	0	Parallel	1500	30	Cont.	72	8	X	2.86	5000
387-1	2	25	8	3	0	Parallel	750	20	Cont.	72	8	X	2.86	3600
387-2	2	25	8	3	0	Parallel	750	20	Cont.	72	8	X	2.86	5000
387-3	2	25	8	3	0	Parallel	750	20	Cont.	72	10	X	2.86	5000
387-4	2	25	8	3	0	Parallel	750	20	Cont.	72	8	K	2.86	5000

Model ID	Geometry									Cross-section		CF detail		Mat'l
	n_{span}	L/d ratio	s_g [ft]	n_{girder}	Support skew [deg]; Layout		R [ft]	s_{cf} [ft]	CF layout	d_w [in]	t_{deck} [in]	CF type	A_{cf} [in^2]	E_c [ksi]
387-5	2	25	8	3	0	Parallel	750	20	Cont.	72	8	X	4.79	5000
388-1	2	25	8	3	0	Parallel	750	30	Cont.	72	8	X	2.86	5000
389-1	2	25	8	3	30	Parallel	1500	20	Cont.	72	8	X	2.86	3600
389-2	2	25	8	3	30	Parallel	1500	20	Cont.	72	8	X	2.86	5000
389-3	2	25	8	3	30	Parallel	1500	20	Cont.	72	10	X	2.86	5000
389-4	2	25	8	3	30	Parallel	1500	20	Cont.	72	8	K	2.86	5000
389-5	2	25	8	3	30	Parallel	1500	20	Cont.	72	8	X	4.79	5000
390-1	2	25	8	3	30	Parallel	1500	30	Cont.	72	8	X	2.86	5000
391-1	2	25	8	3	30	Parallel	750	20	Cont.	72	8	X	2.86	3600
391-2	2	25	8	3	30	Parallel	750	20	Cont.	72	8	X	2.86	5000
391-3	2	25	8	3	30	Parallel	750	20	Cont.	72	10	X	2.86	5000
391-4	2	25	8	3	30	Parallel	750	20	Cont.	72	8	K	2.86	5000
391-5	2	25	8	3	30	Parallel	750	20	Cont.	72	8	X	4.79	5000
392-1	2	25	8	3	30	Parallel	750	30	Cont.	72	8	X	2.86	5000
393-1	2	25	8	3	60	Parallel	1500	20	Cont.	72	8	X	2.86	3600
393-2	2	25	8	3	60	Parallel	1500	20	Cont.	72	8	X	2.86	5000
393-3	2	25	8	3	60	Parallel	1500	20	Cont.	72	10	X	2.86	5000
393-4	2	25	8	3	60	Parallel	1500	20	Cont.	72	8	K	2.86	5000
393-5	2	25	8	3	60	Parallel	1500	20	Cont.	72	8	X	4.79	5000
394-1	2	25	8	3	60	Parallel	1500	30	Cont.	72	8	X	2.86	5000
395-1	2	25	8	3	60	Parallel	750	20	Cont.	72	8	X	2.86	3600
395-2	2	25	8	3	60	Parallel	750	20	Cont.	72	8	X	2.86	5000
395-3	2	25	8	3	60	Parallel	750	20	Cont.	72	10	X	2.86	5000
395-4	2	25	8	3	60	Parallel	750	20	Cont.	72	8	K	2.86	5000
395-5	2	25	8	3	60	Parallel	750	20	Cont.	72	8	X	4.79	5000
396-1	2	25	8	3	60	Parallel	750	30	Cont.	72	8	X	2.86	5000
397-1	2	25	8	3	60	Trap.	1500	20	Cont.	72	8	X	2.86	3600
397-2	2	25	8	3	60	Trap.	1500	20	Cont.	72	8	X	2.86	5000
397-3	2	25	8	3	60	Trap.	1500	20	Cont.	72	10	X	2.86	5000
397-4	2	25	8	3	60	Trap.	1500	20	Cont.	72	8	K	2.86	5000
397-5	2	25	8	3	60	Trap.	1500	20	Cont.	72	8	X	4.79	5000
398-1	2	25	8	3	60	Trap.	1500	30	Cont.	72	8	X	2.86	5000
399-1	2	25	8	3	60	Trap.	750	20	Cont.	72	8	X	2.86	3600
399-2	2	25	8	3	60	Trap.	750	20	Cont.	72	8	X	2.86	5000
399-3	2	25	8	3	60	Trap.	750	20	Cont.	72	10	X	2.86	5000
399-4	2	25	8	3	60	Trap.	750	20	Cont.	72	8	K	2.86	5000
399-5	2	25	8	3	60	Trap.	750	20	Cont.	72	8	X	4.79	5000
400-1	2	25	8	3	60	Trap.	750	30	Cont.	72	8	X	2.86	5000
401-1	2	25	8	5	0	Parallel	1500	20	Cont.	72	8	X	2.86	3600
401-2	2	25	8	5	0	Parallel	1500	20	Cont.	72	8	X	2.86	5000
401-3	2	25	8	5	0	Parallel	1500	20	Cont.	72	10	X	2.86	5000
401-4	2	25	8	5	0	Parallel	1500	20	Cont.	72	8	K	2.86	5000
401-5	2	25	8	5	0	Parallel	1500	20	Cont.	72	8	X	4.79	5000
402-1	2	25	8	5	0	Parallel	1500	30	Cont.	72	8	X	2.86	5000
403-1	2	25	8	5	0	Parallel	750	20	Cont.	72	8	X	2.86	3600
403-2	2	25	8	5	0	Parallel	750	20	Cont.	72	8	X	2.86	5000
403-3	2	25	8	5	0	Parallel	750	20	Cont.	72	10	X	2.86	5000
403-4	2	25	8	5	0	Parallel	750	20	Cont.	72	8	K	2.86	5000
403-5	2	25	8	5	0	Parallel	750	20	Cont.	72	8	X	4.79	5000
404-1	2	25	8	5	0	Parallel	750	30	Cont.	72	8	X	2.86	5000
405-1	2	25	8	5	30	Parallel	1500	20	Cont.	72	8	X	2.86	3600
405-2	2	25	8	5	30	Parallel	1500	20	Cont.	72	8	X	2.86	5000
405-3	2	25	8	5	30	Parallel	1500	20	Cont.	72	10	X	2.86	5000
405-4	2	25	8	5	30	Parallel	1500	20	Cont.	72	8	K	2.86	5000
405-5	2	25	8	5	30	Parallel	1500	20	Cont.	72	8	X	4.79	5000
406-1	2	25	8	5	30	Parallel	1500	30	Cont.	72	8	X	2.86	5000
407-1	2	25	8	5	30	Parallel	750	20	Cont.	72	8	X	2.86	3600
407-2	2	25	8	5	30	Parallel	750	20	Cont.	72	8	X	2.86	5000
407-3	2	25	8	5	30	Parallel	750	20	Cont.	72	10	X	2.86	5000
407-4	2	25	8	5	30	Parallel	750	20	Cont.	72	8	K	2.86	5000
407-5	2	25	8	5	30	Parallel	750	20	Cont.	72	8	X	4.79	5000
408-1	2	25	8	5	30	Parallel	750	30	Cont.	72	8	X	2.86	5000
409-1	2	25	8	5	60	Parallel	1500	20	Cont.	72	8	X	2.86	3600
409-2	2	25	8	5	60	Parallel	1500	20	Cont.	72	8	X	2.86	5000
409-3	2	25	8	5	60	Parallel	1500	20	Cont.	72	10	X	2.86	5000
409-4	2	25	8	5	60	Parallel	1500	20	Cont.	72	8	K	2.86	5000
409-5	2	25	8	5	60	Parallel	1500	20	Cont.	72	8	X	4.79	5000
410-1	2	25	8	5	60	Parallel	1500	30	Cont.	72	8	X	2.86	5000
411-1	2	25	8	5	60	Parallel	750	20	Cont.	72	8	X	2.86	3600
411-2	2	25	8	5	60	Parallel	750	20	Cont.	72	8	X	2.86	5000
411-3	2	25	8	5	60	Parallel	750	20	Cont.	72	10	X	2.86	5000
411-4	2	25	8	5	60	Parallel	750	20	Cont.	72	8	K	2.86	5000
411-5	2	25	8	5	60	Parallel	750	20	Cont.	72	8	X	4.79	5000

Model ID	Geometry									Cross-section		CF detail		Mat'l
	n_{span}	L/d ratio	s_g [ft]	n_{girder}	Support skew [deg]; Layout		R [ft]	s_{cf} [ft]	CF layout	d_w [in]	t_{deck} [in]	CF type	A_{cf} [in^2]	E_c [ksi]
412-1	2	25	8	5	60	Parallel	750	30	Cont.	72	8	X	2.86	5000
413-1	2	25	8	5	60	Trap.	1500	20	Cont.	72	8	X	2.86	3600
413-2	2	25	8	5	60	Trap.	1500	20	Cont.	72	8	X	2.86	5000
413-3	2	25	8	5	60	Trap.	1500	20	Cont.	72	10	X	2.86	5000
413-4	2	25	8	5	60	Trap.	1500	20	Cont.	72	8	K	2.86	5000
413-5	2	25	8	5	60	Trap.	1500	20	Cont.	72	8	X	4.79	5000
414-1	2	25	8	5	60	Trap.	1500	30	Cont.	72	8	X	2.86	5000
415-1	2	25	8	5	60	Trap.	750	20	Cont.	72	8	X	2.86	3600
415-2	2	25	8	5	60	Trap.	750	20	Cont.	72	8	X	2.86	5000
415-3	2	25	8	5	60	Trap.	750	20	Cont.	72	10	X	2.86	5000
415-4	2	25	8	5	60	Trap.	750	20	Cont.	72	8	K	2.86	5000
415-5	2	25	8	5	60	Trap.	750	20	Cont.	72	8	X	4.79	5000
416-1	2	25	8	5	60	Trap.	750	30	Cont.	72	8	X	2.86	5000
417-1	2	25	8	7	0	Parallel	1500	20	Cont.	72	8	X	2.86	3600
417-2	2	25	8	7	0	Parallel	1500	20	Cont.	72	8	X	2.86	5000
417-3	2	25	8	7	0	Parallel	1500	20	Cont.	72	10	X	2.86	5000
417-4	2	25	8	7	0	Parallel	1500	20	Cont.	72	8	K	2.86	5000
417-5	2	25	8	7	0	Parallel	1500	20	Cont.	72	8	X	4.79	5000
418-1	2	25	8	7	0	Parallel	1500	30	Cont.	72	8	X	2.86	5000
419-1	2	25	8	7	0	Parallel	750	20	Cont.	72	8	X	2.86	3600
419-2	2	25	8	7	0	Parallel	750	20	Cont.	72	8	X	2.86	5000
419-3	2	25	8	7	0	Parallel	750	20	Cont.	72	10	X	2.86	5000
419-4	2	25	8	7	0	Parallel	750	20	Cont.	72	8	K	2.86	5000
419-5	2	25	8	7	0	Parallel	750	20	Cont.	72	8	X	4.79	5000
420-1	2	25	8	7	0	Parallel	750	30	Cont.	72	8	X	2.86	5000
421-1	2	25	8	7	30	Parallel	1500	20	Cont.	72	8	X	2.86	3600
421-2	2	25	8	7	30	Parallel	1500	20	Cont.	72	8	X	2.86	5000
421-3	2	25	8	7	30	Parallel	1500	20	Cont.	72	10	X	2.86	5000
421-4	2	25	8	7	30	Parallel	1500	20	Cont.	72	8	K	2.86	5000
421-5	2	25	8	7	30	Parallel	1500	20	Cont.	72	8	X	4.79	5000
422-1	2	25	8	7	30	Parallel	1500	30	Cont.	72	8	X	2.86	5000
423-1	2	25	8	7	30	Parallel	750	20	Cont.	72	8	X	2.86	3600
423-2	2	25	8	7	30	Parallel	750	20	Cont.	72	8	X	2.86	5000
423-3	2	25	8	7	30	Parallel	750	20	Cont.	72	10	X	2.86	5000
423-4	2	25	8	7	30	Parallel	750	20	Cont.	72	8	K	2.86	5000
423-5	2	25	8	7	30	Parallel	750	20	Cont.	72	8	X	4.79	5000
424-1	2	25	8	7	30	Parallel	750	30	Cont.	72	8	X	2.86	5000
425-1	2	25	8	7	60	Parallel	1500	20	Cont.	72	8	X	2.86	3600
425-2	2	25	8	7	60	Parallel	1500	20	Cont.	72	8	X	2.86	5000
425-3	2	25	8	7	60	Parallel	1500	20	Cont.	72	10	X	2.86	5000
425-4	2	25	8	7	60	Parallel	1500	20	Cont.	72	8	K	2.86	5000
425-5	2	25	8	7	60	Parallel	1500	20	Cont.	72	8	X	4.79	5000
426-1	2	25	8	7	60	Parallel	1500	30	Cont.	72	8	X	2.86	5000
427-1	2	25	8	7	60	Parallel	750	20	Cont.	72	8	X	2.86	3600
427-2	2	25	8	7	60	Parallel	750	20	Cont.	72	8	X	2.86	5000
427-3	2	25	8	7	60	Parallel	750	20	Cont.	72	10	X	2.86	5000
427-4	2	25	8	7	60	Parallel	750	20	Cont.	72	8	K	2.86	5000
427-5	2	25	8	7	60	Parallel	750	20	Cont.	72	8	X	4.79	5000
428-1	2	25	8	7	60	Parallel	750	30	Cont.	72	8	X	2.86	5000
429-1	2	25	8	7	60	Trap.	1500	20	Cont.	72	8	X	2.86	3600
429-2	2	25	8	7	60	Trap.	1500	20	Cont.	72	8	X	2.86	5000
429-3	2	25	8	7	60	Trap.	1500	20	Cont.	72	10	X	2.86	5000
429-4	2	25	8	7	60	Trap.	1500	20	Cont.	72	8	K	2.86	5000
429-5	2	25	8	7	60	Trap.	1500	20	Cont.	72	8	X	4.79	5000
430-1	2	25	8	7	60	Trap.	1500	30	Cont.	72	8	X	2.86	5000
431-1	2	25	8	7	60	Trap.	750	20	Cont.	72	8	X	2.86	3600
431-2	2	25	8	7	60	Trap.	750	20	Cont.	72	8	X	2.86	5000
431-3	2	25	8	7	60	Trap.	750	20	Cont.	72	10	X	2.86	5000
431-4	2	25	8	7	60	Trap.	750	20	Cont.	72	8	K	2.86	5000
431-5	2	25	8	7	60	Trap.	750	20	Cont.	72	8	X	4.79	5000
432-1	2	25	8	7	60	Trap.	750	30	Cont.	72	8	X	2.86	5000
433-1	2	25	10	3	0	Parallel	1500	20	Cont.	72	8	X	2.86	3600
433-2	2	25	10	3	0	Parallel	1500	20	Cont.	72	8	X	2.86	5000
433-3	2	25	10	3	0	Parallel	1500	20	Cont.	72	10	X	2.86	5000
433-4	2	25	10	3	0	Parallel	1500	20	Cont.	72	8	K	2.86	5000
433-5	2	25	10	3	0	Parallel	1500	20	Cont.	72	8	X	4.79	5000
434-1	2	25	10	3	0	Parallel	1500	30	Cont.	72	8	X	2.86	5000
435-1	2	25	10	3	0	Parallel	750	20	Cont.	72	8	X	2.86	3600
435-2	2	25	10	3	0	Parallel	750	20	Cont.	72	8	X	2.86	5000
435-3	2	25	10	3	0	Parallel	750	20	Cont.	72	10	X	2.86	5000
435-4	2	25	10	3	0	Parallel	750	20	Cont.	72	8	K	2.86	5000
435-5	2	25	10	3	0	Parallel	750	20	Cont.	72	8	X	4.79	5000
436-1	2	25	10	3	0	Parallel	750	30	Cont.	72	8	X	2.86	5000

Model ID	Geometry									Cross-section		CF detail		Mat'l
	n_{span}	L/d ratio	s_g [ft]	n_{girder}	Support skew [deg]; Layout		R [ft]	s_{cf} [ft]	CF layout	d_w [in]	t_{deck} [in]	CF type	A_{cf} [in^2]	E_c [ksi]
437-1	2	25	10	3	30	Parallel	1500	20	Cont.	72	8	X	2.86	3600
437-2	2	25	10	3	30	Parallel	1500	20	Cont.	72	8	X	2.86	5000
437-3	2	25	10	3	30	Parallel	1500	20	Cont.	72	10	X	2.86	5000
437-4	2	25	10	3	30	Parallel	1500	20	Cont.	72	8	K	2.86	5000
437-5	2	25	10	3	30	Parallel	1500	20	Cont.	72	8	X	4.79	5000
438-1	2	25	10	3	30	Parallel	1500	30	Cont.	72	8	X	2.86	5000
439-1	2	25	10	3	30	Parallel	750	20	Cont.	72	8	X	2.86	3600
439-2	2	25	10	3	30	Parallel	750	20	Cont.	72	8	X	2.86	5000
439-3	2	25	10	3	30	Parallel	750	20	Cont.	72	10	X	2.86	5000
439-4	2	25	10	3	30	Parallel	750	20	Cont.	72	8	K	2.86	5000
439-5	2	25	10	3	30	Parallel	750	20	Cont.	72	8	X	4.79	5000
440-1	2	25	10	3	30	Parallel	750	30	Cont.	72	8	X	2.86	5000
441-1	2	25	10	3	60	Parallel	1500	20	Cont.	72	8	X	2.86	3600
441-2	2	25	10	3	60	Parallel	1500	20	Cont.	72	8	X	2.86	5000
441-3	2	25	10	3	60	Parallel	1500	20	Cont.	72	10	X	2.86	5000
441-4	2	25	10	3	60	Parallel	1500	20	Cont.	72	8	K	2.86	5000
441-5	2	25	10	3	60	Parallel	1500	20	Cont.	72	8	X	4.79	5000
442-1	2	25	10	3	60	Parallel	1500	30	Cont.	72	8	X	2.86	5000
443-1	2	25	10	3	60	Parallel	750	20	Cont.	72	8	X	2.86	3600
443-2	2	25	10	3	60	Parallel	750	20	Cont.	72	8	X	2.86	5000
443-3	2	25	10	3	60	Parallel	750	20	Cont.	72	10	X	2.86	5000
443-4	2	25	10	3	60	Parallel	750	20	Cont.	72	8	K	2.86	5000
443-5	2	25	10	3	60	Parallel	750	20	Cont.	72	8	X	4.79	5000
444-1	2	25	10	3	60	Parallel	750	30	Cont.	72	8	X	2.86	5000
445-1	2	25	10	3	60	Trap.	1500	20	Cont.	72	8	X	2.86	3600
445-2	2	25	10	3	60	Trap.	1500	20	Cont.	72	8	X	2.86	5000
445-3	2	25	10	3	60	Trap.	1500	20	Cont.	72	10	X	2.86	5000
445-4	2	25	10	3	60	Trap.	1500	20	Cont.	72	8	K	2.86	5000
445-5	2	25	10	3	60	Trap.	1500	20	Cont.	72	8	X	4.79	5000
446-1	2	25	10	3	60	Trap.	1500	30	Cont.	72	8	X	2.86	5000
447-1	2	25	10	3	60	Trap.	750	20	Cont.	72	8	X	2.86	3600
447-2	2	25	10	3	60	Trap.	750	20	Cont.	72	8	X	2.86	5000
447-3	2	25	10	3	60	Trap.	750	20	Cont.	72	10	X	2.86	5000
447-4	2	25	10	3	60	Trap.	750	20	Cont.	72	8	K	2.86	5000
447-5	2	25	10	3	60	Trap.	750	20	Cont.	72	8	X	4.79	5000
448-1	2	25	10	3	60	Trap.	750	30	Cont.	72	8	X	2.86	5000
449-1	2	25	10	5	0	Parallel	1500	20	Cont.	72	8	X	2.86	3600
449-2	2	25	10	5	0	Parallel	1500	20	Cont.	72	8	X	2.86	5000
449-3	2	25	10	5	0	Parallel	1500	20	Cont.	72	10	X	2.86	5000
449-4	2	25	10	5	0	Parallel	1500	20	Cont.	72	8	K	2.86	5000
449-5	2	25	10	5	0	Parallel	1500	20	Cont.	72	8	X	4.79	5000
450-1	2	25	10	5	0	Parallel	1500	30	Cont.	72	8	X	2.86	5000
451-1	2	25	10	5	0	Parallel	750	20	Cont.	72	8	X	2.86	3600
451-2	2	25	10	5	0	Parallel	750	20	Cont.	72	8	X	2.86	5000
451-3	2	25	10	5	0	Parallel	750	20	Cont.	72	10	X	2.86	5000
451-4	2	25	10	5	0	Parallel	750	20	Cont.	72	8	K	2.86	5000
451-5	2	25	10	5	0	Parallel	750	20	Cont.	72	8	X	4.79	5000
452-1	2	25	10	5	0	Parallel	750	30	Cont.	72	8	X	2.86	5000
453-1	2	25	10	5	30	Parallel	1500	20	Cont.	72	8	X	2.86	3600
453-2	2	25	10	5	30	Parallel	1500	20	Cont.	72	8	X	2.86	5000
453-3	2	25	10	5	30	Parallel	1500	20	Cont.	72	10	X	2.86	5000
453-4	2	25	10	5	30	Parallel	1500	20	Cont.	72	8	K	2.86	5000
453-5	2	25	10	5	30	Parallel	1500	20	Cont.	72	8	X	4.79	5000
454-1	2	25	10	5	30	Parallel	1500	30	Cont.	72	8	X	2.86	5000
455-1	2	25	10	5	30	Parallel	750	20	Cont.	72	8	X	2.86	3600
455-2	2	25	10	5	30	Parallel	750	20	Cont.	72	8	X	2.86	5000
455-3	2	25	10	5	30	Parallel	750	20	Cont.	72	10	X	2.86	5000
455-4	2	25	10	5	30	Parallel	750	20	Cont.	72	8	K	2.86	5000
455-5	2	25	10	5	30	Parallel	750	20	Cont.	72	8	X	4.79	5000
456-1	2	25	10	5	30	Parallel	750	30	Cont.	72	8	X	2.86	5000
457-1	2	25	10	5	60	Parallel	1500	20	Cont.	72	8	X	2.86	3600
457-2	2	25	10	5	60	Parallel	1500	20	Cont.	72	8	X	2.86	5000
457-3	2	25	10	5	60	Parallel	1500	20	Cont.	72	10	X	2.86	5000
457-4	2	25	10	5	60	Parallel	1500	20	Cont.	72	8	K	2.86	5000
457-5	2	25	10	5	60	Parallel	1500	20	Cont.	72	8	X	4.79	5000
458-1	2	25	10	5	60	Parallel	1500	30	Cont.	72	8	X	2.86	5000
459-1	2	25	10	5	60	Parallel	750	20	Cont.	72	8	X	2.86	3600
459-2	2	25	10	5	60	Parallel	750	20	Cont.	72	8	X	2.86	5000
459-3	2	25	10	5	60	Parallel	750	20	Cont.	72	10	X	2.86	5000
459-4	2	25	10	5	60	Parallel	750	20	Cont.	72	8	K	2.86	5000
459-5	2	25	10	5	60	Parallel	750	20	Cont.	72	8	X	4.79	5000
460-1	2	25	10	5	60	Parallel	750	30	Cont.	72	8	X	2.86	5000
461-1	2	25	10	5	60	Trap.	1500	20	Cont.	72	8	X	2.86	3600

Model ID	Geometry									Cross-section		CF detail		Mat'l
	n_{span}	L/d ratio	s_g [ft]	n_{girder}	Support skew [deg]; Layout		R [ft]	s_{cf} [ft]	CF layout	d_w [in]	t_{deck} [in]	CF type	A_{cf} [in^2]	E_c [ksi]
461-2	2	25	10	5	60	Trap.	1500	20	Cont.	72	8	X	2.86	5000
461-3	2	25	10	5	60	Trap.	1500	20	Cont.	72	10	X	2.86	5000
461-4	2	25	10	5	60	Trap.	1500	20	Cont.	72	8	K	2.86	5000
461-5	2	25	10	5	60	Trap.	1500	20	Cont.	72	8	X	4.79	5000
462-1	2	25	10	5	60	Trap.	1500	30	Cont.	72	8	X	2.86	5000
463-1	2	25	10	5	60	Trap.	750	20	Cont.	72	8	X	2.86	3600
463-2	2	25	10	5	60	Trap.	750	20	Cont.	72	8	X	2.86	5000
463-3	2	25	10	5	60	Trap.	750	20	Cont.	72	10	X	2.86	5000
463-4	2	25	10	5	60	Trap.	750	20	Cont.	72	8	K	2.86	5000
463-5	2	25	10	5	60	Trap.	750	20	Cont.	72	8	X	4.79	5000
464-1	2	25	10	5	60	Trap.	750	30	Cont.	72	8	X	2.86	5000
465-1	2	25	10	7	0	Parallel	1500	20	Cont.	72	8	X	2.86	3600
465-2	2	25	10	7	0	Parallel	1500	20	Cont.	72	8	X	2.86	5000
465-3	2	25	10	7	0	Parallel	1500	20	Cont.	72	10	X	2.86	5000
465-4	2	25	10	7	0	Parallel	1500	20	Cont.	72	8	K	2.86	5000
465-5	2	25	10	7	0	Parallel	1500	20	Cont.	72	8	X	4.79	5000
466-1	2	25	10	7	0	Parallel	1500	30	Cont.	72	8	X	2.86	5000
467-1	2	25	10	7	0	Parallel	750	20	Cont.	72	8	X	2.86	3600
467-2	2	25	10	7	0	Parallel	750	20	Cont.	72	8	X	2.86	5000
467-3	2	25	10	7	0	Parallel	750	20	Cont.	72	10	X	2.86	5000
467-4	2	25	10	7	0	Parallel	750	20	Cont.	72	8	K	2.86	5000
467-5	2	25	10	7	0	Parallel	750	20	Cont.	72	8	X	4.79	5000
468-1	2	25	10	7	0	Parallel	750	30	Cont.	72	8	X	2.86	5000
469-1	2	25	10	7	30	Parallel	1500	20	Cont.	72	8	X	2.86	3600
469-2	2	25	10	7	30	Parallel	1500	20	Cont.	72	8	X	2.86	5000
469-3	2	25	10	7	30	Parallel	1500	20	Cont.	72	10	X	2.86	5000
469-4	2	25	10	7	30	Parallel	1500	20	Cont.	72	8	K	2.86	5000
469-5	2	25	10	7	30	Parallel	1500	20	Cont.	72	8	X	4.79	5000
470-1	2	25	10	7	30	Parallel	1500	30	Cont.	72	8	X	2.86	5000
471-1	2	25	10	7	30	Parallel	750	20	Cont.	72	8	X	2.86	3600
471-2	2	25	10	7	30	Parallel	750	20	Cont.	72	8	X	2.86	5000
471-3	2	25	10	7	30	Parallel	750	20	Cont.	72	10	X	2.86	5000
471-4	2	25	10	7	30	Parallel	750	20	Cont.	72	8	K	2.86	5000
471-5	2	25	10	7	30	Parallel	750	20	Cont.	72	8	X	4.79	5000
472-1	2	25	10	7	30	Parallel	750	30	Cont.	72	8	X	2.86	5000
473-1	2	25	10	7	60	Parallel	1500	20	Cont.	72	8	X	2.86	3600
473-2	2	25	10	7	60	Parallel	1500	20	Cont.	72	8	X	2.86	5000
473-3	2	25	10	7	60	Parallel	1500	20	Cont.	72	10	X	2.86	5000
473-4	2	25	10	7	60	Parallel	1500	20	Cont.	72	8	K	2.86	5000
473-5	2	25	10	7	60	Parallel	1500	20	Cont.	72	8	X	4.79	5000
474-1	2	25	10	7	60	Parallel	1500	30	Cont.	72	8	X	2.86	5000
475-1	2	25	10	7	60	Parallel	750	20	Cont.	72	8	X	2.86	3600
475-2	2	25	10	7	60	Parallel	750	20	Cont.	72	8	X	2.86	5000
475-3	2	25	10	7	60	Parallel	750	20	Cont.	72	10	X	2.86	5000
475-4	2	25	10	7	60	Parallel	750	20	Cont.	72	8	K	2.86	5000
475-5	2	25	10	7	60	Parallel	750	20	Cont.	72	8	X	4.79	5000
476-1	2	25	10	7	60	Parallel	750	30	Cont.	72	8	X	2.86	5000
477-1	2	25	10	7	60	Trap.	1500	20	Cont.	72	8	X	2.86	3600
477-2	2	25	10	7	60	Trap.	1500	20	Cont.	72	8	X	2.86	5000
477-3	2	25	10	7	60	Trap.	1500	20	Cont.	72	10	X	2.86	5000
477-4	2	25	10	7	60	Trap.	1500	20	Cont.	72	8	K	2.86	5000
477-5	2	25	10	7	60	Trap.	1500	20	Cont.	72	8	X	4.79	5000
478-1	2	25	10	7	60	Trap.	1500	30	Cont.	72	8	X	2.86	5000
479-1	2	25	10	7	60	Trap.	750	20	Cont.	72	8	X	2.86	3600
479-2	2	25	10	7	60	Trap.	750	20	Cont.	72	8	X	2.86	5000
479-3	2	25	10	7	60	Trap.	750	20	Cont.	72	10	X	2.86	5000
479-4	2	25	10	7	60	Trap.	750	20	Cont.	72	8	K	2.86	5000
479-5	2	25	10	7	60	Trap.	750	20	Cont.	72	8	X	4.79	5000
480-1	2	25	10	7	60	Trap.	750	30	Cont.	72	8	X	2.86	5000
481-1	2	25	6	3	0	Parallel	1500	20	Cont.	96	8	X	2.86	3600
481-2	2	25	6	3	0	Parallel	1500	20	Cont.	96	8	X	2.86	5000
481-3	2	25	6	3	0	Parallel	1500	20	Cont.	96	10	X	2.86	5000
481-4	2	25	6	3	0	Parallel	1500	20	Cont.	96	8	K	2.86	5000
481-5	2	25	6	3	0	Parallel	1500	20	Cont.	96	8	X	4.79	5000
482-1	2	25	6	3	0	Parallel	1500	30	Cont.	96	8	X	2.86	5000
483-1	2	25	6	3	0	Parallel	750	20	Cont.	96	8	X	2.86	3600
483-2	2	25	6	3	0	Parallel	750	20	Cont.	96	8	X	2.86	5000
483-3	2	25	6	3	0	Parallel	750	20	Cont.	96	10	X	2.86	5000
483-4	2	25	6	3	0	Parallel	750	20	Cont.	96	8	K	2.86	5000
483-5	2	25	6	3	0	Parallel	750	20	Cont.	96	8	X	4.79	5000
484-1	2	25	6	3	0	Parallel	750	30	Cont.	96	8	X	2.86	5000
485-1	2	25	6	3	30	Parallel	1500	20	Cont.	96	8	X	2.86	3600
485-2	2	25	6	3	30	Parallel	1500	20	Cont.	96	8	X	2.86	5000

Model ID	Geometry									Cross-section		CF detail		Mat'l
	n_{span}	L/d ratio	s_g [ft]	n_{girder}	Support skew [deg]; Layout		R [ft]	s_{cf} [ft]	CF layout	d_w [in]	t_{deck} [in]	CF type	A_{cf} [in^2]	E_c [ksi]
485-3	2	25	6	3	30	Parallel	1500	20	Cont.	96	10	X	2.86	5000
485-4	2	25	6	3	30	Parallel	1500	20	Cont.	96	8	K	2.86	5000
485-5	2	25	6	3	30	Parallel	1500	20	Cont.	96	8	X	4.79	5000
486-1	2	25	6	3	30	Parallel	1500	30	Cont.	96	8	X	2.86	5000
487-1	2	25	6	3	30	Parallel	750	20	Cont.	96	8	X	2.86	3600
487-2	2	25	6	3	30	Parallel	750	20	Cont.	96	8	X	2.86	5000
487-3	2	25	6	3	30	Parallel	750	20	Cont.	96	10	X	2.86	5000
487-4	2	25	6	3	30	Parallel	750	20	Cont.	96	8	K	2.86	5000
487-5	2	25	6	3	30	Parallel	750	20	Cont.	96	8	X	4.79	5000
488-1	2	25	6	3	30	Parallel	750	30	Cont.	96	8	X	2.86	5000
489-1	2	25	6	3	60	Parallel	1500	20	Cont.	96	8	X	2.86	3600
489-2	2	25	6	3	60	Parallel	1500	20	Cont.	96	8	X	2.86	5000
489-3	2	25	6	3	60	Parallel	1500	20	Cont.	96	10	X	2.86	5000
489-4	2	25	6	3	60	Parallel	1500	20	Cont.	96	8	K	2.86	5000
489-5	2	25	6	3	60	Parallel	1500	20	Cont.	96	8	X	4.79	5000
490-1	2	25	6	3	60	Parallel	1500	30	Cont.	96	8	X	2.86	5000
491-1	2	25	6	3	60	Parallel	750	20	Cont.	96	8	X	2.86	3600
491-2	2	25	6	3	60	Parallel	750	20	Cont.	96	8	X	2.86	5000
491-3	2	25	6	3	60	Parallel	750	20	Cont.	96	10	X	2.86	5000
491-4	2	25	6	3	60	Parallel	750	20	Cont.	96	8	K	2.86	5000
491-5	2	25	6	3	60	Parallel	750	20	Cont.	96	8	X	4.79	5000
492-1	2	25	6	3	60	Parallel	750	30	Cont.	96	8	X	2.86	5000
493-1	2	25	6	3	60	Trap.	1500	20	Cont.	96	8	X	2.86	3600
493-2	2	25	6	3	60	Trap.	1500	20	Cont.	96	8	X	2.86	5000
493-3	2	25	6	3	60	Trap.	1500	20	Cont.	96	10	X	2.86	5000
493-4	2	25	6	3	60	Trap.	1500	20	Cont.	96	8	K	2.86	5000
493-5	2	25	6	3	60	Trap.	1500	20	Cont.	96	8	X	4.79	5000
494-1	2	25	6	3	60	Trap.	1500	30	Cont.	96	8	X	2.86	5000
495-1	2	25	6	3	60	Trap.	750	20	Cont.	96	8	X	2.86	3600
495-2	2	25	6	3	60	Trap.	750	20	Cont.	96	8	X	2.86	5000
495-3	2	25	6	3	60	Trap.	750	20	Cont.	96	10	X	2.86	5000
495-4	2	25	6	3	60	Trap.	750	20	Cont.	96	8	K	2.86	5000
495-5	2	25	6	3	60	Trap.	750	20	Cont.	96	8	X	4.79	5000
496-1	2	25	6	3	60	Trap.	750	30	Cont.	96	8	X	2.86	5000
497-1	2	25	6	5	0	Parallel	1500	20	Cont.	96	8	X	2.86	3600
497-2	2	25	6	5	0	Parallel	1500	20	Cont.	96	8	X	2.86	5000
497-3	2	25	6	5	0	Parallel	1500	20	Cont.	96	10	X	2.86	5000
497-4	2	25	6	5	0	Parallel	1500	20	Cont.	96	8	K	2.86	5000
497-5	2	25	6	5	0	Parallel	1500	20	Cont.	96	8	X	4.79	5000
498-1	2	25	6	5	0	Parallel	1500	30	Cont.	96	8	X	2.86	5000
499-1	2	25	6	5	0	Parallel	750	20	Cont.	96	8	X	2.86	3600
499-2	2	25	6	5	0	Parallel	750	20	Cont.	96	8	X	2.86	5000
499-3	2	25	6	5	0	Parallel	750	20	Cont.	96	10	X	2.86	5000
499-4	2	25	6	5	0	Parallel	750	20	Cont.	96	8	K	2.86	5000
499-5	2	25	6	5	0	Parallel	750	20	Cont.	96	8	X	4.79	5000
500-1	2	25	6	5	0	Parallel	750	30	Cont.	96	8	X	2.86	5000
501-1	2	25	6	5	30	Parallel	1500	20	Cont.	96	8	X	2.86	3600
501-2	2	25	6	5	30	Parallel	1500	20	Cont.	96	8	X	2.86	5000
501-3	2	25	6	5	30	Parallel	1500	20	Cont.	96	10	X	2.86	5000
501-4	2	25	6	5	30	Parallel	1500	20	Cont.	96	8	K	2.86	5000
501-5	2	25	6	5	30	Parallel	1500	20	Cont.	96	8	X	4.79	5000
502-1	2	25	6	5	30	Parallel	1500	30	Cont.	96	8	X	2.86	5000
503-1	2	25	6	5	30	Parallel	750	20	Cont.	96	8	X	2.86	3600
503-2	2	25	6	5	30	Parallel	750	20	Cont.	96	8	X	2.86	5000
503-3	2	25	6	5	30	Parallel	750	20	Cont.	96	10	X	2.86	5000
503-4	2	25	6	5	30	Parallel	750	20	Cont.	96	8	K	2.86	5000
503-5	2	25	6	5	30	Parallel	750	20	Cont.	96	8	X	4.79	5000
504-1	2	25	6	5	30	Parallel	750	30	Cont.	96	8	X	2.86	5000
505-1	2	25	6	5	60	Parallel	1500	20	Cont.	96	8	X	2.86	3600
505-2	2	25	6	5	60	Parallel	1500	20	Cont.	96	8	X	2.86	5000
505-3	2	25	6	5	60	Parallel	1500	20	Cont.	96	10	X	2.86	5000
505-4	2	25	6	5	60	Parallel	1500	20	Cont.	96	8	K	2.86	5000
505-5	2	25	6	5	60	Parallel	1500	20	Cont.	96	8	X	4.79	5000
506-1	2	25	6	5	60	Parallel	1500	30	Cont.	96	8	X	2.86	5000
507-1	2	25	6	5	60	Parallel	750	20	Cont.	96	8	X	2.86	3600
507-2	2	25	6	5	60	Parallel	750	20	Cont.	96	8	X	2.86	5000
507-3	2	25	6	5	60	Parallel	750	20	Cont.	96	10	X	2.86	5000
507-4	2	25	6	5	60	Parallel	750	20	Cont.	96	8	K	2.86	5000
507-5	2	25	6	5	60	Parallel	750	20	Cont.	96	8	X	4.79	5000
508-1	2	25	6	5	60	Parallel	750	30	Cont.	96	8	X	2.86	5000
509-1	2	25	6	5	60	Trap.	1500	20	Cont.	96	8	X	2.86	3600
509-2	2	25	6	5	60	Trap.	1500	20	Cont.	96	8	X	2.86	5000
509-3	2	25	6	5	60	Trap.	1500	20	Cont.	96	10	X	2.86	5000

Model ID	Geometry									Cross-section		CF detail		Mat'l
	n_{span}	L/d ratio	s_g [ft]	n_{girder}	Support skew [deg]; Layout		R [ft]	s_{cf} [ft]	CF layout	d_w [in]	t_{deck} [in]	CF type	A_{cf} [in^2]	E_c [ksi]
509-4	2	25	6	5	60	Trap.	1500	20	Cont.	96	8	K	2.86	5000
509-5	2	25	6	5	60	Trap.	1500	20	Cont.	96	8	X	4.79	5000
510-1	2	25	6	5	60	Trap.	1500	30	Cont.	96	8	X	2.86	5000
511-1	2	25	6	5	60	Trap.	750	20	Cont.	96	8	X	2.86	3600
511-2	2	25	6	5	60	Trap.	750	20	Cont.	96	8	X	2.86	5000
511-3	2	25	6	5	60	Trap.	750	20	Cont.	96	10	X	2.86	5000
511-4	2	25	6	5	60	Trap.	750	20	Cont.	96	8	K	2.86	5000
511-5	2	25	6	5	60	Trap.	750	20	Cont.	96	8	X	4.79	5000
512-1	2	25	6	5	60	Trap.	750	30	Cont.	96	8	X	2.86	5000
513-1	2	25	6	7	0	Parallel	1500	20	Cont.	96	8	X	2.86	3600
513-2	2	25	6	7	0	Parallel	1500	20	Cont.	96	8	X	2.86	5000
513-3	2	25	6	7	0	Parallel	1500	20	Cont.	96	10	X	2.86	5000
513-4	2	25	6	7	0	Parallel	1500	20	Cont.	96	8	K	2.86	5000
513-5	2	25	6	7	0	Parallel	1500	20	Cont.	96	8	X	4.79	5000
514-1	2	25	6	7	0	Parallel	1500	30	Cont.	96	8	X	2.86	5000
515-1	2	25	6	7	0	Parallel	750	20	Cont.	96	8	X	2.86	3600
515-2	2	25	6	7	0	Parallel	750	20	Cont.	96	8	X	2.86	5000
515-3	2	25	6	7	0	Parallel	750	20	Cont.	96	10	X	2.86	5000
515-4	2	25	6	7	0	Parallel	750	20	Cont.	96	8	K	2.86	5000
515-5	2	25	6	7	0	Parallel	750	20	Cont.	96	8	X	4.79	5000
516-1	2	25	6	7	0	Parallel	750	30	Cont.	96	8	X	2.86	5000
517-1	2	25	6	7	30	Parallel	1500	20	Cont.	96	8	X	2.86	3600
517-2	2	25	6	7	30	Parallel	1500	20	Cont.	96	8	X	2.86	5000
517-3	2	25	6	7	30	Parallel	1500	20	Cont.	96	10	X	2.86	5000
517-4	2	25	6	7	30	Parallel	1500	20	Cont.	96	8	K	2.86	5000
517-5	2	25	6	7	30	Parallel	1500	20	Cont.	96	8	X	4.79	5000
518-1	2	25	6	7	30	Parallel	1500	30	Cont.	96	8	X	2.86	5000
519-1	2	25	6	7	30	Parallel	750	20	Cont.	96	8	X	2.86	3600
519-2	2	25	6	7	30	Parallel	750	20	Cont.	96	8	X	2.86	5000
519-3	2	25	6	7	30	Parallel	750	20	Cont.	96	10	X	2.86	5000
519-4	2	25	6	7	30	Parallel	750	20	Cont.	96	8	K	2.86	5000
519-5	2	25	6	7	30	Parallel	750	20	Cont.	96	8	X	4.79	5000
520-1	2	25	6	7	30	Parallel	750	30	Cont.	96	8	X	2.86	5000
521-1	2	25	6	7	60	Parallel	1500	20	Cont.	96	8	X	2.86	3600
521-2	2	25	6	7	60	Parallel	1500	20	Cont.	96	8	X	2.86	5000
521-3	2	25	6	7	60	Parallel	1500	20	Cont.	96	10	X	2.86	5000
521-4	2	25	6	7	60	Parallel	1500	20	Cont.	96	8	K	2.86	5000
521-5	2	25	6	7	60	Parallel	1500	20	Cont.	96	8	X	4.79	5000
522-1	2	25	6	7	60	Parallel	1500	30	Cont.	96	8	X	2.86	5000
523-1	2	25	6	7	60	Parallel	750	20	Cont.	96	8	X	2.86	3600
523-2	2	25	6	7	60	Parallel	750	20	Cont.	96	8	X	2.86	5000
523-3	2	25	6	7	60	Parallel	750	20	Cont.	96	10	X	2.86	5000
523-4	2	25	6	7	60	Parallel	750	20	Cont.	96	8	K	2.86	5000
523-5	2	25	6	7	60	Parallel	750	20	Cont.	96	8	X	4.79	5000
524-1	2	25	6	7	60	Parallel	750	30	Cont.	96	8	X	2.86	5000
525-1	2	25	6	7	60	Trap.	1500	20	Cont.	96	8	X	2.86	3600
525-2	2	25	6	7	60	Trap.	1500	20	Cont.	96	8	X	2.86	5000
525-3	2	25	6	7	60	Trap.	1500	20	Cont.	96	10	X	2.86	5000
525-4	2	25	6	7	60	Trap.	1500	20	Cont.	96	8	K	2.86	5000
525-5	2	25	6	7	60	Trap.	1500	20	Cont.	96	8	X	4.79	5000
526-1	2	25	6	7	60	Trap.	1500	30	Cont.	96	8	X	2.86	5000
527-1	2	25	6	7	60	Trap.	750	20	Cont.	96	8	X	2.86	3600
527-2	2	25	6	7	60	Trap.	750	20	Cont.	96	8	X	2.86	5000
527-3	2	25	6	7	60	Trap.	750	20	Cont.	96	10	X	2.86	5000
527-4	2	25	6	7	60	Trap.	750	20	Cont.	96	8	K	2.86	5000
527-5	2	25	6	7	60	Trap.	750	20	Cont.	96	8	X	4.79	5000
528-1	2	25	6	7	60	Trap.	750	30	Cont.	96	8	X	2.86	5000
529-1	2	25	8	3	0	Parallel	1500	20	Cont.	96	8	X	2.86	3600
529-2	2	25	8	3	0	Parallel	1500	20	Cont.	96	8	X	2.86	5000
529-3	2	25	8	3	0	Parallel	1500	20	Cont.	96	10	X	2.86	5000
529-4	2	25	8	3	0	Parallel	1500	20	Cont.	96	8	K	2.86	5000
529-5	2	25	8	3	0	Parallel	1500	20	Cont.	96	8	X	4.79	5000
530-1	2	25	8	3	0	Parallel	1500	30	Cont.	96	8	X	2.86	5000
531-1	2	25	8	3	0	Parallel	750	20	Cont.	96	8	X	2.86	3600
531-2	2	25	8	3	0	Parallel	750	20	Cont.	96	8	X	2.86	5000
531-3	2	25	8	3	0	Parallel	750	20	Cont.	96	10	X	2.86	5000
531-4	2	25	8	3	0	Parallel	750	20	Cont.	96	8	K	2.86	5000
531-5	2	25	8	3	0	Parallel	750	20	Cont.	96	8	X	4.79	5000
532-1	2	25	8	3	0	Parallel	750	30	Cont.	96	8	X	2.86	5000
533-1	2	25	8	3	30	Parallel	1500	20	Cont.	96	8	X	2.86	3600
533-2	2	25	8	3	30	Parallel	1500	20	Cont.	96	8	X	2.86	5000
533-3	2	25	8	3	30	Parallel	1500	20	Cont.	96	10	X	2.86	5000
533-4	2	25	8	3	30	Parallel	1500	20	Cont.	96	8	K	2.86	5000

Model ID	Geometry									Cross-section		CF detail		Mat'l
	n_{span}	L/d ratio	s_g [ft]	n_{girder}	Support skew [deg]; Layout		R [ft]	s_{cf} [ft]	CF layout	d_w [in]	t_{deck} [in]	CF type	A_{cf} [in^2]	E_c [ksi]
533-5	2	25	8	3	30	Parallel	1500	20	Cont.	96	8	X	4.79	5000
534-1	2	25	8	3	30	Parallel	1500	30	Cont.	96	8	X	2.86	5000
535-1	2	25	8	3	30	Parallel	750	20	Cont.	96	8	X	2.86	3600
535-2	2	25	8	3	30	Parallel	750	20	Cont.	96	8	X	2.86	5000
535-3	2	25	8	3	30	Parallel	750	20	Cont.	96	10	X	2.86	5000
535-4	2	25	8	3	30	Parallel	750	20	Cont.	96	8	K	2.86	5000
535-5	2	25	8	3	30	Parallel	750	20	Cont.	96	8	X	4.79	5000
536-1	2	25	8	3	30	Parallel	750	30	Cont.	96	8	X	2.86	5000
537-1	2	25	8	3	60	Parallel	1500	20	Cont.	96	8	X	2.86	3600
537-2	2	25	8	3	60	Parallel	1500	20	Cont.	96	8	X	2.86	5000
537-3	2	25	8	3	60	Parallel	1500	20	Cont.	96	10	X	2.86	5000
537-4	2	25	8	3	60	Parallel	1500	20	Cont.	96	8	K	2.86	5000
537-5	2	25	8	3	60	Parallel	1500	20	Cont.	96	8	X	4.79	5000
538-1	2	25	8	3	60	Parallel	1500	30	Cont.	96	8	X	2.86	5000
539-1	2	25	8	3	60	Parallel	750	20	Cont.	96	8	X	2.86	3600
539-2	2	25	8	3	60	Parallel	750	20	Cont.	96	8	X	2.86	5000
539-3	2	25	8	3	60	Parallel	750	20	Cont.	96	10	X	2.86	5000
539-4	2	25	8	3	60	Parallel	750	20	Cont.	96	8	K	2.86	5000
539-5	2	25	8	3	60	Parallel	750	20	Cont.	96	8	X	4.79	5000
540-1	2	25	8	3	60	Parallel	750	30	Cont.	96	8	X	2.86	5000
541-1	2	25	8	3	60	Trap.	1500	20	Cont.	96	8	X	2.86	3600
541-2	2	25	8	3	60	Trap.	1500	20	Cont.	96	8	X	2.86	5000
541-3	2	25	8	3	60	Trap.	1500	20	Cont.	96	10	X	2.86	5000
541-4	2	25	8	3	60	Trap.	1500	20	Cont.	96	8	K	2.86	5000
541-5	2	25	8	3	60	Trap.	1500	20	Cont.	96	8	X	4.79	5000
542-1	2	25	8	3	60	Trap.	1500	30	Cont.	96	8	X	2.86	5000
543-1	2	25	8	3	60	Trap.	750	20	Cont.	96	8	X	2.86	3600
543-2	2	25	8	3	60	Trap.	750	20	Cont.	96	8	X	2.86	5000
543-3	2	25	8	3	60	Trap.	750	20	Cont.	96	10	X	2.86	5000
543-4	2	25	8	3	60	Trap.	750	20	Cont.	96	8	K	2.86	5000
543-5	2	25	8	3	60	Trap.	750	20	Cont.	96	8	X	4.79	5000
544-1	2	25	8	3	60	Trap.	750	30	Cont.	96	8	X	2.86	5000
545-1	2	25	8	5	0	Parallel	1500	20	Cont.	96	8	X	2.86	3600
545-2	2	25	8	5	0	Parallel	1500	20	Cont.	96	8	X	2.86	5000
545-3	2	25	8	5	0	Parallel	1500	20	Cont.	96	10	X	2.86	5000
545-4	2	25	8	5	0	Parallel	1500	20	Cont.	96	8	K	2.86	5000
545-5	2	25	8	5	0	Parallel	1500	20	Cont.	96	8	X	4.79	5000
546-1	2	25	8	5	0	Parallel	1500	30	Cont.	96	8	X	2.86	5000
547-1	2	25	8	5	0	Parallel	750	20	Cont.	96	8	X	2.86	3600
547-2	2	25	8	5	0	Parallel	750	20	Cont.	96	8	X	2.86	5000
547-3	2	25	8	5	0	Parallel	750	20	Cont.	96	10	X	2.86	5000
547-4	2	25	8	5	0	Parallel	750	20	Cont.	96	8	K	2.86	5000
547-5	2	25	8	5	0	Parallel	750	20	Cont.	96	8	X	4.79	5000
548-1	2	25	8	5	0	Parallel	750	30	Cont.	96	8	X	2.86	5000
549-1	2	25	8	5	30	Parallel	1500	20	Cont.	96	8	X	2.86	3600
549-2	2	25	8	5	30	Parallel	1500	20	Cont.	96	8	X	2.86	5000
549-3	2	25	8	5	30	Parallel	1500	20	Cont.	96	10	X	2.86	5000
549-4	2	25	8	5	30	Parallel	1500	20	Cont.	96	8	K	2.86	5000
549-5	2	25	8	5	30	Parallel	1500	20	Cont.	96	8	X	4.79	5000
550-1	2	25	8	5	30	Parallel	1500	30	Cont.	96	8	X	2.86	5000
551-1	2	25	8	5	30	Parallel	750	20	Cont.	96	8	X	2.86	3600
551-2	2	25	8	5	30	Parallel	750	20	Cont.	96	8	X	2.86	5000
551-3	2	25	8	5	30	Parallel	750	20	Cont.	96	10	X	2.86	5000
551-4	2	25	8	5	30	Parallel	750	20	Cont.	96	8	K	2.86	5000
551-5	2	25	8	5	30	Parallel	750	20	Cont.	96	8	X	4.79	5000
552-1	2	25	8	5	30	Parallel	750	30	Cont.	96	8	X	2.86	5000
553-1	2	25	8	5	60	Parallel	1500	20	Cont.	96	8	X	2.86	3600
553-2	2	25	8	5	60	Parallel	1500	20	Cont.	96	8	X	2.86	5000
553-3	2	25	8	5	60	Parallel	1500	20	Cont.	96	10	X	2.86	5000
553-4	2	25	8	5	60	Parallel	1500	20	Cont.	96	8	K	2.86	5000
553-5	2	25	8	5	60	Parallel	1500	20	Cont.	96	8	X	4.79	5000
554-1	2	25	8	5	60	Parallel	1500	30	Cont.	96	8	X	2.86	5000
555-1	2	25	8	5	60	Parallel	750	20	Cont.	96	8	X	2.86	3600
555-2	2	25	8	5	60	Parallel	750	20	Cont.	96	8	X	2.86	5000
555-3	2	25	8	5	60	Parallel	750	20	Cont.	96	10	X	2.86	5000
555-4	2	25	8	5	60	Parallel	750	20	Cont.	96	8	K	2.86	5000
555-5	2	25	8	5	60	Parallel	750	20	Cont.	96	8	X	4.79	5000
556-1	2	25	8	5	60	Parallel	750	30	Cont.	96	8	X	2.86	5000
557-1	2	25	8	5	60	Trap.	1500	20	Cont.	96	8	X	2.86	3600
557-2	2	25	8	5	60	Trap.	1500	20	Cont.	96	8	X	2.86	5000
557-3	2	25	8	5	60	Trap.	1500	20	Cont.	96	10	X	2.86	5000
557-4	2	25	8	5	60	Trap.	1500	20	Cont.	96	8	K	2.86	5000
557-5	2	25	8	5	60	Trap.	1500	20	Cont.	96	8	X	4.79	5000

Model ID	Geometry									Cross-section		CF detail		Mat'l
	n_{span}	L/d ratio	s_g [ft]	n_{girder}	Support skew [deg]; Layout		R [ft]	s_{cf} [ft]	CF layout	d_w [in]	t_{deck} [in]	CF type	A_{cf} [in^2]	E_c [ksi]
558-1	2	25	8	5	60	Trap.	1500	30	Cont.	96	8	X	2.86	5000
559-1	2	25	8	5	60	Trap.	750	20	Cont.	96	8	X	2.86	3600
559-2	2	25	8	5	60	Trap.	750	20	Cont.	96	8	X	2.86	5000
559-3	2	25	8	5	60	Trap.	750	20	Cont.	96	10	X	2.86	5000
559-4	2	25	8	5	60	Trap.	750	20	Cont.	96	8	K	2.86	5000
559-5	2	25	8	5	60	Trap.	750	20	Cont.	96	8	X	4.79	5000
560-1	2	25	8	5	60	Trap.	750	30	Cont.	96	8	X	2.86	5000
561-1	2	25	8	7	0	Parallel	1500	20	Cont.	96	8	X	2.86	3600
561-2	2	25	8	7	0	Parallel	1500	20	Cont.	96	8	X	2.86	5000
561-3	2	25	8	7	0	Parallel	1500	20	Cont.	96	10	X	2.86	5000
561-4	2	25	8	7	0	Parallel	1500	20	Cont.	96	8	K	2.86	5000
561-5	2	25	8	7	0	Parallel	1500	20	Cont.	96	8	X	4.79	5000
562-1	2	25	8	7	0	Parallel	1500	30	Cont.	96	8	X	2.86	5000
563-1	2	25	8	7	0	Parallel	750	20	Cont.	96	8	X	2.86	3600
563-2	2	25	8	7	0	Parallel	750	20	Cont.	96	8	X	2.86	5000
563-3	2	25	8	7	0	Parallel	750	20	Cont.	96	10	X	2.86	5000
563-4	2	25	8	7	0	Parallel	750	20	Cont.	96	8	K	2.86	5000
563-5	2	25	8	7	0	Parallel	750	20	Cont.	96	8	X	4.79	5000
564-1	2	25	8	7	0	Parallel	750	30	Cont.	96	8	X	2.86	5000
565-1	2	25	8	7	30	Parallel	1500	20	Cont.	96	8	X	2.86	3600
565-2	2	25	8	7	30	Parallel	1500	20	Cont.	96	8	X	2.86	5000
565-3	2	25	8	7	30	Parallel	1500	20	Cont.	96	10	X	2.86	5000
565-4	2	25	8	7	30	Parallel	1500	20	Cont.	96	8	K	2.86	5000
565-5	2	25	8	7	30	Parallel	1500	20	Cont.	96	8	X	4.79	5000
566-1	2	25	8	7	30	Parallel	1500	30	Cont.	96	8	X	2.86	5000
567-1	2	25	8	7	30	Parallel	750	20	Cont.	96	8	X	2.86	3600
567-2	2	25	8	7	30	Parallel	750	20	Cont.	96	8	X	2.86	5000
567-3	2	25	8	7	30	Parallel	750	20	Cont.	96	10	X	2.86	5000
567-4	2	25	8	7	30	Parallel	750	20	Cont.	96	8	K	2.86	5000
567-5	2	25	8	7	30	Parallel	750	20	Cont.	96	8	X	4.79	5000
568-1	2	25	8	7	30	Parallel	750	30	Cont.	96	8	X	2.86	5000
569-1	2	25	8	7	60	Parallel	1500	20	Cont.	96	8	X	2.86	3600
569-2	2	25	8	7	60	Parallel	1500	20	Cont.	96	8	X	2.86	5000
569-3	2	25	8	7	60	Parallel	1500	20	Cont.	96	10	X	2.86	5000
569-4	2	25	8	7	60	Parallel	1500	20	Cont.	96	8	K	2.86	5000
569-5	2	25	8	7	60	Parallel	1500	20	Cont.	96	8	X	4.79	5000
570-1	2	25	8	7	60	Parallel	1500	30	Cont.	96	8	X	2.86	5000
571-1	2	25	8	7	60	Parallel	750	20	Cont.	96	8	X	2.86	3600
571-2	2	25	8	7	60	Parallel	750	20	Cont.	96	8	X	2.86	5000
571-3	2	25	8	7	60	Parallel	750	20	Cont.	96	10	X	2.86	5000
571-4	2	25	8	7	60	Parallel	750	20	Cont.	96	8	K	2.86	5000
571-5	2	25	8	7	60	Parallel	750	20	Cont.	96	8	X	4.79	5000
572-1	2	25	8	7	60	Parallel	750	30	Cont.	96	8	X	2.86	5000
573-1	2	25	8	7	60	Trap.	1500	20	Cont.	96	8	X	2.86	3600
573-2	2	25	8	7	60	Trap.	1500	20	Cont.	96	8	X	2.86	5000
573-3	2	25	8	7	60	Trap.	1500	20	Cont.	96	10	X	2.86	5000
573-4	2	25	8	7	60	Trap.	1500	20	Cont.	96	8	K	2.86	5000
573-5	2	25	8	7	60	Trap.	1500	20	Cont.	96	8	X	4.79	5000
574-1	2	25	8	7	60	Trap.	1500	30	Cont.	96	8	X	2.86	5000
575-1	2	25	8	7	60	Trap.	750	20	Cont.	96	8	X	2.86	3600
575-2	2	25	8	7	60	Trap.	750	20	Cont.	96	8	X	2.86	5000
575-3	2	25	8	7	60	Trap.	750	20	Cont.	96	10	X	2.86	5000
575-4	2	25	8	7	60	Trap.	750	20	Cont.	96	8	K	2.86	5000
575-5	2	25	8	7	60	Trap.	750	20	Cont.	96	8	X	4.79	5000
576-1	2	25	8	7	60	Trap.	750	30	Cont.	96	8	X	2.86	5000
577-1	2	25	10	3	0	Parallel	1500	20	Cont.	96	8	X	2.86	3600
577-2	2	25	10	3	0	Parallel	1500	20	Cont.	96	8	X	2.86	5000
577-3	2	25	10	3	0	Parallel	1500	20	Cont.	96	10	X	2.86	5000
577-4	2	25	10	3	0	Parallel	1500	20	Cont.	96	8	K	2.86	5000
577-5	2	25	10	3	0	Parallel	1500	20	Cont.	96	8	X	4.79	5000
578-1	2	25	10	3	0	Parallel	1500	30	Cont.	96	8	X	2.86	5000
579-1	2	25	10	3	0	Parallel	750	20	Cont.	96	8	X	2.86	3600
579-2	2	25	10	3	0	Parallel	750	20	Cont.	96	8	X	2.86	5000
579-3	2	25	10	3	0	Parallel	750	20	Cont.	96	10	X	2.86	5000
579-4	2	25	10	3	0	Parallel	750	20	Cont.	96	8	K	2.86	5000
579-5	2	25	10	3	0	Parallel	750	20	Cont.	96	8	X	4.79	5000
580-1	2	25	10	3	0	Parallel	750	30	Cont.	96	8	X	2.86	5000
581-1	2	25	10	3	30	Parallel	1500	20	Cont.	96	8	X	2.86	3600
581-2	2	25	10	3	30	Parallel	1500	20	Cont.	96	8	X	2.86	5000
581-3	2	25	10	3	30	Parallel	1500	20	Cont.	96	10	X	2.86	5000
581-4	2	25	10	3	30	Parallel	1500	20	Cont.	96	8	K	2.86	5000
581-5	2	25	10	3	30	Parallel	1500	20	Cont.	96	8	X	4.79	5000
582-1	2	25	10	3	30	Parallel	1500	30	Cont.	96	8	X	2.86	5000

Model ID	Geometry									Cross-section		CF detail		Mat'l
	n_{span}	L/d ratio	s_g [ft]	n_{girder}	Support skew [deg]; Layout		R [ft]	s_{cf} [ft]	CF layout	d_w [in]	t_{deck} [in]	CF type	A_{cf} [in^2]	E_c [ksi]
583-1	2	25	10	3	30	Parallel	750	20	Cont.	96	8	X	2.86	3600
583-2	2	25	10	3	30	Parallel	750	20	Cont.	96	8	X	2.86	5000
583-3	2	25	10	3	30	Parallel	750	20	Cont.	96	10	X	2.86	5000
583-4	2	25	10	3	30	Parallel	750	20	Cont.	96	8	K	2.86	5000
583-5	2	25	10	3	30	Parallel	750	20	Cont.	96	8	X	4.79	5000
584-1	2	25	10	3	30	Parallel	750	30	Cont.	96	8	X	2.86	5000
585-1	2	25	10	3	60	Parallel	1500	20	Cont.	96	8	X	2.86	3600
585-2	2	25	10	3	60	Parallel	1500	20	Cont.	96	8	X	2.86	5000
585-3	2	25	10	3	60	Parallel	1500	20	Cont.	96	10	X	2.86	5000
585-4	2	25	10	3	60	Parallel	1500	20	Cont.	96	8	K	2.86	5000
585-5	2	25	10	3	60	Parallel	1500	20	Cont.	96	8	X	4.79	5000
586-1	2	25	10	3	60	Parallel	1500	30	Cont.	96	8	X	2.86	5000
587-1	2	25	10	3	60	Parallel	750	20	Cont.	96	8	X	2.86	3600
587-2	2	25	10	3	60	Parallel	750	20	Cont.	96	8	X	2.86	5000
587-3	2	25	10	3	60	Parallel	750	20	Cont.	96	10	X	2.86	5000
587-4	2	25	10	3	60	Parallel	750	20	Cont.	96	8	K	2.86	5000
587-5	2	25	10	3	60	Parallel	750	20	Cont.	96	8	X	4.79	5000
588-1	2	25	10	3	60	Parallel	750	30	Cont.	96	8	X	2.86	5000
589-1	2	25	10	3	60	Trap.	1500	20	Cont.	96	8	X	2.86	3600
589-2	2	25	10	3	60	Trap.	1500	20	Cont.	96	8	X	2.86	5000
589-3	2	25	10	3	60	Trap.	1500	20	Cont.	96	10	X	2.86	5000
589-4	2	25	10	3	60	Trap.	1500	20	Cont.	96	8	K	2.86	5000
589-5	2	25	10	3	60	Trap.	1500	20	Cont.	96	8	X	4.79	5000
590-1	2	25	10	3	60	Trap.	1500	30	Cont.	96	8	X	2.86	5000
591-1	2	25	10	3	60	Trap.	750	20	Cont.	96	8	X	2.86	3600
591-2	2	25	10	3	60	Trap.	750	20	Cont.	96	8	X	2.86	5000
591-3	2	25	10	3	60	Trap.	750	20	Cont.	96	10	X	2.86	5000
591-4	2	25	10	3	60	Trap.	750	20	Cont.	96	8	K	2.86	5000
591-5	2	25	10	3	60	Trap.	750	20	Cont.	96	8	X	4.79	5000
592-1	2	25	10	3	60	Trap.	750	30	Cont.	96	8	X	2.86	5000
593-1	2	25	10	5	0	Parallel	1500	20	Cont.	96	8	X	2.86	3600
593-2	2	25	10	5	0	Parallel	1500	20	Cont.	96	8	X	2.86	5000
593-3	2	25	10	5	0	Parallel	1500	20	Cont.	96	10	X	2.86	5000
593-4	2	25	10	5	0	Parallel	1500	20	Cont.	96	8	K	2.86	5000
593-5	2	25	10	5	0	Parallel	1500	20	Cont.	96	8	X	4.79	5000
594-1	2	25	10	5	0	Parallel	1500	30	Cont.	96	8	X	2.86	5000
595-1	2	25	10	5	0	Parallel	750	20	Cont.	96	8	X	2.86	3600
595-2	2	25	10	5	0	Parallel	750	20	Cont.	96	8	X	2.86	5000
595-3	2	25	10	5	0	Parallel	750	20	Cont.	96	10	X	2.86	5000
595-4	2	25	10	5	0	Parallel	750	20	Cont.	96	8	K	2.86	5000
595-5	2	25	10	5	0	Parallel	750	20	Cont.	96	8	X	4.79	5000
596-1	2	25	10	5	0	Parallel	750	30	Cont.	96	8	X	2.86	5000
597-1	2	25	10	5	30	Parallel	1500	20	Cont.	96	8	X	2.86	3600
597-2	2	25	10	5	30	Parallel	1500	20	Cont.	96	8	X	2.86	5000
597-3	2	25	10	5	30	Parallel	1500	20	Cont.	96	10	X	2.86	5000
597-4	2	25	10	5	30	Parallel	1500	20	Cont.	96	8	K	2.86	5000
597-5	2	25	10	5	30	Parallel	1500	20	Cont.	96	8	X	4.79	5000
598-1	2	25	10	5	30	Parallel	1500	30	Cont.	96	8	X	2.86	5000
599-1	2	25	10	5	30	Parallel	750	20	Cont.	96	8	X	2.86	3600
599-2	2	25	10	5	30	Parallel	750	20	Cont.	96	8	X	2.86	5000
599-3	2	25	10	5	30	Parallel	750	20	Cont.	96	10	X	2.86	5000
599-4	2	25	10	5	30	Parallel	750	20	Cont.	96	8	K	2.86	5000
599-5	2	25	10	5	30	Parallel	750	20	Cont.	96	8	X	4.79	5000
600-1	2	25	10	5	30	Parallel	750	30	Cont.	96	8	X	2.86	5000
601-1	2	25	10	5	60	Parallel	1500	20	Cont.	96	8	X	2.86	3600
601-2	2	25	10	5	60	Parallel	1500	20	Cont.	96	8	X	2.86	5000
601-3	2	25	10	5	60	Parallel	1500	20	Cont.	96	10	X	2.86	5000
601-4	2	25	10	5	60	Parallel	1500	20	Cont.	96	8	K	2.86	5000
601-5	2	25	10	5	60	Parallel	1500	20	Cont.	96	8	X	4.79	5000
602-1	2	25	10	5	60	Parallel	1500	30	Cont.	96	8	X	2.86	5000
603-1	2	25	10	5	60	Parallel	750	20	Cont.	96	8	X	2.86	3600
603-2	2	25	10	5	60	Parallel	750	20	Cont.	96	8	X	2.86	5000
603-3	2	25	10	5	60	Parallel	750	20	Cont.	96	10	X	2.86	5000
603-4	2	25	10	5	60	Parallel	750	20	Cont.	96	8	K	2.86	5000
603-5	2	25	10	5	60	Parallel	750	20	Cont.	96	8	X	4.79	5000
604-1	2	25	10	5	60	Parallel	750	30	Cont.	96	8	X	2.86	5000
605-1	2	25	10	5	60	Trap.	1500	20	Cont.	96	8	X	2.86	3600
605-2	2	25	10	5	60	Trap.	1500	20	Cont.	96	8	X	2.86	5000
605-3	2	25	10	5	60	Trap.	1500	20	Cont.	96	10	X	2.86	5000
605-4	2	25	10	5	60	Trap.	1500	20	Cont.	96	8	K	2.86	5000
605-5	2	25	10	5	60	Trap.	1500	20	Cont.	96	8	X	4.79	5000
606-1	2	25	10	5	60	Trap.	1500	30	Cont.	96	8	X	2.86	5000
607-1	2	25	10	5	60	Trap.	750	20	Cont.	96	8	X	2.86	3600

Model ID	Geometry									Cross-section		CF detail		Mat'l
	n_{span}	L/d ratio	s_g [ft]	n_{girder}	Support skew [deg]; Layout		R [ft]	s_{cf} [ft]	CF layout	d_w [in]	t_{deck} [in]	CF type	A_{cf} [in^2]	E_c [ksi]
607-2	2	25	10	5	60	Trap.	750	20	Cont.	96	8	X	2.86	5000
607-3	2	25	10	5	60	Trap.	750	20	Cont.	96	10	X	2.86	5000
607-4	2	25	10	5	60	Trap.	750	20	Cont.	96	8	K	2.86	5000
607-5	2	25	10	5	60	Trap.	750	20	Cont.	96	8	X	4.79	5000
608-1	2	25	10	5	60	Trap.	750	30	Cont.	96	8	X	2.86	5000
609-1	2	25	10	7	0	Parallel	1500	20	Cont.	96	8	X	2.86	3600
609-2	2	25	10	7	0	Parallel	1500	20	Cont.	96	8	X	2.86	5000
609-3	2	25	10	7	0	Parallel	1500	20	Cont.	96	10	X	2.86	5000
609-4	2	25	10	7	0	Parallel	1500	20	Cont.	96	8	K	2.86	5000
609-5	2	25	10	7	0	Parallel	1500	20	Cont.	96	8	X	4.79	5000
610-1	2	25	10	7	0	Parallel	1500	30	Cont.	96	8	X	2.86	5000
611-1	2	25	10	7	0	Parallel	750	20	Cont.	96	8	X	2.86	3600
611-2	2	25	10	7	0	Parallel	750	20	Cont.	96	8	X	2.86	5000
611-3	2	25	10	7	0	Parallel	750	20	Cont.	96	10	X	2.86	5000
611-4	2	25	10	7	0	Parallel	750	20	Cont.	96	8	K	2.86	5000
611-5	2	25	10	7	0	Parallel	750	20	Cont.	96	8	X	4.79	5000
612-1	2	25	10	7	0	Parallel	750	30	Cont.	96	8	X	2.86	5000
613-1	2	25	10	7	30	Parallel	1500	20	Cont.	96	8	X	2.86	3600
613-2	2	25	10	7	30	Parallel	1500	20	Cont.	96	8	X	2.86	5000
613-3	2	25	10	7	30	Parallel	1500	20	Cont.	96	10	X	2.86	5000
613-4	2	25	10	7	30	Parallel	1500	20	Cont.	96	8	K	2.86	5000
613-5	2	25	10	7	30	Parallel	1500	20	Cont.	96	8	X	4.79	5000
614-1	2	25	10	7	30	Parallel	1500	30	Cont.	96	8	X	2.86	5000
615-1	2	25	10	7	30	Parallel	750	20	Cont.	96	8	X	2.86	3600
615-2	2	25	10	7	30	Parallel	750	20	Cont.	96	8	X	2.86	5000
615-3	2	25	10	7	30	Parallel	750	20	Cont.	96	10	X	2.86	5000
615-4	2	25	10	7	30	Parallel	750	20	Cont.	96	8	K	2.86	5000
615-5	2	25	10	7	30	Parallel	750	20	Cont.	96	8	X	4.79	5000
616-1	2	25	10	7	30	Parallel	750	30	Cont.	96	8	X	2.86	5000
617-1	2	25	10	7	60	Parallel	1500	20	Cont.	96	8	X	2.86	3600
617-2	2	25	10	7	60	Parallel	1500	20	Cont.	96	8	X	2.86	5000
617-3	2	25	10	7	60	Parallel	1500	20	Cont.	96	10	X	2.86	5000
617-4	2	25	10	7	60	Parallel	1500	20	Cont.	96	8	K	2.86	5000
617-5	2	25	10	7	60	Parallel	1500	20	Cont.	96	8	X	4.79	5000
618-1	2	25	10	7	60	Parallel	1500	30	Cont.	96	8	X	2.86	5000
619-1	2	25	10	7	60	Parallel	750	20	Cont.	96	8	X	2.86	3600
619-2	2	25	10	7	60	Parallel	750	20	Cont.	96	8	X	2.86	5000
619-3	2	25	10	7	60	Parallel	750	20	Cont.	96	10	X	2.86	5000
619-4	2	25	10	7	60	Parallel	750	20	Cont.	96	8	K	2.86	5000
619-5	2	25	10	7	60	Parallel	750	20	Cont.	96	8	X	4.79	5000
620-1	2	25	10	7	60	Parallel	750	30	Cont.	96	8	X	2.86	5000
621-1	2	25	10	7	60	Trap.	1500	20	Cont.	96	8	X	2.86	3600
621-2	2	25	10	7	60	Trap.	1500	20	Cont.	96	8	X	2.86	5000
621-3	2	25	10	7	60	Trap.	1500	20	Cont.	96	10	X	2.86	5000
621-4	2	25	10	7	60	Trap.	1500	20	Cont.	96	8	K	2.86	5000
621-5	2	25	10	7	60	Trap.	1500	20	Cont.	96	8	X	4.79	5000
622-1	2	25	10	7	60	Trap.	1500	30	Cont.	96	8	X	2.86	5000
623-1	2	25	10	7	60	Trap.	750	20	Cont.	96	8	X	2.86	3600
623-2	2	25	10	7	60	Trap.	750	20	Cont.	96	8	X	2.86	5000
623-3	2	25	10	7	60	Trap.	750	20	Cont.	96	10	X	2.86	5000
623-4	2	25	10	7	60	Trap.	750	20	Cont.	96	8	K	2.86	5000
623-5	2	25	10	7	60	Trap.	750	20	Cont.	96	8	X	4.79	5000
624-1	2	25	10	7	60	Trap.	750	30	Cont.	96	8	X	2.86	5000
625-1	2	30	6	3	0	Parallel	Infinite	20	Cont.	72	8	X	2.86	3600
625-2	2	30	6	3	0	Parallel	Infinite	20	Cont.	72	8	X	2.86	5000
625-3	2	30	6	3	0	Parallel	Infinite	20	Cont.	72	10	X	2.86	5000
625-4	2	30	6	3	0	Parallel	Infinite	20	Cont.	72	8	K	2.86	5000
625-5	2	30	6	3	0	Parallel	Infinite	20	Cont.	72	8	X	4.79	5000
626-1	2	30	6	3	0	Parallel	Infinite	30	Cont.	72	8	X	2.86	5000
627-1	2	30	6	3	0	Parallel	1500	20	Cont.	72	8	X	2.86	3600
627-2	2	30	6	3	0	Parallel	1500	20	Cont.	72	8	X	2.86	5000
627-3	2	30	6	3	0	Parallel	1500	20	Cont.	72	10	X	2.86	5000
627-4	2	30	6	3	0	Parallel	1500	20	Cont.	72	8	K	2.86	5000
627-5	2	30	6	3	0	Parallel	1500	20	Cont.	72	8	X	4.79	5000
628-1	2	30	6	3	0	Parallel	1500	30	Cont.	72	8	X	2.86	5000
629-1	2	30	6	3	0	Parallel	750	20	Cont.	72	8	X	2.86	3600
629-2	2	30	6	3	0	Parallel	750	20	Cont.	72	8	X	2.86	5000
629-3	2	30	6	3	0	Parallel	750	20	Cont.	72	10	X	2.86	5000
629-4	2	30	6	3	0	Parallel	750	20	Cont.	72	8	K	2.86	5000
629-5	2	30	6	3	0	Parallel	750	20	Cont.	72	8	X	4.79	5000
630-1	2	30	6	3	0	Parallel	750	30	Cont.	72	8	X	2.86	5000
631-1	2	30	6	3	30	Parallel	Infinite	20	Cont.	72	8	X	2.86	3600
631-2	2	30	6	3	30	Parallel	Infinite	20	Cont.	72	8	X	2.86	5000

Model ID	Geometry									Cross-section		CF detail		Mat'l
	n_{span}	L/d ratio	s_g [ft]	n_{girder}	Support skew [deg];	Layout	R [ft]	s_{cf} [ft]	CF layout	d_w [in]	t_{deck} [in]	CF type	A_{cf} [in^2]	E_c [ksi]
631-3	2	30	6	3	30	Parallel	Infinite	20	Cont.	72	10	X	2.86	5000
631-4	2	30	6	3	30	Parallel	Infinite	20	Cont.	72	8	K	2.86	5000
631-5	2	30	6	3	30	Parallel	Infinite	20	Cont.	72	8	X	4.79	5000
632-1	2	30	6	3	30	Parallel	Infinite	30	Cont.	72	8	X	2.86	5000
633-1	2	30	6	3	30	Parallel	1500	20	Cont.	72	8	X	2.86	3600
633-2	2	30	6	3	30	Parallel	1500	20	Cont.	72	8	X	2.86	5000
633-3	2	30	6	3	30	Parallel	1500	20	Cont.	72	10	X	2.86	5000
633-4	2	30	6	3	30	Parallel	1500	20	Cont.	72	8	K	2.86	5000
633-5	2	30	6	3	30	Parallel	1500	20	Cont.	72	8	X	4.79	5000
634-1	2	30	6	3	30	Parallel	1500	30	Cont.	72	8	X	2.86	5000
635-1	2	30	6	3	30	Parallel	750	20	Cont.	72	8	X	2.86	3600
635-2	2	30	6	3	30	Parallel	750	20	Cont.	72	8	X	2.86	5000
635-3	2	30	6	3	30	Parallel	750	20	Cont.	72	10	X	2.86	5000
635-4	2	30	6	3	30	Parallel	750	20	Cont.	72	8	K	2.86	5000
635-5	2	30	6	3	30	Parallel	750	20	Cont.	72	8	X	4.79	5000
636-1	2	30	6	3	30	Parallel	750	30	Cont.	72	8	X	2.86	5000
637-1	2	30	6	3	60	Parallel	Infinite	20	Cont.	72	8	X	2.86	3600
637-2	2	30	6	3	60	Parallel	Infinite	20	Cont.	72	8	X	2.86	5000
637-3	2	30	6	3	60	Parallel	Infinite	20	Cont.	72	10	X	2.86	5000
637-4	2	30	6	3	60	Parallel	Infinite	20	Cont.	72	8	K	2.86	5000
637-5	2	30	6	3	60	Parallel	Infinite	20	Cont.	72	8	X	4.79	5000
638-1	2	30	6	3	60	Parallel	Infinite	30	Cont.	72	8	X	2.86	5000
639-1	2	30	6	3	60	Parallel	Infinite	20	Stag.	72	8	X	2.86	3600
639-2	2	30	6	3	60	Parallel	Infinite	20	Stag.	72	8	X	2.86	5000
639-3	2	30	6	3	60	Parallel	Infinite	20	Stag.	72	10	X	2.86	5000
639-4	2	30	6	3	60	Parallel	Infinite	20	Stag.	72	8	K	2.86	5000
639-5	2	30	6	3	60	Parallel	Infinite	20	Stag.	72	8	X	4.79	5000
640-1	2	30	6	3	60	Parallel	Infinite	30	Stag.	72	8	X	2.86	5000
641-1	2	30	6	3	60	Parallel	1500	20	Cont.	72	8	X	2.86	3600
641-2	2	30	6	3	60	Parallel	1500	20	Cont.	72	8	X	2.86	5000
641-3	2	30	6	3	60	Parallel	1500	20	Cont.	72	10	X	2.86	5000
641-4	2	30	6	3	60	Parallel	1500	20	Cont.	72	8	K	2.86	5000
641-5	2	30	6	3	60	Parallel	1500	20	Cont.	72	8	X	4.79	5000
642-1	2	30	6	3	60	Parallel	1500	30	Cont.	72	8	X	2.86	5000
643-1	2	30	6	3	60	Parallel	750	20	Cont.	72	8	X	2.86	3600
643-2	2	30	6	3	60	Parallel	750	20	Cont.	72	8	X	2.86	5000
643-3	2	30	6	3	60	Parallel	750	20	Cont.	72	10	X	2.86	5000
643-4	2	30	6	3	60	Parallel	750	20	Cont.	72	8	K	2.86	5000
643-5	2	30	6	3	60	Parallel	750	20	Cont.	72	8	X	4.79	5000
644-1	2	30	6	3	60	Parallel	750	30	Cont.	72	8	X	2.86	5000
645-1	2	30	6	3	60	Trap.	Infinite	20	Cont.	72	8	X	2.86	3600
645-2	2	30	6	3	60	Trap.	Infinite	20	Cont.	72	8	X	2.86	5000
645-3	2	30	6	3	60	Trap.	Infinite	20	Cont.	72	10	X	2.86	5000
645-4	2	30	6	3	60	Trap.	Infinite	20	Cont.	72	8	K	2.86	5000
645-5	2	30	6	3	60	Trap.	Infinite	20	Cont.	72	8	X	4.79	5000
646-1	2	30	6	3	60	Trap.	Infinite	30	Cont.	72	8	X	2.86	5000
647-1	2	30	6	3	60	Trap.	Infinite	20	Stag.	72	8	X	2.86	3600
647-2	2	30	6	3	60	Trap.	Infinite	20	Stag.	72	8	X	2.86	5000
647-3	2	30	6	3	60	Trap.	Infinite	20	Stag.	72	10	X	2.86	5000
647-4	2	30	6	3	60	Trap.	Infinite	20	Stag.	72	8	K	2.86	5000
647-5	2	30	6	3	60	Trap.	Infinite	20	Stag.	72	8	X	4.79	5000
648-1	2	30	6	3	60	Trap.	Infinite	30	Stag.	72	8	X	2.86	5000
649-1	2	30	6	3	60	Trap.	1500	20	Cont.	72	8	X	2.86	3600
649-2	2	30	6	3	60	Trap.	1500	20	Cont.	72	8	X	2.86	5000
649-3	2	30	6	3	60	Trap.	1500	20	Cont.	72	10	X	2.86	5000
649-4	2	30	6	3	60	Trap.	1500	20	Cont.	72	8	K	2.86	5000
649-5	2	30	6	3	60	Trap.	1500	20	Cont.	72	8	X	4.79	5000
650-1	2	30	6	3	60	Trap.	1500	30	Cont.	72	8	X	2.86	5000
651-1	2	30	6	3	60	Trap.	750	20	Cont.	72	8	X	2.86	3600
651-2	2	30	6	3	60	Trap.	750	20	Cont.	72	8	X	2.86	5000
651-3	2	30	6	3	60	Trap.	750	20	Cont.	72	10	X	2.86	5000
651-4	2	30	6	3	60	Trap.	750	20	Cont.	72	8	K	2.86	5000
651-5	2	30	6	3	60	Trap.	750	20	Cont.	72	8	X	4.79	5000
652-1	2	30	6	3	60	Trap.	750	30	Cont.	72	8	X	2.86	5000
653-1	2	30	6	5	0	Parallel	Infinite	20	Cont.	72	8	X	2.86	3600
653-2	2	30	6	5	0	Parallel	Infinite	20	Cont.	72	8	X	2.86	5000
653-3	2	30	6	5	0	Parallel	Infinite	20	Cont.	72	10	X	2.86	5000
653-4	2	30	6	5	0	Parallel	Infinite	20	Cont.	72	8	K	2.86	5000
653-5	2	30	6	5	0	Parallel	Infinite	20	Cont.	72	8	X	4.79	5000
654-1	2	30	6	5	0	Parallel	Infinite	30	Cont.	72	8	X	2.86	5000
655-1	2	30	6	5	0	Parallel	1500	20	Cont.	72	8	X	2.86	3600
655-2	2	30	6	5	0	Parallel	1500	20	Cont.	72	8	X	2.86	5000
655-3	2	30	6	5	0	Parallel	1500	20	Cont.	72	10	X	2.86	5000

Model ID	Geometry									Cross-section		CF detail		Mat'l
	n_{span}	L/d ratio	s_g [ft]	n_{girder}	Support skew [deg];	Layout	R [ft]	s_{cf} [ft]	CF layout	d_w [in]	t_{deck} [in]	CF type	A_{cf} [in^2]	E_c [ksi]
655-4	2	30	6	5	0	Parallel	1500	20	Cont.	72	8	K	2.86	5000
655-5	2	30	6	5	0	Parallel	1500	20	Cont.	72	8	X	4.79	5000
656-1	2	30	6	5	0	Parallel	1500	30	Cont.	72	8	X	2.86	5000
657-1	2	30	6	5	0	Parallel	750	20	Cont.	72	8	X	2.86	3600
657-2	2	30	6	5	0	Parallel	750	20	Cont.	72	8	X	2.86	5000
657-3	2	30	6	5	0	Parallel	750	20	Cont.	72	10	X	2.86	5000
657-4	2	30	6	5	0	Parallel	750	20	Cont.	72	8	K	2.86	5000
657-5	2	30	6	5	0	Parallel	750	20	Cont.	72	8	X	4.79	5000
658-1	2	30	6	5	0	Parallel	750	30	Cont.	72	8	X	2.86	5000
659-1	2	30	6	5	30	Parallel	Infinite	20	Cont.	72	8	X	2.86	3600
659-2	2	30	6	5	30	Parallel	Infinite	20	Cont.	72	8	X	2.86	5000
659-3	2	30	6	5	30	Parallel	Infinite	20	Cont.	72	10	X	2.86	5000
659-4	2	30	6	5	30	Parallel	Infinite	20	Cont.	72	8	K	2.86	5000
659-5	2	30	6	5	30	Parallel	Infinite	20	Cont.	72	8	X	4.79	5000
660-1	2	30	6	5	30	Parallel	Infinite	30	Cont.	72	8	X	2.86	5000
661-1	2	30	6	5	30	Parallel	1500	20	Cont.	72	8	X	2.86	3600
661-2	2	30	6	5	30	Parallel	1500	20	Cont.	72	8	X	2.86	5000
661-3	2	30	6	5	30	Parallel	1500	20	Cont.	72	10	X	2.86	5000
661-4	2	30	6	5	30	Parallel	1500	20	Cont.	72	8	K	2.86	5000
661-5	2	30	6	5	30	Parallel	1500	20	Cont.	72	8	X	4.79	5000
662-1	2	30	6	5	30	Parallel	1500	30	Cont.	72	8	X	2.86	5000
663-1	2	30	6	5	30	Parallel	750	20	Cont.	72	8	X	2.86	3600
663-2	2	30	6	5	30	Parallel	750	20	Cont.	72	8	X	2.86	5000
663-3	2	30	6	5	30	Parallel	750	20	Cont.	72	10	X	2.86	5000
663-4	2	30	6	5	30	Parallel	750	20	Cont.	72	8	K	2.86	5000
663-5	2	30	6	5	30	Parallel	750	20	Cont.	72	8	X	4.79	5000
664-1	2	30	6	5	30	Parallel	750	30	Cont.	72	8	X	2.86	5000
665-1	2	30	6	5	60	Parallel	Infinite	20	Cont.	72	8	X	2.86	3600
665-2	2	30	6	5	60	Parallel	Infinite	20	Cont.	72	8	X	2.86	5000
665-3	2	30	6	5	60	Parallel	Infinite	20	Cont.	72	10	X	2.86	5000
665-4	2	30	6	5	60	Parallel	Infinite	20	Cont.	72	8	K	2.86	5000
665-5	2	30	6	5	60	Parallel	Infinite	20	Cont.	72	8	X	4.79	5000
666-1	2	30	6	5	60	Parallel	Infinite	30	Cont.	72	8	X	2.86	5000
667-1	2	30	6	5	60	Parallel	Infinite	20	Stag.	72	8	X	2.86	3600
667-2	2	30	6	5	60	Parallel	Infinite	20	Stag.	72	8	X	2.86	5000
667-3	2	30	6	5	60	Parallel	Infinite	20	Stag.	72	10	X	2.86	5000
667-4	2	30	6	5	60	Parallel	Infinite	20	Stag.	72	8	K	2.86	5000
667-5	2	30	6	5	60	Parallel	Infinite	20	Stag.	72	8	X	4.79	5000
668-1	2	30	6	5	60	Parallel	Infinite	30	Stag.	72	8	X	2.86	5000
669-1	2	30	6	5	60	Parallel	1500	20	Cont.	72	8	X	2.86	3600
669-2	2	30	6	5	60	Parallel	1500	20	Cont.	72	8	X	2.86	5000
669-3	2	30	6	5	60	Parallel	1500	20	Cont.	72	10	X	2.86	5000
669-4	2	30	6	5	60	Parallel	1500	20	Cont.	72	8	K	2.86	5000
669-5	2	30	6	5	60	Parallel	1500	20	Cont.	72	8	X	4.79	5000
670-1	2	30	6	5	60	Parallel	1500	30	Cont.	72	8	X	2.86	5000
671-1	2	30	6	5	60	Parallel	750	20	Cont.	72	8	X	2.86	3600
671-2	2	30	6	5	60	Parallel	750	20	Cont.	72	8	X	2.86	5000
671-3	2	30	6	5	60	Parallel	750	20	Cont.	72	10	X	2.86	5000
671-4	2	30	6	5	60	Parallel	750	20	Cont.	72	8	K	2.86	5000
671-5	2	30	6	5	60	Parallel	750	20	Cont.	72	8	X	4.79	5000
672-1	2	30	6	5	60	Parallel	750	30	Cont.	72	8	X	2.86	5000
673-1	2	30	6	5	60	Trap.	Infinite	20	Cont.	72	8	X	2.86	3600
673-2	2	30	6	5	60	Trap.	Infinite	20	Cont.	72	8	X	2.86	5000
673-3	2	30	6	5	60	Trap.	Infinite	20	Cont.	72	10	X	2.86	5000
673-4	2	30	6	5	60	Trap.	Infinite	20	Cont.	72	8	K	2.86	5000
673-5	2	30	6	5	60	Trap.	Infinite	20	Cont.	72	8	X	4.79	5000
674-1	2	30	6	5	60	Trap.	Infinite	30	Cont.	72	8	X	2.86	5000
675-1	2	30	6	5	60	Trap.	Infinite	20	Stag.	72	8	X	2.86	3600
675-2	2	30	6	5	60	Trap.	Infinite	20	Stag.	72	8	X	2.86	5000
675-3	2	30	6	5	60	Trap.	Infinite	20	Stag.	72	10	X	2.86	5000
675-4	2	30	6	5	60	Trap.	Infinite	20	Stag.	72	8	K	2.86	5000
675-5	2	30	6	5	60	Trap.	Infinite	20	Stag.	72	8	X	4.79	5000
676-1	2	30	6	5	60	Trap.	Infinite	30	Stag.	72	8	X	2.86	5000
677-1	2	30	6	5	60	Trap.	1500	20	Cont.	72	8	X	2.86	3600
677-2	2	30	6	5	60	Trap.	1500	20	Cont.	72	8	X	2.86	5000
677-3	2	30	6	5	60	Trap.	1500	20	Cont.	72	10	X	2.86	5000
677-4	2	30	6	5	60	Trap.	1500	20	Cont.	72	8	K	2.86	5000
677-5	2	30	6	5	60	Trap.	1500	20	Cont.	72	8	X	4.79	5000
678-1	2	30	6	5	60	Trap.	1500	30	Cont.	72	8	X	2.86	5000
679-1	2	30	6	5	60	Trap.	750	20	Cont.	72	8	X	2.86	3600
679-2	2	30	6	5	60	Trap.	750	20	Cont.	72	8	X	2.86	5000
679-3	2	30	6	5	60	Trap.	750	20	Cont.	72	10	X	2.86	5000
679-4	2	30	6	5	60	Trap.	750	20	Cont.	72	8	K	2.86	5000

Model ID	Geometry									Cross-section		CF detail		Mat'l
	n_{span}	L/d ratio	s_g [ft]	n_{girder}	Support skew [deg];	Layout	R [ft]	s_{cf} [ft]	CF layout	d_w [in]	t_{deck} [in]	CF type	A_{cf} [in^2]	E_c [ksi]
679-5	2	30	6	5	60	Trap.	750	20	Cont.	72	8	X	4.79	5000
680-1	2	30	6	5	60	Trap.	750	30	Cont.	72	8	X	2.86	5000
681-1	2	30	6	7	0	Parallel	Infinite	20	Cont.	72	8	X	2.86	3600
681-2	2	30	6	7	0	Parallel	Infinite	20	Cont.	72	8	X	2.86	5000
681-3	2	30	6	7	0	Parallel	Infinite	20	Cont.	72	10	X	2.86	5000
681-4	2	30	6	7	0	Parallel	Infinite	20	Cont.	72	8	K	2.86	5000
681-5	2	30	6	7	0	Parallel	Infinite	20	Cont.	72	8	X	4.79	5000
682-1	2	30	6	7	0	Parallel	Infinite	30	Cont.	72	8	X	2.86	5000
683-1	2	30	6	7	0	Parallel	1500	20	Cont.	72	8	X	2.86	3600
683-2	2	30	6	7	0	Parallel	1500	20	Cont.	72	8	X	2.86	5000
683-3	2	30	6	7	0	Parallel	1500	20	Cont.	72	10	X	2.86	5000
683-4	2	30	6	7	0	Parallel	1500	20	Cont.	72	8	K	2.86	5000
683-5	2	30	6	7	0	Parallel	1500	20	Cont.	72	8	X	4.79	5000
684-1	2	30	6	7	0	Parallel	1500	30	Cont.	72	8	X	2.86	5000
685-1	2	30	6	7	0	Parallel	750	20	Cont.	72	8	X	2.86	3600
685-2	2	30	6	7	0	Parallel	750	20	Cont.	72	8	X	2.86	5000
685-3	2	30	6	7	0	Parallel	750	20	Cont.	72	10	X	2.86	5000
685-4	2	30	6	7	0	Parallel	750	20	Cont.	72	8	K	2.86	5000
685-5	2	30	6	7	0	Parallel	750	20	Cont.	72	8	X	4.79	5000
686-1	2	30	6	7	0	Parallel	750	30	Cont.	72	8	X	2.86	5000
687-1	2	30	6	7	30	Parallel	Infinite	20	Cont.	72	8	X	2.86	3600
687-2	2	30	6	7	30	Parallel	Infinite	20	Cont.	72	8	X	2.86	5000
687-3	2	30	6	7	30	Parallel	Infinite	20	Cont.	72	10	X	2.86	5000
687-4	2	30	6	7	30	Parallel	Infinite	20	Cont.	72	8	K	2.86	5000
687-5	2	30	6	7	30	Parallel	Infinite	20	Cont.	72	8	X	4.79	5000
688-1	2	30	6	7	30	Parallel	Infinite	30	Cont.	72	8	X	2.86	5000
689-1	2	30	6	7	30	Parallel	1500	20	Cont.	72	8	X	2.86	3600
689-2	2	30	6	7	30	Parallel	1500	20	Cont.	72	8	X	2.86	5000
689-3	2	30	6	7	30	Parallel	1500	20	Cont.	72	10	X	2.86	5000
689-4	2	30	6	7	30	Parallel	1500	20	Cont.	72	8	K	2.86	5000
689-5	2	30	6	7	30	Parallel	1500	20	Cont.	72	8	X	4.79	5000
690-1	2	30	6	7	30	Parallel	1500	30	Cont.	72	8	X	2.86	5000
691-1	2	30	6	7	30	Parallel	750	20	Cont.	72	8	X	2.86	3600
691-2	2	30	6	7	30	Parallel	750	20	Cont.	72	8	X	2.86	5000
691-3	2	30	6	7	30	Parallel	750	20	Cont.	72	10	X	2.86	5000
691-4	2	30	6	7	30	Parallel	750	20	Cont.	72	8	K	2.86	5000
691-5	2	30	6	7	30	Parallel	750	20	Cont.	72	8	X	4.79	5000
692-1	2	30	6	7	30	Parallel	750	30	Cont.	72	8	X	2.86	5000
693-1	2	30	6	7	60	Parallel	Infinite	20	Cont.	72	8	X	2.86	3600
693-2	2	30	6	7	60	Parallel	Infinite	20	Cont.	72	8	X	2.86	5000
693-3	2	30	6	7	60	Parallel	Infinite	20	Cont.	72	10	X	2.86	5000
693-4	2	30	6	7	60	Parallel	Infinite	20	Cont.	72	8	K	2.86	5000
693-5	2	30	6	7	60	Parallel	Infinite	20	Cont.	72	8	X	4.79	5000
694-1	2	30	6	7	60	Parallel	Infinite	30	Cont.	72	8	X	2.86	5000
695-1	2	30	6	7	60	Parallel	Infinite	20	Stag.	72	8	X	2.86	3600
695-2	2	30	6	7	60	Parallel	Infinite	20	Stag.	72	8	X	2.86	5000
695-3	2	30	6	7	60	Parallel	Infinite	20	Stag.	72	10	X	2.86	5000
695-4	2	30	6	7	60	Parallel	Infinite	20	Stag.	72	8	K	2.86	5000
695-5	2	30	6	7	60	Parallel	Infinite	20	Stag.	72	8	X	4.79	5000
696-1	2	30	6	7	60	Parallel	Infinite	30	Stag.	72	8	X	2.86	5000
697-1	2	30	6	7	60	Parallel	1500	20	Cont.	72	8	X	2.86	3600
697-2	2	30	6	7	60	Parallel	1500	20	Cont.	72	8	X	2.86	5000
697-3	2	30	6	7	60	Parallel	1500	20	Cont.	72	10	X	2.86	5000
697-4	2	30	6	7	60	Parallel	1500	20	Cont.	72	8	K	2.86	5000
697-5	2	30	6	7	60	Parallel	1500	20	Cont.	72	8	X	4.79	5000
698-1	2	30	6	7	60	Parallel	1500	30	Cont.	72	8	X	2.86	5000
699-1	2	30	6	7	60	Parallel	750	20	Cont.	72	8	X	2.86	3600
699-2	2	30	6	7	60	Parallel	750	20	Cont.	72	8	X	2.86	5000
699-3	2	30	6	7	60	Parallel	750	20	Cont.	72	10	X	2.86	5000
699-4	2	30	6	7	60	Parallel	750	20	Cont.	72	8	K	2.86	5000
699-5	2	30	6	7	60	Parallel	750	20	Cont.	72	8	X	4.79	5000
700-1	2	30	6	7	60	Parallel	750	30	Cont.	72	8	X	2.86	5000
701-1	2	30	6	7	60	Trap.	Infinite	20	Cont.	72	8	X	2.86	3600
701-2	2	30	6	7	60	Trap.	Infinite	20	Cont.	72	8	X	2.86	5000
701-3	2	30	6	7	60	Trap.	Infinite	20	Cont.	72	10	X	2.86	5000
701-4	2	30	6	7	60	Trap.	Infinite	20	Cont.	72	8	K	2.86	5000
701-5	2	30	6	7	60	Trap.	Infinite	20	Cont.	72	8	X	4.79	5000
702-1	2	30	6	7	60	Trap.	Infinite	30	Cont.	72	8	X	2.86	5000
703-1	2	30	6	7	60	Trap.	Infinite	20	Stag.	72	8	X	2.86	3600
703-2	2	30	6	7	60	Trap.	Infinite	20	Stag.	72	8	X	2.86	5000
703-3	2	30	6	7	60	Trap.	Infinite	20	Stag.	72	10	X	2.86	5000
703-4	2	30	6	7	60	Trap.	Infinite	20	Stag.	72	8	K	2.86	5000
703-5	2	30	6	7	60	Trap.	Infinite	20	Stag.	72	8	X	4.79	5000

Model ID	Geometry									Cross-section		CF detail		Mat'l
	n_{span}	L/d ratio	s_g [ft]	n_{girder}	Support skew [deg]; Layout		R [ft]	s_{cf} [ft]	CF layout	d_w [in]	t_{deck} [in]	CF type	A_{cf} [in^2]	E_c [ksi]
704-1	2	30	6	7	60	Trap.	Infinite	30	Stag.	72	8	X	2.86	5000
705-1	2	30	6	7	60	Trap.	1500	20	Cont.	72	8	X	2.86	3600
705-2	2	30	6	7	60	Trap.	1500	20	Cont.	72	8	X	2.86	5000
705-3	2	30	6	7	60	Trap.	1500	20	Cont.	72	10	X	2.86	5000
705-4	2	30	6	7	60	Trap.	1500	20	Cont.	72	8	K	2.86	5000
705-5	2	30	6	7	60	Trap.	1500	20	Cont.	72	8	X	4.79	5000
706-1	2	30	6	7	60	Trap.	1500	30	Cont.	72	8	X	2.86	5000
707-1	2	30	6	7	60	Trap.	750	20	Cont.	72	8	X	2.86	3600
707-2	2	30	6	7	60	Trap.	750	20	Cont.	72	8	X	2.86	5000
707-3	2	30	6	7	60	Trap.	750	20	Cont.	72	10	X	2.86	5000
707-4	2	30	6	7	60	Trap.	750	20	Cont.	72	8	K	2.86	5000
707-5	2	30	6	7	60	Trap.	750	20	Cont.	72	8	X	4.79	5000
708-1	2	30	6	7	60	Trap.	750	30	Cont.	72	8	X	2.86	5000
709-1	2	30	8	3	0	Parallel	Infinite	20	Cont.	72	8	X	2.86	3600
709-2	2	30	8	3	0	Parallel	Infinite	20	Cont.	72	8	X	2.86	5000
709-3	2	30	8	3	0	Parallel	Infinite	20	Cont.	72	10	X	2.86	5000
709-4	2	30	8	3	0	Parallel	Infinite	20	Cont.	72	8	K	2.86	5000
709-5	2	30	8	3	0	Parallel	Infinite	20	Cont.	72	8	X	4.79	5000
710-1	2	30	8	3	0	Parallel	Infinite	30	Cont.	72	8	X	2.86	5000
711-1	2	30	8	3	0	Parallel	1500	20	Cont.	72	8	X	2.86	3600
711-2	2	30	8	3	0	Parallel	1500	20	Cont.	72	8	X	2.86	5000
711-3	2	30	8	3	0	Parallel	1500	20	Cont.	72	10	X	2.86	5000
711-4	2	30	8	3	0	Parallel	1500	20	Cont.	72	8	K	2.86	5000
711-5	2	30	8	3	0	Parallel	1500	20	Cont.	72	8	X	4.79	5000
712-1	2	30	8	3	0	Parallel	1500	30	Cont.	72	8	X	2.86	5000
713-1	2	30	8	3	0	Parallel	750	20	Cont.	72	8	X	2.86	3600
713-2	2	30	8	3	0	Parallel	750	20	Cont.	72	8	X	2.86	5000
713-3	2	30	8	3	0	Parallel	750	20	Cont.	72	10	X	2.86	5000
713-4	2	30	8	3	0	Parallel	750	20	Cont.	72	8	K	2.86	5000
713-5	2	30	8	3	0	Parallel	750	20	Cont.	72	8	X	4.79	5000
714-1	2	30	8	3	0	Parallel	750	30	Cont.	72	8	X	2.86	5000
715-1	2	30	8	3	30	Parallel	Infinite	20	Cont.	72	8	X	2.86	3600
715-2	2	30	8	3	30	Parallel	Infinite	20	Cont.	72	8	X	2.86	5000
715-3	2	30	8	3	30	Parallel	Infinite	20	Cont.	72	10	X	2.86	5000
715-4	2	30	8	3	30	Parallel	Infinite	20	Cont.	72	8	K	2.86	5000
715-5	2	30	8	3	30	Parallel	Infinite	20	Cont.	72	8	X	4.79	5000
716-1	2	30	8	3	30	Parallel	Infinite	30	Cont.	72	8	X	2.86	5000
717-1	2	30	8	3	30	Parallel	1500	20	Cont.	72	8	X	2.86	3600
717-2	2	30	8	3	30	Parallel	1500	20	Cont.	72	8	X	2.86	5000
717-3	2	30	8	3	30	Parallel	1500	20	Cont.	72	10	X	2.86	5000
717-4	2	30	8	3	30	Parallel	1500	20	Cont.	72	8	K	2.86	5000
717-5	2	30	8	3	30	Parallel	1500	20	Cont.	72	8	X	4.79	5000
718-1	2	30	8	3	30	Parallel	1500	30	Cont.	72	8	X	2.86	5000
719-1	2	30	8	3	30	Parallel	750	20	Cont.	72	8	X	2.86	3600
719-2	2	30	8	3	30	Parallel	750	20	Cont.	72	8	X	2.86	5000
719-3	2	30	8	3	30	Parallel	750	20	Cont.	72	10	X	2.86	5000
719-4	2	30	8	3	30	Parallel	750	20	Cont.	72	8	K	2.86	5000
719-5	2	30	8	3	30	Parallel	750	20	Cont.	72	8	X	4.79	5000
720-1	2	30	8	3	30	Parallel	750	30	Cont.	72	8	X	2.86	5000
721-1	2	30	8	3	60	Parallel	Infinite	20	Cont.	72	8	X	2.86	3600
721-2	2	30	8	3	60	Parallel	Infinite	20	Cont.	72	8	X	2.86	5000
721-3	2	30	8	3	60	Parallel	Infinite	20	Cont.	72	10	X	2.86	5000
721-4	2	30	8	3	60	Parallel	Infinite	20	Cont.	72	8	K	2.86	5000
721-5	2	30	8	3	60	Parallel	Infinite	20	Cont.	72	8	X	4.79	5000
722-1	2	30	8	3	60	Parallel	Infinite	30	Cont.	72	8	X	2.86	5000
723-1	2	30	8	3	60	Parallel	Infinite	20	Stag.	72	8	X	2.86	3600
723-2	2	30	8	3	60	Parallel	Infinite	20	Stag.	72	8	X	2.86	5000
723-3	2	30	8	3	60	Parallel	Infinite	20	Stag.	72	10	X	2.86	5000
723-4	2	30	8	3	60	Parallel	Infinite	20	Stag.	72	8	K	2.86	5000
723-5	2	30	8	3	60	Parallel	Infinite	20	Stag.	72	8	X	4.79	5000
724-1	2	30	8	3	60	Parallel	Infinite	30	Stag.	72	8	X	2.86	5000
725-1	2	30	8	3	60	Parallel	1500	20	Cont.	72	8	X	2.86	3600
725-2	2	30	8	3	60	Parallel	1500	20	Cont.	72	8	X	2.86	5000
725-3	2	30	8	3	60	Parallel	1500	20	Cont.	72	10	X	2.86	5000
725-4	2	30	8	3	60	Parallel	1500	20	Cont.	72	8	K	2.86	5000
725-5	2	30	8	3	60	Parallel	1500	20	Cont.	72	8	X	4.79	5000
726-1	2	30	8	3	60	Parallel	1500	30	Cont.	72	8	X	2.86	5000
727-1	2	30	8	3	60	Parallel	750	20	Cont.	72	8	X	2.86	3600
727-2	2	30	8	3	60	Parallel	750	20	Cont.	72	8	X	2.86	5000
727-3	2	30	8	3	60	Parallel	750	20	Cont.	72	10	X	2.86	5000
727-4	2	30	8	3	60	Parallel	750	20	Cont.	72	8	K	2.86	5000
727-5	2	30	8	3	60	Parallel	750	20	Cont.	72	8	X	4.79	5000
728-1	2	30	8	3	60	Parallel	750	30	Cont.	72	8	X	2.86	5000

Model ID	Geometry									Cross-section		CF detail		Mat'l
	n_{span}	L/d ratio	s_g [ft]	n_{girder}	Support skew [deg]; Layout		R [ft]	s_{cf} [ft]	CF layout	d_w [in]	t_{deck} [in]	CF type	A_{cf} [in^2]	E_c [ksi]
729-1	2	30	8	3	60	Trap.	Infinite	20	Cont.	72	8	X	2.86	3600
729-2	2	30	8	3	60	Trap.	Infinite	20	Cont.	72	8	X	2.86	5000
729-3	2	30	8	3	60	Trap.	Infinite	20	Cont.	72	10	X	2.86	5000
729-4	2	30	8	3	60	Trap.	Infinite	20	Cont.	72	8	K	2.86	5000
729-5	2	30	8	3	60	Trap.	Infinite	20	Cont.	72	8	X	4.79	5000
730-1	2	30	8	3	60	Trap.	Infinite	30	Cont.	72	8	X	2.86	5000
731-1	2	30	8	3	60	Trap.	Infinite	20	Stag.	72	8	X	2.86	3600
731-2	2	30	8	3	60	Trap.	Infinite	20	Stag.	72	8	X	2.86	5000
731-3	2	30	8	3	60	Trap.	Infinite	20	Stag.	72	10	X	2.86	5000
731-4	2	30	8	3	60	Trap.	Infinite	20	Stag.	72	8	K	2.86	5000
731-5	2	30	8	3	60	Trap.	Infinite	20	Stag.	72	8	X	4.79	5000
732-1	2	30	8	3	60	Trap.	Infinite	30	Stag.	72	8	X	2.86	5000
733-1	2	30	8	3	60	Trap.	1500	20	Cont.	72	8	X	2.86	3600
733-2	2	30	8	3	60	Trap.	1500	20	Cont.	72	8	X	2.86	5000
733-3	2	30	8	3	60	Trap.	1500	20	Cont.	72	10	X	2.86	5000
733-4	2	30	8	3	60	Trap.	1500	20	Cont.	72	8	K	2.86	5000
733-5	2	30	8	3	60	Trap.	1500	20	Cont.	72	8	X	4.79	5000
734-1	2	30	8	3	60	Trap.	1500	30	Cont.	72	8	X	2.86	5000
735-1	2	30	8	3	60	Trap.	750	20	Cont.	72	8	X	2.86	3600
735-2	2	30	8	3	60	Trap.	750	20	Cont.	72	8	X	2.86	5000
735-3	2	30	8	3	60	Trap.	750	20	Cont.	72	10	X	2.86	5000
735-4	2	30	8	3	60	Trap.	750	20	Cont.	72	8	K	2.86	5000
735-5	2	30	8	3	60	Trap.	750	20	Cont.	72	8	X	4.79	5000
736-1	2	30	8	3	60	Trap.	750	30	Cont.	72	8	X	2.86	5000
737-1	2	30	8	5	0	Parallel	Infinite	20	Cont.	72	8	X	2.86	3600
737-2	2	30	8	5	0	Parallel	Infinite	20	Cont.	72	8	X	2.86	5000
737-3	2	30	8	5	0	Parallel	Infinite	20	Cont.	72	10	X	2.86	5000
737-4	2	30	8	5	0	Parallel	Infinite	20	Cont.	72	8	K	2.86	5000
737-5	2	30	8	5	0	Parallel	Infinite	20	Cont.	72	8	X	4.79	5000
738-1	2	30	8	5	0	Parallel	Infinite	30	Cont.	72	8	X	2.86	5000
739-1	2	30	8	5	0	Parallel	1500	20	Cont.	72	8	X	2.86	3600
739-2	2	30	8	5	0	Parallel	1500	20	Cont.	72	8	X	2.86	5000
739-3	2	30	8	5	0	Parallel	1500	20	Cont.	72	10	X	2.86	5000
739-4	2	30	8	5	0	Parallel	1500	20	Cont.	72	8	K	2.86	5000
739-5	2	30	8	5	0	Parallel	1500	20	Cont.	72	8	X	4.79	5000
740-1	2	30	8	5	0	Parallel	1500	30	Cont.	72	8	X	2.86	5000
741-1	2	30	8	5	0	Parallel	750	20	Cont.	72	8	X	2.86	3600
741-2	2	30	8	5	0	Parallel	750	20	Cont.	72	8	X	2.86	5000
741-3	2	30	8	5	0	Parallel	750	20	Cont.	72	10	X	2.86	5000
741-4	2	30	8	5	0	Parallel	750	20	Cont.	72	8	K	2.86	5000
741-5	2	30	8	5	0	Parallel	750	20	Cont.	72	8	X	4.79	5000
742-1	2	30	8	5	0	Parallel	750	30	Cont.	72	8	X	2.86	5000
743-1	2	30	8	5	30	Parallel	Infinite	20	Cont.	72	8	X	2.86	3600
743-2	2	30	8	5	30	Parallel	Infinite	20	Cont.	72	8	X	2.86	5000
743-3	2	30	8	5	30	Parallel	Infinite	20	Cont.	72	10	X	2.86	5000
743-4	2	30	8	5	30	Parallel	Infinite	20	Cont.	72	8	K	2.86	5000
743-5	2	30	8	5	30	Parallel	Infinite	20	Cont.	72	8	X	4.79	5000
744-1	2	30	8	5	30	Parallel	Infinite	30	Cont.	72	8	X	2.86	5000
745-1	2	30	8	5	30	Parallel	1500	20	Cont.	72	8	X	2.86	3600
745-2	2	30	8	5	30	Parallel	1500	20	Cont.	72	8	X	2.86	5000
745-3	2	30	8	5	30	Parallel	1500	20	Cont.	72	10	X	2.86	5000
745-4	2	30	8	5	30	Parallel	1500	20	Cont.	72	8	K	2.86	5000
745-5	2	30	8	5	30	Parallel	1500	20	Cont.	72	8	X	4.79	5000
746-1	2	30	8	5	30	Parallel	1500	30	Cont.	72	8	X	2.86	5000
747-1	2	30	8	5	30	Parallel	750	20	Cont.	72	8	X	2.86	3600
747-2	2	30	8	5	30	Parallel	750	20	Cont.	72	8	X	2.86	5000
747-3	2	30	8	5	30	Parallel	750	20	Cont.	72	10	X	2.86	5000
747-4	2	30	8	5	30	Parallel	750	20	Cont.	72	8	K	2.86	5000
747-5	2	30	8	5	30	Parallel	750	20	Cont.	72	8	X	4.79	5000
748-1	2	30	8	5	30	Parallel	750	30	Cont.	72	8	X	2.86	5000
749-1	2	30	8	5	60	Parallel	Infinite	20	Cont.	72	8	X	2.86	3600
749-2	2	30	8	5	60	Parallel	Infinite	20	Cont.	72	8	X	2.86	5000
749-3	2	30	8	5	60	Parallel	Infinite	20	Cont.	72	10	X	2.86	5000
749-4	2	30	8	5	60	Parallel	Infinite	20	Cont.	72	8	K	2.86	5000
749-5	2	30	8	5	60	Parallel	Infinite	20	Cont.	72	8	X	4.79	5000
750-1	2	30	8	5	60	Parallel	Infinite	30	Cont.	72	8	X	2.86	5000
751-1	2	30	8	5	60	Parallel	Infinite	20	Stag.	72	8	X	2.86	3600
751-2	2	30	8	5	60	Parallel	Infinite	20	Stag.	72	8	X	2.86	5000
751-3	2	30	8	5	60	Parallel	Infinite	20	Stag.	72	10	X	2.86	5000
751-4	2	30	8	5	60	Parallel	Infinite	20	Stag.	72	8	K	2.86	5000
751-5	2	30	8	5	60	Parallel	Infinite	20	Stag.	72	8	X	4.79	5000
752-1	2	30	8	5	60	Parallel	Infinite	30	Stag.	72	8	X	2.86	5000
753-1	2	30	8	5	60	Parallel	1500	20	Cont.	72	8	X	2.86	3600

Model ID	Geometry									Cross-section		CF detail		Mat'l
	n_{span}	L/d ratio	s_g [ft]	n_{girder}	Support skew [deg];	Layout	R [ft]	s_{cf} [ft]	CF layout	d_w [in]	t_{deck} [in]	CF type	A_{cf} [in^2]	E_c [ksi]
753-2	2	30	8	5	60	Parallel	1500	20	Cont.	72	8	X	2.86	5000
753-3	2	30	8	5	60	Parallel	1500	20	Cont.	72	10	X	2.86	5000
753-4	2	30	8	5	60	Parallel	1500	20	Cont.	72	8	K	2.86	5000
753-5	2	30	8	5	60	Parallel	1500	20	Cont.	72	8	X	4.79	5000
754-1	2	30	8	5	60	Parallel	1500	30	Cont.	72	8	X	2.86	5000
755-1	2	30	8	5	60	Parallel	750	20	Cont.	72	8	X	2.86	3600
755-2	2	30	8	5	60	Parallel	750	20	Cont.	72	8	X	2.86	5000
755-3	2	30	8	5	60	Parallel	750	20	Cont.	72	10	X	2.86	5000
755-4	2	30	8	5	60	Parallel	750	20	Cont.	72	8	K	2.86	5000
755-5	2	30	8	5	60	Parallel	750	20	Cont.	72	8	X	4.79	5000
756-1	2	30	8	5	60	Parallel	750	30	Cont.	72	8	X	2.86	5000
757-1	2	30	8	5	60	Trap.	Infinite	20	Cont.	72	8	X	2.86	3600
757-2	2	30	8	5	60	Trap.	Infinite	20	Cont.	72	8	X	2.86	5000
757-3	2	30	8	5	60	Trap.	Infinite	20	Cont.	72	10	X	2.86	5000
757-4	2	30	8	5	60	Trap.	Infinite	20	Cont.	72	8	K	2.86	5000
757-5	2	30	8	5	60	Trap.	Infinite	20	Cont.	72	8	X	4.79	5000
758-1	2	30	8	5	60	Trap.	Infinite	30	Cont.	72	8	X	2.86	5000
759-1	2	30	8	5	60	Trap.	Infinite	20	Stag.	72	8	X	2.86	3600
759-2	2	30	8	5	60	Trap.	Infinite	20	Stag.	72	8	X	2.86	5000
759-3	2	30	8	5	60	Trap.	Infinite	20	Stag.	72	10	X	2.86	5000
759-4	2	30	8	5	60	Trap.	Infinite	20	Stag.	72	8	K	2.86	5000
759-5	2	30	8	5	60	Trap.	Infinite	20	Stag.	72	8	X	4.79	5000
760-1	2	30	8	5	60	Trap.	Infinite	30	Stag.	72	8	X	2.86	5000
761-1	2	30	8	5	60	Trap.	1500	20	Cont.	72	8	X	2.86	3600
761-2	2	30	8	5	60	Trap.	1500	20	Cont.	72	8	X	2.86	5000
761-3	2	30	8	5	60	Trap.	1500	20	Cont.	72	10	X	2.86	5000
761-4	2	30	8	5	60	Trap.	1500	20	Cont.	72	8	K	2.86	5000
761-5	2	30	8	5	60	Trap.	1500	20	Cont.	72	8	X	4.79	5000
762-1	2	30	8	5	60	Trap.	1500	30	Cont.	72	8	X	2.86	5000
763-1	2	30	8	5	60	Trap.	750	20	Cont.	72	8	X	2.86	3600
763-2	2	30	8	5	60	Trap.	750	20	Cont.	72	8	X	2.86	5000
763-3	2	30	8	5	60	Trap.	750	20	Cont.	72	10	X	2.86	5000
763-4	2	30	8	5	60	Trap.	750	20	Cont.	72	8	K	2.86	5000
763-5	2	30	8	5	60	Trap.	750	20	Cont.	72	8	X	4.79	5000
764-1	2	30	8	5	60	Trap.	750	30	Cont.	72	8	X	2.86	5000
765-1	2	30	8	7	0	Parallel	Infinite	20	Cont.	72	8	X	2.86	3600
765-2	2	30	8	7	0	Parallel	Infinite	20	Cont.	72	8	X	2.86	5000
765-3	2	30	8	7	0	Parallel	Infinite	20	Cont.	72	10	X	2.86	5000
765-4	2	30	8	7	0	Parallel	Infinite	20	Cont.	72	8	K	2.86	5000
765-5	2	30	8	7	0	Parallel	Infinite	20	Cont.	72	8	X	4.79	5000
766-1	2	30	8	7	0	Parallel	Infinite	30	Cont.	72	8	X	2.86	5000
767-1	2	30	8	7	0	Parallel	1500	20	Cont.	72	8	X	2.86	3600
767-2	2	30	8	7	0	Parallel	1500	20	Cont.	72	8	X	2.86	5000
767-3	2	30	8	7	0	Parallel	1500	20	Cont.	72	10	X	2.86	5000
767-4	2	30	8	7	0	Parallel	1500	20	Cont.	72	8	K	2.86	5000
767-5	2	30	8	7	0	Parallel	1500	20	Cont.	72	8	X	4.79	5000
768-1	2	30	8	7	0	Parallel	1500	30	Cont.	72	8	X	2.86	5000
769-1	2	30	8	7	0	Parallel	750	20	Cont.	72	8	X	2.86	3600
769-2	2	30	8	7	0	Parallel	750	20	Cont.	72	8	X	2.86	5000
769-3	2	30	8	7	0	Parallel	750	20	Cont.	72	10	X	2.86	5000
769-4	2	30	8	7	0	Parallel	750	20	Cont.	72	8	K	2.86	5000
769-5	2	30	8	7	0	Parallel	750	20	Cont.	72	8	X	4.79	5000
770-1	2	30	8	7	0	Parallel	750	30	Cont.	72	8	X	2.86	5000
771-1	2	30	8	7	30	Parallel	Infinite	20	Cont.	72	8	X	2.86	3600
771-2	2	30	8	7	30	Parallel	Infinite	20	Cont.	72	8	X	2.86	5000
771-3	2	30	8	7	30	Parallel	Infinite	20	Cont.	72	10	X	2.86	5000
771-4	2	30	8	7	30	Parallel	Infinite	20	Cont.	72	8	K	2.86	5000
771-5	2	30	8	7	30	Parallel	Infinite	20	Cont.	72	8	X	4.79	5000
772-1	2	30	8	7	30	Parallel	Infinite	30	Cont.	72	8	X	2.86	5000
773-1	2	30	8	7	30	Parallel	1500	20	Cont.	72	8	X	2.86	3600
773-2	2	30	8	7	30	Parallel	1500	20	Cont.	72	8	X	2.86	5000
773-3	2	30	8	7	30	Parallel	1500	20	Cont.	72	10	X	2.86	5000
773-4	2	30	8	7	30	Parallel	1500	20	Cont.	72	8	K	2.86	5000
773-5	2	30	8	7	30	Parallel	1500	20	Cont.	72	8	X	4.79	5000
774-1	2	30	8	7	30	Parallel	1500	30	Cont.	72	8	X	2.86	5000
775-1	2	30	8	7	30	Parallel	750	20	Cont.	72	8	X	2.86	3600
775-2	2	30	8	7	30	Parallel	750	20	Cont.	72	8	X	2.86	5000
775-3	2	30	8	7	30	Parallel	750	20	Cont.	72	10	X	2.86	5000
775-4	2	30	8	7	30	Parallel	750	20	Cont.	72	8	K	2.86	5000
775-5	2	30	8	7	30	Parallel	750	20	Cont.	72	8	X	4.79	5000
776-1	2	30	8	7	30	Parallel	750	30	Cont.	72	8	X	2.86	5000
777-1	2	30	8	7	60	Parallel	Infinite	20	Cont.	72	8	X	2.86	3600
777-2	2	30	8	7	60	Parallel	Infinite	20	Cont.	72	8	X	2.86	5000

Model ID	Geometry									Cross-section		CF detail		Mat'l
	n_{span}	L/d ratio	s_g [ft]	n_{girder}	Support skew [deg]; Layout		R [ft]	s_{cf} [ft]	CF layout	d_w [in]	t_{deck} [in]	CF type	A_{cf} [in^2]	E_c [ksi]
777-3	2	30	8	7	60	Parallel	Infinite	20	Cont.	72	10	X	2.86	5000
777-4	2	30	8	7	60	Parallel	Infinite	20	Cont.	72	8	K	2.86	5000
777-5	2	30	8	7	60	Parallel	Infinite	20	Cont.	72	8	X	4.79	5000
778-1	2	30	8	7	60	Parallel	Infinite	30	Cont.	72	8	X	2.86	5000
779-1	2	30	8	7	60	Parallel	Infinite	20	Stag.	72	8	X	2.86	3600
779-2	2	30	8	7	60	Parallel	Infinite	20	Stag.	72	8	X	2.86	5000
779-3	2	30	8	7	60	Parallel	Infinite	20	Stag.	72	10	X	2.86	5000
779-4	2	30	8	7	60	Parallel	Infinite	20	Stag.	72	8	K	2.86	5000
779-5	2	30	8	7	60	Parallel	Infinite	20	Stag.	72	8	X	4.79	5000
780-1	2	30	8	7	60	Parallel	Infinite	30	Stag.	72	8	X	2.86	5000
781-1	2	30	8	7	60	Parallel	1500	20	Cont.	72	8	X	2.86	3600
781-2	2	30	8	7	60	Parallel	1500	20	Cont.	72	8	X	2.86	5000
781-3	2	30	8	7	60	Parallel	1500	20	Cont.	72	10	X	2.86	5000
781-4	2	30	8	7	60	Parallel	1500	20	Cont.	72	8	K	2.86	5000
781-5	2	30	8	7	60	Parallel	1500	20	Cont.	72	8	X	4.79	5000
782-1	2	30	8	7	60	Parallel	1500	30	Cont.	72	8	X	2.86	5000
783-1	2	30	8	7	60	Parallel	750	20	Cont.	72	8	X	2.86	3600
783-2	2	30	8	7	60	Parallel	750	20	Cont.	72	8	X	2.86	5000
783-3	2	30	8	7	60	Parallel	750	20	Cont.	72	10	X	2.86	5000
783-4	2	30	8	7	60	Parallel	750	20	Cont.	72	8	K	2.86	5000
783-5	2	30	8	7	60	Parallel	750	20	Cont.	72	8	X	4.79	5000
784-1	2	30	8	7	60	Parallel	750	30	Cont.	72	8	X	2.86	5000
785-1	2	30	8	7	60	Trap.	Infinite	20	Cont.	72	8	X	2.86	3600
785-2	2	30	8	7	60	Trap.	Infinite	20	Cont.	72	8	X	2.86	5000
785-3	2	30	8	7	60	Trap.	Infinite	20	Cont.	72	10	X	2.86	5000
785-4	2	30	8	7	60	Trap.	Infinite	20	Cont.	72	8	K	2.86	5000
785-5	2	30	8	7	60	Trap.	Infinite	20	Cont.	72	8	X	4.79	5000
786-1	2	30	8	7	60	Trap.	Infinite	30	Cont.	72	8	X	2.86	5000
787-1	2	30	8	7	60	Trap.	Infinite	20	Stag.	72	8	X	2.86	3600
787-2	2	30	8	7	60	Trap.	Infinite	20	Stag.	72	8	X	2.86	5000
787-3	2	30	8	7	60	Trap.	Infinite	20	Stag.	72	10	X	2.86	5000
787-4	2	30	8	7	60	Trap.	Infinite	20	Stag.	72	8	K	2.86	5000
787-5	2	30	8	7	60	Trap.	Infinite	20	Stag.	72	8	X	4.79	5000
788-1	2	30	8	7	60	Trap.	Infinite	30	Stag.	72	8	X	2.86	5000
789-1	2	30	8	7	60	Trap.	1500	20	Cont.	72	8	X	2.86	3600
789-2	2	30	8	7	60	Trap.	1500	20	Cont.	72	8	X	2.86	5000
789-3	2	30	8	7	60	Trap.	1500	20	Cont.	72	10	X	2.86	5000
789-4	2	30	8	7	60	Trap.	1500	20	Cont.	72	8	K	2.86	5000
789-5	2	30	8	7	60	Trap.	1500	20	Cont.	72	8	X	4.79	5000
790-1	2	30	8	7	60	Trap.	1500	30	Cont.	72	8	X	2.86	5000
791-1	2	30	8	7	60	Trap.	750	20	Cont.	72	8	X	2.86	3600
791-2	2	30	8	7	60	Trap.	750	20	Cont.	72	8	X	2.86	5000
791-3	2	30	8	7	60	Trap.	750	20	Cont.	72	10	X	2.86	5000
791-4	2	30	8	7	60	Trap.	750	20	Cont.	72	8	K	2.86	5000
791-5	2	30	8	7	60	Trap.	750	20	Cont.	72	8	X	4.79	5000
792-1	2	30	8	7	60	Trap.	750	30	Cont.	72	8	X	2.86	5000
793-1	2	30	10	3	0	Parallel	Infinite	20	Cont.	72	8	X	2.86	3600
793-2	2	30	10	3	0	Parallel	Infinite	20	Cont.	72	8	X	2.86	5000
793-3	2	30	10	3	0	Parallel	Infinite	20	Cont.	72	10	X	2.86	5000
793-4	2	30	10	3	0	Parallel	Infinite	20	Cont.	72	8	K	2.86	5000
793-5	2	30	10	3	0	Parallel	Infinite	20	Cont.	72	8	X	4.79	5000
794-1	2	30	10	3	0	Parallel	Infinite	30	Cont.	72	8	X	2.86	5000
795-1	2	30	10	3	0	Parallel	1500	20	Cont.	72	8	X	2.86	3600
795-2	2	30	10	3	0	Parallel	1500	20	Cont.	72	8	X	2.86	5000
795-3	2	30	10	3	0	Parallel	1500	20	Cont.	72	10	X	2.86	5000
795-4	2	30	10	3	0	Parallel	1500	20	Cont.	72	8	K	2.86	5000
795-5	2	30	10	3	0	Parallel	1500	20	Cont.	72	8	X	4.79	5000
796-1	2	30	10	3	0	Parallel	1500	30	Cont.	72	8	X	2.86	5000
797-1	2	30	10	3	0	Parallel	750	20	Cont.	72	8	X	2.86	3600
797-2	2	30	10	3	0	Parallel	750	20	Cont.	72	8	X	2.86	5000
797-3	2	30	10	3	0	Parallel	750	20	Cont.	72	10	X	2.86	5000
797-4	2	30	10	3	0	Parallel	750	20	Cont.	72	8	K	2.86	5000
797-5	2	30	10	3	0	Parallel	750	20	Cont.	72	8	X	4.79	5000
798-1	2	30	10	3	0	Parallel	750	30	Cont.	72	8	X	2.86	5000
799-1	2	30	10	3	30	Parallel	Infinite	20	Cont.	72	8	X	2.86	3600
799-2	2	30	10	3	30	Parallel	Infinite	20	Cont.	72	8	X	2.86	5000
799-3	2	30	10	3	30	Parallel	Infinite	20	Cont.	72	10	X	2.86	5000
799-4	2	30	10	3	30	Parallel	Infinite	20	Cont.	72	8	K	2.86	5000
799-5	2	30	10	3	30	Parallel	Infinite	20	Cont.	72	8	X	4.79	5000
800-1	2	30	10	3	30	Parallel	Infinite	30	Cont.	72	8	X	2.86	5000
801-1	2	30	10	3	30	Parallel	1500	20	Cont.	72	8	X	2.86	3600
801-2	2	30	10	3	30	Parallel	1500	20	Cont.	72	8	X	2.86	5000
801-3	2	30	10	3	30	Parallel	1500	20	Cont.	72	10	X	2.86	5000

Model ID	Geometry									Cross-section		CF detail		Mat'l
	n_{span}	L/d ratio	s_g [ft]	n_{girder}	Support skew [deg]; Layout		R [ft]	s_{cf} [ft]	CF layout	d_w [in]	t_{deck} [in]	CF type	A_{cf} [in^2]	E_c [ksi]
801-4	2	30	10	3	30	Parallel	1500	20	Cont.	72	8	K	2.86	5000
801-5	2	30	10	3	30	Parallel	1500	20	Cont.	72	8	X	4.79	5000
802-1	2	30	10	3	30	Parallel	1500	30	Cont.	72	8	X	2.86	5000
803-1	2	30	10	3	30	Parallel	750	20	Cont.	72	8	X	2.86	3600
803-2	2	30	10	3	30	Parallel	750	20	Cont.	72	8	X	2.86	5000
803-3	2	30	10	3	30	Parallel	750	20	Cont.	72	10	X	2.86	5000
803-4	2	30	10	3	30	Parallel	750	20	Cont.	72	8	K	2.86	5000
803-5	2	30	10	3	30	Parallel	750	20	Cont.	72	8	X	4.79	5000
804-1	2	30	10	3	30	Parallel	750	30	Cont.	72	8	X	2.86	5000
805-1	2	30	10	3	60	Parallel	Infinite	20	Cont.	72	8	X	2.86	3600
805-2	2	30	10	3	60	Parallel	Infinite	20	Cont.	72	8	X	2.86	5000
805-3	2	30	10	3	60	Parallel	Infinite	20	Cont.	72	10	X	2.86	5000
805-4	2	30	10	3	60	Parallel	Infinite	20	Cont.	72	8	K	2.86	5000
805-5	2	30	10	3	60	Parallel	Infinite	20	Cont.	72	8	X	4.79	5000
806-1	2	30	10	3	60	Parallel	Infinite	30	Cont.	72	8	X	2.86	5000
807-1	2	30	10	3	60	Parallel	Infinite	20	Stag.	72	8	X	2.86	3600
807-2	2	30	10	3	60	Parallel	Infinite	20	Stag.	72	8	X	2.86	5000
807-3	2	30	10	3	60	Parallel	Infinite	20	Stag.	72	10	X	2.86	5000
807-4	2	30	10	3	60	Parallel	Infinite	20	Stag.	72	8	K	2.86	5000
807-5	2	30	10	3	60	Parallel	Infinite	20	Stag.	72	8	X	4.79	5000
808-1	2	30	10	3	60	Parallel	Infinite	30	Stag.	72	8	X	2.86	5000
809-1	2	30	10	3	60	Parallel	1500	20	Cont.	72	8	X	2.86	3600
809-2	2	30	10	3	60	Parallel	1500	20	Cont.	72	8	X	2.86	5000
809-3	2	30	10	3	60	Parallel	1500	20	Cont.	72	10	X	2.86	5000
809-4	2	30	10	3	60	Parallel	1500	20	Cont.	72	8	K	2.86	5000
809-5	2	30	10	3	60	Parallel	1500	20	Cont.	72	8	X	4.79	5000
810-1	2	30	10	3	60	Parallel	1500	30	Cont.	72	8	X	2.86	5000
811-1	2	30	10	3	60	Parallel	750	20	Cont.	72	8	X	2.86	3600
811-2	2	30	10	3	60	Parallel	750	20	Cont.	72	8	X	2.86	5000
811-3	2	30	10	3	60	Parallel	750	20	Cont.	72	10	X	2.86	5000
811-4	2	30	10	3	60	Parallel	750	20	Cont.	72	8	K	2.86	5000
811-5	2	30	10	3	60	Parallel	750	20	Cont.	72	8	X	4.79	5000
812-1	2	30	10	3	60	Parallel	750	30	Cont.	72	8	X	2.86	5000
813-1	2	30	10	3	60	Trap.	Infinite	20	Cont.	72	8	X	2.86	3600
813-2	2	30	10	3	60	Trap.	Infinite	20	Cont.	72	8	X	2.86	5000
813-3	2	30	10	3	60	Trap.	Infinite	20	Cont.	72	10	X	2.86	5000
813-4	2	30	10	3	60	Trap.	Infinite	20	Cont.	72	8	K	2.86	5000
813-5	2	30	10	3	60	Trap.	Infinite	20	Cont.	72	8	X	4.79	5000
814-1	2	30	10	3	60	Trap.	Infinite	30	Cont.	72	8	X	2.86	5000
815-1	2	30	10	3	60	Trap.	Infinite	20	Stag.	72	8	X	2.86	3600
815-2	2	30	10	3	60	Trap.	Infinite	20	Stag.	72	8	X	2.86	5000
815-3	2	30	10	3	60	Trap.	Infinite	20	Stag.	72	10	X	2.86	5000
815-4	2	30	10	3	60	Trap.	Infinite	20	Stag.	72	8	K	2.86	5000
815-5	2	30	10	3	60	Trap.	Infinite	20	Stag.	72	8	X	4.79	5000
816-1	2	30	10	3	60	Trap.	Infinite	30	Stag.	72	8	X	2.86	5000
817-1	2	30	10	3	60	Trap.	1500	20	Cont.	72	8	X	2.86	3600
817-2	2	30	10	3	60	Trap.	1500	20	Cont.	72	8	X	2.86	5000
817-3	2	30	10	3	60	Trap.	1500	20	Cont.	72	10	X	2.86	5000
817-4	2	30	10	3	60	Trap.	1500	20	Cont.	72	8	K	2.86	5000
817-5	2	30	10	3	60	Trap.	1500	20	Cont.	72	8	X	4.79	5000
818-1	2	30	10	3	60	Trap.	1500	30	Cont.	72	8	X	2.86	5000
819-1	2	30	10	3	60	Trap.	750	20	Cont.	72	8	X	2.86	3600
819-2	2	30	10	3	60	Trap.	750	20	Cont.	72	8	X	2.86	5000
819-3	2	30	10	3	60	Trap.	750	20	Cont.	72	10	X	2.86	5000
819-4	2	30	10	3	60	Trap.	750	20	Cont.	72	8	K	2.86	5000
819-5	2	30	10	3	60	Trap.	750	20	Cont.	72	8	X	4.79	5000
820-1	2	30	10	3	60	Trap.	750	30	Cont.	72	8	X	2.86	5000
821-1	2	30	10	5	0	Parallel	Infinite	20	Cont.	72	8	X	2.86	3600
821-2	2	30	10	5	0	Parallel	Infinite	20	Cont.	72	8	X	2.86	5000
821-3	2	30	10	5	0	Parallel	Infinite	20	Cont.	72	10	X	2.86	5000
821-4	2	30	10	5	0	Parallel	Infinite	20	Cont.	72	8	K	2.86	5000
821-5	2	30	10	5	0	Parallel	Infinite	20	Cont.	72	8	X	4.79	5000
822-1	2	30	10	5	0	Parallel	Infinite	30	Cont.	72	8	X	2.86	5000
823-1	2	30	10	5	0	Parallel	1500	20	Cont.	72	8	X	2.86	3600
823-2	2	30	10	5	0	Parallel	1500	20	Cont.	72	8	X	2.86	5000
823-3	2	30	10	5	0	Parallel	1500	20	Cont.	72	10	X	2.86	5000
823-4	2	30	10	5	0	Parallel	1500	20	Cont.	72	8	K	2.86	5000
823-5	2	30	10	5	0	Parallel	1500	20	Cont.	72	8	X	4.79	5000
824-1	2	30	10	5	0	Parallel	1500	30	Cont.	72	8	X	2.86	5000
825-1	2	30	10	5	0	Parallel	750	20	Cont.	72	8	X	2.86	3600
825-2	2	30	10	5	0	Parallel	750	20	Cont.	72	8	X	2.86	5000
825-3	2	30	10	5	0	Parallel	750	20	Cont.	72	10	X	2.86	5000
825-4	2	30	10	5	0	Parallel	750	20	Cont.	72	8	K	2.86	5000

Model ID	Geometry									Cross-section		CF detail		Mat'l
	n_{span}	L/d ratio	s_g [ft]	n_{girder}	Support skew [deg];	Layout	R [ft]	s_{cf} [ft]	CF layout	d_w [in]	t_{deck} [in]	CF type	A_{cf} [in^2]	E_c [ksi]
825-5	2	30	10	5	0	Parallel	750	20	Cont.	72	8	X	4.79	5000
826-1	2	30	10	5	0	Parallel	750	30	Cont.	72	8	X	2.86	5000
827-1	2	30	10	5	30	Parallel	Infinite	20	Cont.	72	8	X	2.86	3600
827-2	2	30	10	5	30	Parallel	Infinite	20	Cont.	72	8	X	2.86	5000
827-3	2	30	10	5	30	Parallel	Infinite	20	Cont.	72	10	X	2.86	5000
827-4	2	30	10	5	30	Parallel	Infinite	20	Cont.	72	8	K	2.86	5000
827-5	2	30	10	5	30	Parallel	Infinite	20	Cont.	72	8	X	4.79	5000
828-1	2	30	10	5	30	Parallel	Infinite	30	Cont.	72	8	X	2.86	5000
829-1	2	30	10	5	30	Parallel	1500	20	Cont.	72	8	X	2.86	3600
829-2	2	30	10	5	30	Parallel	1500	20	Cont.	72	8	X	2.86	5000
829-3	2	30	10	5	30	Parallel	1500	20	Cont.	72	10	X	2.86	5000
829-4	2	30	10	5	30	Parallel	1500	20	Cont.	72	8	K	2.86	5000
829-5	2	30	10	5	30	Parallel	1500	20	Cont.	72	8	X	4.79	5000
830-1	2	30	10	5	30	Parallel	1500	30	Cont.	72	8	X	2.86	5000
831-1	2	30	10	5	30	Parallel	750	20	Cont.	72	8	X	2.86	3600
831-2	2	30	10	5	30	Parallel	750	20	Cont.	72	8	X	2.86	5000
831-3	2	30	10	5	30	Parallel	750	20	Cont.	72	10	X	2.86	5000
831-4	2	30	10	5	30	Parallel	750	20	Cont.	72	8	K	2.86	5000
831-5	2	30	10	5	30	Parallel	750	20	Cont.	72	8	X	4.79	5000
832-1	2	30	10	5	30	Parallel	750	30	Cont.	72	8	X	2.86	5000
833-1	2	30	10	5	60	Parallel	Infinite	20	Cont.	72	8	X	2.86	3600
833-2	2	30	10	5	60	Parallel	Infinite	20	Cont.	72	8	X	2.86	5000
833-3	2	30	10	5	60	Parallel	Infinite	20	Cont.	72	10	X	2.86	5000
833-4	2	30	10	5	60	Parallel	Infinite	20	Cont.	72	8	K	2.86	5000
833-5	2	30	10	5	60	Parallel	Infinite	20	Cont.	72	8	X	4.79	5000
834-1	2	30	10	5	60	Parallel	Infinite	30	Cont.	72	8	X	2.86	5000
835-1	2	30	10	5	60	Parallel	Infinite	20	Stag.	72	8	X	2.86	3600
835-2	2	30	10	5	60	Parallel	Infinite	20	Stag.	72	8	X	2.86	5000
835-3	2	30	10	5	60	Parallel	Infinite	20	Stag.	72	10	X	2.86	5000
835-4	2	30	10	5	60	Parallel	Infinite	20	Stag.	72	8	K	2.86	5000
835-5	2	30	10	5	60	Parallel	Infinite	20	Stag.	72	8	X	4.79	5000
836-1	2	30	10	5	60	Parallel	Infinite	30	Stag.	72	8	X	2.86	5000
837-1	2	30	10	5	60	Parallel	1500	20	Cont.	72	8	X	2.86	3600
837-2	2	30	10	5	60	Parallel	1500	20	Cont.	72	8	X	2.86	5000
837-3	2	30	10	5	60	Parallel	1500	20	Cont.	72	10	X	2.86	5000
837-4	2	30	10	5	60	Parallel	1500	20	Cont.	72	8	K	2.86	5000
837-5	2	30	10	5	60	Parallel	1500	20	Cont.	72	8	X	4.79	5000
838-1	2	30	10	5	60	Parallel	1500	30	Cont.	72	8	X	2.86	5000
839-1	2	30	10	5	60	Parallel	750	20	Cont.	72	8	X	2.86	3600
839-2	2	30	10	5	60	Parallel	750	20	Cont.	72	8	X	2.86	5000
839-3	2	30	10	5	60	Parallel	750	20	Cont.	72	10	X	2.86	5000
839-4	2	30	10	5	60	Parallel	750	20	Cont.	72	8	K	2.86	5000
839-5	2	30	10	5	60	Parallel	750	20	Cont.	72	8	X	4.79	5000
840-1	2	30	10	5	60	Parallel	750	30	Cont.	72	8	X	2.86	5000
841-1	2	30	10	5	60	Trap.	Infinite	20	Cont.	72	8	X	2.86	3600
841-2	2	30	10	5	60	Trap.	Infinite	20	Cont.	72	8	X	2.86	5000
841-3	2	30	10	5	60	Trap.	Infinite	20	Cont.	72	10	X	2.86	5000
841-4	2	30	10	5	60	Trap.	Infinite	20	Cont.	72	8	K	2.86	5000
841-5	2	30	10	5	60	Trap.	Infinite	20	Cont.	72	8	X	4.79	5000
842-1	2	30	10	5	60	Trap.	Infinite	30	Cont.	72	8	X	2.86	5000
843-1	2	30	10	5	60	Trap.	Infinite	20	Stag.	72	8	X	2.86	3600
843-2	2	30	10	5	60	Trap.	Infinite	20	Stag.	72	8	X	2.86	5000
843-3	2	30	10	5	60	Trap.	Infinite	20	Stag.	72	10	X	2.86	5000
843-4	2	30	10	5	60	Trap.	Infinite	20	Stag.	72	8	K	2.86	5000
843-5	2	30	10	5	60	Trap.	Infinite	20	Stag.	72	8	X	4.79	5000
844-1	2	30	10	5	60	Trap.	Infinite	30	Stag.	72	8	X	2.86	5000
845-1	2	30	10	5	60	Trap.	1500	20	Cont.	72	8	X	2.86	3600
845-2	2	30	10	5	60	Trap.	1500	20	Cont.	72	8	X	2.86	5000
845-3	2	30	10	5	60	Trap.	1500	20	Cont.	72	10	X	2.86	5000
845-4	2	30	10	5	60	Trap.	1500	20	Cont.	72	8	K	2.86	5000
845-5	2	30	10	5	60	Trap.	1500	20	Cont.	72	8	X	4.79	5000
846-1	2	30	10	5	60	Trap.	1500	30	Cont.	72	8	X	2.86	5000
847-1	2	30	10	5	60	Trap.	750	20	Cont.	72	8	X	2.86	3600
847-2	2	30	10	5	60	Trap.	750	20	Cont.	72	8	X	2.86	5000
847-3	2	30	10	5	60	Trap.	750	20	Cont.	72	10	X	2.86	5000
847-4	2	30	10	5	60	Trap.	750	20	Cont.	72	8	K	2.86	5000
847-5	2	30	10	5	60	Trap.	750	20	Cont.	72	8	X	4.79	5000
848-1	2	30	10	5	60	Trap.	750	30	Cont.	72	8	X	2.86	5000
849-1	2	30	10	7	0	Parallel	Infinite	20	Cont.	72	8	X	2.86	3600
849-2	2	30	10	7	0	Parallel	Infinite	20	Cont.	72	8	X	2.86	5000
849-3	2	30	10	7	0	Parallel	Infinite	20	Cont.	72	10	X	2.86	5000
849-4	2	30	10	7	0	Parallel	Infinite	20	Cont.	72	8	K	2.86	5000
849-5	2	30	10	7	0	Parallel	Infinite	20	Cont.	72	8	X	4.79	5000

Model ID	Geometry									Cross-section		CF detail		Mat'l
	n_{span}	L/d ratio	s_g [ft]	n_{girder}	Support skew [deg];	Layout	R [ft]	s_{cf} [ft]	CF layout	d_w [in]	t_{deck} [in]	CF type	A_{cf} [in^2]	E_c [ksi]
850-1	2	30	10	7	0	Parallel	Infinite	30	Cont.	72	8	X	2.86	5000
851-1	2	30	10	7	0	Parallel	1500	20	Cont.	72	8	X	2.86	3600
851-2	2	30	10	7	0	Parallel	1500	20	Cont.	72	8	X	2.86	5000
851-3	2	30	10	7	0	Parallel	1500	20	Cont.	72	10	X	2.86	5000
851-4	2	30	10	7	0	Parallel	1500	20	Cont.	72	8	K	2.86	5000
851-5	2	30	10	7	0	Parallel	1500	20	Cont.	72	8	X	4.79	5000
852-1	2	30	10	7	0	Parallel	1500	30	Cont.	72	8	X	2.86	5000
853-1	2	30	10	7	0	Parallel	750	20	Cont.	72	8	X	2.86	3600
853-2	2	30	10	7	0	Parallel	750	20	Cont.	72	8	X	2.86	5000
853-3	2	30	10	7	0	Parallel	750	20	Cont.	72	10	X	2.86	5000
853-4	2	30	10	7	0	Parallel	750	20	Cont.	72	8	K	2.86	5000
853-5	2	30	10	7	0	Parallel	750	20	Cont.	72	8	X	4.79	5000
854-1	2	30	10	7	0	Parallel	750	30	Cont.	72	8	X	2.86	5000
855-1	2	30	10	7	30	Parallel	Infinite	20	Cont.	72	8	X	2.86	3600
855-2	2	30	10	7	30	Parallel	Infinite	20	Cont.	72	8	X	2.86	5000
855-3	2	30	10	7	30	Parallel	Infinite	20	Cont.	72	10	X	2.86	5000
855-4	2	30	10	7	30	Parallel	Infinite	20	Cont.	72	8	K	2.86	5000
855-5	2	30	10	7	30	Parallel	Infinite	20	Cont.	72	8	X	4.79	5000
856-1	2	30	10	7	30	Parallel	Infinite	30	Cont.	72	8	X	2.86	5000
857-1	2	30	10	7	30	Parallel	1500	20	Cont.	72	8	X	2.86	3600
857-2	2	30	10	7	30	Parallel	1500	20	Cont.	72	8	X	2.86	5000
857-3	2	30	10	7	30	Parallel	1500	20	Cont.	72	10	X	2.86	5000
857-4	2	30	10	7	30	Parallel	1500	20	Cont.	72	8	K	2.86	5000
857-5	2	30	10	7	30	Parallel	1500	20	Cont.	72	8	X	4.79	5000
858-1	2	30	10	7	30	Parallel	1500	30	Cont.	72	8	X	2.86	5000
859-1	2	30	10	7	30	Parallel	750	20	Cont.	72	8	X	2.86	3600
859-2	2	30	10	7	30	Parallel	750	20	Cont.	72	8	X	2.86	5000
859-3	2	30	10	7	30	Parallel	750	20	Cont.	72	10	X	2.86	5000
859-4	2	30	10	7	30	Parallel	750	20	Cont.	72	8	K	2.86	5000
859-5	2	30	10	7	30	Parallel	750	20	Cont.	72	8	X	4.79	5000
860-1	2	30	10	7	30	Parallel	750	30	Cont.	72	8	X	2.86	5000
861-1	2	30	10	7	60	Parallel	Infinite	20	Cont.	72	8	X	2.86	3600
861-2	2	30	10	7	60	Parallel	Infinite	20	Cont.	72	8	X	2.86	5000
861-3	2	30	10	7	60	Parallel	Infinite	20	Cont.	72	10	X	2.86	5000
861-4	2	30	10	7	60	Parallel	Infinite	20	Cont.	72	8	K	2.86	5000
861-5	2	30	10	7	60	Parallel	Infinite	20	Cont.	72	8	X	4.79	5000
862-1	2	30	10	7	60	Parallel	Infinite	30	Cont.	72	8	X	2.86	5000
863-1	2	30	10	7	60	Parallel	Infinite	20	Stag.	72	8	X	2.86	3600
863-2	2	30	10	7	60	Parallel	Infinite	20	Stag.	72	8	X	2.86	5000
863-3	2	30	10	7	60	Parallel	Infinite	20	Stag.	72	10	X	2.86	5000
863-4	2	30	10	7	60	Parallel	Infinite	20	Stag.	72	8	K	2.86	5000
863-5	2	30	10	7	60	Parallel	Infinite	20	Stag.	72	8	X	4.79	5000
864-1	2	30	10	7	60	Parallel	Infinite	30	Stag.	72	8	X	2.86	5000
865-1	2	30	10	7	60	Parallel	1500	20	Cont.	72	8	X	2.86	3600
865-2	2	30	10	7	60	Parallel	1500	20	Cont.	72	8	X	2.86	5000
865-3	2	30	10	7	60	Parallel	1500	20	Cont.	72	10	X	2.86	5000
865-4	2	30	10	7	60	Parallel	1500	20	Cont.	72	8	K	2.86	5000
865-5	2	30	10	7	60	Parallel	1500	20	Cont.	72	8	X	4.79	5000
866-1	2	30	10	7	60	Parallel	1500	30	Cont.	72	8	X	2.86	5000
867-1	2	30	10	7	60	Parallel	750	20	Cont.	72	8	X	2.86	3600
867-2	2	30	10	7	60	Parallel	750	20	Cont.	72	8	X	2.86	5000
867-3	2	30	10	7	60	Parallel	750	20	Cont.	72	10	X	2.86	5000
867-4	2	30	10	7	60	Parallel	750	20	Cont.	72	8	K	2.86	5000
867-5	2	30	10	7	60	Parallel	750	20	Cont.	72	8	X	4.79	5000
868-1	2	30	10	7	60	Parallel	750	30	Cont.	72	8	X	2.86	5000
869-1	2	30	10	7	60	Trap.	Infinite	20	Cont.	72	8	X	2.86	3600
869-2	2	30	10	7	60	Trap.	Infinite	20	Cont.	72	8	X	2.86	5000
869-3	2	30	10	7	60	Trap.	Infinite	20	Cont.	72	10	X	2.86	5000
869-4	2	30	10	7	60	Trap.	Infinite	20	Cont.	72	8	K	2.86	5000
869-5	2	30	10	7	60	Trap.	Infinite	20	Cont.	72	8	X	4.79	5000
870-1	2	30	10	7	60	Trap.	Infinite	30	Cont.	72	8	X	2.86	5000
871-1	2	30	10	7	60	Trap.	Infinite	20	Stag.	72	8	X	2.86	3600
871-2	2	30	10	7	60	Trap.	Infinite	20	Stag.	72	8	X	2.86	5000
871-3	2	30	10	7	60	Trap.	Infinite	20	Stag.	72	10	X	2.86	5000
871-4	2	30	10	7	60	Trap.	Infinite	20	Stag.	72	8	K	2.86	5000
871-5	2	30	10	7	60	Trap.	Infinite	20	Stag.	72	8	X	4.79	5000
872-1	2	30	10	7	60	Trap.	Infinite	30	Stag.	72	8	X	2.86	5000
873-1	2	30	10	7	60	Trap.	1500	20	Cont.	72	8	X	2.86	3600
873-2	2	30	10	7	60	Trap.	1500	20	Cont.	72	8	X	2.86	5000
873-3	2	30	10	7	60	Trap.	1500	20	Cont.	72	10	X	2.86	5000
873-4	2	30	10	7	60	Trap.	1500	20	Cont.	72	8	K	2.86	5000
873-5	2	30	10	7	60	Trap.	1500	20	Cont.	72	8	X	4.79	5000
874-1	2	30	10	7	60	Trap.	1500	30	Cont.	72	8	X	2.86	5000

Model ID	Geometry									Cross-section		CF detail		Mat'l
	n_{span}	L/d ratio	s_g [ft]	n_{girder}	Support skew [deg]; Layout		R [ft]	s_{cf} [ft]	CF layout	d_w [in]	t_{deck} [in]	CF type	A_{cf} [in^2]	E_c [ksi]
875-1	2	30	10	7	60	Trap.	750	20	Cont.	72	8	X	2.86	3600
875-2	2	30	10	7	60	Trap.	750	20	Cont.	72	8	X	2.86	5000
875-3	2	30	10	7	60	Trap.	750	20	Cont.	72	10	X	2.86	5000
875-4	2	30	10	7	60	Trap.	750	20	Cont.	72	8	K	2.86	5000
875-5	2	30	10	7	60	Trap.	750	20	Cont.	72	8	X	4.79	5000
876-1	2	30	10	7	60	Trap.	750	30	Cont.	72	8	X	2.86	5000
877-1	2	30	6	3	0	Parallel	Infinite	20	Cont.	96	8	X	2.86	3600
877-2	2	30	6	3	0	Parallel	Infinite	20	Cont.	96	8	X	2.86	5000
877-3	2	30	6	3	0	Parallel	Infinite	20	Cont.	96	10	X	2.86	5000
877-4	2	30	6	3	0	Parallel	Infinite	20	Cont.	96	8	K	2.86	5000
877-5	2	30	6	3	0	Parallel	Infinite	20	Cont.	96	8	X	4.79	5000
878-1	2	30	6	3	0	Parallel	Infinite	30	Cont.	96	8	X	2.86	5000
879-1	2	30	6	3	0	Parallel	1500	20	Cont.	96	8	X	2.86	3600
879-2	2	30	6	3	0	Parallel	1500	20	Cont.	96	8	X	2.86	5000
879-3	2	30	6	3	0	Parallel	1500	20	Cont.	96	10	X	2.86	5000
879-4	2	30	6	3	0	Parallel	1500	20	Cont.	96	8	K	2.86	5000
879-5	2	30	6	3	0	Parallel	1500	20	Cont.	96	8	X	4.79	5000
880-1	2	30	6	3	0	Parallel	1500	30	Cont.	96	8	X	2.86	5000
881-1	2	30	6	3	0	Parallel	750	20	Cont.	96	8	X	2.86	3600
881-2	2	30	6	3	0	Parallel	750	20	Cont.	96	8	X	2.86	5000
881-3	2	30	6	3	0	Parallel	750	20	Cont.	96	10	X	2.86	5000
881-4	2	30	6	3	0	Parallel	750	20	Cont.	96	8	K	2.86	5000
881-5	2	30	6	3	0	Parallel	750	20	Cont.	96	8	X	4.79	5000
882-1	2	30	6	3	0	Parallel	750	30	Cont.	96	8	X	2.86	5000
883-1	2	30	6	3	30	Parallel	Infinite	20	Cont.	96	8	X	2.86	3600
883-2	2	30	6	3	30	Parallel	Infinite	20	Cont.	96	8	X	2.86	5000
883-3	2	30	6	3	30	Parallel	Infinite	20	Cont.	96	10	X	2.86	5000
883-4	2	30	6	3	30	Parallel	Infinite	20	Cont.	96	8	K	2.86	5000
883-5	2	30	6	3	30	Parallel	Infinite	20	Cont.	96	8	X	4.79	5000
884-1	2	30	6	3	30	Parallel	Infinite	30	Cont.	96	8	X	2.86	5000
885-1	2	30	6	3	30	Parallel	1500	20	Cont.	96	8	X	2.86	3600
885-2	2	30	6	3	30	Parallel	1500	20	Cont.	96	8	X	2.86	5000
885-3	2	30	6	3	30	Parallel	1500	20	Cont.	96	10	X	2.86	5000
885-4	2	30	6	3	30	Parallel	1500	20	Cont.	96	8	K	2.86	5000
885-5	2	30	6	3	30	Parallel	1500	20	Cont.	96	8	X	4.79	5000
886-1	2	30	6	3	30	Parallel	1500	30	Cont.	96	8	X	2.86	5000
887-1	2	30	6	3	30	Parallel	750	20	Cont.	96	8	X	2.86	3600
887-2	2	30	6	3	30	Parallel	750	20	Cont.	96	8	X	2.86	5000
887-3	2	30	6	3	30	Parallel	750	20	Cont.	96	10	X	2.86	5000
887-4	2	30	6	3	30	Parallel	750	20	Cont.	96	8	K	2.86	5000
887-5	2	30	6	3	30	Parallel	750	20	Cont.	96	8	X	4.79	5000
888-1	2	30	6	3	30	Parallel	750	30	Cont.	96	8	X	2.86	5000
889-1	2	30	6	3	60	Parallel	Infinite	20	Cont.	96	8	X	2.86	3600
889-2	2	30	6	3	60	Parallel	Infinite	20	Cont.	96	8	X	2.86	5000
889-3	2	30	6	3	60	Parallel	Infinite	20	Cont.	96	10	X	2.86	5000
889-4	2	30	6	3	60	Parallel	Infinite	20	Cont.	96	8	K	2.86	5000
889-5	2	30	6	3	60	Parallel	Infinite	20	Cont.	96	8	X	4.79	5000
890-1	2	30	6	3	60	Parallel	Infinite	30	Cont.	96	8	X	2.86	5000
891-1	2	30	6	3	60	Parallel	Infinite	20	Stag.	96	8	X	2.86	3600
891-2	2	30	6	3	60	Parallel	Infinite	20	Stag.	96	8	X	2.86	5000
891-3	2	30	6	3	60	Parallel	Infinite	20	Stag.	96	10	X	2.86	5000
891-4	2	30	6	3	60	Parallel	Infinite	20	Stag.	96	8	K	2.86	5000
891-5	2	30	6	3	60	Parallel	Infinite	20	Stag.	96	8	X	4.79	5000
892-1	2	30	6	3	60	Parallel	Infinite	30	Stag.	96	8	X	2.86	5000
893-1	2	30	6	3	60	Parallel	1500	20	Cont.	96	8	X	2.86	3600
893-2	2	30	6	3	60	Parallel	1500	20	Cont.	96	8	X	2.86	5000
893-3	2	30	6	3	60	Parallel	1500	20	Cont.	96	10	X	2.86	5000
893-4	2	30	6	3	60	Parallel	1500	20	Cont.	96	8	K	2.86	5000
893-5	2	30	6	3	60	Parallel	1500	20	Cont.	96	8	X	4.79	5000
894-1	2	30	6	3	60	Parallel	1500	30	Cont.	96	8	X	2.86	5000
895-1	2	30	6	3	60	Parallel	750	20	Cont.	96	8	X	2.86	3600
895-2	2	30	6	3	60	Parallel	750	20	Cont.	96	8	X	2.86	5000
895-3	2	30	6	3	60	Parallel	750	20	Cont.	96	10	X	2.86	5000
895-4	2	30	6	3	60	Parallel	750	20	Cont.	96	8	K	2.86	5000
895-5	2	30	6	3	60	Parallel	750	20	Cont.	96	8	X	4.79	5000
896-1	2	30	6	3	60	Parallel	750	30	Cont.	96	8	X	2.86	5000
897-1	2	30	6	3	60	Trap.	Infinite	20	Cont.	96	8	X	2.86	3600
897-2	2	30	6	3	60	Trap.	Infinite	20	Cont.	96	8	X	2.86	5000
897-3	2	30	6	3	60	Trap.	Infinite	20	Cont.	96	10	X	2.86	5000
897-4	2	30	6	3	60	Trap.	Infinite	20	Cont.	96	8	K	2.86	5000
897-5	2	30	6	3	60	Trap.	Infinite	20	Cont.	96	8	X	4.79	5000
898-1	2	30	6	3	60	Trap.	Infinite	30	Cont.	96	8	X	2.86	5000
899-1	2	30	6	3	60	Trap.	Infinite	20	Stag.	96	8	X	2.86	3600

Model ID	Geometry									Cross-section		CF detail		Mat'l
	n_{span}	L/d ratio	s_g [ft]	n_{girder}	Support skew [deg];	Layout	R [ft]	s_{cf} [ft]	CF layout	d_w [in]	t_{deck} [in]	CF type	A_{cf} [in^2]	E_c [ksi]
899-2	2	30	6	3	60	Trap.	Infinite	20	Stag.	96	8	X	2.86	5000
899-3	2	30	6	3	60	Trap.	Infinite	20	Stag.	96	10	X	2.86	5000
899-4	2	30	6	3	60	Trap.	Infinite	20	Stag.	96	8	K	2.86	5000
899-5	2	30	6	3	60	Trap.	Infinite	20	Stag.	96	8	X	4.79	5000
900-1	2	30	6	3	60	Trap.	Infinite	30	Stag.	96	8	X	2.86	5000
901-1	2	30	6	3	60	Trap.	1500	20	Cont.	96	8	X	2.86	3600
901-2	2	30	6	3	60	Trap.	1500	20	Cont.	96	8	X	2.86	5000
901-3	2	30	6	3	60	Trap.	1500	20	Cont.	96	10	X	2.86	5000
901-4	2	30	6	3	60	Trap.	1500	20	Cont.	96	8	K	2.86	5000
901-5	2	30	6	3	60	Trap.	1500	20	Cont.	96	8	X	4.79	5000
902-1	2	30	6	3	60	Trap.	1500	30	Cont.	96	8	X	2.86	5000
903-1	2	30	6	3	60	Trap.	750	20	Cont.	96	8	X	2.86	3600
903-2	2	30	6	3	60	Trap.	750	20	Cont.	96	8	X	2.86	5000
903-3	2	30	6	3	60	Trap.	750	20	Cont.	96	10	X	2.86	5000
903-4	2	30	6	3	60	Trap.	750	20	Cont.	96	8	K	2.86	5000
903-5	2	30	6	3	60	Trap.	750	20	Cont.	96	8	X	4.79	5000
904-1	2	30	6	3	60	Trap.	750	30	Cont.	96	8	X	2.86	5000
905-1	2	30	6	5	0	Parallel	Infinite	20	Cont.	96	8	X	2.86	3600
905-2	2	30	6	5	0	Parallel	Infinite	20	Cont.	96	8	X	2.86	5000
905-3	2	30	6	5	0	Parallel	Infinite	20	Cont.	96	10	X	2.86	5000
905-4	2	30	6	5	0	Parallel	Infinite	20	Cont.	96	8	K	2.86	5000
905-5	2	30	6	5	0	Parallel	Infinite	20	Cont.	96	8	X	4.79	5000
906-1	2	30	6	5	0	Parallel	Infinite	30	Cont.	96	8	X	2.86	5000
907-1	2	30	6	5	0	Parallel	1500	20	Cont.	96	8	X	2.86	3600
907-2	2	30	6	5	0	Parallel	1500	20	Cont.	96	8	X	2.86	5000
907-3	2	30	6	5	0	Parallel	1500	20	Cont.	96	10	X	2.86	5000
907-4	2	30	6	5	0	Parallel	1500	20	Cont.	96	8	K	2.86	5000
907-5	2	30	6	5	0	Parallel	1500	20	Cont.	96	8	X	4.79	5000
908-1	2	30	6	5	0	Parallel	1500	30	Cont.	96	8	X	2.86	5000
909-1	2	30	6	5	0	Parallel	750	20	Cont.	96	8	X	2.86	3600
909-2	2	30	6	5	0	Parallel	750	20	Cont.	96	8	X	2.86	5000
909-3	2	30	6	5	0	Parallel	750	20	Cont.	96	10	X	2.86	5000
909-4	2	30	6	5	0	Parallel	750	20	Cont.	96	8	K	2.86	5000
909-5	2	30	6	5	0	Parallel	750	20	Cont.	96	8	X	4.79	5000
910-1	2	30	6	5	0	Parallel	750	30	Cont.	96	8	X	2.86	5000
911-1	2	30	6	5	30	Parallel	Infinite	20	Cont.	96	8	X	2.86	3600
911-2	2	30	6	5	30	Parallel	Infinite	20	Cont.	96	8	X	2.86	5000
911-3	2	30	6	5	30	Parallel	Infinite	20	Cont.	96	10	X	2.86	5000
911-4	2	30	6	5	30	Parallel	Infinite	20	Cont.	96	8	K	2.86	5000
911-5	2	30	6	5	30	Parallel	Infinite	20	Cont.	96	8	X	4.79	5000
912-1	2	30	6	5	30	Parallel	Infinite	30	Cont.	96	8	X	2.86	5000
913-1	2	30	6	5	30	Parallel	1500	20	Cont.	96	8	X	2.86	3600
913-2	2	30	6	5	30	Parallel	1500	20	Cont.	96	8	X	2.86	5000
913-3	2	30	6	5	30	Parallel	1500	20	Cont.	96	10	X	2.86	5000
913-4	2	30	6	5	30	Parallel	1500	20	Cont.	96	8	K	2.86	5000
913-5	2	30	6	5	30	Parallel	1500	20	Cont.	96	8	X	4.79	5000
914-1	2	30	6	5	30	Parallel	1500	30	Cont.	96	8	X	2.86	5000
915-1	2	30	6	5	30	Parallel	750	20	Cont.	96	8	X	2.86	3600
915-2	2	30	6	5	30	Parallel	750	20	Cont.	96	8	X	2.86	5000
915-3	2	30	6	5	30	Parallel	750	20	Cont.	96	10	X	2.86	5000
915-4	2	30	6	5	30	Parallel	750	20	Cont.	96	8	K	2.86	5000
915-5	2	30	6	5	30	Parallel	750	20	Cont.	96	8	X	4.79	5000
916-1	2	30	6	5	30	Parallel	750	30	Cont.	96	8	X	2.86	5000
917-1	2	30	6	5	60	Parallel	Infinite	20	Cont.	96	8	X	2.86	3600
917-2	2	30	6	5	60	Parallel	Infinite	20	Cont.	96	8	X	2.86	5000
917-3	2	30	6	5	60	Parallel	Infinite	20	Cont.	96	10	X	2.86	5000
917-4	2	30	6	5	60	Parallel	Infinite	20	Cont.	96	8	K	2.86	5000
917-5	2	30	6	5	60	Parallel	Infinite	20	Cont.	96	8	X	4.79	5000
918-1	2	30	6	5	60	Parallel	Infinite	30	Cont.	96	8	X	2.86	5000
919-1	2	30	6	5	60	Parallel	Infinite	20	Stag.	96	8	X	2.86	3600
919-2	2	30	6	5	60	Parallel	Infinite	20	Stag.	96	8	X	2.86	5000
919-3	2	30	6	5	60	Parallel	Infinite	20	Stag.	96	10	X	2.86	5000
919-4	2	30	6	5	60	Parallel	Infinite	20	Stag.	96	8	K	2.86	5000
919-5	2	30	6	5	60	Parallel	Infinite	20	Stag.	96	8	X	4.79	5000
920-1	2	30	6	5	60	Parallel	Infinite	30	Stag.	96	8	X	2.86	5000
921-1	2	30	6	5	60	Parallel	1500	20	Cont.	96	8	X	2.86	3600
921-2	2	30	6	5	60	Parallel	1500	20	Cont.	96	8	X	2.86	5000
921-3	2	30	6	5	60	Parallel	1500	20	Cont.	96	10	X	2.86	5000
921-4	2	30	6	5	60	Parallel	1500	20	Cont.	96	8	K	2.86	5000
921-5	2	30	6	5	60	Parallel	1500	20	Cont.	96	8	X	4.79	5000
922-1	2	30	6	5	60	Parallel	1500	30	Cont.	96	8	X	2.86	5000
923-1	2	30	6	5	60	Parallel	750	20	Cont.	96	8	X	2.86	3600
923-2	2	30	6	5	60	Parallel	750	20	Cont.	96	8	X	2.86	5000

Model ID	Geometry									Cross-section		CF detail		Mat'l
	n_{span}	L/d ratio	s_g [ft]	n_{girder}	Support skew [deg];	Layout	R [ft]	s_{cf} [ft]	CF layout	d_w [in]	t_{deck} [in]	CF type	A_{cf} [in^2]	E_c [ksi]
923-3	2	30	6	5	60	Parallel	750	20	Cont.	96	10	X	2.86	5000
923-4	2	30	6	5	60	Parallel	750	20	Cont.	96	8	K	2.86	5000
923-5	2	30	6	5	60	Parallel	750	20	Cont.	96	8	X	4.79	5000
924-1	2	30	6	5	60	Parallel	750	30	Cont.	96	8	X	2.86	5000
925-1	2	30	6	5	60	Trap.	Infinite	20	Cont.	96	8	X	2.86	3600
925-2	2	30	6	5	60	Trap.	Infinite	20	Cont.	96	8	X	2.86	5000
925-3	2	30	6	5	60	Trap.	Infinite	20	Cont.	96	10	X	2.86	5000
925-4	2	30	6	5	60	Trap.	Infinite	20	Cont.	96	8	K	2.86	5000
925-5	2	30	6	5	60	Trap.	Infinite	20	Cont.	96	8	X	4.79	5000
926-1	2	30	6	5	60	Trap.	Infinite	30	Cont.	96	8	X	2.86	5000
927-1	2	30	6	5	60	Trap.	Infinite	20	Stag.	96	8	X	2.86	3600
927-2	2	30	6	5	60	Trap.	Infinite	20	Stag.	96	8	X	2.86	5000
927-3	2	30	6	5	60	Trap.	Infinite	20	Stag.	96	10	X	2.86	5000
927-4	2	30	6	5	60	Trap.	Infinite	20	Stag.	96	8	K	2.86	5000
927-5	2	30	6	5	60	Trap.	Infinite	20	Stag.	96	8	X	4.79	5000
928-1	2	30	6	5	60	Trap.	Infinite	30	Stag.	96	8	X	2.86	5000
929-1	2	30	6	5	60	Trap.	1500	20	Cont.	96	8	X	2.86	3600
929-2	2	30	6	5	60	Trap.	1500	20	Cont.	96	8	X	2.86	5000
929-3	2	30	6	5	60	Trap.	1500	20	Cont.	96	10	X	2.86	5000
929-4	2	30	6	5	60	Trap.	1500	20	Cont.	96	8	K	2.86	5000
929-5	2	30	6	5	60	Trap.	1500	20	Cont.	96	8	X	4.79	5000
930-1	2	30	6	5	60	Trap.	1500	30	Cont.	96	8	X	2.86	5000
931-1	2	30	6	5	60	Trap.	750	20	Cont.	96	8	X	2.86	3600
931-2	2	30	6	5	60	Trap.	750	20	Cont.	96	8	X	2.86	5000
931-3	2	30	6	5	60	Trap.	750	20	Cont.	96	10	X	2.86	5000
931-4	2	30	6	5	60	Trap.	750	20	Cont.	96	8	K	2.86	5000
931-5	2	30	6	5	60	Trap.	750	20	Cont.	96	8	X	4.79	5000
932-1	2	30	6	5	60	Trap.	750	30	Cont.	96	8	X	2.86	5000
933-1	2	30	6	7	0	Parallel	Infinite	20	Cont.	96	8	X	2.86	3600
933-2	2	30	6	7	0	Parallel	Infinite	20	Cont.	96	8	X	2.86	5000
933-3	2	30	6	7	0	Parallel	Infinite	20	Cont.	96	10	X	2.86	5000
933-4	2	30	6	7	0	Parallel	Infinite	20	Cont.	96	8	K	2.86	5000
933-5	2	30	6	7	0	Parallel	Infinite	20	Cont.	96	8	X	4.79	5000
934-1	2	30	6	7	0	Parallel	Infinite	30	Cont.	96	8	X	2.86	5000
935-1	2	30	6	7	0	Parallel	1500	20	Cont.	96	8	X	2.86	3600
935-2	2	30	6	7	0	Parallel	1500	20	Cont.	96	8	X	2.86	5000
935-3	2	30	6	7	0	Parallel	1500	20	Cont.	96	10	X	2.86	5000
935-4	2	30	6	7	0	Parallel	1500	20	Cont.	96	8	K	2.86	5000
935-5	2	30	6	7	0	Parallel	1500	20	Cont.	96	8	X	4.79	5000
936-1	2	30	6	7	0	Parallel	1500	30	Cont.	96	8	X	2.86	5000
937-1	2	30	6	7	0	Parallel	750	20	Cont.	96	8	X	2.86	3600
937-2	2	30	6	7	0	Parallel	750	20	Cont.	96	8	X	2.86	5000
937-3	2	30	6	7	0	Parallel	750	20	Cont.	96	10	X	2.86	5000
937-4	2	30	6	7	0	Parallel	750	20	Cont.	96	8	K	2.86	5000
937-5	2	30	6	7	0	Parallel	750	20	Cont.	96	8	X	4.79	5000
938-1	2	30	6	7	0	Parallel	750	30	Cont.	96	8	X	2.86	5000
939-1	2	30	6	7	30	Parallel	Infinite	20	Cont.	96	8	X	2.86	3600
939-2	2	30	6	7	30	Parallel	Infinite	20	Cont.	96	8	X	2.86	5000
939-3	2	30	6	7	30	Parallel	Infinite	20	Cont.	96	10	X	2.86	5000
939-4	2	30	6	7	30	Parallel	Infinite	20	Cont.	96	8	K	2.86	5000
939-5	2	30	6	7	30	Parallel	Infinite	20	Cont.	96	8	X	4.79	5000
940-1	2	30	6	7	30	Parallel	Infinite	30	Cont.	96	8	X	2.86	5000
941-1	2	30	6	7	30	Parallel	1500	20	Cont.	96	8	X	2.86	3600
941-2	2	30	6	7	30	Parallel	1500	20	Cont.	96	8	X	2.86	5000
941-3	2	30	6	7	30	Parallel	1500	20	Cont.	96	10	X	2.86	5000
941-4	2	30	6	7	30	Parallel	1500	20	Cont.	96	8	K	2.86	5000
941-5	2	30	6	7	30	Parallel	1500	20	Cont.	96	8	X	4.79	5000
942-1	2	30	6	7	30	Parallel	1500	30	Cont.	96	8	X	2.86	5000
943-1	2	30	6	7	30	Parallel	750	20	Cont.	96	8	X	2.86	3600
943-2	2	30	6	7	30	Parallel	750	20	Cont.	96	8	X	2.86	5000
943-3	2	30	6	7	30	Parallel	750	20	Cont.	96	10	X	2.86	5000
943-4	2	30	6	7	30	Parallel	750	20	Cont.	96	8	K	2.86	5000
943-5	2	30	6	7	30	Parallel	750	20	Cont.	96	8	X	4.79	5000
944-1	2	30	6	7	30	Parallel	750	30	Cont.	96	8	X	2.86	5000
945-1	2	30	6	7	60	Parallel	Infinite	20	Cont.	96	8	X	2.86	3600
945-2	2	30	6	7	60	Parallel	Infinite	20	Cont.	96	8	X	2.86	5000
945-3	2	30	6	7	60	Parallel	Infinite	20	Cont.	96	10	X	2.86	5000
945-4	2	30	6	7	60	Parallel	Infinite	20	Cont.	96	8	K	2.86	5000
945-5	2	30	6	7	60	Parallel	Infinite	20	Cont.	96	8	X	4.79	5000
946-1	2	30	6	7	60	Parallel	Infinite	30	Cont.	96	8	X	2.86	5000
947-1	2	30	6	7	60	Parallel	Infinite	20	Stag.	96	8	X	2.86	3600
947-2	2	30	6	7	60	Parallel	Infinite	20	Stag.	96	8	X	2.86	5000
947-3	2	30	6	7	60	Parallel	Infinite	20	Stag.	96	10	X	2.86	5000

Model ID	Geometry									Cross-section		CF detail		Mat'l
	n_{span}	L/d ratio	s_g [ft]	n_{girder}	Support skew [deg]; Layout		R [ft]	s_{cf} [ft]	CF layout	d_w [in]	t_{deck} [in]	CF type	A_{cf} [in^2]	E_c [ksi]
947-4	2	30	6	7	60	Parallel	Infinite	20	Stag.	96	8	K	2.86	5000
947-5	2	30	6	7	60	Parallel	Infinite	20	Stag.	96	8	X	4.79	5000
948-1	2	30	6	7	60	Parallel	Infinite	30	Stag.	96	8	X	2.86	5000
949-1	2	30	6	7	60	Parallel	1500	20	Cont.	96	8	X	2.86	3600
949-2	2	30	6	7	60	Parallel	1500	20	Cont.	96	8	X	2.86	5000
949-3	2	30	6	7	60	Parallel	1500	20	Cont.	96	10	X	2.86	5000
949-4	2	30	6	7	60	Parallel	1500	20	Cont.	96	8	K	2.86	5000
949-5	2	30	6	7	60	Parallel	1500	20	Cont.	96	8	X	4.79	5000
950-1	2	30	6	7	60	Parallel	1500	30	Cont.	96	8	X	2.86	5000
951-1	2	30	6	7	60	Parallel	750	20	Cont.	96	8	X	2.86	3600
951-2	2	30	6	7	60	Parallel	750	20	Cont.	96	8	X	2.86	5000
951-3	2	30	6	7	60	Parallel	750	20	Cont.	96	10	X	2.86	5000
951-4	2	30	6	7	60	Parallel	750	20	Cont.	96	8	K	2.86	5000
951-5	2	30	6	7	60	Parallel	750	20	Cont.	96	8	X	4.79	5000
952-1	2	30	6	7	60	Parallel	750	30	Cont.	96	8	X	2.86	5000
953-1	2	30	6	7	60	Trap.	Infinite	20	Cont.	96	8	X	2.86	3600
953-2	2	30	6	7	60	Trap.	Infinite	20	Cont.	96	8	X	2.86	5000
953-3	2	30	6	7	60	Trap.	Infinite	20	Cont.	96	10	X	2.86	5000
953-4	2	30	6	7	60	Trap.	Infinite	20	Cont.	96	8	K	2.86	5000
953-5	2	30	6	7	60	Trap.	Infinite	20	Cont.	96	8	X	4.79	5000
954-1	2	30	6	7	60	Trap.	Infinite	30	Cont.	96	8	X	2.86	5000
955-1	2	30	6	7	60	Trap.	Infinite	20	Stag.	96	8	X	2.86	3600
955-2	2	30	6	7	60	Trap.	Infinite	20	Stag.	96	8	X	2.86	5000
955-3	2	30	6	7	60	Trap.	Infinite	20	Stag.	96	10	X	2.86	5000
955-4	2	30	6	7	60	Trap.	Infinite	20	Stag.	96	8	K	2.86	5000
955-5	2	30	6	7	60	Trap.	Infinite	20	Stag.	96	8	X	4.79	5000
956-1	2	30	6	7	60	Trap.	Infinite	30	Stag.	96	8	X	2.86	5000
957-1	2	30	6	7	60	Trap.	1500	20	Cont.	96	8	X	2.86	3600
957-2	2	30	6	7	60	Trap.	1500	20	Cont.	96	8	X	2.86	5000
957-3	2	30	6	7	60	Trap.	1500	20	Cont.	96	10	X	2.86	5000
957-4	2	30	6	7	60	Trap.	1500	20	Cont.	96	8	K	2.86	5000
957-5	2	30	6	7	60	Trap.	1500	20	Cont.	96	8	X	4.79	5000
958-1	2	30	6	7	60	Trap.	1500	30	Cont.	96	8	X	2.86	5000
959-1	2	30	6	7	60	Trap.	750	20	Cont.	96	8	X	2.86	3600
959-2	2	30	6	7	60	Trap.	750	20	Cont.	96	8	X	2.86	5000
959-3	2	30	6	7	60	Trap.	750	20	Cont.	96	10	X	2.86	5000
959-4	2	30	6	7	60	Trap.	750	20	Cont.	96	8	K	2.86	5000
959-5	2	30	6	7	60	Trap.	750	20	Cont.	96	8	X	4.79	5000
960-1	2	30	6	7	60	Trap.	750	30	Cont.	96	8	X	2.86	5000
961-1	2	30	8	3	0	Parallel	Infinite	20	Cont.	96	8	X	2.86	3600
961-2	2	30	8	3	0	Parallel	Infinite	20	Cont.	96	8	X	2.86	5000
961-3	2	30	8	3	0	Parallel	Infinite	20	Cont.	96	10	X	2.86	5000
961-4	2	30	8	3	0	Parallel	Infinite	20	Cont.	96	8	K	2.86	5000
961-5	2	30	8	3	0	Parallel	Infinite	20	Cont.	96	8	X	4.79	5000
962-1	2	30	8	3	0	Parallel	Infinite	30	Cont.	96	8	X	2.86	5000
963-1	2	30	8	3	0	Parallel	1500	20	Cont.	96	8	X	2.86	3600
963-2	2	30	8	3	0	Parallel	1500	20	Cont.	96	8	X	2.86	5000
963-3	2	30	8	3	0	Parallel	1500	20	Cont.	96	10	X	2.86	5000
963-4	2	30	8	3	0	Parallel	1500	20	Cont.	96	8	K	2.86	5000
963-5	2	30	8	3	0	Parallel	1500	20	Cont.	96	8	X	4.79	5000
964-1	2	30	8	3	0	Parallel	1500	30	Cont.	96	8	X	2.86	5000
965-1	2	30	8	3	0	Parallel	750	20	Cont.	96	8	X	2.86	3600
965-2	2	30	8	3	0	Parallel	750	20	Cont.	96	8	X	2.86	5000
965-3	2	30	8	3	0	Parallel	750	20	Cont.	96	10	X	2.86	5000
965-4	2	30	8	3	0	Parallel	750	20	Cont.	96	8	K	2.86	5000
965-5	2	30	8	3	0	Parallel	750	20	Cont.	96	8	X	4.79	5000
966-1	2	30	8	3	0	Parallel	750	30	Cont.	96	8	X	2.86	5000
967-1	2	30	8	3	30	Parallel	Infinite	20	Cont.	96	8	X	2.86	3600
967-2	2	30	8	3	30	Parallel	Infinite	20	Cont.	96	8	X	2.86	5000
967-3	2	30	8	3	30	Parallel	Infinite	20	Cont.	96	10	X	2.86	5000
967-4	2	30	8	3	30	Parallel	Infinite	20	Cont.	96	8	K	2.86	5000
967-5	2	30	8	3	30	Parallel	Infinite	20	Cont.	96	8	X	4.79	5000
968-1	2	30	8	3	30	Parallel	Infinite	30	Cont.	96	8	X	2.86	5000
969-1	2	30	8	3	30	Parallel	1500	20	Cont.	96	8	X	2.86	3600
969-2	2	30	8	3	30	Parallel	1500	20	Cont.	96	8	X	2.86	5000
969-3	2	30	8	3	30	Parallel	1500	20	Cont.	96	10	X	2.86	5000
969-4	2	30	8	3	30	Parallel	1500	20	Cont.	96	8	K	2.86	5000
969-5	2	30	8	3	30	Parallel	1500	20	Cont.	96	8	X	4.79	5000
970-1	2	30	8	3	30	Parallel	1500	30	Cont.	96	8	X	2.86	5000
971-1	2	30	8	3	30	Parallel	750	20	Cont.	96	8	X	2.86	3600
971-2	2	30	8	3	30	Parallel	750	20	Cont.	96	8	X	2.86	5000
971-3	2	30	8	3	30	Parallel	750	20	Cont.	96	10	X	2.86	5000
971-4	2	30	8	3	30	Parallel	750	20	Cont.	96	8	K	2.86	5000

Model ID	Geometry									Cross-section		CF detail		Mat'l
	n_{span}	L/d ratio	s_g [ft]	n_{girder}	Support skew [deg];	Layout	R [ft]	s_{cf} [ft]	CF layout	d_w [in]	t_{deck} [in]	CF type	A_{cf} [in^2]	E_c [ksi]
971-5	2	30	8	3	30	Parallel	750	20	Cont.	96	8	X	4.79	5000
972-1	2	30	8	3	30	Parallel	750	30	Cont.	96	8	X	2.86	5000
973-1	2	30	8	3	60	Parallel	Infinite	20	Cont.	96	8	X	2.86	3600
973-2	2	30	8	3	60	Parallel	Infinite	20	Cont.	96	8	X	2.86	5000
973-3	2	30	8	3	60	Parallel	Infinite	20	Cont.	96	10	X	2.86	5000
973-4	2	30	8	3	60	Parallel	Infinite	20	Cont.	96	8	K	2.86	5000
973-5	2	30	8	3	60	Parallel	Infinite	20	Cont.	96	8	X	4.79	5000
974-1	2	30	8	3	60	Parallel	Infinite	30	Cont.	96	8	X	2.86	5000
975-1	2	30	8	3	60	Parallel	Infinite	20	Stag.	96	8	X	2.86	3600
975-2	2	30	8	3	60	Parallel	Infinite	20	Stag.	96	8	X	2.86	5000
975-3	2	30	8	3	60	Parallel	Infinite	20	Stag.	96	10	X	2.86	5000
975-4	2	30	8	3	60	Parallel	Infinite	20	Stag.	96	8	K	2.86	5000
975-5	2	30	8	3	60	Parallel	Infinite	20	Stag.	96	8	X	4.79	5000
976-1	2	30	8	3	60	Parallel	Infinite	30	Stag.	96	8	X	2.86	5000
977-1	2	30	8	3	60	Parallel	1500	20	Cont.	96	8	X	2.86	3600
977-2	2	30	8	3	60	Parallel	1500	20	Cont.	96	8	X	2.86	5000
977-3	2	30	8	3	60	Parallel	1500	20	Cont.	96	10	X	2.86	5000
977-4	2	30	8	3	60	Parallel	1500	20	Cont.	96	8	K	2.86	5000
977-5	2	30	8	3	60	Parallel	1500	20	Cont.	96	8	X	4.79	5000
978-1	2	30	8	3	60	Parallel	1500	30	Cont.	96	8	X	2.86	5000
979-1	2	30	8	3	60	Parallel	750	20	Cont.	96	8	X	2.86	3600
979-2	2	30	8	3	60	Parallel	750	20	Cont.	96	8	X	2.86	5000
979-3	2	30	8	3	60	Parallel	750	20	Cont.	96	10	X	2.86	5000
979-4	2	30	8	3	60	Parallel	750	20	Cont.	96	8	K	2.86	5000
979-5	2	30	8	3	60	Parallel	750	20	Cont.	96	8	X	4.79	5000
980-1	2	30	8	3	60	Parallel	750	30	Cont.	96	8	X	2.86	5000
981-1	2	30	8	3	60	Trap.	Infinite	20	Cont.	96	8	X	2.86	3600
981-2	2	30	8	3	60	Trap.	Infinite	20	Cont.	96	8	X	2.86	5000
981-3	2	30	8	3	60	Trap.	Infinite	20	Cont.	96	10	X	2.86	5000
981-4	2	30	8	3	60	Trap.	Infinite	20	Cont.	96	8	K	2.86	5000
981-5	2	30	8	3	60	Trap.	Infinite	20	Cont.	96	8	X	4.79	5000
982-1	2	30	8	3	60	Trap.	Infinite	30	Cont.	96	8	X	2.86	5000
983-1	2	30	8	3	60	Trap.	Infinite	20	Stag.	96	8	X	2.86	3600
983-2	2	30	8	3	60	Trap.	Infinite	20	Stag.	96	8	X	2.86	5000
983-3	2	30	8	3	60	Trap.	Infinite	20	Stag.	96	10	X	2.86	5000
983-4	2	30	8	3	60	Trap.	Infinite	20	Stag.	96	8	K	2.86	5000
983-5	2	30	8	3	60	Trap.	Infinite	20	Stag.	96	8	X	4.79	5000
984-1	2	30	8	3	60	Trap.	Infinite	30	Stag.	96	8	X	2.86	5000
985-1	2	30	8	3	60	Trap.	1500	20	Cont.	96	8	X	2.86	3600
985-2	2	30	8	3	60	Trap.	1500	20	Cont.	96	8	X	2.86	5000
985-3	2	30	8	3	60	Trap.	1500	20	Cont.	96	10	X	2.86	5000
985-4	2	30	8	3	60	Trap.	1500	20	Cont.	96	8	K	2.86	5000
985-5	2	30	8	3	60	Trap.	1500	20	Cont.	96	8	X	4.79	5000
986-1	2	30	8	3	60	Trap.	1500	30	Cont.	96	8	X	2.86	5000
987-1	2	30	8	3	60	Trap.	750	20	Cont.	96	8	X	2.86	3600
987-2	2	30	8	3	60	Trap.	750	20	Cont.	96	8	X	2.86	5000
987-3	2	30	8	3	60	Trap.	750	20	Cont.	96	10	X	2.86	5000
987-4	2	30	8	3	60	Trap.	750	20	Cont.	96	8	K	2.86	5000
987-5	2	30	8	3	60	Trap.	750	20	Cont.	96	8	X	4.79	5000
988-1	2	30	8	3	60	Trap.	750	30	Cont.	96	8	X	2.86	5000
989-1	2	30	8	5	0	Parallel	Infinite	20	Cont.	96	8	X	2.86	3600
989-2	2	30	8	5	0	Parallel	Infinite	20	Cont.	96	8	X	2.86	5000
989-3	2	30	8	5	0	Parallel	Infinite	20	Cont.	96	10	X	2.86	5000
989-4	2	30	8	5	0	Parallel	Infinite	20	Cont.	96	8	K	2.86	5000
989-5	2	30	8	5	0	Parallel	Infinite	20	Cont.	96	8	X	4.79	5000
990-1	2	30	8	5	0	Parallel	Infinite	30	Cont.	96	8	X	2.86	5000
991-1	2	30	8	5	0	Parallel	1500	20	Cont.	96	8	X	2.86	3600
991-2	2	30	8	5	0	Parallel	1500	20	Cont.	96	8	X	2.86	5000
991-3	2	30	8	5	0	Parallel	1500	20	Cont.	96	10	X	2.86	5000
991-4	2	30	8	5	0	Parallel	1500	20	Cont.	96	8	K	2.86	5000
991-5	2	30	8	5	0	Parallel	1500	20	Cont.	96	8	X	4.79	5000
992-1	2	30	8	5	0	Parallel	1500	30	Cont.	96	8	X	2.86	5000
993-1	2	30	8	5	0	Parallel	750	20	Cont.	96	8	X	2.86	3600
993-2	2	30	8	5	0	Parallel	750	20	Cont.	96	8	X	2.86	5000
993-3	2	30	8	5	0	Parallel	750	20	Cont.	96	10	X	2.86	5000
993-4	2	30	8	5	0	Parallel	750	20	Cont.	96	8	K	2.86	5000
993-5	2	30	8	5	0	Parallel	750	20	Cont.	96	8	X	4.79	5000
994-1	2	30	8	5	0	Parallel	750	30	Cont.	96	8	X	2.86	5000
995-1	2	30	8	5	30	Parallel	Infinite	20	Cont.	96	8	X	2.86	3600
995-2	2	30	8	5	30	Parallel	Infinite	20	Cont.	96	8	X	2.86	5000
995-3	2	30	8	5	30	Parallel	Infinite	20	Cont.	96	10	X	2.86	5000
995-4	2	30	8	5	30	Parallel	Infinite	20	Cont.	96	8	K	2.86	5000
995-5	2	30	8	5	30	Parallel	Infinite	20	Cont.	96	8	X	4.79	5000

Model ID	Geometry									Cross-section		CF detail		Mat'l
	n_{span}	L/d ratio	s_g [ft]	n_{girder}	Support skew [deg]; Layout		R [ft]	s_{cf} [ft]	CF layout	d_w [in]	t_{deck} [in]	CF type	A_{cf} [in^2]	E_c [ksi]
996-1	2	30	8	5	30	Parallel	Infinite	30	Cont.	96	8	X	2.86	5000
997-1	2	30	8	5	30	Parallel	1500	20	Cont.	96	8	X	2.86	3600
997-2	2	30	8	5	30	Parallel	1500	20	Cont.	96	8	X	2.86	5000
997-3	2	30	8	5	30	Parallel	1500	20	Cont.	96	10	X	2.86	5000
997-4	2	30	8	5	30	Parallel	1500	20	Cont.	96	8	K	2.86	5000
997-5	2	30	8	5	30	Parallel	1500	20	Cont.	96	8	X	4.79	5000
998-1	2	30	8	5	30	Parallel	1500	30	Cont.	96	8	X	2.86	5000
999-1	2	30	8	5	30	Parallel	750	20	Cont.	96	8	X	2.86	3600
999-2	2	30	8	5	30	Parallel	750	20	Cont.	96	8	X	2.86	5000
999-3	2	30	8	5	30	Parallel	750	20	Cont.	96	10	X	2.86	5000
999-4	2	30	8	5	30	Parallel	750	20	Cont.	96	8	K	2.86	5000
999-5	2	30	8	5	30	Parallel	750	20	Cont.	96	8	X	4.79	5000
1000-1	2	30	8	5	30	Parallel	750	30	Cont.	96	8	X	2.86	5000
1001-1	2	30	8	5	60	Parallel	Infinite	20	Cont.	96	8	X	2.86	3600
1001-2	2	30	8	5	60	Parallel	Infinite	20	Cont.	96	8	X	2.86	5000
1001-3	2	30	8	5	60	Parallel	Infinite	20	Cont.	96	10	X	2.86	5000
1001-4	2	30	8	5	60	Parallel	Infinite	20	Cont.	96	8	K	2.86	5000
1001-5	2	30	8	5	60	Parallel	Infinite	20	Cont.	96	8	X	4.79	5000
1002-1	2	30	8	5	60	Parallel	Infinite	30	Cont.	96	8	X	2.86	5000
1003-1	2	30	8	5	60	Parallel	Infinite	20	Stag.	96	8	X	2.86	3600
1003-2	2	30	8	5	60	Parallel	Infinite	20	Stag.	96	8	X	2.86	5000
1003-3	2	30	8	5	60	Parallel	Infinite	20	Stag.	96	10	X	2.86	5000
1003-4	2	30	8	5	60	Parallel	Infinite	20	Stag.	96	8	K	2.86	5000
1003-5	2	30	8	5	60	Parallel	Infinite	20	Stag.	96	8	X	4.79	5000
1004-1	2	30	8	5	60	Parallel	Infinite	30	Stag.	96	8	X	2.86	5000
1005-1	2	30	8	5	60	Parallel	1500	20	Cont.	96	8	X	2.86	3600
1005-2	2	30	8	5	60	Parallel	1500	20	Cont.	96	8	X	2.86	5000
1005-3	2	30	8	5	60	Parallel	1500	20	Cont.	96	10	X	2.86	5000
1005-4	2	30	8	5	60	Parallel	1500	20	Cont.	96	8	K	2.86	5000
1005-5	2	30	8	5	60	Parallel	1500	20	Cont.	96	8	X	4.79	5000
1006-1	2	30	8	5	60	Parallel	1500	30	Cont.	96	8	X	2.86	5000
1007-1	2	30	8	5	60	Parallel	750	20	Cont.	96	8	X	2.86	3600
1007-2	2	30	8	5	60	Parallel	750	20	Cont.	96	8	X	2.86	5000
1007-3	2	30	8	5	60	Parallel	750	20	Cont.	96	10	X	2.86	5000
1007-4	2	30	8	5	60	Parallel	750	20	Cont.	96	8	K	2.86	5000
1007-5	2	30	8	5	60	Parallel	750	20	Cont.	96	8	X	4.79	5000
1008-1	2	30	8	5	60	Parallel	750	30	Cont.	96	8	X	2.86	5000
1009-1	2	30	8	5	60	Trap.	Infinite	20	Cont.	96	8	X	2.86	3600
1009-2	2	30	8	5	60	Trap.	Infinite	20	Cont.	96	8	X	2.86	5000
1009-3	2	30	8	5	60	Trap.	Infinite	20	Cont.	96	10	X	2.86	5000
1009-4	2	30	8	5	60	Trap.	Infinite	20	Cont.	96	8	K	2.86	5000
1009-5	2	30	8	5	60	Trap.	Infinite	20	Cont.	96	8	X	4.79	5000
1010-1	2	30	8	5	60	Trap.	Infinite	30	Cont.	96	8	X	2.86	5000
1011-1	2	30	8	5	60	Trap.	Infinite	20	Stag.	96	8	X	2.86	3600
1011-2	2	30	8	5	60	Trap.	Infinite	20	Stag.	96	8	X	2.86	5000
1011-3	2	30	8	5	60	Trap.	Infinite	20	Stag.	96	10	X	2.86	5000
1011-4	2	30	8	5	60	Trap.	Infinite	20	Stag.	96	8	K	2.86	5000
1011-5	2	30	8	5	60	Trap.	Infinite	20	Stag.	96	8	X	4.79	5000
1012-1	2	30	8	5	60	Trap.	Infinite	30	Stag.	96	8	X	2.86	5000
1013-1	2	30	8	5	60	Trap.	1500	20	Cont.	96	8	X	2.86	3600
1013-2	2	30	8	5	60	Trap.	1500	20	Cont.	96	8	X	2.86	5000
1013-3	2	30	8	5	60	Trap.	1500	20	Cont.	96	10	X	2.86	5000
1013-4	2	30	8	5	60	Trap.	1500	20	Cont.	96	8	K	2.86	5000
1013-5	2	30	8	5	60	Trap.	1500	20	Cont.	96	8	X	4.79	5000
1014-1	2	30	8	5	60	Trap.	1500	30	Cont.	96	8	X	2.86	5000
1015-1	2	30	8	5	60	Trap.	750	20	Cont.	96	8	X	2.86	3600
1015-2	2	30	8	5	60	Trap.	750	20	Cont.	96	8	X	2.86	5000
1015-3	2	30	8	5	60	Trap.	750	20	Cont.	96	10	X	2.86	5000
1015-4	2	30	8	5	60	Trap.	750	20	Cont.	96	8	K	2.86	5000
1015-5	2	30	8	5	60	Trap.	750	20	Cont.	96	8	X	4.79	5000
1016-1	2	30	8	5	60	Trap.	750	30	Cont.	96	8	X	2.86	5000
1017-1	2	30	8	7	0	Parallel	Infinite	20	Cont.	96	8	X	2.86	3600
1017-2	2	30	8	7	0	Parallel	Infinite	20	Cont.	96	8	X	2.86	5000
1017-3	2	30	8	7	0	Parallel	Infinite	20	Cont.	96	10	X	2.86	5000
1017-4	2	30	8	7	0	Parallel	Infinite	20	Cont.	96	8	K	2.86	5000
1017-5	2	30	8	7	0	Parallel	Infinite	20	Cont.	96	8	X	4.79	5000
1018-1	2	30	8	7	0	Parallel	Infinite	30	Cont.	96	8	X	2.86	5000
1019-1	2	30	8	7	0	Parallel	1500	20	Cont.	96	8	X	2.86	3600
1019-2	2	30	8	7	0	Parallel	1500	20	Cont.	96	8	X	2.86	5000
1019-3	2	30	8	7	0	Parallel	1500	20	Cont.	96	10	X	2.86	5000
1019-4	2	30	8	7	0	Parallel	1500	20	Cont.	96	8	K	2.86	5000
1019-5	2	30	8	7	0	Parallel	1500	20	Cont.	96	8	X	4.79	5000
1020-1	2	30	8	7	0	Parallel	1500	30	Cont.	96	8	X	2.86	5000

Model ID	Geometry									Cross-section		CF detail		Mat'l
	n_{span}	L/d ratio	s_g [ft]	n_{girder}	Support skew [deg]; Layout		R [ft]	s_{cf} [ft]	CF layout	d_w [in]	t_{deck} [in]	CF type	A_{cf} [in^2]	E_c [ksi]
1021-1	2	30	8	7	0	Parallel	750	20	Cont.	96	8	X	2.86	3600
1021-2	2	30	8	7	0	Parallel	750	20	Cont.	96	8	X	2.86	5000
1021-3	2	30	8	7	0	Parallel	750	20	Cont.	96	10	X	2.86	5000
1021-4	2	30	8	7	0	Parallel	750	20	Cont.	96	8	K	2.86	5000
1021-5	2	30	8	7	0	Parallel	750	20	Cont.	96	8	X	4.79	5000
1022-1	2	30	8	7	0	Parallel	750	30	Cont.	96	8	X	2.86	5000
1023-1	2	30	8	7	30	Parallel	Infinite	20	Cont.	96	8	X	2.86	3600
1023-2	2	30	8	7	30	Parallel	Infinite	20	Cont.	96	8	X	2.86	5000
1023-3	2	30	8	7	30	Parallel	Infinite	20	Cont.	96	10	X	2.86	5000
1023-4	2	30	8	7	30	Parallel	Infinite	20	Cont.	96	8	K	2.86	5000
1023-5	2	30	8	7	30	Parallel	Infinite	20	Cont.	96	8	X	4.79	5000
1024-1	2	30	8	7	30	Parallel	Infinite	30	Cont.	96	8	X	2.86	5000
1025-1	2	30	8	7	30	Parallel	1500	20	Cont.	96	8	X	2.86	3600
1025-2	2	30	8	7	30	Parallel	1500	20	Cont.	96	8	X	2.86	5000
1025-3	2	30	8	7	30	Parallel	1500	20	Cont.	96	10	X	2.86	5000
1025-4	2	30	8	7	30	Parallel	1500	20	Cont.	96	8	K	2.86	5000
1025-5	2	30	8	7	30	Parallel	1500	20	Cont.	96	8	X	4.79	5000
1026-1	2	30	8	7	30	Parallel	1500	30	Cont.	96	8	X	2.86	5000
1027-1	2	30	8	7	30	Parallel	750	20	Cont.	96	8	X	2.86	3600
1027-2	2	30	8	7	30	Parallel	750	20	Cont.	96	8	X	2.86	5000
1027-3	2	30	8	7	30	Parallel	750	20	Cont.	96	10	X	2.86	5000
1027-4	2	30	8	7	30	Parallel	750	20	Cont.	96	8	K	2.86	5000
1027-5	2	30	8	7	30	Parallel	750	20	Cont.	96	8	X	4.79	5000
1028-1	2	30	8	7	30	Parallel	750	30	Cont.	96	8	X	2.86	5000
1029-1	2	30	8	7	60	Parallel	Infinite	20	Cont.	96	8	X	2.86	3600
1029-2	2	30	8	7	60	Parallel	Infinite	20	Cont.	96	8	X	2.86	5000
1029-3	2	30	8	7	60	Parallel	Infinite	20	Cont.	96	10	X	2.86	5000
1029-4	2	30	8	7	60	Parallel	Infinite	20	Cont.	96	8	K	2.86	5000
1029-5	2	30	8	7	60	Parallel	Infinite	20	Cont.	96	8	X	4.79	5000
1030-1	2	30	8	7	60	Parallel	Infinite	30	Cont.	96	8	X	2.86	5000
1031-1	2	30	8	7	60	Parallel	Infinite	20	Stag.	96	8	X	2.86	3600
1031-2	2	30	8	7	60	Parallel	Infinite	20	Stag.	96	8	X	2.86	5000
1031-3	2	30	8	7	60	Parallel	Infinite	20	Stag.	96	10	X	2.86	5000
1031-4	2	30	8	7	60	Parallel	Infinite	20	Stag.	96	8	K	2.86	5000
1031-5	2	30	8	7	60	Parallel	Infinite	20	Stag.	96	8	X	4.79	5000
1032-1	2	30	8	7	60	Parallel	Infinite	30	Stag.	96	8	X	2.86	5000
1033-1	2	30	8	7	60	Parallel	1500	20	Cont.	96	8	X	2.86	3600
1033-2	2	30	8	7	60	Parallel	1500	20	Cont.	96	8	X	2.86	5000
1033-3	2	30	8	7	60	Parallel	1500	20	Cont.	96	10	X	2.86	5000
1033-4	2	30	8	7	60	Parallel	1500	20	Cont.	96	8	K	2.86	5000
1033-5	2	30	8	7	60	Parallel	1500	20	Cont.	96	8	X	4.79	5000
1034-1	2	30	8	7	60	Parallel	1500	30	Cont.	96	8	X	2.86	5000
1035-1	2	30	8	7	60	Parallel	750	20	Cont.	96	8	X	2.86	3600
1035-2	2	30	8	7	60	Parallel	750	20	Cont.	96	8	X	2.86	5000
1035-3	2	30	8	7	60	Parallel	750	20	Cont.	96	10	X	2.86	5000
1035-4	2	30	8	7	60	Parallel	750	20	Cont.	96	8	K	2.86	5000
1035-5	2	30	8	7	60	Parallel	750	20	Cont.	96	8	X	4.79	5000
1036-1	2	30	8	7	60	Parallel	750	30	Cont.	96	8	X	2.86	5000
1037-1	2	30	8	7	60	Trap.	Infinite	20	Cont.	96	8	X	2.86	3600
1037-2	2	30	8	7	60	Trap.	Infinite	20	Cont.	96	8	X	2.86	5000
1037-3	2	30	8	7	60	Trap.	Infinite	20	Cont.	96	10	X	2.86	5000
1037-4	2	30	8	7	60	Trap.	Infinite	20	Cont.	96	8	K	2.86	5000
1037-5	2	30	8	7	60	Trap.	Infinite	20	Cont.	96	8	X	4.79	5000
1038-1	2	30	8	7	60	Trap.	Infinite	30	Cont.	96	8	X	2.86	5000
1039-1	2	30	8	7	60	Trap.	Infinite	20	Stag.	96	8	X	2.86	3600
1039-2	2	30	8	7	60	Trap.	Infinite	20	Stag.	96	8	X	2.86	5000
1039-3	2	30	8	7	60	Trap.	Infinite	20	Stag.	96	10	X	2.86	5000
1039-4	2	30	8	7	60	Trap.	Infinite	20	Stag.	96	8	K	2.86	5000
1039-5	2	30	8	7	60	Trap.	Infinite	20	Stag.	96	8	X	4.79	5000
1040-1	2	30	8	7	60	Trap.	Infinite	30	Stag.	96	8	X	2.86	5000
1041-1	2	30	8	7	60	Trap.	1500	20	Cont.	96	8	X	2.86	3600
1041-2	2	30	8	7	60	Trap.	1500	20	Cont.	96	8	X	2.86	5000
1041-3	2	30	8	7	60	Trap.	1500	20	Cont.	96	10	X	2.86	5000
1041-4	2	30	8	7	60	Trap.	1500	20	Cont.	96	8	K	2.86	5000
1041-5	2	30	8	7	60	Trap.	1500	20	Cont.	96	8	X	4.79	5000
1042-1	2	30	8	7	60	Trap.	1500	30	Cont.	96	8	X	2.86	5000
1043-1	2	30	8	7	60	Trap.	750	20	Cont.	96	8	X	2.86	3600
1043-2	2	30	8	7	60	Trap.	750	20	Cont.	96	8	X	2.86	5000
1043-3	2	30	8	7	60	Trap.	750	20	Cont.	96	10	X	2.86	5000
1043-4	2	30	8	7	60	Trap.	750	20	Cont.	96	8	K	2.86	5000
1043-5	2	30	8	7	60	Trap.	750	20	Cont.	96	8	X	4.79	5000
1044-1	2	30	8	7	60	Trap.	750	30	Cont.	96	8	X	2.86	5000
1045-1	2	30	10	3	0	Parallel	Infinite	20	Cont.	96	8	X	2.86	3600

Model ID	Geometry									Cross-section		CF detail		Mat'l
	n_{span}	L/d ratio	s_g [ft]	n_{girder}	Support skew [deg]; Layout		R [ft]	s_{cf} [ft]	CF layout	d_w [in]	t_{deck} [in]	CF type	A_{cf} [in^2]	E_c [ksi]
1045-2	2	30	10	3	0	Parallel	Infinite	20	Cont.	96	8	X	2.86	5000
1045-3	2	30	10	3	0	Parallel	Infinite	20	Cont.	96	10	X	2.86	5000
1045-4	2	30	10	3	0	Parallel	Infinite	20	Cont.	96	8	K	2.86	5000
1045-5	2	30	10	3	0	Parallel	Infinite	20	Cont.	96	8	X	4.79	5000
1046-1	2	30	10	3	0	Parallel	Infinite	30	Cont.	96	8	X	2.86	5000
1047-1	2	30	10	3	0	Parallel	1500	20	Cont.	96	8	X	2.86	3600
1047-2	2	30	10	3	0	Parallel	1500	20	Cont.	96	8	X	2.86	5000
1047-3	2	30	10	3	0	Parallel	1500	20	Cont.	96	10	X	2.86	5000
1047-4	2	30	10	3	0	Parallel	1500	20	Cont.	96	8	K	2.86	5000
1047-5	2	30	10	3	0	Parallel	1500	20	Cont.	96	8	X	4.79	5000
1048-1	2	30	10	3	0	Parallel	1500	30	Cont.	96	8	X	2.86	5000
1049-1	2	30	10	3	0	Parallel	750	20	Cont.	96	8	X	2.86	3600
1049-2	2	30	10	3	0	Parallel	750	20	Cont.	96	8	X	2.86	5000
1049-3	2	30	10	3	0	Parallel	750	20	Cont.	96	10	X	2.86	5000
1049-4	2	30	10	3	0	Parallel	750	20	Cont.	96	8	K	2.86	5000
1049-5	2	30	10	3	0	Parallel	750	20	Cont.	96	8	X	4.79	5000
1050-1	2	30	10	3	0	Parallel	750	30	Cont.	96	8	X	2.86	5000
1051-1	2	30	10	3	30	Parallel	Infinite	20	Cont.	96	8	X	2.86	3600
1051-2	2	30	10	3	30	Parallel	Infinite	20	Cont.	96	8	X	2.86	5000
1051-3	2	30	10	3	30	Parallel	Infinite	20	Cont.	96	10	X	2.86	5000
1051-4	2	30	10	3	30	Parallel	Infinite	20	Cont.	96	8	K	2.86	5000
1051-5	2	30	10	3	30	Parallel	Infinite	20	Cont.	96	8	X	4.79	5000
1052-1	2	30	10	3	30	Parallel	Infinite	30	Cont.	96	8	X	2.86	5000
1053-1	2	30	10	3	30	Parallel	1500	20	Cont.	96	8	X	2.86	3600
1053-2	2	30	10	3	30	Parallel	1500	20	Cont.	96	8	X	2.86	5000
1053-3	2	30	10	3	30	Parallel	1500	20	Cont.	96	10	X	2.86	5000
1053-4	2	30	10	3	30	Parallel	1500	20	Cont.	96	8	K	2.86	5000
1053-5	2	30	10	3	30	Parallel	1500	20	Cont.	96	8	X	4.79	5000
1054-1	2	30	10	3	30	Parallel	1500	30	Cont.	96	8	X	2.86	5000
1055-1	2	30	10	3	30	Parallel	750	20	Cont.	96	8	X	2.86	3600
1055-2	2	30	10	3	30	Parallel	750	20	Cont.	96	8	X	2.86	5000
1055-3	2	30	10	3	30	Parallel	750	20	Cont.	96	10	X	2.86	5000
1055-4	2	30	10	3	30	Parallel	750	20	Cont.	96	8	K	2.86	5000
1055-5	2	30	10	3	30	Parallel	750	20	Cont.	96	8	X	4.79	5000
1056-1	2	30	10	3	30	Parallel	750	30	Cont.	96	8	X	2.86	5000
1057-1	2	30	10	3	60	Parallel	Infinite	20	Cont.	96	8	X	2.86	3600
1057-2	2	30	10	3	60	Parallel	Infinite	20	Cont.	96	8	X	2.86	5000
1057-3	2	30	10	3	60	Parallel	Infinite	20	Cont.	96	10	X	2.86	5000
1057-4	2	30	10	3	60	Parallel	Infinite	20	Cont.	96	8	K	2.86	5000
1057-5	2	30	10	3	60	Parallel	Infinite	20	Cont.	96	8	X	4.79	5000
1058-1	2	30	10	3	60	Parallel	Infinite	30	Cont.	96	8	X	2.86	5000
1059-1	2	30	10	3	60	Parallel	Infinite	20	Stag.	96	8	X	2.86	3600
1059-2	2	30	10	3	60	Parallel	Infinite	20	Stag.	96	8	X	2.86	5000
1059-3	2	30	10	3	60	Parallel	Infinite	20	Stag.	96	10	X	2.86	5000
1059-4	2	30	10	3	60	Parallel	Infinite	20	Stag.	96	8	K	2.86	5000
1059-5	2	30	10	3	60	Parallel	Infinite	20	Stag.	96	8	X	4.79	5000
1060-1	2	30	10	3	60	Parallel	Infinite	30	Stag.	96	8	X	2.86	5000
1061-1	2	30	10	3	60	Parallel	1500	20	Cont.	96	8	X	2.86	3600
1061-2	2	30	10	3	60	Parallel	1500	20	Cont.	96	8	X	2.86	5000
1061-3	2	30	10	3	60	Parallel	1500	20	Cont.	96	10	X	2.86	5000
1061-4	2	30	10	3	60	Parallel	1500	20	Cont.	96	8	K	2.86	5000
1061-5	2	30	10	3	60	Parallel	1500	20	Cont.	96	8	X	4.79	5000
1062-1	2	30	10	3	60	Parallel	1500	30	Cont.	96	8	X	2.86	5000
1063-1	2	30	10	3	60	Parallel	750	20	Cont.	96	8	X	2.86	3600
1063-2	2	30	10	3	60	Parallel	750	20	Cont.	96	8	X	2.86	5000
1063-3	2	30	10	3	60	Parallel	750	20	Cont.	96	10	X	2.86	5000
1063-4	2	30	10	3	60	Parallel	750	20	Cont.	96	8	K	2.86	5000
1063-5	2	30	10	3	60	Parallel	750	20	Cont.	96	8	X	4.79	5000
1064-1	2	30	10	3	60	Parallel	750	30	Cont.	96	8	X	2.86	5000
1065-1	2	30	10	3	60	Trap.	Infinite	20	Cont.	96	8	X	2.86	3600
1065-2	2	30	10	3	60	Trap.	Infinite	20	Cont.	96	8	X	2.86	5000
1065-3	2	30	10	3	60	Trap.	Infinite	20	Cont.	96	10	X	2.86	5000
1065-4	2	30	10	3	60	Trap.	Infinite	20	Cont.	96	8	K	2.86	5000
1065-5	2	30	10	3	60	Trap.	Infinite	20	Cont.	96	8	X	4.79	5000
1066-1	2	30	10	3	60	Trap.	Infinite	30	Cont.	96	8	X	2.86	5000
1067-1	2	30	10	3	60	Trap.	Infinite	20	Stag.	96	8	X	2.86	3600
1067-2	2	30	10	3	60	Trap.	Infinite	20	Stag.	96	8	X	2.86	5000
1067-3	2	30	10	3	60	Trap.	Infinite	20	Stag.	96	10	X	2.86	5000
1067-4	2	30	10	3	60	Trap.	Infinite	20	Stag.	96	8	K	2.86	5000
1067-5	2	30	10	3	60	Trap.	Infinite	20	Stag.	96	8	X	4.79	5000
1068-1	2	30	10	3	60	Trap.	Infinite	30	Stag.	96	8	X	2.86	5000
1069-1	2	30	10	3	60	Trap.	1500	20	Cont.	96	8	X	2.86	3600
1069-2	2	30	10	3	60	Trap.	1500	20	Cont.	96	8	X	2.86	5000

Model ID	Geometry									Cross-section		CF detail		Mat'l
	n_{span}	L/d ratio	s_g [ft]	n_{girder}	Support skew [deg]; Layout		R [ft]	s_{cf} [ft]	CF layout	d_w [in]	t_{deck} [in]	CF type	A_{cf} [in^2]	E_c [ksi]
1069-3	2	30	10	3	60	Trap.	1500	20	Cont.	96	10	X	2.86	5000
1069-4	2	30	10	3	60	Trap.	1500	20	Cont.	96	8	K	2.86	5000
1069-5	2	30	10	3	60	Trap.	1500	20	Cont.	96	8	X	4.79	5000
1070-1	2	30	10	3	60	Trap.	1500	30	Cont.	96	8	X	2.86	5000
1071-1	2	30	10	3	60	Trap.	750	20	Cont.	96	8	X	2.86	3600
1071-2	2	30	10	3	60	Trap.	750	20	Cont.	96	8	X	2.86	5000
1071-3	2	30	10	3	60	Trap.	750	20	Cont.	96	10	X	2.86	5000
1071-4	2	30	10	3	60	Trap.	750	20	Cont.	96	8	K	2.86	5000
1071-5	2	30	10	3	60	Trap.	750	20	Cont.	96	8	X	4.79	5000
1072-1	2	30	10	3	60	Trap.	750	30	Cont.	96	8	X	2.86	5000
1073-1	2	30	10	5	0	Parallel	Infinite	20	Cont.	96	8	X	2.86	3600
1073-2	2	30	10	5	0	Parallel	Infinite	20	Cont.	96	8	X	2.86	5000
1073-3	2	30	10	5	0	Parallel	Infinite	20	Cont.	96	10	X	2.86	5000
1073-4	2	30	10	5	0	Parallel	Infinite	20	Cont.	96	8	K	2.86	5000
1073-5	2	30	10	5	0	Parallel	Infinite	20	Cont.	96	8	X	4.79	5000
1074-1	2	30	10	5	0	Parallel	Infinite	30	Cont.	96	8	X	2.86	5000
1075-1	2	30	10	5	0	Parallel	1500	20	Cont.	96	8	X	2.86	3600
1075-2	2	30	10	5	0	Parallel	1500	20	Cont.	96	8	X	2.86	5000
1075-3	2	30	10	5	0	Parallel	1500	20	Cont.	96	10	X	2.86	5000
1075-4	2	30	10	5	0	Parallel	1500	20	Cont.	96	8	K	2.86	5000
1075-5	2	30	10	5	0	Parallel	1500	20	Cont.	96	8	X	4.79	5000
1076-1	2	30	10	5	0	Parallel	1500	30	Cont.	96	8	X	2.86	5000
1077-1	2	30	10	5	0	Parallel	750	20	Cont.	96	8	X	2.86	3600
1077-2	2	30	10	5	0	Parallel	750	20	Cont.	96	8	X	2.86	5000
1077-3	2	30	10	5	0	Parallel	750	20	Cont.	96	10	X	2.86	5000
1077-4	2	30	10	5	0	Parallel	750	20	Cont.	96	8	K	2.86	5000
1077-5	2	30	10	5	0	Parallel	750	20	Cont.	96	8	X	4.79	5000
1078-1	2	30	10	5	0	Parallel	750	30	Cont.	96	8	X	2.86	5000
1079-1	2	30	10	5	30	Parallel	Infinite	20	Cont.	96	8	X	2.86	3600
1079-2	2	30	10	5	30	Parallel	Infinite	20	Cont.	96	8	X	2.86	5000
1079-3	2	30	10	5	30	Parallel	Infinite	20	Cont.	96	10	X	2.86	5000
1079-4	2	30	10	5	30	Parallel	Infinite	20	Cont.	96	8	K	2.86	5000
1079-5	2	30	10	5	30	Parallel	Infinite	20	Cont.	96	8	X	4.79	5000
1080-1	2	30	10	5	30	Parallel	Infinite	30	Cont.	96	8	X	2.86	5000
1081-1	2	30	10	5	30	Parallel	1500	20	Cont.	96	8	X	2.86	3600
1081-2	2	30	10	5	30	Parallel	1500	20	Cont.	96	8	X	2.86	5000
1081-3	2	30	10	5	30	Parallel	1500	20	Cont.	96	10	X	2.86	5000
1081-4	2	30	10	5	30	Parallel	1500	20	Cont.	96	8	K	2.86	5000
1081-5	2	30	10	5	30	Parallel	1500	20	Cont.	96	8	X	4.79	5000
1082-1	2	30	10	5	30	Parallel	1500	30	Cont.	96	8	X	2.86	5000
1083-1	2	30	10	5	30	Parallel	750	20	Cont.	96	8	X	2.86	3600
1083-2	2	30	10	5	30	Parallel	750	20	Cont.	96	8	X	2.86	5000
1083-3	2	30	10	5	30	Parallel	750	20	Cont.	96	10	X	2.86	5000
1083-4	2	30	10	5	30	Parallel	750	20	Cont.	96	8	K	2.86	5000
1083-5	2	30	10	5	30	Parallel	750	20	Cont.	96	8	X	4.79	5000
1084-1	2	30	10	5	30	Parallel	750	30	Cont.	96	8	X	2.86	5000
1085-1	2	30	10	5	60	Parallel	Infinite	20	Cont.	96	8	X	2.86	3600
1085-2	2	30	10	5	60	Parallel	Infinite	20	Cont.	96	8	X	2.86	5000
1085-3	2	30	10	5	60	Parallel	Infinite	20	Cont.	96	10	X	2.86	5000
1085-4	2	30	10	5	60	Parallel	Infinite	20	Cont.	96	8	K	2.86	5000
1085-5	2	30	10	5	60	Parallel	Infinite	20	Cont.	96	8	X	4.79	5000
1086-1	2	30	10	5	60	Parallel	Infinite	30	Cont.	96	8	X	2.86	5000
1087-1	2	30	10	5	60	Parallel	Infinite	20	Stag.	96	8	X	2.86	3600
1087-2	2	30	10	5	60	Parallel	Infinite	20	Stag.	96	8	X	2.86	5000
1087-3	2	30	10	5	60	Parallel	Infinite	20	Stag.	96	10	X	2.86	5000
1087-4	2	30	10	5	60	Parallel	Infinite	20	Stag.	96	8	K	2.86	5000
1087-5	2	30	10	5	60	Parallel	Infinite	20	Stag.	96	8	X	4.79	5000
1088-1	2	30	10	5	60	Parallel	Infinite	30	Stag.	96	8	X	2.86	5000
1089-1	2	30	10	5	60	Parallel	1500	20	Cont.	96	8	X	2.86	3600
1089-2	2	30	10	5	60	Parallel	1500	20	Cont.	96	8	X	2.86	5000
1089-3	2	30	10	5	60	Parallel	1500	20	Cont.	96	10	X	2.86	5000
1089-4	2	30	10	5	60	Parallel	1500	20	Cont.	96	8	K	2.86	5000
1089-5	2	30	10	5	60	Parallel	1500	20	Cont.	96	8	X	4.79	5000
1090-1	2	30	10	5	60	Parallel	1500	30	Cont.	96	8	X	2.86	5000
1091-1	2	30	10	5	60	Parallel	750	20	Cont.	96	8	X	2.86	3600
1091-2	2	30	10	5	60	Parallel	750	20	Cont.	96	8	X	2.86	5000
1091-3	2	30	10	5	60	Parallel	750	20	Cont.	96	10	X	2.86	5000
1091-4	2	30	10	5	60	Parallel	750	20	Cont.	96	8	K	2.86	5000
1091-5	2	30	10	5	60	Parallel	750	20	Cont.	96	8	X	4.79	5000
1092-1	2	30	10	5	60	Parallel	750	30	Cont.	96	8	X	2.86	5000
1093-1	2	30	10	5	60	Trap.	Infinite	20	Cont.	96	8	X	2.86	3600
1093-2	2	30	10	5	60	Trap.	Infinite	20	Cont.	96	8	X	2.86	5000
1093-3	2	30	10	5	60	Trap.	Infinite	20	Cont.	96	10	X	2.86	5000

Model ID	Geometry									Cross-section		CF detail		Mat'l
	n_{span}	L/d ratio	s_g [ft]	n_{girder}	Support skew [deg]; Layout		R [ft]	s_{cf} [ft]	CF layout	d_w [in]	t_{deck} [in]	CF type	A_{cf} [in^2]	E_c [ksi]
1093-4	2	30	10	5	60	Trap.	Infinite	20	Cont.	96	8	K	2.86	5000
1093-5	2	30	10	5	60	Trap.	Infinite	20	Cont.	96	8	X	4.79	5000
1094-1	2	30	10	5	60	Trap.	Infinite	30	Cont.	96	8	X	2.86	5000
1095-1	2	30	10	5	60	Trap.	Infinite	20	Stag.	96	8	X	2.86	3600
1095-2	2	30	10	5	60	Trap.	Infinite	20	Stag.	96	8	X	2.86	5000
1095-3	2	30	10	5	60	Trap.	Infinite	20	Stag.	96	10	X	2.86	5000
1095-4	2	30	10	5	60	Trap.	Infinite	20	Stag.	96	8	K	2.86	5000
1095-5	2	30	10	5	60	Trap.	Infinite	20	Stag.	96	8	X	4.79	5000
1096-1	2	30	10	5	60	Trap.	Infinite	30	Stag.	96	8	X	2.86	5000
1097-1	2	30	10	5	60	Trap.	1500	20	Cont.	96	8	X	2.86	3600
1097-2	2	30	10	5	60	Trap.	1500	20	Cont.	96	8	X	2.86	5000
1097-3	2	30	10	5	60	Trap.	1500	20	Cont.	96	10	X	2.86	5000
1097-4	2	30	10	5	60	Trap.	1500	20	Cont.	96	8	K	2.86	5000
1097-5	2	30	10	5	60	Trap.	1500	20	Cont.	96	8	X	4.79	5000
1098-1	2	30	10	5	60	Trap.	1500	30	Cont.	96	8	X	2.86	5000
1099-1	2	30	10	5	60	Trap.	750	20	Cont.	96	8	X	2.86	3600
1099-2	2	30	10	5	60	Trap.	750	20	Cont.	96	8	X	2.86	5000
1099-3	2	30	10	5	60	Trap.	750	20	Cont.	96	10	X	2.86	5000
1099-4	2	30	10	5	60	Trap.	750	20	Cont.	96	8	K	2.86	5000
1099-5	2	30	10	5	60	Trap.	750	20	Cont.	96	8	X	4.79	5000
1100-1	2	30	10	5	60	Trap.	750	30	Cont.	96	8	X	2.86	5000
1101-1	2	30	10	7	0	Parallel	Infinite	20	Cont.	96	8	X	2.86	3600
1101-2	2	30	10	7	0	Parallel	Infinite	20	Cont.	96	8	X	2.86	5000
1101-3	2	30	10	7	0	Parallel	Infinite	20	Cont.	96	10	X	2.86	5000
1101-4	2	30	10	7	0	Parallel	Infinite	20	Cont.	96	8	K	2.86	5000
1101-5	2	30	10	7	0	Parallel	Infinite	20	Cont.	96	8	X	4.79	5000
1102-1	2	30	10	7	0	Parallel	Infinite	30	Cont.	96	8	X	2.86	5000
1103-1	2	30	10	7	0	Parallel	1500	20	Cont.	96	8	X	2.86	3600
1103-2	2	30	10	7	0	Parallel	1500	20	Cont.	96	8	X	2.86	5000
1103-3	2	30	10	7	0	Parallel	1500	20	Cont.	96	10	X	2.86	5000
1103-4	2	30	10	7	0	Parallel	1500	20	Cont.	96	8	K	2.86	5000
1103-5	2	30	10	7	0	Parallel	1500	20	Cont.	96	8	X	4.79	5000
1104-1	2	30	10	7	0	Parallel	1500	30	Cont.	96	8	X	2.86	5000
1105-1	2	30	10	7	0	Parallel	750	20	Cont.	96	8	X	2.86	3600
1105-2	2	30	10	7	0	Parallel	750	20	Cont.	96	8	X	2.86	5000
1105-3	2	30	10	7	0	Parallel	750	20	Cont.	96	10	X	2.86	5000
1105-4	2	30	10	7	0	Parallel	750	20	Cont.	96	8	K	2.86	5000
1105-5	2	30	10	7	0	Parallel	750	20	Cont.	96	8	X	4.79	5000
1106-1	2	30	10	7	0	Parallel	750	30	Cont.	96	8	X	2.86	5000
1107-1	2	30	10	7	30	Parallel	Infinite	20	Cont.	96	8	X	2.86	3600
1107-2	2	30	10	7	30	Parallel	Infinite	20	Cont.	96	8	X	2.86	5000
1107-3	2	30	10	7	30	Parallel	Infinite	20	Cont.	96	10	X	2.86	5000
1107-4	2	30	10	7	30	Parallel	Infinite	20	Cont.	96	8	K	2.86	5000
1107-5	2	30	10	7	30	Parallel	Infinite	20	Cont.	96	8	X	4.79	5000
1108-1	2	30	10	7	30	Parallel	Infinite	30	Cont.	96	8	X	2.86	5000
1109-1	2	30	10	7	30	Parallel	1500	20	Cont.	96	8	X	2.86	3600
1109-2	2	30	10	7	30	Parallel	1500	20	Cont.	96	8	X	2.86	5000
1109-3	2	30	10	7	30	Parallel	1500	20	Cont.	96	10	X	2.86	5000
1109-4	2	30	10	7	30	Parallel	1500	20	Cont.	96	8	K	2.86	5000
1109-5	2	30	10	7	30	Parallel	1500	20	Cont.	96	8	X	4.79	5000
1110-1	2	30	10	7	30	Parallel	1500	30	Cont.	96	8	X	2.86	5000
1111-1	2	30	10	7	30	Parallel	750	20	Cont.	96	8	X	2.86	3600
1111-2	2	30	10	7	30	Parallel	750	20	Cont.	96	8	X	2.86	5000
1111-3	2	30	10	7	30	Parallel	750	20	Cont.	96	10	X	2.86	5000
1111-4	2	30	10	7	30	Parallel	750	20	Cont.	96	8	K	2.86	5000
1111-5	2	30	10	7	30	Parallel	750	20	Cont.	96	8	X	4.79	5000
1112-1	2	30	10	7	30	Parallel	750	30	Cont.	96	8	X	2.86	5000
1113-1	2	30	10	7	60	Parallel	Infinite	20	Cont.	96	8	X	2.86	3600
1113-2	2	30	10	7	60	Parallel	Infinite	20	Cont.	96	8	X	2.86	5000
1113-3	2	30	10	7	60	Parallel	Infinite	20	Cont.	96	10	X	2.86	5000
1113-4	2	30	10	7	60	Parallel	Infinite	20	Cont.	96	8	K	2.86	5000
1113-5	2	30	10	7	60	Parallel	Infinite	20	Cont.	96	8	X	4.79	5000
1114-1	2	30	10	7	60	Parallel	Infinite	30	Cont.	96	8	X	2.86	5000
1115-1	2	30	10	7	60	Parallel	Infinite	20	Stag.	96	8	X	2.86	3600
1115-2	2	30	10	7	60	Parallel	Infinite	20	Stag.	96	8	X	2.86	5000
1115-3	2	30	10	7	60	Parallel	Infinite	20	Stag.	96	10	X	2.86	5000
1115-4	2	30	10	7	60	Parallel	Infinite	20	Stag.	96	8	K	2.86	5000
1115-5	2	30	10	7	60	Parallel	Infinite	20	Stag.	96	8	X	4.79	5000
1116-1	2	30	10	7	60	Parallel	Infinite	30	Stag.	96	8	X	2.86	5000
1117-1	2	30	10	7	60	Parallel	1500	20	Cont.	96	8	X	2.86	3600
1117-2	2	30	10	7	60	Parallel	1500	20	Cont.	96	8	X	2.86	5000
1117-3	2	30	10	7	60	Parallel	1500	20	Cont.	96	10	X	2.86	5000
1117-4	2	30	10	7	60	Parallel	1500	20	Cont.	96	8	K	2.86	5000

Model ID	Geometry									Cross-section		CF detail		Mat'l
	n_{span}	L/d ratio	s_g [ft]	n_{girder}	Support skew [deg];	Layout	R [ft]	s_{cf} [ft]	CF layout	d_w [in]	t_{deck} [in]	CF type	A_{cf} [in^2]	E_c [ksi]
1117-5	2	30	10	7	60	Parallel	1500	20	Cont.	96	8	X	4.79	5000
1118-1	2	30	10	7	60	Parallel	1500	30	Cont.	96	8	X	2.86	5000
1119-1	2	30	10	7	60	Parallel	750	20	Cont.	96	8	X	2.86	3600
1119-2	2	30	10	7	60	Parallel	750	20	Cont.	96	8	X	2.86	5000
1119-3	2	30	10	7	60	Parallel	750	20	Cont.	96	10	X	2.86	5000
1119-4	2	30	10	7	60	Parallel	750	20	Cont.	96	8	K	2.86	5000
1119-5	2	30	10	7	60	Parallel	750	20	Cont.	96	8	X	4.79	5000
1120-1	2	30	10	7	60	Parallel	750	30	Cont.	96	8	X	2.86	5000
1121-1	2	30	10	7	60	Trap.	Infinite	20	Cont.	96	8	X	2.86	3600
1121-2	2	30	10	7	60	Trap.	Infinite	20	Cont.	96	8	X	2.86	5000
1121-3	2	30	10	7	60	Trap.	Infinite	20	Cont.	96	10	X	2.86	5000
1121-4	2	30	10	7	60	Trap.	Infinite	20	Cont.	96	8	K	2.86	5000
1121-5	2	30	10	7	60	Trap.	Infinite	20	Cont.	96	8	X	4.79	5000
1122-1	2	30	10	7	60	Trap.	Infinite	30	Cont.	96	8	X	2.86	5000
1123-1	2	30	10	7	60	Trap.	Infinite	20	Stag.	96	8	X	2.86	3600
1123-2	2	30	10	7	60	Trap.	Infinite	20	Stag.	96	8	X	2.86	5000
1123-3	2	30	10	7	60	Trap.	Infinite	20	Stag.	96	10	X	2.86	5000
1123-4	2	30	10	7	60	Trap.	Infinite	20	Stag.	96	8	K	2.86	5000
1123-5	2	30	10	7	60	Trap.	Infinite	20	Stag.	96	8	X	4.79	5000
1124-1	2	30	10	7	60	Trap.	Infinite	30	Stag.	96	8	X	2.86	5000
1125-1	2	30	10	7	60	Trap.	1500	20	Cont.	96	8	X	2.86	3600
1125-2	2	30	10	7	60	Trap.	1500	20	Cont.	96	8	X	2.86	5000
1125-3	2	30	10	7	60	Trap.	1500	20	Cont.	96	10	X	2.86	5000
1125-4	2	30	10	7	60	Trap.	1500	20	Cont.	96	8	K	2.86	5000
1125-5	2	30	10	7	60	Trap.	1500	20	Cont.	96	8	X	4.79	5000
1126-1	2	30	10	7	60	Trap.	1500	30	Cont.	96	8	X	2.86	5000
1127-1	2	30	10	7	60	Trap.	750	20	Cont.	96	8	X	2.86	3600
1127-2	2	30	10	7	60	Trap.	750	20	Cont.	96	8	X	2.86	5000
1127-3	2	30	10	7	60	Trap.	750	20	Cont.	96	10	X	2.86	5000
1127-4	2	30	10	7	60	Trap.	750	20	Cont.	96	8	K	2.86	5000
1127-5	2	30	10	7	60	Trap.	750	20	Cont.	96	8	X	4.79	5000
1128-1	2	30	10	7	60	Trap.	750	30	Cont.	96	8	X	2.86	5000
1129-1	2	35	6	3	0	Parallel	Infinite	20	Cont.	72	8	X	2.86	3600
1129-2	2	35	6	3	0	Parallel	Infinite	20	Cont.	72	8	X	2.86	5000
1129-3	2	35	6	3	0	Parallel	Infinite	20	Cont.	72	10	X	2.86	5000
1129-4	2	35	6	3	0	Parallel	Infinite	20	Cont.	72	8	K	2.86	5000
1129-5	2	35	6	3	0	Parallel	Infinite	20	Cont.	72	8	X	4.79	5000
1130-1	2	35	6	3	0	Parallel	Infinite	30	Cont.	72	8	X	2.86	5000
1131-1	2	35	6	3	30	Parallel	Infinite	20	Cont.	72	8	X	2.86	3600
1131-2	2	35	6	3	30	Parallel	Infinite	20	Cont.	72	8	X	2.86	5000
1131-3	2	35	6	3	30	Parallel	Infinite	20	Cont.	72	10	X	2.86	5000
1131-4	2	35	6	3	30	Parallel	Infinite	20	Cont.	72	8	K	2.86	5000
1131-5	2	35	6	3	30	Parallel	Infinite	20	Cont.	72	8	X	4.79	5000
1132-1	2	35	6	3	30	Parallel	Infinite	30	Cont.	72	8	X	2.86	5000
1133-1	2	35	6	3	60	Parallel	Infinite	20	Cont.	72	8	X	2.86	3600
1133-2	2	35	6	3	60	Parallel	Infinite	20	Cont.	72	8	X	2.86	5000
1133-3	2	35	6	3	60	Parallel	Infinite	20	Cont.	72	10	X	2.86	5000
1133-4	2	35	6	3	60	Parallel	Infinite	20	Cont.	72	8	K	2.86	5000
1133-5	2	35	6	3	60	Parallel	Infinite	20	Cont.	72	8	X	4.79	5000
1134-1	2	35	6	3	60	Parallel	Infinite	30	Cont.	72	8	X	2.86	5000
1135-1	2	35	6	3	60	Parallel	Infinite	20	Stag.	72	8	X	2.86	3600
1135-2	2	35	6	3	60	Parallel	Infinite	20	Stag.	72	8	X	2.86	5000
1135-3	2	35	6	3	60	Parallel	Infinite	20	Stag.	72	10	X	2.86	5000
1135-4	2	35	6	3	60	Parallel	Infinite	20	Stag.	72	8	K	2.86	5000
1135-5	2	35	6	3	60	Parallel	Infinite	20	Stag.	72	8	X	4.79	5000
1136-1	2	35	6	3	60	Parallel	Infinite	30	Stag.	72	8	X	2.86	5000
1137-1	2	35	6	3	60	Trap.	Infinite	20	Cont.	72	8	X	2.86	3600
1137-2	2	35	6	3	60	Trap.	Infinite	20	Cont.	72	8	X	2.86	5000
1137-3	2	35	6	3	60	Trap.	Infinite	20	Cont.	72	10	X	2.86	5000
1137-4	2	35	6	3	60	Trap.	Infinite	20	Cont.	72	8	K	2.86	5000
1137-5	2	35	6	3	60	Trap.	Infinite	20	Cont.	72	8	X	4.79	5000
1138-1	2	35	6	3	60	Trap.	Infinite	30	Cont.	72	8	X	2.86	5000
1139-1	2	35	6	3	60	Trap.	Infinite	20	Stag.	72	8	X	2.86	3600
1139-2	2	35	6	3	60	Trap.	Infinite	20	Stag.	72	8	X	2.86	5000
1139-3	2	35	6	3	60	Trap.	Infinite	20	Stag.	72	10	X	2.86	5000
1139-4	2	35	6	3	60	Trap.	Infinite	20	Stag.	72	8	K	2.86	5000
1139-5	2	35	6	3	60	Trap.	Infinite	20	Stag.	72	8	X	4.79	5000
1140-1	2	35	6	3	60	Trap.	Infinite	30	Stag.	72	8	X	2.86	5000
1141-1	2	35	6	5	0	Parallel	Infinite	20	Cont.	72	8	X	2.86	3600
1141-2	2	35	6	5	0	Parallel	Infinite	20	Cont.	72	8	X	2.86	5000
1141-3	2	35	6	5	0	Parallel	Infinite	20	Cont.	72	10	X	2.86	5000
1141-4	2	35	6	5	0	Parallel	Infinite	20	Cont.	72	8	K	2.86	5000
1141-5	2	35	6	5	0	Parallel	Infinite	20	Cont.	72	8	X	4.79	5000

Model ID	Geometry									Cross-section		CF detail		Mat'l
	n_{span}	L/d ratio	s_g [ft]	n_{girder}	Support skew [deg]; Layout		R [ft]	s_{cf} [ft]	CF layout	d_w [in]	t_{deck} [in]	CF type	A_{cf} [in^2]	E_c [ksi]
1142-1	2	35	6	5	0	Parallel	Infinite	30	Cont.	72	8	X	2.86	5000
1143-1	2	35	6	5	30	Parallel	Infinite	20	Cont.	72	8	X	2.86	3600
1143-2	2	35	6	5	30	Parallel	Infinite	20	Cont.	72	8	X	2.86	5000
1143-3	2	35	6	5	30	Parallel	Infinite	20	Cont.	72	10	X	2.86	5000
1143-4	2	35	6	5	30	Parallel	Infinite	20	Cont.	72	8	K	2.86	5000
1143-5	2	35	6	5	30	Parallel	Infinite	20	Cont.	72	8	X	4.79	5000
1144-1	2	35	6	5	30	Parallel	Infinite	30	Cont.	72	8	X	2.86	5000
1145-1	2	35	6	5	60	Parallel	Infinite	20	Cont.	72	8	X	2.86	3600
1145-2	2	35	6	5	60	Parallel	Infinite	20	Cont.	72	8	X	2.86	5000
1145-3	2	35	6	5	60	Parallel	Infinite	20	Cont.	72	10	X	2.86	5000
1145-4	2	35	6	5	60	Parallel	Infinite	20	Cont.	72	8	K	2.86	5000
1145-5	2	35	6	5	60	Parallel	Infinite	20	Cont.	72	8	X	4.79	5000
1146-1	2	35	6	5	60	Parallel	Infinite	30	Cont.	72	8	X	2.86	5000
1147-1	2	35	6	5	60	Parallel	Infinite	20	Stag.	72	8	X	2.86	3600
1147-2	2	35	6	5	60	Parallel	Infinite	20	Stag.	72	8	X	2.86	5000
1147-3	2	35	6	5	60	Parallel	Infinite	20	Stag.	72	10	X	2.86	5000
1147-4	2	35	6	5	60	Parallel	Infinite	20	Stag.	72	8	K	2.86	5000
1147-5	2	35	6	5	60	Parallel	Infinite	20	Stag.	72	8	X	4.79	5000
1148-1	2	35	6	5	60	Parallel	Infinite	30	Stag.	72	8	X	2.86	5000
1149-1	2	35	6	5	60	Trap.	Infinite	20	Cont.	72	8	X	2.86	3600
1149-2	2	35	6	5	60	Trap.	Infinite	20	Cont.	72	8	X	2.86	5000
1149-3	2	35	6	5	60	Trap.	Infinite	20	Cont.	72	10	X	2.86	5000
1149-4	2	35	6	5	60	Trap.	Infinite	20	Cont.	72	8	K	2.86	5000
1149-5	2	35	6	5	60	Trap.	Infinite	20	Cont.	72	8	X	4.79	5000
1150-1	2	35	6	5	60	Trap.	Infinite	30	Cont.	72	8	X	2.86	5000
1151-1	2	35	6	5	60	Trap.	Infinite	20	Stag.	72	8	X	2.86	3600
1151-2	2	35	6	5	60	Trap.	Infinite	20	Stag.	72	8	X	2.86	5000
1151-3	2	35	6	5	60	Trap.	Infinite	20	Stag.	72	10	X	2.86	5000
1151-4	2	35	6	5	60	Trap.	Infinite	20	Stag.	72	8	K	2.86	5000
1151-5	2	35	6	5	60	Trap.	Infinite	20	Stag.	72	8	X	4.79	5000
1152-1	2	35	6	5	60	Trap.	Infinite	30	Stag.	72	8	X	2.86	5000
1153-1	2	35	6	7	0	Parallel	Infinite	20	Cont.	72	8	X	2.86	3600
1153-2	2	35	6	7	0	Parallel	Infinite	20	Cont.	72	8	X	2.86	5000
1153-3	2	35	6	7	0	Parallel	Infinite	20	Cont.	72	10	X	2.86	5000
1153-4	2	35	6	7	0	Parallel	Infinite	20	Cont.	72	8	K	2.86	5000
1153-5	2	35	6	7	0	Parallel	Infinite	20	Cont.	72	8	X	4.79	5000
1154-1	2	35	6	7	0	Parallel	Infinite	30	Cont.	72	8	X	2.86	5000
1155-1	2	35	6	7	30	Parallel	Infinite	20	Cont.	72	8	X	2.86	3600
1155-2	2	35	6	7	30	Parallel	Infinite	20	Cont.	72	8	X	2.86	5000
1155-3	2	35	6	7	30	Parallel	Infinite	20	Cont.	72	10	X	2.86	5000
1155-4	2	35	6	7	30	Parallel	Infinite	20	Cont.	72	8	K	2.86	5000
1155-5	2	35	6	7	30	Parallel	Infinite	20	Cont.	72	8	X	4.79	5000
1156-1	2	35	6	7	30	Parallel	Infinite	30	Cont.	72	8	X	2.86	5000
1157-1	2	35	6	7	60	Parallel	Infinite	20	Cont.	72	8	X	2.86	3600
1157-2	2	35	6	7	60	Parallel	Infinite	20	Cont.	72	8	X	2.86	5000
1157-3	2	35	6	7	60	Parallel	Infinite	20	Cont.	72	10	X	2.86	5000
1157-4	2	35	6	7	60	Parallel	Infinite	20	Cont.	72	8	K	2.86	5000
1157-5	2	35	6	7	60	Parallel	Infinite	20	Cont.	72	8	X	4.79	5000
1158-1	2	35	6	7	60	Parallel	Infinite	30	Cont.	72	8	X	2.86	5000
1159-1	2	35	6	7	60	Parallel	Infinite	20	Stag.	72	8	X	2.86	3600
1159-2	2	35	6	7	60	Parallel	Infinite	20	Stag.	72	8	X	2.86	5000
1159-3	2	35	6	7	60	Parallel	Infinite	20	Stag.	72	10	X	2.86	5000
1159-4	2	35	6	7	60	Parallel	Infinite	20	Stag.	72	8	K	2.86	5000
1159-5	2	35	6	7	60	Parallel	Infinite	20	Stag.	72	8	X	4.79	5000
1160-1	2	35	6	7	60	Parallel	Infinite	30	Stag.	72	8	X	2.86	5000
1161-1	2	35	6	7	60	Trap.	Infinite	20	Cont.	72	8	X	2.86	3600
1161-2	2	35	6	7	60	Trap.	Infinite	20	Cont.	72	8	X	2.86	5000
1161-3	2	35	6	7	60	Trap.	Infinite	20	Cont.	72	10	X	2.86	5000
1161-4	2	35	6	7	60	Trap.	Infinite	20	Cont.	72	8	K	2.86	5000
1161-5	2	35	6	7	60	Trap.	Infinite	20	Cont.	72	8	X	4.79	5000
1162-1	2	35	6	7	60	Trap.	Infinite	30	Cont.	72	8	X	2.86	5000
1163-1	2	35	6	7	60	Trap.	Infinite	20	Stag.	72	8	X	2.86	3600
1163-2	2	35	6	7	60	Trap.	Infinite	20	Stag.	72	8	X	2.86	5000
1163-3	2	35	6	7	60	Trap.	Infinite	20	Stag.	72	10	X	2.86	5000
1163-4	2	35	6	7	60	Trap.	Infinite	20	Stag.	72	8	K	2.86	5000
1163-5	2	35	6	7	60	Trap.	Infinite	20	Stag.	72	8	X	4.79	5000
1164-1	2	35	6	7	60	Trap.	Infinite	30	Stag.	72	8	X	2.86	5000
1165-1	2	35	8	3	0	Parallel	Infinite	20	Cont.	72	8	X	2.86	3600
1165-2	2	35	8	3	0	Parallel	Infinite	20	Cont.	72	8	X	2.86	5000
1165-3	2	35	8	3	0	Parallel	Infinite	20	Cont.	72	10	X	2.86	5000
1165-4	2	35	8	3	0	Parallel	Infinite	20	Cont.	72	8	K	2.86	5000
1165-5	2	35	8	3	0	Parallel	Infinite	20	Cont.	72	8	X	4.79	5000
1166-1	2	35	8	3	0	Parallel	Infinite	30	Cont.	72	8	X	2.86	5000

Model ID	Geometry								Cross-section		CF detail		Mat'l
	n_{span}	L/d ratio	s_g [ft]	n_{girder}	Support skew [deg]; Layout	R [ft]	s_{cf} [ft]	CF layout	d_w [in]	t_{deck} [in]	CF type	A_{cf} [in^2]	E_c [ksi]
1167-1	2	35	8	3	30 Parallel	Infinite	20	Cont.	72	8	X	2.86	3600
1167-2	2	35	8	3	30 Parallel	Infinite	20	Cont.	72	8	X	2.86	5000
1167-3	2	35	8	3	30 Parallel	Infinite	20	Cont.	72	10	X	2.86	5000
1167-4	2	35	8	3	30 Parallel	Infinite	20	Cont.	72	8	K	2.86	5000
1167-5	2	35	8	3	30 Parallel	Infinite	20	Cont.	72	8	X	4.79	5000
1168-1	2	35	8	3	30 Parallel	Infinite	30	Cont.	72	8	X	2.86	5000
1169-1	2	35	8	3	60 Parallel	Infinite	20	Cont.	72	8	X	2.86	3600
1169-2	2	35	8	3	60 Parallel	Infinite	20	Cont.	72	8	X	2.86	5000
1169-3	2	35	8	3	60 Parallel	Infinite	20	Cont.	72	10	X	2.86	5000
1169-4	2	35	8	3	60 Parallel	Infinite	20	Cont.	72	8	K	2.86	5000
1169-5	2	35	8	3	60 Parallel	Infinite	20	Cont.	72	8	X	4.79	5000
1170-1	2	35	8	3	60 Parallel	Infinite	30	Cont.	72	8	X	2.86	5000
1171-1	2	35	8	3	60 Parallel	Infinite	20	Stag.	72	8	X	2.86	3600
1171-2	2	35	8	3	60 Parallel	Infinite	20	Stag.	72	8	X	2.86	5000
1171-3	2	35	8	3	60 Parallel	Infinite	20	Stag.	72	10	X	2.86	5000
1171-4	2	35	8	3	60 Parallel	Infinite	20	Stag.	72	8	K	2.86	5000
1171-5	2	35	8	3	60 Parallel	Infinite	20	Stag.	72	8	X	4.79	5000
1172-1	2	35	8	3	60 Parallel	Infinite	30	Stag.	72	8	X	2.86	5000
1173-1	2	35	8	3	60 Trap.	Infinite	20	Cont.	72	8	X	2.86	3600
1173-2	2	35	8	3	60 Trap.	Infinite	20	Cont.	72	8	X	2.86	5000
1173-3	2	35	8	3	60 Trap.	Infinite	20	Cont.	72	10	X	2.86	5000
1173-4	2	35	8	3	60 Trap.	Infinite	20	Cont.	72	8	K	2.86	5000
1173-5	2	35	8	3	60 Trap.	Infinite	20	Cont.	72	8	X	4.79	5000
1174-1	2	35	8	3	60 Trap.	Infinite	30	Cont.	72	8	X	2.86	5000
1175-1	2	35	8	3	60 Trap.	Infinite	20	Stag.	72	8	X	2.86	3600
1175-2	2	35	8	3	60 Trap.	Infinite	20	Stag.	72	8	X	2.86	5000
1175-3	2	35	8	3	60 Trap.	Infinite	20	Stag.	72	10	X	2.86	5000
1175-4	2	35	8	3	60 Trap.	Infinite	20	Stag.	72	8	K	2.86	5000
1175-5	2	35	8	3	60 Trap.	Infinite	20	Stag.	72	8	X	4.79	5000
1176-1	2	35	8	3	60 Trap.	Infinite	30	Stag.	72	8	X	2.86	5000
1177-1	2	35	8	5	0 Parallel	Infinite	20	Cont.	72	8	X	2.86	3600
1177-2	2	35	8	5	0 Parallel	Infinite	20	Cont.	72	8	X	2.86	5000
1177-3	2	35	8	5	0 Parallel	Infinite	20	Cont.	72	10	X	2.86	5000
1177-4	2	35	8	5	0 Parallel	Infinite	20	Cont.	72	8	K	2.86	5000
1177-5	2	35	8	5	0 Parallel	Infinite	20	Cont.	72	8	X	4.79	5000
1178-1	2	35	8	5	0 Parallel	Infinite	30	Cont.	72	8	X	2.86	5000
1179-1	2	35	8	5	30 Parallel	Infinite	20	Cont.	72	8	X	2.86	3600
1179-2	2	35	8	5	30 Parallel	Infinite	20	Cont.	72	8	X	2.86	5000
1179-3	2	35	8	5	30 Parallel	Infinite	20	Cont.	72	10	X	2.86	5000
1179-4	2	35	8	5	30 Parallel	Infinite	20	Cont.	72	8	K	2.86	5000
1179-5	2	35	8	5	30 Parallel	Infinite	20	Cont.	72	8	X	4.79	5000
1180-1	2	35	8	5	30 Parallel	Infinite	30	Cont.	72	8	X	2.86	5000
1181-1	2	35	8	5	60 Parallel	Infinite	20	Cont.	72	8	X	2.86	3600
1181-2	2	35	8	5	60 Parallel	Infinite	20	Cont.	72	8	X	2.86	5000
1181-3	2	35	8	5	60 Parallel	Infinite	20	Cont.	72	10	X	2.86	5000
1181-4	2	35	8	5	60 Parallel	Infinite	20	Cont.	72	8	K	2.86	5000
1181-5	2	35	8	5	60 Parallel	Infinite	20	Cont.	72	8	X	4.79	5000
1182-1	2	35	8	5	60 Parallel	Infinite	30	Cont.	72	8	X	2.86	5000
1183-1	2	35	8	5	60 Parallel	Infinite	20	Stag.	72	8	X	2.86	3600
1183-2	2	35	8	5	60 Parallel	Infinite	20	Stag.	72	8	X	2.86	5000
1183-3	2	35	8	5	60 Parallel	Infinite	20	Stag.	72	10	X	2.86	5000
1183-4	2	35	8	5	60 Parallel	Infinite	20	Stag.	72	8	K	2.86	5000
1183-5	2	35	8	5	60 Parallel	Infinite	20	Stag.	72	8	X	4.79	5000
1184-1	2	35	8	5	60 Parallel	Infinite	30	Stag.	72	8	X	2.86	5000
1185-1	2	35	8	5	60 Trap.	Infinite	20	Cont.	72	8	X	2.86	3600
1185-2	2	35	8	5	60 Trap.	Infinite	20	Cont.	72	8	X	2.86	5000
1185-3	2	35	8	5	60 Trap.	Infinite	20	Cont.	72	10	X	2.86	5000
1185-4	2	35	8	5	60 Trap.	Infinite	20	Cont.	72	8	K	2.86	5000
1185-5	2	35	8	5	60 Trap.	Infinite	20	Cont.	72	8	X	4.79	5000
1186-1	2	35	8	5	60 Trap.	Infinite	30	Cont.	72	8	X	2.86	5000
1187-1	2	35	8	5	60 Trap.	Infinite	20	Stag.	72	8	X	2.86	3600
1187-2	2	35	8	5	60 Trap.	Infinite	20	Stag.	72	8	X	2.86	5000
1187-3	2	35	8	5	60 Trap.	Infinite	20	Stag.	72	10	X	2.86	5000
1187-4	2	35	8	5	60 Trap.	Infinite	20	Stag.	72	8	K	2.86	5000
1187-5	2	35	8	5	60 Trap.	Infinite	20	Stag.	72	8	X	4.79	5000
1188-1	2	35	8	5	60 Trap.	Infinite	30	Stag.	72	8	X	2.86	5000
1189-1	2	35	8	7	0 Parallel	Infinite	20	Cont.	72	8	X	2.86	3600
1189-2	2	35	8	7	0 Parallel	Infinite	20	Cont.	72	8	X	2.86	5000
1189-3	2	35	8	7	0 Parallel	Infinite	20	Cont.	72	10	X	2.86	5000
1189-4	2	35	8	7	0 Parallel	Infinite	20	Cont.	72	8	K	2.86	5000
1189-5	2	35	8	7	0 Parallel	Infinite	20	Cont.	72	8	X	4.79	5000
1190-1	2	35	8	7	0 Parallel	Infinite	30	Cont.	72	8	X	2.86	5000
1191-1	2	35	8	7	30 Parallel	Infinite	20	Cont.	72	8	X	2.86	3600

Model ID	Geometry								Cross-section		CF detail		Mat'l
	n_{span}	L/d ratio	s_g [ft]	n_{girder}	Support skew [deg]; Layout	R [ft]	s_{cf} [ft]	CF layout	d_w [in]	t_{deck} [in]	CF type	A_{cf} [in^2]	E_c [ksi]
1191-2	2	35	8	7	30 Parallel	Infinite	20	Cont.	72	8	X	2.86	5000
1191-3	2	35	8	7	30 Parallel	Infinite	20	Cont.	72	10	X	2.86	5000
1191-4	2	35	8	7	30 Parallel	Infinite	20	Cont.	72	8	K	2.86	5000
1191-5	2	35	8	7	30 Parallel	Infinite	20	Cont.	72	8	X	4.79	5000
1192-1	2	35	8	7	30 Parallel	Infinite	30	Cont.	72	8	X	2.86	5000
1193-1	2	35	8	7	60 Parallel	Infinite	20	Cont.	72	8	X	2.86	3600
1193-2	2	35	8	7	60 Parallel	Infinite	20	Cont.	72	8	X	2.86	5000
1193-3	2	35	8	7	60 Parallel	Infinite	20	Cont.	72	10	X	2.86	5000
1193-4	2	35	8	7	60 Parallel	Infinite	20	Cont.	72	8	K	2.86	5000
1193-5	2	35	8	7	60 Parallel	Infinite	20	Cont.	72	8	X	4.79	5000
1194-1	2	35	8	7	60 Parallel	Infinite	30	Cont.	72	8	X	2.86	5000
1195-1	2	35	8	7	60 Parallel	Infinite	20	Stag.	72	8	X	2.86	3600
1195-2	2	35	8	7	60 Parallel	Infinite	20	Stag.	72	8	X	2.86	5000
1195-3	2	35	8	7	60 Parallel	Infinite	20	Stag.	72	10	X	2.86	5000
1195-4	2	35	8	7	60 Parallel	Infinite	20	Stag.	72	8	K	2.86	5000
1195-5	2	35	8	7	60 Parallel	Infinite	20	Stag.	72	8	X	4.79	5000
1196-1	2	35	8	7	60 Parallel	Infinite	30	Stag.	72	8	X	2.86	5000
1197-1	2	35	8	7	60 Trap.	Infinite	20	Cont.	72	8	X	2.86	3600
1197-2	2	35	8	7	60 Trap.	Infinite	20	Cont.	72	8	X	2.86	5000
1197-3	2	35	8	7	60 Trap.	Infinite	20	Cont.	72	10	X	2.86	5000
1197-4	2	35	8	7	60 Trap.	Infinite	20	Cont.	72	8	K	2.86	5000
1197-5	2	35	8	7	60 Trap.	Infinite	20	Cont.	72	8	X	4.79	5000
1198-1	2	35	8	7	60 Trap.	Infinite	30	Cont.	72	8	X	2.86	5000
1199-1	2	35	8	7	60 Trap.	Infinite	20	Stag.	72	8	X	2.86	3600
1199-2	2	35	8	7	60 Trap.	Infinite	20	Stag.	72	8	X	2.86	5000
1199-3	2	35	8	7	60 Trap.	Infinite	20	Stag.	72	10	X	2.86	5000
1199-4	2	35	8	7	60 Trap.	Infinite	20	Stag.	72	8	K	2.86	5000
1199-5	2	35	8	7	60 Trap.	Infinite	20	Stag.	72	8	X	4.79	5000
1200-1	2	35	8	7	60 Trap.	Infinite	30	Stag.	72	8	X	2.86	5000
1201-1	2	35	10	3	0 Parallel	Infinite	20	Cont.	72	8	X	2.86	3600
1201-2	2	35	10	3	0 Parallel	Infinite	20	Cont.	72	8	X	2.86	5000
1201-3	2	35	10	3	0 Parallel	Infinite	20	Cont.	72	10	X	2.86	5000
1201-4	2	35	10	3	0 Parallel	Infinite	20	Cont.	72	8	K	2.86	5000
1201-5	2	35	10	3	0 Parallel	Infinite	20	Cont.	72	8	X	4.79	5000
1202-1	2	35	10	3	0 Parallel	Infinite	30	Cont.	72	8	X	2.86	5000
1203-1	2	35	10	3	30 Parallel	Infinite	20	Cont.	72	8	X	2.86	3600
1203-2	2	35	10	3	30 Parallel	Infinite	20	Cont.	72	8	X	2.86	5000
1203-3	2	35	10	3	30 Parallel	Infinite	20	Cont.	72	10	X	2.86	5000
1203-4	2	35	10	3	30 Parallel	Infinite	20	Cont.	72	8	K	2.86	5000
1203-5	2	35	10	3	30 Parallel	Infinite	20	Cont.	72	8	X	4.79	5000
1204-1	2	35	10	3	30 Parallel	Infinite	30	Cont.	72	8	X	2.86	5000
1205-1	2	35	10	3	60 Parallel	Infinite	20	Cont.	72	8	X	2.86	3600
1205-2	2	35	10	3	60 Parallel	Infinite	20	Cont.	72	8	X	2.86	5000
1205-3	2	35	10	3	60 Parallel	Infinite	20	Cont.	72	10	X	2.86	5000
1205-4	2	35	10	3	60 Parallel	Infinite	20	Cont.	72	8	K	2.86	5000
1205-5	2	35	10	3	60 Parallel	Infinite	20	Cont.	72	8	X	4.79	5000
1206-1	2	35	10	3	60 Parallel	Infinite	30	Cont.	72	8	X	2.86	5000
1207-1	2	35	10	3	60 Parallel	Infinite	20	Stag.	72	8	X	2.86	3600
1207-2	2	35	10	3	60 Parallel	Infinite	20	Stag.	72	8	X	2.86	5000
1207-3	2	35	10	3	60 Parallel	Infinite	20	Stag.	72	10	X	2.86	5000
1207-4	2	35	10	3	60 Parallel	Infinite	20	Stag.	72	8	K	2.86	5000
1207-5	2	35	10	3	60 Parallel	Infinite	20	Stag.	72	8	X	4.79	5000
1208-1	2	35	10	3	60 Parallel	Infinite	30	Stag.	72	8	X	2.86	5000
1209-1	2	35	10	3	60 Trap.	Infinite	20	Cont.	72	8	X	2.86	3600
1209-2	2	35	10	3	60 Trap.	Infinite	20	Cont.	72	8	X	2.86	5000
1209-3	2	35	10	3	60 Trap.	Infinite	20	Cont.	72	10	X	2.86	5000
1209-4	2	35	10	3	60 Trap.	Infinite	20	Cont.	72	8	K	2.86	5000
1209-5	2	35	10	3	60 Trap.	Infinite	20	Cont.	72	8	X	4.79	5000
1210-1	2	35	10	3	60 Trap.	Infinite	30	Cont.	72	8	X	2.86	5000
1211-1	2	35	10	3	60 Trap.	Infinite	20	Stag.	72	8	X	2.86	3600
1211-2	2	35	10	3	60 Trap.	Infinite	20	Stag.	72	8	X	2.86	5000
1211-3	2	35	10	3	60 Trap.	Infinite	20	Stag.	72	10	X	2.86	5000
1211-4	2	35	10	3	60 Trap.	Infinite	20	Stag.	72	8	K	2.86	5000
1211-5	2	35	10	3	60 Trap.	Infinite	20	Stag.	72	8	X	4.79	5000
1212-1	2	35	10	3	60 Trap.	Infinite	30	Stag.	72	8	X	2.86	5000
1213-1	2	35	10	5	0 Parallel	Infinite	20	Cont.	72	8	X	2.86	3600
1213-2	2	35	10	5	0 Parallel	Infinite	20	Cont.	72	8	X	2.86	5000
1213-3	2	35	10	5	0 Parallel	Infinite	20	Cont.	72	10	X	2.86	5000
1213-4	2	35	10	5	0 Parallel	Infinite	20	Cont.	72	8	K	2.86	5000
1213-5	2	35	10	5	0 Parallel	Infinite	20	Cont.	72	8	X	4.79	5000
1214-1	2	35	10	5	0 Parallel	Infinite	30	Cont.	72	8	X	2.86	5000
1215-1	2	35	10	5	30 Parallel	Infinite	20	Cont.	72	8	X	2.86	3600
1215-2	2	35	10	5	30 Parallel	Infinite	20	Cont.	72	8	X	2.86	5000

Model ID	Geometry									Cross-section		CF detail		Mat'l
	n_{span}	L/d ratio	s_g [ft]	n_{girder}	Support skew [deg]; Layout		R [ft]	s_{cf} [ft]	CF layout	d_w [in]	t_{deck} [in]	CF type	A_{cf} [in^2]	E_c [ksi]
1215-3	2	35	10	5	30	Parallel	Infinite	20	Cont.	72	10	X	2.86	5000
1215-4	2	35	10	5	30	Parallel	Infinite	20	Cont.	72	8	K	2.86	5000
1215-5	2	35	10	5	30	Parallel	Infinite	20	Cont.	72	8	X	4.79	5000
1216-1	2	35	10	5	30	Parallel	Infinite	30	Cont.	72	8	X	2.86	5000
1217-1	2	35	10	5	60	Parallel	Infinite	20	Cont.	72	8	X	2.86	3600
1217-2	2	35	10	5	60	Parallel	Infinite	20	Cont.	72	8	X	2.86	5000
1217-3	2	35	10	5	60	Parallel	Infinite	20	Cont.	72	10	X	2.86	5000
1217-4	2	35	10	5	60	Parallel	Infinite	20	Cont.	72	8	K	2.86	5000
1217-5	2	35	10	5	60	Parallel	Infinite	20	Cont.	72	8	X	4.79	5000
1218-1	2	35	10	5	60	Parallel	Infinite	30	Cont.	72	8	X	2.86	5000
1219-1	2	35	10	5	60	Parallel	Infinite	20	Stag.	72	8	X	2.86	3600
1219-2	2	35	10	5	60	Parallel	Infinite	20	Stag.	72	8	X	2.86	5000
1219-3	2	35	10	5	60	Parallel	Infinite	20	Stag.	72	10	X	2.86	5000
1219-4	2	35	10	5	60	Parallel	Infinite	20	Stag.	72	8	K	2.86	5000
1219-5	2	35	10	5	60	Parallel	Infinite	20	Stag.	72	8	X	4.79	5000
1220-1	2	35	10	5	60	Parallel	Infinite	30	Stag.	72	8	X	2.86	5000
1221-1	2	35	10	5	60	Trap.	Infinite	20	Cont.	72	8	X	2.86	3600
1221-2	2	35	10	5	60	Trap.	Infinite	20	Cont.	72	8	X	2.86	5000
1221-3	2	35	10	5	60	Trap.	Infinite	20	Cont.	72	10	X	2.86	5000
1221-4	2	35	10	5	60	Trap.	Infinite	20	Cont.	72	8	K	2.86	5000
1221-5	2	35	10	5	60	Trap.	Infinite	20	Cont.	72	8	X	4.79	5000
1222-1	2	35	10	5	60	Trap.	Infinite	30	Cont.	72	8	X	2.86	5000
1223-1	2	35	10	5	60	Trap.	Infinite	20	Stag.	72	8	X	2.86	3600
1223-2	2	35	10	5	60	Trap.	Infinite	20	Stag.	72	8	X	2.86	5000
1223-3	2	35	10	5	60	Trap.	Infinite	20	Stag.	72	10	X	2.86	5000
1223-4	2	35	10	5	60	Trap.	Infinite	20	Stag.	72	8	K	2.86	5000
1223-5	2	35	10	5	60	Trap.	Infinite	20	Stag.	72	8	X	4.79	5000
1224-1	2	35	10	5	60	Trap.	Infinite	30	Stag.	72	8	X	2.86	5000
1225-1	2	35	10	7	0	Parallel	Infinite	20	Cont.	72	8	X	2.86	3600
1225-2	2	35	10	7	0	Parallel	Infinite	20	Cont.	72	8	X	2.86	5000
1225-3	2	35	10	7	0	Parallel	Infinite	20	Cont.	72	10	X	2.86	5000
1225-4	2	35	10	7	0	Parallel	Infinite	20	Cont.	72	8	K	2.86	5000
1225-5	2	35	10	7	0	Parallel	Infinite	20	Cont.	72	8	X	4.79	5000
1226-1	2	35	10	7	0	Parallel	Infinite	30	Cont.	72	8	X	2.86	5000
1227-1	2	35	10	7	30	Parallel	Infinite	20	Cont.	72	8	X	2.86	3600
1227-2	2	35	10	7	30	Parallel	Infinite	20	Cont.	72	8	X	2.86	5000
1227-3	2	35	10	7	30	Parallel	Infinite	20	Cont.	72	10	X	2.86	5000
1227-4	2	35	10	7	30	Parallel	Infinite	20	Cont.	72	8	K	2.86	5000
1227-5	2	35	10	7	30	Parallel	Infinite	20	Cont.	72	8	X	4.79	5000
1228-1	2	35	10	7	30	Parallel	Infinite	30	Cont.	72	8	X	2.86	5000
1229-1	2	35	10	7	60	Parallel	Infinite	20	Cont.	72	8	X	2.86	3600
1229-2	2	35	10	7	60	Parallel	Infinite	20	Cont.	72	8	X	2.86	5000
1229-3	2	35	10	7	60	Parallel	Infinite	20	Cont.	72	10	X	2.86	5000
1229-4	2	35	10	7	60	Parallel	Infinite	20	Cont.	72	8	K	2.86	5000
1229-5	2	35	10	7	60	Parallel	Infinite	20	Cont.	72	8	X	4.79	5000
1230-1	2	35	10	7	60	Parallel	Infinite	30	Cont.	72	8	X	2.86	5000
1231-1	2	35	10	7	60	Parallel	Infinite	20	Stag.	72	8	X	2.86	3600
1231-2	2	35	10	7	60	Parallel	Infinite	20	Stag.	72	8	X	2.86	5000
1231-3	2	35	10	7	60	Parallel	Infinite	20	Stag.	72	10	X	2.86	5000
1231-4	2	35	10	7	60	Parallel	Infinite	20	Stag.	72	8	K	2.86	5000
1231-5	2	35	10	7	60	Parallel	Infinite	20	Stag.	72	8	X	4.79	5000
1232-1	2	35	10	7	60	Parallel	Infinite	30	Stag.	72	8	X	2.86	5000
1233-1	2	35	10	7	60	Trap.	Infinite	20	Cont.	72	8	X	2.86	3600
1233-2	2	35	10	7	60	Trap.	Infinite	20	Cont.	72	8	X	2.86	5000
1233-3	2	35	10	7	60	Trap.	Infinite	20	Cont.	72	10	X	2.86	5000
1233-4	2	35	10	7	60	Trap.	Infinite	20	Cont.	72	8	K	2.86	5000
1233-5	2	35	10	7	60	Trap.	Infinite	20	Cont.	72	8	X	4.79	5000
1234-1	2	35	10	7	60	Trap.	Infinite	30	Cont.	72	8	X	2.86	5000
1235-1	2	35	10	7	60	Trap.	Infinite	20	Stag.	72	8	X	2.86	3600
1235-2	2	35	10	7	60	Trap.	Infinite	20	Stag.	72	8	X	2.86	5000
1235-3	2	35	10	7	60	Trap.	Infinite	20	Stag.	72	10	X	2.86	5000
1235-4	2	35	10	7	60	Trap.	Infinite	20	Stag.	72	8	K	2.86	5000
1235-5	2	35	10	7	60	Trap.	Infinite	20	Stag.	72	8	X	4.79	5000
1236-1	2	35	10	7	60	Trap.	Infinite	30	Stag.	72	8	X	2.86	5000
1237-1	2	35	6	3	0	Parallel	Infinite	20	Cont.	96	8	X	2.86	3600
1237-2	2	35	6	3	0	Parallel	Infinite	20	Cont.	96	8	X	2.86	5000
1237-3	2	35	6	3	0	Parallel	Infinite	20	Cont.	96	10	X	2.86	5000
1237-4	2	35	6	3	0	Parallel	Infinite	20	Cont.	96	8	K	2.86	5000
1237-5	2	35	6	3	0	Parallel	Infinite	20	Cont.	96	8	X	4.79	5000
1238-1	2	35	6	3	0	Parallel	Infinite	30	Cont.	96	8	X	2.86	5000
1239-1	2	35	6	3	30	Parallel	Infinite	20	Cont.	96	8	X	2.86	3600
1239-2	2	35	6	3	30	Parallel	Infinite	20	Cont.	96	8	X	2.86	5000
1239-3	2	35	6	3	30	Parallel	Infinite	20	Cont.	96	10	X	2.86	5000

Model ID	Geometry								Cross-section		CF detail		Mat'l
	n_{span}	L/d ratio	s_g [ft]	n_{girder}	Support skew [deg]; Layout	R [ft]	s_{cf} [ft]	CF layout	d_w [in]	t_{deck} [in]	CF type	A_{cf} [in^2]	E_c [ksi]
1239-4	2	35	6	3	30 Parallel	Infinite	20	Cont.	96	8	K	2.86	5000
1239-5	2	35	6	3	30 Parallel	Infinite	20	Cont.	96	8	X	4.79	5000
1240-1	2	35	6	3	30 Parallel	Infinite	30	Cont.	96	8	X	2.86	5000
1241-1	2	35	6	3	60 Parallel	Infinite	20	Cont.	96	8	X	2.86	3600
1241-2	2	35	6	3	60 Parallel	Infinite	20	Cont.	96	8	X	2.86	5000
1241-3	2	35	6	3	60 Parallel	Infinite	20	Cont.	96	10	X	2.86	5000
1241-4	2	35	6	3	60 Parallel	Infinite	20	Cont.	96	8	K	2.86	5000
1241-5	2	35	6	3	60 Parallel	Infinite	20	Cont.	96	8	X	4.79	5000
1242-1	2	35	6	3	60 Parallel	Infinite	30	Cont.	96	8	X	2.86	5000
1243-1	2	35	6	3	60 Parallel	Infinite	20	Stag.	96	8	X	2.86	3600
1243-2	2	35	6	3	60 Parallel	Infinite	20	Stag.	96	8	X	2.86	5000
1243-3	2	35	6	3	60 Parallel	Infinite	20	Stag.	96	10	X	2.86	5000
1243-4	2	35	6	3	60 Parallel	Infinite	20	Stag.	96	8	K	2.86	5000
1243-5	2	35	6	3	60 Parallel	Infinite	20	Stag.	96	8	X	4.79	5000
1244-1	2	35	6	3	60 Parallel	Infinite	30	Stag.	96	8	X	2.86	5000
1245-1	2	35	6	3	60 Trap.	Infinite	20	Cont.	96	8	X	2.86	3600
1245-2	2	35	6	3	60 Trap.	Infinite	20	Cont.	96	8	X	2.86	5000
1245-3	2	35	6	3	60 Trap.	Infinite	20	Cont.	96	10	X	2.86	5000
1245-4	2	35	6	3	60 Trap.	Infinite	20	Cont.	96	8	K	2.86	5000
1245-5	2	35	6	3	60 Trap.	Infinite	20	Cont.	96	8	X	4.79	5000
1246-1	2	35	6	3	60 Trap.	Infinite	30	Cont.	96	8	X	2.86	5000
1247-1	2	35	6	3	60 Trap.	Infinite	20	Stag.	96	8	X	2.86	3600
1247-2	2	35	6	3	60 Trap.	Infinite	20	Stag.	96	8	X	2.86	5000
1247-3	2	35	6	3	60 Trap.	Infinite	20	Stag.	96	10	X	2.86	5000
1247-4	2	35	6	3	60 Trap.	Infinite	20	Stag.	96	8	K	2.86	5000
1247-5	2	35	6	3	60 Trap.	Infinite	20	Stag.	96	8	X	4.79	5000
1248-1	2	35	6	3	60 Trap.	Infinite	30	Stag.	96	8	X	2.86	5000
1249-1	2	35	6	5	0 Parallel	Infinite	20	Cont.	96	8	X	2.86	3600
1249-2	2	35	6	5	0 Parallel	Infinite	20	Cont.	96	8	X	2.86	5000
1249-3	2	35	6	5	0 Parallel	Infinite	20	Cont.	96	10	X	2.86	5000
1249-4	2	35	6	5	0 Parallel	Infinite	20	Cont.	96	8	K	2.86	5000
1249-5	2	35	6	5	0 Parallel	Infinite	20	Cont.	96	8	X	4.79	5000
1250-1	2	35	6	5	0 Parallel	Infinite	30	Cont.	96	8	X	2.86	5000
1251-1	2	35	6	5	30 Parallel	Infinite	20	Cont.	96	8	X	2.86	3600
1251-2	2	35	6	5	30 Parallel	Infinite	20	Cont.	96	8	X	2.86	5000
1251-3	2	35	6	5	30 Parallel	Infinite	20	Cont.	96	10	X	2.86	5000
1251-4	2	35	6	5	30 Parallel	Infinite	20	Cont.	96	8	K	2.86	5000
1251-5	2	35	6	5	30 Parallel	Infinite	20	Cont.	96	8	X	4.79	5000
1252-1	2	35	6	5	30 Parallel	Infinite	30	Cont.	96	8	X	2.86	5000
1253-1	2	35	6	5	60 Parallel	Infinite	20	Cont.	96	8	X	2.86	3600
1253-2	2	35	6	5	60 Parallel	Infinite	20	Cont.	96	8	X	2.86	5000
1253-3	2	35	6	5	60 Parallel	Infinite	20	Cont.	96	10	X	2.86	5000
1253-4	2	35	6	5	60 Parallel	Infinite	20	Cont.	96	8	K	2.86	5000
1253-5	2	35	6	5	60 Parallel	Infinite	20	Cont.	96	8	X	4.79	5000
1254-1	2	35	6	5	60 Parallel	Infinite	30	Cont.	96	8	X	2.86	5000
1255-1	2	35	6	5	60 Parallel	Infinite	20	Stag.	96	8	X	2.86	3600
1255-2	2	35	6	5	60 Parallel	Infinite	20	Stag.	96	8	X	2.86	5000
1255-3	2	35	6	5	60 Parallel	Infinite	20	Stag.	96	10	X	2.86	5000
1255-4	2	35	6	5	60 Parallel	Infinite	20	Stag.	96	8	K	2.86	5000
1255-5	2	35	6	5	60 Parallel	Infinite	20	Stag.	96	8	X	4.79	5000
1256-1	2	35	6	5	60 Parallel	Infinite	30	Stag.	96	8	X	2.86	5000
1257-1	2	35	6	5	60 Trap.	Infinite	20	Cont.	96	8	X	2.86	3600
1257-2	2	35	6	5	60 Trap.	Infinite	20	Cont.	96	8	X	2.86	5000
1257-3	2	35	6	5	60 Trap.	Infinite	20	Cont.	96	10	X	2.86	5000
1257-4	2	35	6	5	60 Trap.	Infinite	20	Cont.	96	8	K	2.86	5000
1257-5	2	35	6	5	60 Trap.	Infinite	20	Cont.	96	8	X	4.79	5000
1258-1	2	35	6	5	60 Trap.	Infinite	30	Cont.	96	8	X	2.86	5000
1259-1	2	35	6	5	60 Trap.	Infinite	20	Stag.	96	8	X	2.86	3600
1259-2	2	35	6	5	60 Trap.	Infinite	20	Stag.	96	8	X	2.86	5000
1259-3	2	35	6	5	60 Trap.	Infinite	20	Stag.	96	10	X	2.86	5000
1259-4	2	35	6	5	60 Trap.	Infinite	20	Stag.	96	8	K	2.86	5000
1259-5	2	35	6	5	60 Trap.	Infinite	20	Stag.	96	8	X	4.79	5000
1260-1	2	35	6	5	60 Trap.	Infinite	30	Stag.	96	8	X	2.86	5000
1261-1	2	35	6	7	0 Parallel	Infinite	20	Cont.	96	8	X	2.86	3600
1261-2	2	35	6	7	0 Parallel	Infinite	20	Cont.	96	8	X	2.86	5000
1261-3	2	35	6	7	0 Parallel	Infinite	20	Cont.	96	10	X	2.86	5000
1261-4	2	35	6	7	0 Parallel	Infinite	20	Cont.	96	8	K	2.86	5000
1261-5	2	35	6	7	0 Parallel	Infinite	20	Cont.	96	8	X	4.79	5000
1262-1	2	35	6	7	0 Parallel	Infinite	30	Cont.	96	8	X	2.86	5000
1263-1	2	35	6	7	30 Parallel	Infinite	20	Cont.	96	8	X	2.86	3600
1263-2	2	35	6	7	30 Parallel	Infinite	20	Cont.	96	8	X	2.86	5000
1263-3	2	35	6	7	30 Parallel	Infinite	20	Cont.	96	10	X	2.86	5000
1263-4	2	35	6	7	30 Parallel	Infinite	20	Cont.	96	8	K	2.86	5000

Model ID	Geometry									Cross-section		CF detail		Mat'l
	n_{span}	L/d ratio	s_g [ft]	n_{girder}	Support skew [deg]; Layout		R [ft]	s_{cf} [ft]	CF layout	d_w [in]	t_{deck} [in]	CF type	A_{cf} [in^2]	E_c [ksi]
1263-5	2	35	6	7	30	Parallel	Infinite	20	Cont.	96	8	X	4.79	5000
1264-1	2	35	6	7	30	Parallel	Infinite	30	Cont.	96	8	X	2.86	5000
1265-1	2	35	6	7	60	Parallel	Infinite	20	Cont.	96	8	X	2.86	3600
1265-2	2	35	6	7	60	Parallel	Infinite	20	Cont.	96	8	X	2.86	5000
1265-3	2	35	6	7	60	Parallel	Infinite	20	Cont.	96	10	X	2.86	5000
1265-4	2	35	6	7	60	Parallel	Infinite	20	Cont.	96	8	K	2.86	5000
1265-5	2	35	6	7	60	Parallel	Infinite	20	Cont.	96	8	X	4.79	5000
1266-1	2	35	6	7	60	Parallel	Infinite	30	Cont.	96	8	X	2.86	5000
1267-1	2	35	6	7	60	Parallel	Infinite	20	Stag.	96	8	X	2.86	3600
1267-2	2	35	6	7	60	Parallel	Infinite	20	Stag.	96	8	X	2.86	5000
1267-3	2	35	6	7	60	Parallel	Infinite	20	Stag.	96	10	X	2.86	5000
1267-4	2	35	6	7	60	Parallel	Infinite	20	Stag.	96	8	K	2.86	5000
1267-5	2	35	6	7	60	Parallel	Infinite	20	Stag.	96	8	X	4.79	5000
1268-1	2	35	6	7	60	Parallel	Infinite	30	Stag.	96	8	X	2.86	5000
1269-1	2	35	6	7	60	Trap.	Infinite	20	Cont.	96	8	X	2.86	3600
1269-2	2	35	6	7	60	Trap.	Infinite	20	Cont.	96	8	X	2.86	5000
1269-3	2	35	6	7	60	Trap.	Infinite	20	Cont.	96	10	X	2.86	5000
1269-4	2	35	6	7	60	Trap.	Infinite	20	Cont.	96	8	K	2.86	5000
1269-5	2	35	6	7	60	Trap.	Infinite	20	Cont.	96	8	X	4.79	5000
1270-1	2	35	6	7	60	Trap.	Infinite	30	Cont.	96	8	X	2.86	5000
1271-1	2	35	6	7	60	Trap.	Infinite	20	Stag.	96	8	X	2.86	3600
1271-2	2	35	6	7	60	Trap.	Infinite	20	Stag.	96	8	X	2.86	5000
1271-3	2	35	6	7	60	Trap.	Infinite	20	Stag.	96	10	X	2.86	5000
1271-4	2	35	6	7	60	Trap.	Infinite	20	Stag.	96	8	K	2.86	5000
1271-5	2	35	6	7	60	Trap.	Infinite	20	Stag.	96	8	X	4.79	5000
1272-1	2	35	6	7	60	Trap.	Infinite	30	Stag.	96	8	X	2.86	5000
1273-1	2	35	8	3	0	Parallel	Infinite	20	Cont.	96	8	X	2.86	3600
1273-2	2	35	8	3	0	Parallel	Infinite	20	Cont.	96	8	X	2.86	5000
1273-3	2	35	8	3	0	Parallel	Infinite	20	Cont.	96	10	X	2.86	5000
1273-4	2	35	8	3	0	Parallel	Infinite	20	Cont.	96	8	K	2.86	5000
1273-5	2	35	8	3	0	Parallel	Infinite	20	Cont.	96	8	X	4.79	5000
1274-1	2	35	8	3	0	Parallel	Infinite	30	Cont.	96	8	X	2.86	5000
1275-1	2	35	8	3	30	Parallel	Infinite	20	Cont.	96	8	X	2.86	3600
1275-2	2	35	8	3	30	Parallel	Infinite	20	Cont.	96	8	X	2.86	5000
1275-3	2	35	8	3	30	Parallel	Infinite	20	Cont.	96	10	X	2.86	5000
1275-4	2	35	8	3	30	Parallel	Infinite	20	Cont.	96	8	K	2.86	5000
1275-5	2	35	8	3	30	Parallel	Infinite	20	Cont.	96	8	X	4.79	5000
1276-1	2	35	8	3	30	Parallel	Infinite	30	Cont.	96	8	X	2.86	5000
1277-1	2	35	8	3	60	Parallel	Infinite	20	Cont.	96	8	X	2.86	3600
1277-2	2	35	8	3	60	Parallel	Infinite	20	Cont.	96	8	X	2.86	5000
1277-3	2	35	8	3	60	Parallel	Infinite	20	Cont.	96	10	X	2.86	5000
1277-4	2	35	8	3	60	Parallel	Infinite	20	Cont.	96	8	K	2.86	5000
1277-5	2	35	8	3	60	Parallel	Infinite	20	Cont.	96	8	X	4.79	5000
1278-1	2	35	8	3	60	Parallel	Infinite	30	Cont.	96	8	X	2.86	5000
1279-1	2	35	8	3	60	Parallel	Infinite	20	Stag.	96	8	X	2.86	3600
1279-2	2	35	8	3	60	Parallel	Infinite	20	Stag.	96	8	X	2.86	5000
1279-3	2	35	8	3	60	Parallel	Infinite	20	Stag.	96	10	X	2.86	5000
1279-4	2	35	8	3	60	Parallel	Infinite	20	Stag.	96	8	K	2.86	5000
1279-5	2	35	8	3	60	Parallel	Infinite	20	Stag.	96	8	X	4.79	5000
1280-1	2	35	8	3	60	Parallel	Infinite	30	Stag.	96	8	X	2.86	5000
1281-1	2	35	8	3	60	Trap.	Infinite	20	Cont.	96	8	X	2.86	3600
1281-2	2	35	8	3	60	Trap.	Infinite	20	Cont.	96	8	X	2.86	5000
1281-3	2	35	8	3	60	Trap.	Infinite	20	Cont.	96	10	X	2.86	5000
1281-4	2	35	8	3	60	Trap.	Infinite	20	Cont.	96	8	K	2.86	5000
1281-5	2	35	8	3	60	Trap.	Infinite	20	Cont.	96	8	X	4.79	5000
1282-1	2	35	8	3	60	Trap.	Infinite	30	Cont.	96	8	X	2.86	5000
1283-1	2	35	8	3	60	Trap.	Infinite	20	Stag.	96	8	X	2.86	3600
1283-2	2	35	8	3	60	Trap.	Infinite	20	Stag.	96	8	X	2.86	5000
1283-3	2	35	8	3	60	Trap.	Infinite	20	Stag.	96	10	X	2.86	5000
1283-4	2	35	8	3	60	Trap.	Infinite	20	Stag.	96	8	K	2.86	5000
1283-5	2	35	8	3	60	Trap.	Infinite	20	Stag.	96	8	X	4.79	5000
1284-1	2	35	8	3	60	Trap.	Infinite	30	Stag.	96	8	X	2.86	5000
1285-1	2	35	8	5	0	Parallel	Infinite	20	Cont.	96	8	X	2.86	3600
1285-2	2	35	8	5	0	Parallel	Infinite	20	Cont.	96	8	X	2.86	5000
1285-3	2	35	8	5	0	Parallel	Infinite	20	Cont.	96	10	X	2.86	5000
1285-4	2	35	8	5	0	Parallel	Infinite	20	Cont.	96	8	K	2.86	5000
1285-5	2	35	8	5	0	Parallel	Infinite	20	Cont.	96	8	X	4.79	5000
1286-1	2	35	8	5	0	Parallel	Infinite	30	Cont.	96	8	X	2.86	5000
1287-1	2	35	8	5	30	Parallel	Infinite	20	Cont.	96	8	X	2.86	3600
1287-2	2	35	8	5	30	Parallel	Infinite	20	Cont.	96	8	X	2.86	5000
1287-3	2	35	8	5	30	Parallel	Infinite	20	Cont.	96	10	X	2.86	5000
1287-4	2	35	8	5	30	Parallel	Infinite	20	Cont.	96	8	K	2.86	5000
1287-5	2	35	8	5	30	Parallel	Infinite	20	Cont.	96	8	X	4.79	5000

Model ID	Geometry									Cross-section		CF detail		Mat'l
	n_{span}	L/d ratio	s_g [ft]	n_{girder}	Support skew [deg];	Layout	R [ft]	s_{cf} [ft]	CF layout	d_w [in]	t_{deck} [in]	CF type	A_{cf} [in^2]	E_c [ksi]
1288-1	2	35	8	5	30	Parallel	Infinite	30	Cont.	96	8	X	2.86	5000
1289-1	2	35	8	5	60	Parallel	Infinite	20	Cont.	96	8	X	2.86	3600
1289-2	2	35	8	5	60	Parallel	Infinite	20	Cont.	96	8	X	2.86	5000
1289-3	2	35	8	5	60	Parallel	Infinite	20	Cont.	96	10	X	2.86	5000
1289-4	2	35	8	5	60	Parallel	Infinite	20	Cont.	96	8	K	2.86	5000
1289-5	2	35	8	5	60	Parallel	Infinite	20	Cont.	96	8	X	4.79	5000
1290-1	2	35	8	5	60	Parallel	Infinite	30	Cont.	96	8	X	2.86	5000
1291-1	2	35	8	5	60	Parallel	Infinite	20	Stag.	96	8	X	2.86	3600
1291-2	2	35	8	5	60	Parallel	Infinite	20	Stag.	96	8	X	2.86	5000
1291-3	2	35	8	5	60	Parallel	Infinite	20	Stag.	96	10	X	2.86	5000
1291-4	2	35	8	5	60	Parallel	Infinite	20	Stag.	96	8	K	2.86	5000
1291-5	2	35	8	5	60	Parallel	Infinite	20	Stag.	96	8	X	4.79	5000
1292-1	2	35	8	5	60	Parallel	Infinite	30	Stag.	96	8	X	2.86	5000
1293-1	2	35	8	5	60	Trap.	Infinite	20	Cont.	96	8	X	2.86	3600
1293-2	2	35	8	5	60	Trap.	Infinite	20	Cont.	96	8	X	2.86	5000
1293-3	2	35	8	5	60	Trap.	Infinite	20	Cont.	96	10	X	2.86	5000
1293-4	2	35	8	5	60	Trap.	Infinite	20	Cont.	96	8	K	2.86	5000
1293-5	2	35	8	5	60	Trap.	Infinite	20	Cont.	96	8	X	4.79	5000
1294-1	2	35	8	5	60	Trap.	Infinite	30	Cont.	96	8	X	2.86	5000
1295-1	2	35	8	5	60	Trap.	Infinite	20	Stag.	96	8	X	2.86	3600
1295-2	2	35	8	5	60	Trap.	Infinite	20	Stag.	96	8	X	2.86	5000
1295-3	2	35	8	5	60	Trap.	Infinite	20	Stag.	96	10	X	2.86	5000
1295-4	2	35	8	5	60	Trap.	Infinite	20	Stag.	96	8	K	2.86	5000
1295-5	2	35	8	5	60	Trap.	Infinite	20	Stag.	96	8	X	4.79	5000
1296-1	2	35	8	5	60	Trap.	Infinite	30	Stag.	96	8	X	2.86	5000
1297-1	2	35	8	7	0	Parallel	Infinite	20	Cont.	96	8	X	2.86	3600
1297-2	2	35	8	7	0	Parallel	Infinite	20	Cont.	96	8	X	2.86	5000
1297-3	2	35	8	7	0	Parallel	Infinite	20	Cont.	96	10	X	2.86	5000
1297-4	2	35	8	7	0	Parallel	Infinite	20	Cont.	96	8	K	2.86	5000
1297-5	2	35	8	7	0	Parallel	Infinite	20	Cont.	96	8	X	4.79	5000
1298-1	2	35	8	7	0	Parallel	Infinite	30	Cont.	96	8	X	2.86	5000
1299-1	2	35	8	7	30	Parallel	Infinite	20	Cont.	96	8	X	2.86	3600
1299-2	2	35	8	7	30	Parallel	Infinite	20	Cont.	96	8	X	2.86	5000
1299-3	2	35	8	7	30	Parallel	Infinite	20	Cont.	96	10	X	2.86	5000
1299-4	2	35	8	7	30	Parallel	Infinite	20	Cont.	96	8	K	2.86	5000
1299-5	2	35	8	7	30	Parallel	Infinite	20	Cont.	96	8	X	4.79	5000
1300-1	2	35	8	7	30	Parallel	Infinite	30	Cont.	96	8	X	2.86	5000
1301-1	2	35	8	7	60	Parallel	Infinite	20	Cont.	96	8	X	2.86	3600
1301-2	2	35	8	7	60	Parallel	Infinite	20	Cont.	96	8	X	2.86	5000
1301-3	2	35	8	7	60	Parallel	Infinite	20	Cont.	96	10	X	2.86	5000
1301-4	2	35	8	7	60	Parallel	Infinite	20	Cont.	96	8	K	2.86	5000
1301-5	2	35	8	7	60	Parallel	Infinite	20	Cont.	96	8	X	4.79	5000
1302-1	2	35	8	7	60	Parallel	Infinite	30	Cont.	96	8	X	2.86	5000
1303-1	2	35	8	7	60	Parallel	Infinite	20	Stag.	96	8	X	2.86	3600
1303-2	2	35	8	7	60	Parallel	Infinite	20	Stag.	96	8	X	2.86	5000
1303-3	2	35	8	7	60	Parallel	Infinite	20	Stag.	96	10	X	2.86	5000
1303-4	2	35	8	7	60	Parallel	Infinite	20	Stag.	96	8	K	2.86	5000
1303-5	2	35	8	7	60	Parallel	Infinite	20	Stag.	96	8	X	4.79	5000
1304-1	2	35	8	7	60	Parallel	Infinite	30	Stag.	96	8	X	2.86	5000
1305-1	2	35	8	7	60	Trap.	Infinite	20	Cont.	96	8	X	2.86	3600
1305-2	2	35	8	7	60	Trap.	Infinite	20	Cont.	96	8	X	2.86	5000
1305-3	2	35	8	7	60	Trap.	Infinite	20	Cont.	96	10	X	2.86	5000
1305-4	2	35	8	7	60	Trap.	Infinite	20	Cont.	96	8	K	2.86	5000
1305-5	2	35	8	7	60	Trap.	Infinite	20	Cont.	96	8	X	4.79	5000
1306-1	2	35	8	7	60	Trap.	Infinite	30	Cont.	96	8	X	2.86	5000
1307-1	2	35	8	7	60	Trap.	Infinite	20	Stag.	96	8	X	2.86	3600
1307-2	2	35	8	7	60	Trap.	Infinite	20	Stag.	96	8	X	2.86	5000
1307-3	2	35	8	7	60	Trap.	Infinite	20	Stag.	96	10	X	2.86	5000
1307-4	2	35	8	7	60	Trap.	Infinite	20	Stag.	96	8	K	2.86	5000
1307-5	2	35	8	7	60	Trap.	Infinite	20	Stag.	96	8	X	4.79	5000
1308-1	2	35	8	7	60	Trap.	Infinite	30	Stag.	96	8	X	2.86	5000
1309-1	2	35	10	3	0	Parallel	Infinite	20	Cont.	96	8	X	2.86	3600
1309-2	2	35	10	3	0	Parallel	Infinite	20	Cont.	96	8	X	2.86	5000
1309-3	2	35	10	3	0	Parallel	Infinite	20	Cont.	96	10	X	2.86	5000
1309-4	2	35	10	3	0	Parallel	Infinite	20	Cont.	96	8	K	2.86	5000
1309-5	2	35	10	3	0	Parallel	Infinite	20	Cont.	96	8	X	4.79	5000
1310-1	2	35	10	3	0	Parallel	Infinite	30	Cont.	96	8	X	2.86	5000
1311-1	2	35	10	3	30	Parallel	Infinite	20	Cont.	96	8	X	2.86	3600
1311-2	2	35	10	3	30	Parallel	Infinite	20	Cont.	96	8	X	2.86	5000
1311-3	2	35	10	3	30	Parallel	Infinite	20	Cont.	96	10	X	2.86	5000
1311-4	2	35	10	3	30	Parallel	Infinite	20	Cont.	96	8	K	2.86	5000
1311-5	2	35	10	3	30	Parallel	Infinite	20	Cont.	96	8	X	4.79	5000
1312-1	2	35	10	3	30	Parallel	Infinite	30	Cont.	96	8	X	2.86	5000

Model ID	Geometry									Cross-section		CF detail		Mat'l
	n_{span}	L/d ratio	s_g [ft]	n_{girder}	Support skew [deg];	Layout	R [ft]	s_{cf} [ft]	CF layout	d_w [in]	t_{deck} [in]	CF type	A_{cf} [in^2]	E_c [ksi]
1313-1	2	35	10	3	60	Parallel	Infinite	20	Cont.	96	8	X	2.86	3600
1313-2	2	35	10	3	60	Parallel	Infinite	20	Cont.	96	8	X	2.86	5000
1313-3	2	35	10	3	60	Parallel	Infinite	20	Cont.	96	10	X	2.86	5000
1313-4	2	35	10	3	60	Parallel	Infinite	20	Cont.	96	8	K	2.86	5000
1313-5	2	35	10	3	60	Parallel	Infinite	20	Cont.	96	8	X	4.79	5000
1314-1	2	35	10	3	60	Parallel	Infinite	30	Cont.	96	8	X	2.86	5000
1315-1	2	35	10	3	60	Parallel	Infinite	20	Stag.	96	8	X	2.86	3600
1315-2	2	35	10	3	60	Parallel	Infinite	20	Stag.	96	8	X	2.86	5000
1315-3	2	35	10	3	60	Parallel	Infinite	20	Stag.	96	10	X	2.86	5000
1315-4	2	35	10	3	60	Parallel	Infinite	20	Stag.	96	8	K	2.86	5000
1315-5	2	35	10	3	60	Parallel	Infinite	20	Stag.	96	8	X	4.79	5000
1316-1	2	35	10	3	60	Parallel	Infinite	30	Stag.	96	8	X	2.86	5000
1317-1	2	35	10	3	60	Trap.	Infinite	20	Cont.	96	8	X	2.86	3600
1317-2	2	35	10	3	60	Trap.	Infinite	20	Cont.	96	8	X	2.86	5000
1317-3	2	35	10	3	60	Trap.	Infinite	20	Cont.	96	10	X	2.86	5000
1317-4	2	35	10	3	60	Trap.	Infinite	20	Cont.	96	8	K	2.86	5000
1317-5	2	35	10	3	60	Trap.	Infinite	20	Cont.	96	8	X	4.79	5000
1318-1	2	35	10	3	60	Trap.	Infinite	30	Cont.	96	8	X	2.86	5000
1319-1	2	35	10	3	60	Trap.	Infinite	20	Stag.	96	8	X	2.86	3600
1319-2	2	35	10	3	60	Trap.	Infinite	20	Stag.	96	8	X	2.86	5000
1319-3	2	35	10	3	60	Trap.	Infinite	20	Stag.	96	10	X	2.86	5000
1319-4	2	35	10	3	60	Trap.	Infinite	20	Stag.	96	8	K	2.86	5000
1319-5	2	35	10	3	60	Trap.	Infinite	20	Stag.	96	8	X	4.79	5000
1320-1	2	35	10	3	60	Trap.	Infinite	30	Stag.	96	8	X	2.86	5000
1321-1	2	35	10	5	0	Parallel	Infinite	20	Cont.	96	8	X	2.86	3600
1321-2	2	35	10	5	0	Parallel	Infinite	20	Cont.	96	8	X	2.86	5000
1321-3	2	35	10	5	0	Parallel	Infinite	20	Cont.	96	10	X	2.86	5000
1321-4	2	35	10	5	0	Parallel	Infinite	20	Cont.	96	8	K	2.86	5000
1321-5	2	35	10	5	0	Parallel	Infinite	20	Cont.	96	8	X	4.79	5000
1322-1	2	35	10	5	0	Parallel	Infinite	30	Cont.	96	8	X	2.86	5000
1323-1	2	35	10	5	30	Parallel	Infinite	20	Cont.	96	8	X	2.86	3600
1323-2	2	35	10	5	30	Parallel	Infinite	20	Cont.	96	8	X	2.86	5000
1323-3	2	35	10	5	30	Parallel	Infinite	20	Cont.	96	10	X	2.86	5000
1323-4	2	35	10	5	30	Parallel	Infinite	20	Cont.	96	8	K	2.86	5000
1323-5	2	35	10	5	30	Parallel	Infinite	20	Cont.	96	8	X	4.79	5000
1324-1	2	35	10	5	30	Parallel	Infinite	30	Cont.	96	8	X	2.86	5000
1325-1	2	35	10	5	60	Parallel	Infinite	20	Cont.	96	8	X	2.86	3600
1325-2	2	35	10	5	60	Parallel	Infinite	20	Cont.	96	8	X	2.86	5000
1325-3	2	35	10	5	60	Parallel	Infinite	20	Cont.	96	10	X	2.86	5000
1325-4	2	35	10	5	60	Parallel	Infinite	20	Cont.	96	8	K	2.86	5000
1325-5	2	35	10	5	60	Parallel	Infinite	20	Cont.	96	8	X	4.79	5000
1326-1	2	35	10	5	60	Parallel	Infinite	30	Cont.	96	8	X	2.86	5000
1327-1	2	35	10	5	60	Parallel	Infinite	20	Stag.	96	8	X	2.86	3600
1327-2	2	35	10	5	60	Parallel	Infinite	20	Stag.	96	8	X	2.86	5000
1327-3	2	35	10	5	60	Parallel	Infinite	20	Stag.	96	10	X	2.86	5000
1327-4	2	35	10	5	60	Parallel	Infinite	20	Stag.	96	8	K	2.86	5000
1327-5	2	35	10	5	60	Parallel	Infinite	20	Stag.	96	8	X	4.79	5000
1328-1	2	35	10	5	60	Parallel	Infinite	30	Stag.	96	8	X	2.86	5000
1329-1	2	35	10	5	60	Trap.	Infinite	20	Cont.	96	8	X	2.86	3600
1329-2	2	35	10	5	60	Trap.	Infinite	20	Cont.	96	8	X	2.86	5000
1329-3	2	35	10	5	60	Trap.	Infinite	20	Cont.	96	10	X	2.86	5000
1329-4	2	35	10	5	60	Trap.	Infinite	20	Cont.	96	8	K	2.86	5000
1329-5	2	35	10	5	60	Trap.	Infinite	20	Cont.	96	8	X	4.79	5000
1330-1	2	35	10	5	60	Trap.	Infinite	30	Cont.	96	8	X	2.86	5000
1331-1	2	35	10	5	60	Trap.	Infinite	20	Stag.	96	8	X	2.86	3600
1331-2	2	35	10	5	60	Trap.	Infinite	20	Stag.	96	8	X	2.86	5000
1331-3	2	35	10	5	60	Trap.	Infinite	20	Stag.	96	10	X	2.86	5000
1331-4	2	35	10	5	60	Trap.	Infinite	20	Stag.	96	8	K	2.86	5000
1331-5	2	35	10	5	60	Trap.	Infinite	20	Stag.	96	8	X	4.79	5000
1332-1	2	35	10	5	60	Trap.	Infinite	30	Stag.	96	8	X	2.86	5000
1333-1	2	35	10	7	0	Parallel	Infinite	20	Cont.	96	8	X	2.86	3600
1333-2	2	35	10	7	0	Parallel	Infinite	20	Cont.	96	8	X	2.86	5000
1333-3	2	35	10	7	0	Parallel	Infinite	20	Cont.	96	10	X	2.86	5000
1333-4	2	35	10	7	0	Parallel	Infinite	20	Cont.	96	8	K	2.86	5000
1333-5	2	35	10	7	0	Parallel	Infinite	20	Cont.	96	8	X	4.79	5000
1334-1	2	35	10	7	0	Parallel	Infinite	30	Cont.	96	8	X	2.86	5000
1335-1	2	35	10	7	30	Parallel	Infinite	20	Cont.	96	8	X	2.86	3600
1335-2	2	35	10	7	30	Parallel	Infinite	20	Cont.	96	8	X	2.86	5000
1335-3	2	35	10	7	30	Parallel	Infinite	20	Cont.	96	10	X	2.86	5000
1335-4	2	35	10	7	30	Parallel	Infinite	20	Cont.	96	8	K	2.86	5000
1335-5	2	35	10	7	30	Parallel	Infinite	20	Cont.	96	8	X	4.79	5000
1336-1	2	35	10	7	30	Parallel	Infinite	30	Cont.	96	8	X	2.86	5000
1337-1	2	35	10	7	60	Parallel	Infinite	20	Cont.	96	8	X	2.86	3600

Model ID	Geometry									Cross-section		CF detail		Mat'l
	n_{span}	L/d ratio	s_g [ft]	n_{girder}	Support skew [deg];	Layout	R [ft]	s_{cf} [ft]	CF layout	d_w [in]	t_{deck} [in]	CF type	A_{cf} [in^2]	E_c [ksi]
1337-2	2	35	10	7	60	Parallel	Infinite	20	Cont.	96	8	X	2.86	5000
1337-3	2	35	10	7	60	Parallel	Infinite	20	Cont.	96	10	X	2.86	5000
1337-4	2	35	10	7	60	Parallel	Infinite	20	Cont.	96	8	K	2.86	5000
1337-5	2	35	10	7	60	Parallel	Infinite	20	Cont.	96	8	X	4.79	5000
1338-1	2	35	10	7	60	Parallel	Infinite	30	Cont.	96	8	X	2.86	5000
1339-1	2	35	10	7	60	Parallel	Infinite	20	Stag.	96	8	X	2.86	3600
1339-2	2	35	10	7	60	Parallel	Infinite	20	Stag.	96	8	X	2.86	5000
1339-3	2	35	10	7	60	Parallel	Infinite	20	Stag.	96	10	X	2.86	5000
1339-4	2	35	10	7	60	Parallel	Infinite	20	Stag.	96	8	K	2.86	5000
1339-5	2	35	10	7	60	Parallel	Infinite	20	Stag.	96	8	X	4.79	5000
1340-1	2	35	10	7	60	Parallel	Infinite	30	Stag.	96	8	X	2.86	5000
1341-1	2	35	10	7	60	Trap.	Infinite	20	Cont.	96	8	X	2.86	3600
1341-2	2	35	10	7	60	Trap.	Infinite	20	Cont.	96	8	X	2.86	5000
1341-3	2	35	10	7	60	Trap.	Infinite	20	Cont.	96	10	X	2.86	5000
1341-4	2	35	10	7	60	Trap.	Infinite	20	Cont.	96	8	K	2.86	5000
1341-5	2	35	10	7	60	Trap.	Infinite	20	Cont.	96	8	X	4.79	5000
1342-1	2	35	10	7	60	Trap.	Infinite	30	Cont.	96	8	X	2.86	5000
1343-1	2	35	10	7	60	Trap.	Infinite	20	Stag.	96	8	X	2.86	3600
1343-2	2	35	10	7	60	Trap.	Infinite	20	Stag.	96	8	X	2.86	5000
1343-3	2	35	10	7	60	Trap.	Infinite	20	Stag.	96	10	X	2.86	5000
1343-4	2	35	10	7	60	Trap.	Infinite	20	Stag.	96	8	K	2.86	5000
1343-5	2	35	10	7	60	Trap.	Infinite	20	Stag.	96	8	X	4.79	5000
1344-1	2	35	10	7	60	Trap.	Infinite	30	Stag.	96	8	X	2.86	5000
1345-1	3	25	6	3	0	Parallel	1500	20	Cont.	72	8	X	2.86	5000
1345-2	3	25	6	3	0	Parallel	1500	20	Cont.	72	8	X	4.79	5000
1346-1	3	25	6	3	0	Parallel	750	20	Cont.	72	8	X	2.86	5000
1346-2	3	25	6	3	0	Parallel	750	20	Cont.	72	8	X	4.79	5000
1347-1	3	25	6	5	0	Parallel	1500	20	Cont.	72	8	X	2.86	5000
1347-2	3	25	6	5	0	Parallel	1500	20	Cont.	72	8	X	4.79	5000
1348-1	3	25	6	5	0	Parallel	750	20	Cont.	72	8	X	2.86	5000
1348-2	3	25	6	5	0	Parallel	750	20	Cont.	72	8	X	4.79	5000
1349-1	3	25	8	3	0	Parallel	1500	20	Cont.	72	8	X	2.86	5000
1349-2	3	25	8	3	0	Parallel	1500	20	Cont.	72	8	X	4.79	5000
1350-1	3	25	8	3	0	Parallel	750	20	Cont.	72	8	X	2.86	5000
1350-2	3	25	8	3	0	Parallel	750	20	Cont.	72	8	X	4.79	5000
1351-1	3	25	8	5	0	Parallel	1500	20	Cont.	72	8	X	2.86	5000
1351-2	3	25	8	5	0	Parallel	1500	20	Cont.	72	8	X	4.79	5000
1352-1	3	25	8	5	0	Parallel	750	20	Cont.	72	8	X	2.86	5000
1352-2	3	25	8	5	0	Parallel	750	20	Cont.	72	8	X	4.79	5000
1353-1	3	25	10	3	0	Parallel	1500	20	Cont.	72	8	X	2.86	5000
1353-2	3	25	10	3	0	Parallel	1500	20	Cont.	72	8	X	4.79	5000
1354-1	3	25	10	3	0	Parallel	750	20	Cont.	72	8	X	2.86	5000
1354-2	3	25	10	3	0	Parallel	750	20	Cont.	72	8	X	4.79	5000
1355-1	3	25	10	5	0	Parallel	1500	20	Cont.	72	8	X	2.86	5000
1355-2	3	25	10	5	0	Parallel	1500	20	Cont.	72	8	X	4.79	5000
1356-1	3	25	10	5	0	Parallel	750	20	Cont.	72	8	X	2.86	5000
1356-2	3	25	10	5	0	Parallel	750	20	Cont.	72	8	X	4.79	5000
1357-1	3	25	6	3	0	Parallel	1500	20	Cont.	96	8	X	2.86	5000
1357-2	3	25	6	3	0	Parallel	1500	20	Cont.	96	8	X	4.79	5000
1358-1	3	25	6	3	0	Parallel	750	20	Cont.	96	8	X	2.86	5000
1358-2	3	25	6	3	0	Parallel	750	20	Cont.	96	8	X	4.79	5000
1359-1	3	25	6	5	0	Parallel	1500	20	Cont.	96	8	X	2.86	5000
1359-2	3	25	6	5	0	Parallel	1500	20	Cont.	96	8	X	4.79	5000
1360-1	3	25	6	5	0	Parallel	750	20	Cont.	96	8	X	2.86	5000
1360-2	3	25	6	5	0	Parallel	750	20	Cont.	96	8	X	4.79	5000
1361-1	3	25	8	3	0	Parallel	1500	20	Cont.	96	8	X	2.86	5000
1361-2	3	25	8	3	0	Parallel	1500	20	Cont.	96	8	X	4.79	5000
1362-1	3	25	8	3	0	Parallel	750	20	Cont.	96	8	X	2.86	5000
1362-2	3	25	8	3	0	Parallel	750	20	Cont.	96	8	X	4.79	5000
1363-1	3	25	8	5	0	Parallel	1500	20	Cont.	96	8	X	2.86	5000
1363-2	3	25	8	5	0	Parallel	1500	20	Cont.	96	8	X	4.79	5000
1364-1	3	25	8	5	0	Parallel	750	20	Cont.	96	8	X	2.86	5000
1364-2	3	25	8	5	0	Parallel	750	20	Cont.	96	8	X	4.79	5000
1365-1	3	25	10	3	0	Parallel	1500	20	Cont.	96	8	X	2.86	5000
1365-2	3	25	10	3	0	Parallel	1500	20	Cont.	96	8	X	4.79	5000
1366-1	3	25	10	3	0	Parallel	750	20	Cont.	96	8	X	2.86	5000
1366-2	3	25	10	3	0	Parallel	750	20	Cont.	96	8	X	4.79	5000
1367-1	3	25	10	5	0	Parallel	1500	20	Cont.	96	8	X	2.86	5000
1367-2	3	25	10	5	0	Parallel	1500	20	Cont.	96	8	X	4.79	5000
1368-1	3	25	10	5	0	Parallel	750	20	Cont.	96	8	X	2.86	5000
1368-2	3	25	10	5	0	Parallel	750	20	Cont.	96	8	X	4.79	5000
1369-1	3	30	6	3	0	Parallel	Infinite	20	Cont.	72	8	X	2.86	5000
1369-2	3	30	6	3	0	Parallel	Infinite	20	Cont.	72	8	X	4.79	5000

Model ID	Geometry									Cross-section		CF detail		Mat'l
	n_{span}	L/d ratio	s_g [ft]	n_{girder}	Support skew [deg]; Layout		R [ft]	s_{cf} [ft]	CF layout	d_w [in]	t_{deck} [in]	CF type	A_{cf} [in^2]	E_c [ksi]
1370-1	3	30	6	5	0	Parallel	Infinite	20	Cont.	72	8	X	2.86	5000
1370-2	3	30	6	5	0	Parallel	Infinite	20	Cont.	72	8	X	4.79	5000
1371-1	3	30	8	3	0	Parallel	Infinite	20	Cont.	72	8	X	2.86	5000
1371-2	3	30	8	3	0	Parallel	Infinite	20	Cont.	72	8	X	4.79	5000
1372-1	3	30	8	5	0	Parallel	Infinite	20	Cont.	72	8	X	2.86	5000
1372-2	3	30	8	5	0	Parallel	Infinite	20	Cont.	72	8	X	4.79	5000
1373-1	3	30	10	3	0	Parallel	Infinite	20	Cont.	72	8	X	2.86	5000
1373-2	3	30	10	3	0	Parallel	Infinite	20	Cont.	72	8	X	4.79	5000
1374-1	3	30	10	5	0	Parallel	Infinite	20	Cont.	72	8	X	2.86	5000
1374-2	3	30	10	5	0	Parallel	Infinite	20	Cont.	72	8	X	4.79	5000
1375-1	3	30	6	3	0	Parallel	Infinite	20	Cont.	96	8	X	2.86	5000
1375-2	3	30	6	3	0	Parallel	Infinite	20	Cont.	96	8	X	4.79	5000
1376-1	3	30	6	5	0	Parallel	Infinite	20	Cont.	96	8	X	2.86	5000
1376-2	3	30	6	5	0	Parallel	Infinite	20	Cont.	96	8	X	4.79	5000
1377-1	3	30	8	3	0	Parallel	Infinite	20	Cont.	96	8	X	2.86	5000
1377-2	3	30	8	3	0	Parallel	Infinite	20	Cont.	96	8	X	4.79	5000
1378-1	3	30	8	5	0	Parallel	Infinite	20	Cont.	96	8	X	2.86	5000
1378-2	3	30	8	5	0	Parallel	Infinite	20	Cont.	96	8	X	4.79	5000
1379-1	3	30	10	3	0	Parallel	Infinite	20	Cont.	96	8	X	2.86	5000
1379-2	3	30	10	3	0	Parallel	Infinite	20	Cont.	96	8	X	4.79	5000
1380-1	3	30	10	5	0	Parallel	Infinite	20	Cont.	96	8	X	2.86	5000
1380-2	3	30	10	5	0	Parallel	Infinite	20	Cont.	96	8	X	4.79	5000

Appendix C: Fatigue I and II Parameters Calculated from Advanced WIM Studies

Table C-1: Arkansas I-30 Applied to all 20 Bridges - Fatigue I Parameters (365 days).

Bridge ID	Before Filtering 25% CAFL		After Filtering 25% CAFL	
	99.99th Percentile Stress Range (ksi)	99.99th Percentile Stress Range (Normalized)	99.99th Percentile Stress Range (ksi)	99.99th Percentile Stress Range (Normalized)
59-2	3.75	0.78	5.25	1.09
83-3	2.41	0.98	2.76	1.13
115-2	3.16	1.02	3.34	1.07
233-2	2.43	1.10	3.09	1.39
253-3	2.01	0.99	2.30	1.13
277-2	1.56	1.01	1.86	1.21
747-2	4.07	0.95	4.93	1.15
753-2	3.30	0.82	4.38	1.10
755-2	3.53	0.68	4.06	0.78
755-4	3.57	0.61	3.99	0.69
761-2	2.58	0.52	3.24	0.66
825-3	2.24	0.69	2.46	0.76
909-2	2.59	0.65	2.82	0.71
1179-2	5.97	1.22	6.38	1.30
1181-2	7.17	1.17	8.09	1.32
1181-4	9.56	1.26	10.79	1.42
1183-2	3.38	1.17	3.66	1.27
1187-2	1.70	0.57	2.22	0.74
1213-3	1.49	0.72	1.83	0.89
1249-2	1.38	0.88	1.81	1.16

Table C-2: Arkansas I-30 Applied to all 20 Bridges - Fatigue II Parameters (365 days).

Bridge ID	Before Filtering 25% CAFL			After Filtering 25% CAFL		
	Effective Stress Range (ksi)	Effective Stress Range (Normalized)	Number of Cycles	Effective Stress Range (ksi)	Effective Stress Range (Normalized)	Number of Cycles
59-2	1.00	0.33	5,679,165	1.00	0.47	1,704,469
83-3	1.00	0.46	3,868,659	1.30	0.53	1,605,396
115-2	1.12	0.36	4,088,772	1.46	0.47	1,679,812
233-2	0.35	0.16	10,197,262	1.16	0.52	146,644
253-3	0.65	0.32	4,772,670	1.04	0.51	956,535
277-2	0.44	0.29	9,008,034	0.87	0.56	837,170
747-2	1.14	0.27	4,795,381	1.90	0.45	779,895
753-2	0.68	0.17	11,546,714	1.51	0.38	745,369
755-2	0.96	0.18	7,027,497	1.49	0.29	1,670,257
755-4	1.01	0.17	5,569,019	1.45	0.25	1,710,773
761-2	0.69	0.14	14,576,648	1.36	0.28	1,646,990
825-3	0.78	0.24	3,742,007	1.05	0.32	1,388,480
909-2	0.89	0.22	4,946,159	1.23	0.31	1,636,047
1179-2	2.12	0.43	3,434,877	2.58	0.53	1,728,683
1181-2	2.35	0.38	5,046,218	3.22	0.53	1,731,073
1181-4	3.11	0.41	5,235,487	4.32	0.57	1,732,307
1183-2	1.19	0.41	3,564,528	1.49	0.52	1,659,569
1187-2	0.46	0.15	14,710,690	0.94	0.31	1,332,328
1213-3	0.50	0.24	8,883,481	0.86	0.42	955,337
1249-2	0.32	0.21	7,170,726	0.88	0.56	99,107

Table C-3: Arizona I-10 Applied to all 20 Bridges - Fatigue I Parameters (342 days).

Bridge ID	Before Filtering 25% CAFL		After Filtering 25% CAFL	
	99.99th Percentile Stress Range (ksi)	99.99th Percentile Stress Range (Normalized)	99.99th Percentile Stress Range (ksi)	99.99th Percentile Stress Range (Normalized)
59-2	3.78	0.78	5.73	1.18
83-3	2.51	1.03	2.88	1.18
115-2	3.34	1.08	3.62	1.16
233-2	2.60	1.17	3.15	1.42
253-3	2.03	1.00	2.46	1.21
277-2	0.58	0.40	1.02	0.72
747-2	2.39	0.64	2.95	0.79
753-2	3.48	1.06	4.27	1.30
755-2	4.63	1.04	5.89	1.33
755-4	5.32	1.07	6.45	1.30
761-2	4.11	0.98	5.64	1.34
825-3	3.02	1.07	3.26	1.15
909-2	3.53	1.03	4.00	1.17
1179-2	4.29	0.99	5.19	1.20
1181-2	4.95	0.91	6.34	1.17
1181-4	6.60	0.95	8.54	1.23
1183-2	3.58	1.45	3.92	1.59
1187-2	1.76	0.74	2.34	0.98
1213-3	1.53	0.74	1.91	0.93
1249-2	1.46	1.00	1.98	1.36

Table C-4: Arizona I-10 Applied to all 20 Bridges - Fatigue II Parameters (342 days).

Bridge ID	Before Filtering 25% CAFL			After Filtering 25% CAFL		
	Effective Stress Range (ksi)	Effective Stress Range (Normalized)	Number of Cycles	Effective Stress Range (ksi)	Effective Stress Range (Normalized)	Number of Cycles
59-2	1.01	0.21	7,809,717	2.13	0.44	570,917
83-3	0.86	0.35	2,527,626	1.28	0.52	619,769
115-2	1.20	0.39	2,769,204	1.55	0.50	1,187,221
233-2	0.37	0.17	7,377,836	1.20	0.54	119,472
253-3	0.69	0.34	3,438,195	1.10	0.54	716,799
277-2	0.47	0.33	6,545,590	0.91	0.63	681,565
747-2	1.19	0.32	3,376,700	1.98	0.53	550,071
753-2	0.73	0.22	8,107,966	1.59	0.48	546,459
755-2	1.01	0.23	9,938,369	2.25	0.51	636,932
755-4	1.33	0.27	5,657,848	2.45	0.49	660,576
761-2	0.74	0.18	4,610,265	1.46	0.35	384,809
825-3	1.15	0.40	2,681,194	1.46	0.51	1,185,131
909-2	1.20	0.35	3,719,180	1.69	0.49	1,218,719
1179-2	1.27	0.29	3,579,162	1.98	0.46	768,719
1181-2	1.35	0.25	5,705,831	2.30	0.43	1,006,136
1181-4	1.82	0.26	5,452,035	3.04	0.44	702,392
1183-2	1.25	0.51	2,572,406	1.57	0.64	1,194,896
1187-2	0.49	0.20	10,508,836	0.98	0.41	1,018,596
1213-3	0.53	0.26	4,238,007	0.88	0.43	46,470
1249-2	0.35	0.24	5,077,407	0.91	0.63	84,110

Table C-5: California SR-99 Applied to all 20 Bridges - Fatigue I Parameters (363 days).

Bridge ID	Before Filtering 25% CAFL		After Filtering 25% CAFL	
	99.99th Percentile Stress Range (ksi)	99.99th Percentile Stress Range (Normalized)	99.99th Percentile Stress Range (ksi)	99.99th Percentile Stress Range (Normalized)
59-2	5.00	0.68	5.29	0.83
83-3	2.18	0.89	2.35	0.96
115-2	2.58	0.83	2.81	0.90
233-2	0.15	0.07	1.42	0.64
253-3	0.75	0.37	1.30	0.64
277-2	1.24	0.87	1.60	1.12
747-2	3.87	1.03	4.05	1.08
753-2	3.35	1.02	3.55	1.08
755-2	4.46	1.01	4.77	1.08
755-4	5.06	1.02	5.32	1.07
761-2	4.02	0.96	4.46	1.06
825-3	2.49	0.88	2.70	0.95
909-2	2.08	0.61	2.34	0.68
1179-2	4.83	1.12	5.04	1.16
1181-2	5.93	1.10	6.28	1.16
1181-4	7.63	1.10	8.20	1.18
1183-2	2.72	1.10	2.85	1.16
1187-2	1.41	0.59	1.84	0.77
1213-3	1.33	0.64	1.68	0.82
1249-2	1.42	0.97	1.57	1.07

Table C-6: California SR-99 Applied to all 20 Bridges - Fatigue II Parameters (363 days).

Bridge ID	Before Filtering 25% CAFL			After Filtering 25% CAFL		
	Effective Stress Range (ksi)	Effective Stress Range (Normalized)	Number of Cycles	Effective Stress Range (ksi)	Effective Stress Range (Normalized)	Number of Cycles
59-2	0.91	0.19	11,585,243	1.92	0.40	951,558
83-3	0.82	0.33	2,403,821	1.19	0.48	635,756
115-2	1.11	0.36	3,004,698	1.43	0.46	1,287,955
233-2	0.34	0.15	7,947,272	1.19	0.54	103,385
253-3	0.65	0.32	3,481,654	1.10	0.54	557,283
277-2	0.44	0.31	5,440,652	0.92	0.64	528,927
747-2	1.08	0.29	3,680,113	1.80	0.48	614,040
753-2	0.67	0.20	8,726,874	1.48	0.45	571,665
755-2	0.92	0.21	10,590,155	2.03	0.46	714,062
755-4	1.20	0.24	5,989,569	2.20	0.44	709,563
761-2	0.72	0.17	5,226,739	1.43	0.34	420,778
825-3	1.11	0.39	2,608,432	1.38	0.49	1,239,225
909-2	0.89	0.26	3,528,275	1.25	0.37	1,085,175
1179-2	2.03	0.47	2,797,592	2.49	0.57	1,391,435
1181-2	2.26	0.42	4,098,998	3.10	0.57	1,396,245
1181-4	2.98	0.43	4,250,685	4.15	0.60	1,401,470
1183-2	1.13	0.46	2,974,886	1.47	0.60	1,228,191
1187-2	0.45	0.19	11,465,987	0.99	0.42	758,143
1213-3	0.50	0.24	4,637,685	0.87	0.42	72,945
1249-2	0.32	0.22	5,630,226	0.90	0.62	70,131

Table C-7: Colorado I-76 Applied to all 20 Bridges - Fatigue I Parameters (365 days).

Bridge ID	Before Filtering 25% CAFL		After Filtering 25% CAFL	
	99.99th Percentile Stress Range (ksi)	99.99th Percentile Stress Range (Normalized)	99.99th Percentile Stress Range (ksi)	99.99th Percentile Stress Range (Normalized)
59-2	4.14	0.86	5.95	1.23
83-3	2.85	1.16	3.40	1.39
115-2	3.65	1.18	3.85	1.24
233-2	2.45	1.10	3.78	1.70
253-3	2.29	1.12	2.81	1.38
277-2	1.70	1.19	2.18	1.52
747-2	4.41	1.17	5.56	1.48
753-2	3.52	1.07	4.45	1.35
755-2	4.65	1.05	6.09	1.37
755-4	5.56	1.12	6.96	1.40
761-2	4.33	1.03	6.48	1.54
825-3	3.41	1.20	3.60	1.27
909-2	3.89	1.14	4.17	1.22
1179-2	4.58	1.06	5.46	1.26
1181-2	5.25	0.97	6.88	1.27
1181-4	6.87	0.99	8.75	1.26
1183-2	2.41	0.98	3.60	1.46
1187-2	2.48	1.04	4.20	1.76
1213-3	2.40	1.16	3.14	1.53
1249-2	1.72	1.18	2.21	1.52

Table C-8: Colorado I-76 Applied to all 20 Bridges - Fatigue II Parameters (365 days).

Bridge ID	Before Filtering 25% CAFL			After Filtering 25% CAFL		
	Effective Stress Range (ksi)	Effective Stress Range (Normalized)	Number of Cycles	Effective Stress Range (ksi)	Effective Stress Range (Normalized)	Number of Cycles
59-2	0.89	0.18	2,203,212	1.86	0.38	179,759
83-3	0.78	0.32	612,996	1.13	0.46	160,366
115-2	1.06	0.34	788,344	1.38	0.44	328,474
233-2	0.33	0.15	1,821,290	1.18	0.53	22,934
253-3	0.62	0.30	900,275	1.06	0.52	132,342
277-2	0.42	0.29	1,840,599	0.92	0.64	107,868
747-2	1.03	0.27	949,847	1.76	0.47	141,480
753-2	0.65	0.20	2,167,941	1.44	0.44	141,786
755-2	0.89	0.20	2,665,341	1.97	0.44	177,665
755-4	1.18	0.24	1,540,855	2.17	0.44	190,362
761-2	0.70	0.17	1,442,476	1.43	0.34	107,423
825-3	1.06	0.37	661,927	1.32	0.47	313,722
909-2	1.10	0.32	953,635	1.50	0.44	344,757
1179-2	1.10	0.25	1,023,337	1.73	0.40	211,219
1181-2	1.19	0.22	1,605,147	1.98	0.37	301,274
1181-4	1.62	0.23	1,514,611	2.70	0.39	183,060
1183-2	0.47	0.19	2,396,548	1.14	0.46	110,333
1187-2	0.41	0.17	1,420,297	1.16	0.49	20,158
1213-3	0.62	0.30	1,037,376	1.17	0.57	251,080
1249-2	0.46	0.31	1,262,613	0.92	0.63	108,309

Table C-9: Illinois I-57 Applied to all 20 Bridges - Fatigue I Parameters (357 days).

Bridge ID	Before Filtering 25% CAFL		After Filtering 25% CAFL	
	99.99th Percentile Stress Range (ksi)	99.99th Percentile Stress Range (Normalized)	99.99th Percentile Stress Range (ksi)	99.99th Percentile Stress Range (Normalized)
59-2	3.46	0.72	4.96	1.03
83-3	2.29	0.93	2.58	1.05
115-2	2.94	0.95	3.32	1.07
233-2	2.55	1.15	3.06	1.38
253-3	1.89	0.93	2.27	1.12
277-2	1.52	1.06	1.83	1.28
747-2	4.07	1.08	4.77	1.27
753-2	3.45	1.05	3.90	1.18
755-2	0.32	0.07	2.70	0.61
755-4	0.70	0.14	2.97	0.60
761-2	0.61	0.14	1.61	0.38
825-3	1.56	0.55	1.70	0.60
909-2	2.42	0.71	2.90	0.85
1179-2	4.08	0.94	4.55	1.05
1181-2	4.77	0.88	5.45	1.01
1181-4	6.18	0.89	7.51	1.08
1183-2	2.42	0.98	2.96	1.20
1187-2	2.55	1.07	3.23	1.36
1213-3	2.05	0.99	2.61	1.27
1249-2	1.53	1.05	1.83	1.25

Table C-10: Illinois I-57 Applied to all 20 Bridges - Fatigue II Parameters (357 days).

Bridge ID	Before Filtering 25% CAFL			After Filtering 25% CAFL		
	Effective Stress Range (ksi)	Effective Stress Range (Normalized)	Number of Cycles	Effective Stress Range (ksi)	Effective Stress Range (Normalized)	Number of Cycles
59-2	0.98	0.20	4,932,367	2.03	0.42	394,044
83-3	0.84	0.34	1,521,983	1.23	0.50	394,697
115-2	1.15	0.37	1,835,734	1.50	0.48	763,982
233-2	0.36	0.16	4,637,915	1.19	0.54	69,579
253-3	0.67	0.33	2,136,743	1.09	0.54	410,667
277-2	0.46	0.32	4,198,829	0.91	0.64	372,183
747-2	1.15	0.31	2,184,963	1.91	0.51	358,657
753-2	0.70	0.21	5,179,556	1.54	0.47	350,191
755-2	0.98	0.22	6,233,542	2.16	0.49	417,264
755-4	1.29	0.26	3,630,418	2.36	0.47	439,116
761-2	0.73	0.17	3,120,222	1.43	0.34	270,978
825-3	1.13	0.40	1,633,404	1.41	0.50	752,766
909-2	1.17	0.34	2,310,146	1.63	0.48	788,591
1179-2	1.22	0.28	2,325,311	1.90	0.44	495,355
1181-2	1.31	0.24	3,704,330	2.21	0.41	676,734
1181-4	1.77	0.26	3,449,308	2.92	0.42	450,216
1183-2	0.51	0.21	5,415,457	1.22	0.50	257,374
1187-2	0.42	0.18	3,166,306	1.16	0.49	58,055
1213-3	0.66	0.32	2,498,075	1.22	0.59	684,813
1249-2	0.49	0.34	2,977,448	0.91	0.63	372,823

Table C-11: Indiana US-31 (Lane 1) Applied to all 20 Bridges - Fatigue I Parameters (365 days).

Bridge ID	Before Filtering 25% CAFL		After Filtering 25% CAFL	
	99.99th Percentile Stress Range (ksi)	99.99th Percentile Stress Range (Normalized)	99.99th Percentile Stress Range (ksi)	99.99th Percentile Stress Range (Normalized)
59-2	4.71	0.97	5.30	1.10
83-3	2.88	1.18	3.06	1.25
115-2	3.04	0.98	3.25	1.05
233-2	2.99	1.35	3.61	1.63
253-3	2.29	1.13	2.63	1.29
277-2	1.74	1.21	2.01	1.41
747-2	4.59	1.22	5.18	1.38
753-2	3.72	1.13	4.34	1.32
755-2	5.06	1.14	5.90	1.33
755-4	5.76	1.16	6.41	1.29
761-2	5.14	1.22	5.85	1.39
825-3	2.95	1.04	3.12	1.10
909-2	3.25	0.95	3.61	1.06
1179-2	5.21	1.20	5.24	1.21
1181-2	5.67	1.05	6.49	1.20
1181-4	7.44	1.07	8.51	1.23
1183-2	2.86	1.16	3.37	1.37
1187-2	2.96	1.24	3.45	1.45
1213-3	2.35	1.14	2.70	1.31
1249-2	1.77	1.21	2.13	1.46

Table C-12: Indiana US-31 (Lane 1) Applied to all 20 Bridges - Fatigue II Parameters (365 days).

Bridge ID	Before Filtering 25% CAFL			After Filtering 25% CAFL		
	Effective Stress Range (ksi)	Effective Stress Range (Normalized)	Number of Cycles	Effective Stress Range (ksi)	Effective Stress Range (Normalized)	Number of Cycles
59-2	1.54	0.32	1,244,510	2.23	0.46	370,237
83-3	1.08	0.44	701,292	1.35	0.55	328,236
115-2	1.14	0.37	810,697	1.47	0.47	314,802
233-2	0.60	0.27	974,544	1.38	0.62	63,845
253-3	0.80	0.39	945,473	1.17	0.58	252,126
277-2	0.46	0.32	1,466,016	0.95	0.67	136,464
747-2	1.53	0.41	1,081,471	2.12	0.56	367,789
753-2	0.91	0.28	2,456,531	1.66	0.50	341,382
755-2	1.37	0.31	2,269,889	2.39	0.54	369,471
755-4	1.73	0.35	1,494,166	2.64	0.53	369,753
761-2	1.63	0.39	1,309,166	2.39	0.57	370,319
825-3	1.15	0.40	689,219	1.41	0.50	341,106
909-2	1.17	0.34	986,329	1.58	0.46	363,042
1179-2	2.25	0.52	414,433	2.32	0.54	373,659
1181-2	1.91	0.35	3,080,428	2.88	0.53	375,635
1181-4	2.50	0.36	1,452,974	3.74	0.54	376,241
1183-2	0.78	0.31	1,862,665	1.32	0.53	320,768
1187-2	0.94	0.39	1,298,571	1.42	0.60	326,219
1213-3	0.68	0.33	1,062,583	1.23	0.60	293,424
1249-2	0.50	0.34	1,268,964	0.96	0.66	137,178

Table C-13: Indiana US-31 (Lane 3) Applied to all 20 Bridges - Fatigue I Parameters (365 days).

Bridge ID	Before Filtering 25% CAFL		After Filtering 25% CAFL	
	99.99th Percentile Stress Range (ksi)	99.99th Percentile Stress Range (Normalized)	99.99th Percentile Stress Range (ksi)	99.99th Percentile Stress Range (Normalized)
59-2	4.01	0.83	4.81	0.99
83-3	2.71	1.11	3.03	1.24
115-2	3.00	0.96	3.15	1.01
233-2	2.61	1.18	3.41	1.54
253-3	2.23	1.09	2.54	1.25
277-2	1.72	1.20	2.05	1.43
747-2	4.28	1.14	5.01	1.33
753-2	3.56	1.08	4.42	1.34
755-2	4.67	1.05	5.76	1.30
755-4	5.42	1.09	6.56	1.32
761-2	4.20	1.00	5.30	1.26
825-3	3.04	1.07	3.18	1.12
909-2	3.26	0.95	3.47	1.01
1179-2	4.25	0.98	4.84	1.12
1181-2	4.98	0.92	6.04	1.12
1181-4	6.54	0.94	7.72	1.11
1183-2	2.47	1.00	3.18	1.29
1187-2	2.54	1.07	3.41	1.43
1213-3	2.38	1.16	2.75	1.33
1249-2	1.72	1.18	2.03	1.39

Table C-14: Indiana US-31 (Lane 3) Applied to all 20 Bridges - Fatigue II Parameters (365 days).

Bridge ID	Before Filtering 25% CAFL			After Filtering 25% CAFL		
	Effective Stress Range (ksi)	Effective Stress Range (Normalized)	Number of Cycles	Effective Stress Range (ksi)	Effective Stress Range (Normalized)	Number of Cycles
59-2	0.93	0.19	2,205,735	1.92	0.40	184,982
83-3	0.82	0.33	643,962	1.19	0.49	169,507
115-2	1.11	0.36	801,694	1.45	0.47	335,901
233-2	0.35	0.16	1,833,892	1.21	0.54	27,040
253-3	0.65	0.32	930,384	1.09	0.53	155,984
277-2	0.45	0.31	1,445,674	0.93	0.65	132,491
747-2	1.07	0.28	976,239	1.80	0.48	153,237
753-2	0.67	0.20	2,236,118	1.48	0.45	149,285
755-2	0.55	0.12	3,203,727	1.06	0.24	28,376
755-4	1.22	0.25	1,582,086	2.23	0.45	198,202
761-2	0.72	0.17	1,449,827	1.43	0.34	116,678
825-3	1.11	0.39	693,455	1.39	0.49	325,393
909-2	1.15	0.34	972,438	1.57	0.46	351,170
1179-2	1.14	0.26	876,239	1.77	0.41	210,696
1181-2	1.23	0.23	1,664,988	2.07	0.38	301,824
1181-4	1.67	0.24	1,549,428	2.78	0.40	199,101
1183-2	0.50	0.20	2,452,011	1.19	0.48	113,720
1187-2	0.41	0.17	1,434,818	1.17	0.49	23,170
1213-3	0.66	0.32	1,067,272	1.22	0.59	273,956
1249-2	0.49	0.33	1,256,035	0.94	0.64	132,730

Table C-15: Kansas I-70 Applied to all 20 Bridges - Fatigue I Parameters (365 days).

Bridge ID	Before Filtering 25% CAFL		After Filtering 25% CAFL	
	99.99th Percentile Stress Range (ksi)	99.99th Percentile Stress Range (Normalized)	99.99th Percentile Stress Range (ksi)	99.99th Percentile Stress Range (Normalized)
59-2	3.81	0.79	5.34	1.10
83-3	2.50	1.02	2.82	1.15
115-2	3.13	1.01	3.35	1.08
233-2	2.51	1.13	3.30	1.49
253-3	2.10	1.03	2.40	1.18
277-2	1.58	1.10	1.97	1.38
747-2	4.15	1.10	4.77	1.27
753-2	3.38	1.03	4.20	1.28
755-2	4.53	1.02	6.22	1.40
755-4	5.22	1.05	6.49	1.31
761-2	4.11	0.98	5.89	1.40
825-3	2.90	1.02	3.05	1.08
909-2	3.47	1.01	3.82	1.12
1179-2	4.36	1.01	5.27	1.22
1181-2	4.81	0.89	6.39	1.18
1181-4	6.33	0.91	8.34	1.20
1183-2	2.39	0.97	3.09	1.25
1187-2	2.55	1.07	3.77	1.58
1213-3	2.20	1.07	2.56	1.24
1249-2	1.60	1.10	1.97	1.35

Table C-16: Kansas I-70 Applied to all 20 Bridges - Fatigue II Parameters (365 days).

Bridge ID	Before Filtering 25% CAFL			After Filtering 25% CAFL		
	Effective Stress Range (ksi)	Effective Stress Range (Normalized)	Number of Cycles	Effective Stress Range (ksi)	Effective Stress Range (Normalized)	Number of Cycles
59-2	0.97	0.20	2,683,397	2.02	0.42	213,999
83-3	0.83	0.34	846,571	1.22	0.50	214,073
115-2	1.14	0.37	1,009,602	1.49	0.48	417,605
233-2	0.37	0.16	2,169,661	1.19	0.54	37,538
253-3	0.67	0.33	1,187,211	1.08	0.53	228,675
277-2	0.45	0.31	2,326,027	0.90	0.63	206,214
747-2	1.15	0.31	1,180,753	1.90	0.51	196,476
753-2	0.70	0.21	2,784,466	1.53	0.46	189,335
755-2	0.97	0.22	3,423,406	2.15	0.48	226,594
755-4	1.29	0.26	1,957,856	2.35	0.47	239,582
761-2	0.72	0.17	1,669,079	1.44	0.34	131,595
825-3	1.11	0.39	899,601	1.40	0.49	412,368
909-2	1.17	0.34	1,246,314	1.62	0.47	430,910
1179-2	1.21	0.28	1,055,669	1.87	0.43	252,134
1181-2	1.29	0.24	2,031,532	2.19	0.40	361,991
1181-4	1.75	0.25	1,888,650	2.90	0.42	249,109
1183-2	0.51	0.21	3,005,387	1.22	0.50	138,769
1187-2	0.42	0.18	1,692,874	1.15	0.48	31,438
1213-3	0.66	0.32	1,378,488	1.21	0.59	377,068
1249-2	0.48	0.33	1,679,149	0.90	0.62	206,809

Table C-17: Louisiana US-171 Applied to all 20 Bridges - Fatigue I Parameters (365 days).

Bridge ID	Before Filtering 25% CAFL		After Filtering 25% CAFL	
	99.99th Percentile Stress Range (ksi)	99.99th Percentile Stress Range (Normalized)	99.99th Percentile Stress Range (ksi)	99.99th Percentile Stress Range (Normalized)
59-2	5.25	1.09	6.51	1.35
83-3	3.18	1.30	4.24	1.73
115-2	4.08	1.31	4.32	1.39
233-2	2.74	1.24	3.97	1.79
253-3	2.81	1.38	3.33	1.63
277-2	2.03	1.42	2.51	1.75
747-2	5.80	1.54	6.73	1.79
753-2	4.11	1.25	5.62	1.71
755-2	5.43	1.22	7.50	1.69
755-4	6.36	1.28	7.97	1.60
761-2	5.44	1.29	7.73	1.84
825-3	4.02	1.42	4.16	1.47
909-2	4.31	1.26	4.64	1.35
1179-2	6.13	1.42	6.91	1.60
1181-2	6.94	1.28	8.60	1.59
1181-4	8.77	1.26	10.80	1.56
1183-2	2.80	1.14	5.06	2.05
1187-2	3.27	1.37	5.25	2.21
1213-3	2.95	1.43	3.51	1.70
1249-2	2.05	1.40	2.82	1.93

Table C-18: Louisiana US-171 Applied to all 20 Bridges - Fatigue II Parameters (365 days).

Bridge ID	Before Filtering 25% CAFL			After Filtering 25% CAFL		
	Effective Stress Range (ksi)	Effective Stress Range (Normalized)	Number of Cycles	Effective Stress Range (ksi)	Effective Stress Range (Normalized)	Number of Cycles
59-2	0.90	0.19	463,400	1.89	0.39	38,646
83-3	0.85	0.35	109,939	1.24	0.51	29,022
115-2	1.10	0.36	161,351	1.45	0.47	65,032
233-2	0.34	0.15	408,739	1.27	0.57	4,516
253-3	0.67	0.33	172,627	1.20	0.59	21,279
277-2	0.48	0.33	254,841	1.01	0.71	20,529
747-2	1.05	0.28	206,533	1.82	0.48	29,821
753-2	0.67	0.20	441,288	1.50	0.46	27,432
755-2	0.90	0.20	549,963	2.00	0.45	36,965
755-4	1.18	0.24	314,145	2.18	0.44	38,791
761-2	0.77	0.18	307,351	1.60	0.38	23,852
825-3	1.18	0.42	120,149	1.44	0.51	60,057
909-2	1.17	0.34	184,872	1.55	0.45	71,952
1179-2	1.14	0.26	183,671	1.76	0.41	37,826
1181-2	1.21	0.22	359,055	2.09	0.39	58,351
1181-4	1.60	0.23	337,001	2.74	0.40	40,538
1183-2	0.48	0.19	530,536	1.24	0.50	19,005
1187-2	0.45	0.19	297,105	1.27	0.53	4,503
1213-3	0.69	0.33	194,462	1.33	0.64	41,608
1249-2	0.51	0.35	233,211	1.02	0.70	20,609

Table C-19: Maryland US-15 Applied to all 20 Bridges - Fatigue I Parameters (351 days).

Bridge ID	Before Filtering 25% CAFL		After Filtering 25% CAFL	
	99.99th Percentile Stress Range (ksi)	99.99th Percentile Stress Range (Normalized)	99.99th Percentile Stress Range (ksi)	99.99th Percentile Stress Range (Normalized)
59-2	3.64	0.75	4.52	0.93
83-3	2.67	1.09	3.16	1.29
115-2	2.99	0.96	3.25	1.04
233-2	2.52	1.13	3.42	1.54
253-3	2.07	1.02	2.57	1.27
277-2	1.63	1.14	2.01	1.41
747-2	4.28	1.14	4.70	1.25
753-2	3.62	1.10	4.22	1.28
755-2	4.76	1.07	5.25	1.18
755-4	5.45	1.10	5.83	1.17
761-2	4.27	1.02	4.90	1.17
825-3	3.27	1.15	3.37	1.19
909-2	3.25	0.95	3.52	1.03
1179-2	4.27	0.99	4.51	1.04
1181-2	5.06	0.94	5.56	1.03
1181-4	6.54	0.94	7.36	1.06
1183-2	2.53	1.03	3.05	1.24
1187-2	2.56	1.08	4.81	2.02
1213-3	2.25	1.09	2.89	1.40
1249-2	1.64	1.13	2.04	1.40

Table C-20: Maryland US-15 Applied to all 20 Bridges - Fatigue II Parameters (351 days).

Bridge ID	Before Filtering 25% CAFL			After Filtering 25% CAFL		
	Effective Stress Range (ksi)	Effective Stress Range (Normalized)	Number of Cycles	Effective Stress Range (ksi)	Effective Stress Range (Normalized)	Number of Cycles
59-2	0.84	0.17	667,176	1.80	0.37	51,442
83-3	0.79	0.32	157,871	1.11	0.45	47,650
115-2	1.03	0.33	231,460	1.34	0.43	96,113
233-2	0.34	0.15	541,627	1.21	0.55	5,832
253-3	0.63	0.31	243,418	1.08	0.53	34,152
277-2	0.44	0.31	361,682	0.98	0.68	23,574
747-2	0.97	0.26	288,403	1.70	0.45	40,552
753-2	0.62	0.19	642,295	1.40	0.43	39,495
755-2	0.85	0.19	784,708	1.89	0.43	51,703
755-4	1.10	0.22	462,598	2.07	0.42	52,847
761-2	0.70	0.17	416,841	1.45	0.34	31,793
825-3	1.09	0.38	174,399	1.30	0.46	93,138
909-2	1.09	0.32	267,301	1.45	0.42	103,448
1179-2	1.05	0.24	260,796	1.66	0.38	52,660
1181-2	1.13	0.21	505,404	1.94	0.36	83,815
1181-4	1.50	0.22	480,640	2.63	0.38	53,982
1183-2	0.46	0.19	737,604	1.16	0.47	12,608
1187-2	0.41	0.17	407,973	1.21	0.51	5,163
1213-3	0.64	0.31	280,061	1.18	0.57	67,757
1249-2	0.48	0.33	325,962	0.98	0.67	23,470

Table C-21: Minnesota US-2 Applied to all 20 Bridges - Fatigue I Parameters (365 days).

Bridge ID	Before Filtering 25% CAFL		After Filtering 25% CAFL	
	99.99th Percentile Stress Range (ksi)	99.99th Percentile Stress Range (Normalized)	99.99th Percentile Stress Range (ksi)	99.99th Percentile Stress Range (Normalized)
59-2	5.29	1.09	6.53	1.35
83-3	3.52	1.44	4.00	1.63
115-2	4.10	1.32	4.30	1.38
233-2	2.67	1.20	3.86	1.74
253-3	3.14	1.54	3.49	1.72
277-2	2.13	1.49	2.87	2.00
747-2	5.39	1.44	6.05	1.61
753-2	3.88	1.18	4.72	1.43
755-2	5.40	1.22	7.77	1.75
755-4	6.48	1.30	8.64	1.74
761-2	5.47	1.30	7.31	1.74
825-3	3.87	1.37	4.05	1.43
909-2	4.37	1.28	4.52	1.32
1179-2	6.11	1.41	6.56	1.52
1181-2	6.60	1.22	8.20	1.52
1181-4	8.23	1.19	9.92	1.43
1183-2	2.94	1.19	4.68	1.90
1187-2	2.88	1.21	4.31	1.81
1213-3	3.17	1.54	3.58	1.74
1249-2	2.15	1.47	2.80	1.92

Table C-22: Minnesota US-2 Applied to all 20 Bridges - Fatigue II Parameters (365 days).

Bridge ID	Before Filtering 25% CAFL			After Filtering 25% CAFL		
	Effective Stress Range (ksi)	Effective Stress Range (Normalized)	Number of Cycles	Effective Stress Range (ksi)	Effective Stress Range (Normalized)	Number of Cycles
59-2	0.95	0.20	324,738	1.98	0.41	26,972
83-3	0.87	0.35	82,177	1.21	0.50	25,027
115-2	1.14	0.37	115,824	1.48	0.48	48,245
233-2	0.38	0.17	270,783	1.24	0.56	3,835
253-3	0.69	0.34	122,402	1.14	0.56	21,476
277-2	0.48	0.33	187,287	0.98	0.69	17,757
747-2	1.11	0.30	142,695	1.86	0.49	23,474
753-2	0.69	0.21	317,751	1.51	0.46	21,290
755-2	0.95	0.21	385,628	2.09	0.47	26,501
755-4	1.24	0.25	224,355	2.28	0.46	27,828
761-2	0.78	0.18	207,039	1.51	0.36	19,676
825-3	1.18	0.42	90,156	1.43	0.50	47,139
909-2	1.19	0.35	137,187	1.61	0.47	50,934
1179-2	1.23	0.28	124,769	1.79	0.41	35,513
1181-2	1.28	0.24	250,920	2.18	0.40	43,422
1181-4	1.70	0.24	230,129	2.86	0.41	28,928
1183-2	0.51	0.21	363,002	1.23	0.50	17,273
1187-2	0.45	0.19	203,108	1.22	0.51	3,432
1213-3	0.69	0.34	143,107	1.27	0.61	38,376
1249-2	0.51	0.35	169,732	0.99	0.68	17,787

Table C-23: New Mexico I-25 Applied to all 20 Bridges - Fatigue I Parameters (361 days).

Bridge ID	Before Filtering 25% CAFL		After Filtering 25% CAFL	
	99.99th Percentile Stress Range (ksi)	99.99th Percentile Stress Range (Normalized)	99.99th Percentile Stress Range (ksi)	99.99th Percentile Stress Range (Normalized)
59-2	3.77	0.78	5.12	1.06
83-3	2.52	1.03	2.74	1.12
115-2	3.17	1.02	3.39	1.09
233-2	2.40	1.08	3.00	1.35
253-3	2.09	1.03	2.34	1.15
277-2	1.55	1.08	2.10	1.47
747-2	4.22	1.12	4.99	1.33
753-2	3.45	1.05	4.36	1.32
755-2	4.59	1.04	5.78	1.30
755-4	5.28	1.06	6.08	1.22
761-2	4.00	0.95	5.56	1.32
825-3	2.98	1.05	3.11	1.10
909-2	3.39	0.99	3.67	1.07
1179-2	4.21	0.97	5.12	1.18
1181-2	4.87	0.90	6.16	1.14
1181-4	6.36	0.92	8.20	1.18
1183-2	2.40	0.98	3.35	1.36
1187-2	2.39	1.00	3.75	1.58
1213-3	2.22	1.08	2.72	1.32
1249-2	1.58	1.08	2.06	1.41

Table C-24: New Mexico I-25 Applied to all 20 Bridges - Fatigue II Parameters (361 days).

Bridge ID	Before Filtering 25% CAFL			After Filtering 25% CAFL		
	Effective Stress Range (ksi)	Effective Stress Range (Normalized)	Number of Cycles	Effective Stress Range (ksi)	Effective Stress Range (Normalized)	Number of Cycles
59-2	0.87	0.18	907,380	1.81	0.37	75,374
83-3	0.76	0.31	256,930	1.12	0.46	64,802
115-2	1.04	0.34	325,321	1.36	0.44	135,360
233-2	0.33	0.15	751,618	1.17	0.53	9,168
253-3	0.61	0.30	377,578	1.03	0.51	56,949
277-2	0.41	0.29	584,795	0.91	0.64	42,673
747-2	1.01	0.27	391,576	1.72	0.46	60,397
753-2	0.63	0.19	893,550	1.41	0.43	57,606
755-2	0.87	0.20	1,096,566	1.93	0.43	73,504
755-4	1.16	0.23	629,203	2.10	0.42	80,337
761-2	0.68	0.16	589,955	1.40	0.33	42,339
825-3	1.04	0.37	277,993	1.30	0.46	129,225
909-2	1.10	0.32	382,217	1.47	0.43	142,856
1179-2	1.09	0.25	355,440	1.67	0.39	79,958
1181-2	1.16	0.21	672,578	1.96	0.36	119,105
1181-4	1.56	0.22	635,942	2.62	0.38	79,666
1183-2	0.47	0.19	1,014,920	1.14	0.46	45,351
1187-2	0.40	0.17	585,496	1.14	0.48	7,986
1213-3	0.61	0.30	430,858	1.15	0.56	104,461
1249-2	0.45	0.31	515,207	0.91	0.63	43,108

Table C-25: New Mexico I-10 Applied to all 20 Bridges - Fatigue I Parameters (359 days).

Bridge ID	Before Filtering 25% CAFL		After Filtering 25% CAFL	
	99.99th Percentile Stress Range (ksi)	99.99th Percentile Stress Range (Normalized)	99.99th Percentile Stress Range (ksi)	99.99th Percentile Stress Range (Normalized)
59-2	3.91	0.81	5.98	1.24
83-3	2.53	1.03	2.98	1.22
115-2	1.66	0.53	1.80	0.58
233-2	0.16	0.07	1.41	0.63
253-3	0.92	0.45	1.28	0.63
277-2	0.54	0.38	1.02	0.71
747-2	1.58	0.42	2.44	0.65
753-2	0.78	0.24	1.84	0.56
755-2	0.31	0.07	2.72	0.61
755-4	0.65	0.13	2.99	0.60
761-2	0.60	0.14	1.72	0.41
825-3	1.55	0.55	1.70	0.60
909-2	3.78	1.10	4.15	1.21
1179-2	4.60	1.06	6.21	1.43
1181-2	5.15	0.95	7.59	1.40
1181-4	6.71	0.97	9.30	1.34
1183-2	2.46	1.00	3.47	1.41
1187-2	2.56	1.08	4.17	1.75
1213-3	2.28	1.11	2.80	1.36
1249-2	1.60	1.10	2.11	1.45

Table C-26: New Mexico I-10 Applied to all 20 Bridges - Fatigue II Parameters (359 days).

Bridge ID	Before Filtering 25% CAFL			After Filtering 25% CAFL		
	Effective Stress Range (ksi)	Effective Stress Range (Normalized)	Number of Cycles	Effective Stress Range (ksi)	Effective Stress Range (Normalized)	Number of Cycles
59-2	1.00	0.21	5,580,764	2.11	0.44	415,487
83-3	0.85	0.35	1,856,055	1.27	0.52	449,115
115-2	1.18	0.38	2,087,865	1.53	0.49	868,078
233-2	0.37	0.17	5,283,615	1.20	0.54	85,539
253-3	0.69	0.34	2,504,548	1.09	0.54	511,396
277-2	0.47	0.33	4,759,211	0.90	0.63	478,253
747-2	1.19	0.32	2,458,694	1.98	0.53	402,019
753-2	0.72	0.22	5,915,103	1.58	0.48	396,777
755-2	1.01	0.23	7,195,028	2.24	0.50	463,858
755-4	1.32	0.27	4,166,993	2.44	0.49	488,714
761-2	0.74	0.18	3,396,476	1.47	0.35	275,656
825-3	1.13	0.40	1,970,175	1.44	0.51	859,626
909-2	1.19	0.35	2,727,327	1.67	0.49	887,622
1179-2	1.28	0.29	2,610,573	1.98	0.46	568,533
1181-2	1.34	0.25	4,113,081	2.26	0.42	746,591
1181-4	1.82	0.26	3,869,505	3.02	0.44	511,335
1183-2	0.52	0.21	6,014,723	1.26	0.51	276,201
1187-2	0.42	0.18	3,484,735	1.16	0.49	67,778
1213-3	0.67	0.33	5,779,857	1.23	0.60	812,579
1249-2	0.49	0.34	3,531,858	0.91	0.62	480,032

Table C-27: Pennsylvania I-80 Applied to all 20 Bridges - Fatigue I Parameters (275 days).

Bridge ID	Before Filtering 25% CAFL		After Filtering 25% CAFL	
	99.99th Percentile Stress Range (ksi)	99.99th Percentile Stress Range (Normalized)	99.99th Percentile Stress Range (ksi)	99.99th Percentile Stress Range (Normalized)
59-2	4.06	0.84	5.50	1.14
83-3	2.56	1.05	3.21	1.31
115-2	3.31	1.06	3.60	1.16
233-2	2.68	1.21	3.79	1.71
253-3	2.38	1.17	2.66	1.31
277-2	1.87	1.30	2.13	1.49
747-2	4.43	1.18	5.10	1.36
753-2	3.64	1.10	4.37	1.33
755-2	4.86	1.10	5.96	1.35
755-4	5.62	1.13	6.70	1.35
761-2	0.60	0.14	1.58	0.38
825-3	1.51	0.53	1.74	0.61
909-2	1.63	0.48	2.02	0.59
1179-2	3.51	0.81	4.50	1.04
1181-2	5.16	0.95	6.36	1.18
1181-4	6.75	0.97	8.43	1.22
1183-2	2.57	1.04	3.44	1.40
1187-2	2.62	1.10	3.81	1.60
1213-3	2.52	1.22	2.93	1.42
1249-2	1.88	1.29	2.16	1.48

Table C-28: Pennsylvania I-80 Applied to all 20 Bridges - Fatigue II Parameters (275 days).

Bridge ID	Before Filtering 25% CAFL			After Filtering 25% CAFL		
	Effective Stress Range (ksi)	Effective Stress Range (Normalized)	Number of Cycles	Effective Stress Range (ksi)	Effective Stress Range (Normalized)	Number of Cycles
59-2	0.99	0.20	5,141,784	2.03	0.42	429,536
83-3	0.84	0.34	1,716,915	1.25	0.51	416,251
115-2	1.14	0.37	2,123,628	1.51	0.49	819,044
233-2	0.36	0.16	4,998,247	1.23	0.55	72,947
253-3	0.68	0.33	2,355,564	1.12	0.55	419,804
277-2	0.46	0.32	4,577,323	0.95	0.66	365,744
747-2	1.14	0.30	2,403,142	1.91	0.51	390,658
753-2	0.71	0.22	5,444,067	1.55	0.47	374,606
755-2	0.97	0.22	6,610,834	2.14	0.48	442,981
755-4	1.31	0.26	3,824,499	2.35	0.47	493,236
761-2	0.73	0.17	3,500,398	1.42	0.34	318,591
825-3	1.13	0.40	1,825,478	1.45	0.51	791,622
909-2	1.19	0.35	2,514,295	1.65	0.48	848,708
1179-2	1.26	0.29	2,082,954	1.86	0.43	463,220
1181-2	1.31	0.24	4,034,885	2.22	0.41	718,130
1181-4	1.77	0.26	3,720,348	2.97	0.43	499,766
1183-2	0.52	0.21	5,937,430	1.24	0.50	289,363
1187-2	0.42	0.18	3,510,203	1.18	0.49	61,957
1213-3	0.67	0.32	5,536,350	1.26	0.61	701,243
1249-2	0.50	0.34	3,326,882	0.95	0.65	367,045

Table C-29: Tennessee I-40 (Lane 1) Applied to all 20 Bridges - Fatigue I Parameters (268 days).

Bridge ID	Before Filtering 25% CAFL		After Filtering 25% CAFL	
	99.99th Percentile Stress Range (ksi)	99.99th Percentile Stress Range (Normalized)	99.99th Percentile Stress Range (ksi)	99.99th Percentile Stress Range (Normalized)
59-2	3.06	0.63	4.19	0.87
83-3	2.17	0.89	2.32	0.95
115-2	2.54	0.82	2.95	0.95
233-2	2.14	0.96	2.91	1.31
253-3	1.81	0.89	1.99	0.98
277-2	1.44	1.01	1.56	1.09
747-2	3.35	0.89	4.05	1.08
753-2	2.77	0.84	3.32	1.01
755-2	3.73	0.84	4.63	1.04
755-4	4.28	0.86	5.35	1.08
761-2	3.36	0.80	4.85	1.16
825-3	2.41	0.85	2.51	0.89
909-2	2.70	0.79	2.94	0.86
1179-2	3.38	0.78	3.99	0.92
1181-2	3.92	0.72	4.88	0.90
1181-4	5.14	0.74	6.92	1.00
1183-2	1.98	0.80	2.78	1.13
1187-2	2.11	0.88	3.10	1.30
1213-3	1.92	0.93	2.13	1.03
1249-2	1.46	1.00	1.65	1.13

Table C-30: Tennessee I-40 (Lane 1) Applied to all 20 Bridges - Fatigue II Parameters (268 days).

Bridge ID	Before Filtering 25% CAFL			After Filtering 25% CAFL		
	Effective Stress Range (ksi)	Effective Stress Range (Normalized)	Number of Cycles	Effective Stress Range (ksi)	Effective Stress Range (Normalized)	Number of Cycles
59-2	0.79	0.16	1,188,994	1.68	0.35	90,980
83-3	0.68	0.28	361,828	1.07	0.44	72,385
115-2	0.92	0.30	451,978	1.24	0.40	166,054
233-2	0.29	0.13	987,207	1.11	0.50	9,648
253-3	0.55	0.27	509,229	0.95	0.47	71,485
277-2	0.37	0.26	1,009,286	0.82	0.57	50,030
747-2	0.93	0.25	551,670	1.60	0.43	82,690
753-2	0.55	0.17	1,298,324	1.29	0.39	69,860
755-2	0.78	0.18	1,501,290	1.76	0.40	93,186
755-4	1.01	0.20	886,371	1.91	0.38	97,242
761-2	0.58	0.14	757,721	1.28	0.30	39,479
825-3	0.93	0.33	386,959	1.20	0.42	157,301
909-2	0.96	0.28	546,556	1.34	0.39	180,131
1179-2	0.99	0.23	562,086	1.55	0.36	120,778
1181-2	1.05	0.19	935,533	1.88	0.35	137,115
1181-4	1.44	0.21	818,242	2.42	0.35	104,299
1183-2	0.42	0.17	1,318,047	1.06	0.43	48,628
1187-2	0.34	0.14	767,599	1.06	0.44	8,678
1213-3	0.55	0.27	591,627	1.06	0.51	130,634
1249-2	0.41	0.28	705,533	0.82	0.56	50,425

Table C-31: Tennessee I-40 (Lane 3) Applied to all 20 Bridges - Fatigue I Parameters (268 days).

Bridge ID	Before Filtering 25% CAFL		After Filtering 25% CAFL	
	99.99th Percentile Stress Range (ksi)	99.99th Percentile Stress Range (Normalized)	99.99th Percentile Stress Range (ksi)	99.99th Percentile Stress Range (Normalized)
59-2	5.30	1.09	6.03	1.25
83-3	2.57	1.05	2.79	1.14
115-2	2.46	0.79	2.71	0.87
233-2	2.96	1.33	3.51	1.58
253-3	1.61	0.79	1.96	0.96
277-2	1.60	1.12	1.93	1.35
747-2	4.49	1.20	5.11	1.36
753-2	3.49	1.06	4.33	1.31
755-2	4.67	1.05	6.07	1.37
755-4	5.39	1.08	6.39	1.28
761-2	4.16	0.99	5.45	1.30
825-3	3.10	1.09	3.24	1.14
909-2	3.55	1.04	3.94	1.15
1179-2	4.38	1.01	5.25	1.21
1181-2	5.00	0.92	6.45	1.19
1181-4	6.59	0.95	8.55	1.23
1183-2	3.49	1.42	3.80	1.54
1187-2	1.76	0.74	2.26	0.95
1213-3	1.71	0.83	1.88	0.91
1249-2	1.48	1.01	1.93	1.32

Table C-32: Tennessee I-40 (Lane 3) Applied to all 20 Bridges - Fatigue II Parameters (268 days).

Bridge ID	Before Filtering 25% CAFL			After Filtering 25% CAFL		
	Effective Stress Range (ksi)	Effective Stress Range (Normalized)	Number of Cycles	Effective Stress Range (ksi)	Effective Stress Range (Normalized)	Number of Cycles
59-2	1.42	0.29	6,435,998	2.35	0.49	1,149,481
83-3	0.91	0.37	1,423,260	1.21	0.50	1,014,599
115-2	1.13	0.36	2,861,142	1.49	0.48	1,138,006
233-2	0.36	0.16	6,806,186	1.20	0.54	101,260
253-3	0.67	0.33	3,219,858	1.08	0.53	606,062
277-2	0.45	0.32	6,233,358	0.91	0.64	526,154
747-2	1.13	0.30	3,226,843	1.89	0.50	522,353
753-2	0.70	0.21	7,616,375	1.53	0.46	516,166
755-2	0.97	0.22	9,206,491	2.14	0.48	612,401
755-4	1.29	0.26	5,353,358	2.34	0.47	662,451
761-2	0.72	0.17	4,640,426	1.43	0.34	390,607
825-3	1.11	0.39	2,486,176	1.41	0.50	1,108,638
909-2	1.18	0.34	3,412,319	1.63	0.48	1,167,429
1179-2	1.20	0.28	3,431,315	1.87	0.43	726,526
1181-2	1.29	0.24	5,452,202	2.16	0.40	1,000,212
1181-4	1.76	0.25	5,060,645	2.93	0.42	677,391
1183-2	1.20	0.49	2,505,929	1.52	0.62	1,125,612
1187-2	0.47	0.20	10,191,629	0.98	0.41	822,580
1213-3	0.53	0.26	3,998,522	0.88	0.43	614,864
1249-2	0.34	0.23	5,014,767	0.91	0.62	68,030

Table C-33: Virginia US-29 (Lane 1) Applied to all 20 Bridges - Fatigue I Parameters (365 days).

Bridge ID	Before Filtering 25% CAFL		After Filtering 25% CAFL	
	99.99th Percentile Stress Range (ksi)	99.99th Percentile Stress Range (Normalized)	99.99th Percentile Stress Range (ksi)	99.99th Percentile Stress Range (Normalized)
59-2	2.90	0.60	4.86	1.00
83-3	2.59	1.06	3.00	1.23
115-2	3.16	1.02	3.36	1.08
233-2	2.45	1.11	3.27	1.47
253-3	2.09	1.03	2.44	1.20
277-2	1.61	1.12	1.89	1.32
747-2	4.07	1.08	4.57	1.22
753-2	3.39	1.03	3.99	1.21
755-2	4.54	1.02	5.57	1.26
755-4	5.21	1.05	5.79	1.16
761-2	4.18	0.99	5.08	1.21
825-3	3.07	1.08	3.17	1.12
909-2	3.35	0.98	3.60	1.05
1179-2	4.17	0.96	4.89	1.13
1181-2	4.85	0.90	5.70	1.05
1181-4	6.32	0.91	8.01	1.15
1183-2	2.39	0.97	3.26	1.32
1187-2	2.43	1.02	3.39	1.42
1213-3	2.29	1.11	2.83	1.37
1249-2	1.64	1.13	2.32	1.59

Table C-34: Virginia US-29 (Lane 1) Applied to all 20 Bridges - Fatigue II Parameters (365 days).

Bridge ID	Before Filtering 25% CAFL			After Filtering 25% CAFL		
	Effective Stress Range (ksi)	Effective Stress Range (Normalized)	Number of Cycles	Effective Stress Range (ksi)	Effective Stress Range (Normalized)	Number of Cycles
59-2	0.89	0.18	1,401,446	1.86	0.38	113,957
83-3	0.79	0.32	394,386	1.14	0.46	105,710
115-2	1.07	0.34	496,213	1.39	0.45	208,591
233-2	0.34	0.15	1,132,879	1.18	0.53	15,212
253-3	0.63	0.31	576,839	1.06	0.52	88,313
277-2	0.43	0.30	1,149,953	0.92	0.64	70,907
747-2	1.03	0.27	605,483	1.75	0.47	92,999
753-2	0.65	0.20	1,416,126	1.44	0.44	91,498
755-2	0.89	0.20	1,706,904	1.98	0.45	113,761
755-4	1.18	0.24	984,345	2.17	0.44	118,946
761-2	0.70	0.17	881,874	1.42	0.34	67,077
825-3	1.07	0.38	427,476	1.33	0.47	202,763
909-2	1.10	0.32	614,361	1.51	0.44	219,050
1179-2	1.10	0.25	652,715	1.74	0.40	133,685
1181-2	1.19	0.22	1,042,219	1.99	0.37	190,307
1181-4	1.62	0.23	980,221	2.69	0.39	119,238
1183-2	0.48	0.19	1,532,313	1.14	0.46	72,267
1187-2	0.41	0.17	874,221	1.15	0.48	13,099
1213-3	0.63	0.31	653,279	1.17	0.57	167,119
1249-2	0.47	0.32	780,928	0.93	0.64	71,204

Table C-35: Wisconsin SH-29 Applied to all 20 Bridges - Fatigue I Parameters (365 days).

Bridge ID	Before Filtering 25% CAFL		After Filtering 25% CAFL	
	99.99th Percentile Stress Range (ksi)	99.99th Percentile Stress Range (Normalized)	99.99th Percentile Stress Range (ksi)	99.99th Percentile Stress Range (Normalized)
59-2	4.42	0.91	5.64	1.17
83-3	2.92	1.19	3.15	1.29
115-2	3.53	1.13	3.61	1.16
233-2	2.67	1.20	3.69	1.66
253-3	2.36	1.16	2.87	1.41
277-2	1.79	1.25	2.11	1.48
747-2	4.66	1.24	5.36	1.43
753-2	3.63	1.10	5.06	1.54
755-2	4.93	1.11	6.18	1.39
755-4	5.96	1.20	6.88	1.38
761-2	4.54	1.08	6.01	1.43
825-3	3.35	1.18	3.52	1.24
909-2	3.80	1.11	3.99	1.17
1179-2	4.82	1.11	6.07	1.40
1181-2	5.38	0.99	6.57	1.21
1181-4	7.25	1.05	9.33	1.34
1183-2	2.56	1.04	3.45	1.40
1187-2	2.59	1.09	4.14	1.74
1213-3	2.58	1.25	3.06	1.49
1249-2	1.81	1.24	2.21	1.52

Table C-36: Wisconsin SH-29 Applied to all 20 Bridges - Fatigue II Parameters (365 days).

Bridge ID	Before Filtering 25% CAFL			After Filtering 25% CAFL		
	Effective Stress Range (ksi)	Effective Stress Range (Normalized)	Number of Cycles	Effective Stress Range (ksi)	Effective Stress Range (Normalized)	Number of Cycles
59-2	0.92	0.19	741,059	1.92	0.40	61,390
83-3	0.84	0.34	199,888	1.21	0.49	54,209
115-2	1.13	0.36	260,847	1.46	0.47	109,132
233-2	0.34	0.16	626,537	1.23	0.56	8,819
253-3	0.67	0.33	295,436	1.13	0.56	46,248
277-2	0.47	0.33	456,213	0.97	0.68	41,162
747-2	1.06	0.28	329,268	1.82	0.48	49,862
753-2	0.67	0.20	741,814	1.49	0.45	47,688
755-2	0.92	0.21	898,898	2.04	0.46	61,087
755-4	1.20	0.24	529,995	2.22	0.45	64,012
761-2	0.73	0.17	490,345	1.47	0.35	39,378
825-3	1.15	0.41	217,988	1.43	0.50	104,277
909-2	1.16	0.34	324,078	1.58	0.46	115,970
1179-2	1.14	0.26	350,338	1.80	0.42	73,496
1181-2	1.22	0.23	565,660	2.06	0.38	99,964
1181-4	1.67	0.24	525,354	2.79	0.40	64,222
1183-2	0.49	0.20	821,627	1.20	0.49	34,978
1187-2	0.43	0.18	481,822	1.19	0.50	7,772
1213-3	0.68	0.33	340,971	1.28	0.62	83,056
1249-2	0.51	0.35	397,726	0.97	0.67	41,128

References

AASHTO. 2014. *AASHTO LRFD Bridge Design Specifications.* 7th. Washington, D.C.: American Association of State Highway Transportation Officials.

—. 1965. *AASHTO Standard Specifications for Highway Bridges.* 9th. American Association of State Highway Transportation Officials.

—. 1994. *LRFD Bridge Design Specifications.* 1st. American Association of State Highway Transportation Officials.

—. 2012. *LRFD Bridge Design Specifications.* 6th. American Association of State Highway Transportation Officials.

—. 2017. *LRFD Bridge Design Specifications.* 8th. American Association of State Highway Transportation Officials.

—. 2016. *LRFD Bridge Design Specifications, 2016 Interim Revisions.* 6th. American Association of State Highway Transportation Officials.

Abaqus/CAE. 2017. *Abaqus/CAE User's Guide.*

Allen, T., A. Nowak, and R. Bathurst. 2005. *Calibration to Determine Load and Resistance Factors for Geotechnical and Structural Design.* Transportation Research Circular E-C079, Washington, D.C.: Transportation Research Board.

Al-Qadi, I., H. Wang, Y. Ouyang, K. Grimmelsman, and J. Purdy. 2016. *LTBP Program's Literature Review on Weigh-in-Motion Systems.* FHWA-HRT-16-024, McLean, Virginia: Federal Highway Administration.

ASTM. 2017. "Standard Specification for Highway Weigh-in-Motion (WIM) Systems with User Requirements and Test Methods." *E1318.* ASTM International.

Azizinamini, A., S. Kathol, and M. Beacham. 1995. "Influence of Cross Frames on Load Resisting Capacity of Steel Girder Bridges." *Engineering Journal* (American Institute of Steel Construction) 107-116.

Battistini, A., W. Wang, T. Helwig, M. Engelhardt, and K. Frank. 2016. "Stiffness Behavior of Cross Frame in Steel Bridge Systems." *Journal of Bridge Engineering* (American Society of Civil Engineers) 21 (6).

Chavel, B. W., and C. J. Earls. 2006. "Construction of Horizontally Curved Steel I-girder Bridge: Erection Sequence." *Journal of Bridge Engineering* (American Society of Civil Engineers) 81-90.

Chavel, B., D. Coletti, K. Frank, M. Grubb, B McEleney, R. Medlock, and D. White. 2016. *Skewed and Curved Steel I-Girder Bridge Fit.* Chicago, IL: National Steel Bridge Alliance.

Chowdhury, P., and H. Sehitoglu. 2016. "Mechanisms of Fatigue Crack Growth - a Critical Digest of Theoretical Developments." *Fatigue and Fracture of Engineering Materials and Structures.*

Connor, R., and J. Fisher. 2006. "Identifying Effective and Ineffective Retrofits for Distortion Fatigue Cracking in Steel Bridges Using Field Instrumentation." *Journal of Bridge Engineering* (American Society of Civil Engineers) 11 (6): 745-752.

Curtis, R., and R. Till. 2008. *Recommendations for Michican Specific Load and Resistance Factor Design Loads and Load and Resistance Factor Rating Procedures.* MDOT Research Report R-1511, East Lansing, Michigan: Michigan Department of Transportation.

Davis, J. 2007. *Live-Load Models for Design and Fatigue Evaluation of Highway Bridges.* Ph.D. Dissertation, New Brunswick, New Jersey: Rutgers, The State University of New Jersey.

FHWA. 2016. *Design and Evaluatoin of Steel Bridges for Fatigue and Fracture.* Washington, D.C.: U.S. Department of Transportation Federal Highway Administration.

Fisher, J., G. Kulak, and I. Smith. 1998. *A Fatigue Primer for Structural Engineers.* National Steel Bridge Alliance.

Fisher, J., K. Frank, M. Hirt, and B. McNamee. 1969. *Effect of Weldments on the Fatigue Strength of Steel Beams.* NCHRP Project 12-7, Fritz Engineering Laboratory Report No. 334.2, Washington, D.C.: Highway Research Board.

Fisher, J., P. Albrecht, B. Yen, D. Klingerman, and B. McNamee. 1974. *Fatigue Strength of Steel Beams with Welded Stiffeners and Attachments.* NCHRP Report 147, Washington, D.C.: Transportation Research Board.

Freund, L. B. 1990. *Dynamic Fracture Mechanics.* New York Citdy, New York: Cambridge University Press.

Fu, G., and J. van de Lindt. 2006. *LRFD Load Calibration for State of Michigan Trunkline Bridges.* Research Report RC-1466, Lansing, Michigan: Michigan Department of Transportation.

Fu, G., and O. Hag-Elsafi. 1997. *Safety-Based Bridge Overstress Criteria for Non-Divisible Loads.* Final Report R212, New York State Department of Transportation.

Fu, G., and O. Hag-Elsafi. 2000. "Vehicular Overloads: Load Model, Bridge Safety, and Permit Checking." *Journal of Bridge Engineering* (American Society of Civil Engineers) 49.

Fu, G., J. Chi, and Q. Wang. 2019. *Illinois-Specific Live-Load Factors Based on Truck Data.* ICT Project R27-171, Illinois Center for Transportation.

Ghosn, M., B. Sivakumar, and F. Miao. 2011. *Load and Resistance Factor Rating (LRFR) in NYS.* Final Project Report C-06-13, The City College of The City University of New York.

Goble, G., F. Moses, and A. Pavia. 1976. "Applications of a Bridge Measurement System." *Transportation Research Record* 579: 36-47.

Grubb, M. 1984. "Horizontally Curved I-Girder Bridge Analysis: V-Load Method." *Transportation Research Record 982* 26-36.

Hasofer, A., and N. Lind. 1974. "An Exact and Invariant First Order Reliability Format." *Journal of Engineering Mechanics* (American Society of Civil Engineers) 100 (EM1): 111-121.

Helwig, T., and J. Yura. 2015. *Steel Bridge Design Handbook: Bracing System Design.* Technical Report, Washington, D.C.: Federal Highway Administration.

Helwig, T., and L. Wang. 2003. *Cross-Frame and Diaphragm Behavior for Steel Bridges with Skewed Supports.* Research Report 1772-1, Austin, TX: Report for Texas Department of Transporation.

Helwig, T., and Z. Fan. 2000. *Field and Computational Studies of Steel Trapezoidal Box Girder Bridges.* TxDOT Research Report 1395-3, Houston, Texas: The University of Houston.

Keating, P., and J. Fisher. 1986. *Evaluation of Fatigue Tests and Design Criteria on Welded Details.* NCHRP Report 286, Washington, D.C.: Transportation Research Board.

Keating, P., K. Saindon, and S. Wilson. 1997. *Cross Frame Diaphragm Fatigue and Load Distribution Behavior in Steel Highway Bridges.* TxDOT Research Report 1360-2F, College Station, TX: Texas Transportation Institute.

Kulicki, J., and D. Mertz. 1998. "Development of Comprehensive Bridge Specifications and Commentary." *NCHRP Research Results Digest*, May.

Kulicki, J., W. Wassef, A. Nowak, D. Mertz, N. Samtani, and H. Nassif. 2015. *Bridges for Service Life Beyond 100 Years: Service Limit State Design.* SHRP2 Report S2-R19B-RW-1, Washington, D.C.: Transportation Research Board.

Kulicki, J., Z. Prucz, C. Clancy, D. Mertz, and A. Nowak. 2007. *Updating the Calibration Report for AASHTO LRFD Code.* NCHRP Project 20-7/186, Washington, D.C.: NCHRP.

Kwon, S., E. Kim, S. Orton, H. Salim, and T. Hazlett. 2011. *Calibration of the Live Load Factor in LRFD Design Guidelines.* Columbia, Missouri: University of Missouri.

Lee, C. 1966. Vehicle Weighing Scale with Overlapped Load Bearing Plates. United States of America Patent 3,266,584. August 16.

Lee, C., and J. Garner. 1996. *Collection and Analysis of Augmented Weigh-in-Motion Data.* Center for Transportation Research Report 987-8, Austin, Texas: The University of Texas at Austin.

Mahmoud, K. 2011. "Modern Techniques in Bridge Engineering." *Proceedings of 6th New York City Bridge Conference, 25-26 July 2011.* CRC Press.

McConnell, J., M. Radovic, and K. Ambrose. 2016. "Field Evaluation of Cross-Frame and Girder Live-Load Response in Skewed Steel I-Girder Bridges." *Journal of Bridge Engineering* (American Society of Civil Engineers) 21 (3).

McDonald, G., and K. Frank. 2009. *The Fatigue Performance of Angle Cross-Frame Members in Bridges.* MS Thesis, Austin, Texas: The University of Texas at Austin.

Mertz, D. 2008. *Gerald Desmond Bridge Replacement Project Site-Specific Vehicular Live Load Study.* Draft Report, Port of Long Beach, California.

Moses, F. 2001. *Calibration of Load Factors for LRFR Bridge Evaluation.* NCHRP Report 454, Transportation Research Board.

Nassif, H., M. Gindy, and J. Davis. 2008. *Live Load Calibration for the Schuyler Heim Bridge Replacement and State Route 47 Extension.* Final Report, California Department of Transportation.

NBS. 1969. *Mechanisms Leading to the Failure of the Point Pleasant, West Virginia Bridge.* National Bureau of Standards Report.

Normann, O., and R. Hopkins. 1952. *Weighing Vehicles in Motion.* HRB Bulletin 50, Washington, D.C.: Highway Research Board.

Nowak, A. 1999. *Calibration of LRFD Bridge Design Code.* NCHRP Report 368, Washington, D.C.: Transportation Research Board.

Nowak, A., and K. Collins. 2013. *Reliability of Structures.* 2nd. Boca Raton, Florida: CRC Press.

OHBDC. 1979. *Ontario Highway Bridge Design Code.* Downsview, Ontario, Canada: Ministiry of Transportation.

Park, S. 2020. *Modifactions to Cross-Frame Stiffness for Composite Steel Bridges.* PhD Dissertation, Austin, TX: The University of Texas at Austin.

Pelphrey, J., C. Higgins, B. Sivakumar, R. Groff, B. Hartman, J. Charbonneau, J. Rooper, and B.

Johnson. 2008. "State-Specific LRFR Live Load Factors Using Weigh-in-Motion Data." *Journal of Bridge Engineering* (American Society of Civil Engineers) 13: 339-350.

Quadrato, C. 2010. *Stability of Skewed I-shaped Girder Bridges.* Dissertation, Austin, Texas: The University of Texas at Austin.

Quadrato, C., A. Battistini, T. Helwig, M. Engelhardt, and K. Frank. 2014. "Increasing Girder Elastic Buckling Strength using Split Pipe Bearing Stiffeners." *Journal of Bridge Engineering* (American Society of Civil Engineers) 19 (4).

Rackwitz, R., and B. Fiessler. 1978. "Structural Reliability under Combined Random Load Sequences." *Computers and Structures* 9: 489-494.

Reichenbach. 2020. *Experimental and Analytical Evaluation of Cross-Frame Fatigue Behavior in Steel I-Girder Bridges.* Ph.D. Dissertation, Austin, TX: The University of Texas at Austin.

Reichenbach, M., J. White, S. Park, E. Zecchin, M. Moore, Y. Liu, T. Helwig, and M. Engelhardt. 2021. *Proposed Modifications to AASHTO Cross-Frame Analysis and Design.* NCHRP 12-113 Final Report, Washington, D.C.: Transportation Research Board.

Romage, M. 2008. *Field Measurements on Lean-On Bracing System for Steel I-Girder Bridges with Skewed Supports.* Thesis, Austin, TX: The University of Texas at Austin.

Rowles, L. 2014. "Field Load Test of a Curved Steel I-Girder Bridge During Construction and Comparison with 2D Grid Modeling." *Structures Congress.* Boston, MA. 687-698.

Russo, F. 2017. "A Bridge Forward." *Modern Steel Construction* 45-54.

Sivakumar, B., F. Moses, G. Fu, and M. Ghosn. 2007. *Legal Truck Loads and AASHTO Legal Loads for Posting.* NCHRP Report 575, Washington, D.C.: Transportation Research Board.

Sivakumar, B., M. Ghosn, and F. Moses. 2008. *Protocols for Collecting and Using Traffic Data.* NCHRP Web-Only Document 135, Washington, D.C.: Transportation Research Board.

Sivakumar, B., M. Ghosn, and F. Moses. 2011. *Protocols for Collecting and Using Traffic Data in Bridge Design.* NCHRP Report 683, Washington, D.C.: Transportation Research Board.

Stith, J., B. Petruzzi, T. Helwig, M. Engelhardt, K. Frank, and E. Williamson. 2010. *Guidelines for Design and Safe Handling of Curved I-Shaped Steel Girders.* TxDOT Project Report 0-5574, Austin, Texas: Center for Transportation Research, The University of Texas at Austin.

Tedesco, J., J. Stalllings, and D. Tow. 1995. "Finite Element Method Analysis of Bridge Girder-

Diaphragm Interaction." *Computers and Sturctures* 461.

Uddin, N., H. Zhao, C. Waldron, L. Dong, and A. Greer. 2011. *Weign-in-Motion (WIM) Data for Site-Specific LRFR Bridge Load Rating.* UTCA Report No. 10204, Hunstville, Alabama: University Transportation Center for Alabama.

USDOT. 2018. *Transportation Statistics Annual Report.* Ofice of the Secretary of Transportation, Washington, D.C.: U.S. Department of Transportation, Bureau of Transportation Statistics.

Wang, W. 2013. *A Study of Stiffness of Steel Bridge Cross Frames.* PhD Dissertation, Austin, TX: The University of Texas at Austin.

Wassef, W., J. Kulicki, H. Nassif, D. Mertz, and A. Nowak. 2014. *Calibration of AASHTO LRFD Concrete Bridge Design Specifications for Serviceability.* NCHRP Web-Only Document 201, Washington, D.C.: Transportation Research Board.

White, D., D. Coletti, B. Chavel, A. Sanchez, C. Ozgur, J. Jimenez Chong, R. Leon, et al. 2012. *Guidelines for Analysis Methods and Construction Engineering of Curved and Skewed Steel Girder Bridges.* NCHRP Report 725, Washington, D.C.: Transportation Research Board.

White, D., T. Nguyen, D. Coletti, B. Chavel, M. Grubb, and C. Boring. 2015. *Guidelines for Reliable Fit-Up of Steel I-Girder Bridges.* NCHRP 20-07/Task 355, Washington, D.C.: Transportation Research Board, National Research Council.

Wilson, W., and J. Coombe. 1939. "Fatigue Tests of Connection Angles." *Engineering Experiment Station Bulletin Series No. 317.*

Witcher, T. R. 2017. "From Disaster to Prevention: The Silver Bridge." *Civil Engineering*, December: 44-47.

Yura, J. 2001. "Fundamentals of Beam Bracing." *Engineering Journal* (American Institute of Steel Construction) 11-26.

Yura, J., B. Philips, S. Raju, and S. Webb. 1992. *Bracing of Steel Beams in Bridges.* Research Report 1239-4F, Austin, TX: Center for Transportation Research - University of Texas at Austin.

Yura, J., T. Helwig, R. Herman, and C. Zhou. 2008. "Global Lateral Buckling of I-Shaped Girder Systems." *Journal of Structural Engineering* (American Society of Civil Engineerings).

Zhang, L. 2007. *An Evaluation of the Technical and Economic Performance of Weigh-in-Motion Sensing Technology.* M.S. Thesis, Waterloo, Ontario, Canada: Univesity of Waterloo.

Zhou, Y., and A. Biegalski. 2010. "Investigations of Large Web Fractures of Welded Steel Plate Girder Bridge." *Journal of Bridge Engineering.*

Zwerneman, F. 1997. *Fatigue Assessment of Bridge Members.* Final Report: Executive Summary, Oklahoma State University.